On generalisations of the AGT correspondence for non-Lagrangian theories of class $\mathcal{S}$

Dissertation

zur Erlangung des Doktorgrades
an der Fakultät für Mathematik,
Informatik und Naturwissenschaften

Fachbereich Physik
der Universität Hamburg

vorgelegt von

Ioana Coman-Lohi

Hamburg

2018

Gutachter/innen der Dissertation:	Prof. Dr. Joerg Teschner
	Prof. Dr. Volker Schomerus
Zusammensetzung der Prfungskommission:	Prof. Dr. Joerg Teschner
	Prof. Dr. Volker Schomerus
	Prof. Dr. Gleb Arutyunov
	Prof. Dr. Günter H. W. Sigl
	Prof. Dr. Dieter Horns
Vorsitzende/r der Prfungskommission:	Prof. Dr. Dieter Horns
Datum der Disputation:	18.04.2018
Vorsitzender Fach-Promotionsausschusses PHYSIK:	Prof. Dr. Wolfgang Hansen
Leiter des Fachbereichs PHYSIK:	Prof. Dr. Michael Potthoff
Dekan der Fakultät MIN:	Prof. Dr. Heinrich Graener

To Karolina, Nikolas, Ana, Doru and Cristina

Abstract

Non-perturbative aspects of $\mathcal{N} = 2$ supersymmetric field theories of class $\mathcal{S}$ are deeply encoded in the algebra of functions on moduli spaces $\mathcal{M}_{\text{flat}}$ of flat $SL(N)$-connections on Riemann surfaces. Expectation values of Wilson and 't Hooft supersymmetric line operators are related to holonomies of flat connections, while expectation values of line operators in the low energy effective theory are related to Fock-Goncharov coordinates on $\mathcal{M}_{\text{flat}}$. Through the decomposition of UV line operators into IR line operators, we determine their noncommutative algebra from the quantisation of Fock-Goncharov Laurent polynomials, and find that it coincides with the skein algebra studied in the context of Chern-Simons theory through quantum group theory methods.

We also investigate the relations between the quantisation of moduli spaces of flat connections, $\mathfrak{sl}_N$ Toda conformal field theories and quantum group theory, and find that another realisation of the skein algebra is generated by Verlinde network operators on Toda conformal blocks. To arrive here we use the free field representation of $\mathcal{W}$-algebras to define natural bases for spaces of conformal blocks in Toda field theory. For $\mathfrak{sl}_3$ conformal blocks on a three-punctured sphere with generic representations associated to the three punctures we construct operator valued monodromies of degenerate fields which can be used to describe the quantisation of the moduli spaces of flat $SL(3)$-connections. The matrix elements of these quantum monodromy matrices can be expressed as Laurent polynomials of more elementary operators, which have a simple definition in the free field representation and are identified as quantised counterparts of natural higher rank Fenchel-Nielsen type coordinates. Arguments from quantum group theory then lead to the identification of the quantum skein algebra of functions on moduli spaces of flat connections and the algebra of Verlinde network operators. Comparing the spectra of these two realisations provides non-trivial support for their equivalence. Our results can be viewed as evidence for the generalisation of the AGT correspondence to higher-rank class $\mathcal{S}$ theories, in particular those with no known weakly-coupled Lagrangian description.

We investigate possible applications to the study of non-Lagrangian SUSY field theories through their relation to topological string theory. Beginning with the topological string partition functions corresponding to the T_N trinion theories of class $\mathcal{S}$, we explore the relation between the geometric data of the local Calabi-Yau manifold used in the geometric engineering of these theories and certain parameters which enter the free field construction of $\mathfrak{sl}_N$ Toda conformal blocks. A meaningful way to take the geometric engineering limit is discussed in the most simple case.

Zusammenfassung

Nichtperturbative Aspekte $\mathcal{N} = 2$ supersymmetrischer Feldtheorien der Klasse $\mathcal{S}$ sind in der Algebra der Funktionen auf Modulräumen $\mathcal{M}_{\text{flat}}$ flacher $SL(N)$-Zusammenhänge auf Riemannschen Flächen verschlüsselt. Erwartungswerte supersymmetrischer Wilson und 't Hooft Linienoperatoren stehen in Verbindung mit Holonomien flacher Zusammenhänge, während Erwartungswerte von Linienoperatoren in der effektiven Niedrigenergie-Theorie mit Fock-Goncharov Koordinaten auf $\mathcal{M}_{\text{flat}}$ verbunden sind. Über die Zerlegung von UV-Linienoperatoren in IR-Linienoperatoren bestimmen wir ihre nichtkommutative Algebra aus der Quantisierung der Fock-Goncharov Laurent-Polynome und finden mithilfe quantengruppentheoretischer Methoden, dass sie mit der Skein-Algebra übereinstimmt, welche im Kontext von Chern-Simons Theorie behandelt wird.

Darüber hinaus untersuchen wir Verbindungen zwischen der Quantisierung von Modulräumen flacher Zusammenhänge, $\mathfrak{sl}_N$ Toda konformen Feldtheorien und Quantengruppentheorie. Wir finden, dass eine weitere Realisierung der Skein-Algebra durch Verlinde-Netzwerkoperatoren auf konformen Blöcken von Toda konformen Feldtheorien erzeugt wird. Um zu diesem Ergebnis zu gelangen, nutzen wir die freie Felddarstellung von $\mathcal{W}$-Algebren, um eine natürliche Basis für Räume konformer Blöcke in Toda konformen Feldtheorien zu definieren. Für $\mathfrak{sl}_3$ konforme Blöcke auf einer 3-punktierten Sphäre mit beliebigen zu den drei Punkten assoziierten Darstellungen konstruieren wir operatorwertige Monodromien entarteter Felder, welche zur Beschreibung der Quantisierung von Modulräumen flacher $SL(3)$-Zusammenhänge genutzt werden können. Die Matrixelemente dieser Quanten-Monodromiematrizen können als Laurent-Polynome elementarerer Operatoren ausgedrückt werden, welche eine einfache Definition in der freien Felddarstellung haben und die quantisierten Gegenstücke natürlicher Fenchel-Nielsen Koordinaten höheren Ranges sind. Argumente aus der Quantengruppentheorie führen dann zur Identifizierung der Quanten-Skein-Algebra der Funktionen auf Modulräumen flacher Zusammenhänge und der Algebra der Verlinde-Netzwerkoperatoren. Der Vergleich der Spektren dieser beiden Realisierungen liefert nicht-triviale Evidenz für ihre Äquivalenz. Unsere Resultate können als Untermauerung der Verallgemeinerung der AGT Korrespondenz auf Theorien der Klasse $\mathcal{S}$ höheren Rangs, insbesondere für jene ohne bekannte Lagrange-Beschreibung im schwach gekoppelten Regime, verstanden werden.

Wir untersuchen mögliche Anwendungen in der Erforschung supersymmetrischer Theorien ohne Lagrange-Beschreibung durch ihre Verbindung zur topologischen Stringtheorie. Beginnend mit der Zustandssumme des topologischen Strings, welche dem T_N Trinion in Theorien der Klasse $\mathcal{S}$ entspricht, erkunden wir die Verbindung zwischen den geometrischen Daten der lokalen Calabi-Yau Mannigfaltigkeit, welche im Kontext des Geometric Engineering dieser Theorien benutzt werden, und bestimmten Parametern, welche in der freien Feldkonstruktion von $\mathfrak{sl}_N$ Toda konformen Blöcken auftauchen. Für den einfachsten Fall diskutieren wir einen sinnvollen Weg, den Grenzwert für das Geometric Engineering zu bestimmen.

This thesis is based on the publications:

- I. Coman, M. Gabella, J. Teschner, *Line operators in theories of class $\mathcal{S}$, quantized moduli space of flat connections, and Toda field theory*, JHEP **1510** (2015) 143, [arXiv:1505.05898];
- I. Coman, E. Pomoni, J. Teschner, *Toda conformal blocks, quantum groups, and flat connections*, (2017), [arXiv:1712.10225];
- *I. Coman, E. Pomoni, J. Teschner*, *Liouville conformal blocks from topological strings*, to appear;
- *I. Coman, E. Pomoni, J. Teschner*, *Toda conformal blocks from topological strings*, in progress.

Other publications by the author:

- I. Coman, E. Pomoni, F. Yagi, M. Taki, *Spectral curves of N=1 theories of class Sk*, JHEP **1706**, (2017) 136, [arXiv:1512.06079];
- C.I. Lazaroiu, E.M. Babalic, I.A. Coman, *The geometric algebra of supersymmetric backgrounds*, Proceedings of Symposia in Pure Mathematics, Vol. 90 (2015) 227-237;
- C.I. Lazaroiu, E.M. Babalic, I.A. Coman, *The geometric algebra of Fierz identities in arbitrary dimensions and signatures*, JHEP **09** (2013) 156, [arXiv:1304.4403];
- C.I. Lazaroiu, E.M. Babalic, I.A. Coman, *A unified approach to Fierz identities*, AIP Conf. Proc. **1564**, 57 (2013), [arXiv:1303.1575];
- E.M. Babalic, I.A. Coman, C. Condeescu, C.I. Lazaroiu, A. Micu, *On N=2 compactifications of M-theory to AdS3 using geometric algebra techniques*, AIP Conf. Proc. **1564**, 63 (2013);
- C.I. Lazaroiu, E.M. Babalic, I.A. Coman, *Geometric algebra techniques in flux compactifications*, Advances of High Energy Physics (2016), [arXiv:1212.6766v1].

Contents

I Introduction **1**

1 Introduction **1**

1.1 Recent advances 2

1.2 Correspondence to two dimensional conformal field theory 6

1.3 Relation to topological string theory 8

1.4 Parallel developments and an alternative route towards AGT 9

1.5 Overview 13

II Quantisation of moduli spaces of flat connections on punctured Riemann surfaces **17**

2 Algebra of loop and network operators **21**

2.1 Moduli space of flat connections 21

2.2 Trace functions 22

2.3 Poisson structure 24

2.4 Classical skein algebra 25

2.5 Loop and network functions 26

2.6 Commuting Hamiltonians 29

2.7 Tinkertoys 30

2.8 Skein quantisation 31

3 Quantisation of tinkertoys **37**

3.1 Pants networks 37

3.2 One-punctured torus 45

3.3 Four-punctured sphere 50

4 Fock-Goncharov holonomies **53**

4.1 Fock-Goncharov coordinates . . . 53
4.2 Holonomies . . . 54
4.3 Quantisation . . . 56
4.4 Pants networks . . . 58
4.5 One-punctured torus . . . 65
4.6 Four-punctured sphere . . . 72

5 First conclusions **75**

Appendices **77**

A Fock-Goncharov coordinates **79**
A.1 Coordinates associated with N-triangulations . . . 79
A.2 Snakes and projective bases . . . 81

III Toda conformal blocks, moduli spaces of flat connections and quantum groups **87**

6 Relation to conformal field theory **93**
6.1 Toda conformal field theory and $\mathcal{W}_N$-algebra . . . 93
6.2 Conformal blocks . . . 95
6.3 Degenerate representations . . . 99
6.4 Free field construction of conformal blocks . . . 100
6.5 Quantum monodromies . . . 101
6.6 Verlinde operators and quantised moduli spaces of flat connections . . . 102

7 Quantum group background **105**
7.1 Representations . . . 106
7.2 Tensor products of representations . . . 107
7.3 Iterated Clebsch-Gordan maps . . . 109
7.4 R-matrix . . . 109
7.5 Twisted (compositions of) Clebsch-Gordan maps . . . 110

8 Free-field construction of chiral vertex operators **113**
8.1 Basic definitions . . . 113
8.2 Conformal blocks from screened vertex operators . . . 116

8.3 Braiding of screened vertex operators . . . 117
8.4 Construction of conformal blocks . . . 119
8.4.1 Relation to quantum group theory . . . 119
8.4.2 Independence of the choice of base-point . . . 120

9 Computation of monodromies **123**
9.1 Conformal blocks with degenerate fields . . . 124
9.2 Braiding with fundamental representation . . . 124
9.3 Form of the monodromy matrix . . . 125

10 Verlinde line and network operators and their algebra **127**
10.1 Braiding and fusion of degenerate fields . . . 127
10.2 Conformal blocks with degenerate fields . . . 129
10.3 Verlinde network operators . . . 131
10.4 Relation to skein algebra . . . 132

11 Spectrum **135**
11.1 Spectrum in Toda field theory . . . 135
11.2 Spectrum of quantised trace functions . . . 137
11.3 Remarks . . . 141

12 More relations to the quantisation of moduli spaces of flat connections **143**
12.1 The notion of Fenchel-Nielsen type coordinates . . . 143
12.2 Quantum Fenchel-Nielsen type coordinates . . . 144
12.3 Yang's functions and isomonodromic tau functions from classical limits . . . 145

13 Conclusions and outlook **147**
13.1 More punctures . . . 147
13.2 Continuous bases for spaces of conformal blocks in Toda CFT . . . 148
13.2.1 Continuation in screening numbers . . . 148
13.2.2 Relation to quantum group theory and higher Teichmüller theory . . . 149

Appendices **151**

B Useful relations **153**

C Clebsch-Gordan coefficients **155**
C.1 Clebsch-Gordan coefficients for generic weights λ 155
C.2 Clebsch-Gordan coefficients for the case $\lambda_2 = \omega_1$ 156

D Braid matrix derivation **157**

E Realisation of the generators e_i on screened vertex operators **163**

IV Toda conformal blocks and topological strings **165**

14 Liouville conformal blocks and topological strings **171**

15 The topological vertex result **175**
15.1 Resummation into a product formula 177
15.2 The four dimensional limit 178
15.2.1 A useful factorisation 179
15.2.2 The limit of the regular part 180
15.2.3 Renormalising the singular part 181

16 From topological strings to a matrix integral **183**
16.1 Imposing the specialisation condition on the topological strings 183
16.2 The matrix integral as a sum of residues 184

17 The free field representation **189**
17.1 The $\mathfrak{q} \to 1$ limit of the matrix integral 190

18 Integral form of the T_N topological strings partition function **193**
18.1 Defining of the functions $\mathcal{I}_a$, $\mathcal{I}_{m_a}$, $\mathcal{I}_{a,a}$ 196
18.2 Reduction of $\mathcal{Z}_N^{\text{pert}}$ 198
18.3 Poles and residues of $\mathcal{I}_N$ 198

19 The free field representation of $\mathfrak{sl}_N$ $\mathfrak{q}$-Toda **201**
19.1 Geometrical interpretation for the screening numbers 202

20 Conclusions and outlook **207**

Appendices **209**

F Special functions **211**

F.1 The limit $\mathfrak{q} \to 1$ 213

G Variants of Jackson integrals and the $\mathfrak{q} \to 1$ limit **215**

H Useful identities **217**

H.1 Face relations among Kähler parameters 217

V Final thoughts and perspectives **221**

Part I

Introduction

Chapter 1

Introduction

Motivated by the quest to understand the fundamental nature in which the universe works, physicists have constructed frameworks to explain observed phenomena and enable the computation of quantitative predictions. A prominent example is that of gauge theories whose role in the frame of theoretical physics is to describe interactions between elementary particles. The current paradigm is extremely successful when applied to weakly-interacting theories, where perturbative approaches based on a Lagrangian formulation are appropriate. It is however not well suited to explain strong coupling phenomena, a notable example of which occurs in quantum chromodynamics. Its formulation displays asymptotic freedom at high energies where colour interactions between quarks are weak, but exhibits confinement at low energies, which holds quarks in a bound state. Confinement is a non-perturbative effect that emerges in strongly interacting regimes and which is not accounted for by perturbation theory. Further effects whose understanding is so far outside the reach of perturbation theory are *instantons*, which are exponentially suppressed contributions to effective interactions caused by nontrivial solutions to the Euclidean equations of motion. Our knowledge of gauge theories is therefore so far incomplete without a grasp of their strong coupling behaviour.

Nevertheless, advances have been made in this direction in the past decades, with important physical quantities being calculated exactly for theories that have a certain amount of supersymmetry. The additional constraints that are imposed by this symmetry describing relations between bosons and fermions have allowed physicists to mitigate some of the current technical difficulties. Highlights of recent success include exact results on the expectation values of certain physical observables like Wilson and 't Hooft loop operators and powerful algorithms for the computation of the spectra of BPS states which yield non-perturbative results. There exist also examples from Seiberg-Witten theory where instanton corrections and confinement are understood. The hope is that by developing new theoretical techniques through the analysis of supersymmetric field theories, the resulting insights will be applicable to more realistic scenarios. In this context, the success story in the study of $\mathcal{N} = 2$ supersymmetric field theories in four dimensions has placed these at the centre of a harmonious and enduring interplay between physics and mathematics. We will review below some of these advances, a survey of which can be found in [1].

1.1 Recent advances

Seiberg-Witten theory

Beginning with the two publications [2], [3], Seiberg and Witten discovered exact results for the low energy effective actions of certain four dimensional $\mathcal{N} = 2$ supersymmetric gauge theories. A nice pedagogical introduction can be found in [4]. The content of such theories with generic gauge group G, is distributed into vector multiplets $(A_\mu, \phi, \lambda^{\mathcal{I}})_r$ and hypermultiplets $(Q_{\mathcal{I}}, \psi.\tilde{\psi})$, where the label r is in the range $1, \ldots,$ rank(G) and $\mathcal{I} = 1, 2$. The former are the gauge multiplets and contain a gauge field A_μ with spacetime parameter $\mu = 1, \ldots, 4$, a scalar field ϕ in the adjoint representation of the gauge group and the two fermions $\lambda^{\mathcal{I}}$, while the latter contain matter fields $Q_{\mathcal{I}}$ and fermions $\psi, \tilde{\psi}$. Such gauge theories admit families of supersymmetric vacua which form a moduli space $\mathcal{M}_{\text{vac}}$. This space splits into the Coulomb branch, which is parameterised by vacuum expectation values of gauge invariant functions of the scalars ϕ, the Higgs branch, where matter fields receive non-vanishing mass parameters, and branches of mixed type. Considering for example theories with $SU(2)$ gauge groups, the Coulomb branch of $\mathcal{M}_{\text{vac}}$ is parametrised by $u \equiv \langle \text{Tr}(\phi^2) \rangle$, while the matter fields have vanishing vacuum expectation values $\langle Q \rangle = 0$. When the gauge groups are replaced by $SU(N)$, there are $N - 1$ such functions $u^{(k)} = \langle \text{Tr}(\phi^k) \rangle$, with $k = 2, \ldots, N$.

The gauge group $SU(N)$ breaks to $U(1)^{N-1}$ at low energy, where the physics at generic points $u^{(k)}$ on the Coulomb branch is described by an effective action functional whose bosonic part

$$S_{\text{b}}^{\text{eff}} = \frac{1}{4\pi} \int d^4x \big(\text{Im}(\tau^{kl}) \partial_\mu \bar{a}_k \partial^\mu a_l + \frac{1}{2} \text{Im}(\tau^{kl}) F_{k,\mu\nu} F_l^{\mu\nu} + \frac{1}{2} \text{Re}(\tau^{kl}) F_{k,\mu\nu} \tilde{F}_l^{\mu\nu} \big) \qquad (1.1.1)$$

depends on a matrix of couplings τ^{kl} and the $N-1$ vector multiplets A_k with scalar components a_k and field strength F_k. The fermionic counterpart $S_{\text{f}}^{\text{eff}}$ is fully determined by the constraints of $\mathcal{N} = 2$ supersymmetry and the full effective action that describes the quantum field theory at low energies is the combination $S^{\text{eff}} = S_{\text{b}}^{\text{eff}} + S_{\text{f}}^{\text{eff}}$.

The low energy physics for generic values of the parameters $u^{(k)}$ is captured by the prepotential $\mathcal{F}(a)$, which is a holomorphic function whose argument denotes collectively the scalar components $a = (a_1, ..., a_{N-1})$ of the vector multiplets and which determines the matrix of couplings through $\tau^{kl}(a) = \partial_{a_k} \partial_{a_l} \mathcal{F}(a)$. For large classes of $\mathcal{N} = 2$ supersymmetric gauge theories, the function $\mathcal{F}(a)$ is in turn specified by an auxiliary Riemann surface called the Seiberg-Witten (SW) curve Σ which is defined by a polynomial equation $P(v, t) = 0$ in two complex variables and with coefficients determined by $u^{(k)}$, the mass parameters m of the flavour fields and the matrix τ of gauge couplings. For a canonical one-form $\lambda_{SW} = v dt/t$ and a chosen basis of the first homology group $H_1(\Sigma, \mathbb{Z})$ represented by pairs of curves $\{\alpha, \beta\}_r$ with intersection index $\alpha_r \cap \beta_s = \delta_{rs}$, the periods $a_r(u) = \int_{\alpha_r} \lambda_{SW}$ and $a_r^D(u) = \int_{\beta_r} \lambda_{SW}$ define pairs of dual complex coordinates on the space of vacua $\mathcal{M}_{\text{vac}}$. Such a basis of cycles $\{\alpha, \beta\}$ can be seen on the torus at the top of Figure 1.1. The prepotential relates the corresponding dual coordinates through $a_r^D = \partial_{a_r} \mathcal{F}(a)$. The parameters (a, a^D) are called *electric-magnetic* dual in the sense that they enter descriptions of the low energy physics at different points in the moduli space.

Supersymmetric field theories can be realised in the context of string or M-theory through com-

pactifications of Hanany-Witten brane constructions, where physical parameters receive a geometric interpretation. One may take the example of $SU(N)$ gauge theories embedded in type IIA superstring theory and which emerge from a D4 – NS5 brane construction [5]. This is illustrated for the simple and elegant case of the $SU(2)$ gauge theory with four flavours on the left of Figure 1.1. The table specifies the space-time directions which are spanned by the branes and marked by "–" and the coordinates where the branes are located at a point, marked by "·". The construction is depicted in the 45 plane, in which the NS5 branes extend and the D4 branes are point-like, and the x^6 direction which is spanned by the D4 branes but where the NS5 branes are located at a point. The geometrical parameters are the separation of the NS5 branes in the direction x^6 proportional to the effective gauge coupling $\ell \sim 1/g^2$ which enters $\tau = \frac{4\pi i}{g^2} + \frac{\theta}{2\pi}$, the separation a of the D4 branes suspended between the two NS5s and the positions in the 45 plane of the semi-infinite D4 branes which represent the mass parameters m_i.

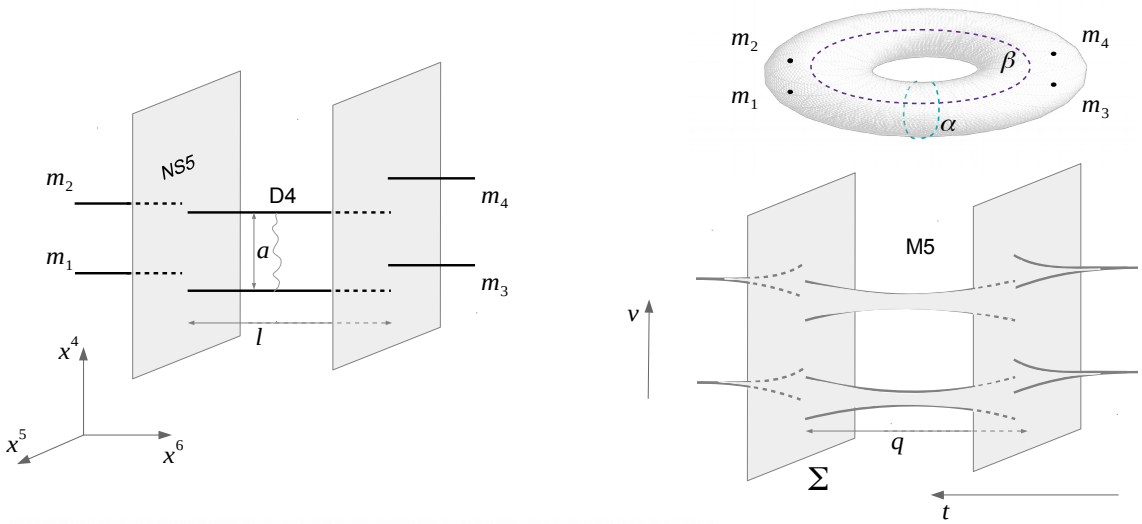

IIA	x^0	x^1	x^2	x^3	x^4	x^5	x^6	x^7	x^8	x^9	(x^{10})
NS5-branes	–	–	–	–	–	–	·	·	·	·	·
D4-branes	–	–	–	–	·	·	–	·	·	·	–

$v = x^4 + i x^5$

$t = e^{-(x^6 + i x^{10})/r}$

Figure 1.1: Left: *The type IIA brane realisation of the $d = 4$, $\mathcal{N} = 2$, $SU(2)$ four flavour gauge theory as D4 branes intersecting NS5 branes.* Right: *The eleven dimensional realisation of this theory is though an M5 brane with non-trivial topology which wraps the Seiberg-Witten curve Σ.* Top: *The curve Σ is topologically equivalent to a four punctured torus, with a basis for $H_1(\Sigma, \mathbb{Z})$ represented by the curves $\{\alpha, \beta\}$.* Bottom: *The table summarises the brane configuration in the spacetime directions, with r the radius of compactification for the direction x^{10}.*

A non-perturbative completion of type IIA string theory is provided in eleven dimensions by an underlying fundamental theory called *M-theory*. Type IIA brane constructions like those depicted in Figure 1.1 can be embedded in M-theory by adding the spacetime direction x^{10} which is compactified on a circle of radius r. The set of D4 – NS5 branes on the left of Figure 1.1 thereby becomes a single M5 brane on the right, which has non-trivial topology and wraps a Riemann surface. This surface is identified with the SW curve Σ defined by a polynomial equation $P(v, t) = 0$ in two complex variables which are specified by the spacetime coordinates

$v = x^4 + \mathrm{i}x^5$ and $t = \exp(-(x^6 + \mathrm{i}x^{10})/r)$. The precise form of the polynomial $P(v,t)$ is determined by the asymptotic behaviour of the curve with respect to the parameters (v,t) at the positions of the branes. The SW curve for the particular case depicted in Figure 1.1 is[1] topologically a punctured torus with punctures at the two lifts of the positions $t \in \{0,\infty\}$. The parameter q is related to the UV coupling τ as $q = e^{2\pi i\tau}$, while the masses m_i are given by the integrals around the locations of the punctures at $t \in \{0,\infty\}$ of the meromorphic differential λ_{SW}.

Alternative realisation of $\mathcal{N} = 2$ field theories

Assuming that M-theory exists and also the existence of a low energy supergravity limit which preserves a certain amount of supersymmetry, then it is often possible to predict the quantum field theories given by various low energy limits. This reasoning has provided powerful insights into the behaviour of such quantum field theories. It can furthermore predict the existence of low energy limits of M-theory which have some amount of supersymmetry even when there is no otherwise known description of the corresponding field theory. An interesting class of interacting six dimensional theories with $(2,0)$ superconformal symmetry and which live on the world volume of stacks of M5 branes emerged in this context [6], [7], [8]. These have no known Lagrangian description since even their field content is so far unclear, yet they have represented a subject of great interest in recent years.

The mere existence of such theories has led to highly non-trivial predictions in the work of Gaiotto [9] who introduced a rich and interesting class of four dimensional $\mathcal{N} = 2$ supersymmetric field theories $\mathfrak{X}(\mathcal{C}_{g,n}, \mathfrak{g})$, nowadays often referred to as class $\mathcal{S}$. Such theories arise from the twisted compactification of the six dimensional $(2,0)$ superconformal field theory with Lie algebra $\mathfrak{g}$ of ADE type on a background $M^4 \times \mathcal{C}_{g,n}$, where $\mathcal{C}_{g,n}$ is a Riemann surface of genus g with n punctures [10]. The field theory $\mathfrak{X}(\mathcal{C}_{g,n}, \mathfrak{g})$ lives on the four-manifold M^4 and provides an effective description for the six dimensional theory associated to $\mathfrak{g}$ on a stack of N M5 branes which wrap the Riemann surface $\mathcal{C}_{g,n}$, when the area of this surface is small and the rank of $\mathfrak{g}$ is $N-1$.

The surfaces $\mathcal{C}_{g,n}$ in Gaiotto's classification [9] are related to the SW curves $\Sigma : P(v,t) = 0$ for the corresponding field theories. The former provide a UV description, whereas the latter appear in the IR regime generally as ramified N-sheeted covers of the curves $\mathcal{C}_{g,n}$. The relation can be seen as a result of a coordinate transformation for the equation which defines the curve Σ. In the case of $SU(N)$ gauge theories of the type presented in Figure 1.1, this equation is of degree N in parameter v and can be brought into the form $x^N = \sum_{\ell=2}^{N} \phi_\ell(z) x^{N-\ell}$, where $\phi_\ell(z)$ are meromorphic functions on a sphere $\mathcal{C}_{0,n}$ with poles at the locations of the punctures [2]. More generally, this curve becomes a punctured Riemann surface $\mathcal{C}_{g,n}$ of higher genus when

[1] The Seiberg-Witten curve Σ in this case is defined by the equation

$$(m_1 - v)(m_2 - v)t^2 + \big(-(1+q)v^2 + q\sum_{i=1}^{4} m_i + u\big)t + q(m_3 - v)(m_4 - v) = 0\,, \tag{1.1.2}$$

with the correct asymptotic behaviour in the limits $t \to 0, \infty$ and also where $v \to m_i$.

[2] The transformation combines a shift of v which removes the next to leading order with a reparametrisation $(v,t) \to (x,t)$,

the corresponding gauge theories can be represented by quiver diagrams with loops [9]. In the simple example presented in Figure 1.1 the UV curve is a four punctured sphere $\mathcal{C}_{0,4}$.

Class $\mathcal{S}$ theories of type $\mathfrak{g} = \mathfrak{sl}_2$ admit weakly-coupled Lagrangian descriptions specified by pair of pants decompositions $\mathcal{P}_{g,n}$ of the surface $\mathcal{C}_{g,n}$ combined with a choice of trivalent graph Γ. Each of the $h = 3g - 3 + n$ cutting curves defining the pants decomposition corresponds to an $SU(2)$ gauge group, while each of the n punctures corresponds to an $SU(2)$ flavour group like in Table 1.1.

Riemann surface $\mathcal{C}_{g,n}$	$d = 4$, $\mathcal{N} = 2$ gauge theory $\mathfrak{X}(\mathcal{C}_{g,n}, \mathfrak{sl}_2)$
Pants decomposition $\mathcal{P}_{g,n}$ a trivalent graph Γ on $\mathcal{C}_{g,n}$	Lagrangian description with action functional $S_\tau^{\mathcal{P},\Gamma}$
Gluing parameters $q_r = e^{2\pi i \tau_r}$, $r = 1, \ldots, h$	UV couplings τ_r
h cutting curves on connecting tubes	h vector multiplets $(A_\mu, \phi)_r$
n punctures	n hypermultiplets

Table 1.1: *Correspondence between data associated to $\mathcal{C}_{g,n}$ and the gauge theory $\mathfrak{X}(\mathcal{C}_{g,n}, \mathfrak{sl}_2)$.*

Results from localisation

The development of localisation techniques [11] has allowed the computation of important physical quantities in $\mathcal{N} = 2$ field theories exactly, with important recent advances notably in [12], [13]. It relies on the existence of a supersymmetry generator $\mathcal{Q}$, which squares to a bosonic generator and which is a non-anomalous symmetry for the action functional $S[\Phi]$ such that $\mathcal{Q}S[\Phi] = 0$. If this requirement is satisfied, then the action can be deformed through $S[\Phi] \to S[\Phi] + t\mathcal{Q}V[\Phi]$, where the auxiliary fermionic functional $V[\Phi]$ is such that $\mathcal{Q}^2 V[\Phi] = 0$ and $t \in \mathbb{R}$. The partition function defined by the path integral

$$\mathcal{Z}(t) = \int [\mathcal{D}\Phi] e^{-S[\Phi] - t\mathcal{Q}V[\Phi]}\,, \qquad \frac{d\mathcal{Z}(t)}{dt} = 0 \tag{1.1.3}$$

is then independent of t as a consequence of the unbroken supersymmetry [13]. It is thus possible to calculate $\mathcal{Z}(t)$ with $t \to \infty$, where the integral localises on the moduli space $\mathcal{M}_{\text{sol}}$ of field configurations which are solutions to $\mathcal{Q}V = 0$. It is furthermore possible to argue along similar lines that expectation values of supersymmetric observables $\mathcal{O}[\Phi]$ which obey $\mathcal{Q}\mathcal{O} = 0$ and which are defined with the deformed action by

$$\langle \mathcal{O} \rangle = \int [\mathcal{D}\Phi] e^{-S[\Phi] - t\mathcal{Q}V[\Phi]} \mathcal{O} \tag{1.1.4}$$

are independent of the parameter t. Depending on the model and on the existence of a good choice for the functional $V[\Phi]$, the space $\mathcal{M}_{\text{sol}}$ can be finite dimensional and such expectation values thus become ordinary integrals.

where $v = xt$, and a subsequent $SL(2,\mathbb{Z})$ transformation $t \to \frac{az+b}{cz+d}$, $x \to (cz+d)^2 x$.

The localisation procedure was applied by Pestun in [13] to calculate the partition function $\mathcal{Z}$ of a quantum field theory on particular finite-volume spacetime backgrounds, which have sufficient symmetry to preserve unbroken a supersymmetry $\mathcal{Q}$. Certain IR divergences were regularised as a result of this. Examples of such backgrounds are the four-sphere and more generally the four-ellipsoids $E^4_{\epsilon_1,\epsilon_2} = \{x_0^2 + \epsilon_1^2(x_1^2 + x_2^2) + \epsilon_2^2(x_3^2 + x_4^2) = 1\}$, where ϵ_1, ϵ_2 are called Omega deformation parameters. When $SU(N)$ gauge theories are placed on such a background, the partition function localises as $\mathcal{Z} = \int da \mathcal{Z}(a)$, with the integrand $\mathcal{Z}(a) = \mathcal{Z}(a, m, \tau; \epsilon_1, \epsilon_2)$ reduced to a sum

$$\mathcal{Z}(a, m, \tau; \epsilon_1, \epsilon_2) = \mathcal{Z}^{\text{pert}}(a, m, \tau; \epsilon_1, \epsilon_2)\big(1 + \sum_{k=1}^{\infty} q^k \mathcal{Z}^{(k)}(a, m; \epsilon_1, \epsilon_2)\big) \,. \tag{1.1.5}$$

The perturbative component $\mathcal{Z}^{\text{pert}}$ contains exactly a tree-level and one-loop contributions, while the instanton part $\sum_k q^k \mathcal{Z}^{(k)}$ contains the series of instanton corrections. This is related to the prepotential $\mathcal{F}(a)$ from [2], [3] in the limit of vanishing deformation parameters $\epsilon_1, \epsilon_2 \to 0$ as

$$\mathcal{F}(a) \equiv \mathcal{F}(a, m; \tau) = -\lim_{\epsilon_1,\epsilon_2 \to 0} \epsilon_1 \epsilon_2 \mathcal{Z}(a, m, \tau; \epsilon_1, \epsilon_2) \,. \tag{1.1.6}$$

1.2 Correspondence to two dimensional conformal field theory

Alday, Gaiotto, and Tachikawa (AGT) made the striking observation that the four-sphere partition functions of $SU(2)$ class $\mathcal{S}$ theories can be expressed in terms of correlation functions of Liouville conformal field theory on $\mathcal{C}_{g,n}$ [14].

Liouville field theory (see [15] for a recent review) is the most simple example of $\mathfrak{sl}_N$ Toda conformal field theories, where $N = 2$, and is formally defined by the Lagrangian

$$\mathcal{L}_{\text{Liouv}} = \frac{1}{4\pi}(\partial_a \phi)^2 + \mu e^{2b\phi} \tag{1.2.7}$$

in terms of the Liouville two dimensional scalar field $\phi(z, \bar{z})$, the dimensionless coupling constant b and the scale parameter μ. The field $\phi(z, \bar{z})$ can be constructed using a free chiral field $\varphi(z)$ and the corresponding anti-chiral field $\bar{\varphi}(\bar{z})$ [16], [17]. Correlation functions of the chiral primary fields $V_\alpha(z) = e^{2\alpha\varphi(z)}$ can be represented in a holomorphically factorised form

$$\langle V_{\alpha_4}(\infty) V_{\alpha_3}(1) V_{\alpha_2}(q) V_{\alpha_1}(0) \rangle = \int_{\mathbb{R}^+} \frac{d\alpha}{2\pi} C_{21}(\alpha) C_{43}(-\alpha) |\mathcal{F}_\alpha^{\alpha_{\text{ext}}}(q)|^2 \tag{1.2.8}$$

where $\alpha_{\text{ext}} = (\alpha_4, \alpha_3, \alpha_2, \alpha_1)$ and the coefficients $C_{ij}(\alpha) \equiv C_{\alpha_i, \alpha_j, Q/2 + \mathrm{i}\alpha}$ with $Q = b + b^{-1}$ are the DOZZ three point structure constants which are known explicitly, having been conjectured by [18], [19] and derived in the free field representation of Liouville CFT in [16]. They specify the tree point functions[3]

$$\langle V_{\alpha_3}(z_3) V_{\alpha_2}(z_2) V_{\alpha_1}(z_1) \rangle = \frac{C_{\alpha_3, \alpha_2, \alpha_1}}{|z_1 - z_2|^{2\Delta_{12,3}} |z_1 - z_3|^{2\Delta_{13,2}} |z_2 - z_3|^{2\Delta_{23,1}}} \,. \tag{1.2.9}$$

[3] The exponents $\Delta_{ij,k} = \Delta_{\alpha_i} + \Delta_{\alpha_j} - \Delta_{\alpha_k}$ are given by the conformal dimension of the primaries $\Delta_\alpha = \alpha(Q - \alpha)$.

The conformal blocks $\mathcal{F}_{\alpha}^{\alpha_{\text{ext}}}(q)$ can be represented as a power series in the parameter q

$$\mathcal{F}_{\alpha}^{\alpha_{\text{ext}}}(q) = q^{\frac{Q^2}{4}+\alpha^2-\Delta_{\alpha_1}-\Delta_{\alpha_2}}\left(1+\sum_{k=1}^{\infty} q^k \mathcal{F}_{\alpha,k}^{\alpha_{\text{ext}}}\right) , \tag{1.2.10}$$

where the coefficients $\mathcal{F}_{\alpha,k}^{\alpha_{\text{ext}}}$ are determined by conformal symmetry.

Returning to the $SU(2)$ four flavour gauge theory example presented in Figure 1.1, the authors in [14] identified the instanton contributions $\mathcal{Z}^{(k)}(a, m; \epsilon_1, \epsilon_2)$ with the coefficients in the power series expansion of the four point conformal block $\mathcal{Z}^{(k)} = \mathcal{F}_{\alpha,k}^{\alpha_{\text{ext}}}$. The AGT correspondence is more generally a relation between partition functions for $\mathfrak{X}(\mathcal{C}_{g,n}, \mathfrak{sl}_2)$ field theories on $E^4_{\epsilon_1,\epsilon_2}$ and Liouville n-point functions of the form

$$\mathcal{Z}_{E^4_{\epsilon_1,\epsilon_2}}[\mathfrak{X}(\mathcal{C}_{g,n}, \mathfrak{sl}_2)] = \int da \mathcal{Z}^{\text{pert}} |\mathcal{Z}^{\text{inst}}|^2 = \int d\alpha C \cdots C |\mathcal{F}_{\alpha}^{\alpha_{\text{ext}}}|^2 = \langle \prod_{i=1}^{n} V_{\alpha_i}(z_i) \rangle_{\mathcal{C}_{g,n}} . \tag{1.2.11}$$

The dictionary is summarised in Table 1.2.

$d = 4$, $\mathcal{N} = 2$ gauge theory $\mathfrak{X}(\mathcal{C}_{g,n}, \mathfrak{sl}_2)$	Liouville conformal field theory
Ω-deformation parameters $\epsilon_{1,2}$	Coupling constants b, b^{-1}
Mass parameters m_i	External momenta α_i of correlation functions
Coulomb branch parameters a	Internal moments α
Four-sphere partition function	Full correlation function
Instanton partition function	Conformal block

Table 1.2: *Correspondence between gauge theory data and Liouville CFT parameters.*

Higher rank generalisation

An important goal is the generalisation of the AGT correspondence to cases where $\mathfrak{g}$ is a finite dimensional Lie algebra of higher rank, such as $\mathfrak{g} = \mathfrak{sl}_N$. The origin of class $\mathcal{S}$ theories from the six dimensional $(2, 0)$ theory suggests that the relations to two dimensional conformal field theory may have interesting generalisations for $N > 2$. In particular, for A_{N-1} theories one expects to find a picture similar to that for the $\mathfrak{sl}_2$ story, but with Liouville CFT replaced by the conformal Toda field theories associated to the Lie algebras $\mathfrak{g} = \mathfrak{sl}_N$ [20]. Strong evidence has been accumulated for this conjecture, including [21], [22], [23], [24], [25], [26], [27], [28], [29], [30], [31], [32], [33], [34], [35]. In particular in [29] it has been proven for a certain subclass of the A_{N-1} theories in class $\mathcal{S}$ which may be represented as quiver gauge theories with linear or circular quiver diagrams. However, neither side of this higher rank AGT correspondence is fully understood beyond this subclass. In particular for non-Lagrangian theories, even in the simplest case $\mathfrak{g} = \mathfrak{sl}_3$ one encounters considerable additional difficulties obstructing direct generalisations of the results known for $\mathfrak{g} = \mathfrak{sl}_2$.

Usual methods do not apply on the side of $\mathcal{N} = 2$ SUSY field theory because among class $\mathcal{S}$ theories of type $\mathfrak{g} = \mathfrak{sl}_N$ with $N > 2$ one generically finds interacting field theories not having a weak coupling limit with a useful Lagrangian description. It is therefore unclear what should play the role of instanton partition functions in these non-Lagrangian cases. This difficulty has a counterpart on the side of $\mathfrak{sl}_N$ Toda field theories where the spaces of conformal blocks are known to be infinite dimensional generically, but otherwise poorly understood up to now.

1.3 Relation to topological string theory

Four dimensional $\mathcal{N} = 2$ field theories emerge as low energy descriptions of Hanany–Witten type brane constructions in type IIA string theory, like depicted for exmple in Figure 1.1. There exist however various string theoretic descriptions of the same quantum field theory and which are related to one another by a web of string dualities, a nice presentation of which can be found in [36]. Physical quantities of interest which are protected by supersymmetry – such as partition functions – play an important role in establishing these dualities, since the absence of quantum corrections means they can be computed exactly and identified across the different dual descriptions.

In particular, type IIA brane constructions are related by a series of string dualities [37] to compactifications of type IIA string theory on non-compact Calabi-Yau three manifolds CY_3, without any branes. The latter represent the geometric engineering point of view [38], [39], [40] which describes four dimensional gauge theories as decoupling limits of string theory. In this fully geometric type IIA description it is possible to calculate the topological string partition function using the (refined) topological vertex [41], [42], [43], [44], [45], [46]. The partition functions of $d = 4$, $\mathcal{N} = 2$ field theories should emerge as a limit of topological strings partition functions on CY_3 manifolds of toric type, which are algebraic manifolds that can be easily described in terms of a finite amount of combinatorial data, as suggested by Nekrasov in [12].

Topological strings partition functions can be computed graphically in the style of Feynman calculus using brane diagrams like the examples depicted in Figure 1.2, where the integrals that appear when computing Feynman diagrams are replaced by sums over Young tableaux. The brane (or *web*) diagrams are graphs which consist of a collection of trivalent vertices joined by straight oriented edges and which are dual to the toric diagram that encodes the combinatorial data specifying the corresponding CY_3. Such a dual pair of diagrams is drawn in Figure 1.2b, where the toric diagram is depicted by a dashed line. By associating a vertex function to the vertices of the web diagram and edge factors to the oriented edges, where these edges are furthermore decorated by Young tableaux, the associated topological strings partition functions schematically take the form of a sum over the Young tableaux on internal edges

$$\mathcal{Z}^{\text{top}} = \sum_{\text{partitions}} \text{three-vertices} \times \text{edge factors} \, . \tag{1.3.12}$$

The topological vertex formalism thus enables an alternative derivation of instanton partition functions based on the geometry of toric diagrams. It further provides tools to make predictions

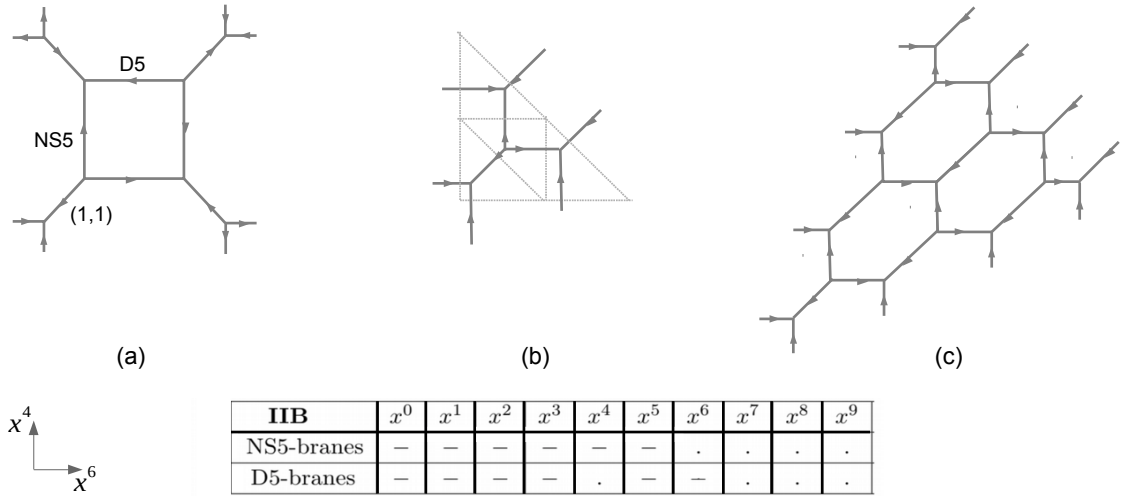

IIB	x^0	x^1	x^2	x^3	x^4	x^5	x^6	x^7	x^8	x^9
NS5-branes	–	–	–	–	–	–	.	.	.	.
D5-branes	–	–	–	–	.	–	–	.	.	.

Figure 1.2: (a) *The type IIB web diagram realising the $d = 4$, $\mathcal{N} = 2$, $SU(2)$ four flavour gauge theory on junctions of NS5, D5 and (1,1) branes.* (b) *The web diagram realising the T_2 theory of class $\mathcal{S}$ and the dual (dashed) toric diagram.* (c) *The web diagram realising the T_4 theory.* Bottom: *The table lists the brane configuration in the spacetime directions and the direction x^5 is compactification on a circle.*

for the currently undefined instanton partition functions of non-Lagrangian theories. The T_N theories of class $\mathcal{S}$ for example are strongly coupled, have $SU(N)^3$ global symmetry and no known weakly-coupled Lagrangian description. The low energy dynamics of a circle uplift to five dimensions of these theories is captured by web diagrams [47] of the type sketched in Figure 1.2c. The fifth dimension which is compactified on a circle is given by the spacetime direction x^5 in the table summarising the brane configuration, while the 4d theories live in the spacetime dimensions $x^0 - x^3$. The topological string partition functions for such theories were calculated in [48], giving an ansatz for the instanton partition functions of the T_N theories.

The topological string partition functions computed in [48] can be in principle be related to three point conformal blocks of $\mathfrak{sl}_N$ Toda conformal field theory by passing to a particular integral formulation, following the approach of [34], [49]. This can serve to identify a preferred basis in the space of conformal blocks from the point of view of the topological string.

1.4 Parallel developments and an alternative route towards AGT

Parallel developments have come from the insight of Gaiotto, Moore and Neitzke (GMN) that the BPS spectrum of a class $\mathcal{S}$ theory is encoded in geometrical structures on the moduli space $\mathcal{M}_{\text{vac}}$ of vacua of the theory on $\mathbb{R}^3 \times S^1$ [50], [10], [51], [52]. BPS states in the Hilbert space of a supersymmetric field theory are special since they form distinguished small representations of the supersymmetry algebra and so do not mix with other generic states in the spectrum.

The six dimensional description of class $\mathcal{S}$ theories implies that $\mathcal{M}_{\text{vac}}$ is isomorphic to Hitchin's moduli space $\mathcal{M}_{\text{H}}$ of solutions to the self-duality equations on $\mathcal{C}_{g,n}$ (see [53] for a review). This space has a hyperkähler structure and in one of its complex structures it can be identified with

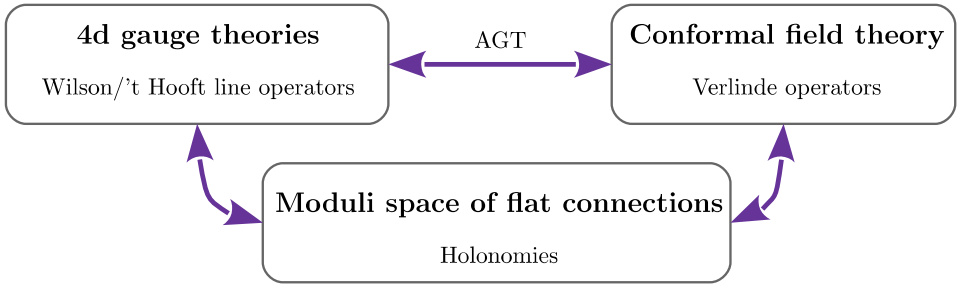

Figure 1.3: *Triangle of relations between 4d $\mathcal{N}=2$ supersymmetric gauge theories labeled by Riemann surfaces $\mathcal{C}_{g,n}$* (left)*, conformal field theory (Liouville or Toda) on $\mathcal{C}_{g,n}$* (right)*, and the moduli space of flat $SL(N,\mathbb{C})$-connections on $\mathcal{C}_{g,n}$* (bottom)*. We also indicate the interpretation of line defects in each description.*

Field theory $\mathfrak{X}(\mathcal{C},\mathfrak{sl}_2)$	Liouville theory	Moduli of flat connections on $\mathcal{C}$
Algebra $\mathcal{A}_{\mathfrak{X}}$ generated by SUSY loop observables	Algebra $\mathcal{A}_V$ of Verlinde line operators	Quantised algebra $\mathcal{A}_{\text{flat}}$ of functions on $\mathcal{M}_{\text{flat}}(\mathrm{SL}(2),\mathcal{C})$
Instanton partition functions	Liouville conformal blocks	Natural bases for modules of $\mathcal{A}_{\text{flat}}$

Table 1.3: *Isomorphic algebras appear in different contexts.*

the moduli space $\mathcal{M}_{\text{flat}}$ of complex flat connections. This leads to the key relation

$$\mathcal{M}_{\text{vac}}(\mathbb{R}^3\times S^1)=\mathcal{M}_{\text{flat}}(\mathcal{C}_{g,n})\ . \tag{1.4.13}$$

An important manifestation of this relation is that vacuum expectation values of BPS line operators in class $\mathcal{S}$ theories can be expressed as holonomies of flat connections on $\mathcal{C}_{g,n}$.

It has subsequently been observed in [54], [55] that the origin of the AGT correspondence can be understood in the simplest case, where $\mathfrak{g}=\mathfrak{sl}_2$, from the relation to $\mathcal{M}_{\text{flat}}$. An essential role in this story is played by the algebra $\mathcal{A}_{\mathfrak{X}}$ of supersymmetric Wilson- and 't Hooft loops representing an important sub-algebra of the algebra of all observables in $\mathfrak{X}(\mathcal{C}_{g,n},\mathfrak{g})$. The algebra $\mathcal{A}_{\mathfrak{X}}$ turns out to be isomorphic to the algebra $\mathcal{A}_V$ of Verlinde line operators in Liouville CFT [56], [57], [58], [59], which is furthermore isomorphic to the algebra $\mathcal{A}_{\text{flat}}$ of quantised functions on the moduli space of flat $SL(2)$-connections on Riemann surfaces [54], as summarised in Table 1.3. One can argue [54] that the isomorphisms between the algebras $\mathcal{A}_{\mathfrak{X}}$, $\mathcal{A}_V$ and $\mathcal{A}_{\text{flat}}$ imply the relations between instanton partition functions for $\mathfrak{X}(\mathcal{C}_{g,n},\mathfrak{sl}_2)$ and conformal blocks of Liouville CFT observed in [14] and discussed in many subsequent works. Thus there appears to be a triangle of relations between $\mathcal{N}=2$ supersymmetric gauge theories, conformal field theories, and moduli spaces of flat connections, as depicted in Figure 1.3. Further discussion regarding line operators and their role in the AGT correspondence is presented below.

Line operators and framed BPS states

BPS line operators in class $\mathcal{S}$ theories $\mathfrak{X}(\mathcal{C}_{g,n}, \mathfrak{g})$ are supersymmetric generalisations of Wilson and 't Hooft line observables, describing the effect of inserting heavy dyonic probe particles labeled by electric and magnetic charge vectors.[4] Supersymmetric Wilson loops can be defined as path ordered exponentials

$$W_{\mathcal{R}} = \mathrm{tr}_{\mathcal{R}} \mathcal{P} \mathrm{exp} \oint_{S^1} ds(\phi + \mathrm{i}A) \tag{1.4.14}$$

in terms of the gauge field A_μ and scalar field ϕ of a vector multiplet. Magnetic dual 't Hooft loop observables can be defined semiclassically through a path integral over field configurations with specific singular behaviour near the supporting curve and describe the effect of transporting a magnetically charged probe particle along this curve.

Such a supersymmetric line operator can be viewed as descending from a surface operator in the six dimensional $(2,0)$ theory, which is labeled by a representation $\mathcal{R}$ of $\mathfrak{g}$ and supported on $S^1 \times \wp$, with $\wp$ a path on $\mathcal{C}_{g,n}$. This leads to a relation between the vacuum expectation value (vev) of the line operator $L(\mathcal{R}; \wp)$ on S^1 and the classical holonomy of a flat connection $\mathcal{A}$ along the path $\wp$ on $\mathcal{C}_{g,n}$:

$$\left\langle\, L(\mathcal{R}; \wp) \,\right\rangle = \mathrm{tr}_{\mathcal{R}} \mathrm{Hol}_{\wp} \mathcal{A} \,. \tag{1.4.15}$$

BPS line operators thus provide natural coordinate functions on $\mathcal{M}_{\text{flat}}$.

As argued in [51], [62], the vev of a UV line operator L can be represented in the IR in terms of a set of vevs of line operators $\mathcal{X}_\gamma$ with charge γ defined using the low-energy abelian gauge fields:

$$L = \sum_\gamma \overline{\Omega}(L, \gamma) \mathcal{X}_\gamma \,. \tag{1.4.16}$$

The coefficients $\overline{\Omega}(L, \gamma)$ are integers which count the BPS states supported by the line operator L, called *framed BPS states*. The IR line operators $\mathcal{X}_\gamma$ are Darboux coordinates on $\mathcal{M}_{\mathrm{flat}}$ that are closely related to the coordinates constructed by Fock and Goncharov in their study of higher Teichmüller spaces [63].[5]

The line operators can be quantised by twisting $\mathbb{R}^3 \times S^1$ into the fibered product $\mathbb{R} \times \mathbb{C} \times_q S^1$ such that a coordinate z on $\mathbb{C}$ rotates as $z \to qz$ after going around S^1 [66], [51], [59]. BPS conditions then constrain line operators on S^1 to be located at points along the axis $\mathbb{R}$ and at the origin of $\mathbb{C}$ (see Figure 1.4). The relation (1.4.16) between UV and IR line operators becomes

$$\hat{L} = \sum_\gamma \overline{\Omega}(L, \gamma; q) \hat{\mathcal{X}}_\gamma \,, \tag{1.4.17}$$

[4] Note that allowed sets of "mutually local" line operators are specified by a certain topological data, which impose some restrictions on the representations [51], [60], [61]. This subtlety will not affect our conclusions in an essential way, as noted for the A_1 case in [55].

[5] Teichmüller spaces are the spaces of deformations of complex structures on Riemann surfaces and appear as one of the components in the moduli space of flat $SL(2, \mathbb{R})$ connections [64], [65].

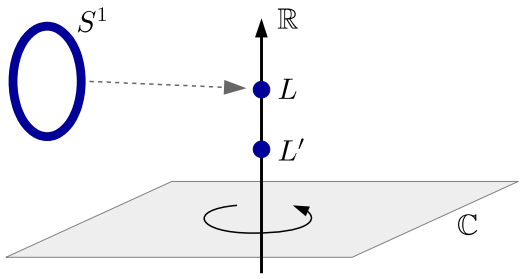

Figure 1.4: *The algebra of line operators can be quantised by twisting $\mathbb{R}^3 \times S^1$ such that a plane $\mathbb{C} \subset \mathbb{R}^3$ rotates as one moves along the S^1. BPS line operators wrap S^1 and align along the axis $\mathbb{R}$ at the origin of $\mathbb{C}$.*

where the noncommutative variables $\hat{\mathcal{X}}_\gamma$ satisfy the relation $\hat{\mathcal{X}}_\gamma \hat{\mathcal{X}}_{\gamma'} = q^{\frac{1}{2}\langle\gamma,\gamma'\rangle}\hat{\mathcal{X}}_{\gamma+\gamma'}$. The coefficients $\overline{\underline{\Omega}}(L,\gamma;q)$ are the *framed protected spin characters* defined in [51] as

$$\overline{\underline{\Omega}}(L,\gamma;q) = \mathrm{tr}_{\mathcal{H}_L^{\mathrm{BPS}}} q^{J_3}(-q^{\frac{1}{2}})^{2I_3} \ , \tag{1.4.18}$$

where $\mathcal{H}_L^{\mathrm{BPS}}$ is the Hilbert space of framed BPS states, and J_3 and I_3 are generators of the $SO(3)$ and $SU(2)_R$ symmetries. GMN conjectured that framed BPS states have $I_3 = 0$ ("no exotics conjecture"), which implies in particular that the $\overline{\underline{\Omega}}(L,\gamma;q)$ are linear combinations of $su(2)$ characters with positive integral coefficients. The coefficients of $q^m X_\gamma$ in the decomposition (1.4.17) of a line operator are dimensions of Hilbert spaces graded by the IR electromagnetic charges γ and the $so(3)$ spins m.

The noncommutative algebra of IR line operators $\hat{\mathcal{X}}_\gamma$ determines via (1.4.17) the algebra of UV line operators, which may be represented by relations of the form

$$\hat{L} * \hat{L}' = \sum_{L''} c(L,L',L'';q)\hat{L}'' \ . \tag{1.4.19}$$

The order in which we multiply operators corresponds to their ordering along the axis $\mathbb{R}$. The algebra generated by the operators $\hat{L}$ can be viewed as a noncommutative deformation of the algebra of functions on $\mathcal{M}_{\text{flat}}$, with q the deformation parameter.

The role of line operators in the AGT correspondence

Expectation values of line operators in A_1 theories on the four-ellipsoid $E^4_{\epsilon_1,\epsilon_2}$ can be calculated by localization [13], [58], [67] and take the schematic form

$$\left\langle\, L \,\right\rangle_{\epsilon_1,\epsilon_2} \ = \ \int \mathrm{d}a \ (\Psi(a))^* \, \mathsf{L} \, \Psi(a) \ . \tag{1.4.20}$$

The integration is performed over variables $a = (a_1, \ldots, a_h)$ representing the zero modes of the $h = 3g-3+n$ scalar fields in the vector multiplets. $\Psi(a)$ represents the contribution of the path integral over the lower half-ellipsoid with $x_0 < 0$, and L is a finite difference operator acting on the variables a. It is natural to interpret the right hand side of (1.4.20) as an expectation value in an effective zero-mode quantum mechanics. By localization, this quantum mechanics

in finite volume can be shown to represent the exact result for $\langle L \rangle_{\epsilon_1,\epsilon_2}$. The functions $\Psi(a)$ can be identified with the instanton partition functions (see [68] for a review and references) that were found to be related to Liouville conformal blocks by AGT.

The approach proposed in [54] establishes the relation between the wave-functions $\Psi(a)$ in (1.4.20) and the Liouville conformal blocks without using the relation to the instanton partition functions observed in [13]. It is based on the observation that the effective zero-mode quantum mechanics in which line operators take the form (1.4.20) coincides with the quantum-mechanical system obtained by quantising a real slice $\mathcal{M}^{\mathbb{R}}_{\text{flat}}$ in $\mathcal{M}_{\text{flat}}$. This follows from the fact that the algebra $\mathcal{A}^{\mathfrak{X}}_{\epsilon_1\epsilon_2}$ generated by the supersymmetric line operators on $E^4_{\epsilon_1,\epsilon_2}$ factorizes as $\mathcal{A}^{\mathfrak{X}}_{\epsilon_1\epsilon_2} \simeq \mathcal{A}^{\epsilon_1/\epsilon_2}_{\text{flat}} \times \mathcal{A}^{\epsilon_2/\epsilon_1}_{\text{flat}}$ into two copies of the noncommutative algebra $\mathcal{A}^{\hbar}_{\text{flat}}$ obtained in the quantisation of the algebra of coordinate functions on $\mathcal{M}_{\text{flat}}$, as argued for instance in [69]. The two copies correspond to line operators supported on $x_0 = x_1 = x_2 = 0$ and $x_0 = x_3 = x_4 = 0$, respectively. The same conclusion can be reached from the observation made in [59] that the algebra of line operators supported on $x_0 = x_1 = x_2 = 0$, for example, is isomorphic as a noncommutative algebra to the algebra of line operators in $\mathbb{R}^3 \times S^1$ defined via (1.4.19) with $\hbar = \epsilon_1/\epsilon_2$. The twisting of $\mathbb{R}^3 \times S^1$ inducing the noncommutativity models the residual effect of the curvature near the support of the line operators on $E^4_{\epsilon_1,\epsilon_2}$.

Duality invariance of the expectation values (1.4.20) may then be combined with the representation theory of $\mathcal{A}^{\text{line}}_{\epsilon_1\epsilon_2}$ to obtain a precise mathematical characterisation of the wave functions $\Psi(a) \equiv \Psi_\tau(a)$, now considered as multivalued analytic functions of the gauge coupling constants $\tau = (\tau_1, \ldots, \tau_h)$ [54]. It was furthermore shown in [54] that the Virasoro conformal blocks represent the same mathematical objects. Within conformal field theory one may, in particular, define a natural family of operators called the Verlinde loop operators representing the action of the quantised algebra of functions on $\mathcal{M}_{\text{flat}}$ on spaces of conformal blocks.

Having established the relation between wave-functions $\Psi_\tau(a)$ and the Liouville conformal blocks it remains to notice that the functions $\Psi(a)$ in (1.4.20) must coincide with the instanton partition functions defined in [12]. Different arguments in favour of this identification can be found in [13] and in [69]. This line of argument establishes the validity of the relations between conformal blocks and instanton partition functions conjectured in [14] and discussed in many subsequent works for all A_1 theories of class $\mathcal{S}$.[6] A crucial role is played by the relation of the algebra $\mathcal{A}^{\hbar}_{\text{flat}}$ to the algebra $\mathcal{A}_V$ generated by the Verlinde line operators. This relation is generalised to theories of higher rank in this thesis, thereby supporting the natural generalisation of the AGT correspondence to class $\mathcal{S}$ theories of type A_{N-1}.

1.5 Overview

This thesis begins a program to generalise the AGT correspondence to higher rank based on the central role of line operators and the moduli space of flat connections in the approach of [54]. It looks at relations between the theories $\mathfrak{X}(\mathcal{C}_{g,n}, \mathfrak{g})$ and $\mathfrak{sl}_N$ Toda conformal field theory in the triangle in Figure 1.3 for higher rank cases, with particular interest for those cases where no

[6] A somewhat similar approach to the case $\epsilon_2 = 0$ had previously been outlined in [70].

weakly-coupled Lagrangian description is known. Given the difficulties in tackling directly higher rank gauge theories and Toda CFTs, and also motivated by the six dimensional description, we focus first on flat connections and take the quantised algebra of functions $\mathcal{A}_{\text{flat}}$ as an ansatz for the algebra $\mathcal{A}_{\mathfrak{X}}$. This is perfectly consistent with previous work on the cases which do have a Lagrangian description [71], [24], [35], [72].

Part II will describe in detail the quantum algebra $\mathcal{A}_{\text{flat}}$ of functions on the moduli spaces of flat $SL(N,\mathbb{C})$ connections on Riemann surfaces $\mathcal{C}_{g,n}$ in terms of their generators and the relations which these satisfy. It will employ quantum group theoretic tools [73] in order to achieve this and, independently, an explicit representation of the algebra $\mathcal{A}_{\text{flat}}$ provided by Fock-Goncharov coordinates [63]. The representation in terms of Fock-Goncharov coordinates presents a further separate interest, as it will allow us to study many higher rank examples of the *framed protected spin characters* which were defined in [51].

The arguments of GMN relate $\mathcal{A}_{\text{flat}}$ to the algebra $\mathcal{A}_{\mathfrak{X}}$ of supersymmetric line operators in class $\mathcal{S}$ theories of type A_{N-1} and we will show in Part III that $\mathcal{A}_{\text{flat}}$ can be identified with the algebra $\mathcal{A}_V$ of Verlinde loop and network operators in $\mathfrak{sl}_N$ Toda conformal field theory. After introducing the relevant background, we will construct within the free field representation:

- natural bases for the space of Toda conformal blocks associated to punctured Riemann surfaces;
- operator valued monodromy matrices of degenerate fields which can be used to describe the quantisation of the space $\mathcal{M}_{\text{flat}}$ and
- given such "quantum" monodromy matrices, Verlinde network operators which act on the spaces of Toda conformal blocks.

Studying the algebra generated by these operators using the same quantum group theoretic tools as in Part II will then prove the isomorphism $\mathcal{A}_{\text{flat}} \simeq \mathcal{A}_V$. Given the central role played by these algebras in the approach of [54], we may regard the relations

$$\mathcal{A}_{\mathfrak{X}} \simeq \mathcal{A}_{\text{flat}} \simeq \mathcal{A}_V \tag{1.5.21}$$

as support for a higher-rank AGT correspondence. The relations between representations of $\mathcal{A}_{\text{flat}}$ and the algebra of Verlinde line operators in Toda CFT suggest that suitable Toda conformal blocks represent natural candidates for the yet unknown partition functions of the strongly coupled theories $\mathfrak{X}(\mathcal{C}_{g,n},\mathfrak{g})$.

As a result of constructing the "quantum" monodromy matrices, we will furthermore find a direct link between the free field realisation of conformal field theories and the non-commutative geometry of flat connections on Riemann surfaces. This is due to a simple relation between a particular set of parameters in the free field construction of conformal blocks for $\mathfrak{sl}_3$ Toda CFT and a generalisation of coordinates of Fenchel-Nielsen type on the moduli space of flat $SL(3)$-connections on $\mathcal{C}_{0,3}$. These Fenchel-Nielsen type coordinates are coordinates compatible with pair of pants decompositions of $\mathcal{C}_{g,n}$ and they enter the operator valued monodromy matrices as basic building blocks.

Part IV will then address connections to topological string theory, motivated by [74], [48], [75] which propose that conformal blocks of Toda CFT can be obtained in a certain limit from the partition functions of topological string theory on certain toric Calabi-Yau manifolds used for the geometric engineering of four dimensional theories $\mathfrak{X}(\mathcal{C}_{g,n}, \mathfrak{g})$. Of particular interest will once more be the theories $\mathfrak{X}(\mathcal{C}_{0,3}, \mathfrak{sl}_N)$, which have no known weakly-coupled Lagrangian description when $N \geq 3$. With the help of the refined topological vertex one may represent the relevant topological string partition functions as infinite series admitting partial resummations. We will investigate mapping these partition functions to conformal blocks for a deformed version of Toda field theory and, in the most simple of cases, explore meaningful ways to take the geometric engineering limit and find the precise relation between the partition function from topological strings corresponding to the T_2 theory of class $\mathcal{S}$ and Liouville three point conformal blocks. As a result, this exercise will lead to an identification of some of the geometric data of the local Calabi-Yau used in the geometric engineering of the theories $\mathfrak{X}(\mathcal{C}_{0,3}, \mathfrak{sl}_N)$ with parameters which enter the free field construction of Toda conformal blocks.

Part II

Quantisation of moduli spaces of flat connections on punctured Riemann surfaces

Introduction

The six dimensional origin of class $\mathcal{S}$ theories $\mathfrak{X}(\mathcal{C}_{g,n}, \mathfrak{sl}_N)$ suggests that there should exist a family of supersymmetric line operators that correspond to coordinate functions on the moduli space $\mathcal{M}^N_{g,n} \equiv \mathcal{M}^{SL(N,\mathbb{C})}_{\text{flat}}(\mathcal{C}_{g,n})$ of flat $SL(N,\mathbb{C})$-connections on the Riemann surface $\mathcal{C}_{g,n}$. This follows from the arguments presented in Section 1.4. For $\mathfrak{sl}_2$ theories traces of holonomies along simple, non-self-intersecting, closed loops suffice to parameterise the space $\mathcal{M}^2_{g,n}$. For higher rank however, we need to consider in addition some functions associated with *networks* on $\mathcal{C}_{g,n}$. These network functions are constructed from a collection of holonomies along open paths that are contracted at junctions with $SL(N)$-invariant tensors. Such networks arise naturally from products of simple curves by applying $SL(N)$ skein relations at their intersections.

In the following chapters we will study the algebra of functions associated to such loops and networks. Since the quantised form of this algebra can be identified with the algebra of supersymmetric line operators $\mathcal{A}_{\mathfrak{X}}$ in theories $\mathfrak{X}(\mathcal{C}_{g,n}, \mathfrak{sl}_N)$ (see Section 1.4), describing this will play a central role in supporting a generalisation of the AGT correspondence to higher rank.

Contents of Part II

The algebra $\mathcal{A}^N_{g,n}$ of functions on $\mathcal{M}^N_{g,n}$ can be described in terms of a set of generators (loop and network functions) and the relations that they satisfy, as we will see in Charpter 2. A standard way to quantise $\mathcal{A}^N_{g,n}$ into a noncommutative algebra is to use quantum skein relations to resolve intersections in a product of operators. This deformation can be defined using the Reshetikhin-Turaev construction of knot invariants [73] in terms of quantum group theory and gives a product of the form (1.4.19)

$$\hat{L} * \hat{L}' = \sum_{L''} c(L, L', L''; q) \hat{L}'' \ ,$$

where the operators $\hat{L}$ may also be network operators.

In Chapter 3, we give several explicit examples of algebras $\mathcal{A}^N_{g,n}$ and their quantisations for the basic surfaces: three-punctured sphere $\mathcal{C}_{0,3}$, one-punctured torus $\mathcal{C}_{1,1}$ and four-punctured sphere $\mathcal{C}_{0,4}$. Using pants decompositions of surfaces $\mathcal{C}_{g,n}$, we can build the algebras $\mathcal{A}^N_{g,n}$ from these basic building blocks, in the spirit of the "tinkertoys" approach [76].

In Chapter 4, we describe an explicit representation of the algebra $\mathcal{A}^N_{g,n}$ in terms of Fock-Goncharov coordinates [63]. Loop and network functions are expressed in terms of positive

Laurent polynomials, as in the relation (1.4.16) between UV and IR line operators. The natural quantisation of Fock-Goncharov coordinates then determines uniquely the quantisation of $\mathcal{A}^N_{g,n}$. For all the cases that we compare, we find that the resulting quantum relations coincide with the ones obtained from skein quantisation. Furthermore, the existence of such quantum relations turns out to lead to a unique quantisation of the Fock-Goncharov polynomials, as in (1.4.17)

$$\hat{L} = \sum_{\gamma} \underline{\overline{\Omega}}(L, \gamma; q) \hat{\mathcal{X}}_{\gamma} \ .$$

This allows us obtain many examples of framed protected spin characters $\underline{\overline{\Omega}}(L, \gamma; q)$ in higher-rank theories, which is an interesting application in its own right.

The appendices collect the relevant background about Fock-Goncharov coordinates. Part II of this thesis largely reproduces Sections 2 – 4 of [77].

Chapter 2

Algebra of loop and network operators

This chapter describes the relevant background on the algebra $\mathcal{A}^N_{g,n}$ of functions on the moduli space $\mathcal{M}^N_{g,n}$ of flat connections on a punctured Riemann surface $\mathcal{C}_{g,n}$, which can be described in terms of generators and relations. We construct a set of generators for $\mathcal{A}^N_{g,n}$ consisting of functions associated with simple loops and networks naturally associated with a pair of pants decomposition of $\mathcal{C}_{g,n}$. Other functions can then be obtained by taking products of generators and resolving intersections with skein relations. The number of generators obtained in this way typically exceeds the dimension of the moduli space, as is reflected in the existence of polynomial relations between the coordinate functions. The algebra $\mathcal{A}^N_{g,n}$ has a Poisson structure, and it can be deformed into a noncommutative algebra $\mathcal{A}^N_{g,n}(q)$ by applying the skein relations that encode the representation theory of the quantum group $\mathcal{U}_q(\mathfrak{sl}_N)$. We study in detail the case of the pair of pants $\mathcal{C}_{0,3}$, which is the building block for any $\mathcal{C}_{g,n}$. This will illustrate the crucial role of networks at higher rank. We also present some results for the punctured torus $\mathcal{C}_{1,1}$ and the four-punctured sphere $\mathcal{C}_{0,4}$. Using pants decompositions one may use these results to get a set of coordinates allowing us to cover $\mathcal{M}^N_{g,n}$ at least locally.

2.1 Moduli space of flat connections

The close relationship between 4d $\mathcal{N} = 2$ supersymmetric theories in class $\mathcal{S}$ and Hitchin systems is revealed by compactifying on a circle S^1. The moduli space $\mathcal{M}_{\text{vac}}$ of vacua of such theories with gauge group G on $\mathbb{R}^3 \times S^1$ can be identified with the moduli space of solutions to Hitchin's equations on $\mathcal{C}_{g,n}$ [10], [51]. These equations imply that the complex connections $\mathcal{A}(\zeta)$ built out of a connection A and a one-form φ,

$$\mathcal{A}(\zeta) = R\zeta^{-1}\varphi + A + R\zeta\bar{\varphi}\,, \tag{2.1.1}$$

are flat for all values of the parameter $\zeta \in \mathbb{C}^*$ (R is the radius of S^1).[1] $\mathcal{M}_{\text{vac}}$ is a hyper-Kähler space, and with the appropriate choice of complex structure it is identified with the moduli space of flat $G_{\mathbb{C}}$-connections on $\mathcal{C}_{g,n}$, with singularities at the punctures. We will only consider the cases where the singularities at the punctures are of regular type[2].

[1] We will restrict to the case $\zeta = 1$ henceforth.

[2] Regularity means that the connection is gauge-equivalent to a meromorphic connection with simple poles at the punctures.

Flat connections modulo gauge transformations are then completely characterised by the representation of the fundamental group $\pi_1(\mathcal{C}_{g,n})$ generated by the holonomy matrices. If we denote the space of holomorphic connections on $\mathbb{P}^1$ of the form

$$\nabla' = \partial_y + A(y), \qquad A(y) = \sum_{r=1}^{n} \frac{A_r}{y - z_r}, \qquad \sum_{r=1}^{n} A_r = 0, \tag{2.1.2}$$

with $A_r \in \mathfrak{g}$ modulo overall conjugation by elements of $G_{\mathbb{C}}$ by $\mathcal{M}_{dR}(\mathfrak{g}, \mathcal{C}_{0,n})$, then computing the holonomy defines a map $\mathcal{M}_{dR}(\mathfrak{g}, \mathcal{C}_{0,n}) \to \mathcal{M}_B(G_{\mathbb{C}}, \mathcal{C}_{0,n})$, with $\mathcal{M}_B(G_{\mathbb{C}}, \mathcal{C}_{0,n})$ being the character variety. The holonomy of a flat $G_{\mathbb{C}}$-connection $\nabla = \mathrm{d} + \mathcal{A}$ along a closed curve $\gamma \in \pi_1(\mathcal{C}_{g,n})$ is given by $\mathrm{Hol}(\gamma) = \mathcal{P}\exp \int_\gamma \mathcal{A} \in G_{\mathbb{C}}$. The moduli space $\mathcal{M}_{\text{vac}}$ of vacua is thereby identified with the space of representations $\rho : \pi_1(\mathcal{C}_{g,n}) \to G_{\mathbb{C}}$, modulo overall conjugation:

$$\mathcal{M}_{\text{vac}} \simeq \mathcal{M}_B(G_{\mathbb{C}}, \mathcal{C}_{g,n}) = \mathrm{Hom}\big(\pi_1(\mathcal{C}_{g,n}), G_{\mathbb{C}}\big)/G_{\mathbb{C}} \ . \tag{2.1.3}$$

More explicitly, we have

$$\mathcal{M} = \left\{ (\mathbf{A}_1, \ldots, \mathbf{A}_g, \mathbf{B}_1, \ldots, \mathbf{B}_g, \mathbf{M}_1, \ldots, \mathbf{M}_n) \,|\, \prod_{i=1}^{g} \mathbf{A}_i \mathbf{B}_i \mathbf{A}_i^{-1} \mathbf{B}_i^{-1} = \prod_{a=1}^{n} \mathbf{M}_a \right\} \Big/ G_{\mathbb{C}},$$

where $\mathbf{A}_i, \mathbf{B}_i \in G_{\mathbb{C}}$ are holonomy matrices for based loops going around the A- and B-cycles for each of the g handles, and $\mathbf{M}_a \in G_{\mathbb{C}}$ are holonomy matrices for based loops going around each of the n punctures. These matrices are considered modulo the action of $G_{\mathbb{C}}$ by simultaneous conjugation.

For 4d $\mathcal{N} = 2$ theories of type A_{N-1}, the complexified gauge group is $G_{\mathbb{C}} = SL(N, \mathbb{C})$. We are thus interested in the moduli space $\mathcal{M}_{g,n}^N \equiv \mathcal{M}_{\text{flat}}(SL(N, \mathbb{C}), \mathcal{C}_{g,n})$ of flat $SL(N, \mathbb{C})$-connections on a Riemann surface $\mathcal{C}_{g,n}$, modulo gauge transformations. It has a dimension given by

$$\dim[\mathcal{M}_{g,n}^N] \ = \ -\chi(\mathcal{C}_{g,n}) \dim[SL(N, \mathbb{C})] = (2g + n - 2)(N^2 - 1) \ , \tag{2.1.4}$$

with the Euler characteristic $\chi(\mathcal{C}_{g,n}) = 2 - 2g - n$. We can furthermore fix the conjugacy classes of the holonomies $\mathbf{M}_a$ around the punctures (as we will see, this amounts to restricting to a symplectic leaf of the Poisson variety $\mathcal{M}_{g,n}^N$). The moduli space $\bar{\mathcal{M}}_{g,n}^N$ of flat connections with $\mathbf{M}_a$ in fixed conjugacy classes has the dimension

$$\begin{aligned} \dim[\bar{\mathcal{M}}_{g,n}^N] \ &= \ -\chi(\mathcal{C}_{g,n}) \dim[SL(N, \mathbb{C})] - n\mathrm{rank}[SL(N, \mathbb{C})] \\ &= \ (2g + n - 2)(N^2 - 1) - n(N - 1) \ . \end{aligned} \tag{2.1.5}$$

2.2 Trace functions

The algebra $\mathcal{A}_{g,n}^N \equiv \mathrm{Fun}^{\text{alg}}(\mathcal{M}_{g,n}^N)$ of algebraic functions on $\mathcal{M}_{g,n}^N$ can be described in terms of generators and relations, as we now review. Traces of holonomy matrices provide coordinate functions for $\mathcal{M}_{g,n}^N$ (see e.g. [78] for a review). They can be expressed as traces of words

made out of letters given by the holonomy matrices $\mathbf{A}_i, \mathbf{B}_i, \mathbf{M}_a$. The relation coming from the fundamental group $\pi_1(\mathcal{C}_{g,n})$ allows us to eliminate one of the holonomy matrices, say $\mathbf{M}_n$, which leaves $(1-\chi)$ independent letters (for $n>0$). General upper bounds are known for the maximal length of words that form a generating set of $\mathcal{A}^N_{g,n}$. The generators can be taken to be traces of words with lengths up to $N(N+1)/2$ for $N \leq 4$, or up to N^2 for $N > 4$ (see references in [79]). The difference between the number of generators and the dimension of $\mathcal{M}^N_{g,n}$ is then accounted for by the existence of polynomial relations $\mathcal{P}_\alpha = 0$, which are consequences of the Cayley-Hamilton theorem. The algebra $\mathcal{A}^N_{g,n}$ is thus described as the polynomial ring generated by trace functions quotiented by polynomial relations:

$$\mathcal{A}^N_{g,n} = \mathbb{C}\left[\mathrm{tr}\mathbf{A}_i, \mathrm{tr}\mathbf{A}_i\mathbf{B}_j, \cdots\right]/\{\mathcal{P}_\alpha\}. \tag{2.2.6}$$

Note that this algebraic structure of $\mathcal{M}^N_{g,n}$ does not distinguish between different surfaces with the same number of letters. For example, the description of $\mathcal{A}^N_{g,n}$ in terms of generators and relations is the same for the one-punctured torus $\mathcal{C}_{1,1}$ and for the three-punctured sphere $\mathcal{C}_{0,3}$, which both have $(1-\chi)=2$ letters.

Examples for $N = 2$: Let us first consider the particularly simple example of $SL(2,\mathbb{C})$-connections on the one-punctured torus $\mathcal{C}_{1,1}$. The moduli space is given by

$$\mathcal{M}^2_{1,1} = \{(\mathbf{A},\mathbf{B},\mathbf{M}) | \mathbf{A}\mathbf{B}\mathbf{A}^{-1}\mathbf{B}^{-1} = \mathbf{M}\}/SL(2,\mathbb{C})\ . \tag{2.2.7}$$

The algebra of functions $\mathcal{A}^2_{1,1}$ is generated by the trace functions

$$\mathrm{tr}\mathbf{A},\ \mathrm{tr}\mathbf{B},\ \mathrm{tr}\mathbf{A}\mathbf{B}\ . \tag{2.2.8}$$

Since the dimension of $\mathcal{M}^2_{1,1}$ is 3, there is no relation between these 3 generators. However, the generators are related to the trace of the holonomy around the puncture via

$$(\mathrm{tr}\mathbf{A})^2 + (\mathrm{tr}\mathbf{B})^2 + (\mathrm{tr}\mathbf{A}\mathbf{B})^2 - \mathrm{tr}\mathbf{A}\mathrm{tr}\mathbf{B}\mathrm{tr}\mathbf{A}\mathbf{B} = -\mathrm{tr}\mathbf{M} + 2\ , \tag{2.2.9}$$

and therefore they do satisfy a relation once we fix the conjugacy class of $\mathbf{M}$ to obtain $\bar{\mathcal{M}}^2_{1,1}$.

A more typical example is the sphere $\mathcal{C}_{0,4}$ with four punctures, which we label by A, B, C, D. The moduli space is

$$\mathcal{M}^2_{0,4} = \{(\mathbf{A},\mathbf{B},\mathbf{C},\mathbf{D}) | \mathbf{A}\mathbf{B}\mathbf{C}\mathbf{D} = \mathbf{I}\}/SL(2,\mathbb{C})\ . \tag{2.2.10}$$

The holonomies $\mathbf{A}$, $\mathbf{B}$, $\mathbf{C}$ can be taken to be 3 independent letters, while $\mathbf{D} = (\mathbf{A}\mathbf{B}\mathbf{C})^{-1}$. The algebra of functions $\mathcal{A}^2_{0,4}$ is generated by traces of words with maximal length equal to 3:

$$\mathbf{A},\ \mathbf{B},\ \mathbf{C},\ \mathbf{A}\mathbf{B} \equiv \mathbf{S},\ \mathbf{B}\mathbf{C} \equiv \mathbf{T},\ \mathbf{C}\mathbf{A} \equiv \mathbf{U},\ \mathbf{A}\mathbf{B}\mathbf{C} = \mathbf{D}^{-1},\ \mathbf{C}\mathbf{B}\mathbf{A}\ . \tag{2.2.11}$$

These 8 trace functions satisfy 2 polynomial relations (we use the notation $A_1 \equiv \mathrm{tr}\mathbf{A}$):

$$\begin{aligned} D_1 + \mathrm{tr}\mathbf{C}\mathbf{B}\mathbf{A} &= A_1T_1 + B_1U_1 + C_1S_1 - A_1B_1C_1\ , \\ D_1 \cdot \mathrm{tr}\mathbf{C}\mathbf{B}\mathbf{A} &= S_1T_1U_1 + S_1^2 + T_1^2 + U_1^2 + A_1^2 + B_1^2 + C_1^2 \\ &\quad - A_1B_1S_1 - B_1C_1T_1 - C_1A_1U_1 - 4\ . \end{aligned} \tag{2.2.12}$$

The first relation allows to eliminate $\mathrm{tr}\mathbf{CBA}$ since it is linear. The algebra of functions $\mathcal{A}^2_{0,4}$ is then described as the quotient of the polynomial ring

$$\mathbb{C}[A_1, B_1, C_1, D_1, S_1, T_1, U_1] \tag{2.2.13}$$

by the quartic polynomial

$$\begin{aligned}\mathcal{P}_1 &= S_1T_1U_1 + S_1^2 + T_1^2 + U_1^2 + A_1B_1C_1D_1 + A_1^2 + B_1^2 + C_1^2 + D_1^2 \\ &\quad -(A_1B_1 + C_1D_1)S_1 - (B_1C_1 + D_1A_1)T_1 - (C_1A_1 + B_1D_1)U_1 - 4\ .\end{aligned} \tag{2.2.14}$$

This gives a 6-dimensional quartic hypersurface in $\mathbb{C}^7$.

In general, the number of words in r letters of length up to 3 is

$$r + \binom{r}{2} + \binom{r}{3} = \frac{r(r^2+5)}{6}\ . \tag{2.2.15}$$

This number of generators becomes quickly much larger than the dimension $3(r-1)$ of $\mathcal{M}^2_{g,n}$, which implies that there are many polynomial relations.

Example for $N = 3$: The description of $\mathcal{A}^3_{g,n}$ for surfaces with 2 letters is very similar to that of $\mathcal{A}^2_{g,n}$ for surfaces with 3 letters (see for example [80] and references therein). The generators of $\mathcal{A}^3_{1,1}$ can be taken to be the traces of the 10 following words with length up to 6 (note that the Cayley-Hamilton theorem implies that $\mathbf{A}^{-1} \sim \mathbf{A}^2$ so it counts as 2 letters):

$$\mathbf{A}^{\pm 1},\ \mathbf{B}^{\pm 1},\ (\mathbf{AB})^{\pm 1},\ (\mathbf{AB}^{-1})^{\pm 1},\ (\mathbf{ABA}^{-1}\mathbf{B}^{-1})^{\pm 1}\ . \tag{2.2.16}$$

These generators satisfy 2 relations (similar to the relations (2.2.12) for $\mathcal{A}^2_{0,4}$):

$$\begin{aligned}\mathrm{tr}\mathbf{ABA}^{-1}\mathbf{B}^{-1} + \mathrm{tr}\mathbf{BAB}^{-1}\mathbf{A}^{-1} &= (\ldots)\ , \\ \mathrm{tr}\mathbf{ABA}^{-1}\mathbf{B}^{-1} \cdot \mathrm{tr}\mathbf{BAB}^{-1}\mathbf{A}^{-1} &= (\ldots)\ .\end{aligned} \tag{2.2.17}$$

Eliminating $\mathrm{tr}\mathbf{BAB}^{-1}\mathbf{A}^{-1}$ with the first relation, we can then describe $\mathcal{A}^3_{1,1}$ as an 8-dimensional sextic hypersurface in $\mathbb{C}^9$.

2.3 Poisson structure

There is a Poisson structure on the moduli space $\mathcal{M}^N_{g,n}$, see [81] for a review and further references. Note that unlike the algebraic structure described in the previous section, the Poisson structure does distinguish between surfaces with the same $\chi(\mathcal{C}_{g,n})$. The Poisson algebra has a Poisson bracket defined using the Atiyah-Bott symplectic structure. Goldman gave a general formula for the Poisson bracket of trace functions in terms of intersections of curves [82]:

$$\{\mathrm{trHol}(\alpha), \mathrm{trHol}(\beta)\} = \sum_{p \in \alpha \cap \beta} \epsilon(p; \alpha, \beta) \left[\mathrm{trHol}(\alpha_p\beta_p) - \frac{1}{N}\mathrm{trHol}(\alpha)\mathrm{trHol}(\beta)\right]\ , \tag{2.3.18}$$

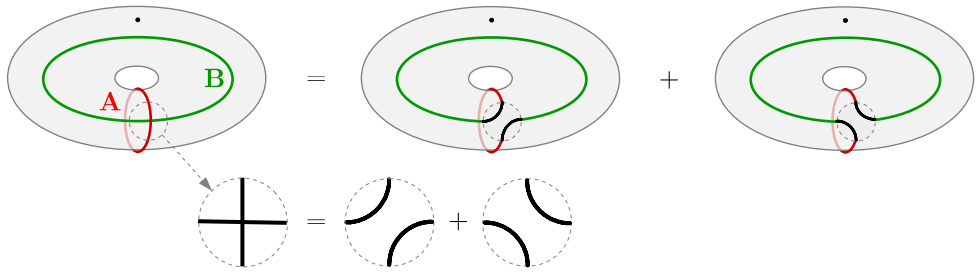

Figure 2.1: Top*: The product of the trace functions for the A- and B-cycles on $\mathcal{C}_{1,1}$ gives the trace functions associated with the curves obtained by resolving the intersection.* Bottom*: Locally, the crossing is replaced by two pairs of non-intersecting segments. This is the classical skein relation for $N = 2$.*

where $\epsilon(p;\alpha,\beta) = \pm 1$ is the oriented intersection number at the point p, and α_p, β_p are the curves α, β based at p.

As an illustration we can consider $\mathcal{C}_{1,1}$ with $N = 2$. Since the A- and B-cycles intersect once, Goldman's formula gives

$$\{\mathrm{tr}\mathbf{A}, \mathrm{tr}\mathbf{B}\} = \mathrm{tr}\mathbf{AB} - \frac{1}{2}\mathrm{tr}\mathbf{A}\mathrm{tr}\mathbf{B}\ . \tag{2.3.19}$$

Note that the right-hand side can be written as the derivative of the relation (2.2.9) by $\mathrm{tr}\mathbf{AB}$. This indicates that the Poisson structure on $\mathcal{M}^2_{1,1}$ is compatible with its structure as an algebraic variety. The Poisson algebra for the traces functions (2.2.16) on $\mathcal{M}^3_{0,3}$ and $\mathcal{M}^3_{1,1}$ has been studied in [83].

2.4 Classical skein algebra

Relations between functions in $\mathcal{A}^N_{g,n}$ have a topological origin. Let us take again the example of $\mathcal{C}_{1,1}$ with $N = 2$. The product of the traces associated with the A- and B-cycles is given by

$$\mathrm{tr}\mathbf{A}\mathrm{tr}\mathbf{B} = \mathrm{tr}\mathbf{AB} + \mathrm{tr}\mathbf{AB}^{-1}\ . \tag{2.4.20}$$

Graphically, we can interpret this as resolving the intersection of the A- and B-cycles into a pair of curves that curl up around the torus in two ways (see Figure 2.1). This procedure is reminiscent of the classical skein relations in knot theory, which are linear relations between knot diagrams (projections of knots onto a plane) that differ only locally around an intersection. In fact, skein relations are nothing else than graphical representations of ϵ-tensor identities such as $\epsilon_{ab}\epsilon^{cd} = \delta^c_a\delta^d_b - \delta^d_a\delta^c_b$, which can be used to derive the relation (2.4.20).

The $SL(2)$ skein relation implies that $\mathcal{A}^2_{g,n}$ can be described in terms of simple curves without self-intersections. In the case of $\mathcal{C}_{0,3}$ with $N = 2$, the trace function $\mathrm{tr}\mathbf{AB}^{-1}$, which corresponds to a Figure-8 curve surrounding the punctures A and B and intersecting itself once, can be expressed in terms of non-intersecting curves as

$$\begin{aligned}\mathrm{tr}\mathbf{AB}^{-1} &= \mathbf{A}^a_d\mathbf{B}^{-1b}{}_c\delta^c_a\delta^d_b = \mathbf{A}^a_d\mathbf{B}^{-1b}{}_c(\epsilon_{ab}\epsilon^{cd} + \delta^d_a\delta^c_b)\\ &= -\mathrm{tr}\mathbf{AB} + \mathrm{tr}\mathbf{A}\mathrm{tr}\mathbf{B}\ ,\end{aligned} \tag{2.4.21}$$

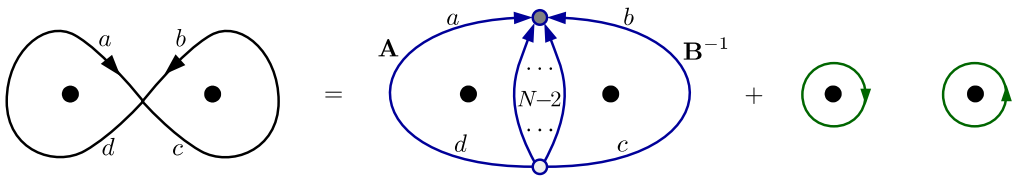

Figure 2.2: *The application of the skein relation for general N to a self-intersecting curve produces a network with two N-valent junctions connected by an edge with multiplicity $N-2$.*

where we used $\mathbf{B} = -\epsilon(\mathbf{B}^{\mathrm{t}})^{-1}\epsilon$ and $\mathrm{tr}\mathbf{B}^{-1} = \mathrm{tr}\mathbf{B}$. Similarly, $\mathrm{tr}\mathbf{CBA}$ on $\mathcal{C}_{0,4}$ corresponds to the Pochhammer curve with three self-intersections and can be expressed in terms of simple curves by applying the skein relation, as in (2.2.12).

An important difference for $N > 2$ is that the skein relations involve N-valent junctions, associated with $SL(N)$-invariant ϵ-tensors (see for example [84]). In the case $N = 3$, the ϵ-tensor identity

$$\delta_a^c\delta_b^d = \epsilon_{abm}\epsilon^{cdm} + \delta_a^d\delta_b^c \tag{2.4.22}$$

corresponds to the skein relation expressed graphically as

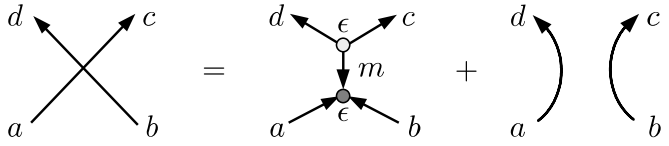

(2.4.23)

For general $N > 2$, the resolution of a self-intersection via skein relations therefore produces a network with two junctions. Let us consider again a Figure-8 curve around two punctures:

$$\mathrm{tr}\mathbf{AB}^{-1} \;=\; \mathbf{A}_a^d\mathbf{B}^{-1c}{}_b\delta_c^a\delta_d^b = \mathbf{A}_a^d\mathbf{B}^{-1c}{}_b\left(\frac{1}{(N-2)!}\epsilon^{abm_1\cdots m_{N-2}}\epsilon_{cdm_1\cdots m_{N-2}} + \delta_d^a\delta_c^b\right) \tag{2.4.24}$$

This relation can be represented graphically as in Figure 2.2.

The natural appearance of junctions in the algebra $\mathcal{A}_{g,n}^N$ motivates us to adopt a set of generators for $\mathcal{A}_{g,n}^N$ which does not consist exclusively of trace functions, but also includes network functions.

2.5 Loop and network functions

The set of generators of $\mathcal{A}_{g,n}^N$ described in section 2.2 involves traces of large words of the holonomy matrices $\mathbf{A}_i$, $\mathbf{B}_i$, $\mathbf{M}_a$, which are generally associated with curves that have self-intersections. In this section, we will mostly trade such self-intersecting curves for networks with junctions using the skein relations. Our generators are thus associated with simple loops (without self-intersections) and with networks.

Loops: Each loop on $\mathcal{C}_{g,n}$ gives $N-1$ trace functions A_i, $i = 1,\dots N-1$, which can be taken to be the coefficients of the characteristic polynomial of the associated holonomy matrix

Figure 2.3: Left: *Loop functions are depicted as oriented simple closed curves labeled by integers* $i = 1, \ldots, N-1$. *Reversing the orientation amounts to replacing* i *by* $N-i$. Right: *Trivalent junctions with all outgoing edges (source) or all incoming edges (sink). Edges are labeled by integers* i, j, k *that sum to* N.

$\mathbf{A} \in SL(N, \mathbb{C})$:

$$\det(\mathbf{A} - \lambda \mathbf{I}) = (-\lambda)^N + (-\lambda)^{N-1} A_1 + (-\lambda)^{N-2} A_2 + \cdots - \lambda A_{N-1} + 1 \ . \tag{2.5.25}$$

The coefficients A_i are sums of all principal $i \times i$ minors of $\mathbf{A}$:

$$A_i \ = \sum_{n_1, \cdots, n_{N-i}} [\mathbf{A}]_{n_1 \cdots n_{N-i}} \ , \tag{2.5.26}$$

where we denote the determinant of $\mathbf{A}$ with the rows and columns $n_1, \ldots, n_{N-i}$ removed by

$$[\mathbf{A}]_{n_1 \cdots n_{N-i}} = \frac{1}{i!} \epsilon_{n_1 \cdots n_{N-i} m_1 \cdots m_i} \mathbf{A}^{m_1}_{l_1} \cdots \mathbf{A}^{m_i}_{l_i} \epsilon^{n_1 \cdots n_{N-i} l_1 \cdots l_i} \ . \tag{2.5.27}$$

We can also write the loop functions A_i as traces of exterior powers of $\mathbf{A}$:

$$A_1 \ = \ \mathrm{tr}\mathbf{A} \ , \qquad A_2 = \frac{1}{2}[(\mathrm{tr}\mathbf{A})^2 - \mathrm{tr}(\mathbf{A}^2)] \ , \quad \ldots \ , \quad A_i = \mathrm{tr}(\wedge^i \mathbf{A}) \ . \tag{2.5.28}$$

The loop function A_i corresponds to the i^{th} fundamental antisymmetric representation $\wedge^i \square$ of $SL(N, \mathbb{C})$. Note that if we replace $\mathbf{A}$ by its inverse $\mathbf{A}^{-1}$ in the expression for A_i we obtain the complex conjugate representation A_{N-i}. For example, the fundamental representation corresponds to $A_1 = \mathrm{tr}\mathbf{A}$, while the antifundamental representation corresponds to $A_{N-1} = \mathrm{tr}\mathbf{A}^{-1}$. We can thus represent loop functions graphically by an oriented loop labeled by an integer $i = 1, \ldots, \lfloor N/2 \rfloor$, where $\lfloor N/2 \rfloor$ is the integral part of $N/2$. Reversing the orientation corresponds to replacing $\mathbf{A}$ by $\mathbf{A}^{-1}$, the fundamental A_1 by the antifundamental A_{N-1}, and so on (see Figure 2.3 left). For even N, the $(N/2)^{\text{th}}$ representation is self-adjoint, and so the corresponding loop does not need an orientation.

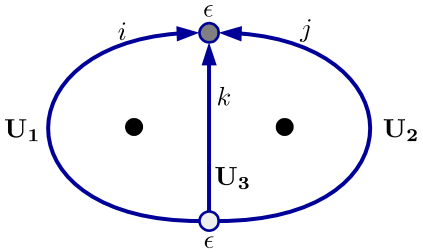

Figure 2.4: *Network with two trivalent junctions and three edges surrounding two punctures. The edges carry the* i^{th}, j^{th}, *and* k^{th} *antisymmetric representations of* $SL(N, \mathbb{C})$, *with* $i + j + k = N$. *The network function* N_{ijk} *is constructed by contracting* i *copies of the holonomy matrix* $\mathbf{U_1}$, j *copies of* $\mathbf{U_2}$, *and* k *copies of* $\mathbf{U_3}$ *with the two* ϵ*-tensors at the junctions.*

Networks: We also construct functions associated with networks. By a *network*[3] we mean a closed directed graph whose edges carry antisymmetric representations and whose vertices carry invariant tensors.[4] The vertices, or junctions, are in principle N-valent but they can always be resolved into trivalent junctions, on which we therefore focus. The three edges that meet at a junction (either all outgoing or all incoming) are labeled by positive integers i, j, k satisfying $i+j+k=N$, which indicate that they carry respectively the i^{th}, j^{th}, k^{th} antisymmetric representations (see Figure 2.3 right). Junctions do not have labels since there is only one invariant tensor $\epsilon_{m_1\cdots m_N}$ in $\wedge^i\square\otimes\wedge^j\square\otimes\wedge^k\square$. A network function is defined by contracting the holonomy matrices along the edges with the ϵ-tensors at the junctions. The resulting function is invariant under simultaneous conjugation of the holonomy matrices. For example, a network consisting of two junctions connected by three oriented edges as in Figure 2.4 gives $(N-1)(N-2)/2$ network functions N_{ijk} of the form

$$N_{ijk}=\frac{1}{i!j!k!}\epsilon_{m_1\cdots m_N}\mathbf{U}_{\mathbf{1}\ n_1}^{m_1}\cdots\mathbf{U}_{\mathbf{1}\ n_i}^{m_i}\mathbf{U}_{\mathbf{2}\ n_{i+1}}^{m_{i+1}}\cdots\mathbf{U}_{\mathbf{2}\ n_{i+j}}^{m_{i+j}}\mathbf{U}_{\mathbf{3}\ n_{i+j+1}}^{m_{i+j+1}}\cdots\mathbf{U}_{\mathbf{3}\ n_N}^{m_N}\epsilon^{n_1\cdots n_N}\ , \tag{2.5.29}$$

where $\mathbf{U_1},\mathbf{U_2},\mathbf{U_3}$ are the holonomy matrices (in the fundamental representation) along the three edges. If we reverse the orientation of the edges we obtain another set of $(N-1)(N-2)/2$ network functions, which we denote by $\bar{N}_{ijk}$.

From networks to self-intersecting curves: Network functions can also be expressed in terms of the holonomy matrices $\mathbf{A}_i$, $\mathbf{B}_i$, $\mathbf{M}_a$ generating a representation of $\pi_1(\mathcal{C}_{g,n})$. In order to do this, let us recall that a flat $SL(N)$-connection can always be trivialized by gauge transformations in any simply-connected domain. Covering $\mathcal{C}_{g,n}$ by simply-connected domains one may describe the flat connections in terms of the constant transition functions from one domain to another. Equivalently, one may describe flat connections using branch-cuts, a collection of curves or arcs on $\mathcal{C}_{g,n}$ such that cutting along the branch-cuts produces a simply-connected domain. The holonomy $\mathrm{Hol}(\gamma)$ will then receive contributions only when the curve γ crosses branch-cuts. $\mathrm{Hol}(\gamma)$ can therefore be represented as the product of "jump"-matrices associated with the branch-cuts crossed by γ, taken in the order in which the different branch-cuts are crossed.

Considering the network N_{ijk} defined in (2.5.29), for example, we can use the branch-cuts depicted in Figure 2.5. The "jump"-matrices associated with these branch-cuts coincide with the holonomy matrices $\mathbf{A}$ and $\mathbf{B}$ around the two punctures depicted in Figure 2.5. The holonomy matrix associated with the middle arc labeled by the letter k is the identity, as no branch-cut is crossed. It follows that we can express N_{ijk} as

$$\begin{aligned}
N_{ijk} &= \frac{1}{i!j!k!}\epsilon_{m_1\cdots m_N}\mathbf{A}^{m_1}_{\ n_1}\cdots\mathbf{A}^{m_i}_{\ n_i}\mathbf{B}^{-1m_{i+1}}_{\qquad n_{i+1}}\cdots\mathbf{B}^{-1m_{i+j}}_{\qquad n_{i+j}}\delta^{m_{i+j+1}}_{n_{i+j+1}}\cdots\delta^{m_N}_{n_N}\epsilon^{n_1\cdots n_N}\ ,\\
&= \frac{1}{i!j!}\delta^{n_1\cdots n_{i+j}}_{m_1\cdots m_{i+j}}\mathbf{A}^{m_1}_{\ n_1}\cdots\mathbf{A}^{m_i}_{\ n_i}\mathbf{B}^{-1m_{i+1}}_{\qquad n_{i+1}}\cdots\mathbf{B}^{-1m_{i+j}}_{\qquad n_{i+j}}\\
&= \mathrm{tr}\mathbf{A}^i\mathbf{B}^{-j}-\mathrm{tr}\mathbf{A}^{i-1}\mathbf{B}^{-1}\mathbf{A}\mathbf{B}^{-j+1}+\cdots
\end{aligned} \tag{2.5.30}$$

[3] Closely related objects go under the names of spin networks, trace diagrams, tensor diagrams, webs, etc.

[4] We prefer this definition to the one given by Samuel Johnson in his *Dictionary of the English Language* (1755): "Network: Any thing reticulated or decussated, at equal distances, with interstices between the intersections."

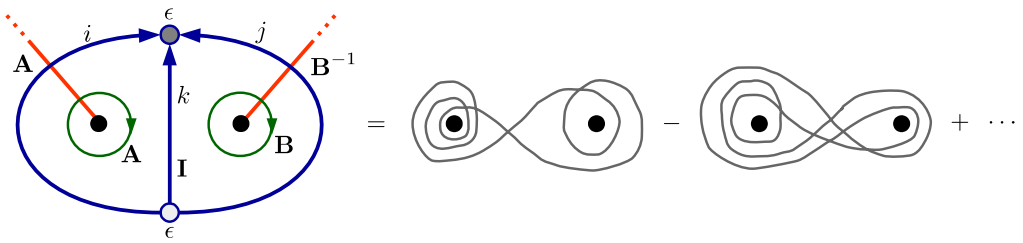

Figure 2.5: *The branch-cuts (orange lines) encode the holonomies* $\mathbf{A}$ *and* $\mathbf{B}$ *around the punctures. The edges of the network* N_{ijk} *are associated with the holonomies of the branch-cuts that they cross:* i *times* $\mathbf{A}$*,* j *times* $\mathbf{B}^{-1}$*, and* k *times the identity* $\mathbf{I}$*. The right-hand side shows two of the self-intersecting curves that appear in the expansion of the network function in terms of traces.*

We thus see that this point of view relates network functions to trace functions associated with self-intersecting curves as in section 2.2. As illustrated on the right of Figure 2.5, the corresponding trace functions are typically associated with very complicated curves with many self-intersections. This is one of the advantages of working with networks instead of self-intersecting curves. Different labelings of a network with a given topology account for a family of intricate curves. Notice that the relation (2.5.30) between network and trace functions can also be seen as a consequence of skein relations, given that it involves contractions of ϵ-tensors. We have shown a simple example in Figure 2.2.

2.6 Commuting Hamiltonians

The moduli space $\bar{\mathcal{M}}^N_{g,n}$ with fixed conjugacy classes for the holonomies around the punctures exhibits the key features of an integrable Hamiltonian system. Firstly, $\bar{\mathcal{M}}^N_{g,n}$ is a symplectic manifold. Fixing the conjugacy classes of the holonomies around the punctures corresponds to restricting to a symplectic leaf of the Poisson manifold $\mathcal{M}^N_{g,n}$ viewed as a symplectic foliation.

We can moreover find a maximal set of Hamiltonians, that is a number of Poisson-commuting functions equal to half the dimension of the moduli space $\bar{\mathcal{M}}^N_{g,n}$. Goldman's formula (2.3.18) implies that trace functions associated with curves that do not intersect each other automatically Poisson-commute. In the case $N = 2$ we can simply consider the trace functions associated to a maximal number of mutually non-intersecting closed curves on $\mathcal{C}_{g,n}$. Cutting $\mathcal{C}_{g,n}$ along such a collection of curves defines a decomposition of $\mathcal{C}_{g,n}$ into $(2g - 2 + n)$ pairs of pants with $(3g - 3 + n)$ cutting curves. The traces of holonomies associated with these curves thus provides a maximal set of Poisson-commuting Hamiltonians:

$$\#\{\text{cutting loops}\} = 3g - 3 + n = \frac{1}{2}\dim \bar{\mathcal{M}}^2_{g,n} \,. \tag{2.6.31}$$

However, for $N > 2$, the cutting curves alone do not suffice to get a maximal set of commuting Hamiltonians. We therefore supplement them by the two-junction networks (2.5.29) that can be put on each pair of pants (see Figure 2.6). Each cutting curve provides $(N - 1)$ trace functions, and each pants network provides $(N - 1)(N - 2)/2$ network functions. They add up to give a number of functions which is precisely half the dimension (2.1.5) of the moduli space of flat

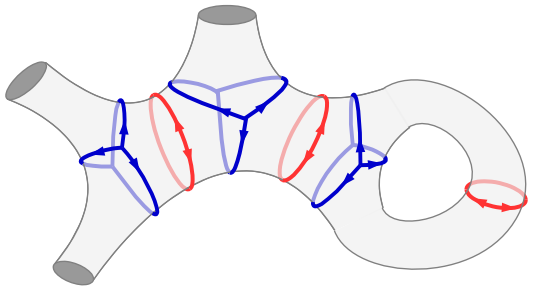

Figure 2.6: *A maximal set of commuting Hamiltonians is provided by the functions associated with cutting curves (red) and with pants networks (blue) in a pair of pants decomposition of the surface $\mathcal{C}_{g,n}$.*

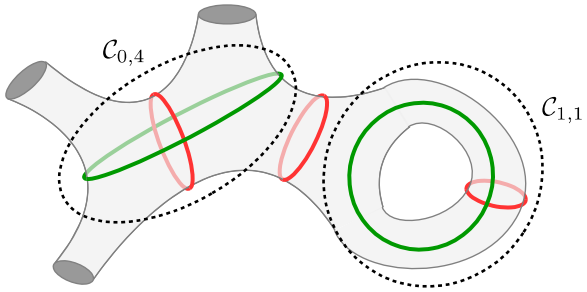

Figure 2.7: *The neighborhood of a cutting loop (red) on $\mathcal{C}_{g,n}$ can look either like $\mathcal{C}_{0,4}$ or like $\mathcal{C}_{1,1}$. In each case we can find a natural conjugate loop (green).*

connections with fixed holonomies around the punctures:

$$(3g-3+n)(N-1)+(2g-2+n)\frac{(N-1)(N-2)}{2} \;=\; \frac{1}{2}\dim \bar{\mathcal{M}}^N_{g,n}\,. \quad (2.6.32)$$

The Poisson-commutativity of the trace functions associated to cutting curves among themselves and with the networks is obvious from the fact that they do not intersect (Goldman's formula (2.3.18) applies to self-intersecting curves, and hence to the networks as well). On the other hand, it is not obvious that the network functions associated with pants networks Poisson-commute among themselves, $\{N_{ijk}, N_{lmn}\} = 0$. Although we do not have a general proof, we checked that they commute up to the case $N = 6$.

2.7 Tinkertoys

In order to get a complete system of coordinates for $\bar{\mathcal{M}}^N_{g,n}$ we need to supplement the maximal set of commuting Hamiltonians described in the previous section by sufficiently many additional coordinate functions. A natural way to find additional variables that do not Poisson-commute with the pants networks N_{ijk} on $\mathcal{C}_{0,3}$ is to take the pants networks $\bar{N}_{ijk}$ with reverse orientation.

Simple additional coordinates that do not Poisson-commute with the trace functions associated to the cutting curves defining the pants decomposition can also be defined in a simple way. Each cutting curve is contained in a subsurface isomorphic either to a four-holed sphere or a one-holed torus embedded in $\mathcal{C}_{g,n}$, see Figure 2.7 for an illustration. In the case of $\mathcal{C}_{0,4}$, natural

additional coordinates are associated with curves surrounding another pair of holes than the cutting curve under consideration. In the case of $\mathcal{C}_{1,1}$ one may, for example consider an additional coordinate associated with the B-cycle if the cutting curve is the A-cycle, see Figure 2.7.

Altogether, the cutting loops and their conjugate loops, together with the pants networks of both orientations provide a complete set of coordinates on $\bar{\mathcal{M}}^N_{g,n}$ that cover this space at least locally. We can therefore reduce the study of $\bar{\mathcal{M}}^N_{g,n}$ for a generic Riemann surface $\mathcal{C}_{g,n}$ to the study of pants networks on $\mathcal{C}_{0,3}$, and of pairs of conjugate loops on $\mathcal{C}_{0,4}$ and $\mathcal{C}_{1,1}$. This motivates us to focus on these three cases in the following sections.

Note that the additional coordinates on $\bar{\mathcal{M}}^N_{g,n}$ that we introduced above are not *canonically* conjugate. However, it should be possible to define generalisations of the Fenchel-Nielsen coordinates, a set of Darboux coordinates for $\bar{\mathcal{M}}^N_{g,n}$ in terms of which one may parameterise the coordinate functions defined above. Such Darboux coordinates were shown in the case $N = 2$ to play a key role in the relation to integrable systems [70].[5]

2.8 Skein quantisation

Motivated by the applications to supersymmetric gauge theories, we will next discuss the quantisation of the moduli space $\mathcal{M}^N_{g,n}$ of flat $SL(N,\mathbb{C})$-connections on a Riemann surface $\mathcal{C}_{g,n}$. This means in particular to construct a family of noncommutative deformations $\mathcal{A}^N_{g,n}(q)$ of the algebra $\mathcal{A}^N_{g,n}$ of functions on $\mathcal{M}^N_{g,n}$ parameterized by one parameter $q \equiv \mathrm{e}^{\hbar}$. The loop and network functions get replaced by generators of the noncommutative algebra $\mathcal{A}^N_{g,n}(q)$. In the classical limit $q \to 1$ ($\hbar \to 0$), the product $\hat{A}\hat{B}$ of two operators reduces to the commutative product AB of the corresponding functions, while the commutator $[\hat{A},\hat{B}] = \hat{A}\hat{B} - \hat{B}\hat{A}$ should reproduce the Poisson bracket $\{A, B\}$.

This problem has been extensively studied in the past, starting from [85], and motivated in particular by the relation to Chern-Simons theory[6] [86], [87]. Considering Chern-Simons theory on three-manifolds M_3 of the form $\mathcal{C}_{g,n} \times I$, with I an interval with coordinate t, one may note that parameterised closed curves on $\mathcal{C}_{g,n}$ naturally define knots in M_3. In the context of Chern-Simons theory it is natural to relate the ordering of the factors in a product of generators in $\mathcal{A}^N_{g,n}(q)$ to the ordering of observables according to the value of their "time"-coordinates t. Given two knots K_A and K_B one may define their formal product $K_A K_B$ to be the link composed of K_A in $\mathcal{C}_{g,n} \times [1/2, 1]$ and K_B in $\mathcal{C}_{g,n} \times [0, 1/2]$,

$$K_A K_B = \left\{ (x,t) \in \mathcal{C}_{g,n} \times [0,1] | (x, 2t-1) \in K_A \text{ for } t \geq \tfrac{1}{2} \, ; (x,2t) \in K_B \text{ for } t \leq \tfrac{1}{2} \right\}. \tag{2.8.33}$$

This operation is depicted in Figure 2.8. A natural set of relations to be imposed on the product in $\mathcal{A}^N_{g,n}(q)$ has been identified, severely constrained by the topological nature of Chern-Simons theory and leading to the definition of isotopy invariants of knots and links.

[5] We will define higher rank analogs of Fenchel-Nielsen type coordinates for the case $N = 3$ in Part III of this thesis.

[6] A lot of the research in this direction was devoted to Chern-Simons theories with compact gauge groups like $SU(N)$. However, the resulting algebras $\mathcal{A}^N_{g,n}(q)$ appearing in this context turn out to be independent of the real form of the corresponding complex group (here $SL(N)$) under consideration.

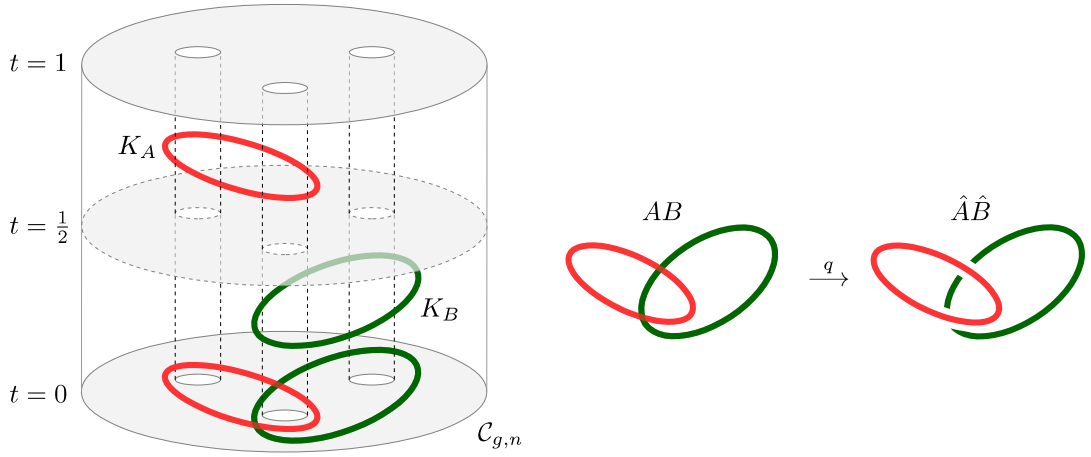

Figure 2.8: Left*: Product of two knots K_A and K_B in the 3-manifold $\mathcal{C}_{g,n} \times [0,1]$.* Right*: The corresponding loop operators that intersect classically are superposed at the quantum level.*

The first constructions of quantum $\mathfrak{sl}_N$ invariants were provided by Reshetikhin and Turaev [73] using the representation theory of the quantum group[7] $\mathcal{U}_q(\mathfrak{sl}_N)$. It was later observed that the resulting algebra can be described without the use of quantum groups in terms of generators and relations. In the following we will briefly describe the work of Sikora [88] on link invariants in $\mathbb{R}^3$ which uses both points of view (see also [84] for $SL(3)$, and [89] for similar formulations).

Sikora describes in [88] a construction of isotopy invariants of certain ribbon graphs called N-webs. The N-webs are composed of oriented ribbons emanating from, or ending in, N-valent vertices called sources or sinks, respectively (see [88] for a more formal definition). We will see that the N-webs are closely related to the networks considered in this section. This construction can be understood as a special case of Reshetikhin and Turaev's constructions. It can be described using the projections of N-webs to $\mathbb{R}^2$ called N-web diagrams. The web-diagram may be decomposed into pieces of three types: (i) crossings, (ii) sinks or sources, and (iii) cups or caps of the form

.

With each of these pieces one associates intertwining maps between tensor products of fundamental representations $\square$ of $\mathcal{U}_q(\mathfrak{sl}_N)$. The maps associated with crossings, in particular, are in a basis $e_1, \ldots, e_N$ for $\mathbb{C}$ represented by

$$\mathsf{B}(e_a \otimes e_b) = q^{\frac{1}{2N}} \begin{cases} e_b \otimes e_a & \text{for } a > b\,, \\ q^{-\frac{1}{2}} e_a \otimes e_b & \text{for } a = b\,, \\ e_b \otimes e_a + (q^{-\frac{1}{2}} - q^{\frac{1}{2}}) e_a \otimes e_b & \text{for } a < b\,, \end{cases} \tag{2.8.34}$$

or by the inverse map B^{-1}, depending on which edge is on top of the other:

(2.8.35)

[7] We summarise in this section a few of the quantum group notions that are relevant for Part II of this thesis. A more detailed account will be given in Chapter 7.

The maps associated with sinks are the unique (up to normalization) intertwining maps from the N-fold tensor product of the fundamental representation of $\mathcal{U}_q(\mathfrak{sl}_N)$ to the trivial representation, while the conjugate of this map is associated with the sources. In a similar way one associates to the caps the unique (up to normalization) intertwining maps from the tensor products of fundamental representations $\square$ with the anti-fundamental representations $\bar{\square}$ to the the trivial representation. The maps associated with the cups are the conjugate intertwining maps, respectively. Explicit formulae can be found in [88]. Using these building blocks one constructs the invariant associated with an N-web by composing the intertwining maps associated to the pieces in the natural way specified by the decomposition of the given N-web diagram into pieces.

The isotopy invariants of N-webs defined in this way satisfy various relations that can be used to calculate them explicitly. These relations relate invariants associated with N-web diagrams that are identical outside of suitable discs $\mathbb{D} \subset \mathbb{R}^2$. A typical example may be graphically represented as

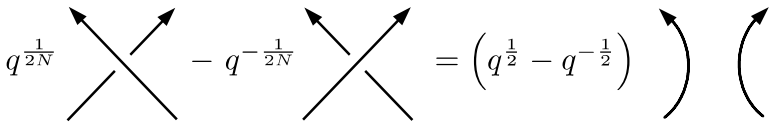

(2.8.36)

Such relations are quantum analogs of the skein relations discussed previously. Before entering into a more detailed description of the skein relations, let us note that the local nature of the skein relations will allow us to use the same relations as defining relations for the algebras $\mathcal{A}^N_{g,n}(q)$ we are interested in. This will be the basis for the approach used in the next chapter, as will be illustrated in particular by Figure 3.11. The three-dimensional isotopy invariance of the N-web invariants ensures that the resulting algebra has a three-dimensional interpretation via (2.8.33). It is easy to see that the relation (2.8.36) reproduces Goldman's bracket (2.3.18) in the limit $\hbar \to 0$.

We shall now turn to a more detailed description of the set of relations proposed in [88]. The first condition in [88] is the crossing condition (2.8.36).[8] Next, the quantum invariant for the union of two unlinked knots must be equal to the product of the quantum invariants for the knots. There are also conditions for the contraction of a trivial knot and for the Reidemeister move of type I:

(2.8.37)

We have been using the notation $[n]_q$ defined as

$$[n]_q \equiv \frac{q^{n/2} - q^{-n/2}}{q^{1/2} - q^{-1/2}} = q^{(n-1)/2} + q^{(n-3)/2} + \cdots + q^{-(n-1)/2} \,. \tag{2.8.38}$$

[8] We choose conventions that agree with the calculations in terms of Fock-Goncharov holonomies in Chapter 4. They are related to the bracket used in [88] by the redefinition $q \to q^{-2}$, and then the renormalization of each junction by $iq^{-N(N-1)/4}$ and of each edge carrying the i^{th} antisymmetric representation by $1/[i]!$. We also introduce some signs in (2.8.37).

Finally, there is a relation between two nearby N-valent junctions (a source and a sink) and a sum of positive braids labeled by permutations σ (with lengths $l(\sigma)$):

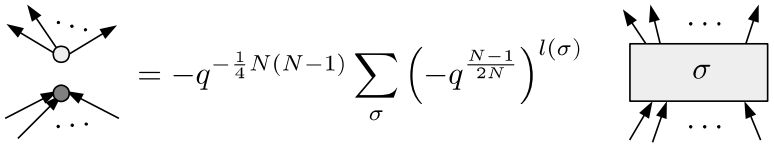

(2.8.39)

It was shown in [88] that the relations above suffice to characterize the resulting invariant of N-webs uniquely.

Note that the edges do not carry labels in Sikora's formulation. For our goals it will be convenient to represent i parallel edges between two junctions by a single edge with label i. This will allow us to define the quantised counterparts of the networks introduced previously. A quantum network corresponding to the network shown in Figure 2.4, for example, may be represented by an N-web obtained by splitting the N edges connecting one source and one sink into three groups of i, j, and k edges.

The relation (2.8.39) allows to derive skein relations for the resolution of all possible crossings in terms of N-web diagrams without crossings. Of particular interest is the following special case of the fundamental skein relation obtained by contracting $(N-2)$ pairs of edges from the upper and lower parts of (2.8.39):

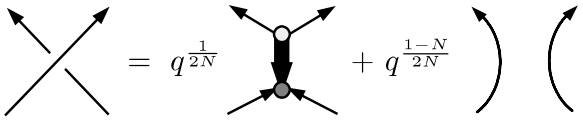

(2.8.40)

We indicate that the edge between the two junctions carries the label $N-2$ by drawing it thicker than the other edges associated with the fundamental representation. The fundamental skein relation with the other ordering at the crossing has q replaced by q^{-1}. A large set of useful relations can be derived from the relations stated above, including reduction moves of contractible bubbles (digons), squares, hexagons, etc. Such relations were worked out in [90], [91], [92]. We show some examples in Figure 2.9.

Sikora's construction allows one to recover the construction of quantum $\mathfrak{sl}_N$ invariants previously given by Murakami, Ohtsuki, and Yamada in [89] (a useful summary is given in [93]). This construction uses trivalent graphs with a "flow" built out of the following two types of vertices:

(2.8.41)

The edges connected at such vertices cary labels with values in $\{0, 1, \ldots, N-1\}$. An edge with label 0 can be removed, and an edge with label i is equivalent to an edge with label $N-i$ with opposite orientation, as depicted on the left of Figure 2.3. The vertices (2.8.41) can be represented in terms of pairs of the sources and sinks used in Sikora's formulation, as explained in [88].

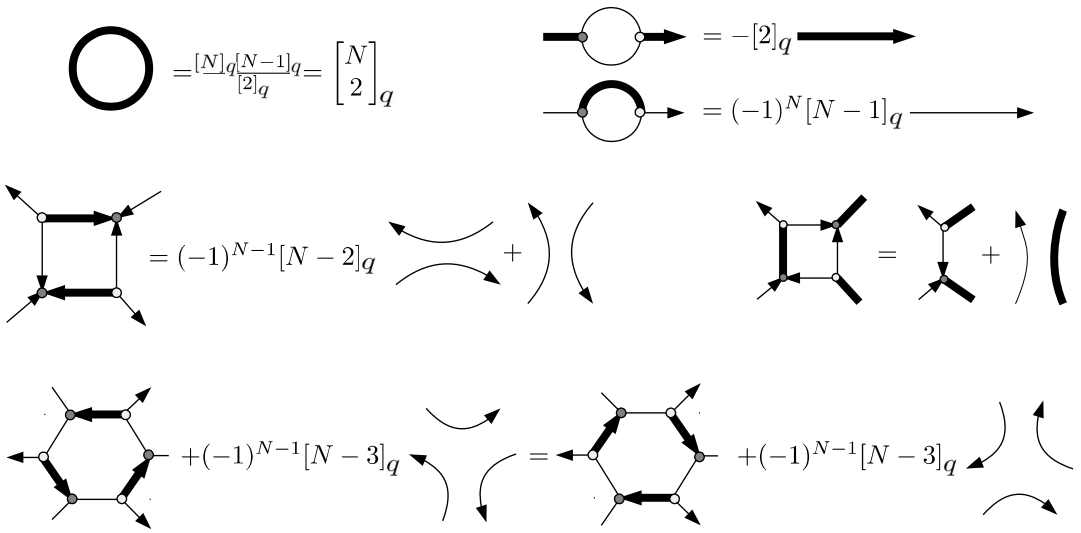

Figure 2.9: *Reduction of contractible cycles. The square reduction on the right is valid for $N = 4$. Our conventions are that thin edges carry the fundamental representation, while thick edges carry the $(N-2)$th antisymmetric representation.*

It is possible to derive an expression for a general skein relation resolving the crossing of lines labeled by arbitrary $i, j \in \{0, 1, \ldots, N-1\}$ [89] (see [93] for the normalization):

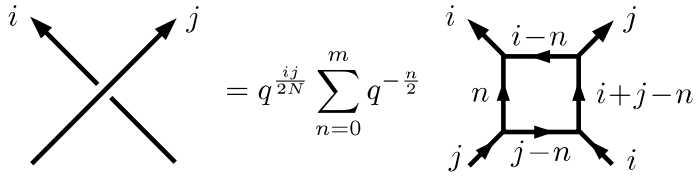

(2.8.42)

with $m = \min\{i, j, N-i, N-j\}$. For the other ordering at the crossing, one should replace q by q^{-1}. When $i = j = 1$ this expression reproduces the fundamental skein relation (2.8.40). We will also need skein relations for $N = 4$ with $i = 2$ (thick line) and $j = 1$ or $j = 2$:

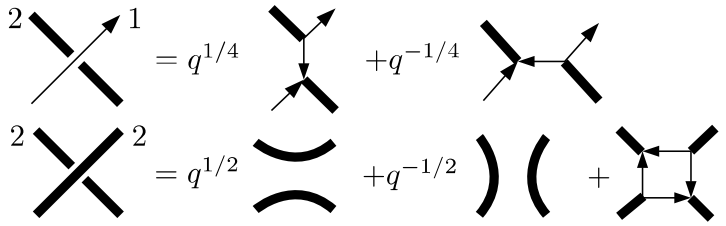

(2.8.43)

Let us finally note that the link invariants constructed in [89] also correspond to simple special cases of the Reshetikhin-Turaev construction. The label $i \in \{0, 1, \ldots, N-1\}$ assigned to an edge of a colored N-web is identified with the label for one of the irreducible representation $M_i \equiv \wedge^i \square$ of the quantum group $\mathcal{U}_q(\mathfrak{sl}_N)$ that is obtained as the i^{th} antisymmetric tensor power of the fundamental representation $\square$. The linear map $\mathsf{B}_{ij} : M_j \otimes M_i \to M_i \otimes M_j$ appearing on the left hand side of (2.8.42) can be obtained from the universal R-matrix R of $\mathcal{U}_q(\mathfrak{sl}_N)$ via

$$\mathsf{B}_{ij} \;=\; \mathsf{P}_{ij}(\pi_j \otimes \pi_i)(\mathsf{R})\,, \tag{2.8.44}$$

with P_{ij} the permutation of tensor factors, $\mathsf{P}_{ij} : M_j \otimes M_i \to M_i \otimes M_j$. The trivalent vertices in (2.8.41) are associated with the Clebsch-Gordan maps (with $k = i + j$):

$$C_{ij}^{k} : \ M_i \otimes M_j \to M_k \ , \qquad C_{k}^{ij} : \ M_k \to M_i \otimes M_j \ . \tag{2.8.45}$$

In the case where $i+j = N$, one edge carries the trivial representation and can thus be removed. This gives cap and cup maps:

$$C_{i,N-i}^{0} : \ M_i \otimes M_{N-i} \to \mathbb{C} \ , \qquad C_{0}^{N-j,j} : \ \mathbb{C} \to M_{N-j} \otimes M_j \ . \tag{2.8.46}$$

Quantum invariants of a network are then obtained by composing the intertwining maps associated with the pieces of the network.

Chapter 3

Quantisation of tinkertoys

In this chapter we will describe the quantised algebras of functions $\mathcal{A}^N_{g,n}(q)$ on the moduli space $\mathcal{M}^N_{g,n}$ of flat connections on a punctured Riemann surface $\mathcal{C}_{g,n}$ obtained by using skein quantisation in some simple examples. These will be associated with surface $\mathcal{C}_{g,n}$ with (g,n) being $(0,3)$, $(1,1)$ and $(0,4)$. As explained previously, it is reasonable to regard the results as basic building blocks for the description of the algebras associated with more general surfaces $\mathcal{C}_{g,n}$.

3.1 Pants networks

As the prototypical illustration of the role of network operators, we consider flat $SL(N,\mathbb{C})$-connections on a three-punctured sphere $\mathcal{C}_{0,3}$, also known as the pair of pants, or pants for short. As we mentioned in Section 2.6, any Riemann surface $\mathcal{C}_{g,n}$ can be decomposed into pants by choosing a maximal set of simple loops that do not intersect. The pair of pants $\mathcal{C}_{0,3}$ is hence not merely the simplest example, but also the most essential one, from which any other surface can in principle be understood. The main novelties for the case $N > 2$ will be apparent in this example. Indeed, any simple loop on $\mathcal{C}_{0,3}$ can be deformed into a loop surrounding a puncture, so networks are the only relevant objects in this case. A particularly important network has two trivalent junctions and three edges, running between every pair of punctures; we call it the *pants network* (see Figure 3.1). The number of possible pants network operators is given by the partition of N into three strictly positive integers $i + j + k = N$, which gives $\binom{N-1}{2} = (N-1)(N-2)/2$.

In terms of 4d $\mathcal{N} = 2$ gauge theories, $\mathcal{C}_{0,3}$ corresponds to the theory T_N studied by Gaiotto [9], which can be used as a fundamental building block for more general theories. T_N is a strongly coupled $\mathcal{N} = 2$ superconformal field theory with no known weakly-coupled Lagrangian description (except for T_2, which is free). It has $SU(N)^3$ flavor symmetry and $SU(2) \times U(1)$ R-symmetry. It contains operators Q and $\tilde{Q}$ with scaling dimension $(N-1)$ that transform in the trifundamental representations $(\square, \square, \square)$ and $(\bar{\square}, \bar{\square}, \bar{\square})$ of $SU(N)^3$. There are also Higgs branch operators μ_1, μ_2, μ_3, which have scaling dimension 2 and transform in the adjoint of one $SU(N)$. Finally, there are Coulomb branch operators $u_k^{(i)}$ with dimension k; the labels take the

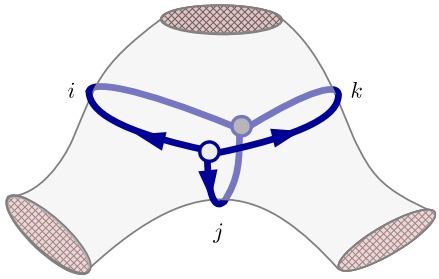

Figure 3.1: *Pants network on a pair of pants* $\mathcal{C}_{0,3}$.

values $k = 3, \ldots, N$ and $i = 1, \ldots, k-2$, so their number is $(N-1)(N-2)/2$. We see that this matches nicely the number of pants networks.

The fundamental group of the sphere $\mathcal{C}_{0,3}$ with three punctures A, B, C is represented by the loops $\gamma_A, \gamma_B, \gamma_C$ around each puncture satisfying one relation:

$$\pi_1(\mathcal{C}_{0,3}) = \{(\gamma_A, \gamma_B, \gamma_C) | \gamma_A \gamma_B \gamma_C = \gamma_\circ\} \,, \tag{3.1.1}$$

where $\gamma_\circ$ denotes a contractible loop. The corresponding holonomy matrices $\mathbf{A}$, $\mathbf{B}$, $\mathbf{C}$ satisfy $\mathbf{ABC} = (-1)^{N-1}\mathbf{I}$ (the sign is chosen for consistency with (2.8.41) and (4.2.6)). The moduli space of flat $SL(N, \mathbb{C})$-connections has the dimension

$$\dim[\mathcal{M}^N_{0,3}] = N^2 - 1 \,. \tag{3.1.2}$$

The functions coming from the loops around the punctures, A_i, B_i, C_i, with $i = 1, \ldots, N-1$, and from the pants network with both orientations, N_a, $\bar{N}_a$, with $a = 1, \ldots, (N-1)(N-2)/2$, provide the correct number of coordinates on $\mathcal{M}^N_{0,3}$:

$$3(N-1) + 2\frac{(N-1)(N-2)}{2} \quad = \quad N^2 - 1 \,. \tag{3.1.3}$$

Fixing the eigenvalues of the holonomies around the punctures then gives $3(N-1)$ constraints and leaves us with only the pants networks:

$$\dim[\bar{\mathcal{M}}^N_{0,3}] = (N-2)(N-1) \,. \tag{3.1.4}$$

SL(3)

The first non-trivial case is $N = 3$. We will show how to obtain a closed Poisson algebra involving the loops and pants network, together with an extra six-junction network. This gives 10 generators satisfying 2 polynomial relations, which can be quantised using quantum skein relations.

Loop and network functions: There are two loop functions for each holonomy matrix, namely the coefficients of the characteristic polynomial, which can be expressed in terms of traces as in (2.5.28): $A_1 = \mathrm{tr}\mathbf{A}$ and $A_2 = \mathrm{tr}\mathbf{A}^{-1}$ (and similarly for $\mathbf{B}$ and $\mathbf{C}$). The network function N_1

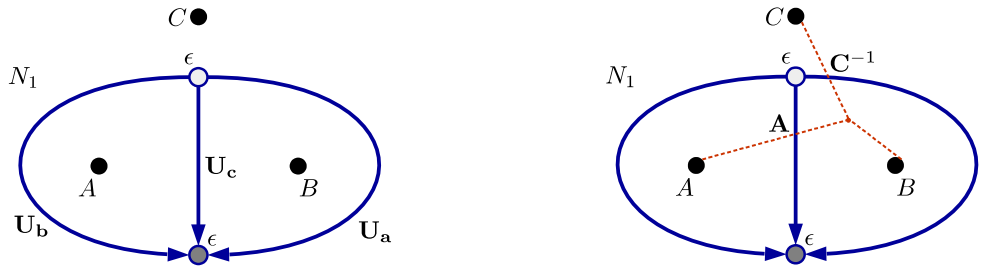

Figure 3.2: Left*: Construction of the network operator N_1 on $\mathcal{C}_{0,3}$ from the holonomy matrices $\mathbf{U_a}$, $\mathbf{U_b}$, $\mathbf{U_c}$ along its edges contracted with ϵ-tensors at the junctions.* Right*: The holonomy matrices $\mathbf{A}$, $\mathbf{B}$, $\mathbf{C}$ are associated with the branch-cuts (dashed) starting at the punctures A, B, C. Two edges of the network N_1 intersect the branch-cuts and are thus associated with $\mathbf{A}$ and $\mathbf{C}^{-1}$.*

and its reverse $\bar{N}_1$ can be constructed as in (2.5.29) by fusing the three edges at the two trivalent junctions with ϵ-tensors (see Figure 3.2 left):[1]

$$\begin{aligned} N_1 &= -\epsilon_{mnp}\mathbf{U}^m_{\mathbf{a}\,r}\mathbf{U}^n_{\mathbf{b}\,s}\mathbf{U}^p_{\mathbf{c}\,t}\epsilon^{rst}\,, \\ \bar{N}_1 &= -\epsilon_{mnp}(\mathbf{U}^{-1}_{\mathbf{a}})^m_r(\mathbf{U}^{-1}_{\mathbf{b}})^n_s(\mathbf{U}^{-1}_{\mathbf{c}})^p_t\epsilon^{rst}\,. \end{aligned} \tag{3.1.5}$$

Alternatively, we can construct the network functions as in (2.5.30) by associating holonomy matrices with the edges of the network according to which branch-cuts they cross (see Figure 3.2 right). This gives the following expressions:

$$\begin{aligned} N_1 &= -\epsilon_{mnp}\mathbf{A}^m_r\delta^n_s(\mathbf{C}^{-1})^p_t\epsilon^{rst} = \mathrm{tr}\mathbf{A}\mathbf{C}^{-\mathbf{1}} - A_1C_2\,, \\ \bar{N}_1 &= -\epsilon_{mnp}(\mathbf{A}^{-1})^m_r\delta^n_s\mathbf{C}^p_t\epsilon^{rst} = \mathrm{tr}\mathbf{A}^{-\mathbf{1}}\mathbf{C} - A_2C_1\,. \end{aligned} \tag{3.1.6}$$

The several possible choices for the position of the branch-cuts all lead to the same network function:

$$N_1 = \mathrm{tr}\mathbf{A}\mathbf{C}^{-\mathbf{1}} - A_1C_2 = \mathrm{tr}\mathbf{B}\mathbf{A}^{-\mathbf{1}} - B_1A_2 = \mathrm{tr}\mathbf{C}\mathbf{B}^{-\mathbf{1}} - C_1B_2\,. \tag{3.1.7}$$

A term such as $\mathrm{tr}\mathbf{B}\mathbf{A}^{-\mathbf{1}}$ corresponds to a self-intersecting Figure-8 loop going around the punctures B clockwise and A anticlockwise. Resolving the intersection with the skein relation in (2.4.23) produces the relation (3.1.7) (see Figure 3.3).

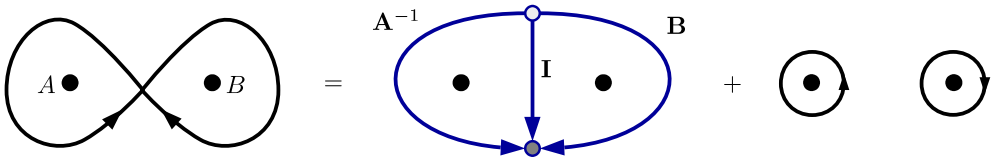

Figure 3.3: *Applying the skein relation to a self-intersecting loop going around two punctures produces a network and pair of loops around the punctures.*

[1]The overall sign is chosen for later convenience, so that N_1 will be expressed as a *positive* Laurent polynomial in the Fock-Goncharov coordinates, as in (4.4.24).

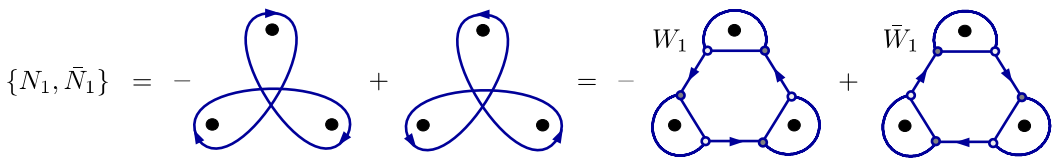

Figure 3.4: *The Poisson bracket of the pants networks N_1 and $\bar{N}_1$ can be expressed in terms of Pochhammer curves or in terms of the 6-junction network W_1 and its reverse $\bar{W}_1$.*

Closed Poisson algebra: We would like to find a set of generators including A_i, B_i, C_i and N_1, $\bar{N}_1$ that forms a closed Poisson algebra. The Poisson brackets can be obtained from Goldman's formula (2.3.18). Since the Poisson bracket is proportional to the intersection number, the loop functions A_i, B_i, C_i around the punctures obviously Poisson-commute with everything:

$$\{A_i, \bullet\} = \{B_i, \bullet\} = \{C_i, \bullet\} = 0 \,. \tag{3.1.8}$$

To apply Goldman's formula to the pants networks we use their expressions (3.1.6) in terms of trace functions. We get

$$\{N_1, \bar{N}_1\} \;=\; \{\mathrm{tr}\mathbf{A}\mathbf{C}^{-1}, \mathrm{tr}\mathbf{A}^{-1}\mathbf{C}\} = -\mathrm{tr}\mathbf{C}\mathbf{B}\mathbf{A} + \mathrm{tr}(\mathbf{C}\mathbf{B}\mathbf{A})^{-1} = -W_1 + \bar{W}_1 \,, \tag{3.1.9}$$

where the functions W_1 and $\bar{W}_1$ correspond to the six-junction networks shown in Figure 3.4 and are related to the so-called Pochhammer curves $\mathrm{tr}\mathbf{C}\mathbf{B}\mathbf{A}$ and $\mathrm{tr}(\mathbf{C}\mathbf{B}\mathbf{A})^{-1}$ via the skein relation and reductions in (2.8.40) and Figure 2.9 (with $q = 1$):

$$\begin{aligned} W_1 &= \mathrm{tr}\mathbf{C}\mathbf{B}\mathbf{A} - A_1A_2 - B_1B_2 - C_1C_2 \,, \\ \bar{W}_1 &= \mathrm{tr}(\mathbf{C}\mathbf{B}\mathbf{A})^{-1} - A_1A_2 - B_1B_2 - C_1C_2 \,. \end{aligned} \tag{3.1.10}$$

If we want to obtain a closed Poisson algebra we thus need to add W_1 and $\bar{W}_1$ to the set of generators and compute their Poisson brackets. We find that they indeed close:[2]

$$\begin{aligned} \{N_1, W_1\} &= \mathrm{tr}\mathbf{B}^{-1}\mathbf{C}^{2}\mathbf{B}\mathbf{A} - \mathrm{tr}\mathbf{C}\mathbf{B}^{-1}\mathbf{C}\mathbf{B}\mathbf{A} + \mathrm{tr}\mathbf{A}^{-1}\mathbf{B}^{-1}\mathbf{A}\mathbf{C} - \mathrm{tr}\mathbf{C}\mathbf{B}^{-1} \\ &= -N_1W_1 + 3\bar{N}_1^2 + 2\bar{N}_1(A_1B_2 + B_1C_2 + C_1A_2) - 6N_1 + \Lambda \,, \\ \{N_1, \bar{W}_1\} &= -\mathrm{tr}\mathbf{C}\mathbf{B}^{-2}\mathbf{C}^{-1}\mathbf{A}^{-1} + \mathrm{tr}\mathbf{B}^{-1}\mathbf{C}\mathbf{B}^{-1}\mathbf{C}^{-1}\mathbf{A}^{-1} - \mathrm{tr}\mathbf{A}^{-1}\mathbf{B}^{-1}\mathbf{A}\mathbf{C} + \mathrm{tr}\mathbf{C}\mathbf{B}^{-1} \\ &= N_1\bar{W}_1 - 3\bar{N}_1^2 - 2\bar{N}_1(A_1B_2 + B_1C_2 + C_1A_2) + 6N_1 - \Lambda \,, \\ \{W_1, \bar{W}_1\} &= \mathrm{tr}(\mathbf{B}\mathbf{A}\mathbf{C})^{-1}\mathbf{A}\mathbf{C}\mathbf{B} - \mathrm{tr}(\mathbf{C}\mathbf{B}\mathbf{A})^{-1}\mathbf{A}\mathbf{C}\mathbf{B} + \mathrm{tr}(\mathbf{A}\mathbf{C}\mathbf{B})^{-1}\mathbf{C}\mathbf{B}\mathbf{A} \\ &\quad -\mathrm{tr}(\mathbf{B}\mathbf{A}\mathbf{C})^{-1}\mathbf{C}\mathbf{B}\mathbf{A} + \mathrm{tr}(\mathbf{C}\mathbf{B}\mathbf{A})^{-1}\mathbf{B}\mathbf{A}\mathbf{C} - \mathrm{tr}(\mathbf{A}\mathbf{C}\mathbf{B})^{-1}\mathbf{B}\mathbf{A}\mathbf{C} \\ &= 3(N_1^3 - \bar{N}_1^3) + 2N_1^2(A_2B_1 + B_2C_1 + C_2A_1) \\ &\quad -2\bar{N}_1^2(A_1B_2 + B_1C_2 + C_1A_2) + N_1\bar{\Lambda} - \bar{N}_1\Lambda \,, \end{aligned} \tag{3.1.11}$$

and the remaining Poisson brackets can be deduced by replacing every object by its reverse: $\mathbf{A} \to \mathbf{A}^{-1}$, $A_1 \to A_2$, $N_1 \to \bar{N}_1$, $W_1 \to \bar{W}_1$, and so on. Here we have defined

$$\begin{aligned} \Lambda \;\equiv\; & A_1A_2B_2C_1 + B_1B_2C_2A_1 + C_1C_2A_2B_1 + A_1^2B_1 + B_1^2C_1 + C_1^2A_1 \\ & + A_2B_2^2 + B_2C_2^2 + C_2A_2^2 - 3(A_2B_1 + B_2C_1 + C_2A_1) \,. \end{aligned} \tag{3.1.12}$$

[2]Because of the large number of self-intersections to resolve, it is tedious to get the expressions in terms of networks (second lines) from applying skein relations. However, they can be derived easily with Mathematica in the explicit representation of loop and network functions as Fock-Goncharov polynomials that we will present in Chapter 4.

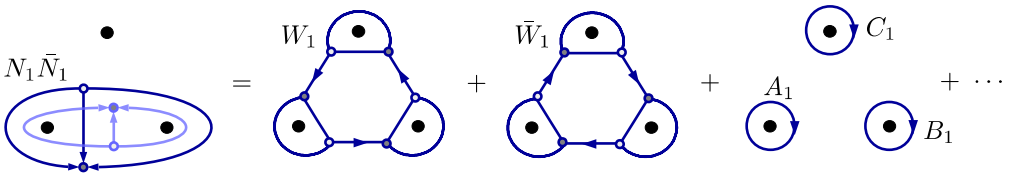

Figure 3.5: *The product $N_1\bar{N}_1$ can be expressed in terms of the networks W_1 and $\bar{W}_1$ via the skein relation.*

In conclusion, we have obtained a closed Poisson algebra with the generators

$$A_i, B_i, C_i, N_1, \bar{N}_1, W_1, \bar{W}_1 \ . \tag{3.1.13}$$

Since the dimension of the moduli space $\mathcal{M}^3_{0,3}$ is 8, there must be 2 relations between these 10 generators.

Relations: A simple way to obtain a relation is to consider the product of N_1 and $\bar{N}_1$. We can draw these networks on $\mathcal{C}_{0,3}$ such that they have two intersections, which we resolve by applying the skein relation (see Figure 3.5). The resulting networks can be simplified via the square reduction of Figure 2.9 (with $q = 1$), and the polynomial relation is then $\mathcal{P}_1 = 0$ with

$$\mathcal{P}_1 \ = \ N_1\bar{N}_1 - \big(W_1 + \bar{W}_1 + A_1B_1C_1 + A_2B_2C_2 + A_1A_2 + B_1B_2 + C_1C_2 + 3\big) \tag{3.1.14}$$

The second relation $\mathcal{P}_2 = 0$ comes from the product of W_1 and $\bar{W}_1$:[3]

$$\begin{aligned}\mathcal{P}_2 \ = \ & (W_1+6)(\bar{W}_1+6) - \Big[N_1^3 + N_1^2(A_2B_1 + B_2C_1 + A_1C_2) + N_1\bar{\Lambda} \\ & + A_1^3 + B_1^3 + C_1^3 + A_1^2A_2B_1C_1 + A_1B_1^2B_2C_1 + A_1B_1C_1^2C_2 \\ & + A_1^2B_1^2C_2 + A_2B_1^2C_1^2 + A_1^2B_2C_1^2 - 2(A_1^2B_2C_2 + A_2B_1^2C_2 + A_2B_2C_1^2) + \text{reverse} \\ & + A_1A_2B_1B_2C_1C_2 + A_1A_2B_1B_2 + B_1B_2C_1C_2 + C_1C_2A_1A_2 \\ & - 3(A_1B_1C_1 + A_2B_2C_2) - 9(A_1A_2 + B_1B_2 + C_1C_2) + 27\Big] \ ,\end{aligned} \tag{3.1.15}$$

Here "+reverse" means that all the previous terms should be added with reverse orientation.

We have therefore arrived at a description of the algebra $\mathcal{A}^3_{0,3}$ in terms of the 10 generators (3.1.13) satisfying the 2 relations $\mathcal{P}_1$ and $\mathcal{P}_2$:

$$\mathcal{A}^3_{0,3} = \mathbb{C}\left[A_i, B_i, C_i, N_1, \bar{N}_1, W_1, \bar{W}_1\right] / \{\mathcal{P}_1, \mathcal{P}_2\} \ . \tag{3.1.16}$$

It is straightforward to relate our description involving networks to the description in terms of trace functions as in (2.2.16) and (2.2.17).

Remarkably, we can write the Poisson brackets in terms of derivatives of the polynomial relations (this can be compared with [83]):

$$\begin{aligned}\{N_1, \bar{N}_1\} \ &= \ \frac{\partial\mathcal{P}_1}{\partial W_1}\frac{\partial\mathcal{P}_2}{\partial\bar{W}_1} - \frac{\partial\mathcal{P}_1}{\partial\bar{W}_1}\frac{\partial\mathcal{P}_2}{\partial W_1} \ , \qquad \{N_1, W_1\} = \frac{\partial\mathcal{P}_1}{\partial\bar{W}_1}\frac{\partial\mathcal{P}_2}{\partial\bar{N}_1} - \frac{\partial\mathcal{P}_1}{\partial\bar{N}_1}\frac{\partial\mathcal{P}_2}{\partial\bar{W}_1} \ , \\ \{N_1, \bar{W}_1\} \ &= \ \frac{\partial\mathcal{P}_1}{\partial\bar{N}_1}\frac{\partial\mathcal{P}_2}{\partial W_1} - \frac{\partial\mathcal{P}_1}{\partial W_1}\frac{\partial\mathcal{P}_2}{\partial\bar{N}_1} \ , \qquad \{W_1, \bar{W}_1\} = \frac{\partial\mathcal{P}_1}{\partial N_1}\frac{\partial\mathcal{P}_2}{\partial\bar{N}_1} - \frac{\partial\mathcal{P}_1}{\partial\bar{N}_1}\frac{\partial\mathcal{P}_2}{\partial N_1}\end{aligned} \tag{3.1.17}$$

[3] This complicated expression is also more readily obtained in the explicit representation presented in Chapter 4.

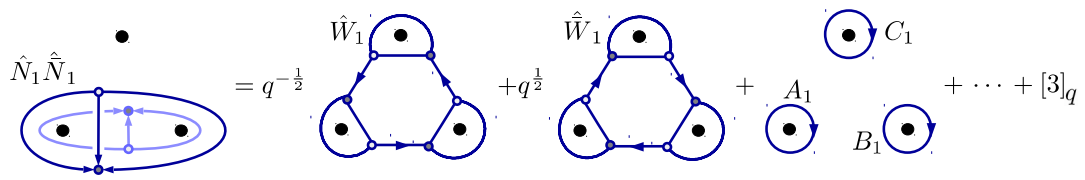

Figure 3.6: *The quantum product of $\hat{N}_1\hat{\bar{N}}_1$ resolved via the quantum skein relation.*

This indicates that that the Poisson structure of $\mathcal{M}^3_{0,3}$ is compatible with its structure as an algebraic variety.

Quantisation: Quantum versions of the polynomial relations $\mathcal{P}_1$ and $\mathcal{P}_2$, in which the network functions are replaced by noncommuting operators, can be obtained by applying the quantum skein relations in (2.8.40) and Figure 2.9.

The quantum relation $\hat{\mathcal{P}}_1$ is obtained by superposing the operators $\hat{N}_1$ and $\hat{\bar{N}}_1$ and resolving their two intersections via the quantum skein relation (see Figure 3.6):

$$\hat{N}_1\hat{\bar{N}}_1 = q^{-\frac{1}{2}}\hat{W}_1 + q^{\frac{1}{2}}\hat{\bar{W}}_1 + \hat{A}_1\hat{B}_1\hat{C}_1 + \hat{A}_2\hat{B}_2\hat{C}_2 + \hat{A}_1\hat{A}_2 + \hat{B}_1\hat{B}_2 + \hat{C}_1\hat{C}_2 + [3]_q\,. \quad (3.1.18)$$

The operator $\hat{N}_1$, which appears first in the product, is drawn on top of the second operator $\hat{\bar{N}}_1$. Note that the product $\hat{\bar{N}}_1\hat{N}_1$ with inverted order would give the same expression but with the replacement $q \to q^{-1}$.

The quantisation of the second relation $\mathcal{P}_2$ gives

$$\begin{aligned}\left(\hat{W}_1 + [6]_q\right)\left(\hat{\bar{W}}_1 + [6]_q\right) \;=\; & q^{\frac{3}{2}}\hat{N}_1^3 + \hat{q}\hat{N}_1^2(\hat{A}_2\hat{B}_1 + \hat{B}_2\hat{C}_1 + \hat{A}_1\hat{C}_2) + q^{\frac{1}{2}}\hat{N}_1\hat{\bar{\Lambda}}' \\ & +\hat{A}_1^3 + \hat{B}_1^3 + \hat{C}_1^3 + \hat{A}_1^2\hat{A}_2\hat{B}_1\hat{C}_1 + \hat{A}_1\hat{B}_1^2\hat{B}_2\hat{C}_1 + \hat{A}_1\hat{B}_1\hat{C}_1^2\hat{C}_2 \\ & +\hat{A}_1^2\hat{B}_1^2\hat{C}_2 + \hat{A}_2\hat{B}_1^2\hat{C}_1^2 + \hat{A}_1^2\hat{B}_2\hat{C}_1^2 \\ & -(q+q^{-1})(\hat{A}_1^2\hat{B}_2\hat{C}_2 + \hat{A}_2\hat{B}_1^2\hat{C}_2 + \hat{A}_2\hat{B}_2\hat{C}_1^2) + \text{reverse} \\ & +\hat{A}_1\hat{A}_2\hat{B}_1\hat{B}_2\hat{C}_1\hat{C}_2 \\ & -(q-3+q^{-1})(\hat{A}_1\hat{A}_2\hat{B}_1\hat{B}_2 + \hat{B}_1\hat{B}_2\hat{C}_1\hat{C}_2 + \hat{C}_1\hat{C}_2\hat{A}_1\hat{A}_2) \\ & -(2q^2+q-3+q^{-1}+2q^{-2})(\hat{A}_1\hat{B}_1\hat{C}_1 + \hat{A}_2\hat{B}_2\hat{C}_2) \\ & -(2q^2+q+3+q^{-1}+2q^{-2})(\hat{A}_1\hat{A}_2 + \hat{B}_1\hat{B}_2 + \hat{C}_1\hat{C}_2) \\ & +q^5 + 2q^4 + q^3 + 3q^2 + 3q + 7 \\ & +3q^{-1} + 3q^{-2} + q^{-3} + 2q^{-4} + q^{-5}\,, \end{aligned} \quad (3.1.19)$$

where now "+ reverse" also implies the replacement $q \to q^{-1}$, and in $\hat{\bar{\Lambda}}'$ we have replaced the coefficient of 3 by $2q + q^{-2}$.

We also find the following quantum commutators:

$$\begin{aligned}
\hat{N}_1\hat{\bar{N}}_1 - \hat{\bar{N}}_1\hat{N}_1 &= (q^{\frac{1}{2}} - q^{-\frac{1}{2}})(\hat{\bar{W}}_1 - \hat{W}_1)\,, \\
q^{\frac{1}{2}}\hat{N}_1\hat{W}_1 - q^{-\frac{1}{2}}\hat{W}_1\hat{N}_1 &= (q^{\frac{3}{2}} - q^{-\frac{3}{2}})\hat{\bar{N}}_1^2 + (q - q^{-1})\hat{\bar{N}}_1(\hat{A}_1\hat{B}_2 + \hat{B}_1\hat{C}_2 + \hat{C}_1\hat{A}_2) \\
&\quad -(q^2 + q - q^{-1} - q^{-2})\hat{N}_1 + (q^{\frac{1}{2}} - q^{-\frac{1}{2}})\hat{\Lambda}\,, \\
q^{-\frac{1}{2}}\hat{N}_1\hat{\bar{W}}_1 - q^{\frac{1}{2}}\hat{\bar{W}}_1\hat{N}_1 &= (q^{-\frac{3}{2}} - q^{\frac{3}{2}})\hat{\bar{N}}_1^2 + (q^{-1} - q)\hat{\bar{N}}_1(\hat{A}_1\hat{B}_2 + \hat{B}_1\hat{C}_2 + \hat{C}_1\hat{A}_2) \\
&\quad -(q^{-2} + q^{-1} - q - q^2)\hat{N}_1 + (q^{-\frac{1}{2}} - q^{\frac{1}{2}})\hat{\Lambda}\,,
\end{aligned} \tag{3.1.20}$$

and

$$\begin{aligned}
\hat{W}_1\hat{\bar{W}}_1 - \hat{\bar{W}}_1\hat{W}_1 &= (q^{\frac{3}{2}} - q^{-\frac{3}{2}})(\hat{N}_1^3 - \hat{\bar{N}}_1^3) + (q - q^{-1})\hat{N}_1^2(\hat{A}_2\hat{B}_1 + \hat{B}_2\hat{C}_1 + \hat{C}_2\hat{A}_1) \\
&\quad -(q - q^{-1})\hat{\bar{N}}_1^2(\hat{A}_1\hat{B}_2 + \hat{B}_1\hat{C}_2 + \hat{C}_1\hat{A}_2) \\
&\quad +(q^{\frac{1}{2}} - q^{-\frac{1}{2}})(\hat{N}_1\hat{\bar{\Lambda}} - \hat{\bar{N}}_1\hat{\Lambda})\,,
\end{aligned} \tag{3.1.21}$$

where in $\hat{\Lambda}$ we have made the replacement $3 \to [3]_q$. These relations reduce at first order in $\hbar$ to the Poisson brackets (3.1.9) and (3.1.11). For example, with a little bit of rewriting we obtain

$$\begin{aligned}
[\hat{N}_1, \hat{W}_1] &= (1-q)\hat{W}_1\hat{N}_1 + (q - q^{-2})\hat{\bar{N}}_1^2 + (q^{\frac{1}{2}} - q^{-\frac{3}{2}})\hat{\bar{N}}_1(\hat{A}_1\hat{B}_2 + \hat{B}_1\hat{C}_2 + \hat{C}_1\hat{A}_2) \\
&\quad -(q^{\frac{3}{2}} + q^{\frac{1}{2}} - q^{-\frac{3}{2}} - q^{-\frac{5}{2}})\hat{N}_1 + (1 - q^{-1})\hat{\Lambda} \\
&= \hbar\Big[-\hat{W}_1\hat{N}_1 + 3\hat{\bar{N}}_1^2 + 2\hat{\bar{N}}_1(\hat{A}_1\hat{B}_2 + \hat{B}_1\hat{C}_2 + \hat{C}_1\hat{A}_2) - 6\hat{N}_1 + \hat{\Lambda}\Big] + \mathcal{O}(\hbar^2) \\
&= \hbar\{N_1, W_1\} + \mathcal{O}(\hbar^2)\,.
\end{aligned} \tag{3.1.22}$$

SL(4)

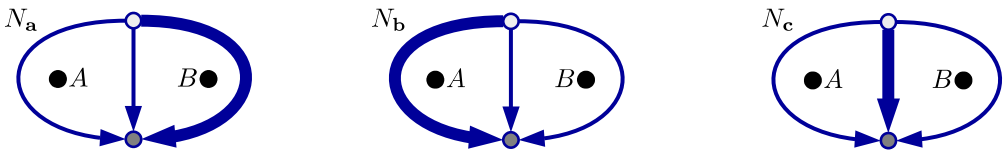

Figure 3.7: *The pants networks $N_{\mathbf{a}}$, $N_{\mathbf{b}}$, $N_{\mathbf{c}}$ differ from one another by the choice of the edge (thick) that carries the second antisymmetric representation of $SL(4)$.*

We find a similar structure for $SL(4)$ loop and network operators. The loop functions A_i around the puncture A are

$$A_1 = \mathrm{tr}\mathbf{A}\,, \qquad A_2 = \frac{1}{2}\left[(\mathrm{tr}\mathbf{A})^2 - \mathrm{tr}(\mathbf{A}^2)\right]\,, \qquad A_3 = \mathrm{tr}\mathbf{A}^{-1}\,. \tag{3.1.23}$$

We can construct three pants networks $N_{\mathbf{a}}$, $N_{\mathbf{b}}$, $N_{\mathbf{c}}$, differing by the choice of the edge that carries the second antisymmetric representation of $SL(4)$ (see Figure 3.7):

$$\begin{aligned}
N_{\mathbf{a}} &= -\frac{1}{2}\epsilon_{mnpq}\mathbf{U}^m_{\mathbf{a}\,r}\mathbf{U}^n_{\mathbf{a}\,s}\mathbf{U}^p_{\mathbf{b}\,t}\mathbf{U}^q_{\mathbf{c}\,u}\epsilon^{rstu} = \mathrm{tr}\mathbf{C}\mathbf{B}^{-1} - C_1B_3\,, \\
N_{\mathbf{b}} &= -\frac{1}{2}\epsilon_{mnpq}\mathbf{U}^m_{\mathbf{a}\,r}\mathbf{U}^n_{\mathbf{b}\,s}\mathbf{U}^p_{\mathbf{b}\,t}\mathbf{U}^q_{\mathbf{c}\,u}\epsilon^{rstu} = \mathrm{tr}\mathbf{A}\mathbf{C}^{-1} - A_1C_3\,, \\
N_{\mathbf{c}} &= -\frac{1}{2}\epsilon_{mnpq}\mathbf{U}^m_{\mathbf{a}\,r}\mathbf{U}^n_{\mathbf{b}\,s}\mathbf{U}^p_{\mathbf{c}\,t}\mathbf{U}^q_{\mathbf{c}\,u}\epsilon^{rstu} = \mathrm{tr}\mathbf{B}\mathbf{A}^{-1} - B_1A_3\,.
\end{aligned} \tag{3.1.24}$$

Pants networks with the same orientation Poisson-commute with each other:

$$\{N_{\mathbf{a}}, N_{\mathbf{b}}\} = \{N_{\mathbf{b}}, N_{\mathbf{c}}\} = \{N_{\mathbf{c}}, N_{\mathbf{a}}\} \;\; = \;\; 0 \,, \tag{3.1.25}$$

but they do not commute with their reverses:

$$\begin{aligned}
\{N_{\mathbf{a}}, \bar{N}_{\mathbf{a}}\} &= \{N_{\mathbf{b}}, \bar{N}_{\mathbf{b}}\} = \{N_{\mathbf{c}}, \bar{N}_{\mathbf{c}}\} = \mathrm{tr}\mathbf{CBA} - \mathrm{tr}\,(\mathbf{CBA})^{-1} \,, \\
\{N_{\mathbf{a}}, \bar{N}_{\mathbf{c}}\} &= \mathrm{tr}\mathbf{C}\mathbf{B}^{-1}\mathbf{A}\mathbf{B}^{-1} - \mathrm{tr}\mathbf{C}\mathbf{B}^{-2}\mathbf{A} \,, \\
\{N_{\mathbf{c}}, \bar{N}_{\mathbf{b}}\} &= \mathrm{tr}\mathbf{B}\mathbf{A}^{-1}\mathbf{C}\mathbf{A}^{-1} - \mathrm{tr}\mathbf{B}\mathbf{A}^{-2}\mathbf{C} \,, \\
\{N_{\mathbf{b}}, \bar{N}_{\mathbf{a}}\} &= \mathrm{tr}\mathbf{A}\mathbf{C}^{-1}\mathbf{B}\mathbf{C}^{-1} - \mathrm{tr}\mathbf{A}\mathbf{C}^{-2}\mathbf{B} \,.
\end{aligned} \tag{3.1.26}$$

As in the $SL(3)$ case, to obtain a closed Poisson algebra we would need to add the functions appearing in the Poisson brackets of the pants networks to the set of generators, compute their Poisson brackets, and so on. Repeating this procedure until the Poisson algebra closes would lead to a large number of generators, satisfying many polynomial relations. Ultimately, it should be possible to choose the set of 15 *independent* generators of $\mathcal{A}^4_{0,3}$ to be given by the loop functions around the punctures and by the pants networks:

$$A_i, B_i, C_i, N_{\mathbf{a}}, \bar{N}_{\mathbf{a}}, N_{\mathbf{b}}, \bar{N}_{\mathbf{b}}, N_{\mathbf{c}}, \bar{N}_{\mathbf{c}} \,. \tag{3.1.27}$$

This can be compared with the 15 generators of the ring of invariants of two matrices given in [94].

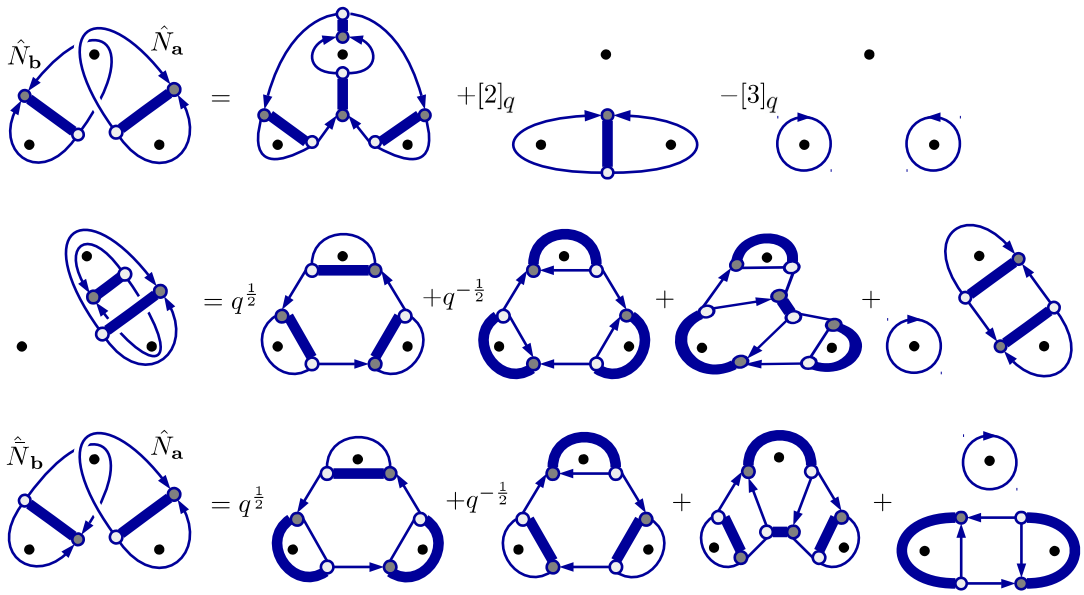

Figure 3.8: *Product of pants networks:* $\hat{N}_{\mathbf{a}}\hat{N}_{\mathbf{b}}$ *(top),* $\hat{N}_{\mathbf{a}}\hat{\bar{N}}_{\mathbf{a}}$ *(middle),* $\hat{N}_{\mathbf{a}}\hat{\bar{N}}_{\mathbf{b}}$ *(bottom).*

Many quantum relations can be easily obtained by applying quantum skein relations to products of pants networks. We show a few examples in Figure 3.8.

3.2 One-punctured torus

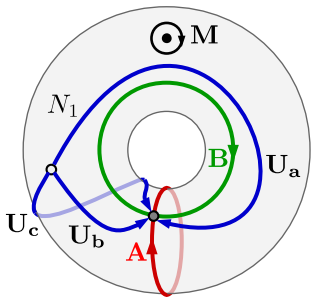

Figure 3.9: *One-punctured torus $\mathcal{C}_{1,1}$. The A- and B-cycles are shown, together with a network operator N_1, consisting of three edges and two junctions.*

Our next simple example is the torus with one full puncture, denoted by $\mathcal{C}_{1,1}$ (see Figure 3.9). The corresponding 4d gauge theory is the so-called $\mathcal{N} = 2^*$ $SU(N)$ gauge theory, which can be obtained from the $\mathcal{N} = 4$ theory by giving a mass to an adjoint hypermultiplet.

The fundamental group of $\mathcal{C}_{1,1}$ consists of three loops, the A-cycle γ_A (meridian), the B-cycle γ_B (longitude), and the loop γ_M around the puncture, subject to one relation:

$$\pi_1(\mathcal{C}_{1,1}) = \{(\gamma_A, \gamma_B, \gamma_M) | \gamma_A \gamma_B \gamma_A^{-1} \gamma_B^{-1} = \gamma_M\} \, . \tag{3.2.28}$$

The holonomy matrices by $\mathbf{A}$, $\mathbf{B}$, and $\mathbf{M}$ satisfy $\mathbf{ABA}^{-1}\mathbf{B}^{-1} = \mathbf{M}$. We can also combine the matrices $\mathbf{A}$ and $\mathbf{B}$ into matrices $\mathbf{C} \equiv (\mathbf{AB})^{-1}$ and $\mathbf{C}' \equiv \mathbf{AB}^{-1}$ associated with the curves $\gamma_C = (\gamma_A \gamma_B)^{-1}$ and $\gamma_{C'} = \gamma_A \gamma_B^{-1}$, respectively. Each of these holonomy matrices gives $(N-1)$ loop functions.

We also consider a particular two-junction network N_1 with two junctions whose edges go around the A- and B-cycles (in contrast to the case of $\mathcal{C}_{0,3}$, there are many two-junction networks that we can consider on $\mathcal{C}_{1,1}$). The network N_1 and its reverse $\bar{N}_1$ each contributes $(N-1)(N-2)/2$ operators. Together, the operators coming from $\mathbf{A}$, $\mathbf{B}$, $\mathbf{C}$ and from the networks N_1, $\bar{N}_1$ add up to the dimension (2.1.4) of the moduli space of flat $SL(N)$-connections on $\mathcal{C}_{1,1}$:

$$3(N-1) + 2\frac{(N-1)(N-2)}{2} \quad = \quad N^2 - 1 = \dim[\mathcal{M}^N_{1,1}] \, . \tag{3.2.29}$$

SL(2)

We start by briefly reviewing the well-studied case of flat $SL(2,\mathbb{C})$-connections on the one-punctured torus $\mathcal{C}_{1,1}$ [51] (see also [95], [70], [54]). The Poisson bracket of the A-cycle function $A_1 = \mathrm{tr}\mathbf{A}$ and the B-cycle function $B_1 = \mathrm{tr}\mathbf{B}$ is (by Goldman's formula (2.3.18)):

$$\{A_1, B_1\} = \mathrm{tr}\mathbf{AB} - \frac{1}{2}A_1 B_1 = -\mathrm{tr}\mathbf{AB}^{-1} + \frac{1}{2}A_1 B_1 \, . \tag{3.2.30}$$

The extra traces $C_1 = \mathrm{tr}\mathbf{AB}$ and $C_1' = \mathrm{tr}\mathbf{AB}^{-1}$ correspond to curves that go once around the A-cycle and once around the B-cycle (in different directions). Applying the skein relation to

products of loop functions gives

$$A_1 B_1 \;=\; C_1 + C_1' \,, \qquad C_1 C_1' = A_1^2 + B_1^2 + M_1 - 2 \,, \tag{3.2.31}$$

which can be combined to obtain the relation $\mathcal{P}_1 = 0$ with

$$\mathcal{P}_1 = A_1 B_1 C_1 - (A_1^2 + B_1^2 + C_1^2 + M_1 - 2) \,. \tag{3.2.32}$$

The Poisson bracket between the generators A_1, B_1, C_1 can be written as

$$\{A_1, B_1\} = -\frac{1}{2}\frac{\partial \mathcal{P}_1}{C_1} \,, \tag{3.2.33}$$

and cyclic permutations of A_1, B_1, C_1.

To obtain quantum relations, we apply the quantum skein relation:

$$\hat{A}_1 \hat{B}_1 = q^{\frac{1}{4}} \hat{C}_1 + q^{-\frac{1}{4}} \hat{C}_1' \,. \tag{3.2.34}$$

Inverting the order in the product amounts to exchanging $q \leftrightarrow q^{-1}$, so we can obtain the q-deformed commutation relation

$$q^{\frac{1}{4}} \hat{A}_1 \hat{B}_1 - q^{-\frac{1}{4}} \hat{B}_1 \hat{A}_1 = \left(q^{\frac{1}{2}} - q^{-\frac{1}{2}}\right) \hat{C}_1 \,. \tag{3.2.35}$$

Note that this relation can be written as a quantum commutator

$$[\hat{A}_1, \hat{B}_1] = (q^{-\frac{1}{2}} - 1)\hat{B}_1 \hat{A}_1 + (q^{\frac{1}{4}} - q^{-\frac{3}{4}})\hat{C}_1 \,, \tag{3.2.36}$$

which reproduces the Poisson bracket (3.2.30) at first order in $\hbar$. Similarly, the quantum skein relation leads to the quantisation of the cubic relation (3.2.32):

$$\hat{\mathcal{P}}_1 = q^{\frac{1}{4}} \hat{A}_1 \hat{B}_1 \hat{C}_1 - \left(q^{\frac{1}{2}} \hat{A}_1^2 + q^{-\frac{1}{2}} \hat{B}_1^2 + q^{\frac{1}{2}} \hat{C}_1^2 + M_1 - [2]_q\right) \,. \tag{3.2.37}$$

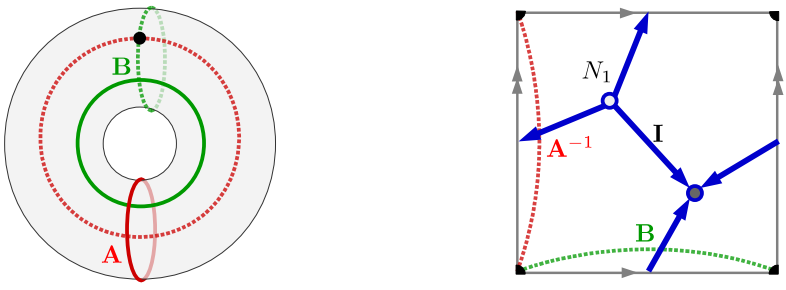

Figure 3.10: Left*: Covering of $\mathcal{C}_{1,1}$ with two branch-cuts (dashed lines). Each branch-cut is associated with a holonomy matrix* $\mathbf{A}$ *or* $\mathbf{B}$. Right*: $\mathcal{C}_{1,1}$ described as a square with opposite sides identified, and with the puncture at the corners. The holonomy matrices associated with the three edges of the network N_1 are determined by the branch-cuts that they cross.*

SL(3)

We now have the loop functions $A_1 = \mathrm{tr}\mathbf{A}$ and $A_2 = \mathrm{tr}\mathbf{A}^{-1}$ and similarly for B_i, M_i, C_i, and C_i'. There are many different two-junction networks that can be put on $\mathcal{C}_{1,1}$. A natural choice is the network that goes once around the A-cycle and once around the B-cycle. The associated network function N_1 and its reverse $\bar{N}_1$ can be expressed as

$$\begin{aligned} N_1 &= \epsilon_{mnp}\mathbf{U}^m_{\mathbf{a}\,r}\mathbf{U}^n_{\mathbf{b}\,s}\mathbf{U}^p_{\mathbf{c}\,t}\epsilon^{rst}\,, \\ \bar{N}_1 &= \epsilon_{mnp}(\mathbf{U}^{-1}_{\mathbf{a}})^m_r(\mathbf{U}^{-1}_{\mathbf{b}})^n_s(\mathbf{U}^{-1}_{\mathbf{c}})^p_t\epsilon^{rst}\,. \end{aligned} \tag{3.2.38}$$

As explained in Section (2.5), the network functions N_1 and $\bar{N}_1$ can also be obtained from the transition functions in a covering of $\mathcal{C}_{1,1}$. We can for example cover $\mathcal{C}_{1,1}$ with one patch that overlaps itself along two branch-cuts that go around the A- and B-cycles and intersect at the puncture (see Figure 3.10). The network N_1 has one edge that crosses the branch-cut associated with $\mathbf{A}$ (with reverse orientation), one that crosses the branch-cut associated with $\mathbf{B}$, and one that does not cross any branch-cut. This gives the following expressions

$$\begin{aligned} N_1 &= \epsilon_{mnp}(\mathbf{A}^{-1})^m_r\mathbf{B}^n_{\ s}\delta^p_t\epsilon^{rst} = A_2B_1 - C_2'\,, \\ \bar{N}_1 &= \epsilon_{mnp}\mathbf{A}^m_{\ r}(\mathbf{B}^{-1})^n_{\ s}\delta^p_t\epsilon^{rst} = A_1B_2 - C_1'\,, \end{aligned} \tag{3.2.39}$$

with $C_1' = \mathrm{tr}\mathbf{A}\mathbf{B}^{-1}$ and $C_2' = \mathrm{tr}\mathbf{A}^{-1}\mathbf{B}$. Such relations between networks and products of intersecting loops can of course also be understood as arising from the skein relation (2.4.23) (see Figure 3.11):

$$A_2B_1 = N_1 + C_2'\,, \qquad A_1B_2 = \bar{N}_1 + C_1'\,. \tag{3.2.40}$$

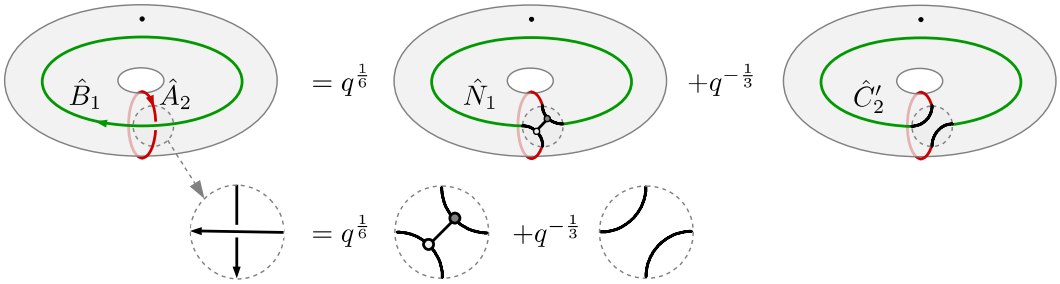

Figure 3.11: *Relations between loop and network operators arise from the skein relation.*

The quantisation of relations such as (3.2.40) can be obtained by applying quantum skein relations to resolve the intersection of the A- and B-cycles:

$$\begin{aligned} \hat{A}_2\hat{B}_1 &= q^{\frac{1}{6}}\hat{N}_1 + q^{-\frac{1}{3}}\hat{C}_2'\,, \qquad \hat{A}_1\hat{B}_1 = q^{-\frac{1}{6}}\hat{N}_1' + q^{\frac{1}{3}}\hat{C}_2\,, \\ \hat{A}_1\hat{B}_2 &= q^{\frac{1}{6}}\hat{\bar{N}}_1 + q^{-\frac{1}{3}}\hat{C}_1'\,, \qquad \hat{A}_2\hat{B}_2 = q^{-\frac{1}{6}}\hat{\bar{N}}_1' + q^{\frac{1}{3}}\hat{C}_1\,. \end{aligned} \tag{3.2.41}$$

Here the operator $\hat{N}_1'$ corresponds to the flipped network shown on the left of Figure 3.12.

Changing the ordering in the product of two operators simply inverts q, so we can deduce expressions for commutators, whose leading terms in $\hbar$ correspond to the Poisson brackets. For

example we obtain

$$[\hat{A}_2, \hat{B}_1] \;=\; (q^{\frac{1}{6}} - q^{-\frac{1}{6}})\hat{N}_1 + (q^{-\frac{1}{3}} - q^{\frac{1}{3}})\hat{C}_2' \quad \to \quad \{A_2, B_1\} = \frac{1}{3}(N_1 - 2C_2') \; . \tag{3.2.42}$$

We can also apply the quantum skein relation to the product of $\hat{N}_1$ and $\hat{\bar{N}}_1$:

$$\hat{N}_1\hat{\bar{N}}_1 = q^{-\frac{1}{2}}\hat{W}_6 + q^{\frac{1}{2}}\hat{\bar{W}}_6 + \hat{A}_1\hat{A}_2 + \hat{B}_1\hat{B}_2 + \hat{C}_1\hat{C}_2 + \hat{M}_1 + \hat{M}_2 + [3]_q \; , \tag{3.2.43}$$

where W_6 is a network with six junctions shown on the right of Figure 3.12. The same network W_6 also appears in the product

$$\hat{\bar{N}}_1'\hat{C}_2 = \hat{W}_6 + q^{\frac{1}{2}}\hat{A}_1\hat{A}_2 + q^{-\frac{1}{2}}\hat{B}_1\hat{B}_2 \; . \tag{3.2.44}$$

More complicated relations are impractical to derive in this way, but can be computed in the explicit representation of the loop and network operators in terms of Fock-Goncharov polynomials, as we will discuss in Chapter 4. We have for example the classical relation (also given in [80], [96])

$$\begin{aligned} A_1A_2B_1B_2C_1C_2 \;=\; & \Big[N_1^3 + N_1^2(A_2B_1 + B_2C_1 + C_2A_1) \\ & + N_1(A_1A_2B_1C_2 + A_1^2C_1 + A_2^2B_2 - 3A_1B_2 + \text{cyclic}) \\ & - (A_1B_2^2C_2^2 - 2A_1^2B_2C_2 + A_1^3 + \text{cyclic}) + \text{reverse}\Big] \\ & - N_1\bar{N}_1(A_1A_2 + \text{cyclic}) - (A_1A_2B_1B_2 + \text{cyclic}) \\ & + 3(A_1B_1C_1 + A_2B_2C_2) + M_1M_2 + 6(M_1 + M_2) + 9 \; . \end{aligned} \tag{3.2.45}$$

Here "+cyclic" means adding the terms obtained by cyclic permutation of A, B, C, and "+reverse" the terms obtained by reversing the orientation, $A_1 \leftrightarrow A_2$, $N_1 \leftrightarrow \bar{N}_1$, and so on. Recall that at the classical level the algebraic structures of $\mathcal{M}^N_{0,3}$ and $\mathcal{M}^N_{1,1}$ are the same, so that the relation (3.2.45) is the counterpart of the relation (3.1.15) for the 3-punctured sphere. The Poisson structures on $\mathcal{M}^N_{0,3}$ and $\mathcal{M}^N_{1,1}$ can also be related via a symplectic quotient, as explained in [97].

In conclusion, we can describe the algebra $\mathcal{A}^3_{1,1}$ in terms of the 10 generators A_i, B_i, M_i, C_i, N_1, $\bar{N}_1$ satisfying the relations (3.2.43) and (3.2.45). Classically, these generators form a closed

Figure 3.12: Left*: Flipped network N_1'.* Right*: Network W_6 appearing in the product $N_1\bar{N}_1$.*

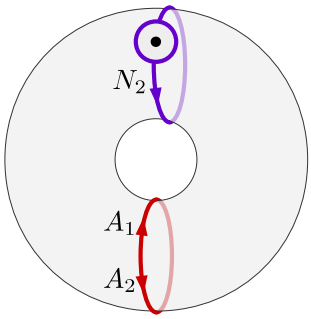

Figure 3.13: *A maximal set of commutting Hamiltonians on $\bar{\mathcal{M}}^3_{1,1}$ is provided by the A-cycle functions A_i and the pants network N_2.*

Poisson algebra (as noted in [96]):

$$\begin{aligned}
\{A_1,B_1\} &= C_2-\frac{1}{3}A_1B_1\ , & \{A_2,B_1\} &= N_1-\frac{2}{3}A_2B_1\ ,\\
\{B_1,C_1\} &= A_2-\frac{1}{3}B_1C_1\ , & \{B_2,C_1\} &= N_1-\frac{2}{3}B_2C_1\ ,\\
\{C_1,A_1\} &= B_2-\frac{1}{3}C_1A_1\ , & \{C_2,A_1\} &= N_1-\frac{2}{3}C_2A_1\ ,\\
\{A_1,N_1\} &= -\frac{1}{3}A_1N_1+A_2C_2-B_1\ , & \{A_1,\bar{N}_1\} &= \frac{1}{3}A_1\bar{N}_1-A_2B_2+C_1\ ,\\
\{B_1,N_1\} &= -\frac{1}{3}B_1N_1+A_2B_2-C_1\ , & \{B_1,\bar{N}_1\} &= \frac{1}{3}B_1\bar{N}_1-B_2C_2+A_1\ ,\\
\{C_1,N_1\} &= -\frac{1}{3}C_1N_1+B_2C_2-A_1\ , & \{C_1,\bar{N}_1\} &= \frac{1}{3}C_1\bar{N}_1-A_2C_2+B_1\ ,\\
& & \{N_1,\bar{N}_1\} &= A_1B_1C_1-A_2B_2C_2\ .
\end{aligned} \tag{3.2.46}$$

The remaining Poisson brackets can be obtained by reversing the orientation. In addition, the functions M_i associated with the curve around the puncture are central elements of the Poisson algebra, $\{M_i,\bullet\}=0$.

Fixing the values of the central elements M_i leaves us with a 6-dimensional moduli space $\bar{\mathcal{M}}^3_{1,1}$ which is symplectic. A natural maximal set of commuting Hamiltonians consists of the A-cycle functions A_i together with a network N_2 that surrounds the puncture and has one edge along the A-cycle (see Figure 3.13):

$$N_2=-\epsilon_{mnp}\mathbf{A}^m_{\ r}\mathbf{M}^n_{\ s}\delta^p_{\ t}\epsilon^{rst}=\mathrm{tr}\mathbf{AM}-A_1M_1\ . \tag{3.2.47}$$

This network is the pants network in the pants decomposition obtained by cutting $\mathcal{C}_{1,1}$ along the A-cycle. It is related to the network N_1 defined above via

$$N_2 \;=\; -N_1C_1-\bar{N}_1B_1+A_2B_1C_1+B_2C_2-A_2^2+A_1\ . \tag{3.2.48}$$

The A-cycle functions A_i and the pants network N_2 Poisson-commute, as is obvious from the fact that they do not intersect:

$$\{A_1,A_2\}=\{A_1,P_1\}=\{A_2,P_1\}=0\ . \tag{3.2.49}$$

SL(4)

The A-cycle functions are $A_1 = \mathrm{tr}\mathbf{A}$, $A_2 = \frac{1}{2}\left[(\mathrm{tr}\mathbf{A})^2 - \mathrm{tr}(\mathbf{A}^2)\right]$, $A_3 = \mathrm{tr}\mathbf{A}^{-1}$. We define three networks which are going once around the A-cycle and once around the B-cycle, and differ by the choice of the branch that is doubled:

$$\begin{aligned} N_a &= \tfrac{1}{2}\epsilon_{mnpq}\mathbf{U}^m_{\mathbf{a}\,r}\mathbf{U}^n_{\mathbf{a}\,s}\mathbf{U}^p_{\mathbf{b}\,t}\mathbf{U}^q_{\mathbf{c}\,u}\epsilon^{rstu}\,, \\ N_{\mathbf{b}} &= \tfrac{1}{2}\epsilon_{mnpq}\mathbf{U}^m_{\mathbf{a}\,r}\mathbf{U}^n_{\mathbf{b}\,s}\mathbf{U}^p_{\mathbf{b}\,t}\mathbf{U}^q_{\mathbf{c}\,u}\epsilon^{rstu}\,, \\ N_{\mathbf{c}} &= \tfrac{1}{2}\epsilon_{mnpq}\mathbf{U}^m_{\mathbf{a}\,r}\mathbf{U}^n_{\mathbf{b}\,s}\mathbf{U}^p_{\mathbf{c}\,t}\mathbf{U}^q_{\mathbf{c}\,u}\epsilon^{rstu}\,. \end{aligned} \tag{3.2.50}$$

Quantum relations between the loop and network operators can be obtained by applying quantum skein relations:

$$\begin{aligned} \hat{A}_1\hat{B}_3 &= q^{-\frac{1}{8}}\hat{\hat{N}}_{\mathbf{b}} + q^{\frac{3}{8}}\hat{C}'_1\,, \quad \hat{A}_1\hat{B}_1 = q^{\frac{1}{8}}\hat{N}'_{\mathbf{b}} + q^{-\frac{3}{8}}\hat{C}_3\,, \quad \hat{A}_3\hat{B}_1 = q^{-\frac{1}{8}}\hat{N}_{\mathbf{b}} + q^{\frac{3}{8}}\hat{C}'_3 \\ \hat{A}_1\hat{B}_2 &= q^{-\frac{1}{4}}\hat{\hat{N}}_{\mathbf{a}} + q^{\frac{1}{4}}\hat{N}'_{\mathbf{a}}\,, \quad \hat{A}_3\hat{B}_3 = q^{\frac{1}{8}}\hat{\hat{N}}'_{\mathbf{b}} + q^{-\frac{3}{8}}\hat{C}_1\,, \quad \hat{A}_2\hat{B}_1 = q^{-1/4}\hat{N}_{\mathbf{c}} + q^{\frac{1}{4}}\hat{N}'_{\mathbf{c}}\,, \\ \hat{A}_3\hat{B}_2 &= q^{-\frac{1}{4}}\hat{N}_{\mathbf{a}} + q^{\frac{1}{4}}\hat{\hat{N}}'_{\mathbf{a}}\,, \quad \hat{A}_2\hat{B}_3 = q^{-1/4}\hat{\hat{N}}_{\mathbf{c}} + q^{\frac{1}{4}}\hat{\hat{N}}'_{\mathbf{c}}\,, \quad \hat{A}_2\hat{B}_2 = q^{\frac{1}{2}}\hat{C}'_2 + q^{-\frac{1}{2}}\hat{C}_2 + \hat{N}_4\,. \end{aligned} \tag{3.2.51}$$

Here the networks with a prime are flipped and N_4 is the four-junction network in Figure 3.14.

3.3 Four-punctured sphere

The next example (with $\chi = -2$) is the sphere $\mathcal{C}_{0,4}$ with four full punctures, denoted by A, B, C, D. Its fundamental group can be expressed in terms of the loops $\gamma_A, \gamma_B, \gamma_C, \gamma_D$ surrounding the punctures clockwise, subject to one relation:

$$\pi_1(\mathcal{C}_{0,4}) = \{(\gamma_A, \gamma_B, \gamma_C, \gamma_D)|\gamma_A\gamma_B\gamma_C\gamma_D = \gamma_\circ\}\,. \tag{3.3.52}$$

We associate holonomy matrices $\mathbf{A}, \mathbf{B}, \mathbf{C}, \mathbf{D}$ to these loops, satisfying $\mathbf{ABCD} = (-1)^{N-1}\mathbf{I}$. In addition, we consider the loops γ_S and γ_T surrounding pairs of punctures: $\mathbf{S} \equiv \mathbf{AB}$ and $\mathbf{T} \equiv \mathbf{BC}$ (see Figure 3.15). We also define the two networks N_{AB}, N_{CD} (and their inverses $\bar{N}_{AB}, \bar{N}_{CD}$) around punctures A, B, and C, D, respectively, which are adapted to the pants decomposition determined by the curve γ_S. Each of the holonomy matrices $\mathbf{A}, \mathbf{B}, \mathbf{C}, \mathbf{D}, \mathbf{S}, \mathbf{T}$ gives $(N-1)$ functions, while each of the four networks $N_{AB}, N_{CD}, \bar{N}_{AB}, \bar{N}_{CD}$ gives $(N-1)(N-2)/2$ functions. This gives the following number of functions:

$$6(N-1) + 4\frac{(N-1)(N-2)}{2} \;=\; 2(N^2-1) = \dim[\mathcal{M}^N_{0,4}]\,. \tag{3.3.53}$$

Fixing the conjugacy classes of $\mathbf{A}, \mathbf{B}, \mathbf{C}, \mathbf{D}$ gives $4(N-1)$ constraints.

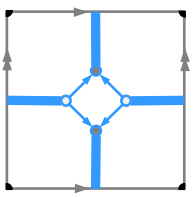

Figure 3.14: *Network N_4 that appears in the product A_2B_2 (thick lines carry $\wedge^2\square$).*

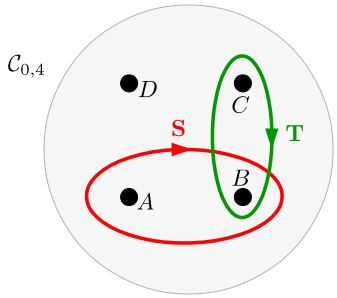

Figure 3.15: *Sphere $\mathcal{C}_{0,4}$ with 4 punctures A, B, C, D. The holonomy matrices* $\mathbf{S}$ *and* $\mathbf{T}$ *are associated with loops surrounding pairs of punctures.*

SL(2)

The generators $A_1, B_1, C_1, D_1, S_1, T_1$ do not form a closed Poisson algebra on their own. Indeed, applying the quantum skein relation gives

$$\hat{S}_1\hat{T}_1 \;=\; q^{-\frac{1}{2}}\hat{U}_1 + q^{\frac{1}{2}}\hat{U}_1' + \hat{A}_1\hat{C}_1 + \hat{B}_1\hat{D}_1 \,, \tag{3.3.54}$$

with $U_1 \equiv \mathrm{tr}\mathbf{BD}$ and $U_1' \equiv \mathrm{tr}\mathbf{AC}$ (up to an overall sign for later convenience). The leading order in $\hbar$ gives the Poisson bracket

$$\{S_1, T_1\} = -U_1 + U_1' \,. \tag{3.3.55}$$

We can eliminate U_1' via the relation (3.3.54), but then we must include U_1 in the set of generators in order to obtain a closed Poisson algebra. The closure of the Poison algebra with the 7 generators $A_1, B_1, C_1, D_1, S_1, T_1, U_1$ is implied by the following q-deformed commutators:

$$\begin{aligned}
q^{-\frac{1}{2}}\hat{S}_1\hat{T}_1 - q^{\frac{1}{2}}\hat{T}_1\hat{S}_1 &= (q^{-1}-q)\hat{U}_1 - (q^{\frac{1}{2}}-q^{-\frac{1}{2}})(\hat{A}_1\hat{C}_1 + \hat{B}_1\hat{D}_1) \,, \\
q^{-\frac{1}{2}}\hat{T}_1\hat{U}_1 - q^{\frac{1}{2}}\hat{U}_1\hat{T}_1 &= (q^{-1}-q)\hat{S}_1 - (q^{\frac{1}{2}}-q^{-\frac{1}{2}})(\hat{A}_1\hat{B}_1 + \hat{C}_1\hat{D}_1) \,, \\
q^{-\frac{1}{2}}\hat{U}_1\hat{S}_1 - q^{\frac{1}{2}}\hat{S}_1\hat{U}_1 &= (q^{-1}-q)\hat{T}_1 - (q^{\frac{1}{2}}-q^{-\frac{1}{2}})(\hat{B}_1\hat{C}_1 + \hat{A}_1\hat{D}_1) \,.
\end{aligned} \tag{3.3.56}$$

Since $\dim[\mathcal{M}^2_{0,4}] = 6$, there must be one relation between the 7 generators. It is provided by the product of U_1 and U_1':

$$\begin{aligned}
\hat{U}_1\hat{U}_1' \;=\; & q\hat{S}_1^2 + q^{-1}\hat{T}_1^2 + q^{\frac{1}{2}}\hat{S}_1(\hat{A}_1\hat{B}_1 + \hat{C}_1\hat{D}_1) + q^{-\frac{1}{2}}\hat{T}_1(\hat{B}_1\hat{C}_1 + \hat{A}_1\hat{D}_1) \\
& + \hat{A}_1\hat{B}_1\hat{C}_1\hat{D}_1 + \hat{A}_1^2 + \hat{B}_1^2 + \hat{C}_1^2 + \hat{D}_1^2 - [2]_q^2 \,.
\end{aligned} \tag{3.3.57}$$

Eliminating U_1' with the relation (3.3.54) we obtain the familiar cubic relation (see [54])

$$\begin{aligned}
\hat{\mathcal{P}}_1 \;=\; & q^{-\frac{1}{2}}\hat{S}_1\hat{T}_1\hat{U}_1 - q^{-1}\hat{S}_1^2 - q\hat{T}_1^2 - q^{-1}\hat{U}_1^2 \\
& - q^{-\frac{1}{2}}\hat{S}_1(\hat{A}_1\hat{B}_1 + \hat{C}_1\hat{D}_1) - q^{\frac{1}{2}}\hat{T}_1(\hat{B}_1\hat{C}_1 + \hat{A}_1\hat{D}_1) - q^{-\frac{1}{2}}\hat{U}_1(\hat{A}_1\hat{C}_1 + \hat{B}_1\hat{D}_1) \\
& - \hat{A}_1\hat{B}_1\hat{C}_1\hat{D}_1 - \hat{A}_1^2 - \hat{B}_1^2 - \hat{C}_1^2 - \hat{D}_1^2 + [2]_q^2 \,.
\end{aligned} \tag{3.3.58}$$

Note that the same relation holds with U_1 replaced by U_1' and q by q^{-1}. We thus have a presentation of the algebra $\mathcal{A}^2_{0,4}$ in terms of 7 generators satisfying the cubic relation $\mathcal{P}_1$:

$$\mathcal{A}^2_{0,4} = \mathbb{C}\left[A_1, B_1, C_1, D_1, S_1, T_1, U_1\right]/\mathcal{P}_1 \,. \tag{3.3.59}$$

The Poisson brackets can be expressed as derivatives of $\mathcal{P}_1$, for example

$$\{S_1, T_1\} \;=\; \frac{\partial \mathcal{P}_1}{\partial U_1} = S_1T_1 - 2U_1 - (A_1C_1 + B_1D_1) \,. \tag{3.3.60}$$

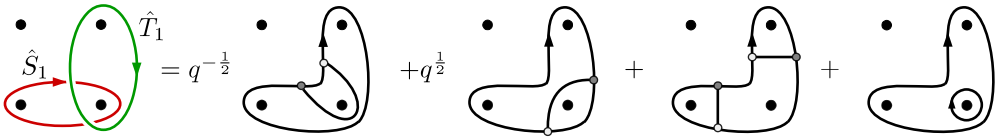

Figure 3.16: *The product $\hat{S}_1\hat{T}_1$ generates networks via skein relations.*

SL(3)

For Riemann surfaces with $\dim[\pi_1(\mathcal{C}_{g,n})] = 3$ such as $\mathcal{C}_{0,4}$, the $SL(3)$ character variety has dimension 16, and is generated by a minimal number of 45 trace functions, see [94], [98]. This implies the existence of 29 relations between the generators. Choices for the 16 *independent* generators were given in [99]. In terms our description, we can take the following loop and pants network functions $\{A_i, B_i, C_i, S_i, T_i, U_i', N_{AB}, \bar{N}_{AB}, N_{AC}, \bar{N}_{AC}\}$, with

$$N_{AB} = \mathrm{tr}\mathbf{A}\mathbf{B}^{-1} - A_1B_2\,, \qquad N_{AC} = \mathrm{tr}\mathbf{A}\mathbf{C}^{-1} - A_1C_2\,. \tag{3.3.61}$$

We can then apply quantum skein relations to products of generators to obtain relations. For example we get (see Figure 3.16)

$$\hat{S}_1\hat{T}_1 = q^{-\frac{1}{2}}\hat{N}_{BD} + q^{\frac{1}{2}}\hat{N}'_{BD} + \hat{N}_{ABC} + \hat{B}_1\hat{D}_2\,, \tag{3.3.62}$$

with

$$\begin{aligned} N_{BD} &= \mathrm{tr}\mathbf{B}\mathbf{D}^{-1} - B_1D_2\,, \qquad N'_{BD} = \mathrm{tr}\mathbf{A}\mathbf{B}^{-1}\mathbf{C} - B_2U_1'\,, \\ N_{ABC} &= \mathrm{tr}\mathbf{C}\mathbf{B}^{-1}\mathbf{A} - A_1\bar{N}_{BC} - C_1N_{AB} - A_1B_2C_1\,. \end{aligned} \tag{3.3.63}$$

We also find

$$\hat{N}_{AB}\hat{\bar{N}}_{AB} = q^{-\frac{1}{2}}\hat{N}_6 + q^{\frac{1}{2}}\hat{\bar{N}}_6 + \hat{S}_1\hat{A}_2\hat{B}_2 + \hat{S}_2\hat{A}_1\hat{B}_1 + \hat{S}_1\hat{S}_2 + \hat{A}_1\hat{A}_2 + \hat{B}_1\hat{B}_2 + [3]_q\,, \tag{3.3.64}$$

with (see Figure 3.17)

$$N_6 = \mathrm{tr}\mathbf{A}\mathbf{B}\mathbf{A}^{-1}\mathbf{B}^{-1} - S_1S_2 - A_1A_2 - B_1B_2\,. \tag{3.3.65}$$

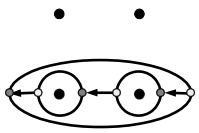

Figure 3.17: *The six-junction network N_6 that appears in the product $N_{AB}\bar{N}_{AB}$.*

Chapter 4

Fock-Goncharov holonomies

We now give an explicit representation of the algebra $\mathcal{A}_{g,n}^N$ in terms of polynomials in the coordinates defined by Fock and Goncharov in their seminal work on higher Teichmüller theory [63]. The holonomy matrices constructed with their methods have some nice positivity properties, which imply that all loop and network functions are given by Laurent polynomials with positive integral coefficients. Relations between generators can then be easily obtained (with the help of Mathematica for higher rank). Thanks to the natural quantisation of the Fock-Goncharov coordinates, these relations can be quantised uniquely. In all examples we have studied perfect agreement is found with the results of skein quantisation presented in the previous chapter. The most non-trivial part of the quantisation concerns the positive integral coefficients in the loop and network polynomials. We will see that they get quantised to positive integral Laurent polynomials in $q^{1/2}$ – as expected from their interpretation as the framed protected spin characters of Gaiotto, Moore, and Neitzke [51]. We give many examples up to $N = 4$ for the surfaces $\mathcal{C}_{0,3}$, $\mathcal{C}_{1,1}$, and $\mathcal{C}_{0,4}$.

4.1 Fock-Goncharov coordinates

Fock and Goncharov defined useful systems of coordinates for $\mathcal{M}_{g,n}^N$ associated with triangulations of $\mathcal{C}_{g,n}$. Provided that $\mathcal{C}_{g,n}$ is a hyperbolic surface with at least one puncture, it can be decomposed into triangles with vertices at the punctures. There are -2χ triangles and -3χ edges in this ideal triangulation. Each ideal triangle can then be further decomposed into N^2 small triangles, which produces a so-called N-triangulation (see Figure 4.1). The Fock-Goncharov coordinates x_α, with $\alpha = 1, \ldots, d$, are associated with the vertices of these small triangles (excluding the punctures of $\mathcal{C}_{g,n}$). There are $(N-1)$ coordinates on each edge, and $\binom{N-1}{2}$ coordinates inside each face, which add up to $d \equiv \dim[\mathcal{M}_{g,n}^N]$ (see appendix A for more details).

The Poisson structure on $\mathcal{M}_{g,n}^N$ can be neatly encoded in a system of oriented arrows on the edges of the small triangles of the N-triangulation (see Figure 4.1 right). The Poisson bracket between two Fock-Goncharov coordinates is given by

$$\{x_\alpha, x_\beta\} = \varepsilon_{\alpha\beta} x_\alpha x_\beta \,, \tag{4.1.1}$$

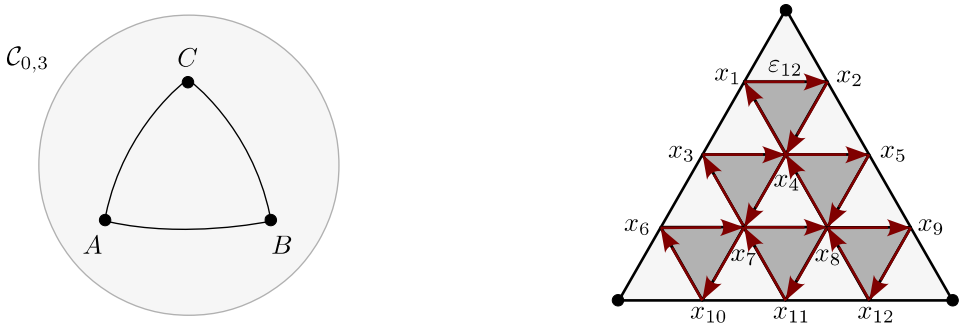

Figure 4.1: Left*: ideal triangulation of the three-punctured sphere $\mathcal{C}_{0,3}$ into two triangles.* Right*: N-triangulation of an ideal triangle into N^2 small black and white triangles (here for $N = 4$). The Poisson structure ε is encoded in the arrows circulating clockwise around the small black triangles.*

with

$$\varepsilon_{\alpha\beta} = \#(\text{arrows from } x_\alpha \text{ to } x_\beta) - \#(\text{arrows from } x_\beta \text{ to } x_\alpha) \quad \in \{0, \pm 1, \pm 2\} \,. \tag{4.1.2}$$

A monomial $x_1^{\mathsf{a}_1} \cdots x_d^{\mathsf{a}_d}$ can be encoded in a vector of exponents $\mathbf{a} = (\mathsf{a}_1, \ldots, \mathsf{a}_d)$, called tropical a-coordinates.[1] The Poisson bracket between two monomials $x_\mathbf{a} \equiv \prod_\alpha x_\alpha^{\mathsf{a}_\alpha}$ and $x_\mathbf{b} \equiv \prod_\alpha x_\alpha^{\mathsf{b}_\alpha}$ is given by

$$\{x_\mathbf{a}, x_\mathbf{b}\} = \sum_{\alpha,\beta} (\mathsf{a}_\alpha \varepsilon_{\alpha\beta} \mathsf{b}_\beta) x_\mathbf{a} x_\mathbf{b} = (\mathbf{a}^{\mathrm{t}} \varepsilon \mathbf{b}) x_\mathbf{a} x_\mathbf{b} = -\sum_\alpha (\mathsf{x}_\alpha \mathsf{b}_\alpha) x_\mathbf{a} x_\mathbf{b} \,. \tag{4.1.3}$$

In the last expression, the combinations $\mathsf{x}_\alpha \equiv \sum_\beta \varepsilon_{\alpha\beta} \mathsf{a}_\beta$ are the tropical x-coordinates of the monomial $x_\mathbf{a}$. Clearly, monomials with $\mathsf{x}_\alpha = 0$ for all α are central elements of the Poisson algebra (we will see below that they correspond to traces of holonomies around the punctures). The moduli space $\mathcal{M}_{g,n}^N$ is a symplectic fibration over the space of central monomials.

4.2 Holonomies

Fock and Goncharov constructed holonomies on the triangulated surface $\mathcal{C}_{g,n}$ using the snake matrices reviewed in appendix A. The general procedure to obtain the holonomy for a curve γ is to choose a curve homotopic to γ on the graph Γ that is dual to the triangulation and multiply the matrices assigned to the corresponding edges and vertices of the dual graph.

More precisely, the dual graph Γ must be fattened and decomposed into rectangles along its edges and hexagons around its vertices (see Figure 4.2). There are three types of segments in the decomposed fat graph: the segments e crossing an edge of the triangulation, the segments s intersecting the dual graph, and the segments v around the vertices of the dual graph. The segments e and v are oriented clockwise around the punctures, while the segments s are not oriented. The matrices $\mathbf{e}, \mathbf{s}, \mathbf{v} \in SL(N, \mathbb{C})$ assigned to the segments e, s, v of the decomposed fat graph are the snake matrices defined in appendix A (normalized to have unit determinant):

$$\mathbf{e}_{x_1} \;=\; H_1(x_1) H_2(x_2) \cdots H_{N-1}(x_{N-1}) \,, \qquad \mathbf{s} = S \,, \qquad \mathbf{v}_x = \mathcal{F} \,. \tag{4.2.4}$$

[1] The a_i are coordinates for the tropicalization of the $\mathcal{A}$-space defined by Fock and Goncharov, which is dual to the $\mathcal{X}$-space parameterized by the x_i. The $\mathcal{A}$-space is isomorphic to the space of laminations on $\mathcal{C}_{g,n}$.

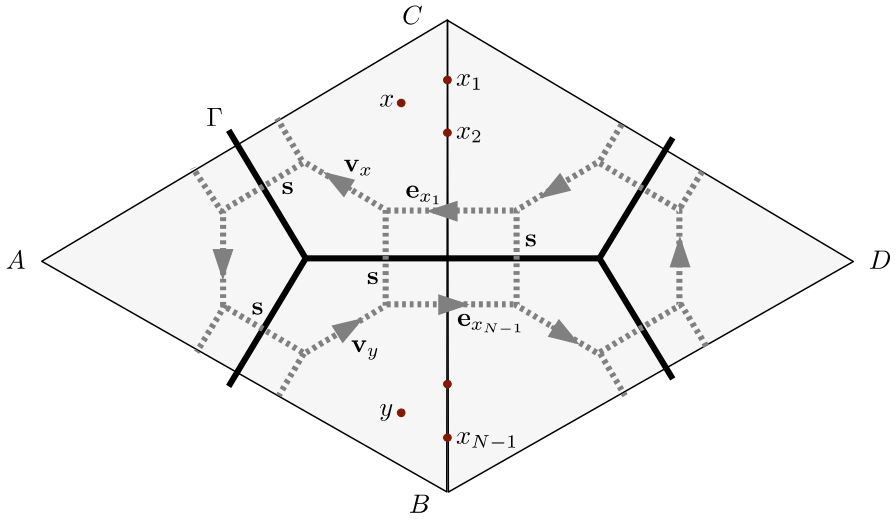

Figure 4.2: *Two triangles in a triangulation and the corresponding dual graph* Γ *(black). The fat dual graph (dashed) is decomposed into rectangles and hexagons, and its segments are associated with matrices* $\mathbf{e}$*,* $\mathbf{s}$*,* $\mathbf{v}$*.*

Here the matrix $\mathbf{e}_{x_1}$ depends on the $(N-1)$ coordinates $x_1, \ldots, x_{N-1}$ along the relevant edge in the triangulation (for conciseness we only indicate the coordinate that is closest to the puncture around which it rotates). Similarly, the matrix $\mathbf{v}_x$ depends on all the coordinates inside the relevant face in the triangulation. For example, for $N = 3$ we have

$$\mathbf{e}_{x_1} = \begin{pmatrix} 1 & 0 & 0 \\ 0 & x_1 & 0 \\ 0 & 0 & x_1 x_2 \end{pmatrix} , \qquad \mathbf{s} = \begin{pmatrix} 0 & 0 & 1 \\ 0 & -1 & 0 \\ 1 & 0 & 0 \end{pmatrix} , \qquad \mathbf{v}_x = \begin{pmatrix} 1 & 0 & 0 \\ 1 & 1 & 0 \\ 1 & 1+x & x \end{pmatrix} . \quad (4.2.5)$$

The holonomy for a path on the fat graph with successive segments $(s_1, s_2, \cdots, s_m)$, where $s_i \in \{e, s, v\}$, is given by the product of the corresponding matrices: $\mathbf{s_m} \cdots \mathbf{s_2 s_1}$. The holonomy around a rectangle or an hexagon is (projectively) equal to the identity:

$$\mathbf{eses} = \mathbf{vsvsvs} = (-1)^{N-1}\mathbf{I} \, . \quad (4.2.6)$$

Note that this sign is consistent with our conventions for the contraction of a fundamental loop in (2.8.40) (in the classical case $q = 1$).

The holonomy for any curve γ on the surface $\mathcal{C}_{g,n}$ is obtained by choosing a curve homotopic to γ on the fat graph and multiplying the corresponding matrices (the properties (4.2.6) ensure that the choice of curve on the graph is irrelevant). Fock and Goncharov showed that the resulting holonomy matrix is conjugate to a matrix whose minors are given by Laurent polynomials with positive integral coefficients (in any coordinate system, that is for any triangulation).[2] It follows that the loop functions A_i that we defined in (2.5.26) as sums of principal minors (invariant under conjugation) will also be given by positive integral Laurent polynomials in the variables $x_\alpha^{1/N}$. We will moreover observe in explicit examples below that the network functions (2.5.29)

[2] In the case of a holonomy for a loop running around a puncture, the resulting matrix is moreover conjugate to a triangular matrix.

also turn out to be positive integral Laurent polynomials, but we did not find an easy derivation of this property from the positivity of the minors.

A loop or network function L will always contain a highest term with unit coefficient, that is a monomial $x_{\mathbf{a}} = \prod_\alpha x_\alpha^{\mathsf{a}_\alpha}$ such that any other monomial $x_{\mathbf{b}} = \prod_\alpha x_\alpha^{\mathsf{b}_\alpha}$ has $\mathsf{b}_\alpha \leq \mathsf{a}_\alpha$ for all α:

$$L = x_1^{\mathsf{a}_1} x_2^{\mathsf{a}_2} \cdots x_d^{\mathsf{a}_d} + \cdots \tag{4.2.7}$$

In contrast, other monomials in L have integral coefficients $\underline{\Omega}$ that can be larger than 1:

$$L = x_{\mathbf{a}} + \underline{\Omega}_{\mathbf{b}} x_{\mathbf{b}} + \underline{\Omega}_{\mathbf{c}} x_{\mathbf{c}} + \cdots \ . \tag{4.2.8}$$

The product of two loop or network functions L and L' can be expanded as

$$LL' = \sum_{L''} c(L, L'; L'') L'' \ . \tag{4.2.9}$$

For $SL(2)$, Fock and Goncharov proved the positivity of the coefficients $c(L, L'; L'')$ by applying the skein relation shown in Figure 2.1 to the intersections between the loops associated with L and L' and by reducing contractible loops as in (2.8.37).[3] Note that the positivity of the $SL(N)$ skein relation (2.4.23) immediately implies that a product of loop or network functions can be written as a finite sum with positive coefficients. However, reduction moves such as those shown in Figure 2.9 can spoil this positivity since they involve negative signs.

4.3 Quantisation

The Fock-Goncharov coordinates admit a natural quantisation. The algebra $\mathcal{A}_{g,n}^N$ of functions on $\mathcal{M}_{g,n}^N$ can be q-deformed into a noncommutative algebra $\mathcal{A}_{g,n}^N(q)$ by promoting the coordinates x_α to operators $\hat{x}_\alpha$ satisfying the relations

$$\hat{x}_\alpha \hat{x}_\beta = q^{\varepsilon_{\alpha\beta}} \hat{x}_\beta \hat{x}_\alpha \ . \tag{4.3.10}$$

It is convenient to work with logarithmic coordinates X_α, defined via $x_\alpha = \exp X_\alpha$, and the corresponding operators $\hat{X}_\alpha$, which satisfy the commutation relation (recall $q = \exp\hbar$)

$$[\hat{X}_\alpha, \hat{X}_\beta] = \hbar \{X_\alpha, X_\beta\} = \hbar \varepsilon_{\alpha\beta} \ . \tag{4.3.11}$$

A monomial in the Fock-Goncharov coordinates can be quantised by first expressing it as an exponential of a sum of logarithmic coordinates, and then promoting them to operators (as in [95] for example):

$$x_{\mathbf{a}} = \prod_{\alpha=1}^n x_\alpha^{\mathsf{a}_\alpha} = \exp \sum_\alpha \mathsf{a}_\alpha X_\alpha \quad \longrightarrow^{q} \quad \hat{x}_{\mathbf{a}} = \exp \sum_\alpha \mathsf{a}_\alpha \hat{X}_\alpha = q^{-\frac{1}{2}\sum_{\alpha<\beta} \mathsf{a}_\alpha \varepsilon_{\alpha\beta} \mathsf{a}_\beta} \prod_\alpha \hat{x}_\alpha^{\mathsf{a}_\alpha} \ , \tag{4.3.12}$$

[3] More precisely, their proof does not apply to the loop functions A_i that we are using, but to their slightly different "canonical maps" $\mathbf{I} = \mathrm{tr}(\mathbf{A}^i)$ from the space of integral $\mathcal{A}$-laminations to the space of positive Laurent polynomials.

where in the last step we used the Baker-Campbell-Hausdorff formula. Similarly, the quantum product of two monomials is given by

$$\begin{aligned}\hat{x}_{\mathbf{a}} * \hat{x}_{\mathbf{b}} &= \exp\sum_{\alpha} \mathsf{a}_\alpha \hat{X}_\alpha * \exp\sum_{\beta} \mathsf{b}_\beta \hat{X}_\beta = \mathsf{e}^{\frac{1}{2}\sum_{\alpha,\beta}[\mathsf{a}_\alpha \hat{X}_\alpha, \mathsf{b}_\beta \hat{X}_\beta]} \exp\sum_{\alpha} (\mathsf{a}_\alpha + \mathsf{b}_\alpha)\hat{X}_\alpha \\ &= q^{\frac{1}{2}\mathbf{a}^{\mathsf{t}}\varepsilon\mathbf{b}} \hat{x}_{\mathbf{a}+\mathbf{b}} \,. \end{aligned} \tag{4.3.13}$$

The loop and network functions that we want to quantise are positive integral Laurent polynomials in the Fock-Goncharov coordinates. The monomials $x_{\mathbf{a}}$ that they involve can simply be quantised as in (4.3.12). It is much less obvious to determine how to quantise the positive integral coefficients $\overline{\Omega}$ of the monomials. Fock and Goncharov conjectured that these quantum coefficients are positive Laurent polynomials in $q^{1/2}$. They also conjectured that the highest term, which has a unit coefficient classically, has a unit coefficient in the quantum operator too. We will make the assumption that all the unit coefficients in a loop or network polynomial remain unit coefficients in the quantised operator (as expected from the interpretation of these coefficients as protected spin characters in [51]). What remains to find is how the non-unit coefficients $\overline{\Omega}$ get quantised:

$$L = x_{\mathbf{a}} + \overline{\Omega}_{\mathbf{b}} x_{\mathbf{b}} + \cdots \qquad \stackrel{q}{\longrightarrow} \qquad \hat{L} = \hat{x}_{\mathbf{a}} + \overline{\Omega}^q_{\mathbf{b}} \hat{x}_{\mathbf{b}} + \cdots \,. \tag{4.3.14}$$

Our strategy is to demand that the classical loop and network functions, which satisfy some relations of the form (4.2.9) (such as (3.1.14) and (3.1.15) for $\mathcal{C}_{0,3}$), get quantised into operators satisfying quantised versions of these relations. This requirement turns out to be powerful enough to determine uniquely the coefficients in expansions of the loop and network generators into monomials of quantised Fock-Goncharov-coordinates. We will illustrate this quantisation procedure in many examples in the following sections.

We first need to determine how the quantised relations look like. The classical relations are typically of the form (4.2.9) and get quantised to

$$\hat{L} * \hat{L}' = \sum_{\hat{L}''} c^q(\hat{L}, \hat{L}'; \hat{L}'') \hat{L}'' \,, \tag{4.3.15}$$

where the $c^q(\hat{L}, \hat{L}'; \hat{L}'')$ are some functions of q. On the left-hand side, the quantum product $\hat{L}\hat{L}'$ generates some powers of q as in (4.3.13). Focusing on the monomials in $\hat{L}$, $\hat{L}'$, and $\hat{L}''$ with unit coefficients, we can then read off the quantum coefficients $c^q(\hat{L}, \hat{L}'; \hat{L}'')$. We will see that they are integral Laurent polynomials in $q^{1/2N}$. The resulting quantum relations agree with the ones that we could obtain from skein quantisation, such as (3.1.18).

We can then determine the quantum coefficients $\overline{\Omega}^q$ by comparing coefficients of monomials with the same exponents on both sides of the quantum relations. We will find that the $\overline{\Omega}^q$ are always finite positive integral Laurent polynomials in $q^{1/2}$ which are invariant under $q \leftrightarrow q^{-1}$. This is in agreement with the positivity conjectures made in [51] for the protected spin characters.

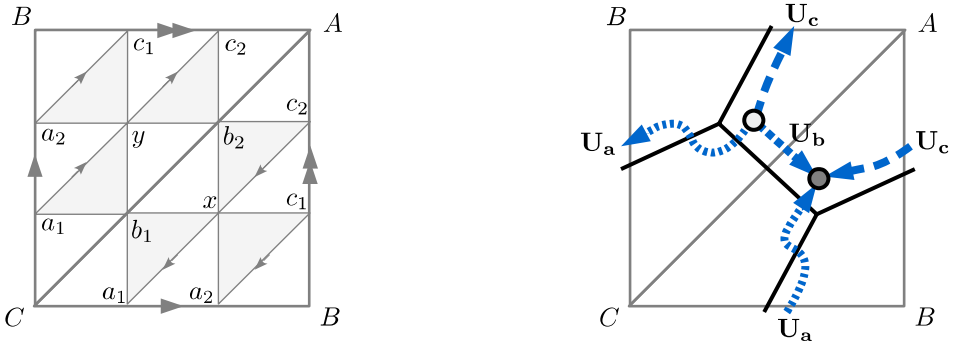

Figure 4.3: Left*: 3-triangulation of the sphere $\mathcal{C}_{0,3}$ with three punctures labeled by A, B, C. The edges carry two coordinates each, a_i, b_i, c_i and the faces one each, x, y.* Right*: The dual graph, and the branches $\mathbf{U_a}, \mathbf{U_b}, \mathbf{U_c}$ projected on the fat graph. The white junction indicates the base point for the loops in $\pi_1(\mathcal{C}_{0,3})$.*

4.4 Pants networks

We come back to the basic example of flat $SL(N,\mathbb{C})$-connections on the pair of pants $\mathcal{C}_{0,3}$. The abstract structure of the algebra of loop and network operators was discussed in Section 3.1.

SL(3)

A 3-triangulation of the pair of pants $\mathcal{C}_{0,3}$ is shown in Figure 4.3 left. We denote the Fock-Goncharov coordinates on the edges of the triangles by a_i, b_i, c_i, with $i = 1, 2$, and on the faces by x, y.

Loop functions: The dual graph consists of three edges $\mathbf{U_a}, \mathbf{U_b}, \mathbf{U_c}$, which we can project on segments of the fat graph to obtain the following holonomy matrices:

$$\mathbf{U_a} \;=\; \mathbf{s}\mathbf{v}_x^{-1}\mathbf{s}\mathbf{e}_{a_2}\mathbf{s}\mathbf{v}_y^{-1}\mathbf{s}\;, \qquad \mathbf{U_b} = \mathbf{e}_{b_2}^{-1}\;, \qquad \mathbf{U_c} = \mathbf{v}_x\mathbf{e}_{c_2}\mathbf{v}_y\;. \tag{4.4.16}$$

The holonomy matrices for the three clockwise loops around the punctures can then be expressed as

$$\mathbf{A} = \mathbf{U_b}^{-1}\mathbf{U_c}\;, \qquad \mathbf{B} = \mathbf{U_c}^{-1}\mathbf{U_a}\;, \qquad \mathbf{C} = \mathbf{U_a}^{-1}\mathbf{U_b}\;, \tag{4.4.17}$$

so that they satisfy the relation $\mathbf{ABC} = \mathbf{I}$ from $\pi_1(\mathcal{C}_{0,3})$. The eigenvalues of these matrices correspond (up to normalizations) to products of coordinates along parallel loops around the punctures in the 3-triangulation (see Figure 4.4 left):

$$\begin{aligned}
\mathbf{A} \;&:\quad (1, \alpha_1, \alpha_1\alpha_2)\;, \qquad \alpha_1 = b_2c_2\;, \quad \alpha_2 = b_1c_1xy\;,\\
\mathbf{B} \;&:\quad (1, \beta_1, \beta_1\beta_2)\;, \qquad \beta_1 = c_1a_2\;, \quad \beta_2 = c_2a_1xy\;,\\
\mathbf{C} \;&:\quad (1, \gamma_1, \gamma_1\gamma_2)\;, \qquad \gamma_1 = a_1b_1\;, \quad \gamma_2 = a_2b_2xy\;.
\end{aligned} \tag{4.4.18}$$

Defining the loop functions $A_1 = \mathrm{tr}\mathbf{A}$ and $A_2 = \mathrm{tr}\mathbf{A}^{-1}$, we can write the compact expression

$$A_i = \prod_j \alpha_j^{-\kappa_{ij}^{-1}}\,(1 + \alpha_i + \alpha_1\alpha_2)\;, \tag{4.4.19}$$

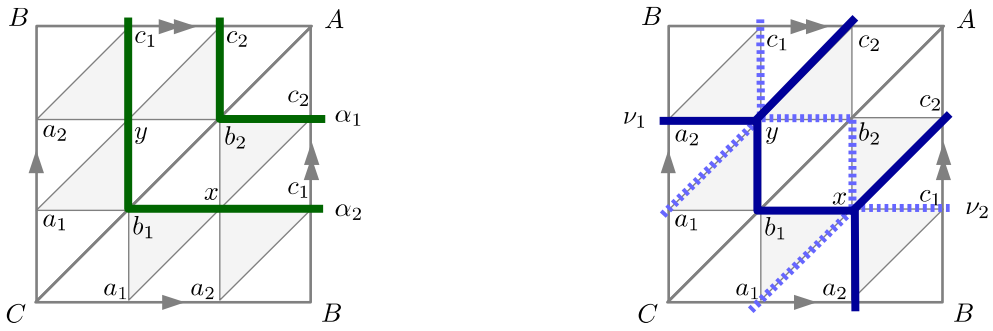

Figure 4.4: Left*: Paths homotopic to the loop around the puncture A on the 3-triangulation of $\mathcal{C}_{0,3}$, which correspond to the monomials $\alpha_1 = b_2c_2$ and $\alpha_2 = b_1c_1xy$.* Right*: Paths homotopic to the network N_1, corresponding to $\nu_1 = a_2b_1c_2xy$ (dark) and $\nu_2 = a_1b_2c_1xy$ (dashed).*

where the normalization factor is determined by the Cartan matrix κ of $SL(3)$:

$$\kappa = \begin{pmatrix} 2 & -1 \\ -1 & 2 \end{pmatrix} , \qquad \kappa^{-1} = \frac{1}{3}\begin{pmatrix} 2 & 1 \\ 1 & 2 \end{pmatrix} . \tag{4.4.20}$$

This simple interpretation of the loop functions comes from the fact that for a path around a puncture the Fock-Goncharov holonomy matrix can be written as a triangular matrix:

$$\mathbf{A} = \prod_j \alpha_j^{-\kappa^{-1}_{1j}} \begin{pmatrix} 1 & 0 & 0 \\ b_2 + \alpha_1 & \alpha_1 & 0 \\ b_1b_2(1 + c_2 + c_2x + c_1c_2x) & b_1\alpha_1(1 + x + c_1x + c_1xy) & \alpha_1\alpha_2 \end{pmatrix} \tag{4.4.21}$$

The normalization factor ensures that $\det \mathbf{A} = 1$. Note that the tropical x-coordinates all vanish for A_i, B_i, C_i, which implies that they are central elements of the Poisson algebra (recall (4.1.3)).

Network functions: We construct the network function N_1 and its reverse $\bar{N}_1$ by fusing the three edges at the two trivalent junctions with ϵ-tensors (see (3.1.5), or alternatively (3.1.6)):

$$\begin{aligned} N_1 &= -\epsilon_{mnp}\mathbf{U}^m_{\mathbf{a}\,r}\mathbf{U}^n_{\mathbf{b}\,s}\mathbf{U}^p_{\mathbf{c}\,t}\epsilon^{rst} , \\ \bar{N}_1 &= -\epsilon_{mnp}(\mathbf{U}^{-1}_{\mathbf{a}})^m_r(\mathbf{U}^{-1}_{\mathbf{b}})^n_s(\mathbf{U}^{-1}_{\mathbf{c}})^p_t\epsilon^{rst} . \end{aligned} \tag{4.4.22}$$

This gives polynomials with 25 terms each. Three of these terms stand out: the highest term, the lowest term, and the middle term (which also happens to be the only term with a non-unit coefficient). They can be written in terms of monomials ν_1 and ν_2 that have a geometric interpretation as paths homotopic to the network on the 3-triangulation (see Figure 4.4 right):

$$\begin{aligned} N_1 &\ni \prod_i \nu_i^{-\kappa^{-1}_{1i}} (1 + 2\nu_1 + \nu_1\nu_2) , \qquad \nu_1 = a_2b_1c_2xy , \\ \bar{N}_1 &\ni \prod_i \nu_i^{-\kappa^{-1}_{2i}} (1 + 2\nu_2 + \nu_1\nu_2) , \qquad \nu_2 = a_1b_2c_1xy . \end{aligned} \tag{4.4.23}$$

The full expression for N_1 is

$$\begin{aligned} N_1 \;=\; \prod_i \nu_i^{-\kappa_{1i}^{-1}} \big(1 + y + a_2 y + b_1 y + c_2 y + a_2 b_1 y + a_2 c_2 y + b_1 c_2 y + a_2 b_1 c_2 y + a_2 b_1 x y \\ + a_2 c_2 x y + b_1 c_2 x y + 2\nu_1 + a_1 a_2 b_1 c_2 x y + a_2 b_1 b_2 c_2 x y + a_2 b_1 c_1 c_2 x y \\ + a_2 b_1 c_2 x^2 y + a_1 a_2 b_1 c_2 x^2 y + a_2 b_1 b_2 c_2 x^2 y + a_1 a_2 b_1 b_2 c_2 x^2 y + a_2 b_1 c_1 c_2 x^2 y \\ + a_1 a_2 b_1 c_1 c_2 x^2 y + a_2 b_1 b_2 c_1 c_2 x^2 y + a_1 a_2 b_1 b_2 c_1 c_2 x^2 y + \nu_1 \nu_2 \big) \,. \end{aligned} \tag{4.4.24}$$

This is consistent with the expression obtained in [96] from products of trace functions (see also [100]). The tropical a-coordinates of N_1 (the exponents of its highest term) and its tropical x-coordinates are given by

$$\mathbf{a}(N_1) \;=\; \frac{1}{3}(2,1,1,2,2,1,3,3) \,, \qquad \mathbf{x}(N_1) = (0,0,0,0,0,0,1,-1) \,. \tag{4.4.25}$$

Poisson brackets: The Poisson bracket for the pants networks is computed by using (4.1.3). The Poisson tensor (4.1.2) can be read off from the 3-triangulation in Figure 4.3, and is given in the basis $\{a_1, a_2, b_1, b_2, c_1, c_2, x, y\}$ by

$$\varepsilon = \begin{pmatrix} 0 & 0 & 0 & 0 & 0 & 0 & -1 & 1 \\ 0 & 0 & 0 & 0 & 0 & 0 & 1 & -1 \\ 0 & 0 & 0 & 0 & 0 & 0 & 1 & -1 \\ 0 & 0 & 0 & 0 & 0 & 0 & -1 & 1 \\ 0 & 0 & 0 & 0 & 0 & 0 & -1 & 1 \\ 0 & 0 & 0 & 0 & 0 & 0 & 1 & -1 \\ 1 & -1 & -1 & 1 & 1 & -1 & 0 & 0 \\ -1 & 1 & 1 & -1 & -1 & 1 & 0 & 0 \end{pmatrix} \tag{4.4.26}$$

This gives the Poisson bracket (3.1.9)

$$\{N_1, \bar{N}_1\} \;=\; -W_1 + \bar{W}_1 \,. \tag{4.4.27}$$

The network functions W_1 and $\bar{W}_1$ have 187 terms each, with the following highest, lowest, and middle terms:

$$\begin{aligned} W_1 \;&\ni\; \prod_j \sigma_j^{-\kappa_{1j}^{-1}} \,(1 + 8\sigma_1 + \sigma_1\sigma_2) \,, \qquad \sigma_1 = a_1 a_2 b_1 b_2 c_1 c_2 y^3 \,, \\ \bar{W}_1 \;&\ni\; \prod_j \sigma_j^{-\kappa_{2j}^{-1}} \,(1 + 8\sigma_2 + \sigma_1\sigma_2) \,, \qquad \sigma_2 = a_1 a_2 b_1 b_2 c_1 c_2 x^3 \,. \end{aligned} \tag{4.4.28}$$

All the Poisson brackets (3.1.11) between the generators $N_1, \bar{N}_1, W_1, \bar{W}_1$ can be easily computed in this way.

Classical relations: It is easy to obtain the polynomial relations between the generators $A_i, B_i, C_i, N_1, \bar{N}_1, W_1, \bar{W}_1$. One useful method is to start with a product, say $N_1\bar{N}_1$, and to look for a combination of generators with the same highest term, in this case $A_1 B_1 C_1$, in order

to cancel it. Then we find that the highest terms in $N_1\bar{N}_1 - A_1B_1C_1$ can be cancelled by W_1 and $\bar{W}_1$. Repeating this procedure a few more times leads to the relation $\mathcal{P}_1$ given in (3.1.14). After implementing this algorithm in Mathematica we can obtain relatively complicated relations such as $\mathcal{P}_2$ given in (3.1.15). In contrast, it would be very laborious to derive this relation purely from applying skein relations, because it would require the resolution of many intersections in the products $W_1\bar{W}_1$, N_1^3, and N_1^2. Of course, the fact that $\mathcal{P}_2$ is a combination of several product expansions of the form (4.2.9) implies that its coefficients can appear somewhat unnatural (this comment applies even more for the quantised relation (3.1.19)).

Quantisation of the relations: We now want to obtain quantum versions of the polynomial relations $\mathcal{P}_1$ and $\mathcal{P}_2$, in which the network functions are replaced by noncommuting operators. Each term in the classical relations can acquire at the quantum level a coefficient that is an arbitrary function of the quantisation parameter $q = \mathrm{e}^{\hbar}$ and that reduces to the classical integral coefficient in the limit $q \to 1$.

The quantum product of polynomials in the Fock-Goncharov coordinates can be obtained by applying the product (4.3.13) to each pair of monomials. For example, the quantum product $\hat{N}_1\hat{\bar{N}}_1$ will produce a certain power of q for each pair of monomials coming from $\hat{N}_1$ and $\hat{\bar{N}}_1$. Let us consider first the highest terms $x_{\mathbf{a}}$ and $x_{\bar{\mathbf{a}}}$ in N_1 and $\bar{N}_1$ with tropical a-coordinates

$$\mathbf{a} \;=\; \frac{1}{3}(2,1,1,2,2,1,3,3)\,, \qquad \bar{\mathbf{a}} = \frac{1}{3}(1,2,2,1,1,2,3,3)\,. \tag{4.4.29}$$

These two monomials Poisson-commute, $\{x_{\mathbf{a}}, x_{\bar{\mathbf{a}}}\} = 0$, which implies that their quantum product does not produce any power of q:

$$\hat{x}_{\mathbf{a}}\hat{x}_{\bar{\mathbf{a}}} \;=\; \hat{x}_{\mathbf{a}+\bar{\mathbf{a}}}\,. \tag{4.4.30}$$

This implies that the corresponding term in $\hat{\mathcal{P}}_1$ with tropical a-coordinate

$$\mathbf{a} + \bar{\mathbf{a}} = (1,1,1,1,1,1,2,2) \tag{4.4.31}$$

must have the same coefficient as $\hat{N}_1\hat{\bar{N}}_1$. This term turns out to be the highest term in $\hat{A}_1\hat{B}_1\hat{C}_1$, and so, by an overall rescaling, we can set the coefficients of $\hat{N}_1\hat{\bar{N}}_1$ and $\hat{A}_1\hat{B}_1\hat{C}_1$ to one in the quantum relation $\hat{\mathcal{P}}_1$. The next highest terms in the relation have tropical a-coordinates $(1,1,1,1,1,1,2,1)$ and $(1,1,1,1,1,1,1,2)$. They correspond respectively to the highest terms of the operators $\hat{W}_1$ and $\hat{\bar{W}}_1$, as well as to two products of monomials in $\hat{N}_1\hat{\bar{N}}_1$ with coefficients $q^{-1/2}$ and $q^{1/2}$. This fixes the quantum coefficients of $\hat{W}_1$ and $\hat{\bar{W}}_1$ in $\hat{\mathcal{P}}_1$.

Repeating this procedure for the next highest terms in the relation allows us to determine all the quantum coefficients, except for the constant term 3 in $\mathcal{P}_1$. We find that it should quantise as $Q_2\bar{Q}_2 - 1$, where Q_2 and $\bar{Q}_2$ are the quantisations of the coefficients of 2 that appear in the expansion of the network operators $\hat{N}_1$ and $\hat{\bar{N}}_1$ (recall (4.4.23)). We will show momentarily that $Q_2 = \bar{Q}_2 = [2]_q$ and thus the 3 should quantise as $[2]_q^2 - 1 = [3]_q$. The quantum relation $\hat{\mathcal{P}}_1$ finally takes the form

$$\hat{N}_1\hat{\bar{N}}_1 = q^{-\frac{1}{2}}\hat{W}_1 + q^{\frac{1}{2}}\hat{\bar{W}}_1 + \hat{A}_1\hat{B}_1\hat{C}_1 + \hat{A}_2\hat{B}_2\hat{C}_2 + \hat{A}_1\hat{A}_2 + \hat{B}_1\hat{B}_2 + \hat{C}_1\hat{C}_2 + [3]_q\,. \tag{4.4.32}$$

Pleasingly, this quantum relation agrees exactly with the result (3.1.18) that we obtained in Section 3.1 by applying the quantum skein relation.

Applying the same procedure (with the help of Mathematica) to the second relation $\mathcal{P}_2$ leads to the quantum relation given in (3.1.19).

Quantisation of the generators: Having quantised the relations, we would now like to quantise the generators themselves, as described in Section 4.3. The generators are polynomials in the Fock-Goncharov coordinates with integer coefficients. The unit coefficients should not be affected by the quantisation, but we need to find how to quantise the non-integral coefficients that appear in front of some monomials. We will see how the quantum relation (3.1.18) can be used to determine these quantum coefficients uniquely.

There is only one term in the expansion for N_1 with a non-unit coefficient, namely the middle term with the factor of 2 in (4.4.23). In the quantum operator $\hat{N}_1$, this coefficient of 2 will be replaced by a function Q_2 of q. We can determine Q_2 by finding a term in the quantum relation that is linear in it. For example, the monomial $1/a_1$ appears in $\hat{N}_1\hat{\bar{N}}_1$ with the coefficient Q_2, and also in $\hat{W}_1$ and $\hat{\bar{W}}_1$ with unit coefficient. Since W_1 and $\bar{W}_1$ appear in the quantum relation (3.1.18) with factors of $q^{1/2}$ and $q^{-1/2}$, we deduce that the coefficient of 2 in N_1 simply becomes a quantum $[2]_q$ in $\hat{N}_1$:

$$2 \in N_1 \quad \xrightarrow{q} \quad Q_2 = q^{\frac{1}{2}} + q^{-\frac{1}{2}} \equiv [2]_q \in \hat{N}_1 \,. \tag{4.4.33}$$

The coefficient of 2 in $\bar{N}_1$ similarly quantises to $\bar{Q}_2 = [2]_q$. So we have (up to normalization)

$$\begin{aligned} N_1 &\ni 1 + 2\nu_1 + \nu_1\nu_2 \quad \xrightarrow{q} \quad \hat{N}_1 \ni 1 + [2]_q\hat{\nu}_1 + \hat{\nu}_1\hat{\nu}_2 \,, \\ \bar{N}_1 &\ni 1 + 2\nu_2 + \nu_1\nu_2 \quad \xrightarrow{q} \quad \hat{N}_1 \ni 1 + [2]_q\hat{\nu}_2 + \hat{\nu}_1\hat{\nu}_2 \,. \end{aligned} \tag{4.4.34}$$

Among the 187 monomials in the network W_1, 24 have a coefficient 2, 4 a 3, 12 a 4, 6 a 5, 2 a 6, and 1 an 8. Let us focus on the monomial $8y/x$ in W_1. In the classical relation $\mathcal{P}_1$ given in (3.1.14), the coefficient of 8 is cancelled by 8 pairs of monomials in $N_1\bar{N}_1$, $x_{\mathbf{a}_i}$ from N_1 and $x_{\bar{\mathbf{a}}_i}$ from $\hat{\bar{N}}_1$, whose products give y/x. For example we have

$$\mathbf{a}_1 \;=\; -\frac{1}{3}(1,2,2,1,1,2,3,0) \,, \qquad \bar{\mathbf{a}}_1 = \frac{1}{3}(1,2,2,1,1,2,0,3) \tag{4.4.35}$$

satisfying $\mathbf{a}_1 + \bar{\mathbf{a}}_1 = (0,0,0,0,0,0,-1,1)$. In the quantum relation, however, the quantum product of the corresponding monomials in $\hat{N}_1\hat{\bar{N}}_1$ produces some power of q as in (4.3.13):

$$\hat{x}_{\mathbf{a}_1}\hat{x}_{\bar{\mathbf{a}}_1} \;=\; q^{\frac{1}{2}\mathbf{a}_1^{\mathrm{t}}\varepsilon\bar{\mathbf{a}}_1}\hat{x}_{\mathbf{a}_1+\bar{\mathbf{a}}_1} = q\hat{x}_{\mathbf{a}_1+\bar{\mathbf{a}}_1} \,. \tag{4.4.36}$$

Summing over the contributions of all such pairs $(\mathbf{a}_i, \bar{\mathbf{a}}_i)$, we obtain the expression for the quantisation of the term $8y/x$ in $\hat{W}_1$ (recall there is a factor of $q^{-1/2}$ in front of $\hat{W}_1$ in the quantum relation (3.1.18)):

$$8 \in W_1 \quad \xrightarrow{q} \quad q^{\frac{1}{2}}\sum_{i=1}^{8} q^{\frac{1}{2}\mathbf{a}_i^{\mathrm{t}}\varepsilon\bar{\mathbf{a}}_i} = q^{\frac{3}{2}} + 3q^{\frac{1}{2}} + 3q^{-\frac{1}{2}} + q^{-\frac{3}{2}} = [2]_q^3 \in \hat{W}_1 \,. \tag{4.4.37}$$

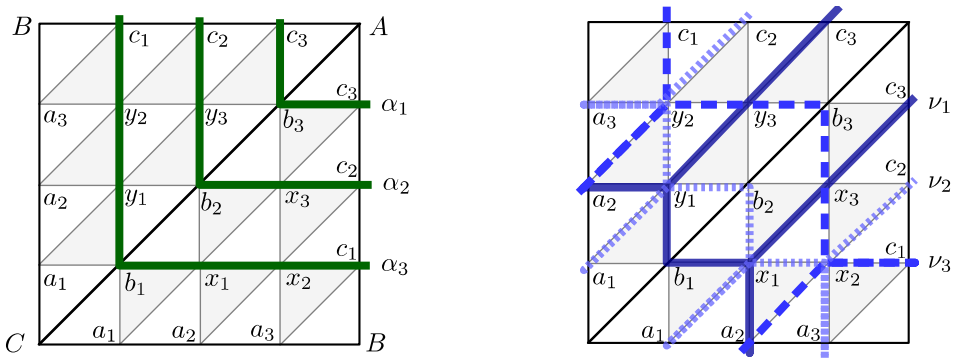

Figure 4.5: *4-triangulation of $\mathcal{C}_{0,3}$.* Left*: The green lines represent the eigenvalues α_i of the holonomy matrix* $\mathbf{A}$ *around the puncture A.* Right*: Paths corresponding to ν_1 (continuous), ν_2 (fine dashed), and ν_3 (dashed) appearing in N_1.*

The quantisation of all the non-unit coefficients in the network operators $\hat{W}_1$ and $\hat{\bar{W}}_1$ can be determined in the same way. We find

$$\begin{aligned} &2 \to q^{\frac{1}{2}} + q^{-\frac{1}{2}} = [2]_q \,, && 8 \to q^{\frac{3}{2}} + 3q^{\frac{1}{2}} + 3q^{-\frac{1}{2}} + q^{-\frac{3}{2}} = [2]_q^3 \,, \\ &3 \to q + 1 + q^{-1} = [3]_q \,, && 4 \to q + 2 + q^{-1} = [3]_q + 1 = [2]_q^2 \,, \\ &5 \to q + 3 + q^{-1} = [3]_q + 2 \,, && 6 \to q + 4 + q^{-1} = [3]_q + 3 \,. \end{aligned} \tag{4.4.38}$$

We see that all the quantised coefficients in the loop and network operators are positive integral Laurent polynomials in $q^{1/2}$, and are also invariant under $q \to q^{-1}$.

This provides further evidence for the positivity conjectures of Gaiotto, Moore, and Neitzke [51] about the framed protected spin characters (1.4.18), which should take the form

$$\underline{\Omega}(L, \gamma; q) = \mathrm{tr}_{\mathcal{H}_L^{\mathrm{BPS}}} q^{J_3} \,, \tag{4.4.39}$$

with J_3 a generator of $so(3)$.

SL(4)

We find a similar structure for $SL(4)$ loop and network operators. For example, the holonomy matrix $\mathbf{A}$ around the puncture A has the following eigenvalues (see Figure 4.5):

$$\begin{aligned} \mathbf{A} \quad : \quad & \prod_i \alpha_i^{-\kappa_{1i}^{-1}} (1, \alpha_1, \alpha_1\alpha_2, \alpha_1\alpha_2\alpha_3) \,, \\ & \alpha_1 = b_3 c_3 \,, \quad \alpha_2 = b_2 c_2 x_3 y_3 \,, \quad \alpha_3 = b_1 c_1 x_1 x_2 y_1 y_2 \,, \end{aligned} \tag{4.4.40}$$

with the $SL(4)$ Cartan matrix

$$\kappa = \begin{pmatrix} 2 & -1 & 0 \\ -1 & 2 & -1 \\ 0 & -1 & 2 \end{pmatrix} \,, \qquad \kappa^{-1} = \frac{1}{4} \begin{pmatrix} 3 & 2 & 1 \\ 2 & 4 & 2 \\ 1 & 2 & 3 \end{pmatrix} \,. \tag{4.4.41}$$

The loop functions A_i can be expressed in terms of the α_i:

$$\begin{aligned} A_1 &= \mathrm{tr}\mathbf{A} = \prod_i \alpha_i^{-\kappa_{1i}^{-1}} (1 + \alpha_1 + \alpha_1\alpha_2 + \alpha_1\alpha_2\alpha_3) \,, \\ A_2 &= \frac{1}{2}\left[(\mathrm{tr}\mathbf{A})^2 - \mathrm{tr}(\mathbf{A}^2)\right] = \prod_i \alpha_i^{-\kappa_{2i}^{-1}} (1 + \alpha_2 + \alpha_1\alpha_2 + \alpha_2\alpha_3 + \alpha_1\alpha_2\alpha_3 + \alpha_1\alpha_2^2\alpha_3) \,, \\ A_3 &= \mathrm{tr}\mathbf{A}^{-1} = \prod_i \alpha_i^{-\kappa_{3i}^{-1}} (1 + \alpha_3 + \alpha_2\alpha_3 + \alpha_1\alpha_2\alpha_3) \,. \end{aligned} \tag{4.4.42}$$

We can construct three pants networks $N_{\mathbf{a}}$, $N_{\mathbf{b}}$, $N_{\mathbf{c}}$ (and their reverses), differing by the choice of the edge that carries the second antisymmetric representation of $SL(4)$ (recall Figure 3.7):

$$\begin{aligned} N_{\mathbf{a}} &= -\frac{1}{2}\epsilon_{mnpq}\mathbf{U}^m_{\mathbf{a}\,r}\mathbf{U}^n_{\mathbf{a}\,s}\mathbf{U}^p_{\mathbf{b}\,t}\mathbf{U}^q_{\mathbf{c}\,u}\epsilon^{rstu} = \mathrm{tr}\mathbf{C}\mathbf{B}^{-1} - C_1B_3 \,, \\ N_{\mathbf{b}} &= -\frac{1}{2}\epsilon_{mnpq}\mathbf{U}^m_{\mathbf{a}\,r}\mathbf{U}^n_{\mathbf{b}\,s}\mathbf{U}^p_{\mathbf{b}\,t}\mathbf{U}^q_{\mathbf{c}\,u}\epsilon^{rstu} = \mathrm{tr}\mathbf{A}\mathbf{C}^{-1} - A_1C_3 \,, \\ N_{\mathbf{c}} &= -\frac{1}{2}\epsilon_{mnpq}\mathbf{U}^m_{\mathbf{a}\,r}\mathbf{U}^n_{\mathbf{b}\,s}\mathbf{U}^p_{\mathbf{c}\,t}\mathbf{U}^q_{\mathbf{c}\,u}\epsilon^{rstu} = \mathrm{tr}\mathbf{B}\mathbf{A}^{-1} - B_1A_3 \,. \end{aligned} \tag{4.4.43}$$

These pants network functions contain 176 terms each, all with unit coefficient apart from 12 that have a coefficient of 2. Some of the terms have an interpretation as paths homotopic to the network (see Figure 4.5), and we can write for example

$$N_{\mathbf{a}} \ni \prod_i \nu_i^{-\kappa_{1i}^{-1}} (1 + 2\nu_1 + 2\nu_1\nu_2 + \nu_1\nu_2\nu_3) \,, \tag{4.4.44}$$

$$\bar{N}_{\mathbf{a}} \ni \prod_i \nu_i^{-\kappa_{3i}^{-1}} (1 + 2\nu_3 + 2\nu_2\nu_3 + \nu_1\nu_2\nu_3) \,, \tag{4.4.45}$$

with $\nu_1 = a_2b_1c_3x_1x_3y_1y_3$, $\nu_2 = a_1a_3b_2c_2x_1x_2y_1y_2$, and $\nu_3 = a_2b_3c_1x_2x_3y_2y_3$.

Quantum relations can be obtained by using the quantum skein relations for $\mathcal{U}_q(\mathfrak{sl}_4)$ (see Figure 3.8). The quantisation of the network operators can then be obtained from these relations. In particular, the 12 coefficients of 2 appearing in each pants operator get quantised to $[2]_q = q^{1/2} + q^{-1/2}$, much in the same way as for $SL(3)$. A more elaborate illustration is provided by the network that appears with a factor of $q^{1/2}$ in the relation for $\hat{N}_a\hat{\bar{N}}_b$ (see Figure 3.8). This network operator contains 2344 terms with a coefficient of 2, 184 with a 3, 815 with a 4, 123 with a 5, 91 with a 6, 115 with an 8, 6 with a 9, 14 with a 10, 8 with a 12, and 4 with a 16. Every coefficient gets quantised in a unique way. Note however that coefficients that are the

same classically can quantise in different ways:

$$
\begin{aligned}
2 &\to q^{\frac{1}{2}} + q^{-\frac{1}{2}} \quad \text{or} \quad 2\,, \\
3 &\to q + 1 + q^{-1} \quad \text{or} \quad 3\,, \\
4 &\to q + 2 + q^{-1} \quad \text{or} \quad 2q^{\frac{1}{2}} + 2q^{-\frac{1}{2}}\,, \\
5 &\to q + 3 + q^{-1}\,, \\
6 &\to q^{\frac{3}{2}} + 2q^{\frac{1}{2}} + 2q^{-\frac{1}{2}} + q^{-\frac{3}{2}} \quad \text{or} \quad 3q^{\frac{1}{2}} + 3q^{-\frac{1}{2}} \quad \text{or} \quad q + 4 + q^{-1}\,, \\
8 &\to 2q + 4 + 2q^{-1} \quad \text{or} \quad q^{\frac{3}{2}} + 3q^{\frac{1}{2}} + 3q^{-\frac{1}{2}} + q^{-\frac{3}{2}}\,, \\
9 &\to 2q + 5 + 2q^{-1}\,, \\
10 &\to q^{\frac{3}{2}} + 4q^{\frac{1}{2}} + 4q^{-\frac{1}{2}} + q^{-\frac{3}{2}}\,, \\
12 &\to q^2 + 3q + 4 + 3q^{-1} + q^{-2} \quad \text{or} \quad 2q^{\frac{3}{2}} + 4q^{\frac{1}{2}} + 4q^{-\frac{1}{2}} + 2q^{-\frac{3}{2}}\,, \\
16 &\to q^2 + 4q + 6 + 4q^{-1} + q^{-2} \quad \text{or} \quad 2q^{\frac{3}{2}} + 6q^{\frac{1}{2}} + 6q^{-\frac{1}{2}} + 2q^{-\frac{3}{2}}\,,
\end{aligned}
\tag{4.4.46}
$$

4.5 One-punctured torus

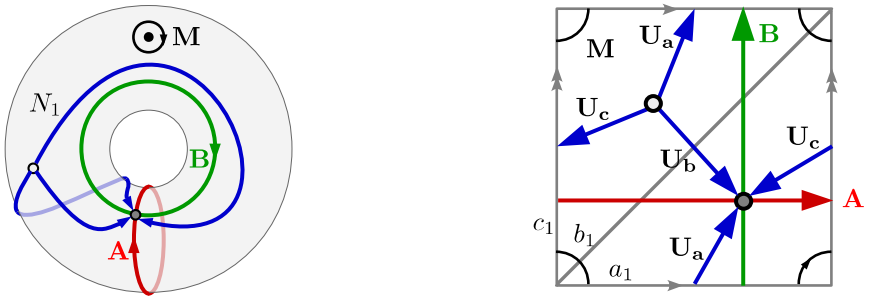

Figure 4.6: Left*: One-punctured torus $\mathcal{C}_{1,1}$. The A- and B-cycles are shown, together with a network operator N_1.* Right*: A triangulation of $\mathcal{C}_{1,1}$ into two triangles. The dual graph consists of the edges $\mathbf{U}_a$, $\mathbf{U}_b$, $\mathbf{U}_c$, and corresponds to the network N_1.*

SL(2)

We start by briefly reviewing the well-studied case of flat $SL(2,\mathbb{C})$-connections on the one-punctured torus $\mathcal{C}_{1,1}$ [51] (see also [95]). A triangulation of $\mathcal{C}_{1,1}$ and its dual graph are shown on the right of Figure 4.6. The three edges of the dual graph can be used to express all the loop and network functions. After projecting the edges on the fat graph, we can express the corresponding holonomy matrices as products of (normalized) snake matrices:

$$
\mathbf{U_a} = \mathbf{s}\mathbf{v}^{-1}\mathbf{s}\mathbf{e}_a\mathbf{v}_y\,, \qquad \mathbf{U_b} = \mathbf{e}_b^{-1}\,, \qquad \mathbf{U_c} = \mathbf{v}\mathbf{e}_c\mathbf{s}\mathbf{v}^{-1}\mathbf{s}\,. \tag{4.5.47}
$$

The holonomy matrices for the A- and B-cycles, and for the clockwise closed loop around the puncture (all based at the black junction in Figure 3.9) are expressed as

$$
\mathbf{A} = \mathbf{U_b}\mathbf{U_c}^{-1}\,, \qquad \mathbf{B} = \mathbf{U_a}\mathbf{U_b}^{-1}\,, \qquad \mathbf{M} = \mathbf{U_b}\mathbf{U_c}^{-1}\mathbf{U_a}\mathbf{U_b}^{-1}\mathbf{U_c}\mathbf{U_a}^{-1}\,. \tag{4.5.48}
$$

In terms of the Fock-Goncharov coordinates a, b, c on the edges of the triangulation, these loop functions are given by

$$A_1 = \sqrt{bc} + \sqrt{\frac{b}{c}} + \frac{1}{\sqrt{bc}}\,, \quad B_1 = \sqrt{ab} + \sqrt{\frac{a}{b}} + \frac{1}{\sqrt{ab}}\,, \quad M_1 = abc + \frac{1}{abc} \tag{4.5.49}$$

These results were already derived by Gaiotto, Moore, and Neitzke [51], who emphasized that they were unexpected from classical reasoning. Indeed, the vev of a Wilson line operator in a representation $\mathcal{R}$ of the gauge group would naively correspond in the IR theory (where the gauge group is broken to its Cartan subgroup) to a sum of vevs of Wilson lines labeled by the weights of $\mathcal{R}$. In the case of A_1 in (4.5.49), these IR Wilson lines correspond to the terms $\sqrt{bc}$ and $1/\sqrt{bc}$. However, extra contributions, such as $\sqrt{b/c}$, come as a surprise. They were attributed to interesting bound states in [51].

The Poisson bracket of A_1 and B_1 can be obtained by direct calculation from (4.1.1) and agrees with (3.2.30):

$$\{A_1, B_1\} = \mathrm{tr}\mathbf{AB} - \frac{1}{2}A_1B_1 = -\mathrm{tr}\mathbf{AB}^{-1} + \frac{1}{2}A_1B_1\,. \tag{4.5.50}$$

The traces $C_1 = \mathrm{tr}\mathbf{AB}$ and $C_1' = \mathrm{tr}\mathbf{AB}^{-1}$ correspond to curves that go once around the A-cycle and once around the B-cycle (in different directions) and take the form

$$C_1 = \sqrt{ca} + \sqrt{\frac{c}{a}} + \frac{1}{\sqrt{ca}}\,, \qquad C_1' = \sqrt{\frac{a}{c}}\left(bc + b + 2 + \frac{1}{b} + \frac{1}{ab}\right)\,. \tag{4.5.51}$$

As explained in Section 4.3, in order to quantise the generators we first write them in terms of logarithmic coordinates A, B, C defined via $a = \mathrm{e}^A$, $b = \mathrm{e}^B$, $c = \mathrm{e}^C$, and then promote these coordinates to operators $\hat{A}, \hat{B}, \hat{C}$ satisfying the commutation relations

$$[\hat{A}, \hat{B}] = [\hat{B}, \hat{C}] = [\hat{C}, \hat{A}] = 2\hbar\,. \tag{4.5.52}$$

For example, the quantised A-cycle operator is given by

$$\hat{A}_1 = \mathrm{e}^{-\frac{1}{2}(\hat{B}+\hat{C})} + \mathrm{e}^{\frac{1}{2}(\hat{B}-\hat{C})} + \mathrm{e}^{\frac{1}{2}(\hat{B}+\hat{C})}\,. \tag{4.5.53}$$

We can explicitly check that the quantum relation (3.2.37) is satisfied by using the quantum product (4.3.13).

A key point is that the loop function C_1' contains a coefficient of 2 in (4.5.51), and it is not clear a priori how to quantise it. However, the quantum relation (3.2.34) imposes that this 2 in C_1' be replaced by the quantum integer $[2]_q = q^{1/2} + q^{-1/2}$ in $\hat{C}_1'$.

SL(3)

A 3-triangulation of $\mathcal{C}_{1,1}$ is shown in Figure 4.7. There are now two Fock-Goncharov coordinates for each edge, a_i, b_i, c_i, with $i = 1, 2$, and one for each triangle, x, y. We express the holonomy matrices corresponding to the three branches of the dual graph as

$$\mathbf{U_a} = \mathbf{s}\mathbf{v}_x^{-1}\mathbf{s}\mathbf{e}_{a_2}\mathbf{v}_y\,, \qquad \mathbf{U_b} = \mathbf{e}_{b_2}^{-1}\,, \qquad \mathbf{U_c} = \mathbf{v}_x\mathbf{e}_{c_2}\mathbf{s}\mathbf{v}_y^{-1}\mathbf{s}\,. \tag{4.5.54}$$

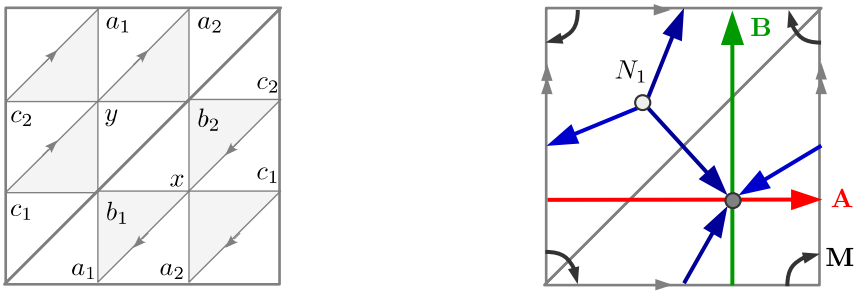

Figure 4.7: Left*: 3-triangulation of $\mathcal{C}_{1,1}$. The edges carry two coordinates each, a_i, b_i, c_i, and the faces one each, x, y.* Right*: the A-cycle (red), the B-cycle (green), the loop around the puncture (black), and the network N_1 corresponding to the dual graph (blue).*

These three branches can be used to construct all the loop and network functions, exactly as in (4.5.48) for the $SL(2)$ case.

The loop functions $M_1 = \mathrm{tr}\mathbf{M}$ and $M_2 = \mathrm{tr}\mathbf{M}^{-1}$ can be expressed compactly as

$$M_i = \prod_j \mu_j^{-\kappa_{ij}^{-1}} (1 + \mu_i + \mu_1\mu_2) \ , \tag{4.5.55}$$

where $\mu_1 = a_1a_2b_1b_2c_1c_2$ and $\mu_2 = a_1a_2b_1b_2c_1c_2x^3y^3$ correspond to products of coordinates along paths surrounding the puncture. The A-cycle functions $A_1 = \mathrm{tr}\mathbf{A}$ and $A_2 = \mathrm{tr}\mathbf{A}^{-1}$ similarly involve the monomials $\alpha_1 = b_1c_1x$ and $\alpha_2 = b_2c_2y$, which are products of coordinates along paths homotopic to the A-cycle (see Figure 4.8):

$$\begin{aligned} A_1 &= \prod_j \alpha_j^{-\kappa_{1j}^{-1}} \left[1 + b_1 + b_1x + b_1b_2x + \alpha_1(1 + b_2 + b_2y + \alpha_2)\right] \ , \\ A_2 &= \prod_j \alpha_j^{-\kappa_{2j}^{-1}} \left[1 + b_2 + b_2y + b_1b_2y + \alpha_2(1 + b_1 + b_1x + \alpha_1)\right] \ . \end{aligned} \tag{4.5.56}$$

Interestingly, the tropical x-coordinates of the terms in A_i involving only the α_i (namely the highest, middle, and lowest terms) reproduce the weight systems of the fundamental and anti-fundamental representations. More specifically, the tropical x-coordinates $(\mathsf{b}_1, \mathsf{b}_2)$ are

$$A_1 \ni \prod_j \alpha_j^{-\kappa_{1j}^{-1}} \begin{cases} \alpha_1\alpha_2 & : \quad (0,1) \\ \alpha_1 & : \quad (1,-1) \\ 1 & : \quad (-1,0) \ , \end{cases} \qquad A_2 \ni \prod_j \alpha_j^{-\kappa_{2j}^{-1}} \begin{cases} \alpha_1\alpha_2 & : \quad (1,0) \\ \alpha_2 & : \quad (-1,1) \\ 1 & : \quad (0,-1) \ . \end{cases} \tag{4.5.57}$$

The B-cycle functions B_i have similar expressions, involving the monomials $\beta_1 = a_1b_1x$ and $\beta_2 = a_2b_2y$. The Poisson bracket between β_i and α_j can be neatly expressed in terms of the Cartan matrix κ (as in [101]):

$$\{\beta_i, \alpha_j\} = \kappa_{ij}\beta_i\alpha_j \ , \qquad \{\beta_i, \beta_j\} = \{\alpha_i, \alpha_j\} = 0 \ . \tag{4.5.58}$$

The network function N_1 and its reverse $\bar{N}_1$ defined as

$$\begin{aligned} N_1 &= \epsilon_{mnp}\mathbf{U}^m_{\mathbf{a}\,r}\mathbf{U}^n_{\mathbf{b}\,s}\mathbf{U}^p_{\mathbf{c}\,t}\epsilon^{rst} \ , \\ \bar{N}_1 &= \epsilon_{mnp}(\mathbf{U}^{-1}_{\mathbf{a}})^m_r(\mathbf{U}^{-1}_{\mathbf{b}})^n_s(\mathbf{U}^{-1}_{\mathbf{c}})^p_t\epsilon^{rst} \end{aligned} \tag{4.5.59}$$

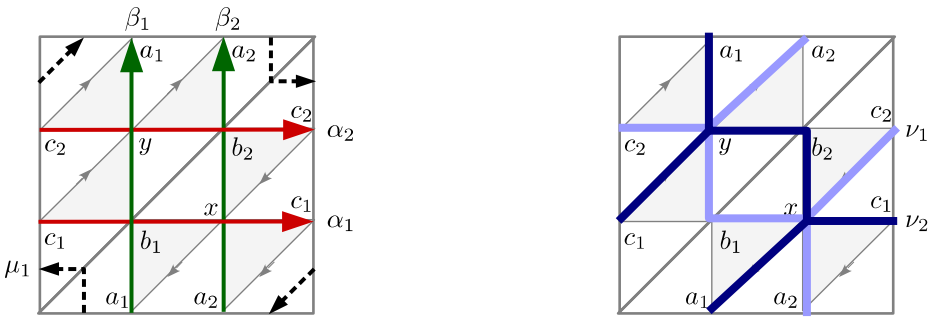

Figure 4.8: Left*: Paths corresponding to the monomials* $\alpha_1 = b_1c_1x$, $\alpha_2 = b_2c_2y$, $\beta_1 = a_1b_1x$, $\beta_2 = a_2b_2y$, *and* $\mu_1 = a_1a_2b_1b_2c_1c_2$. Right*: Paths corresponding to* $\nu_1 = a_2b_1c_2xy$ *and* $\nu_2 = a_1b_2c_1xy$.

contain 28 terms each, only one of which has a non-unit coefficient of 2. The full expression for N_1 is precisely the same as the expression (4.4.24) for the pants network function on $\mathcal{C}_{0,3}$, apart from three extra terms:

$$N_1(\mathcal{C}_{1,1}) = N_1(\mathcal{C}_{0,3}) + \prod_j \nu_j^{-\kappa_{1j}^{-1}} (a_2b_1b_2xy + b_1c_1c_2xy + c_2a_1a_2xy) \ . \tag{4.5.60}$$

The loop functions $C_1' = \mathrm{tr}\mathbf{A}\mathbf{B}^{-1}$ and $C_2' = \mathrm{tr}\mathbf{A}^{-1}\mathbf{B}$ are polynomials with 27 terms, 8 of which have a coefficient of 2.

The quantisation of relations such as (3.2.40) can be obtained by using the quantum product:

$$\begin{aligned} \hat{A}_2\hat{B}_1 &= q^{\frac{1}{6}}\hat{N}_1 + q^{-\frac{1}{3}}\hat{C}_2' \ , \qquad \hat{A}_1\hat{B}_1 = q^{-\frac{1}{6}}\hat{N}_1' + q^{\frac{1}{3}}\hat{C}_2 \ , \\ \hat{A}_1\hat{B}_2 &= q^{\frac{1}{6}}\hat{\bar{N}}_1 + q^{-\frac{1}{3}}\hat{C}_1' \ , \qquad \hat{A}_2\hat{B}_2 = q^{-\frac{1}{6}}\hat{\bar{N}}_1' + q^{\frac{1}{3}}\hat{C}_1 \ . \end{aligned} \tag{4.5.61}$$

Here the network operator $\hat{N}_1'$ corresponds to the flipped dual graph (see Figure 3.12). This agrees with the relations (3.2.41) obtained by applying the quantum skein relation.

In order for these quantum relations to hold, the coefficients of 2 appearing in the classical functions N_1, C_i', and N_1' must be replaced by the quantum integer $[2]_q = q^{1/2} + q^{-1/2}$ in the operators $\hat{N}_1$, $\hat{C}_i'$, and $\hat{N}_1'$.

We can also reproduce the quantum relations (3.2.43):

$$\hat{N}_1\hat{\bar{N}}_1 = q^{-\frac{1}{2}}\hat{W}_6 + q^{\frac{1}{2}}\hat{\bar{W}}_6 + \hat{A}_1\hat{A}_2 + \hat{B}_1\hat{B}_2 + \hat{C}_1\hat{C}_2 + \hat{M}_1 + \hat{M}_2 + [3]_q \ , \tag{4.5.62}$$

where W_6 is a network with six junctions shown in Figure 3.12. The same network W_6 also appears in the product

$$\hat{\bar{N}}_1'\hat{C}_2 = \hat{W}_6 + q^{\frac{1}{2}}\hat{A}_1\hat{A}_2 + q^{-\frac{1}{2}}\hat{B}_1\hat{B}_2 \ . \tag{4.5.63}$$

We can further compute the classical relation (also obtained in [80] and [96])

$$\begin{aligned} A_1A_2B_1B_2C_1C_2 \ = \ & \Big[N_1^3 + N_1^2(A_2B_1 + B_2C_1 + C_2A_1) \\ & + N_1(A_1A_2B_1C_2 + A_1^2C_1 + A_2^2B_2 - 3A_1B_2 + \text{cyclic}) \\ & - (A_1B_2^2C_2^2 - 2A_1^2B_2C_2 + A_1^3 + \text{cyclic}) + \text{reverse}\Big] \\ & - N_1\bar{N}_1(A_1A_2 + \text{cyclic}) - (A_1A_2B_1B_2 + \text{cyclic}) \\ & + 3(A_1B_1C_1 + A_2B_2C_2) + M_1M_2 + 6(M_1 + M_2) + 9 \ . \end{aligned} \tag{4.5.64}$$

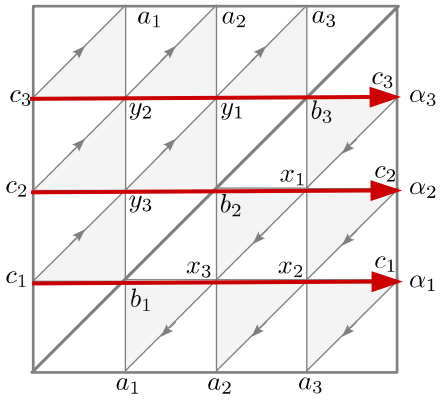

Figure 4.9: *4-triangulation of $\mathcal{C}_{1,1}$. The edges carry three coordinates each, a_i, b_i, c_i, and the faces three each, x_i and y_i. The paths corresponding to the monomials $\alpha_1 = b_1c_1x_2x_3$, $\alpha_2 = b_2c_2x_1y_3$, and $\alpha_3 = b_3c_3y_1y_2$ appearing in the loop functions A_i are indicated.*

Here "+cyclic" means adding the terms obtained by cyclic permutation of A, B, C, and "+reverse" the terms obtained by reversing the orientation, $A_1 \leftrightarrow A_2$, $N_1 \leftrightarrow \bar{N}_1$ and so on. We also computed a quantisation of the relation (4.5.64) in a basis where each monomial is ordered alphabetically and where we need to add terms that vanish in the classical limit $q \to 1$. This is a rather long relation, which is included for completeness at the end of this section.

SL(4)

The 4-triangulation of $\mathcal{C}_{1,1}$ has 15 coordinates, 3 for each edge, a_i, b_i, c_i, and 3 for each face, $\{x_i, y_i\}$, with $i = 1, 2, 3$ (see Figure 4.9). The A-cycle functions A_1 and A_3 have 21 terms each, while A_2 has 56 terms, some of which can be expressed as

$$\begin{aligned} A_1 &\ni \prod_i \alpha_i^{-\kappa_{1i}^{-1}} (1 + \alpha_1 + \alpha_1\alpha_2 + \alpha_1\alpha_2\alpha_3) \,, \\ A_2 &\ni \prod_i \alpha_i^{-\kappa_{2i}^{-1}} (1 + \alpha_2 + \alpha_1\alpha_2 + \alpha_2\alpha_3 + \alpha_1\alpha_2\alpha_3 + \alpha_1\alpha_2^2\alpha_3) \,, \\ A_3 &\ni \prod_i \alpha_i^{-\kappa_{3i}^{-1}} (1 + \alpha_3 + \alpha_2\alpha_3 + \alpha_1\alpha_2\alpha_3) \,, \end{aligned} \tag{4.5.65}$$

with $\alpha_1 = b_1c_1x_2x_3$, $\alpha_2 = b_2c_2x_1y_3$, and $\alpha_3 = b_3c_3y_1y_2$. The tropical x-coordinates $\{\mathsf{b}_1, \mathsf{b}_2, \mathsf{b}_3\}$ of these terms in A_1 and A_3 reproduce the weight systems of the fundamental and anti-fundamental representations (similarly to (4.5.57)), while those in A_2 form the weight system of the second antisymmetric representation:

$$A_2 \ni \prod_i \alpha_i^{-\kappa_{2i}^{-1}} \begin{cases} \alpha_1\alpha_2^2\alpha_3 & : & (0,1,0) \\ \alpha_1\alpha_2\alpha_3 & : & (1,-1,1) \\ \alpha_1\alpha_2, \alpha_2\alpha_3 & : & (-1,0,1), (1,0,-1) \\ \alpha_2 & : & (-1,1,-1) \\ 1 & : & (0,-1,0) \,. \end{cases} \tag{4.5.66}$$

We define three networks homotopic to the dual graph, differing by the choice of the branch that is doubled (their expansions contain 223 monomials each):

$$\begin{aligned} N_a &= \frac{1}{2}\epsilon_{mnpq}\mathbf{U}^m_{\mathbf{a}\,r}\mathbf{U}^n_{\mathbf{a}\,s}\mathbf{U}^p_{\mathbf{b}\,t}\mathbf{U}^q_{\mathbf{c}\,u}\epsilon^{rstu}\,, \\ N_b &= \frac{1}{2}\epsilon_{mnpq}\mathbf{U}^m_{\mathbf{a}\,r}\mathbf{U}^n_{\mathbf{b}\,s}\mathbf{U}^p_{\mathbf{b}\,t}\mathbf{U}^q_{\mathbf{c}\,u}\epsilon^{rstu}\,, \\ N_c &= \frac{1}{2}\epsilon_{mnpq}\mathbf{U}^m_{\mathbf{a}\,r}\mathbf{U}^n_{\mathbf{b}\,s}\mathbf{U}^p_{\mathbf{c}\,t}\mathbf{U}^q_{\mathbf{c}\,u}\epsilon^{rstu}\,. \end{aligned} \tag{4.5.67}$$

The quantum relations in (3.2.51) allow to uniquely determine how all the integral coefficients of 2, 4, and 8 appearing in the Fock-Goncharov expansions of the network functions get quantised:

$$\begin{gathered} 2 \to [2]_q = q^{\frac{1}{2}} + q^{-\frac{1}{2}}\,, \qquad 4 \to [2]^2_q = q + 2 + q^{-1}\,, \\ 8 \to [2]^3_q = q^{\frac{3}{2}} + 3q^{\frac{1}{2}} + 3q^{-\frac{1}{2}} + q^{-\frac{3}{2}}\,. \end{gathered} \tag{4.5.68}$$

Quantisation of the relation (4.5.64)

The quantisation of the $SL(3)$ relation (4.5.64) which involves monomials of length at most six can be performed in a basis where each monomial is ordered alphabetically, as mentioned on the previous page, and the result is:

$$
\begin{aligned}
A_1A_2B_1B_2C_1C_2 = \frac{q-1}{q^{1/3}}\left(A_1^2A_2B_1C_1 - q^{-1}A_2B_1B_2^2C_2 + A_1B_1C_1^2C_2\right)\\
+\Big[q^{-1/2}\hat{N}_1^3 - q^{-2/3}\hat{N}_1^2(A_2B_1+B_2C_1+q^{1/3}A_1C_2) + \text{reverse}\Big]\\
+N_1\Big[q^{-1/6}(A_1A_2B_1C_2+q^{-2/3}A_2B_1B_2C_1+A_1B_2C_1C_2)\\
\quad+q^{-1/6}\Big((q^{-2}-q+1)A_1B_1^2+q^{-5/3}(-1+3q-q^2)A_1^2C_1+B_1C_1^2\Big)\\
\quad+q^{-7/6}((1-q+q^2)A_2^2B_2+B_2^2C_2+q^{1/3}A_2C_2^2)\\
\quad-q^{-7/6}\Big((q^{-3}-2q^{-2}+q+2+q)A_1B_2+(3-q+q^2)B_1C_2\\
\qquad+q^{-5/3}(1-4q+6q^2-2q^3+q^4+q^5)A_2C_1\Big)\Big]\\
+\bar{N}_1\Big[q^{-1/6}(A_1A_2B_2C_1+q^{-2/3}A_1B_1B_2C_2+A_2B_1C_1C_2)\\
\quad+q^{-1/6}\Big((q^{-3}-q^{-2}+1)A_2B_2^2+q^{-2/3}A_2^2C_2+B_2C_2^2\Big)\\
\quad+q^{-7/6}((1-q^2+q^3)A_1^2B_1+B_1^2C_1+q^{1/3}A_1C_1^2)\\
\quad-q^{-7/6}\Big((q^{-2}-2q^{-1}+3+2q-3q^2+3q^3-q^4)A_2B_1+(3-q+q^2)B_2C_1\\
\qquad+q^{-2/3}(-1+3q-q^2+q^3+q^4)A_1C_2\Big)\Big]\\
-q^{-1/3}\Big(A_1B_2^2C_2^2+A_2^2B_1C_2^2+A_2B_1^2C_1^2+A_1^2B_2C_1^2\\
\quad+(q^{-1}-1+q)A_2^2B_2^2C_1+(q^{-1}-1+q)A_1^2B_1^2C_2\Big)\\
+q^{-1/3}\Big((q^{-1}-2+4q-q^2)A_1^2B_2C_2+(q^{-1}+q)A_2B_1^2C_2+(2-q+q^2)A_2B_2C_1^2\\
\quad+(-q^{-2}+4q^{-1}-2+q)A_1B_2^2C_1+(1+q)A_2^2B_1C_1+(2-q+q^2)A_1B_1C_2^2\Big)\\
-\Big((q^{-1}-2+3q-q^2)A_1^3+A_2^3+q^{-2}B_1^3+(-q^{-4}+3q^{-3}-2q^{-2}+q^{-1})B_2^3+C_1^3+C_2^3\Big)\\
-N_1\bar{N}_1(A_1A_2+q^{-2}B_1B_2+C_1C_2)\\
-\Big((q^{-3}-q^{-2}+1-q^2+q^3)A_1A_2B_1B_2+(-q^{-1}+3-q)B_1B_2C_1C_2\\
\quad+(-q^{-3}+3q^{-2}+q^{-1}-4+2q)A_1A_2C_1C_2\Big)\\
+q^{-13/3}\Big((-q+4q^2-3q^3+3q^5-q^7+q^8)A_1B_1C_1\\
\quad+(1-3q+5q^2-5q^3+6q^4-3q^5+q^6+q^7)A_2B_2C_2\Big)\\
+q^{-1}M_1M_2+(q^{-2}+2q^{-1}+2+q)(M_1+M_2)+(q^{-2}+2q^{-1}+3+2q+q^2)\\
+(q^{-5}-3q^{-4}+4q^{-3}-q^{-2}+q^{-1}-2+3q-5q^2+3q^3-q^4)A_1A_2\\
-(q^{-5}-2q^{-4}-q^{-3}+4q^{-2}-2q^{-1}-1+2q-q^2)B_1B_2\\
-(q^{-2}-3q^{-1}+q-q^2+2q^3)C_1C_2\,.
\end{aligned}
$$

4.6 Four-punctured sphere

Another example is a sphere $\mathcal{C}_{0,4}$ with four full punctures, A, B, C, D. It can be triangulated into four triangles, as shown in Figure 4.10.

SL(2)

The loop around the punctures give the following trace functions:

$$\begin{aligned} A_1 &= \sqrt{acf} + \frac{1}{\sqrt{acf}} , \qquad B_1 = \sqrt{bce} + \frac{1}{\sqrt{bce}} , \\ C_1 &= \sqrt{def} + \frac{1}{\sqrt{def}} , \qquad D_1 = \sqrt{abd} + \frac{1}{\sqrt{abd}} . \end{aligned} \tag{4.6.69}$$

We also consider loops surrounding pairs of punctures, $\mathbf{S} = \mathbf{AB}$, $\mathbf{T} = \mathbf{BC}$, and $\mathbf{U} = \mathbf{BD}$ (see [51]):

$$\begin{aligned} S_1 &= \frac{1}{\sqrt{abef}}(1 + a + e + ae + abe + aef + abef) , \\ T_1 &= \frac{1}{\sqrt{bcdf}}(1 + b + f + bf + bcf + bdf + bcdf) , \\ U_1 &= \frac{1}{\sqrt{acde}}(1 + c + d + cd + acd + cde + acde) . \end{aligned} \tag{4.6.70}$$

These polynomials do not contain any non-unit coefficients, so their quantisation is straightforward. In particular, we can reproduce the quantum relation $\hat{\mathcal{P}}_1$ (3.3.58).

The loop function associated with the holonomy $\mathbf{U}' = \mathbf{AC}$ does however contain coefficients of 2 and 4:

$$\begin{aligned} U_1' = \frac{1}{\sqrt{a}b\sqrt{c}\sqrt{d}\sqrt{e}f}(&ab^2cdef^2 + ab^2cef^2 + ab^2cef + ab^2def^2 + ab^2def + ab^2ef^2 \\ &+2ab^2ef + ab^2e + abcef^2 + abcef + abdef^2 + abdef + 2abef^2 \\ &+4abef + 2abe + abf + ab + aef^2 \\ &+2aef + ae + af + a + bef + be + ef + e + 1) . \end{aligned} \tag{4.6.71}$$

The quantisation of these non-unit coefficients can be determined by demanding that the quantum relation (3.3.54) holds. We find that we must make the following replacements:

$$2 \to q^{\frac{1}{2}} + q^{-\frac{1}{2}} , \qquad 4 \to q + 2 + q^{-1} . \tag{4.6.72}$$

SL(3)

A 3-triangulation of $\mathcal{C}_{0,4}$ is shown in Figure 4.10. Each holonomy matrix gives two loop functions, for example

$$A_i = \prod_j \alpha_j^{-\kappa_{ij}^{-1}} (1 + \alpha_i + \alpha_1\alpha_2) , \qquad \alpha_1 = a_2c_1f_2 , \quad \alpha_2 = a_1c_2f_1x_1x_3x_4 . \tag{4.6.73}$$

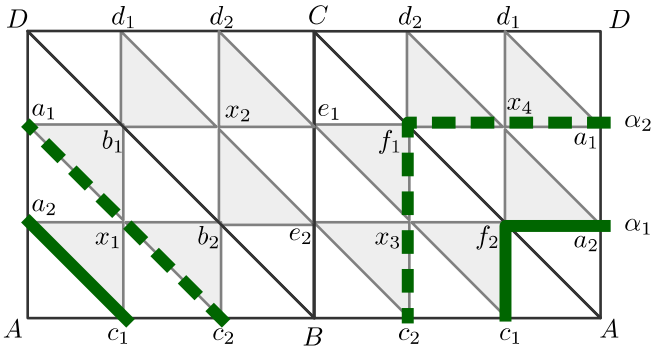

Figure 4.10: 3-*triangulation of* $\mathcal{C}_{0,4}$. *The edges on the left and on the right are glued together. The paths corresponding to the monomials* $\alpha_1 = a_2c_1f_2$ *and* $\alpha_2 = a_1c_2f_1x_1x_3x_4$ *are indicated.*

The monomials α_i are products of coordinates along paths surrounding the puncture on the 3-triangulation (see Figure 4.10). The operators coming from $\mathbf{S}, \mathbf{T}, \mathbf{U}$ have 48 terms each. The operators S_i contain the terms

$$S_i \ni \prod_j \sigma_j^{-\kappa_{ij}^{-1}} (1 + \sigma_i + \sigma_1\sigma_2) \,, \qquad \sigma_1 = a_2b_2e_2f_2x_1x_3 \,, \quad \sigma_2 = a_1b_1e_1f_1x_2x_4 \,. \tag{4.6.74}$$

We can reproduce the quantum relations (3.3.62) and (3.3.64), provided that we quantise the non-unit integer coefficients appearing in the network operators as follows:

$$\begin{aligned} &2 \to q^{\frac{1}{2}} + q^{-\frac{1}{2}} \,, \qquad 3 \to q + 1 + q^{-1}, \qquad 4 \to q + 2 + q^{-1} \,, \\ &5 \to q + 3 + q^{-1} \,, \qquad 6 \to q + 4 + q^{-1} \quad \text{or} \quad q^{\frac{3}{2}} + 2q^{\frac{1}{2}} + 2q^{-\frac{1}{2}} + q^{-\frac{3}{2}} \,, \\ &7 \to q + 5 + q^{-1} \,, \qquad 8 \to q^{\frac{3}{2}} + 3q^{\frac{1}{2}} + 3q^{-\frac{1}{2}} + q^{-\frac{3}{2}} \,, \qquad 10 \to q^{\frac{3}{2}} + 4q^{\frac{1}{2}} + 4q^{-\frac{1}{2}} + q^{-\frac{3}{2}} \,. \end{aligned} \tag{4.6.75}$$

Note that among the 21 coefficients of 6 appearing in N_6, 13 are quantised to $q + 4 + q^{-1}$ and 8 to $q^{3/2} + 2q^{1/2} + 2q^{-1/2} + q^{-3/2}$.

Chapter 5

First conclusions

Thus far we have studied the algebras $\mathcal{A}_{\text{flat}} \equiv \mathcal{A}^N_{g,n}$ of functions on moduli spaces of flat $SL(N,\mathbb{C})$-connections $\mathcal{M}^N_{g,n}$ on punctured Riemann surfaces $\mathcal{C}_{g,n}$, both at the classical and quantum levels, for the three basic cases $\mathcal{C}_{0,3}$, $\mathcal{C}_{1,1}$ and $\mathcal{C}_{0,4}$. More general surfaces with arbitrary genus and number of punctures may be constructed by gluing these essential building blocks. The algebras of functions corresponding to these basic blocks were described in terms of generators and relations, where the sets of generating functions comprised loop and network operators which have nice locality properties with respect to a pair of pants decomposition of the surface $\mathcal{C}_{g,n}$. We have furthermore identified maximal sets of commuting functions that parametrise half of the reduced moduli space $\bar{\mathcal{M}}^N_{g,n}$, which has fixed conjugacy classes for the holonomies around the punctures and which therefore exhibits the key features of an integrable Hamiltonian system.

In order to quantise the algebras $\mathcal{A}_{\text{flat}}$, we have used two independent methods: the skein quantisation based on the Reshetikhin-Turaev construction of knot invariants and the quantisation obtained in the explicit parametrisation provided by Fock-Goncharov coordinates. Reassuringly, the results obtained coincide in all of the cases.

The parametrisation through Fock-Goncharov coordinates has moreover allowed us to find many examples for higher rank theories of class $\mathcal{S}$ of framed protected spin characters, which were discussed in Section 1.4. The study of such counting tools represents an interesting application of the Fock-Goncharov coordinates which is of independent interest, as mentioned in Section 1.5.

Having determined a description of the algebra of functions $\mathcal{A}_{\text{flat}}$ on the moduli space $\mathcal{M}^N_{g,n}$, we would like to remind the reader that the arguments of Section 1.4 identified this with the algebra $\mathcal{A}_{\mathfrak{X}}$ of supersymmetric line operators in theories $\mathfrak{X}(\mathcal{C}_{g,n}, \mathfrak{sl}_N)$ of class $\mathcal{S}$. Part III of this thesis will now look at relations between quantised moduli spaces of flat connections on Riemann surfaces and $\mathfrak{sl}_N$ Toda conformal field theories. It will in particular construct a proof that the quantised algebras $\mathcal{A}_{\text{flat}}$ are isomorphic to the algebras $\mathcal{A}_V$ of Verlinde operators acting on spaces of conformal blocks which are associated to $\mathcal{C}_{g,n}$. This isomorphism will then constitute evidence to support a higher rank generalisation of the AGT correspondence, which was outlined at the beginning of Section 1.5 as one of the focal points of this thesis.

Appendices

Appendix A

Fock-Goncharov coordinates

In [63], Fock and Goncharov constructed coordinates systems on the moduli space of flat connections over a punctured surface $\mathcal{C}_{g,n}$. They assume that the surface is hyperbolic, that is $\chi(\mathcal{C}_{g,n}) = 2-2g-n < 0$, and has at least one puncture, $n \geq 1$. Their approach consists in "localizing" flat connections on the triangles of an ideal triangulation of $\mathcal{C}_{g,n}$ (in which the vertices of the triangles are at punctures). However, since a triangle is contractible, any flat connection on it is trivial. This difficulty can be overcome by considering *framed* flat connections, which means adding on each puncture a flag that is invariant under the holonomy around the puncture.

A.1 Coordinates associated with N-triangulations

Let us review how to build coordinates on the moduli space of framed flat connections over a punctured surface $\mathcal{C}_{g,n}$ (We mostly follow section 4 in [101], and appendix A in [52]). Given an $\mathfrak{sl}_N$-vector bundle with a framed flat connection over $\mathcal{C}_{g,n}$, each triangle of an ideal triangulation of $\mathcal{C}_{g,n}$ gives rise to a (generic) configuration of three flags $\{A, B, C\}$ associated with the vertices. A flag A in an N-dimensional complex vector space V_N is a collection of nested subspaces

$$A: \qquad 0 = A_0 \subset A_1 \subset A_2 \subset \cdots \subset A_N = V_N \ , \tag{A.1.1}$$

with $\dim[A_a] = a$. An N-triangulation consists in a further decomposition of each triangle into small triangles, whose vertices are at the $\binom{N+2}{2}$ lattice points p_{abc} with

$$a+b+c = N \ , \qquad a, b, c \in \mathbb{Z}_{\geq 0} \ . \tag{A.1.2}$$

See Figure A.1 for an example with $N = 3$.

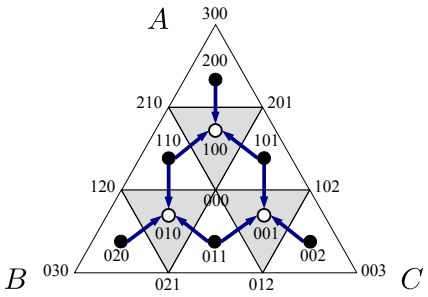

Figure A.1: *N-triangulation of a triangle (here for $N = 3$). The triples of non-negative integers a, b, c sum to 3 on lattice points p_{abc}, to 2 on white triangles associated with lines l_{abc} (black dots), and to 1 on black triangles associated with planes P_{abc} (white dots). The internal lattice point is associated with the 3-space V_{000}. Arrows between dots indicate incidence relations.*

There are N^2 small triangles for each ideal triangle, $\binom{N+1}{2}$ of which are "upright" (white) and labeled by the solutions of $a+b+c = N-1$, while $\binom{N}{2}$ are "upside-down" (black) and labeled by the solutions of $a + b + c = N - 2$. To every white triangle we associate a line l_{abc} in V_N arising as the intersection of the corresponding subspaces of the flags $\{A, B, C\}$. More explicitly, writing $A^a \equiv A_{N-a}$ with $\text{codim}[A^a] = a$, we have

$$l_{abc} = A^a \cap B^b \cap C^c \,, \qquad a + b + c = N - 1 \,. \tag{A.1.3}$$

Similarly, we associate to every black triangle a plane P_{abc}, and to every internal lattice point with $a + b + c = N - 3$ a 3-space V_{abc}:

$$P_{abc} = A^a \cap B^b \cap C^c \,, \qquad a + b + c = N - 2 \,, V_{abc} = A^a \cap B^b \cap C^c \,, \qquad a + b + c = N - 3 \,.$$

The plane P_{abc} on a black triangle contains all three lines $l_{(a+1)bc}$, $l_{a(b+1)c}$, and $l_{ab(c+1)}$ on the adjacent white triangles. In turn, the 3-space V_{abc} on an internal lattice point contains all three planes on the surrounding black triangles, and thus all six lines on the surrounding white triangles.

This collection of subspaces on the N-triangulation allows us to associate coordinates to every lattice point (excluding the vertices at the punctures). We can define coordinates x_{abc} associated with the internal lattice points p_{abc} with $a + b + c = N - 3$ as the triple-ratio of the six surrounding lines contained in V_{abc} (the neighborhood of an internal lattice point looks like the 3-triangulation shown in Figure A.1). The 3-space V_{abc} contains the three flags

$$\begin{aligned} \tilde{A}: &\quad 0 \subset l_{(a+2)bc} \subset P_{(a+1)bc} \subset V_{abc} \,, \\ \tilde{B}: &\quad 0 \subset l_{a(b+2)c} \subset P_{a(b+1)c} \subset V_{abc} \,, \\ \tilde{C}: &\quad 0 \subset l_{ab(c+2)} \subset P_{ab(c+1)} \subset V_{abc} \,. \end{aligned} \tag{A.1.4}$$

Fixing the flags to be $\tilde{A} = (\mathbf{a_1}, \mathbf{a_1} \wedge \mathbf{a_2})$, with $\mathbf{a_i}$ vectors in V_{abc}, we can write the triple-ratio as

$$x_{abc} = \frac{\langle \mathbf{a_1} \wedge \mathbf{a_2} \wedge \mathbf{b_1} \rangle \langle \mathbf{b_1} \wedge \mathbf{b_2} \wedge \mathbf{c_1} \rangle \langle \mathbf{c_1} \wedge \mathbf{c_2} \wedge \mathbf{a_1} \rangle}{\langle \mathbf{a_1} \wedge \mathbf{a_2} \wedge \mathbf{c_1} \rangle \langle \mathbf{b_1} \wedge \mathbf{b_2} \wedge \mathbf{a_1} \rangle \langle \mathbf{c_1} \wedge \mathbf{c_2} \wedge \mathbf{b_1} \rangle} \,. \tag{A.1.5}$$

Here the notation $\langle \mathbf{v_1} \wedge \mathbf{v_2} \wedge \mathbf{v_3} \rangle$ means the determinant of the matrix expressing the vectors $\mathbf{v_1}, \mathbf{v_2}, \mathbf{v_3}$ in a unimodular basis for the 3-space containing them (this triple-ratio is the inverse of the one originally defined by Fock and Goncharov, see appendix A in [52]).

It remains to define coordinates for the lattice points on the edges of the ideal triangulation. Along the common edge of two glued N-triangulated triangles, adjacent white triangles are associated with the same lines, and adjacent black triangles to the same planes (see Figure A.2).

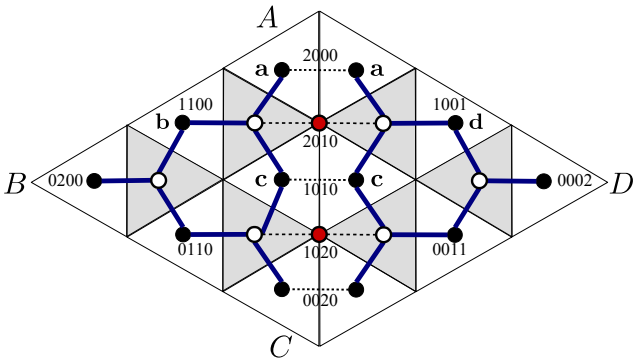

Figure A.2: *Two 3-triangulated triangles ABC and ACD glued along the edge AC. The quadruples of non-negative integers a, b, c, d sum to 3 on lattice points p_{abcd}, and to 2 on white triangles associated with lines l_{abcd}. Lines and planes adjacent across the edge are identical. Each edge point is surrounded by four lines.*

A lattice point on an edge is thus surrounded by four lines, which allows us to define a cross-ratio coordinate. For example, at the point p_{2010} on Figure A.2, we choose four vectors $\mathbf{a} \in l_{2000}$, $\mathbf{b} \in l_{1100}$, $\mathbf{c} \in l_{1010}$, $\mathbf{d} \in l_{1001}$, all contained in the plane P_{1000}, which give the cross-ratio

$$x_{2010} = \frac{\langle \mathbf{a} \wedge \mathbf{b} \rangle \langle \mathbf{c} \wedge \mathbf{d} \rangle}{\langle \mathbf{a} \wedge \mathbf{d} \rangle \langle \mathbf{b} \wedge \mathbf{c} \rangle} \,. \tag{A.1.6}$$

An ideal triangulation of the surface $\mathcal{C}_{g,n}$ has $-2\chi(\mathcal{C}_{g,n})$ triangles and $-3\chi(\mathcal{C}_{g,n})$ edges. There are $\binom{N-1}{2}$ internal lattice points in each triangle and $N-1$ lattice points on each edge, so the total number of independent coordinates provided by triple-ratios and cross-ratios is

$$\#\{x\text{-coordinates}\} = -\chi(\mathcal{C}_{g,n}) \dim[SL(N,\mathbb{C})] \,. \tag{A.1.7}$$

This agrees with the dimension (2.1.4) of the moduli space of flat $SL(N,\mathbb{C})$-connections on $\mathcal{C}_{g,n}$.

A.2 Snakes and projective bases

Fock and Goncharov showed how to construct projective bases in the N-dimensional vector space V_N related to three flags A, B, C at the vertices of a triangle. Each basis is represented by a *snake*, that is an oriented path on the edges of the $(N-1)$-triangulation from one vertex to the opposite side (see Figure A.3 for an example).

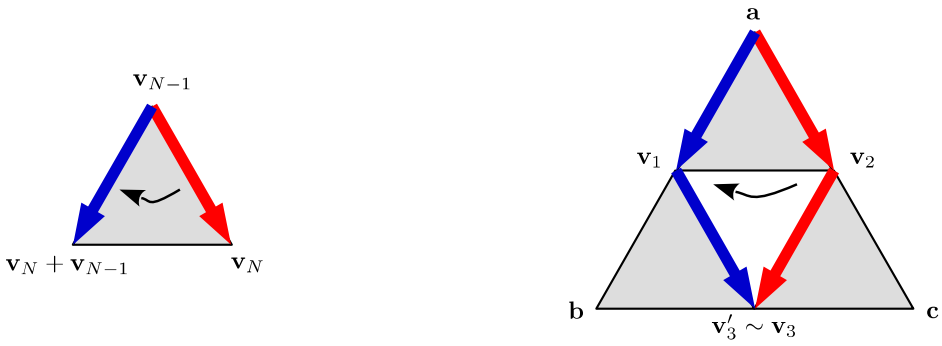

Figure A.5: *Elementary moves for segments of a snake.* Left*: Move I can only occur on the last segment of a snake.* Right*: Move II can occur on any two consecutive segments of a snake.*

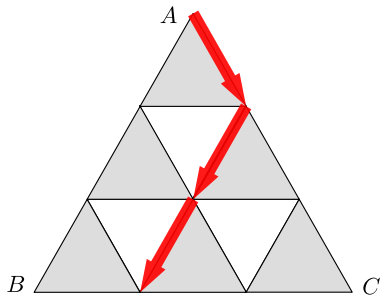

Figure A.3: *Example of a snake on the* $(N-1)$*-triangulation of a triangle (here for* $N = 4$*).*

Notice that in the $(N-1)$-triangulation the vertices correspond to lines, and the upright (black) triangles to planes. Each segment of the snake goes from a line l_1 to a line l_2, and the plane they define also contains a third line l_3 at the third vertex of the black triangles. Given a vector $\mathbf{v}_1 \in l_1$, a vector $\mathbf{v}_2 \in l_2$ is determined by the rule that $\mathbf{v}_2 + \mathbf{v}_1 \in l_3$ if the segment is oriented clockwise around the black triangle, and $\mathbf{v}_2 - \mathbf{v}_1 \in l_3$ if it is oriented counterclockwise (see Figure A.4).

Figure A.4: *Segment of a snake along an edge of a black triangle in an* $(N-1)$*-triangulation. The vertices of the triangles correspond to 3 coplanar lines* l_1, l_2, l_3*. Picking a vector* $\mathbf{v}_1 \in l_1$ *at the start of the segment determines* $\mathbf{v}_2 \in l_2$ *by the rule that* $\mathbf{v}_2 \pm \mathbf{v}_1 \in l_3$ *depending on whether the segment is oriented clockwise or counterclockwise around the triangle.*

To construct the projective basis $\{\mathbf{v}_1, \mathbf{v}_2, \cdots, \mathbf{v}_N\}$ defined by a snake, we can choose any vector $\mathbf{v_1}$ at the first vertex of the snake and use this rule to determine all the subsequent vectors.

A projective basis can be transformed into another one by a sequence of simple moves. The moves I and II shown in Figure A.5 can be expressed in terms of two types of elementary

$GL(N)$ matrices. Let $\varphi_i : SL(2) \to GL(N)$ be the canonical embedding corresponding to the i^{th} root $\lambda_i - \lambda_{i+1}$. Then the two types of elementary matrices can be written as

$$F_i = \varphi_i \begin{pmatrix} 1 & 0 \\ 1 & 1 \end{pmatrix} , \qquad H_i(x) = \text{diag}(\underbrace{1, \cdots, 1}_{i \text{ times}}, x, \cdots, x) . \tag{A.2.8}$$

For example, for $N = 3$ we have the following elementary matrices:

$$F_1 = \begin{pmatrix} 1 & 0 & 0 \\ 1 & 1 & 0 \\ 0 & 0 & 1 \end{pmatrix} , \quad F_2 = \begin{pmatrix} 1 & 0 & 0 \\ 0 & 1 & 0 \\ 0 & 1 & 1 \end{pmatrix} ,$$
$$H_1(x) = \begin{pmatrix} 1 & 0 & 0 \\ 0 & x & 0 \\ 0 & 0 & x \end{pmatrix} , \quad H_2(x) = \begin{pmatrix} 1 & 0 & 0 \\ 0 & 1 & 0 \\ 0 & 0 & x \end{pmatrix} . \tag{A.2.9}$$

Note that F_i and $H_j(x)$ commute unless $i = j$.

Move I flips the last segment of a snake across a black triangle, which according to the rule in Figure A.4 transforms the projective basis as

$$\begin{pmatrix} \mathbf{v}_1 \\ \vdots \\ \mathbf{v}_{N-1} \\ \mathbf{v}_N \end{pmatrix} \mapsto \begin{pmatrix} \mathbf{v}_1 \\ \vdots \\ \mathbf{v}_{N-1} \\ \mathbf{v}_N + \mathbf{v}_{N-1} \end{pmatrix} = F_{N-1} \begin{pmatrix} \mathbf{v}_1 \\ \vdots \\ \mathbf{v}_{N-1} \\ \mathbf{v}_N \end{pmatrix} . \tag{A.2.10}$$

Move II takes any two consecutive segments of a snake across a pair of adjacent black and white triangles, see Figure A.5. For a choice of vector $\mathbf{a}$ at their first common vertex, the initial and final snakes define two vectors $\mathbf{v}_3$ and $\mathbf{v}'_3$ spanning the line at the vertex where the snakes meet again. The proportionality function is precisely the coordinate x_{abc} for the internal lattice point associated with the white triangle

$$\mathbf{v}'_3 = x_{abc} \mathbf{v}_3 . \tag{A.2.11}$$

This can be checked by writing down the triple-ratio (A.1.5) for the choice of flags $A = (\mathbf{a}, \mathbf{v}_1)$, $B = (\mathbf{b}, \mathbf{v}_3)$, $C = (\mathbf{c}, \mathbf{v}_2)$ and using the relations provided by the black triangles as in Figure A.4 (that is $\mathbf{v}_1 = \mathbf{v}_2 + \mathbf{a}$, $\mathbf{b} = \mathbf{v}'_3 + \mathbf{v}_1$, $\mathbf{c} = \mathbf{v}_3 - \mathbf{v}_2$). The transformation between the bases associated with the two snakes in Figure A.5 acts as

$$\begin{pmatrix} \mathbf{a} \\ \mathbf{v}_2 \\ \mathbf{v}_3 \end{pmatrix} \mapsto \begin{pmatrix} \mathbf{a} \\ \mathbf{v}_1 \\ \mathbf{v}'_3 \end{pmatrix} = F_1 H_2(x_{abc}) \begin{pmatrix} \mathbf{a} \\ \mathbf{v}_2 \\ \mathbf{v}_3 \end{pmatrix} . \tag{A.2.12}$$

More generally, we can see that moving the i^{th} segment of snake across a black triangle corresponds to acting with a matrix F_i, while moving it across a white triangle corresponds to acting with a matrix $H_i(x)$, where x is the face coordinate associated with the white triangle. An important snake transformation consists in moving a snake from one edge of a triangle across the entire face to the next edge, rotating clockwise around the initial vertex (see Figure A.6).

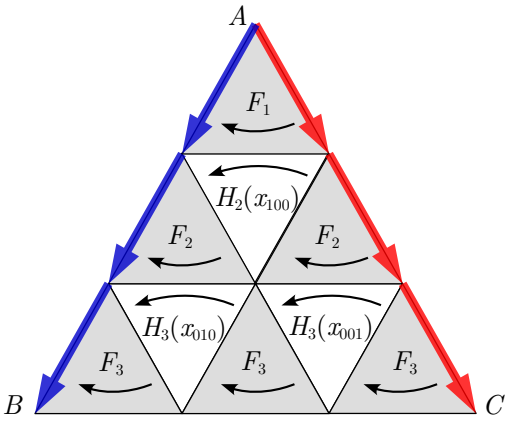

Figure A.6: *Elementary matrices F_i and $H_i(x)$ in an $(N-1)$-triangulation (here for $N=4$). The transformation $\mathcal{F}$ from the snake along the edge AC to the snake along AB can be decomposed into a sequence of moves across the black and white triangles, corresponding to matrices F_i and $H_i(x)$.*

For $N=2$ this gives simply $\mathcal{F}=F_1$. For $N=3$, this gives

$$\mathcal{F}=F_2F_1H_2(x_{000})F_2=\begin{pmatrix}1 & 0 & 0\\ 1 & 1 & 0\\ 1 & 1+x_{000} & x_{000}\end{pmatrix}. \tag{A.2.13}$$

For $N=4$ as in Figure A.6 this gives

$$\mathcal{F}=F_3F_2H_3(x_{010})F_3F_1H_2(x_{100})F_2H_3(x_{001})F_3\,. \tag{A.2.14}$$

Another type of move is the reversal of the orientation of a snake along an edge of a triangle, see Figure A.7.

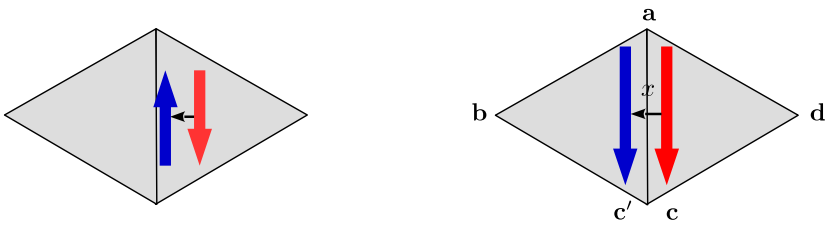

Figure A.7: Left*: reversal of the orientation of the snake along an edge of a triangle.* Right*: snake crossing an edge of a triangle with a cross-ratio coordinate x.*

This reverses the order of the basis vectors, and changes the sign of every even-numbered vector, thus multiplying by an anti-diagonal matrix

$$S=\begin{pmatrix}\cdots & 0 & 0 & 1\\ \cdots & 0 & -1 & 0\\ \cdots & 1 & 0 & 0\\ \iddots & \vdots & \vdots & \vdots\end{pmatrix}. \tag{A.2.15}$$

Finally, we can move a snake from one triangle to another across their common edge. If the coordinates along the edge followed by the snake are $\{x_1, x_2, \ldots, x_{N-1}\}$ (in this order), this transformation acts as

$$H_1(x_1)H_2(x_2)\cdots H_{N-1}(x_{N-1}) = \text{diag}(1, x_1, x_1x_2, \ldots, x_1x_2\cdots x_{N-1})\ . \qquad \text{(A.2.16)}$$

This can again be checked by writing down the cross-ratio (A.1.6) for the edge coordinate x in Figure A.7 and using the relations provided by the black triangles as in Figure A.4.

Part III

Toda conformal blocks, moduli spaces of flat connections and quantum groups

Introduction

The third part of this thesis investigates the relations between Toda conformal field theories, the quantisation of moduli spaces of flat connections and quantum group theory. As outlined at the end of Part I, one of the main goals in this thesis is to bring evidence supporting a higher rank generalisation of the AGT correspondence, in particular relating non-Lagrangian theories $\mathfrak{X}(\mathcal{C}_{g,n}, \mathfrak{sl}_N)$ of class $\mathcal{S}$ to $\mathfrak{sl}_N$ Toda field theories. The approach taken to achieve this aim studies algebras of operators on the two sides of the correspondence, whose isomorphism for rank one theories was argued [54] to imply the AGT relations between instanton partition functions for $\mathfrak{X}(\mathcal{C}_{g,n}, \mathfrak{sl}_2)$ and conformal blocks of Liouville CFT, discussed in Section 1.2. In Part II we have studied the non-commutative algebra $\mathcal{A}_{\mathfrak{X}}$ of supersymmetric line operators in theories $\mathfrak{X}(\mathcal{C}_{g,n}, \mathfrak{sl}_N)$ indirectly, making use of the identification between $\mathcal{A}_{\mathfrak{X}}$ and the quantised algebra of functions on moduli spaces of flat connections $\mathcal{A}_{\text{flat}}$ (see Section 1.4) and explicitly describing the latter in terms of generators and relations. We will now demonstrate that $\mathcal{A}_{\text{flat}}$ is isomorphic to the algebra of Verlinde operators which act on conformal blocks of $\mathfrak{sl}_N$ of Toda CFT, which can then be seen as support for a generalisation of the AGT correspondence.

One of our aims will thus be to establish a precise relation between conformal blocks in Toda CFT and specific states in the space of states obtained by quantising the moduli spaces of flat connections on Riemann surfaces $\mathcal{C}$. The use of pants decompositions reduces the problem to the basic case $\mathcal{C} = \mathcal{C}_{0,3}$. Some guidance is provided by the paradigm well-studied in the case of rational conformal field theories summarised in Table 5.1.

Conformal field theory	Quantum group theory	Moduli of flat connections
Invariants in tensor products of $\mathcal{W}$-algebra representations (conformal blocks)	Invariants in tensor products of quantum group representations	Spaces of states

Table 5.1: *Comparison of modular functors from conformal field theory, quantum group theory (Reshetikhin-Turaev construction) and quantisation of the moduli spaces of flat connections on Riemann surfaces.*

However, the Toda CFTs of interest in this context are not expected to be rational and we will therefore need a non-rational analog of the set of relations indicated in Table 5.1 generalising the situation encountered in the case of Liouville theory (see [54] and references therein). The experiences made in this case suggest that a very useful role will be played in the non-rational cases by the Verlinde line operators, a natural family of operators V_γ on the spaces of conformal

blocks labelled by closed curves γ on the Riemann surface $\mathcal{C}$. The relevant spaces of conformal blocks can be abstractly characterised as modules for the algebra $\mathcal{A}_V$ of Verlinde line operators [54]. This means that these spaces of conformal blocks have a natural scalar product making the Verlinde line operators self-adjoint. Natural representations of $\mathcal{A}_V$ diagonalise maximal commutative sub-algebras of $\mathcal{A}_V$ and such sub-algebras of $\mathcal{A}_V$ are labelled by pair of pants decompositions. Different pants decompositions give different representations of $\mathcal{A}_V$ intertwined by unitary operators representing the fusion, braiding and modular transformations.

A key step towards understanding the relation between conformal field theory and the quantum theory of flat connections is therefore to establish the isomorphism between the algebra of Verlinde line operators $\mathcal{A}_V$ and the algebra of quantised functions on the corresponding moduli spaces of flat connections. In the case of Liouville theory this was established in [54] using the explicit computations of Verlinde line operators performed in [56], [57]. As discussed in [54] one finds that the Verlinde line operators generate a representation of the quantised algebra $\mathcal{A}_{\text{flat}}$ of functions on $\mathcal{M}_{\text{flat}}^{PSL(2,\mathbb{R})}$. The generator of $\mathcal{A}_{\text{flat}}$ corresponding to the Verlinde line operator V_γ is the quantised counterpart L_γ of a trace function on $\mathcal{M}_{\text{flat}}^{PSL(2,\mathbb{R})}$. The situation is schematically summarised in Table 5.2.

We investigate in Part III of this thesis the relations between representations of $\mathcal{A}_{\text{flat}}$ and the algebra of Verlinde line operators in the case of $\mathfrak{sl}_N$ Toda CFT, following [77]. In doing so we define Verlinde network operators, which are natural generalizations of Verlinde line operators [56], [57] acting on spaces of Toda conformal blocks, and show that the algebra $\mathcal{A}_{\text{V}}$ that they generate can be identified with the quantised algebra $\mathcal{A}_{\text{flat}}$.

An important feature of the representations associated to pants decompositions is the fact that the Verlinde line operators, in the case of $\mathfrak{sl}_2$ Toda (which is Liouville), get expressed in terms of a set of more basic operators representing quantised counterparts of certain coordinates on $\mathcal{M}_{\text{flat}}^{PSL(2,\mathbb{R})}$, which are close relatives of the Fenchel-Nielsen coordinates for the Teichmüller spaces [54]. [1] The relevance of such coordinates has previously been emphasised in a related context in [70]. The distinguished role of these coordinates in our context is explained by the fact that they have two important features: (i) they represent the algebraic structure of the moduli spaces of flat connections in the simplest possible way, and (ii) they are compatible with pants decompositions.

The free field representation of the $\mathcal{W}_N$ algebra of symmetry of $\mathfrak{sl}_N$ Toda CFT allows us to define convenient bases for spaces of conformal blocks. Further developing known connections between free field representations of conformal field theories and quantum group theory, we will relate the spaces of conformal blocks to spaces of intertwining maps between tensor products of quantum group representations to irreducible representations. This reduces the computation of monodromies to a quantum group problem. The monodromy transformations get represented in terms of operator-valued matrices with matrix elements represented as finite-difference operators acting on the multiplicity labels for bases of conformal blocks. Our explicit computations

[1] In Part II of this thesis, an important role in the study of $\mathcal{A}_{\text{flat}}$ was played by Fock-Goncharov coordinates on the moduli space of flat connections $\mathcal{M}_{\text{flat}}$ [63], which are coordinates associated to triangulations of the Riemann surface $\mathcal{C}_{g,n}$. From the point of view of conformal field theory, it turns out that Fenchel-Nielsen coordinates are nicer, being associated to pair of pants decompositions of $\mathcal{C}_{g,n}$.

	Conformal field theory	Moduli of flat connections on $\mathcal{C}$
Algebra	$\mathcal{A}_V$ of Verlinde line operators	Quantised algebra $\mathcal{A}_{\text{flat}}$ of functions on $\mathcal{M}_{\text{flat}}^{SL(2)}(\mathcal{C})$
Generators	Verlinde line operators V_γ	Quantised trace functions L_γ
Module	Spaces of conformal blocks	Spaces of states

Table 5.2: *The vector spaces listed in the row at the bottom can be abstractly characterised as modules of isomorphic algebras $\mathcal{A}_{flat} \simeq \mathcal{A}_V$.*

then allow us to identify basic building blocks for the operator-valued monodromies, which can be identified with (quantised) coordinates for moduli spaces of flat connections generalising the Fenchel-Nielsen coordinates mentioned above.

It should be noted that coordinates for $\mathcal{M}_{\text{flat}}^{PSL(3,\mathbb{R})}$ satisfying the conditions (i), (ii) characterising coordinates of Fenchel-Nielsen type have been previously introduced in [102], [103]. A systematic geometric approach to the definition of higher rank analogs of the Fenchel-Nielsen coordinates was proposed in [104], [105] and it would be very interesting to understand the relation between the coordinates defined in these references and the ones presented here.

As a final observation, let us also note that some of the braid matrices that enter monodromy transformations in Toda CFT have been calculated in [24], [35], [72]. However, in all these cases the two representations associated to the punctures involved in the braiding operations are degenerate or semi-degenerate. These correspond to four dimensional $\mathcal{N} = 2$ field theories $\mathfrak{X}(\mathcal{C}, \mathfrak{g})$ which have a Lagrangian description.

Contents Part III

We summarise below the contents of the chapters which form Part III of this thesis.

Chapter 6 introduces the relevant background[2] from conformal field theory. It explains how to use conformal blocks with degenerate field insertions to define operator-valued analogs of monodromy matrices and construct Verlinde line operators with these, summarising some of the main results which lead to the isomorphism $\mathcal{A}_{\text{flat}} \simeq \mathcal{A}_V$. Chapter 7 then collects the definitions and notations concerning the quantum group $\mathcal{U}_q(\mathfrak{sl}_N)$ relevant for our goals. A construction of conformal blocks for the $\mathcal{W}_3$ algebra using the free field representation is introduced in Chapter 8. It is explained how this construction relates bases for the spaces of conformal blocks on $\mathcal{C}_{0,3}$ to bases in the space of Clebsch-Gordan maps for the quantum group $\mathcal{U}_q(\mathfrak{sl}_3)$. The connection to quantum group theory provided by the free field representation is then used in Chapter 9 to calculate basic cases of the monodromies of degenerate fields around generic chiral vertex operators in $\mathfrak{sl}_3$ Toda CFT.

We then define Verlinde network operators which are natural generalisations of Verlinde line operators in Chapter 10 and use the monodromy matrices of Chapter 9, together existing results for the braiding of degenerate chiral vertex operators in $\mathfrak{sl}_N$ Toda CFT, to show that the

[2] A somewhat different approach leading to important results is described in [106] and references therein.

algebra of Verlinde network operators $\mathcal{A}_V$ is equivalent to the quantum skein algebra described in Section 2.8.[3] To see this, we will first observe that the braid matrices in Toda field theory, from which Verlinde network operators are constructed, are related by a twist to the standard R-matrix of the quantum group $\mathcal{U}_q(\mathfrak{sl}_N)$. In turn, this R-matrix is used to construct the quantum skein algebra defining the quantised algebra $\mathcal{A}_{\text{flat}}$.

Having demonstrated the isomorphism $\mathcal{A}_{\text{flat}} \simeq \mathcal{A}_V$, the identification $\mathcal{A}_{\text{flat}} \simeq \mathcal{A}_{\mathfrak{X}}$ from Section 1.4 in Part I completes the set of relations $\mathcal{A}_{\mathfrak{X}} \simeq \mathcal{A}_{\text{flat}} \simeq \mathcal{A}_V$, which we may regard as support for a higher-rank AGT correspondence, one of the main goals outlined for this thesis in Section 1.5. Following the proof of this isomorphism on the level of operator algebras, we will make a few further observations in Chapter 11 comparing the spectra of operators generating the algebra $\mathcal{A}_V$ in Toda field theory and $\mathcal{A}_{\text{flat}}$ in the quantum theory of moduli spaces of flat connections, respectively.

Chapter 12 will then further use the results of the monodromy computation in Chapter 9 in order to relate the basic building blocks of the operator valued monodromy matrices to coordinates of Fenchel-Nielsen type on the moduli spaces of flat $SL(3)$-connections. There exist two different limits in Toda CFT corresponding to a classical limit for $\mathcal{A}_V$, $b \to 0$ and $b \to i$, which both yield a deformation parameter $q^2 = e^{-2\pi \mathrm{i} b^2}$ equal to 1. We point out relations to the Yang's function for the Hitchin system, and to the isomonodromic tau-function for holomorphic $SL(3)$-connections on $\mathcal{C}_{0,3}$ arising in the two limits, respectively.

To conclude, in Chapter 13 we discuss the extension of our results to continuous families of conformal blocks, which is expected to be relevant for a full understanding of Toda CFT. The appendices collect some useful relations relevant to the quantum groups calculations and provide more detail for the technical points that occur in the conformal field theory calculations. Part III of this thesis largely reproduces Sections 5-6 of [77] and combines these with [107].

[3] To avoid potential notational confusion, let us observe here that $\mathcal{A}_{\text{flat}}$ and $\mathcal{A}^N_{g,n}(q)$ in Section 2.8 are both used to denote the same quantised algebras. The former notation is generic, while the latter is better suited when discussing examples with specific rank or Riemann surfaces $\mathcal{C}_{g,n}$.

Chapter 6

Relation to conformal field theory

This chapter contains the essential background for $\mathfrak{sl}_N$ Toda conformal field theory necessary to outline the main results in Part III of this thesis. It briefly explains the construction of conformal blocks with degenerate field insertions, how this is used to define quantum monodromy matrices and how these enter the construction of Verlinde line operators. The combination of these results allows to state the algebra isomorphism $\mathcal{A}_{\text{flat}} \simeq \mathcal{A}_V$ between quantised algebras of functions on moduli spaces of flat connections and algebras of Verlinde operators on spaces of conformal blocks, for which a proof will be presented in Chapter 10.

6.1 Toda conformal field theory and $\mathcal{W}_N$-algebra

The Lagrangian which defines $\mathfrak{sl}_N$ Toda conformal field theory is

$$\mathcal{L} = \frac{1}{8\pi}(\partial_a\phi, \partial^a\phi) + \mu \sum_{i=1}^{N-1} \mathrm{e}^{b(e_i,\phi)} \,, \tag{6.1.1}$$

where $\phi = (\phi_1, \ldots, \phi_{N-1})$ is a two dimensional scalar field and the parameters are the dimensionless coupling constant b and the scale parameter μ. $(\cdot,\cdot)$ denotes here the scalar product in $\mathbb{R}^{N-1}$.

Lie algebra conventions: The vectors e_i with $i = 1, \ldots, N-1$ are the simple roots of the Lie algebra $\mathfrak{sl}_N$ and their scalar product on the Cartan subalgebra of $\mathfrak{sl}_N$ is the Cartan matrix given by $\kappa_{ij} = (e_i, e_j)$. It is often useful to represent the root/weight subspace of $\mathfrak{sl}_N$ as a hyperplane in $\mathbb{R}^N$, allowing us to represent the simple roots as $e_i = u_i - u_{i+1}$ with u_i a unit vector of $\mathbb{R}^N$. The simple roots are dual to the fundamental weights ω_i in the sense that $(e_i, \omega_j) = \delta_{ij}$. In general they can be written as $\omega_i = \sum_{j=1}^{i} u_j - \frac{i}{N}\sum_{k=1}^{N} u_k$. Their inner product is given by the inverse Cartan matrix $(\omega_i, \omega_j) = \kappa_{ij}^{-1}$ and their sum is the Weyl vector $\rho_W = \sum_i \omega_i$. The weights of the fundamental representation of $\mathfrak{sl}_N$ with highest weight ω_1 are $h_i = \omega_1 - \sum_{j=1}^{i-1} e_j$, with $i = 1, \ldots, N$ and $(h_i, h_j) = \delta_{ij} - \frac{1}{N}$.

Chiral algebra $\mathcal{W}_N$ and its free field construction

The example of Liouville theory corresponding to the case $N = 2$ [16], [17] suggests that we should to be able to construct the Toda field $\phi(z, \bar{z})$ using the chiral free fields $\varphi_j(z)$, for $j = 1, \ldots, N-1$, with mode expansion

$$\varphi_j(z) = q_j - \mathrm{i}p_j \ln z + \sum_{n \neq 0} \frac{\mathrm{i}}{n} a_n^j z^{-n} , \tag{6.1.2}$$

where the modes satisfy the commutation relations

$$[a_n^i, a_m^j] = n\delta_{ij}\delta_{n+m} , \qquad [p_j, q_k] = -\mathrm{i}\delta_{jk} \tag{6.1.3}$$

and $a_n^{i\dagger} = a_{-n}^i$. In order to build the non-chiral fields $\phi_i(z, \bar{z})$ out of the chiral free fields $\varphi_j(z)$ one must supplement them with a similar collection of anti-chiral fields $\bar{\varphi}_j(\bar{z})$.

The chiral symmetry algebra of $\mathfrak{sl}_N$ Toda conformal field theory is a $\mathcal{W}_N$-algebra. It is an associative algebra generated by holomorphic currents $W_d(z)$ of spin $d = 2, \ldots, N$ (see [108] for a review). These can be constructed in the free-field representation through a deformed version of the Miura transformations

$$: \prod_{i=0}^{N-1} (Q\partial + (h_{N-i}, \partial\varphi(z))) : = \sum_{k=0}^{N} W_{N-k}(z)(Q\partial)^k , \tag{6.1.4}$$

where : : denotes Wick ordering. The holomorphic currents of spins 0 and 1 are $W_0(z) = 1$, $W_1(z) = 0$, while the currents $W_d(z)$ with $d = 2, \ldots, N$, have mode expansions

$$W_d(z) = \sum_{n=-\infty}^{\infty} W_{d,n} z^{-n-d} . \tag{6.1.5}$$

The chiral algebra $\mathcal{W}_N$ defined in this way is the chiral symmetry algebra of Toda CFT if the parameter Q in equation (6.1.4) is related to the parameter b in the Lagrangian (6.1.1) through $Q = b + b^{-1}$. The modes $L_n \equiv W_{2,n}$ of the stress energy tensor

$$T(z) \equiv W_2(z) = (Q\rho, \partial^2\varphi) - \frac{1}{2}(\partial\varphi, \partial\varphi) \tag{6.1.6}$$

generate a Virasoro subalgebra within $\mathcal{W}_N$

$$[L_n, L_m] = (n-m)L_{n+m} + \frac{c}{12}(n^3 - n)\delta_{n+m} \tag{6.1.7}$$

with central charge

$$c = (N-1)(1 + N(N+1)Q^2) .$$

The modes of the currents $W_d(z)$ satisfy nonlinear commutation relations which contain a quadratic term and therefore the $\mathcal{W}_N$-algebra is not a Lie algebra.

In the following sections, wherever we restrict discussion to the case $N = 3$ corresponding to $\mathfrak{sl}_3$ Toda theory we will use the simplified notations

$$T(y) \equiv W_2(y) = \sum_{n \in \mathbb{Z}} y^{-n-2} L_n , \qquad W(y) = W_3(y) = \sum_{n \in \mathbb{Z}} y^{-n-3} W_n . \tag{6.1.8}$$

Representations: Irreducible representations $\mathcal{V}_\alpha$ of the $\mathcal{W}_N$-algebra are labeled by an $(N-1)$-component vector α in the Cartan subalgebra of $\mathfrak{sl}_N$. The representations $\mathcal{V}_\alpha$ are generated from highest-weight vectors $\mathfrak{e}_\alpha$ which are annihilated by the positive modes of $W_d(z)$ and which are eigenvectors of $W_{d,0}$ with eigenvalues determined by α

$$W_{d,n}\mathfrak{e}_\alpha = 0\,, \quad n>0, \qquad W_{d,0}\mathfrak{e}_\alpha = w_d(\alpha)\mathfrak{e}_\alpha\,, \qquad d=2,\dots,N, \tag{6.1.9}$$

where $w_d(\alpha)$ are polynomials of α of degree d, with

$$w_2(\alpha) = \frac{1}{2}(2Q\rho_W - \alpha, \alpha) \tag{6.1.10}$$

being the conformal dimension. The representation space of $\mathcal{V}_\alpha$ is generated by acting on $\mathfrak{e}_\alpha$ with the modes $W_{d,-n}$ for $n>0$, as usual.

The space of states of the Toda CFTs will then be of the form $\mathcal{H} = \int_{\mathbb{S}} d\alpha\, \mathcal{V}_\alpha \otimes \bar{\mathcal{V}}_\alpha$, where $\bar{\mathcal{V}}_\alpha$ is a representation for the algebra $\mathcal{W}_N$ generated by the anti-holomorphic currents $\bar{W}_d(\bar{z})$. The set of labels $\mathbb{S}$ for the representations appearing in $\mathcal{H}$ is expected to be the set of vectors α of the form $\alpha = \mathcal{Q} + i\mathfrak{p}$, $\mathfrak{p}\in\mathbb{R}^2$, $\mathcal{Q} = \rho_W(b+b^{-1})$.

6.2 Conformal blocks

Conformal blocks can be introduced elegantly as certain invariants in the tensor product of representations of $\mathcal{W}_N$-algebras associated with Riemann surfaces $\mathcal{C}_{g,n}$. The definition will be given explicitly only for the case $C_{0,n} = \mathbb{P}^1 \setminus \{z_1,\dots z_n\}$, as the solutions to the Ward identities expressing the $\mathcal{W}$-algebra symmetry of $\mathfrak{sl}_N$ Toda CFT under the $\mathcal{W}_N$-algebra. The formulation is to a large extent analogous to the one presented in [109] for the case of the Virasoro algebra. More general cases are discussed in [110]. We shall associate a highest-weight representation $\mathcal{V}_r \equiv \mathcal{V}_{\alpha_r}$ of the $\mathcal{W}_N$-algebra with the r^{th} puncture z_r of $\mathcal{C}_{0,n}$ for $r=1,\dots,n$ and define the tensor product $\mathcal{R} = \bigotimes_{i=1}^n \mathcal{V}_{\alpha_i}$. Conformal blocks can then be defined as linear functionals[1]

$$f_{0,n} : \mathcal{R} \to \mathbb{C} \tag{6.2.11}$$

satisfying an invariance condition of the form

$$f_{0,n}\big(W_d[\eta_d]\cdot v\big) = 0\,, \qquad \forall\ v\in\mathcal{R}\,,\ \ \forall\ d=2,\dots N\,, \tag{6.2.12}$$

where $W_d[\eta_d]$ is defined for holomorphic $(1-d)$-differentials $\eta_d = \eta_d(y)(dy)^{1-d}$ on $\mathcal{C}_{0,n}$, for $d=2,\dots,N$, by introducing the coefficients of the Laurent expansion of η_d around z_r through

$$\eta_d(y) = \sum_{k\in\mathbb{Z}} \eta_{d,k}^{(r)}\,(y-z_r)^{d+k-1} \tag{6.2.13}$$

and setting

$$W_d[\eta_d] = \sum_{r=1}^n \sum_{k\in\mathbb{Z}} \eta_{d,k}^{(r)}\, W_{d,k}(z_r)\,, \tag{6.2.14}$$

[1] This is the definition often given in the mathematical literature. The relation to the conformal Ward identities is discussed for the case $N=2$ for example in [109].

with $W_{d,k}(z_r)$ acting only on the r-th tensor factor of $\mathcal{R}$ associated to the puncture z_r,

$$W_{d,k}(z_r) \;=\; \mathrm{id}\otimes\cdots\otimes\mathrm{id}\otimes\underset{\text{r-th}}{W_{d,k}}\otimes\mathrm{id}\otimes\cdots\otimes\mathrm{id}\;. \tag{6.2.15}$$

The conditions (6.2.12) generalize the conformal Ward identities [111]. The subscript label for the conformal blocks will generally be omitted, as this will be clear from context.

We will often find it convenient to assume that $z_n = \infty$ which does not restrict the generality in any serious way. By using a part of the defining invariance conditions (6.2.12) one may reduce the computation of the linear functionals $f(v)$, $v \in \mathcal{R}$, to the special values

$$g_f(v_\infty) = f(\mathfrak{e}_1 \otimes \cdots \otimes \mathfrak{e}_{n-1} \otimes v_\infty), \qquad v_\infty \in \mathcal{V}_{\alpha_n}. \tag{6.2.16}$$

There is a one-to-one correspondence between functionals $f : \mathcal{R} \to \mathbb{C}$ satisfying (6.2.12), and functionals $g : \mathcal{V}_{\alpha_n} \to \mathbb{C}$ satisfying a reduced system of invariance conditions following from (6.2.12). We will therefore also call such functionals g conformal blocks.

Space of conformal blocks: The invariance conditions (6.2.12) represent an infinite system of linear equations defining a subspace $\mathrm{CB}(\mathcal{C}_{0,n}, \mathcal{R})$ of the dual $\mathcal{R}'$ to the vector space $\mathcal{R}$. The vector space defined in this way is called the space of conformal blocks $\mathrm{CB}(\mathcal{C}_{0,n}, \mathcal{R})$ associated with the Riemann surface $\mathcal{C}_{0,n}$ with representations $\mathcal{V}_i$ at the punctures. This space is infinite-dimensional, in general. We now want to get a first idea about the "size" of this space.

In the case $N = 2$, the conformal block for $\mathcal{C}_{0,3}$ is known to be defined uniquely up to normalisation by the invariance property (6.2.12). Using this same equation one may express all values $f(v_1 \otimes v_2 \otimes v_3 \otimes v_4)$ associated with $\mathcal{C}_{0,4}$ in terms of

$$f(\mathfrak{e}_{\alpha_1} \otimes \mathfrak{e}_{\alpha_2} \otimes L_{-1}^k \mathfrak{e}_{\alpha_3} \otimes \mathfrak{e}_{\alpha_4}) \equiv F_k\;, \qquad F_k \in \mathbb{C}\;, \qquad k \in \mathbb{Z}_{>0}\;. \tag{6.2.17}$$

One therefore finds that the space of conformal blocks associated with $\mathcal{C}_{0,4}$ is infinite-dimensional and isomorphic as a vector space to the space of formal power series in one variable. This space is far too big to be interesting for physical applications, as stressed in [54], [112]. Only if the growth of the complex numbers F_k ensures convergence of series like $F(z) = \sum_k \frac{1}{k!} F_k z^k$, can one integrate the canonical connection on spaces of conformal blocks defined by the energy-momentum tensor at least locally. Further conditions like existence of an analytic continuation of $F(z)$ to the Teichmüller space $\mathcal{T}_{0,4}$, and reasonable growth at the boundaries of $\mathcal{T}_{0,4}$ characterise the subspaces of $\mathrm{CB}(\mathcal{C}_{0,4}, \bigotimes_{i=1}^4 \mathcal{V}_{\alpha_i})$ of potential physical interest.

In the case $N = 3$, one generically finds an infinite-dimensional space of conformal blocks already for the three-punctured sphere. Using the invariance property (6.2.12), it is possible to express the values of the conformal blocks $f(v)$ on arbitrary $v \in \mathcal{V}_{\alpha_1} \otimes \mathcal{V}_{\alpha_2} \otimes \mathcal{V}_{\alpha_3}$ associated with $\mathcal{C}_{0,3}$ in terms of the particular values $F_{f,l}$ (see [113])

$$F_{f,l} = f(\mathfrak{e}_{\alpha_1} \otimes \mathfrak{e}_{\alpha_2} \otimes (W_{-1})^l \mathfrak{e}_{\alpha_3}) \in \mathbb{C}\;. \tag{6.2.18}$$

This means that any conformal block f on $\mathcal{C}_{0,3}$ is uniquely defined by the sequence of complex numbers $F_f = (F_{f,l})_{l\in\mathbb{N}}$. Therefore, similarly to (6.2.17), the space of conformal blocks associated with $\mathcal{C}_{0,3}$ is infinite-dimensional and can be identified with the space of formal Taylor series

in one variable. In analogy to the case $N = 2$, $n = 4$ mentioned above we may expect that the physically relevant subspaces of $\mathrm{CB}(\mathcal{C}_{0,3}, \bigotimes_{i=1}^{3} \mathcal{V}_{\alpha_i})$ may have a representation as spaces of analytic functions in one variable.

The representation of the $\mathcal{W}_3$-algebra attached to the puncture z_r generated by the operators $W_{d,n}(z_r)$ induces an action on the spaces of conformal blocks $\mathrm{CB}(\mathcal{C}, \mathcal{R})$ via

$$(W_{d,n}(z_r)f)(v) = f(W_{d,n}(z_r)v). \tag{6.2.19}$$

The conformal block $W_{d,n}(z_r)f$ obtained by acting on f with $W_{d,n}(z_r)$ is characterised by a sequence $(F_{W_{d,n}(z_r)f,l})_{l\in\mathbb{N}}$ which may be computed by specialising the definition (6.2.19) to vectors of the form $v = \mathfrak{e}_{\alpha_1} \otimes \mathfrak{e}_{\alpha_2} \otimes (W_{-1})^l \mathfrak{e}_{\alpha_3}$ and using (6.2.12) to express the right hand side of (6.2.19) as a linear combination of the $F_{f,l'}$, $l' \in \mathbb{N}$.

At general rank $(N-1)$, the number of extra variables required to get similar representations for the spaces of conformal blocks associated with $\mathcal{C}_{0,3}$ is equal to half of the dimension[2] of the moduli space of flat connections $(N-1)(N-2)/2$. One way to understand this is by considering, as in [22], [74], the difference between the number of basic three point functions and the number of constraints from the Ward identities (6.2.12) and corresponding to generators of the $\mathcal{W}_N$-algebra. There are $N(N-1)/2$ descendant operators constructed by acting with the modes $(W_{d,-l})^n$ on a highest-weight state, for $l = 1, 2, \ldots, d-1$ and $d = 2, 3, \ldots, N$, which lead to $3N(N-1)/2$ basic three point functions after taking into account the three primaries. Subtracting $N^2 - 1$ constraints corresponding to generators $W_{d,l}$, $l = -d+1, -d+2, \ldots, d-1$ and $d = 2, \ldots, N$, gives precisely the number $(N-1)(N-2)/2$ of unconstrained positive integers parameterising the conformal block associated with $\mathcal{C}_{0,3}$.

The infinite-dimensionality of the spaces of conformal blocks corresponding to the three-punctured spheres, for $N \geq 3$, leads to one of the basic problems in $\mathfrak{sl}_3$ Toda CFT. It implies that the Toda CFT three-point function can be represented in the following form

$$\begin{aligned} &\langle\, V_{\alpha_3}(v_3 \otimes w_3; z_3, \bar{z}_3) V_{\alpha_2}(v_2 \otimes w_2; z_2, \bar{z}_2) V_{\alpha_1}(v_1 \otimes w_1; z_1, \bar{z}_1) \,\rangle = \\ &\quad = \int dk d\bar{k}\; C_\rho(k, \bar{k}) f_k^\rho(v_3 \otimes v_2 \otimes v_1; z_3, z_2, z_1) \bar{f}_{\bar{k}}^\rho(w_3 \otimes w_2 \otimes w_1; \bar{z}_3, \bar{z}_2, \bar{z}_1). \end{aligned} \tag{6.2.20}$$

In (6.2.20) we are using the notation $V_\alpha(v \otimes w; z, \bar{z})$ for the vertex operator associated to a state $v \otimes w \in \mathcal{V}_\alpha \otimes \mathcal{V}_\alpha$ by the state-operator correspondence. It can be represented as a normal ordered product of the primary field $V_\alpha(z, \bar{z}) = V_\alpha(\mathfrak{e}_\alpha \otimes \mathfrak{e}_\alpha; z, \bar{z})$ associated to the highest weight state $\mathfrak{e}_\alpha \otimes \mathfrak{e}_\alpha$ with differential polynomials in the fields representing the $\mathcal{W}_3$-algebra. The superscript ρ refers to the triple of labels $\rho = (\alpha_3, \alpha_2, \alpha_1)$ for the representations of the $\mathcal{W}$-algebra associated to the vertex operators appearing in the correlation function (6.2.20). f_k^ρ and $\bar{f}_{\bar{k}}^\rho$ are bases for the relevant (sub-)spaces of the spaces of conformal blocks on the three-punctured spheres $\mathcal{C}_{0,3} = \mathbb{P}^1 \setminus \{z_1, z_2, z_3\}$ having $\mathcal{W}$-algebra representations with labels α_i assigned to the punctures z_i for $i = 1, 2, 3$, respectively.

[2]This number is equal to the dimension of the Coulomb branch of the T_N gauge theory. Together with the $3(N-1)$ parameters of the momenta α, it gives the $(N+4)(N-1)/2$ parameters of the T_N theory [22].

Gluing construction: We expect to be able to reduce the case of an n-punctured sphere to the one for the three-punctured sphere by means of the gluing construction. Given a possibly disconnected Riemann surface with two marked points P_0^i, $i = 1, 2$, surrounded by parameterized discs one can construct a new Riemann surface by pairwise identifying the points in suitable annular regions around the two marked points, respectively. Having conformal blocks associated with two surfaces $\mathcal{C}_i$ with $n_i + 1$ punctures $P_0^i, P_1^i, \ldots, P_{n_i}^i$ one may construct a conformal block associated with the surface $\mathcal{C}_{12}$ obtained by gluing annular neighborhoods of P_0^i, $i = 1, 2$ as follows

$$\begin{aligned} f_{\mathcal{C}_{12}}(v_1 \otimes \cdots \otimes v_{n_1} \otimes w_1 \otimes \cdots \otimes w_{n_2}) = \\ = \sum_{\nu \in \mathcal{I}_\beta} f_{\mathcal{C}_1}(v_1 \otimes \cdots \otimes v_{n_1} \otimes v_\nu)\, f_{\mathcal{C}_2}(\mathrm{e}^{2\pi i \tau L_0} v_\nu^\vee \otimes w_1 \otimes \cdots \otimes w_{n_2})\,. \end{aligned} \tag{6.2.21}$$

The vectors v_ν and $v_\nu^\vee$ are elements of bases $\{v_\nu; \nu \in \mathcal{I}_\beta\}$ and $\{v_\nu^\vee; \nu \in \mathcal{I}_\beta\}$ for the representation $\mathcal{V}_\beta$ which are dual with respect to the invariant bilinear form $\langle ., . \rangle_\beta$ on $\mathcal{V}_\beta$. The parameter τ in (6.2.21) is the modulus of the annular region used in the gluing construction of $\mathcal{C}_{12}$. The rest of the notations in (6.2.21) are hopefully self-explanatory. The case where P_0^i, $i = 1, 2$, are on a connected surface can be treated in a similar way.

A general Riemann surface $\mathcal{C}_{g,n}$ can be obtained by gluing $2g - 2 + n$ pairs of pants $\mathcal{C}_{0,3}^v$, $v = 1, \ldots, 2g - 2 + n$. It is possible to construct conformal blocks for the resulting Riemann surface from the conformal blocks associated with the pairs of pants $\mathcal{C}_{0,3}^v$ by recursive use of the gluing construction outlined above. This yields families of conformal blocks parameterized by (i) the choices of representations $\mathcal{V}_\beta$ used in the gluing construction, and (ii) the choices of elements of the spaces $\mathrm{CB}(\mathcal{C}_{0,3}^v)$, $v = 1, \ldots, 2g - 2 + n$.

Chiral vertex operators: Closely related to the gluing construction of conformal blocks are constructions of conformal blocks using chiral vertex operators. There is a one-to-one correspondence between the conformal blocks $f \in \mathrm{CB}(\mathcal{C}_{0,3})$ for three-punctured spheres $\mathcal{C}_{0,3} = \mathbb{P}^1 \setminus \{0, z_2, \infty\}$ and chiral vertex operators $V^\rho(v_2, z_2) : \mathcal{V}_{\alpha_1} \to \mathcal{V}_{\alpha_3}$, $\rho = (\alpha_3, \alpha_2, \alpha_1)$, $v_2 \in \mathcal{V}_{\alpha_2}$, defined by the relation

$$f(v_1 \otimes v_2 \otimes v_3) = \langle v_3, V^\rho(v_2, z_2) v_1 \rangle_{\mathcal{V}_{\alpha_3}}\,, \tag{6.2.22}$$

for all $v_i \in \mathcal{V}_{\alpha_i}$, $i = 1, 2, 3$, using an invariant bilinear form $\langle\, .\,,\, .\,\rangle_{\mathcal{V}_{\alpha_3}}$ on $\mathcal{V}_{\alpha_3}$. The field $V^\rho(v_2, z_2)$ associated with the highest-weight vector $v_{\alpha_2} \in \mathcal{V}_{\alpha_2}$ is called a primary field, and all other fields are called descendants. A graphical representation is given in Figure 6.1. One may, more generally, relate conformal blocks f_V associated with n-punctured spheres $\mathcal{C}_{0,n}$ to families of multi-local chiral vertex operators $V(w; z) : \mathcal{V}_{\alpha_1} \to \mathcal{V}_{\alpha_n}$, $w \in \mathcal{V}_{\alpha_2} \otimes \cdots \otimes \mathcal{V}_{\alpha_{n-1}}$, $z = (z_1, \ldots, z_{n-1})$, defined such that

$$f_V(v_1 \otimes \cdots \otimes v_n) = \langle v_n, V(w; z) v_1 \rangle_{\mathcal{V}_{\alpha_n}}. \tag{6.2.23}$$

Such multi-local vertex operators can be constructed as compositions of vertex operators $V^\rho(v, z)$

$$\langle v_n\,,\, V^{(\alpha_n, \alpha_{n-1}, \beta_{n-3})}(v_{n-1}, z_{n-1}) \cdots V^{(\beta_1, \alpha_2, \alpha_1)}(v_2, z_2)\, v_1 \rangle_{\mathcal{V}_{\alpha_n}}\,, \tag{6.2.24}$$

assuming that $z_n = \infty$ and $z_1 = 0$. We may therefore construct large families of conformal blocks by constructing the chiral vertex operators $V^\rho(v, z)$, or equivalently the conformal blocks associated to $\mathcal{C}_{0,3}$. This will be one of our main goals here.

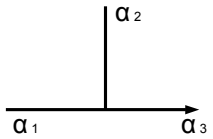

Figure 6.1: *Vertex operator as an intertwiner of highest-weight representations* $\mathcal{V}_{\alpha_i}$.

6.3 Degenerate representations

It will be useful to distinguish three types of representations. A distinguished role will be played by the representations which have $\alpha = -b\omega_i - b^{-1}\omega_j$, where ω_i and ω_j are weights of finite-dimensional representations of $\mathfrak{sl}_N$. Such representations are called *fully degenerate* to reflect the fact that the vectors in these representations satisfy the maximal possible number of inequivalent relations of the form $\mathcal{P}_l(W_{d,-n})\mathfrak{e}_\alpha = 0$ for certain polynomials $\mathcal{P}_l$. These are called called null vectors among the vectors generated by the algebra $\mathcal{W}_N$ from the highest weight vector $\mathfrak{e}_\alpha$. For generic α one has no such relations in the representations $\mathcal{V}_\alpha$, which are then called *fully non-degenerate*. There are various intermediate cases, called *semi-degenerate*, in which there exist relations of the form $\mathcal{P}_l(W_{d,-n})\mathfrak{e}_\alpha = 0$, but the number of inequivalent relations of this type is smaller than in fully degenerate representations. This happens for example if $\alpha = \kappa\omega_1$, with $\kappa \in \mathbb{C}$.

A special role is played by the vertex operators associated to degenerate representations of the $\mathcal{W}_N$-algebra where the representation label α is equal to either $-b\omega_1$ or $-b\omega_{N-1}$, with ω_1 and ω_{N-1} being the weights associated to the fundamental and anti-fundamental representation of $\mathfrak{sl}_N$, respectively. In the case $N = 3$ one will find the following three null vectors in the representation $\mathcal{V}_{-b\omega_1}$:

$$\mathfrak{n}_1 : \qquad 0 = (L_{-1} + \kappa_{1,1}W_{-1})\mathfrak{e}_{-b\omega_1}\,, \tag{6.3.25}$$

$$\mathfrak{n}_2 : \qquad 0 = (L_{-1}^2 + \kappa_{2,1}L_{-2} + \kappa_{2,2}W_{-2})\mathfrak{e}_{-b\omega_1}\,, \tag{6.3.26}$$

$$\mathfrak{n}_3 : \qquad 0 = (L_{-1}^3 + \kappa_{3,1}L_{-2}L_{-1} + \kappa_{3,2}L_{-3} + \kappa_{3,3}W_{-3})\mathfrak{e}_{-b\omega_1}\,. \tag{6.3.27}$$

Explicit formulae for the coefficients can be found for example in [106]. The relations in the representation $\mathcal{V}_{-b\omega_{N-1}}$ take a similar form, obtained by replacing $\kappa_{i,i}$ by $-\kappa_{i,i}$, $i = 1, 2, 3$.

The null vectors in degenerate representations have well-known consequences for the vertex operators associated to such representations. If $\alpha_2 = -b\omega_1$, for example, it follows from the relations above that $V^\rho(v_2, z_2) : \mathcal{V}_{\alpha_1} \to \mathcal{V}_{\alpha_3}$ can only be non-vanishing if $\alpha_3 = \alpha_1 - bh_\imath$ where $h_\imath$ are the weights of the fundamental representation of $\mathfrak{sl}_3$ for $\imath = 1, 2, 3$. For $\alpha_2 = -b\omega_{N-1}$ one will similarly find $\alpha_3 = \alpha_1 + bh_\imath$ for $\imath = 1, 2, 3$. We may therefore abbreviate the notations for the corresponding vertex operators to $D_\imath(y)$ and $\bar{D}_\imath(y)$, respectively. They map

$$D_\imath : \mathcal{V}_\alpha \to \mathcal{V}_{\alpha - bh_\imath}, \qquad \bar{D}_\imath : \mathcal{V}_\alpha \to \mathcal{V}_{\alpha + bh_\imath}, \qquad \imath = 1, 2, 3. \tag{6.3.28}$$

It is furthermore well-known that these relations imply differential equations satisfied by the conformal blocks if some of the tensor factors of $\mathcal{R} = \bigotimes_{r=1}^{n} \mathcal{V}_{\alpha_r}$ are degenerate in the sense above. To be specific we will in the following consider conformal blocks on a sphere with $n+2$ punctures $z_1 = 0, z_2, \ldots, z_{n-1}, y, y_0, \infty$, with representation $\mathcal{V}_{-b\omega_{N-1}}$ associated to y_0 and representation $\mathcal{V}_{-b\omega_1}$ associated to y. As in (6.2.23) we may then consider the conformal blocks

$$\mathcal{F}_V(y, y_0; z)_{\bar{\imath}u} = \left\langle \mathfrak{e}_n, \bar{D}_{\bar{\imath}}(y_0) D_i(y)\, V(\mathfrak{e}_2 \otimes \cdots \otimes \mathfrak{e}_{n-1}; z)\, \mathfrak{e}_1 \right\rangle_{\mathcal{V}_{\alpha_n}}. \tag{6.3.29}$$

The differential equations following from the null vectors include, in particular,

$$\left(\frac{\partial^3}{\partial y^3} + \kappa_{3,1}\, \mathsf{T}(y) \frac{\partial}{\partial y} + \kappa_{3,2}\, \mathsf{T}'(y) + \kappa_{3,3}\, \mathsf{W}(y) \right) \mathcal{F}_V(y; y_0; z)_{\bar{\imath}u} \;=\; 0\,, \tag{6.3.30}$$

where

$$\begin{aligned} \mathsf{W}(y) =& \frac{w_3(-b\omega_1)}{(y-t_0)^3} + \frac{\mathsf{W}_{-1}(y_0)}{(y-y_0)^2} + \frac{\mathsf{W}_{-2}(y_0)}{y-y_0} + \sum_{r=1}^{n-1} \left(\frac{w_3(\alpha_r)}{(y-z_r)^3} + \frac{\mathsf{W}_{-1}(z_r)}{(y-z_r)^2} + \frac{\mathsf{W}_{-2}(z_r)}{y-z_r} \right), \\ \mathsf{T}(y) =& \frac{w_2(-b\omega_1)}{(y-y_0)^2} + \frac{1}{y-y_0} \frac{\partial}{\partial y_0} + \sum_{r=1}^{n-1} \left(\frac{w_2(\alpha_r)}{(y-z_r)^2} + \frac{1}{y-z_r} \frac{\partial}{\partial z_r} \right). \end{aligned} \tag{6.3.31}$$

Note that the null vectors $\mathfrak{n}_1$ allow us to express $\mathsf{W}_{-1}(y_0)$ in terms of $\mathsf{L}_{-1}(y_0) \sim \frac{\partial}{\partial y_0}$. We may furthermore use the null vector $\mathfrak{n}_2$ together with the Ward identities to express $\mathsf{W}_{-2}(y_0)$ in terms of a differential operator $\mathcal{W}_{-2}(y_0)$ constructed out of derivatives $\frac{\partial}{\partial y_0}$ and $\mathsf{L}_{-1}(z_r)$. However, even in the case $n = 3$ one can not use the invariance conditions defining the conformal blocks to express all $\mathsf{W}_{-i}(z_r)\mathcal{F}_V(y; u; z)_{\bar{\imath}u}$, $i = 1, 2$ in terms of derivatives of $\mathcal{F}_V(y; u; z)_{\bar{\imath}u}$, in general.

Not having a closed system of differential equations represents an obstacle for the use of the differential equations (6.3.30). One of our goals is to define the analytic continuation of $\mathcal{F}_V(y; y_0; z)_{\bar{\imath}u}$ with respect to y and compute the resulting monodromies. Without a more explicit description of the action of the algebra $\mathcal{W}_3$ on spaces of conformal blocks one can not use the differential equations discussed above to reach this goal. This is the main difference to the case where $N = 2$. Other methods are needed to reach this aim, as will be introduced next.

6.4 Free field construction of conformal blocks

We propose that promising candidates for useful bases for the spaces of conformal blocks can be defined using the free field representation of the algebra $\mathcal{W}_N$. This section gives an outline for $N = 3$ of the necessary constructions which is sufficient for the formulation of some of our main results. A more detailed description will be given in Chapter 8 below.

Key elements are the normal ordered exponentials

$$V_\alpha(z) = e^{(\alpha, \varphi(z))}. \tag{6.4.32}$$

One of the most important properties for the following will be the exchange relation

$$V_\beta(z') V_\alpha(z) = \mathrm{e}^{-\pi \mathrm{i}(\alpha,\beta)} V_\alpha(z) V_\beta(z')\,, \tag{6.4.33}$$

where the left hand side is understood as the analytic continuation from a region $|z'| > |z|$ and z' moves in a counter-clockwise direction around z. The special fields $S_i(z) = V_{be_i}(z)$ will be referred to as the screening currents. From the screening currents $S_i(z)$ one can construct screening charges $Q_i(\gamma)$ as

$$Q_i(\gamma) = \int_\gamma dz\ e^{b(e_i,\varphi(z))}, \tag{6.4.34}$$

γ being a suitable contour. Apart from the screening charges associated to the simple roots e_i, $i = 1, 2$, it will frequently be useful to consider the composite screening charge Q_{12} defined as

$$Q_{12}(\gamma) = \int_\gamma dy\ S_{12}(y), \qquad S_{12}(y) = \int_{\gamma_y} dy'\ S_1(y)S_2(y'), \tag{6.4.35}$$

with γ_y a suitable contour encircling the point y which will be specified more precisely below.

We may use these ingredients to construct conformal blocks on $\mathcal{C}_{0,3}$ by expressions of the following form

$$\begin{aligned} g(v_\infty) = \int_{\mathcal{C}_{u_1}} du_1 \cdots \int_{\mathcal{C}_{u_m}} du_m \int_{\mathcal{C}_{v_1}} dv_1 \cdots \int_{\mathcal{C}_{v_n}} dv_n \int_{\mathcal{C}_{w_1}} dw_1 \cdots \int_{\mathcal{C}_{w_p}} dw_p \\ \big\langle v_\infty\,,\ S_1(u_1)\dots S_1(u_m)S_{12}(v_1)\dots S_{12}(v_n)S_2(w_1)\dots S_2(w_p)V_{\alpha_2}(z_2)V_{\alpha_1}(z_1)\,\mathfrak{e}_0\big\rangle. \end{aligned} \tag{6.4.36}$$

The precise definition of the expression on the right hand side of (6.4.36) requires further explanations. The integrand is the multi-valued analytic function obtained by standard normal ordering of the exponential fields appearing in the matrix element on the right hand side of (6.4.36). Both the contours of integration and the precise choice of branch defining the integrand still need to be specified. All this will be discussed in more detail in Chapter 8 below.

The vertex operators appearing in (6.4.36) map from a module $\mathcal{V}_{\alpha_1}$ of the $\mathcal{W}_3$ algebra to the module $\mathcal{F}_{\alpha_3}$, where α_3 is related to α_2, α_1 and $\mathbf{n} = (m, n, p)$ by the conservation of the free field momentum,

$$\alpha_3 = \alpha_1 + \alpha_2 + b(s_1e_1 + s_2e_2), \qquad \begin{aligned} s_1 &:= n + m, \\ s_2 &:= n + p. \end{aligned} \tag{6.4.37}$$

Fixing the triple $\rho = (\alpha_3, \alpha_2, \alpha_1)$ of representation labels only fixes the two combinations $s_1 = m + n$ and $s_2 = n + p$ of the three parameters $\mathbf{n} = (m, n, p)$. It is therefore natural to parameterise $\mathbf{n}$ in terms of s_1, s_2 and an additional multiplicity label k such that

$$\begin{aligned} m &= s_1 - k, \\ p &= s_2 - k, \end{aligned} \qquad n = k. \tag{6.4.38}$$

For fixed external parameters $\rho = (\alpha_3, \alpha_2, \alpha_1)$ one may therefore use (6.4.36) to construct a one-parameter family of conformal blocks F_k^ρ.

6.5 Quantum monodromies

A useful probe for the conformal blocks F_k^ρ will be the 3×3 matrix of conformal blocks on $\mathcal{C}_{0,3+2}$ having matrix elements denoted by $\mathcal{F}_k^\rho(y; y_0)_{\bar\imath u}$, $\imath, \bar\imath = 1, 2, 3$, defined as

$$\mathcal{F}_k^\rho(y; y_0)_{\bar\imath u} = \langle\, \mathfrak{e}_{\alpha_3}\,,\ \bar D_{\bar\imath}(y_0) D_\imath(y)\, V_k^\rho(z)\, \mathfrak{e}_{\alpha_1}\rangle. \tag{6.5.39}$$

We will regard y_0 as a base-point, typically assumed to be near ∞ on $\mathcal{C}_{0,3}$ and sometimes use the abbreviated notation $\mathcal{F}^\rho_k(y)_{\bar{\imath}\imath} \equiv \mathcal{F}^\rho_k(y;y_0)_{\bar{\imath}\imath}$. We are going to demonstrate in Chapter 9 below that $\mathcal{F}^\rho_k(y)_{\jmath,\imath}$ has an analytic continuation with respect to y generating a representation of the fundamental group $\pi_1(\mathcal{C}_{0,3})$ of the form

$$\mathcal{F}^\rho_k(\gamma.y)_{\bar{\imath}\imath} = \sum_\jmath \sum_l (M_\gamma)^{\jmath,l}_{\imath,k}\, \mathcal{F}^\rho_l(y)_{\bar{\imath}\jmath}. \tag{6.5.40}$$

We will see that only finitely many terms are nonzero in the summation over l. It will be useful to regard the coefficients $(M_\gamma)^{\jmath,k}_{\imath,l}$ as matrix elements of operators $(\mathsf{M}_\gamma)_\imath{}^\jmath$, $\imath,\jmath = 1,2,3$, acting on a vector space with a basis labelled by k, allowing us to write (6.5.40) in the form

$$\mathbf{F}^\rho(\gamma.y)_{\bar{\imath}\imath} = \sum_\jmath (\mathsf{M}_\gamma)_\imath{}^\jmath \cdot \mathbf{F}^\rho(y)_{\bar{\imath}\jmath}. \tag{6.5.41}$$

We may anticipate at this point that the matrices $(\mathsf{M}_\gamma)_\imath{}^\jmath$ will turn out to be "quantum" analogs of the monodromy matrices of a flat $SL(3)$-connection on $\mathcal{C}_{0,3}$.

The derivation of the relations (6.5.41) described below will allow us to show that the elements $(\mathsf{M}_\gamma)_\imath{}^\jmath$ of the quantum monodromy matrices can be expressed as functions $M_\gamma(\mathsf{u},\mathsf{v})_\imath{}^\jmath$ of the two operators

$$\mathsf{u}\,\mathcal{F}^\rho_k = q^{-2k}\mathcal{F}^\rho_k, \qquad \mathsf{v}\,\mathcal{F}^\rho_k = q^{-k}\mathcal{F}^\rho_{k+1}, \tag{6.5.42}$$

generating a Weyl algebra $\mathcal{W}_\hbar$ characterised by the commutation relation $\mathsf{uv} = q^{-2}\mathsf{vu}$, using the notation $q = e^{-\mathrm{i}\pi b^2}$. It turns out that the $M_\gamma(\mathsf{u},\mathsf{v})_\imath{}^\jmath$ are Laurent polynomials of low orders in u, v. This property will be essential for the interpretation of u and v as quantised analogs of Fenchel-Nielsen type coordinates on moduli spaces of flat connections to be discussed in Chapter 12.

6.6 Verlinde operators and quantised moduli spaces of flat connections

Spaces of conformal blocks carry two natural module structures. One type of module structure is canonically associated to the definition of conformal blocks as solutions to the conformal and $\mathcal{W}$-algebra Ward identities, as defined in Section 6.2. Of particular interest for us is another type of module structure defined in terms of the so-called Verlinde line operators and their generalisations. This section will present the definition of the Verlinde line operators, and explain why the algebra of Verlinde line operators is a quantum deformation of the algebra of regular functions on $\mathcal{M}^{SL(3)}_{\text{flat}}(\mathcal{C}_{0,3})$ following [77].

In order to define the Verlinde line operators let us note that the identity operator appears in the operator product expansion

$$\begin{aligned}\bar{D}_{\bar{\imath}}(y_0)D_\imath(y) = {}& \delta_{\bar{\imath},\imath}\, P_\imath\, (y_0-y)^{\lambda_0}(\mathrm{id} + Y(y_0-y)) \\ & + \sum_{l=2}^{3} C^l_{\bar{\imath},\imath}\,(y_0-y)^{\lambda_l}(V_l(y) + \mathcal{O}(y_0-y)),\end{aligned} \tag{6.6.43}$$

where $Y(y_0-y) = \sum_{n=1}^\infty (y_0-y)^n Y_n(y)$, with $Y_n(y)$ being combinations of the generators of the $\mathcal{W}_3$ algebra. The chiral vertex operators $V_l(y)$ correspond to the other finite-dimensional

representations appearing in the tensor product of fundamental and anti-fundamental representation of $\mathfrak{sl}_3$. This shows that a canonical projection $\mathbb{P}$ from the space of conformal blocks on $\mathcal{C}_{0,3+2}$ spanned by the $\mathcal{F}_k^\rho(y)_{\bar\imath\bar\imath}$ to the space of conformal blocks on $\mathcal{C}_{0,3}$ spanned by F_k^ρ can be defined by setting $\mathbb{P}(\mathcal{F}_k^\rho(y)_{\bar\imath\bar\imath}) = \delta_{\bar\imath\bar\imath} P_\imath F_k^\rho$.

By taking linear combinations of (6.6.43) one may eliminate the terms containing the chiral vertex operators $V_l(y)$, leading to a relation of the form

$$\sum_{\imath=1}^{3} E^\imath\, \bar D_\imath(y_0) D_\imath(y) = (y_0 - y)^{\lambda_0}(\mathrm{id} + Y(y_0 - y)). \tag{6.6.44}$$

This allows us to define an embedding $\mathbb{E}$ of the space of conformal blocks on $\mathcal{C}_{0,3}$ into the space of conformal blocks on $\mathcal{C}_{0,3+2}$ by setting $\mathbb{E}(F_k^\rho) = \sum_{\imath=1}^3 E^\imath\, \mathcal{F}_k^\rho(y)_{\imath\imath}$.

As before we find it convenient to regard the functions $\mathcal{F}_k^\rho$ as components of a vector $\mathbf{F}^\rho$ with respect to a basis labelled by k. We have observed in the previous section that the analytic continuation of $\mathbf{F}^\rho(y)_{\imath,\imath}$ along $\gamma \in \pi_1(\mathcal{C}_{0,3})$ defines an operator M_γ on the space of conformal blocks on $\mathcal{C}_{0,3+2}$,

$$\mathsf{M}_\gamma\big(\mathbf{F}^\rho(y)_{\bar\imath\bar\imath}\big) \equiv \mathbf{F}^\rho(\gamma.y)_{\bar\imath\bar\imath} = \sum_{\jmath} (\mathsf{M}_\gamma)_\imath{}^\jmath \cdot \mathbf{F}^\rho(y)_{\bar\imath\bar\jmath}. \tag{6.6.45}$$

The composition $\mathbb{P} \circ \mathsf{M}_\gamma \circ \mathbb{E}$ will then be an operator from the space of conformal blocks on $\mathcal{C}_{0,3}$ to itself which may be represented in the form

$$(\mathbb{P} \circ \mathsf{M}_\gamma \circ \mathbb{E})(\mathcal{F}_\mu) = \mathsf{V}_\gamma \cdot \mathcal{F}_\mu, \qquad \mathsf{V}_\gamma = \sum_{\imath=1}^{3} E^\imath\, (\mathsf{M}_\gamma)_\imath{}^\imath\, P_\imath. \tag{6.6.46}$$

The operators V_γ will be called Verlinde line operators. They can be regarded as as "quantum" versions of the traces of the monodromy matrices M_γ of a flat $SL(3)$-connection.

Assuming the validity of the mondromy relations like (6.5.41) for general rank, we will show in Chapter 10 following [77] that the algebra generated by the operators V_γ is isomorphic to the algebra of quantised functions on $\mathcal{M}_{\mathrm{flat}}^{SL(N)}(\mathcal{C}_{0,3})$, the moduli space of flat $SL(N)$-connections on $\mathcal{C}_{0,3}$. This means in particular that, for $N = 3$, the operators V_γ satisfy the deformed relations (3.1.18) and (3.1.19)

$$\mathcal{P}_i^\hbar\big(\{\mathsf{V}_\gamma, \gamma \in \pi_1(C_{0,3})\}\big) = 0, \qquad i = 1, 2\,, \tag{6.6.47}$$

where the polynomials $\mathcal{P}_i^\hbar$ differ from the polynomials $\mathcal{P}_i$ in the corresponding classical relations (3.1.14) and (3.1.15) by fixing an operator ordering and $\hbar$-dependent deformations of the coefficients. It was furthermore shown in Part II that the operators V_γ satisfy (q-)commutation relations reproducing the Poisson brackets of the corresponding trace functions to leading order in $\hbar$.

We had observed in Section 6.5 that the elements of the quantum monodromy matrices can be expressed as functions of two operators u and v. It follows from (6.6.46) that the same is true for the Verlinde line operators V_γ. We will argue in Chapter 12 that the classical limits of u and v are closely related to natural higher rank analogs of the Fenchel-Nielsen coordinates.

Chapter 7

Quantum group background

We review here some relevant basic notions about quantum groups. These are ubiquitous in the following chapters, entering the construction of chiral vertex operators and conformal blocks in the free field representation in Chapter 8 and the computation of quantum monodromy matrices in Chapter 9. They will furthermore play a central role in the identification of the quantised algebra of functions $\mathcal{A}_{\text{flat}}$ studied in Part II of this thesis with the algebra of Verlinde operators $\mathcal{A}_V$ in Chapter 10.

For a complete background and set of axioms we refer the reader to one of the standard references [114].

Abstractly, a *Hopf algebra* is a collection $(\mathcal{U}, m, \eta, \Delta, \epsilon, S)$, with unit $\eta : \mathbb{C}(q) \to \mathcal{U}$, product $m : \mathcal{U} \otimes \mathcal{U} \to \mathcal{U}$, co-product $\Delta : \mathcal{U} \to \mathcal{U} \otimes \mathcal{U}$, counit $\epsilon : \mathcal{U} \to \mathbb{C}(q)$ and an algebra anti-automorphism called antipode $S : \mathcal{U} \to \mathcal{U}$. The triple $(\mathcal{U}, m, \eta)$ is a unital associative algebra and $(\mathcal{U}, \Delta, \epsilon)$ is a counital associative coalgebra. Δ, ϵ are unital algebra homomorphisms and satisfy the following relations

$$\begin{aligned} (\Delta \otimes \mathrm{id}) \circ \Delta &= (\mathrm{id} \otimes \Delta) \circ \Delta \qquad \text{(co-associativity)} \\ (\epsilon \otimes \mathrm{id}) \circ \Delta &= (\mathrm{id} \otimes \epsilon) \circ \Delta = \mathrm{id} \\ m \circ (S \otimes \mathrm{id}) \circ \Delta &= \eta \circ \epsilon = m \circ (\mathrm{id} \otimes S) \circ \Delta \qquad \text{(pentagon)} \,. \end{aligned} \tag{7.0.1}$$

The quantum group $\mathcal{U} = \mathcal{U}_q(\mathfrak{sl}_N)$ is a Hopf algebra, generated as an associative algebra over $\mathbb{C}(q)$ by e_i, f_i and $\mathsf{k}_i^{\pm}$ for $i = 1, \ldots, N-1$ which satisfy the relations

$$[\mathsf{e}_i, \mathsf{f}_j] = \delta_{ij} \frac{\mathsf{k}_i - \mathsf{k}_i^{-1}}{q - q^{-1}}, \qquad \begin{matrix} \mathsf{k}_i^{\pm} \mathsf{e}_j = q^{\pm \kappa_{ij}} \mathsf{e}_j \mathsf{k}_i^{\pm} \\ \mathsf{k}_i^{\pm} \mathsf{f}_j = q^{\mp \kappa_{ij}} \mathsf{f}_j \mathsf{k}_i^{\pm} \end{matrix} \,, \qquad \mathsf{k}_i \mathsf{k}_i^{-1} = 1 = \mathsf{k}_i^{-1} \mathsf{k}_i \tag{7.0.2}$$

for $i = 1, \ldots, N-1$ and where we recall κ is the $\mathfrak{sl}_N$ Cartan matrix $\kappa_{ij} = 2\delta_{ij} - \delta_{i+1,j} - \delta_{i,j+1}$. The Serre relations are

$$\mathsf{e}_i^2 \mathsf{e}_j - (q + q^{-1}) \mathsf{e}_i \mathsf{e}_j \mathsf{e}_i + \mathsf{e}_j \mathsf{e}_i^2 = 0 \,, \quad \mathsf{f}_i^2 \mathsf{f}_j - (q + q^{-1}) \mathsf{f}_i \mathsf{f}_j \mathsf{f}_i + \mathsf{f}_j \mathsf{f}_i^2 = 0 \,, \tag{7.0.3}$$

with $|i - j| = 1$. The Hopf algebra structure is given by $\epsilon(\mathsf{k}_i) = 1,\ \epsilon(\mathsf{e}_i) = 0 = \epsilon(\mathsf{f}_i)$ and

$$S(K_i) = \mathsf{k}_i^{-1} \quad , \quad S(\mathsf{e}_i) = -\mathsf{e}_i \mathsf{k}_i^{-1} \quad , \quad S(\mathsf{f}_i) = -\mathsf{k}_i \mathsf{f}_i$$

and by the action of the co-product Δ on the generators, which we specify below.

Let us now restrict for a moment to the case $N = 3$. Defining

$$\mathsf{e}_{12} = \mathsf{e}_1\mathsf{e}_2 - q\mathsf{e}_2\mathsf{e}_1 \ , \qquad \mathsf{f}_{12} = \mathsf{f}_1\mathsf{f}_2 - q\mathsf{f}_2\mathsf{f}_1 \ , \tag{7.0.4}$$

it follows from the quantum Serre relations that

$$\mathsf{e}_1\mathsf{e}_{12} = q^{-1}\mathsf{e}_{12}\mathsf{e}_1 \ , \qquad \mathsf{e}_2\mathsf{e}_{12} = q\mathsf{e}_{12}\mathsf{e}_2 \ , \tag{7.0.5}$$

$$\mathsf{f}_1\mathsf{f}_{12} = q^{-1}\mathsf{f}_{12}\mathsf{f}_1 \ , \qquad \mathsf{f}_2\mathsf{f}_{12} = q\mathsf{f}_{12}\mathsf{f}_2 \ . \tag{7.0.6}$$

Using these relations it is possible to show that arbitrary monomials formed out of the basic generators f_i, $i = 1, 2$ can be represented as linear combinations of the ordered monomials $\mathsf{f}_1^{n_1}\mathsf{f}_{12}^{n}\mathsf{f}_2^{n_2}$ with $(n_1, n_{12}, n_2) \in \mathbb{N}^3$. This statement generalises straightforwardly to higher rank, where for $\mathcal{U}_q(\mathfrak{sl}_N)$ it is possible to define $\frac{1}{2}(N-1)(N-2)$ generators f_{ij}, with $i < j$, through

$$\mathsf{f}_{ij} = \mathsf{f}_{ik}\mathsf{f}_{kj} - q\mathsf{f}_{kj}\mathsf{f}_{ik} \ , \qquad 1 \leq i < k < j < N$$

and similarly for e_{ij}. Then arbitrary monomials of the basic generators f_i for $i = 1, \ldots, N-1$ can be represented as weighted sums over the ordered monomials

$$\mathsf{f}_1^{n_1}\mathsf{f}_{12}^{n_{12}} \ldots \mathsf{f}_{1\ N-1}^{n_1\ N-1}\mathsf{f}_2^{n_2} \ldots \mathsf{f}_{2\ N-1}^{n_2\ N-1} \ldots \mathsf{f}_{N-1\ N-1}^{n_{N-1}\ N-1} \ .$$

7.1 Representations

With each algebra $\mathcal{U}$, we can associate the category Rep$\mathcal{U}$ of its finite dimensional linear representations, with objects V, $W, \ldots$ that are finitely generated left $\mathcal{U}$-modules and with morphisms that are $\mathcal{U}$-linear homomorphisms. The action of $\mathcal{U}$ on a $\mathcal{U}$-module V induces a representation $\pi_V : \mathcal{U} \to \text{End}\, V$.

Restricting once more to the case $N = 3$, the irreducible highest weight representation of $\mathcal{U}_q(\mathfrak{sl}_3)$ with highest weight λ will be denoted by $\mathcal{R}_\lambda$. The highest weight vector $v_\lambda \in \mathcal{R}_\lambda$ is annihilated by the generators e_i, $\mathsf{e}_i v_\lambda = 0$ and the action of k_i is

$$\mathsf{k}_i v_\lambda = q^{(e_i,\lambda)} v_\lambda \ . \tag{7.1.7}$$

The representations $\mathcal{R}_\lambda$ are irreducible for generic weights λ. We will use a basis for the $\mathcal{U}_q(\mathfrak{sl}_3)$ Verma module $\mathcal{R}_\lambda$ which consists of the following vectors

$$e^\lambda_{\mathbf{n}} = \mathsf{f}_1^{n_1}\mathsf{f}_{12}^{n}\mathsf{f}_2^{n_2} v_\lambda \ , \qquad \mathbf{n} = (n_1, n, n_2) \ . \tag{7.1.8}$$

The vector $e^\lambda_{\mathbf{n}}$ has weight

$$\nu = \nu(\lambda, \mathbf{n}) = \lambda - (n + n_1)e_1 - (n + n_2)e_2 \ . \tag{7.1.9}$$

It will sometimes be useful to parameterise the labels $\mathbf{n} = (n_1, n, n_2)$ in terms another pair of data $\mathbf{n} = [\delta, m]$ consisting of the shift of weights $\delta = -s_1 e_1 - s_2 e_2$ together with a multiplicity label m such that $s_1 = n_1 + n$, $s_2 = n_2 + n$ and $n = m$. For fixed weight $\nu = \lambda + \delta$

parameterised by positive integers s_1 and s_2, one can only have finitely many values of m between 0 and $d_\nu - 1 = \min(s_1, s_2)$. The multiplicity space of a weight ν has dimension d_ν and will be denoted by $\mathcal{M}^\nu_\lambda$.

The action of the generators x of $\mathcal{U}_q(\mathfrak{sl}_3)$ is represented in the basis (7.1.8) by the matrices $R^{\lambda,\mathbf{n}'}_{(x),\mathbf{n}}$ defined by

$$\pi_\lambda(x)e^\lambda_{\mathbf{n}} = \sum_{\mathbf{n}'} R^{\lambda,\mathbf{n}'}_{(x),\mathbf{n}} e^\lambda_{\mathbf{n}'}. \tag{7.1.10}$$

Lists with the matrix elements of $R^{\lambda,\mathbf{n}'}_{(x),\mathbf{n}}$ for $x = \mathsf{e}_i, \mathsf{f}_i$ can be found in appendix B. Here we will only note the following important feature concerning the dependence on the multiplicity labels k. The action of $\pi_\lambda(x)$ on the basis vector $e^\lambda_{\mathbf{n}}$ can for $x = \mathsf{e}_i, \mathsf{f}_i$, $i = 1, 2$, be represented in the following form

$$\begin{aligned} \pi_\lambda(\mathsf{e}_i)e^\lambda_{[\delta,k]} &= E_i(\lambda,\delta,u_k)\, e^\lambda_{[\delta+e_i,k]} + E'_i(\lambda,\delta,u_k)\, \mathsf{v}^{-1}\, e^\lambda_{[\delta+e_i,k]}\ , \\ \pi_\lambda(\mathsf{f}_i)e^\lambda_{[\delta,k]} &= F_i(\lambda,\delta,u_k)\, e^\lambda_{[\delta-e_i,k]} + F'_i(\lambda,\delta,u_k)\, \mathsf{v}^{+1}\, e^\lambda_{[\delta-e_i,k]}\ , \end{aligned} \tag{7.1.11}$$

where $u_k = q^{-2k}$, $\mathsf{v}e^\lambda_{[\delta,k]} = q^{-k}e^\lambda_{[\delta,k+1]}$, and the coefficient functions E_i, E'_i, F_i and F'_i are Laurent polynomials in the variable u_k. This simple feature will play a crucial role for us in the following chapters.

We call a weight λ generic if it is not the highest weight of a finite-dimensional highest weight representation of $\mathfrak{sl}_3$. Apart from the representations associated to generic weights λ we will be interested in particular in the fundamental representation generated from the highest weight vector v_{ω_1} and having a basis $\{v_{\omega_1}, \mathsf{f}_1 v_{\omega_1}, \mathsf{f}_{12} v_{\omega_1}\}$.

7.2 Tensor products of representations

The co-product in a Hopf algebra $\mathcal{U}$ induces the tensor product in Rep$\mathcal{U}$, where for $\mathcal{U}$-modules U, V and $\forall a \in \mathcal{U}$, $\pi_{U\otimes V}(a) = (\pi_U \otimes \pi_V)(\Delta(a))$. The unit object in Rep$\mathcal{U}$ is the ground field $\mathbb{C}(q)$ equipped with the action of $\mathcal{U}$ by means of the counit ϵ. Furthermore, there exist associativity and left and right action homomorphisms that make Rep$\mathcal{U}$ a monoidal category (see for example [73]).

The co-product Δ of $\mathcal{U} = \mathcal{U}_q(\mathfrak{sl}_3)$ is defined by

$$\Delta(\mathsf{e}_i) = \mathsf{k}_i \otimes \mathsf{e}_i + \mathsf{e}_i \otimes 1\ , \quad \Delta(\mathsf{f}_i) = \mathsf{f}_i \otimes \mathsf{k}_i^{-1} + 1 \otimes \mathsf{f}_i\ , \quad \Delta(\mathsf{k}_i) = \mathsf{k}_i \otimes \mathsf{k}_i. \tag{7.2.12}$$

The co-product is an algebra homomorphism, so equations (7.2.12) imply, for example,

$$\begin{aligned} \Delta(\mathsf{e}_{12}) &= \mathsf{k}_1\mathsf{k}_2 \otimes \mathsf{e}_{12} + \mathsf{e}_{12} \otimes 1 + (q^{-1} - q)\mathsf{e}_2\mathsf{k}_1 \otimes \mathsf{e}_1 \\ \Delta(\mathsf{f}_{12}) &= \mathsf{f}_{12} \otimes \mathsf{k}_1^{-1}\mathsf{k}_2^{-1} + 1 \otimes \mathsf{e}_{12} + (q^{-1} - q)\mathsf{f}_1 \otimes \mathsf{f}_2\mathsf{k}_1^{-1}\ . \end{aligned} \tag{7.2.13}$$

The Clebsch-Gordan (CG) maps describe the embedding of irreducible representations into tensor products of representations.

For triples of $\mathcal{U}$-modules U, V, W, where $U \subset V \otimes W$, a Clebsch-Gordan map $C^U_{VW} : V \otimes W \to U$ intertwines the actions on $V \otimes W$ and U,

$$C^U_{VW}(\pi_V \otimes \pi_W)\Delta(x) = \pi_U(x)C^U_{VW}, \qquad x \in \mathcal{U}\ . \tag{7.2.14}$$

Clebsch-Gordan maps are represented graphically as trivalent vertices in Figure 7.1.

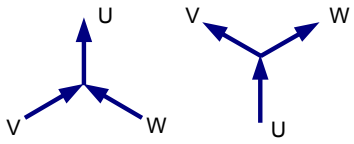

Figure 7.1: *Clebsch-Gordan maps intertwining tensor products of representations.*

We note that the representations V, W and U may be reducible, in general. We may, in particular, consider cases where V, W and U can be tensor products of representations such as $V = V_1 \otimes \cdots \otimes V_m$, for example. Such Clebsch-Gordan maps C^U_{VW} can be constructed as compositions of Clebsch-Gordan maps intertwining the respective representations on the tensor factors. Avoiding cases where q is a root of unity, one may find any irreducible finite-dimensional representation in a sufficiently high tensor power of the fundamental representation.

The conjugate Clebsch-Gordan maps $C_U^{VW} : U \to V \otimes W$ satisfy the property

$$C_U^{VW} \pi_U(x) = (\pi_V \otimes \pi_W)\Delta(x) C_U^{VW} \ . \tag{7.2.15}$$

A special subset of intertwiners are the *cap* and *cup* maps intertwining between a tensor product $V \otimes \bar{V}$ and the trivial representation $\mathbf{1} \simeq \mathbb{C}(q)$, respectively, where $\bar{V}$ is the conjugate representation to V. In the Reshetikhin-Turaev construction, one considers general morphisms M in Rep$\mathcal{U}$ between tensor products of modules $V_1 \otimes \ldots \otimes V_m$ and $W_1 \otimes \ldots \otimes W_n$.

In the case of the highest weight representations introduced above for $N = 3$, one may represent the CG maps $\mathsf{C}^{\lambda_1\lambda_2}_{\lambda_3} : \mathcal{R}_{\lambda_3} \to \mathcal{R}_{\lambda_1} \otimes \mathcal{R}_{\lambda_2}$ in the form

$$e^{\lambda_3}_{\mathbf{n}_3}(\lambda_2, \lambda_1) = \sum_{\substack{\mathbf{n}_2, \mathbf{n}_1 \\ \nu_3 = \nu_2 + \nu_1}} \left(\begin{smallmatrix} \lambda_3 \\ \mathbf{n}_3 \end{smallmatrix} \middle| \begin{smallmatrix} \lambda_2 & \lambda_1 \\ \mathbf{n}_2 & \mathbf{n}_1 \end{smallmatrix} \right) e^{\lambda_1}_{\mathbf{n}_1} \otimes e^{\lambda_2}_{\mathbf{n}_2} \ , \tag{7.2.16}$$

Here and below we use the notation $\nu_i = \nu_i(\lambda_i, \mathbf{n}_i)$ with $\nu(\lambda, \mathbf{n})$ defined in (7.1.9).

A set of equations for the Clebsch-Gordan coefficients (CGC) $\left(\begin{smallmatrix} \lambda_3 \\ \mathbf{n}_3 \end{smallmatrix} \middle| \begin{smallmatrix} \lambda_2 & \lambda_1 \\ \mathbf{n}_2 & \mathbf{n}_1 \end{smallmatrix} \right)$ follows from the intertwining property

$$\Delta(x) e^{\lambda_3}_{\mathbf{n}_3}(\lambda_2, \lambda_1) = \sum_{\mathbf{n}'_3} R^{\lambda_3, \mathbf{n}'_3}_{(x), \mathbf{n}_3} e^{\lambda_3}_{\mathbf{n}'_3}(\lambda_2, \lambda_1) \ , \tag{7.2.17}$$

for any element $x \in \mathcal{U}_q(\mathfrak{sl}_3)$. When $x = \mathsf{e}_i \in \{\mathsf{e}_1, \mathsf{e}_2\}$ and $\mathbf{n}_3 = 0$, this equation implies that for every fixed pair $(\mathbf{n}_1, \mathbf{n}_2)$

$$0 = \sum_{\mathbf{n}'_2} \left(\begin{smallmatrix} \lambda_3 \\ 0 \end{smallmatrix} \middle| \begin{smallmatrix} \lambda_2 & \lambda_1 \\ \mathbf{n}'_2 & \mathbf{n}_1 \end{smallmatrix} \right) q^{(e_i, \nu_1)} R^{\lambda_2, \mathbf{n}_2}_{(\mathsf{e}_i), \mathbf{n}'_2} + \sum_{\mathbf{n}'_1} \left(\begin{smallmatrix} \lambda_3 \\ 0 \end{smallmatrix} \middle| \begin{smallmatrix} \lambda_2 & \lambda_1 \\ \mathbf{n}_2 & \mathbf{n}'_1 \end{smallmatrix} \right) R^{\lambda_1, \mathbf{n}_1}_{(\mathsf{e}_i), \mathbf{n}'_1} \ . \tag{7.2.18}$$

Equations (7.2.18) can be regarded as a set of recursion relations. For generic values of λ_i, $i = 1, 2, 3$ one can show that these equations determine $\left(\begin{smallmatrix} \lambda_3 \\ 0 \end{smallmatrix} \middle| \begin{smallmatrix} \lambda_2 & \lambda_1 \\ \mathbf{n}_2 & \mathbf{n}_1 \end{smallmatrix} \right)$ uniquely in terms of $\left(\begin{smallmatrix} \lambda_3 \\ 0 \end{smallmatrix} \middle| \begin{smallmatrix} \lambda_2 & \lambda_1 \\ \mathbf{n}_2 & 0 \end{smallmatrix} \right)$. Indeed, it is not hard to see (see Appendix B for further details) that one can use equations (7.2.18) to derive a recursion relation expressing $\left(\begin{smallmatrix} \lambda_3 \\ 0 \end{smallmatrix} \middle| \begin{smallmatrix} \lambda_2 & \lambda_1 \\ \mathbf{n}_2 & \mathbf{n}_1 \end{smallmatrix} \right)$ with $\mathbf{n}_1 = [-s_1 e_1 - s_2 e_2, k_1]$ in terms of the CGC $\left(\begin{smallmatrix} \lambda_3 \\ 0 \end{smallmatrix} \middle| \begin{smallmatrix} \lambda_2 & \lambda_1 \\ \mathbf{m}_2 & \mathbf{m}_1 \end{smallmatrix} \right)$ having $\mathbf{m}_1 = [-s'_1 e_1 - s'_2 e_2, k'_1]$ with $s'_1 + s'_2 = s_1 + s_2 - 1$.

The value of $\left(\begin{smallmatrix}\lambda_3\\0\end{smallmatrix}\middle|\begin{smallmatrix}\lambda_2&\lambda_1\\\mathbf{n}_2&0\end{smallmatrix}\right)$ is not further constrained by (7.2.18). A basis for the space of CG maps $\mathsf{C}^{\lambda_1\lambda_2}_{\lambda_3}$ is therefore obtained from the CGC $\left(\begin{smallmatrix}\lambda_3\\\mathbf{n}_3\end{smallmatrix}\middle|\begin{smallmatrix}\lambda_2&\lambda_1\\\mathbf{n}_2&\mathbf{n}_1\end{smallmatrix}\right)_k$ characterised by the property that

$$\left(\begin{smallmatrix}\lambda_3\\0\end{smallmatrix}\middle|\begin{smallmatrix}\lambda_2&\lambda_1\\\mathbf{n}_2&0\end{smallmatrix}\right)_k = \delta_{k,k_2}, \quad \text{if} \quad \mathbf{n}_2 = [\delta_2, k_2], \quad \delta_2 = \lambda_3 - \lambda_1 - \lambda_2\ . \tag{7.2.19}$$

As k_2 can only take a finite set of values determined by δ_2 we see that the coefficients $\left(\begin{smallmatrix}\lambda_3\\\mathbf{n}_3\end{smallmatrix}\middle|\begin{smallmatrix}\lambda_2&\lambda_1\\\mathbf{n}_2&\mathbf{n}_1\end{smallmatrix}\right)_k$ generate a basis for the space of CG maps. For generic weights λ_1, λ_2, λ_3 there is an isomorphism between the space of CG maps and the subspace with weight $\lambda_3 - \lambda_1$ within $\mathcal{R}_{\lambda_2}$, or equivalently the subspace with weight $\lambda_3 - \lambda_2$ within $\mathcal{R}_{\lambda_1}$.

It will be important to keep in mind that the $\left(\begin{smallmatrix}\lambda_3\\0\end{smallmatrix}\middle|\begin{smallmatrix}\lambda_2&\lambda_1\\\mathbf{n}_2&\mathbf{n}_1\end{smallmatrix}\right)_k$ depend on the multiplicity labels only through the matrix elements $R^{\lambda,\mathbf{n}}_{(\mathsf{e}_i),\mathbf{n}'}$. The features concerning the dependence of $R^{\lambda,\mathbf{n}}_{(\mathsf{e}_i),\mathbf{n}'}$ on the multiplicity labels observed in (7.1.11) will be inherited. Note furthermore that the recursive procedure determining the CGC $\left(\begin{smallmatrix}\lambda_3\\0\end{smallmatrix}\middle|\begin{smallmatrix}\lambda_2&\lambda_1\\\mathbf{n}_2&\mathbf{n}_1\end{smallmatrix}\right)_k$ proceeds by induction in $s = s_1 + s_2$ if $\mathbf{n}_1 = [-s_1e_1 - s_2e_2, k_1]$. In each step one generically increases the range of values for the multiplicity label k_2 in $\mathbf{n}_2 = [\delta_2, k_2]$ with non-vanishing $\left(\begin{smallmatrix}\lambda_3\\0\end{smallmatrix}\middle|\begin{smallmatrix}\lambda_2&\lambda_1\\\mathbf{n}_2&\mathbf{n}_1\end{smallmatrix}\right)_k$ by one unit. In the case where $\mathbf{n}_1 = [-s_1e_1 - s_2e_2, k_1]$ with $s_1 + s_2 \leq 2$, for example, we find non-vanishing $\left(\begin{smallmatrix}\lambda_3\\0\end{smallmatrix}\middle|\begin{smallmatrix}\lambda_2&\lambda_1\\\mathbf{n}_2&\mathbf{n}_1\end{smallmatrix}\right)_k$ only for $k - 2 \leq k_2 \leq k$. Further details can be found in appendix C.

7.3 Iterated Clebsch-Gordan maps

Families of intertwining maps $\mathsf{C} : \bigotimes_{l=1}^{n-1} \mathcal{R}_l \to \bar{\mathcal{R}}_n$ can be constructed as compositions of the Clebsch-Gordon maps introduced in Section 7.2. For $m = 3$, for example, one may consider linear combinations of the form

$$e^{\lambda_4}_{\mathbf{n}_4}(\lambda_3, \lambda_2, \lambda_1) = \sum_{\substack{\mathbf{n}_3,\mathbf{n}_2,\mathbf{n}_1\\ \nu_4=\nu_1+\nu_2+\nu_3}} \left(\begin{smallmatrix}\lambda_4\\\mathbf{n}_4\end{smallmatrix}\middle|\begin{smallmatrix}\lambda_3&\lambda_2&\lambda_1\\\mathbf{n}_3&\mathbf{n}_2&\mathbf{n}_1\end{smallmatrix}\right) e^{\lambda_1}_{\mathbf{n}_1} \otimes e^{\lambda_2}_{\mathbf{n}_2} \otimes e^{\lambda_3}_{\mathbf{n}_3}, \tag{7.3.20}$$

One may argue in the same way as before that the coefficients in (7.3.20) are uniquely determined in terms of the particular values for $\mathbf{n}_4 = 0$ and $\mathbf{n}_1 = 0$. The space $\mathrm{CG}(\lambda_4|\lambda_3\lambda_2\lambda_1)$ of Clebsch-Gordan maps is therefore isomorphic to the subspace denoted by $\mathcal{R}^{\lambda_4-\lambda_1}_{\lambda_3,\lambda_2}$ in $\mathcal{R}_{\lambda_3} \otimes \mathcal{R}_{\lambda_2}$ with total weight $\lambda_4 - \lambda_1$. It is then easy to see that a basis for this space is provided by the composition of Clebsch-Gordan maps,

$$\left(\begin{smallmatrix}\lambda_4\\0\end{smallmatrix}\middle|\begin{smallmatrix}\lambda_3&\lambda_2&\lambda_1\\\mathbf{n}_3&\mathbf{n}_2&0\end{smallmatrix}\right)^{\lambda_{12}}_{k_3,k_2} = \sum_{\substack{\mathbf{n}_{21}\\ \nu_{12}=\lambda_1+\nu_2}} \left(\begin{smallmatrix}\lambda_4\\0\end{smallmatrix}\middle|\begin{smallmatrix}\lambda_3&\lambda_{12}\\\mathbf{n}_3&\mathbf{n}_{12}\end{smallmatrix}\right)_{k_3} \left(\begin{smallmatrix}\lambda_{12}\\\mathbf{n}_{12}\end{smallmatrix}\middle|\begin{smallmatrix}\lambda_2&\lambda_1\\\mathbf{n}_2&0\end{smallmatrix}\right)_{k_2}. \tag{7.3.21}$$

In order to see this, let us note that the allowed values of λ_{12} are of the form $\lambda_{12} = \lambda_1 + \lambda_2 - \delta_{12}$. The coefficients (7.3.21) represent the matrix elements of a map $\mathsf{D}^{\lambda_4}_{\lambda_3\lambda_2\lambda_1}$ from $\mathrm{CG}(\lambda_4|\lambda_3\lambda_2\lambda_1)$ into $\mathcal{R}^{\lambda_4-\lambda_1}_{\lambda_3,\lambda_2}$.

7.4 R-matrix

A *quasitriangular* Hopf algebra $\mathcal{U}$ additionally has an invertible element $\mathsf{R} \in \mathcal{U} \otimes \mathcal{U}$, the universal R-matrix of $\mathcal{U}$, which satisfies a set of relations. The quantum group $\mathcal{U}_q(\mathfrak{sl}_N)$ is a

quasitriangular Hopf algebra. Its universal R-matrix $\mathsf{R} \in \mathcal{U}_q(\mathfrak{sl}_N) \otimes \mathcal{U}_q(\mathfrak{sl}_N)$ has the property

$$\mathsf{R}\Delta(x)\mathsf{R}^{-1} = (\mathsf{P} \circ \Delta)(x) \,, \qquad x \in \mathcal{U}_q(\mathfrak{sl}_N) \,, \tag{7.4.22}$$

where $\mathsf{P} \in \mathcal{U}_q(\mathfrak{sl}_N) \otimes \mathcal{U}_q(\mathfrak{sl}_N)$ is the permutation that acts as $\mathsf{P}(x \otimes y) = y \otimes x$. It satisfies the Yang-Baxter equation $\mathsf{R}_{12}\mathsf{R}_{13}\mathsf{R}_{23} = \mathsf{R}_{23}\mathsf{R}_{13}\mathsf{R}_{12}$ and the action of the co-product on it is

$$(\Delta \otimes 1)\mathsf{R} = \mathsf{R}_{13}\mathsf{R}_{23} \,, \qquad (1 \otimes \Delta)\mathsf{R} = \mathsf{R}_{13}\mathsf{R}_{12} \,. \tag{7.4.23}$$

It can be shown that the conditions (7.4.22) have a unique solution of the form $\mathsf{R} = q^t\bar{\mathsf{R}}$ with $t = \sum_{ij}(\kappa_{ij}^{-1})\mathsf{h}_i \otimes \mathsf{h}_j$, with κ_{ij} being the Cartan matrix, $\mathsf{k}_i = q^{\mathsf{h}_i}$ and

$$\bar{\mathsf{R}} = 1 + (q - q^{-1})(\mathsf{e}_1 \otimes \mathsf{f}_1 + \mathsf{e}_2 \otimes \mathsf{f}_2 - q^{-1}\mathsf{e}_{12} \otimes \mathsf{f}_{12}) + (q - q^{-1})^2\mathsf{e}_2\mathsf{e}_1 \otimes \mathsf{f}_2\mathsf{f}_1 + \dots \tag{7.4.24}$$

for $N = 3$.[1] The omitted terms in the expression (7.4.24) are of higher order in e_i, $i = 1, 2$. The universal R-matrix is related to the braid matrices $\mathsf{B}_{\lambda_1\lambda_2} : \mathcal{R}_{\lambda_1} \otimes \mathcal{R}_{\lambda_2} \to \mathcal{R}_{\lambda_2} \otimes \mathcal{R}_{\lambda_1}$ through

$$\mathsf{B}_{\lambda_1\lambda_2} = \mathsf{P} \circ \mathsf{r}_{\lambda_1\lambda_2}, \quad \text{where} \quad \mathsf{r}_{\lambda_1\lambda_2} = (\pi_{\lambda_1} \otimes \pi_{\lambda_2})(\mathsf{R}) \tag{7.4.27}$$

is the evaluation of the universal R-matrix in the tensor product of representations $\mathcal{R}_{\lambda_1} \otimes \mathcal{R}_{\lambda_2}$ and P is the permutation of tensor factors. Our notation for the matrix elements of $\mathsf{B}_{\lambda_1\lambda_2}$ is defined such that

$$\mathsf{B}_{\lambda_1\lambda_2}\, e^{\lambda_1}_{\mathbf{n}_1} \otimes e^{\lambda_2}_{\mathbf{n}_2} = \sum_{\mathbf{m}_1,\mathbf{m}_2} (B_{\lambda_1\lambda_2})^{\mathbf{m}_1\,\mathbf{m}_2}_{\mathbf{n}_1\,\mathbf{n}_2} e^{\lambda_2}_{\mathbf{m}_2} \otimes e^{\lambda_1}_{\mathbf{m}_1} \,. \tag{7.4.28}$$

The existence of the braiding map, which is a morphism of Rep$\mathcal{U}$, turns this into a braided monoidal category.

7.5 Twisted (compositions of) Clebsch-Gordan maps

A key element which will be required to demonstrate the isomorphism $\mathcal{A}_{\text{flat}} \simeq \mathcal{A}_V$ between quantised algebras of functions on moduli spaces of flat connections and algebras of Verlinde operators for $\mathfrak{sl}_N$ Toda CFT in Chapter 10 is represented by twisted compositions of Clebsch-Gordan maps. We discuss such compositions below.

Two quasitriangular Hopf algebras $\mathcal{U}$ and $\tilde{\mathcal{U}}$ are related by a Drinfeld twist $\mathcal{J} \in \mathcal{U} \otimes \mathcal{U}$ if the co-products and R-matrices are related by

$$\tilde{\Delta}(\cdot) = \mathcal{J}^{-1}\Delta(\cdot)\mathcal{J}, \qquad \tilde{\mathsf{R}}_{12} = \mathcal{J}_{21}^{-1}\mathsf{R}_{12}\mathcal{J}_{12} \,. \tag{7.5.29}$$

[1] The expression for general N is

$$\mathsf{R} = q^t\, \mathrm{e}^{(q-q^{-1})\mathsf{e}_2\otimes\mathsf{f}_2}_{q^{-2}}\, \mathrm{e}^{(q^{-2}-1)\mathsf{e}_{12}\otimes\mathsf{f}_{12}}_{q^{-2}}\, \mathrm{e}^{(q-q^{-1})\mathsf{e}_1\otimes\mathsf{f}_1}_{q^{-2}} \,, \tag{7.4.25}$$

with exponentials defined through

$$\mathrm{e}^x_q = \sum_{n=0}^{\infty} \frac{x^n}{[n]!} \,, \qquad [n] = \frac{1 - q^{2n}}{1 - q^2} \,. \tag{7.4.26}$$

Here we are using leg-numbering notation where the subscripts refer to tensor factors. The twist will preserve co-associativity if

$$(\Delta \otimes \mathrm{id})(\mathcal{J}) \cdot \mathcal{J}_{12} \;=\; (\mathrm{id} \otimes \Delta)(\mathcal{J}) \cdot \mathcal{J}_{23}\,, \tag{7.5.30}$$

The action of $\mathcal{J}$ may be extended to m-fold tensor products by defining recursively

$$\mathcal{J}^{(k+1)} := (\mathrm{id}^{\otimes(k-1)} \otimes \Delta)(\mathcal{J}^{(k)}) \cdot (\mathrm{id}^{\otimes(k-1)} \otimes \mathcal{J})\,, \qquad \mathcal{J}^{(2)} := \mathcal{J}\,. \tag{7.5.31}$$

The condition (7.5.30) ensures that the operator

$$J^{(m)}_{V_1 \otimes \cdots \otimes V_m} := (\pi_{V_1} \otimes \cdots \otimes \pi_{V_m})(\mathcal{J}^{(m)})\,, \tag{7.5.32}$$

is independent of the order in which tensor products are taken.

Given a Clebsch-Gordan map $C^U_{VW} : V \otimes W \to U$ we may define [77]

$$\tilde{C}^U_{VW} := C^U_{VW} \cdot J_{VW}\;, \qquad J_{VW} := (\pi_V \otimes \pi_W)(\mathcal{J})\,. \tag{7.5.33}$$

It is easy to see that $\tilde{C}^U_{VW}$ is a Clebsch-Gordan map intertwining the representation defined on $V \otimes W$ using the twisted co-product $\tilde{\Delta}$ with the representation U. Similarly, by defining $\tilde{C}^{VW}_U := J^{-1}_{VW} C^{VW}_U$ one can show that $\tilde{C}^{VW}_U \pi_U(x) = (\pi_V \otimes \pi_W)\tilde{\Delta}(x)\tilde{C}^{VW}_U$.

Given a general intertwining map $C : V_1 \otimes \ldots \otimes V_m \to W_1 \otimes \ldots \otimes W_n$ it seems natural to define

$$\tilde{C} := (J^{(n)}_{W_1 \otimes \ldots \otimes W_n})^{-1} \cdot M \cdot J^{(m)}_{V_1 \otimes \ldots \otimes V_m}\,. \tag{7.5.34}$$

If M is represented as the composition of "more elementary" Clebsch-Gordan maps one needs to verify the consistency of definition (7.5.34) with (7.5.33). This boils down to the consideration of two cases, as will be discussed in the following.

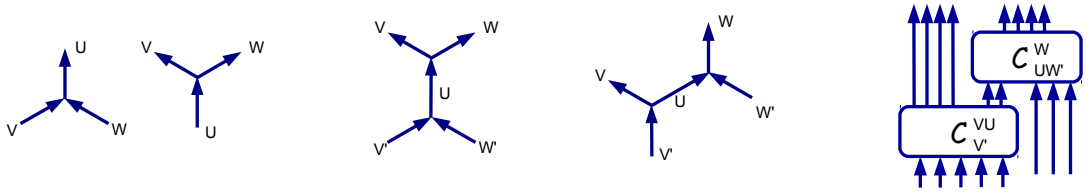

Figure 7.2: Left*: Clebsch-Gordan maps.* Middle*: Glued vertices.* Right*: Generic network.*

Twisting composite intertwiners (I): Let $C^{UVW}_T : T \to U \otimes V \otimes W$ be constructed as $C^{UV}_S C^{SW}_T$. This composition may be re-expressed in terms of $\tilde{C}^{UV}_S \tilde{C}^{SW}_T$ by using

$$C^{UV}_S C^{SW}_T = C^{UV}_S J_{SW} J^{-1}_{SW} C^{SW}_T = C^{UV}_S J_{SW} \tilde{C}^{SW}_T\;. \tag{7.5.35}$$

Decomposing $J_{SW} = \sum_k \pi_S(x_k) \otimes \pi_W(x^k)$, one may use the intertwining property satisfied by C^{UV}_S to calculate

$$\begin{aligned} C^{UV}_S\, J_{SW} &= C^{UV}_S \cdot \sum_k \pi_S(x_k) \otimes \pi_W(x^k) = \\ &= \sum_k (\pi_U \otimes \pi_V)(\Delta(x_k)) \otimes \pi_W(x^k) \cdot C^{UV}_S \;=\; J_{(U \otimes V) \otimes W}\, C^{UV}_S\;. \end{aligned}$$

Noting that $C_S^{UV} = J_{UV}\tilde{C}_S^{UV}$, we arrive at

$$C_S^{UV}C_T^{SW} = J_{(U\otimes V)\otimes W}J_{UV}\tilde{C}_S^{UV}\tilde{C}_T^{SW} \ . \tag{7.5.36}$$

In a similar way one may verify that $C_S^{VW}C_T^{US} = J_{U\otimes(V\otimes W)}J_{VW}\tilde{C}_S^{VW}\tilde{C}_T^{US}$.

Twisted compositions (II): Clebsch-Gordan maps of the type C_U^{VW} and C_{VW}^U can also be composed in the following ways

$$C_{V'W'}^{VW} := C_U^{VW}C_{V'W'}^U \quad , \quad C_{V'W'}^{VW} := C_{UW'}^W C_{V'}^{VU} \ . \tag{7.5.37}$$

The second type of composition is diagrammatically represented in Figure 7.2.

Recall that the representations π_V, $\pi_U, \ldots$ are not necessarily irreducible. As such, the blocks in Figure 7.2 should themselves be thought of as networks with a general number of incoming and outgoing legs and iterated compositions of Clebsch-Gordan maps inside each block. Compositions of the first type in equation (7.5.37) are twisted trough

$$\tilde{N}_{V'W'}^{VW} = \tilde{C}_U^{VW}\tilde{C}_{V'W'}^U = J_{VW}^{-1}C_U^{VW}C_{V'W'}^U J_{V'W'} \ . \tag{7.5.38}$$

Compositions of the second type

$$\hat{N}_{V'W'}^{VW} = C_{UW'}^W C_{V'}^{VU} = \tilde{C}_{UW'}^W J_{UW'}^{-1}J_{VU}\tilde{C}_{V'}^{VU} \tag{7.5.39}$$

also transform by conjugation with the J-factors of equation (7.5.38). To show that $\hat{N}_{V'W'}^{VW}$ is twisted by acting on its free legs as

$$\hat{N}_{V'W',\text{twist}}^{VW} = J_{VW}^{-1}\hat{N}_{V'W'}^{VW}J_{V'W'} \ , \tag{7.5.40}$$

we insert the identity in (7.5.39)

$$\hat{N}_{V'W',\text{twist}}^{VW} = J_{VW}^{-1}C_{UW'}^W J_{V(U\otimes W')}J_{V(U\otimes W')}^{-1}J_{(V\otimes U)W'}J_{(V\otimes U)W'}^{-1}C_{V'}^{VU}J_{V'W'} \ .$$

$J_{V(U\otimes W')}$ and $J_{(V\otimes U)W'}^{-1}$ can be shifted past $C_{UW'}^W$ and $C_{V'}^{VU}$ to cancel J_{VW}^{-1} and $J_{V'W'}$

$$C_{UW'}^W J_{V(U\otimes W')} = C_{UW'}^W \sum_k \pi_V(x_k)\otimes(\pi_U\otimes\pi_{W'})\Delta(x^k) = \sum_k \pi_V(x_k)\otimes\pi_W(x^k)C_{UW'}^W \ ,$$

where $\sum_k \pi_V(x_k)\otimes\pi_W(x^k)C_{UW'}^W = J_{VW}C_{UW'}^W$ and similatly for $J_{(V\otimes U)W'}^{-1}$. So we find

$$\hat{N}_{V'W',\text{twist}}^{VW} \ = \ C_{UW'}^W J_{V(U\otimes W')}^{-1}J_{(V\otimes U)W'}C_{V'}^{VU} = \tilde{C}_{UW'}^W J_{UW'}^{-1}J_{V(U\otimes W')}^{-1}J_{(V\otimes U)W'}J_{VU}\tilde{C}_{V'}^{VU} \ .$$

By the cocycle condition (7.5.30) $J_{UW'}^{-1}J_{V(U\otimes W')}^{-1}J_{(V\otimes U)W'}J_{VU}$ reduces to the identity evaluated on the tensor product of modules $V\otimes U\otimes W'$ and

$$\hat{N}_{V'W',\text{twist}}^{VW} = \tilde{C}_{UW'}^W\tilde{C}_{V'}^{VU} \tag{7.5.41}$$

as claimed. Therefore general networks $\hat{N}_{V'W'}^{VW}$, constructed as iterated compositions of Clebsch-Gordan maps, are twisted by J-factors which act only on their external free legs.

Chapter 8

Free-field construction of chiral vertex operators

With the preliminary notions of conformal field theory in Chapter 6 and the quantum group theoretic background from Chapter 7 on hand, we will now describe how to define the chiral vertex operators (CVOs) precisely in order to compute the monodromies resulting from the analytic continuation of the location of a degenerate chiral vertex operator around the support of a generic CVO. One needs to specify a suitable set of contours for the integration of screening currents in order to complete the construction of the chiral vertex operators. Monodromies may then be calculated by deforming the contours appropriately. The main goal of this chapter, as well as the next, will be to derive the claims about the structure of the quantum monodromy matrices formulated at the end of Chapter 6. Consequences of these results for the relations to moduli spaces of flat connections will be explained in chapters 10 and 12 below.

The approach described below is inspired by the works [115], [116] where the connection between the free field representation of the Virasoro algebra and the quantum group $\mathcal{U}_q(\mathfrak{sl}_2)$ was investigated. Relations between free field representations of other conformal field theories and quantum groups of higher ranks have been studied in [117], [118], [119]. However, the aims and scope of these works are different from ours, making it difficult to extract the results relevant for us from the references above. We therefore give a self-contained treatment below.

8.1 Basic definitions

There is a useful way to construct chiral vertex operators in terms of the free fields $\varphi_j(z)$ in equation (6.1.2), where the basic building blocks are the normal-ordered exponential fields $V_\alpha(z)$ defined in equation (6.4.32). The normal-ordered exponentials represent operators on $\mathcal{M} \equiv \mathcal{F} \otimes L^2(\mathbb{R}^{N-1})$ for $\mathrm{Re}(z) > 0$, $\mathcal{F}$ being the Fock space generated by the oscillators a_n^i. Representing the momenta p_j as multiplication operators on $L^2(\mathbb{R}^{N-1})$ leads to a representation of the operators $\mathrm{e}^{(\alpha,q)}$ appearing in (6.4.32) as finite difference operators on functions $\psi(p)$. For our goals it will often suffice to adopt the closely related definition of the operators $\mathrm{e}^{(\alpha,q)}$ as formal shift operators mapping the highest-weight vector $v_\beta \in \mathcal{V}_\beta$ to $v_{\beta+\alpha} \in \mathcal{V}_{\alpha+\beta}$. The fields

$V_\alpha(z)$ may then be identified with the chiral primary fields $V^{(\beta+\alpha,\alpha,\beta)}(z)$ for the algebra $\mathcal{W}_N$ via

$$V_\alpha(z)v_\beta = z^{\Delta_\alpha}V^{(\beta+\alpha,\alpha,\beta)}(z)v_\beta\,, \qquad v_\beta \in \mathcal{V}_\beta\,. \tag{8.1.1}$$

An important role is furthermore played by the screening charges $Q_i(\gamma) = \int_\gamma dz S_i(z)$ which were defined in equation (6.4.34), where the contour γ begins at a base-point z_0 and encircles the position z in the counter-clockwise direction.

Powers of the screening charges like $Q_i^n(z) \equiv (Q_i(z))^n$ make sense as unbounded self-adjoint operators on $\mathcal{M}$ if the power n is sufficiently small compared to b^{-2}. Higher powers can be defined by analytic continuation in b^2, and the result can be represented explicitly using suitable modifications of the contours of integration in (6.4.34). The key property of the screening charges $Q_i(z)$ follows from the fact that the commutator of the fields $S_i(z)$ with the generators of the $\mathcal{W}_N$-algebra can be represented as a total derivative. This implies that the screening charges commute with the generators $W_{d,k}$.

More general primary fields can therefore be constructed by multiplying normal-ordered exponentials with monomials formed out of the screening charges. In the case $N = 2$ one may consider composite fields of the form $V_s^\alpha(z) = Q^s(\gamma)V_\alpha(z)$, $s \in \mathbb{Z}_{\geq 0}$. For $N = 3$ one could consider, more generally, fields of the form $Q_1^{s_1}Q_2^{s_2}Q_1^{s_3}Q_2^{s_4}\cdots V_\alpha$. We should note, however, that there exist many linear relations among these fields, as follows from the fact that the screening charges Q_i satisfy the Serre relations of the quantum group $\mathcal{U}_q(\mathfrak{sl}_N)$ [118],

$$Q_i^2Q_j = (q+q^{-1})Q_iQ_jQ_i - Q_jQ_i^2\,, \qquad \text{with} \quad |i-j| = 1\,. \tag{8.1.2}$$

Using these relations it is elementary to show that in the case $N = 3$ arbitrary screened vertex operators can be expressed as linear combinations of

$$V_{\mathbf{s}}^\alpha(z) = Q_1^{s_1-k}(\gamma)Q_{12}^k(\gamma)Q_2^{s_2-k}(\gamma)V_\alpha(z)\,, \tag{8.1.3}$$

where $\mathbf{s} = (s_1, s_2, k)$, and

$$Q_{12}(\gamma) = Q_1Q_2 - qQ_2Q_1 = (1-q^2)\int_\gamma \mathrm{d}z \int_{<z} \mathrm{d}z' S_1(z)S_2(z')\,. \tag{8.1.4}$$

Indeed, the relations (8.1.2) can be rewritten as

$$Q_1Q_{12} \;=\; q^{-1}Q_{12}Q_1\,, \qquad Q_2Q_{12} = qQ_{12}Q_2\,. \tag{8.1.5}$$

By making repeated use of these relations together with[1]

$$Q_1Q_2^n = q^nQ_2^nQ_1 + [n]_qQ_2^{n-1}Q_{12}\,, \tag{8.1.6}$$

we can then express an arbitrary product of charges $Q_1^{s_1}Q_2^{s_2}Q_1^{s_3}Q_2^{s_4}\cdots$ as linear combination of monomials of the form $Q_1^{s_1-k}Q_{13}^kQ_2^{s_2-k}$, reducing any screened vertex operator to (8.1.3).

By using the screened vertex operators $V_{\mathbf{s}}^\alpha$ one may represent more general chiral vertex operators via

$$V_{\mathbf{s}}^\alpha(z)v_\beta = z^{\Delta_\alpha}V_k^{(\beta',\alpha,\beta)}(z)v_\beta\,, \qquad \text{with} \quad \beta' = \beta+\alpha+b(s_1e_1+s_2e_2)\,. \tag{8.1.7}$$

[1]Here we are using $[n]_q \equiv \frac{q^n-q^{-n}}{q-q^{-1}} = q^{n-1}+q^{n-3}+\cdots+q^{-n+1}$.

It is furthermore important to note that the difference between β' and β is independent of the parameter k in (8.1.3). By varying k one may therefore define via (8.1.7) an infinite family of chiral vertex operators $V_k^{(\beta',\alpha,\beta)}(z)$ intertwining between the same two representations β' and β. The correspondence (6.2.22) between chiral vertex operators and conformal blocks on the three-punctured sphere associates with each chiral vertex operator $V_k^{(\beta',\alpha,\beta)}(z)$ a conformal block $f_k \in \mathrm{CB}(\mathcal{C}_{0,3})$. It seems plausible that the conformal blocks f_k generate a basis for the physically relevant subspace of conformal blocks on $\mathcal{C}_{0,3}$.

Higher rank: To generalize these observations to $N > 3$ let us note that it directly follows from (8.1.2) that the space of screened vertex operators forms a module for the nilpotent subalgebra of $\mathcal{U}_q(\mathfrak{sl}_N)$, with action of the generators e_i represented by left multiplication with Q_i. One may define screening charges $Q_{ij}(z)$ associated with the generators e_{ij}, $j > i$ of $\mathcal{U}_q(\mathfrak{sl}_N)$ recursively via $Q_{ii}(\gamma) \equiv Q_i(\gamma)$ together with

$$Q_{ij}(\gamma) \;=\; Q_{ik}(\gamma)Q_{k+1\;j}(\gamma) - qQ_{k+1\;j}(\gamma)Q_{ik}(\gamma)\,, \quad 1 \leq i \leq k < j \leq N\,. \tag{8.1.8}$$

There are therefore $\frac{1}{2}(N-1)N$ screening charges Q_{ij}, $j \geq i$, in one-to-one correspondence with the positive roots of $\mathfrak{sl}_N$. More general screened vertex operators can therefore be constructed as

$$\begin{aligned} V_{\mathbf{s}}^{\alpha}(z) = \big[Q_{11}^{s_{11}}(\gamma)Q_{12}^{s_{12}}(\gamma)\cdots Q_{1\;N-1}^{s_{1\;N-1}}(\gamma)\big] \times \cdots \\ \times \big[Q_{22}^{s_{22}}(\gamma)\cdots Q_{2\;N-1}^{s_{2\;N-1}}(\gamma)\big] \times \cdots \times \big[Q_{N-1\;N-1}^{s_{N-1\;N-1}}(\gamma)\big]\, V_\alpha(z)\,, \end{aligned} \tag{8.1.9}$$

where $\mathbf{s} = \{s_{ij}; i \leq j\}$. Different ordering prescriptions for the positive roots of $\mathfrak{sl}_N$ will correspond to different bases in the space of conformal blocks on $\mathcal{C}_{0,3}$. Since physical correlation functions in Toda CFT can however not depend on such choices, this invariance may represent a supplement to the crossing symmetry conditions exploited in the conformal bootstrap approach which may be potentially useful.

The space of screened vertex operators thus constructed may be extended to a module for the Borel-subalgebra of $\mathcal{U}_q(\mathfrak{sl}_N)$ with generators h_i and e_i by identifying h_i with the adjoint action of $-\mathrm{i}p^i/b$. For general α one may identify the resulting module with the Verma module of $\mathcal{U}_q(\mathfrak{sl}_N)$ with weight $\omega_\alpha = -\alpha/b$. The observations above imply a relation between screened vertex operators and representations of $\mathcal{U}_q(\mathfrak{sl}_N)$ on the level of vector spaces. This relation will be strengthened considerably below.

As before one may use the screened vertex operators $V_{\mathbf{s}}^{\alpha}(z)$ to define chiral vertex operators via the obvious generalization of (8.1.7) to $N > 3$. Fixing the difference $\beta' - \beta$ defines a subspace in the space of parameters $\mathbf{s}$ of dimension $\frac{1}{2}(N-1)(N-2)$. This dimension coincides with half of the dimension of the moduli space of flat connections on $\mathcal{C}_{0,3}$, which was previously found to be equal to the dimension of the space of parameters labeling inequivalent elements in $\mathrm{CB}(\mathcal{C}_{0,3})$. This observation raises our hopes that the screened vertex operators $V_{\alpha}^{\mathbf{s}}(\sigma)$ can indeed be used to construct bases for $\mathrm{CB}(\mathcal{C}_{0,3})$.

8.2 Conformal blocks from screened vertex operators

For the remainder of this section we will restrict the discussion to the case $N = 3$. It will be useful to represent conformal blocks as linear combinations of a family of auxiliary matrix elements of the following form

$$\left\langle v_\infty \, , \, V_{k_m}^{\rho_m}(z_m) \cdots V_{k_2}^{\rho_2}(z_2) \mathfrak{e}_{\alpha_1} \right\rangle = \sum_{\mathbf{n}_m,\ldots,\mathbf{n}_1} C\left(\begin{smallmatrix} \rho_m,\ldots,\rho_2 \\ k_m,\ldots,k_2 \end{smallmatrix}\right)_{\mathbf{n}_m,\ldots,\mathbf{n}_1} W_{\mathbf{n}_m,\ldots,\mathbf{n}_1}^{\alpha_m,\ldots,\alpha_1}(z_m,\ldots,z_2,0), \quad (8.2.10)$$

where $\rho_l = (\beta_l, \alpha_l, \beta_{l-1})$ for $l = 2, \ldots, m$, $\beta_m = \alpha_\infty$ and $v_\infty \in \mathcal{F}_{\alpha_\infty}$, both for the purpose of defining chiral vertex operators and for the computation of monodromies that result from the analytic continuation of the location of a degenerate chiral vertex operator around the support of a generic chiral vertex operator. The functions $W_{\mathbf{n}_m,\ldots,\mathbf{n}_1}^{\alpha_m,\ldots,\alpha_1}(z_m,\ldots,z_1)$ in (8.2.10) are defined as multiple integrals

$$\begin{aligned} W_{\mathbf{n_m},\ldots,\mathbf{n_1}}^{\alpha_m,\ldots,\alpha_1}(z_m,\ldots,z_1) = \quad (8.2.11) \\ = \int_{\check{\Gamma}} d\mathbf{y}_m \ldots d\mathbf{y}_1 \left\langle v_\infty \, , \, \mathbf{S}_m^{\mathbf{n}_m}(\mathbf{y}_m) V_{\alpha_m}(z_m) \ldots \mathbf{S}_1^{\mathbf{n}_1}(\mathbf{y}_1) V_{\alpha_1}(z_1) \mathfrak{e}_0 \right\rangle, \end{aligned}$$

over the contours $\check{\Gamma} = \Gamma_m^{\mathbf{n}_m} \times \ldots \times \Gamma_1^{\mathbf{n}_1}$ depicted in Figure 8.1. The crosses in Figure 8.1 indicate normalisation points on the contour $\check{\Gamma}$ where the multi-valued integrand in (8.2.11) is real if $z_r \in \mathbb{R}^+$, $r = 2, \ldots, m$, and $0 < z_2 < \cdots < z_m$. We are using the notations $\mathbf{n}_l = (n_{l,1}, n_{l,12}, n_{l,2})$ for $l = 1, \ldots, m$, and

$$\mathbf{S}_l^{\mathbf{n}_l}(\mathbf{y}_l) := S_1(y_{1,1}^{(l)}) \ldots S_1(y_{1,n_{l,1}}^{(l)}) S_{12}(y_{12,1}^{(l)}) \ldots S_{12}(y_{12,n_{l,12}}^{(l)}) S_2(y_{2,1}^{(l)}) \ldots S_2(y_{2,n_{l,2}}^{(l)}), \quad (8.2.12)$$

and assume that

$$\alpha_\infty = \sum_{l=1}^{m} (\alpha_i + b(n_{l,1} + n_{l,12})e_1 + b(n_{l,2} + n_{l,12})e_2). \quad (8.2.13)$$

The contours used to define the composite screening currents $S_{12}(y)$ in (6.4.35) should be chosen such that the only singular point of the integrand in (8.2.11) encircled by γ_y is the point y.

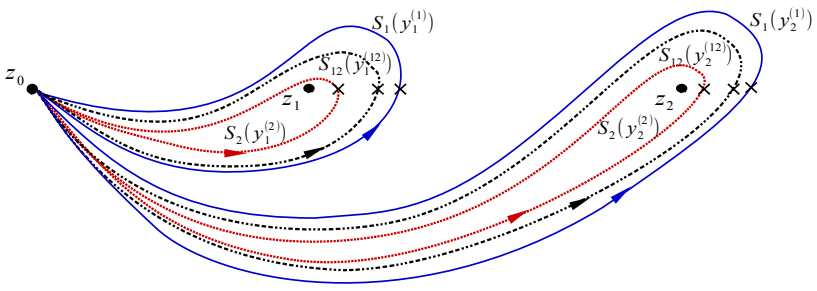

Figure 8.1: *Nested non-intersecting and non-self-intersecting multi-contours for integration over screening currents associated with different vertex operators. The multi-contours around a puncture and which are associated with a particular screening charge are depicted collectively by one loop.*

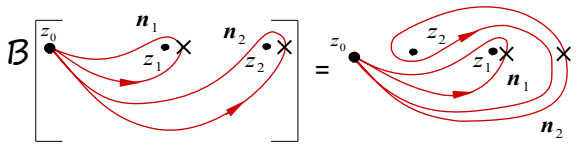

Figure 8.2: *Braiding of two generic multi-contours. The collections of contours associated with general products of screening charges are depicted here are simple loops around the punctures.*

The functions $W^{\alpha_m,\ldots,\alpha_1}_{\mathbf{n_m},\ldots,\mathbf{n_1}}$ do not by themselves represent conformal blocks, as is easily seen by the following considerations. The commutators between screening currents $S_i(z)$ and the generators of the $\mathcal{W}_3$-algebra are total derivatives with respect to the variable z. When the screening currents $S_i(z)$ are integrated over open contours as depicted in Figure 8.1, one will therefore find boundary terms in the commutators between screening charges and the generators of the $\mathcal{W}_3$-algebra supported at the base-point z_0. The boundary terms will spoil the validity of the Ward identities for the $\mathcal{W}_3$-algebra, in general.

However, we will see that the boundary terms all cancel for specific choices of the coefficients C in (8.2.10). Representing compositions of chiral vertex operators in the form (8.2.10) is useful since both the problem to find the coefficients C in (8.2.10) and the calculation of monodromies will be shown to reduce to purely algebraic problems in quantum group theory.

8.3 Braiding of screened vertex operators

The spaces of functions generated by the functions $W^{\alpha_m,\ldots,\alpha_1}_{\mathbf{n_m},\ldots,\mathbf{n_1}}(z_m,\ldots,z_1)$ introduced in (8.2.11) carry a natural action of the braid group which turns out to be related to the representation of the braid group on tensor products of quantum group representations. We will now briefly explain this first crucial link between quantum group theory and free field representation to be used in this section.

Let us consider $W^{\alpha_2\alpha_1}_{\mathbf{n_2}\mathbf{n_1}}(z_2,z_1)$ defined using the contours from Figure 8.1. The braiding operations are defined using the analytic continuation of this function with respect to z_2 and z_1 along a path exchanging their positions. This analytic continuation can be defined by integrating along suitably deformed contours as indicated in Figure 8.2. By means of contour deformations one can represent the result of this operation as a linear combination of integrals over the contours introduced in Figure 8.1.

This can be done by the following recursive procedure. In a first sequence of steps, performed in an induction over $\mathbf{n}_2 = (n_{2,1}, n_{2,21}, n_{2,2})$ one may deform the contours on the right of Figure 8.2 into linear combinations of the contours depicted in Figure 8.3

The induction step is indicated in Figure 8.4.

In a second sequence of steps one may then deform the contours surrounding both z_1 and z_2 in Figure 8.3 into a linear combination of contours surrounding only z_1 or z_2 at a time. The result of this procedure can be represented as linear combination of the original contours introduced

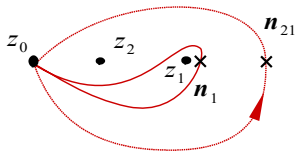

Figure 8.3: *A set of auxiliary contours for the braiding calculation.*

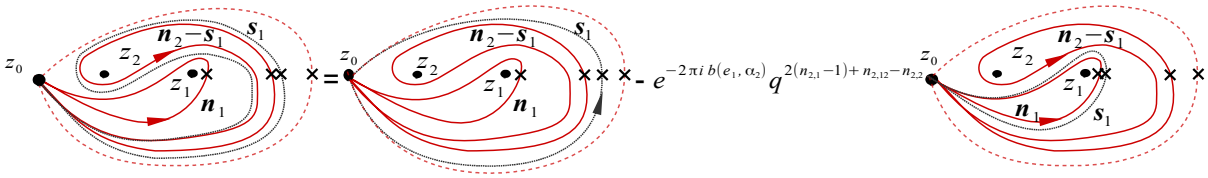

Figure 8.4: *Deformation of the outermost of the contours encircling z_2 representing a step in the passage to linear combinations of the contour depicted in Figure 8.3, where* $\mathbf{s}_1 = (1,0,0)$.

in Figure 8.1, leading to a relation of the form

$$\mathcal{B}\big(W^{\alpha_2\alpha_1}_{\mathbf{n}_2\mathbf{n}_1}(z_2,z_1)\big) = \sum_{\mathbf{m}_1,\mathbf{m}_2} (b_{\alpha_1\alpha_2})^{\mathbf{m}_1\,\mathbf{m}_2}_{\mathbf{n}_1\,\mathbf{n}_2} W^{\alpha_2\alpha_1}_{\mathbf{m}_2\mathbf{m}_1}(z_1,z_2) \tag{8.3.14}$$

We will explain in more detail in appendix D below how such computations can be done and calculate the matrix elements of $b_{\alpha_1\alpha_2}$ for the important special case where $\alpha_2 = -b\omega_1$ with α_1 generic. The result can be compared to the action of the braid group on tensor products of quantum group representations defined in (7.4.28). It turns out that the matrix $b_{\alpha_1\alpha_2}$ appearing in (8.3.14) coincides with the matrix $B_{\lambda_1\lambda_2}$ in (7.4.28) provided that $\lambda_l = -\alpha_l/b$ for $l = 1,2$. This result can easily be generalised to the cases where $\alpha_2 = -b\lambda_2$ with λ_2 being the weight of any finite-dimensional representation of $\mathcal{U}_q(\mathfrak{sl}_3)$ by noting that any finite-dimensional representation of $\mathcal{U}_q(\mathfrak{sl}_3)$ appears in the iterated tensor products of fundamental representations, and that the co-product of the quantum group has a simple representation in terms of the free field representation, as indicated in Figure 8.5 below.

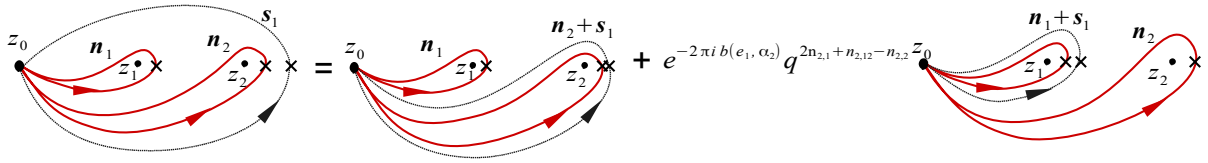

Figure 8.5: *Decomposition of a simple contour* $\mathbf{s}_1 = (1,0,0)$ *associated with the root* e_1 *around two punctures into contours enclosing only one of the punctures. This decomposition represents the co-product* $\Delta(\mathsf{f}_1) = 1 \otimes \mathsf{f}_i + \mathsf{f}_1 \otimes \mathsf{k}_1^{-1}$.

As representations of the braid group one may therefore identify the vector spaces generated by the functions $W^{\alpha_m,\ldots,\alpha_1}_{\mathbf{n}_m,\ldots,\mathbf{n}_1}(z_m,\ldots,z_1)$ with the tensor product of quantum group representations

$\bigotimes_{l=1}^{m} \mathcal{R}_{\lambda_l}$ assuming that the weights are related as $\lambda_l = -\alpha_l/b$, $l = 1, \ldots, m$.

8.4 Construction of conformal blocks

We had noted above that the functions $W^{\alpha_m,\ldots,\alpha_1}_{\mathbf{n_m},\ldots,\mathbf{n_1}}(z_m, \ldots, z_1)$ are not the objects we are ultimately interested in. They do not satisfy the Ward identities for the $\mathcal{W}_3$-algebra characterising the conformal blocks. It turns out, however, that there exist suitable linear combinations of the form (8.2.10) which will indeed represent conformal blocks. We are now going to argue that this will be the case if the coefficients C in (8.2.10) are the matrix elements of the Clebsch-Gordan (CG) maps discussed in the previous chapter, describing the embedding of the irreducible representation with weight $\lambda_\infty = -b^{-1}\alpha_\infty$ into the tensor product $\bigotimes_{l=1}^{m} \mathcal{R}_{\lambda_l}$. For $m = 3$, for example, one may get expressions of the following form

$$\begin{aligned}\langle v_\infty, V^{\rho_3}_{k_3}(z_3) V^{\rho_2}_{k_2}(z_2) \mathfrak{e}_{\alpha_1}\rangle = \\ = \sum_{\substack{\mathbf{n}_3,\mathbf{n}_2,\mathbf{n}_1,\mathbf{n}_{21} \\ \lambda_4=\nu_{12}+\nu_3 \\ \nu_{12}=\nu_1+\nu_2}} \left(\begin{smallmatrix}\lambda_4 \\ 0\end{smallmatrix}\middle|\begin{smallmatrix}\lambda_3 & \lambda_{12} \\ \mathbf{n}_3 & \mathbf{n}_{12}\end{smallmatrix}\right)_{k_3} \left(\begin{smallmatrix}\lambda_{12} \\ \mathbf{n}_{12}\end{smallmatrix}\middle|\begin{smallmatrix}\lambda_2 & \lambda_1 \\ \mathbf{n}_2 & \mathbf{n}_1\end{smallmatrix}\right)_{k_2} W^{\alpha_3,\alpha_2,\alpha_1}_{\mathbf{n}_3,\mathbf{n}_2,\mathbf{n}_1}(z_3, z_2, 0),\end{aligned} \tag{8.4.15}$$

where $\rho_2 = (\alpha_{21}, \alpha_2, \alpha_1)$ and $\rho_3 = (\alpha_\infty, \alpha_3, \alpha_{21})$ with $\alpha_{21} = -b\lambda_{21}$. Note that the summations in (8.4.15) include summations over the multiplicity labels of $\mathbf{n}_3$, $\mathbf{n}_2$, $\mathbf{n}_1$ and $\mathbf{n}_{21}$ together with a summation over two out the three weights ν_1, ν_2 and ν_3.

8.4.1 Relation to quantum group theory

In order to see the relation between the problem to find linear combinations of the form (8.2.10) representing conformal blocks and the Clebsch-Gordan problem one needs to notice that the boundary terms appearing in the commutators of the screening charges with the generators of the algebra $\mathcal{W}_3$ turn out to be related to the action of the generators e_i on tensor products of quantum group representations defined by means of the co-product. In order to formulate a more precise statement, let us introduce some useful notations. Let

$$V^{\alpha_m,\ldots,\alpha_1}_{\mathbf{n}_m,\ldots,\mathbf{n}_1}(z_m, \ldots, z_1) = \int_{\check{\Gamma}} d\mathbf{y}_m \ldots d\mathbf{y}_1 \; \mathbf{S}^{\mathbf{n}_m}_m(\mathbf{y}_m) V_{\alpha_m}(z_m) \ldots \mathbf{S}^{\mathbf{n}_1}_1(\mathbf{y}_1) V_{\alpha_1}(z_1) \tag{8.4.16}$$

be the operator appearing in the matrix elements (8.2.11) defining the functions $W^{\alpha_m,\ldots,\alpha_1}_{\mathbf{n_m},\ldots,\mathbf{n_1}}$. The correspondence with vectors in tensor products of quantum group representations observed above can be schematically represented as

$$V^{\alpha_m,\ldots,\alpha_1}_{\mathbf{n}_m,\ldots,\mathbf{n}_1} \quad \leftrightarrow \quad e^{\lambda_1}_{\mathbf{n}_1} \otimes \ldots \otimes e^{\lambda_m}_{\mathbf{n}_m} \,, \tag{8.4.17}$$

allowing us to introduce the notation

$$\big(\Delta(x) V^{\alpha_m,\ldots,\alpha_1}_{\mathbf{n}_m,\ldots,\mathbf{n}_1}\big)(z_m, \ldots, z_1) \tag{8.4.18}$$

for the vertex operator associated to $\Delta(x) e^{\lambda_1}_{\mathbf{n}_1} \otimes \ldots \otimes e^{\lambda_m}_{\mathbf{n}_m}$ for $x \in \mathcal{U}_q(\mathfrak{sl}_3)$ via the correspondence (8.4.17). In the computation of the commutator of the vertex operators $V^{\alpha_m,\ldots,\alpha_1}_{\mathbf{n}_m,\ldots,\mathbf{n}_1}$ with the

generators of the algebra $\mathcal{W}_3$ one may distinguish terms from the commutators of the screening currents from the terms coming from commutators with other exponential fields. The contribution of the former is then found to be a linear combination of terms which are proportional to $(\Delta(\mathsf{e}_i)V^{\alpha_m,\ldots,\alpha_1}_{\mathbf{n}_m,\ldots,\mathbf{n}_1})(z_m,\ldots,z_1)$. Considering, for example, the commutator with L_{-1} we find

$$\big[\, L_{-1}\,,\, V^{\alpha_m,\ldots,\alpha_1}_{\mathbf{n}_m,\ldots,\mathbf{n}_1}(z_m,\ldots,z_1)\,\big] = \sum_{l=1}^{m} \partial_{z_l} V^{\alpha_m,\ldots,\alpha_1}_{\mathbf{n}_m,\ldots,\mathbf{n}_1}(z_m,\ldots,z_1) + (\text{boundary terms}), \quad (8.4.19)$$

with boundary terms proportional to $(\Delta(x)V^{\alpha_m,\ldots,\alpha_1}_{\mathbf{n}_m,\ldots,\mathbf{n}_1})(z_m,\ldots,z_1)$ for

$$x = (q-q^{-1})(\mathsf{k}_1^{-1}\mathsf{e}_1 + \mathsf{k}_2^{-1}\mathsf{e}_2). \quad (8.4.20)$$

The derivation of these statements is outlined in appendix E. We conclude that the boundary terms in the commutators with generators of the algebra $\mathcal{W}_3$ will vanish if the coefficients C in (8.2.10) are taken to be the expansion coefficients of the images of highest weight vectors under the CG maps.

8.4.2 Independence of the choice of base-point

It is important to observe that the linear combinations (8.2.10) representing conformal blocks do not depend on the position of the base point z_0 indicated in Figure 8.1. Indeed, the derivative of $W^{\alpha_m,\ldots,\alpha_1}_{\mathbf{n_m},\ldots,\mathbf{n_1}}$ with respect to z_0 yields boundary terms which cancel in the linear combinations (8.2.10) by the same arguments as used above.

The independence of z_0 can be used for our advantage in two ways. One may note, on the one hand, that the expressions for conformal blocks resulting from (8.2.10) can be replaced by expressions where different base points z_0 are associated to each individual CG coefficient appearing in expressions like (8.4.15). In (8.4.15), for example, one could have a base-point z_0 for the integrations with screening numbers $\mathbf{n}_1$ and $\mathbf{n}_2$, and another base-point z_0' for those with screening numbers $\mathbf{n}_{12}$ and $\mathbf{n}_3$, as depicted in Figure 8.6. In this form it is manifest that the conformal blocks defined via (8.4.15) factorise into three point conformal blocks, as they should. This representation furthermore exhibits clearly the relation between the intermediate representation $\mathcal{V}_{\alpha_{12}}$ of the algebra $\mathcal{W}_3$ appearing in the conformal blocks on the left side of (8.4.15) and the intermediate representation $\mathcal{R}_{\lambda_{12}}$ appearing in the Clebsch-Gordan coefficients on the right side of (8.4.15), with representation labels related by $\alpha_{12} = -b\lambda_{12}$.

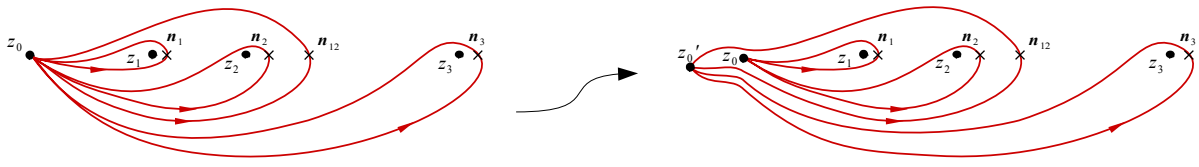

Figure 8.6: *Different base points z_0 and z_0' associated with different integration contours.*

If, furthermore, the components of α_1 are sufficiently negative, one may simplify the expression (8.4.15) by taking the limit where the base-point z_0 used in the definition of the contours

approaches z_1. Taking into account (7.2.19) the expression (8.4.15) gets simplified to

$$\langle v_\infty, V_{k_3}^{\rho_3}(z_3)V_{k_2}^{\rho_2}(z_2)\mathfrak{e}_{\alpha_1}\rangle = \sum_{\substack{\mathbf{n}_3 \\ \nu_3+\nu_2=\lambda_4-\lambda_1}} D_{k_3k_2}^{\lambda_{12}} \left(\begin{smallmatrix} \lambda_4 \\ 0 \end{smallmatrix} \middle| \begin{smallmatrix} \lambda_3 & \lambda_2 & \lambda_1 \\ \mathbf{n}_3 & \mathbf{n}_2 & 0 \end{smallmatrix}\right) W_{\mathbf{n}_3,\mathbf{n}_2,0}^{\alpha_3,\alpha_2,\alpha_1}(z_3,z_2,0), \quad (8.4.21)$$

where $\mathbf{n}_2 = [\lambda_{12}-\lambda_1-\lambda_2, k_2]$, $\rho_2 = (\alpha_{21}, \alpha_2, \alpha_1)$ and $\rho_3 = (\alpha_\infty, \alpha_3, \alpha_{21})$ with $\alpha_{21} = -b\lambda_{21}$. The expression for the coefficients $D_{k_3,k_2}^{\lambda_{12}}$ in (8.4.21) gets simplified to

$$D_{k_3,k_2}^{\lambda_{12}} \left(\begin{smallmatrix} \lambda_4 \\ 0 \end{smallmatrix} \middle| \begin{smallmatrix} \lambda_3 & \lambda_2 & \lambda_1 \\ \mathbf{n}_3 & \mathbf{n}_2 & 0 \end{smallmatrix}\right) = \sum_{\substack{\mathbf{n}_{21} \\ \nu_{12}=\lambda_4-\nu_3}} \left(\begin{smallmatrix} \lambda_4 \\ 0 \end{smallmatrix} \middle| \begin{smallmatrix} \lambda_3 & \lambda_{12} \\ \mathbf{n}_3 & \mathbf{n}_{12} \end{smallmatrix}\right)_{k_3} . \quad (8.4.22)$$

We see that sending z_0 to z_1 is related to the projection of the tensor product $\bigotimes_{l=1}^3 \mathcal{R}_{\lambda_l}$ onto the subspace $v_{\lambda_1} \otimes \bigotimes_{l=2}^3 \mathcal{R}_{\lambda_l}$. This projection obviously commutes with the braiding operation applied to the second and third tensor factors, allowing us to simplify the computations.

It can also be useful to consider the limit where $z_0 \to z_2$, which we will do in Chapter 10. In this case one may use contours supported near the circles around the origin with radius $|z_2|$, allowing us represent the CVOs as composite operators of the form $Q_1^{n_1}(\gamma)Q_{12}^{n_{12}}(\gamma)Q_2^{n_2}(\gamma)V_{\alpha_2}(z_2)$, with the screening charges $Q_i(z) = \int_\gamma S_i(y)$ being defined by integration over $\gamma = \{y \in \mathbb{C}; |y| = |z_2|\}$ for $i = 1, 12, 2$.

Chapter 9

Computation of monodromies

Using the chiral vertex operators that we have constructed in Chapter 8, we will now explain how the connection between the free field representation and quantum group theory helps us to compute the representation of monodromies on spaces of conformal blocks. Recall from Chapter 6 that we are interested in calculating the monodromies of the conformal blocks

$$\mathcal{F}_k^\rho(y;y_0)_{\bar{\imath}\imath} = \langle\, \mathfrak{e}_{\alpha_3}\,,\, \bar{D}_{\bar{\imath}}(y_0) D_\imath(y)\, V_k^\rho(z)\, \mathfrak{e}_{\alpha_1}\rangle, \tag{9.0.1}$$

regarded as functions of y. The task can be simplified slightly by sending the base-point y_0 to infinity, reducing the problem to the computation of the monodronies of the four-point conformal blocks

$$\mathcal{G}_k^\rho(y)_\imath = \langle\, v_\infty\,,\, D_\imath(y)\, V_k^\rho(z)\, \mathfrak{e}_{\alpha_1}\rangle, \tag{9.0.2}$$

where $v_\infty \in \mathcal{V}_{\alpha_4}$ with α_4 being related to the variables α_3 and $\bar{\imath}$ in (9.0.1) as $\alpha_4 = \alpha_3 - bh_{\bar{\imath}}$.

We will therefore consider the space of conformal blocks on the four-punctured sphere $\mathcal{C}_{0,4} = \mathbb{P}^1 \setminus \{z_1 = 0, z_2 = z, z_3 = y, z_4 = \infty\}$ with representation $\mathcal{V}_{\alpha_r}$ assigned to z_r, $r = 1, \ldots, 4$. The free field representation identifies this space with the subspace of $\bigotimes_{l=1}^3 \mathcal{R}_{\lambda_l}$ with weight $\lambda_4 - \lambda_1$, assuming that $\alpha_r = -b\lambda_r$ for $r = 1, \ldots, 4$.

The fundamental group of $\mathcal{C}_{0,3} = \mathbb{P}^1 \setminus \{0, z, \infty\}$ is generated by the loops γ_0, γ_z, γ_∞ around 0, z and ∞. Since the loop $\gamma_0 \circ \gamma_z \circ \gamma_\infty$ is contractible, it suffices to compute the monodromies along two out of the three loops. The monodromy of the conformal blocks $\mathcal{G}_k^\rho(y)_\imath$ introduced in (9.0.2) around ∞ is a simple diagonal matrix. It will therefore suffice to compute the monodromy of $\mathcal{G}_k^\rho(y)_\imath$ along a loop surrounding $z_2 = z$. The free field representation introduced above relates this monodromy to

$$(\mathsf{D}^{\lambda_4}_{\lambda_1\lambda_2\lambda_3})^{-1} \cdot \mathsf{B}_{\lambda_3\lambda_2} \cdot \mathsf{B}_{\lambda_2\lambda_3} \cdot \mathsf{D}^{\lambda_4}_{\lambda_1\lambda_2\lambda_3}\,, \tag{9.0.3}$$

where D is the linear operator defined in (8.4.15), and $\mathsf{B}_{\lambda_3\lambda_2} : \mathcal{R}_{\lambda_3} \otimes \mathcal{R}_{\lambda_2} \to \mathcal{R}_{\lambda_2} \otimes \mathcal{R}_{\lambda_3}$ is the braiding operation.

As explained previously, we will mainly be interested in the case where the representation $\mathcal{R}_{\lambda_3}$ assigned to $z_3 = y$ is the fundamental representation, $\lambda_3 = \omega_1$. The simplifications resulting from $\lambda_3 = \omega_1$ will be discussed next.

9.1 Conformal blocks with degenerate fields

In the case $\lambda_3 = \omega_1$ the weight λ_{12} in (8.4.21) can only take the values $\lambda_\imath = \lambda_4 - h_\imath$, $\imath = 1, 2, 3$. The expansion (8.4.21) further simplifies to

$$\langle v_\infty, D_\imath(y) V_k^{\rho_2}(z) \mathfrak{e}_{\alpha_1} \rangle = \sum_{\jmath=1}^{3} \sum_{\substack{\mathbf{n}_3 \\ \lambda_4 = h_\jmath + \nu_2 + \lambda_1}} D_{k,0}^{\lambda_\imath} \left(\begin{smallmatrix} \lambda_4 \\ 0 \end{smallmatrix} \middle| \begin{smallmatrix} \omega_1 & \lambda_2 & \lambda_1 \\ \mathbf{d}_\jmath & \mathbf{n}_2 & 0 \end{smallmatrix} \right) W_{\delta_\jmath, \mathbf{n}_2, 0}^{-b\omega_1, \alpha_2, \alpha_1}(y, z, 0), \tag{9.1.4}$$

where $\mathbf{d}_i = [\omega_1 - h_i, 0]$, $i = 1, 2$, and $\mathbf{d}_3 = [\omega_1 - h_3, 1]$. One should also remember that $\mathbf{n}_2$ is fixed as $\mathbf{n}_2 = [\lambda_{12} - \lambda_1 - \lambda_2, k]$. Taking this constraint into account, we will in the following replace the notation $W_{\delta_\jmath, \mathbf{n}_2, 0}^{-b\omega_1, \alpha_2, \alpha_1}$ by $W_{\jmath,k}^{\alpha_4, \alpha_2, \alpha_1}$. Noting that $\nu_{12} = \lambda_4 - h_\imath$ one finds that the summation over $\mathbf{n}_{12}$ in (8.4.22) can take only the four possible values $\mathbf{s}_i = [-e_i, 0]$, $i = 1, 2$ and $[-e_{12}, \epsilon]$, $e_{12} = e_1 + e_2$, $\epsilon \in \{0, 1\}$. One may then write (9.1.4) a bit more concisely in the form

$$\langle v_\infty, D_\imath(y) V_k^{\rho}(z) e_{\alpha_1} \rangle = \sum_{\jmath=1}^{3} D_{\imath\jmath}(\lambda_4) W_{\jmath,k}^{\alpha_4, \alpha_2, \alpha_1}(z_3, z_2, z_1). \tag{9.1.5}$$

The remaining coefficients in (9.1.5) are

$$D_{ii} = 1\,, \quad D_{i+1\,i} = \left(\begin{smallmatrix} \lambda_4 \\ 0 \end{smallmatrix} \middle| \begin{smallmatrix} \omega_1 & \lambda_4 - h_{i+1} \\ \mathbf{d}_i & \mathbf{s}_i \end{smallmatrix} \right), \quad D_{31} = \sum_{\epsilon=0}^{1} \left(\begin{smallmatrix} \lambda_4 \\ 0 \end{smallmatrix} \middle| \begin{smallmatrix} \omega_1 & \lambda_4 - h_3 \\ 0 & [-e_{12}, \epsilon] \end{smallmatrix} \right). \tag{9.1.6}$$

Using the notation

$$[n] = \frac{1 - q^{2n}}{1 - q^2}\,. \tag{9.1.7}$$

the non vanishing matrix elements of D can be represented explicitly as

$$\begin{aligned}
D_{21} &= q^{-1}[-(e_1, \lambda_4)]^{-1}\,, \\
D_{32} &= q^{2(e_2, \lambda_4) - 2}\big([1 - (e_2, \lambda_4)] - [1 + (e_1, \lambda_4)]\big)\big([(e_2, \lambda_4) - 1]\mathsf{c}_{\lambda_4}^{(2)}\big)^{-1}\,, \\
D_{31} &= q^{2(e_{12}, \lambda_4) - 1}\left(1 - [1 - (e_2, \lambda_4)]\right)\big([(e_2, \lambda_4) - 1]\mathsf{c}_{\lambda_4}^{(2)}\big)^{-1}\,, \\
\mathsf{c}_{\lambda_4}^{(2)} &= q^{2 + 2(e_1, \lambda_4)}(1 + [1 - (e_{12}, \lambda_4)]) - (1 - q^2)([1 - (e_2, \lambda_4)] - [1 + (e_1, \lambda_4)]).
\end{aligned} \tag{9.1.8}$$

The derivation of these expressions is outlined in appendix C.2.

9.2 Braiding with fundamental representation

The form of the braid relations simplifies when $\lambda_2 = \omega_1$ or $\lambda_3 = \omega_1$. Let us first consider the case $\lambda_2 = \omega_1$. The braid matrix preserves weight subspaces in the tensor product. Recalling that the only allowed weights in the fundamental representation are $h_\imath$, $\imath = 1, 2, 3$ one notes that the subspace in $\mathcal{R}_{\omega_1} \otimes \mathcal{R}_\lambda$ having fixed total weight ν is spanned by vectors of the form $e_{\delta_\imath}^{\omega_1} \otimes e_{\mathbf{n}}^{\lambda}$ with weight of $e_{\mathbf{n}}^{\lambda}$ being $\nu - h_\imath$ for $\imath = 1, 2, 3$. For fixed $\imath$ one gets a subspace of $\mathcal{R}_{\omega_1} \otimes \mathcal{R}_\lambda$ isomorphic to the multiplicity space $\mathcal{M}_\lambda^{\nu - h_\imath}$. The projection of the braiding operator $\mathsf{B}_{\omega_1 \lambda} : \mathcal{R}_{\omega_1} \otimes \mathcal{R}_\lambda \to \mathcal{R}_\lambda \otimes \mathcal{R}_{\omega_1}$ onto a subspace of total weight ν can be represented by a matrix

$\mathsf{b}^+ \equiv \mathsf{b}^+(\lambda,\nu)$ of operators b^+_{ij} mapping from $\mathcal{M}_\lambda^{\nu-h_i}$ to $\mathcal{M}_\lambda^{\nu-h_j}$ for $i,j=1,2,3$. It turns out that b^+ is upper triangular. As $\dim(\mathcal{M}_{\nu-h_i}) \geq \dim(\mathcal{M}_{\nu-h_j})$ for $i<j$ one may define operators v^{-1}, k mapping $\mathcal{M}_{\nu-h_i}$ to $\mathcal{M}_{\nu-h_j}$ by picking bases $\{\mathfrak{m}_{i,k}; k=0,\dots,\dim(\mathcal{M}_{\nu-h_i})-1\}$ and $\{\mathfrak{m}_{j,k}; k=0,\dots,\dim(\mathcal{M}_{\nu-h_j})-1\}$ for $\mathcal{M}_\lambda^{\nu-h_i}$ and $\mathcal{M}_\lambda^{\nu-h_j}$, respectively, and setting

$$\mathsf{v}^{-1}\,\mathfrak{m}_{i,k} = q^k\,\mathfrak{m}_{j,k-1}, \qquad \mathsf{k}\,\mathfrak{m}_{i,k} = k\,\mathfrak{m}_{j,k}. \tag{9.2.9}$$

This allows us to represent the matrix elements b^+_{ij} of b^+ explicitly as

$$\begin{aligned}
\mathsf{b}^+_{11} &= q^{(h_1,\nu)}\,, \qquad \mathsf{b}^+_{22} = q^{(h_2,\nu+e_1)}\,, \qquad \mathsf{b}^+_{33} = q^{(h_3,\nu+e_{12})} \\
\mathsf{b}^+_{12} &= q^{(h_2,\nu+e_1)}(q-q^{-1})q^{-s_2-(e_1,\lambda)}\left(q^{1+2\mathsf{k}}[s_1-\mathsf{k}][1-s_1+s_2-\mathsf{k}+(e_1,\lambda)]+\mathsf{v}^{-1}[\mathsf{k}]\right) \\
\mathsf{b}^+_{23} &= q^{(h_3,\nu+e_{12})}(q^{-1}-q)\left([s_2-\mathsf{k}][1-s_2+\mathsf{k}+(e_2,\lambda)]q^{-(e_2,\lambda)}-\mathsf{v}^{-1}[\mathsf{k}]q^{1-2s_2+(e_2,\lambda)}\right)
\end{aligned} \tag{9.2.10}$$

and

$$\begin{aligned}
\mathsf{b}^+_{13} = q^{(h_3,\nu+e_{12})}(1-q^2)\Big(&[s_1-\mathsf{k}][s_2-\mathsf{k}][s_2-1-\mathsf{k}-(e_2,\lambda)]q^{1+4\mathsf{k}-3s_2+(e_2-e_1,\lambda)} \\
&+\mathsf{v}^{-1}[\mathsf{k}]\big([s_2-2-(e_{12},\lambda)]q^{2-2\mathsf{k}-s_2+(e_{12},\lambda)}-[s_2-\mathsf{k}]q^{-2-s_2-(e_{12},\lambda)} \\
&\qquad +[s_1-\mathsf{k}]q^{2\mathsf{k}-3s_2+(e_2-e_1,\lambda)}+[s_2-\mathsf{k}+1]q^{2\mathsf{k}-2-3s_2+(e_2-e_1,\lambda)}\big) \\
&-q^{-1}\mathsf{v}^{-2}[\mathsf{k}][\mathsf{k}-1]q^{-3s_2-(e_2-e_1,\lambda)}\Big).
\end{aligned} \tag{9.2.11}$$

In the second case $\lambda_3=\omega_1$ one may similarly represent the projection of $\mathsf{B}_{\lambda\omega_1}$ onto the subspace of weight ν by a matrix $\mathsf{b}_- \equiv \mathsf{b}_-(\nu)$ which has matrix elements

$$\begin{aligned}
\mathsf{b}^-_{11} &= q^{(h_1,\nu)}\,, \qquad \mathsf{b}^-_{22} = q^{(h_2,\nu+e_1)}\,, \qquad \mathsf{b}^-_{33} = q^{(h_3,\nu+e_{12})} \\
\mathsf{b}^-_{21} &= q^{(h_1,\nu)}(q-q^{-1})\,, \qquad \mathsf{b}^-_{32} = q^{(h_2,\nu+e_1)}(q^2-1)q^{-s_1+1}\left(\mathsf{v}q^{2\mathsf{k}}[s_1-1-\mathsf{k}]-q^{2\mathsf{k}}\right) \\
\mathsf{b}^-_{31} &= q^{(h_1,\nu)}(q-q^{-1})\mathsf{v}q^{s_1-1}\,.
\end{aligned} \tag{9.2.12}$$

A feature of particular importance for us is the fact that the braid matrix can be represented as a matrix having elements which are finite difference operators of second order in the multiplicity label. This is a direct consequence of (7.1.11) given the relation between braiding and quantum group R-matrix, as is easily seen using (7.4.24).

9.3 Form of the monodromy matrix

With both of the braid matrices b_+ and b_- explicitly derived, we now find that the matrix M_2 representing the monodromy around z_2 takes the form $M_2 = D^{-1}\mathsf{b}_-\mathsf{b}_+D$ with D being a lower triangular matrix with matrix elements acting as pure multiplication operators on the multiplicity spaces. It may be useful to note that

$$\mathsf{b}_- = \begin{pmatrix} q^{(h_1,\nu)} & 0 & 0 \\ \mathsf{b}^-_{21} & q^{(h_2,\nu+e_1)} & 0 \\ \mathsf{b}^-_{31} & \mathsf{b}^-_{32} & q^{(h_3,\nu+e_{12})} \end{pmatrix}, \qquad \mathsf{b}_+ = \begin{pmatrix} q^{(h_1,\nu)} & \mathsf{b}^+_{12} & \mathsf{b}^+_{13} \\ 0 & q^{(h_2,\nu+e_1)} & \mathsf{b}^+_{23} \\ 0 & 0 & q^{(h_3,\nu+e_{12})} \end{pmatrix},$$

We may represent $\mathsf{b}_-\mathsf{b}_+$ as

$$\mathsf{b}_-\mathsf{b}_+ = \begin{pmatrix} q^{2(h_1,\nu)} & q^{(h_1,\nu)}\mathsf{b}^+_{12} & q^{(h_1,\nu)}\mathsf{b}^+_{13} \\ q^{(h_1,\nu)}\mathsf{b}^-_{21} & q^{2(h_2,\nu+e_1)} + \mathsf{b}^-_{21}\mathsf{b}^+_{12} & \mathsf{b}^-_{21}\mathsf{b}^+_{13} + q^{(h_2,\nu+e_1)}\mathsf{b}^+_{23} \\ q^{(h_1,\nu)}\mathsf{b}^-_{31} & \mathsf{b}^-_{31}\mathsf{b}^+_{12} + q^{(h_2,\nu+e_1)}\mathsf{b}^-_{32} & q^{2(h_3,\nu+e_{12})} + \mathsf{b}^-_{32}\mathsf{b}^+_{23} + \mathsf{b}^-_{31}\mathsf{b}^+_{13} \end{pmatrix},$$

It has now become straightforward to derive the claim from Section 6.5 concerning the form of the monodromy matrix, that it has matrix elements which are finite difference operators in the multiplicity labels of low order.

Chapter 10

Verlinde line and network operators and their algebra

We have up to this point collected a series of results pertaining to the construction of chiral vertex operators and conformal blocks for $\mathfrak{sl}_N$ Toda CFT through the free field representation. This has led in Chapter 9 to the explicit derivation of quantum monodromy matrices which describe the effect of moving degenerate fields around generic chiral vertex operators in $\mathfrak{sl}_3$ Toda CFT and which entered the definition of Verlinde line operators at the end of Chapter 6. We will now explain how the quantised algebras of functions $\mathcal{A}_{\text{flat}}$ (also equivalently denoted by $\mathcal{A}^N_{g,n}(q)$) on the moduli spaces of flat connections $\mathcal{M}^N_{g,n}$, discussed in Part II of this thesis, arise naturally in conformal field theory, as stated in Chapter 6. For this purpose, we will define Verlinde network operators, which are natural generalisations of Verlinde line operators, and show that their algebra $\mathcal{A}_V$ is equivalent to the quantum skein algebra described in Section 2.8. Our arguments are formulated in the generic N case and are based on the fact that the braid matrix of degenerate chiral vertex operators, whose construction was described in the previous chapters, is twist-equivalent to the R-matrix of the quantum group $\mathcal{U}_q(\mathfrak{sl}_N)$ defining the skein algebra. The main result of this chapter will therefore be a proof of the isomorphism $\mathcal{A}_{\text{flat}} \simeq \mathcal{A}_V$, which was stated as one of the main aims of this thesis at the end of Section 1.5.

10.1 Braiding and fusion of degenerate fields

In this section we take advantage of the independence of the choice of base-point for the contours of integration that enter the definition of screening charges, as explained in Section 8.4.2, and consider the limit where these contours become of Felder type [120], supported on circles around the origin with radius z. Referring back to Figure 8.6, this means taking the limit $z_0 \to z_2$ and $z_0' \to z_3$ and we further set $z_2 = e^{\mathrm{i}\sigma_2},\ z_3 = e^{\mathrm{i}\sigma_3}$. [1] Notice that this limit process

[1] In this setup, the appropriate variant of the exchange relation (6.4.33) is

$$V_\beta(\sigma')V_\alpha(\sigma) = \mathrm{e}^{-\pi\mathrm{i}(\alpha,\beta)\mathrm{sgn}(\sigma'-\sigma)}V_\alpha(\sigma)V_\beta(\sigma')\,.$$

also implies projecting onto highest weight sates by setting $\mathbf{n}_2 = \mathbf{n}_3 = 0$.

The braid matrix of degenerate screened vertex operators has been calculated in [121] for $\mathfrak{sl}_N$ Toda CFT. Such operators have special values of α and $\mathbf{s}$ and satisfy certain differential equations relating derivatives of $V_{\mathbf{s}}^{\alpha}(\sigma)$ to the W_N-currents, like in Section 6.3 when $N = 3$. The basic example for this phenomenon occurs in the case $\alpha = -b\omega_1$ when $[p_i, V_{\mathbf{s}}^{\alpha}(\sigma)] = \mathrm{i}bh_i V_{\mathbf{s}}^{\alpha}(\sigma)$, where h_i, $i = 1, \ldots, N$ are the weights of the fundamental representation. We will again use the simplified notation $D_i(\sigma)$ for the screened vertex operators $V_{\mathbf{s}}^{\alpha}(\sigma)$ satisfying these conditions. They satisfy an N^{th}-order operator differential equation [121], which is essentially equivalent to the equations expressing the decoupling of null-vectors in the Verma module $\mathcal{V}_{-b\omega_1}$ within the framework of [111], see e.g. [113] [106]. State-operator correspondence in CFT relates the allowed values of β' to the so-called fusion rules, the rules determining the set of labels of the primary fields that can appear in the operator product expansion of fields $V_{-b\omega_1}(z_1)V_{\beta}(z_2)$.

The operator product expansion of degenerate fields generates further degenerate fields. It follows from the fusion rules that the screened vertex operators $V_{\mathbf{s}}^{-b\lambda}(\sigma)$ that can be generated by recursively performing operator product expansions of the operators $D_i(\sigma)$ are labeled by the weights λ of finite-dimensional representations[2] M_λ of $\mathcal{U}_q(\mathfrak{sl}_N)$. The allowed powers of screening charges collected in $\mathbf{s} = \{s_{ij}, i \leq j\}$ are constrained by the fusion rules determining the fields $V_{\beta'}(z_2)$ appearing in the operator product expansion $V_{-b\lambda}(z_1)V_{\beta}(z_2)$. The s_{ij} have to be integers constrained by the condition that $\frac{1}{b}(\beta - \beta')$ coincides with one of the weights of the vectors in the representation M_λ.

It was shown in [121] that the degenerate fields $D_i(\sigma)$ satisfy exchange relations of the form

$$D_i(\sigma_2)D_j(\sigma_1) = \sum_{k,l=1}^{N} B^{\mathrm{D}}(p)_{ij}^{k\ell}\, D_k(\sigma_1)D_\ell(\sigma_2)\,. \tag{10.1.1}$$

Note that the matrix $B^{\mathrm{D}}(p)$ appearing in (11.1.10) is operator-valued in general, being dependent on the zero-mode operator $p = (p_1, \ldots, p_{N-1})$ from the expansion (6.1.2). The limit process described above, which moved the points $z_0 \to z_2$ and $z_0' \to z_3$ in order to define the integration contours for screening charges, obscures the contour manipulation point of view on the braiding calculation. Instead, one should adopt an alternative picture that relies on algebraic manipulations, like in Section 4 of [17]. It is in this picture that the dependence of the braid matrix on the mode p becomes manifest.

The matrix $B^{\mathrm{D}}(p)$ satisfies a modified form of the Yang-Baxter equation called dynamical Yang-Baxter equation and $B^{\mathrm{D}}(p)$ therefore represents an example of what is called a dynamical R-matrix. It was furthermore shown in [122] that there exist linear combinations $\tilde{D}_i(\sigma) = \sum_{j=1}^{N} c(p)_i^j\, D_j(\sigma)$ satisfying exchange relations of the form (11.1.10) with a matrix $\tilde{B}^{\mathrm{D}}$ that is p-independent, and will therefore be denoted by $\tilde{B}$. The matrix $\tilde{B}$ is different from the standard braid-matrix B representing the braiding of two fundamental representations of the quantum group $\mathcal{U} \equiv \mathcal{U}_q(\mathfrak{sl}_N)$ (one can refer back to Chapter 7 for the relevant background on $\mathcal{U}_q(\mathfrak{sl}_N)$). Recall that B can be obtained from the universal R-matrix R of $\mathcal{U}_q(\mathfrak{sl}_N)$ as

$$\mathsf{B} = \mathsf{P}(\pi_{\square} \otimes \pi_{\square})(\mathsf{R})\,, \tag{10.1.2}$$

[2] We identify $M_i \equiv M_{\omega_i}$ in our notations, with ω_i being the weight of the representation $\wedge^i\square$.

when working with the fundamental representation (in the notations of Part II) and where P is the operator permuting the two tensor factors of $\mathbb{C}^N \otimes \mathbb{C}^N$. The relation between $\tilde{B}$ and B was subsequently clarified in [123], where is was shown that $\tilde{B}$ can be obtained in a similar way as (10.1.2) from a universal R-matrix $\tilde{\mathsf{R}}$ that is related to R by a Drinfeld twist $\mathcal{J} \in \mathcal{U} \otimes \mathcal{U}$ such that $\tilde{\mathsf{R}} = \mathcal{J}_{21}{}^{-1} \mathsf{R}\, \mathcal{J}$. Recall that the twist $\mathcal{J}$ that relates R and $\tilde{\mathsf{R}}$ satisfies the cocycle condition

$$(\Delta \otimes \mathrm{id})(\mathcal{J}) \cdot \mathcal{J}_{12} \;=\; (\mathrm{id} \otimes \Delta)(\mathcal{J}) \cdot \mathcal{J}_{23}\,. \tag{10.1.3}$$

It is interesting at this point to observe the following. In Chapter 9 we calculated the similarity transformation which relates the braid matrices derived for chiral vertex operators in the free field representation of $\mathfrak{sl}_3$ Toda CFT to the standard $\mathcal{U}_q(\mathfrak{sl}_3)$ quantum group braid matrices. This similarity transformation was given there in terms of the relevant Clebsch-Gordan coefficients, whereas presently we can observe this type of transformation to be related to the twist $\mathcal{J}$. It is more precisely the combination of this twist with the change of basis from $D_\imath(\sigma)$ to $\tilde{D}_\imath(\sigma)$ removing the p-dependence.

As explained in Section 7.5, one may extend the action of $\mathcal{J}$ to m-fold tensor products, allowing us to define operators

$$J_f^{(m)} := (\pi_f \otimes \cdots \otimes \pi_f)(\mathcal{J}^{(m)})\,. \tag{10.1.4}$$

The cocycle condition (10.1.3) implies that $J_f^{(m)}$ is independent of the order in which tensor products are taken.

Let us consider the space VO_m spanned by the compositions of vertex operators $D_{\imath_m \ldots \imath_1}(\sigma_m, \ldots, \sigma_1) := \tilde{D}_{\imath_m}(\sigma_m)\tilde{D}_{\imath_{m-1}}(\sigma_{m-1}) \cdots \tilde{D}_{\imath_1}(\sigma_1)$ with $\imath_k \in \{1, \ldots, N\}$ for $k = 1, \ldots, m$. The space VO_m carries a representation of the braid group $\mathcal{B}_m$ with m strands represented in terms of the braid matrices $\tilde{B}$. It follows from the fact that R and $\tilde{\mathsf{R}}$ are related by the Drinfeld twist $\mathcal{J}$ that the linear operator $J_f^{(m)}$ maps the braid group representation on VO_m to the standard braid group representation on the m-fold tensor product of fundamental representations of $\mathcal{U}_q(\mathfrak{sl}_N)$.

By repeated use of the operator product expansion one may construct other degenerate vertex operators $D_{\mathbf{s}}^{\lambda}(\sigma)$ starting from the products $D_{\imath_m \ldots \imath_1}(\sigma_m, \ldots, \sigma_1)$. The vertex operators $D_{\mathbf{s}}^{\lambda}(\sigma)$ that can be obtained in this way have weights λ associated with the finite-dimensional irreducible representations of $\mathcal{U}_q(\mathfrak{sl}_N)$. It easily follows from the results described above that the braid group representation generated by products of the vertex operators $D_{\mathbf{s}}^{\lambda}(\sigma)$ is isomorphic to the braid group representation on the tensor product of the corresponding representations of $\mathcal{U}_q(\mathfrak{sl}_N)$. This implies, in particular, that the vector space spanned by the vertex operators $D_{\mathbf{s}}^{\lambda}(\sigma)$ with fixed λ is isomorphic to the space on which the finite-dimensional irreducible representation M_λ with highest weight λ is realised.

10.2 Conformal blocks with degenerate fields

Let us consider conformal blocks associated with a Riemann surface $\mathcal{C}_{g,n+d}$ with $n+d$ punctures (see Figure 10.1). We assume that fully degenerate representations $\mathcal{D}_k$ are associated with the punctures Q_k, $k = 1, \ldots, d$. The remaining n punctures P_r, $r = 1, \ldots, n$ are assumed not

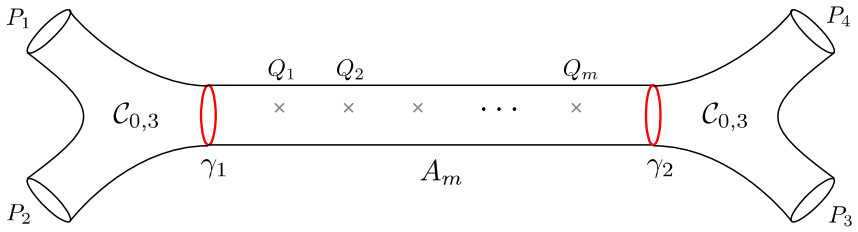

Figure 10.1: *Part of a decomposition of $\mathcal{C}_{g,n+d}$ with n punctures P_r and d marked points Q_k into three-holed spheres $\mathcal{C}_{0,3}$ and annuli A_m with m marked points.*

to be fully degenerate. We may alternatively consider Q_k, $k = 1, \ldots, d$, as a collection of distinguished points on the Riemann surface $\mathcal{C}_{g,n}$ which has punctures only at P_r, $r = 1, \ldots, n$. We may start from a pants decomposition $\sigma = (\gamma, \Gamma)$ of the surface $\mathcal{C}_{g,n}$. Cutting $\mathcal{C}_{g,n}$ along the simple closed curves contained in $\gamma = \{\gamma_1, \ldots, \gamma_{3g-3+n}\}$ decomposes the surface into spheres $\mathcal{C}^v_{0,3}$ with three boundary components which can be holes or punctures. The trivalent graph Γ on $\mathcal{C}_{g,n}$ has exactly one vertex within each $\mathcal{C}^v_{0,3}$; it allows us to distinguish pants decompositions related by Dehn twists. The pants decomposition specified by $\sigma = (\gamma, \Gamma)$ can always be refined to a decomposition into a collection of annuli A^e and three-holed spheres T^v such that each of the fully degenerate punctures is contained in one of the annuli A^e. This can be done by cutting along additional simple closed curves on $\mathcal{C}_{g,n}$ which do not intersect any of the curves in γ, do not mutually intersect and do not contain any Q_k, $k = 1, \ldots, d$. We furthermore need to cut out discs around the punctures P_r, $r = 1, \ldots, n$. A chosen orientation of the edges of Γ allows us to distinguish an incoming and an outgoing boundary component of each annulus A^e.

The gluing construction of conformal blocks allows us to construct families of conformal blocks out of two types of building blocks: The conformal blocks associated with the three-holed spheres, and the conformal blocks associated with the annuli A^e. Of particular interest for us will be the latter. Let $\mathrm{CB}(A_m)$ be the space of conformal blocks associated with an annulus with m marked points associated with fully degenerate representations, and incoming and outgoing boundary components associated with non-degenerate representations. We shall fix the representation associated with the incoming boundary component to be $\mathcal{V}_\beta$, and we assign fully degenerate representations $\mathcal{V}_{-b\lambda_1}, \ldots, \mathcal{V}_{-b\lambda_m}$ to the m marked points, respectively. The set of representations associated with the outgoing boundary component is then restricted by the fusion rules to a finite set. We will assign to the outgoing boundary component the direct sum of all representations allowed by the fusion rules.

It follows from the fusion rules that the resulting space of conformal blocks $\mathrm{CB}(A_m)$ is finite-dimensional. A basis for $\mathrm{CB}(A_m)$ can be constructed explicitly using the degenerate vertex operators defined above,

$$f_{A_m}(v_0 \otimes v_1 \otimes \cdots \otimes v_m \otimes v_{m+1}) = \langle\, v_{m+1}\,,\, D^{\lambda_m}_{\mathbf{s}_m}(v_m, \sigma_m)\ \cdots\ D^{\lambda_1}_{\mathbf{s}_1}(v_1, \sigma_1)\, v_0 \,\rangle_{\beta'}\,, \quad (10.2.5)$$

where $v_0 \in \mathcal{V}_\beta$, $v_{m+1} \in \mathcal{V}_{\beta'}$, and $D^{\lambda_k}_{\mathbf{s}_k}(v_k, \sigma_k)$ are the descendants of the degenerate vertex operators $D^{\lambda_k}_{\mathbf{s}_k}(\sigma_k)$ associated with vectors $v_k \in \mathcal{V}_{-b\lambda_k}$ for $k = 1, \ldots, m$.

It follows from the results discussed in the previous section that the space of conformal blocks $\mathrm{CB}(A_m)$ is naturally isomorphic (as a module for $\mathcal{B}_m$) to the tensor product of the m finite-

dimensional representations $M_{\lambda_1}, \ldots, M_{\lambda_m}$ of the quantum group $\mathcal{U}_q(\mathfrak{sl}_N)$,

$$\mathrm{CB}(A_m) \simeq M_{\lambda_1} \otimes \cdots \otimes M_{\lambda_m} . \tag{10.2.6}$$

This isomorphism is realized by a linear operators $J^{(m)}_{\lambda_1 \ldots \lambda_m}(p)$ that is constructed by combining the change of basis removing the p-dependence with the Drinfeld twist $\mathcal{J}$.

10.3 Verlinde network operators

Verlinde network operators are generalizations of Verlinde loop operators [56], [57] to Toda CFT of higher rank and were previously studied in [71]. In order to define the Verlinde network operators one needs to consider conformal blocks associated with a Riemann surface $\mathcal{C}_{g,n+d}$, as above. Our definition will be based on certain relations between the spaces of conformal blocks with varying number d of fully degenerate insertions. In order to describe these relations we will employ the set-up introduced in the previous section, in particular the decomposition of $\mathcal{C}_{g,n+d}$ into three-holed spheres T_v and annuli A^e, and the isomorphism (10.2.6) which can be applied locally for each annulus A^e.

This needs to be combined with one further ingredient. We will conjecture that there exist at general rank exchange relations between fully degenerate chiral vertex operators and generic chiral vertex operators,

$$D_\imath(z_1) V^\alpha_{\mathbf{s}}(z_2) = \sum_j \sum_{\mathbf{s}'} B^{\jmath,\mathbf{s}'}_{\imath,\mathbf{s}}(\alpha) V^\alpha_{\mathbf{s}'}(z_2) D_\jmath(z_1) , \tag{10.3.7}$$

like those that were derived in Chapter 8 for rank two, where $|z_1| = |z_2|$, and furthermore operator product expansions of the form

$$D_\imath(w)\, V^\alpha_{\mathbf{s}}(z) \;=\; \sum_j \sum_{\mathbf{s}'} F^{\jmath,\mathbf{s}'}_{\imath,\mathbf{s}}(\alpha) V^{\alpha - b h_\jmath}_{\mathbf{s}'} \big(D_\jmath(w-z) v_\alpha, z \big) , \tag{10.3.8}$$

where h_s are the weights of the fundamental representation with highest weight ω_1. These relations would imply that there exist linear relations between the spaces of conformal blocks associated with surfaces $\mathcal{C}_{g,n+d}$ and $\mathcal{C}'_{g,n+d}$ related by moving a degenerate field from one annulus A^e to another one $A^{e'}$. So far we do not have a proof of these relations for general N. We expect that such a direct proof should be possible using the free field representation of the vertex operators. One may furthermore note that the relations (10.3.7), (10.3.8) follow from the results of [71] if the vertex operator $V^\alpha_{\mathbf{s}}$ is associated with a semi-degenerate representation $\mathcal{V}_\alpha$. Further generalizations of these braid relations were found in [35]. The general statement should follow from this special case if the operator product expansion of sufficiently many semi-degenerate vertex operators generates vertex operators associated with fully non-degenerate representations, as is generally expected.

By combining these ingredients we are now ready to define generalisations of the Verlinde line operators as follows (see Figure 10.2). The isomorphisms (10.2.6) allow us to associate maps between spaces of conformal blocks with all the maps between tensor products of representations used in the Reshetikhin-Turaev construction. These maps may be composed with the

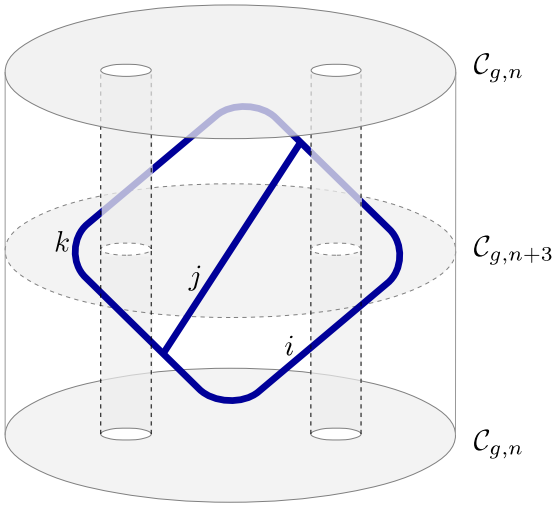

Figure 10.2: *Verlinde network operator.*

moves (10.3.7), (10.3.8) describing the motion of a fully degenerate puncture from one annulus to another. One may in particular consider compositions of these two types of fusion and braiding operations for degenerate fields starting and ending with the space of conformal blocks associated with a surface $\mathcal{C}_{g,n}$ with no fully degenerate insertions. It is clear that such compositions can be labeled by networks of the same type as considered in the previous chapters in Part II. The construction outlined above associates with each network an operator acting on the space $\mathrm{CB}(\mathcal{C}_{g,n})$ of conformal blocks for a surface $\mathcal{C}_{g,n}$ with n non-degenerate punctures.

10.4 Relation to skein algebra

The Verlinde network operators generate an algebra $\mathcal{A}_V$ realized on the spaces $\mathrm{CB}(C_{g,n})$. We are going to argue that this algebra is the same as the quantised algebra of functions on the moduli space of flat connections $\mathcal{M}^N_{g,n}$. Recall that the product of two networks is represented in terms of a network with crossings. It may be assumed that all crossings are located in annuli A^e. In order to describe the resulting algebraic relations we may therefore use the isomorphism (10.2.6) allowing us to describe the operations representing the crossing in terms of the intertwining maps used in the Reshetikhin-Turaev construction. All skein relations valid in the framework of the Reshetikhin-Turaev construction thereby carry over to the Verlinde network operators. In order to verify this claim it suffices to check that the basic skein relations are preserved by the twist $J_{\lambda_1 \dots \lambda_n}$ representing the isomorphism (10.2.6). Recall that the basic skein relations (2.8.42) take the form

$B_{ij} \; =$ 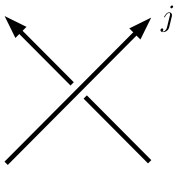 $= q^{\frac{ij}{2N}} \sum_{n=0}^{m} q^{-\frac{n}{2}}$ 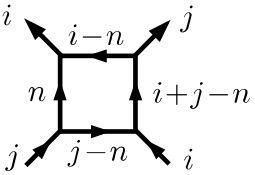 (10.4.9)

with $m = \min\{i, j, N-i, N-j\}$. In the framework of Reshetikhin-Turaev one associates to both sides intertwining maps between the representations $M_j \otimes M_i$ and $M_i \otimes M_j$ of the quantum group $\mathcal{U}_q(\mathfrak{sl}_N)$. The intertwining map on the left of (10.4.9) is represented by the operator B_{ij} defined in (2.8.44), while the operators on the right of (10.4.9), in the following denoted as $C(n)^{ij}_{ji}$, are compositions of Clebsch-Gordan maps as introduced in Section 2.8. If the quasitriangular Hopf algebra $\mathcal{U} = \mathcal{U}_q(\mathfrak{sl}_N)$ is replaced by a quasi-triangular Hopf algebra $\tilde{\mathcal{U}}$ related to $\mathcal{U}$ by a Drinfeld twist one may construct the intertwining maps $\tilde{C}(n)^{ij}_{ji}$ between representations of $\tilde{\mathcal{U}}$ from the intertwining maps $C(n)^{ij}_{ji}$ of $\mathcal{U}$ in a natural way, as explained in Section 7.5. The construction is such that we have $\tilde{C}(n)^{ij}_{ji} = J^{-1}_{ij} C(n)^{ij}_{ji} J_{ji}$, provided that J_{ij} is the similarity transformation relating B_{ij} and $\tilde{B}_{ij}$ as $\tilde{B}_{ij} = J^{-1}_{ij} \mathsf{B}_{ij} J_{ji}$. It follows immediately that $\tilde{C}(n)^{ij}_{ji}$ and $\tilde{B}_{ij}$ will satisfy a relation of the same form as (10.4.9), whereby indeed, we find that $\mathcal{A}_V \simeq \mathcal{A}^N_{g,n}(q)$. The algebra $\mathcal{A}^N_{g,n}(q)$ is non other than the quantised algebra $\mathcal{A}_{\text{flat}}$.

One may in particular consider Verlinde network operators associated with networks that are confined to a disc $\mathbb{D}$ embedded in an annulus A^e. It is easy to see that such network operators will act on $\mathrm{CB}(\mathcal{C}_{g,n})$ as multiplication by a number. This number represents one of the link invariants obtained by using the Reshetikhin-Turaev construction. This construction is thereby recognised as a special case of the definition of the Verlinde network operators given above.

Chapter 11

Spectrum

In the previous chapter we have found that the construction of loop and network operators using Fock-Goncharov coordinates in Part II defines an algebra isomorphic to the algebra generated by the Verlinde network operators in Toda CFT. We have also observed in Section 2.6 that the resulting algebra shares some features with the algebra of operators in a quantum integrable model, containing large commutative sub-algebras. Simultaneously diagonalising these sub-algebras defines natural representations. The next natural step in our program is to compare the representations resulting from the quantisation of the Fock-Goncharov coordinates, and from Toda conformal field theory. As an outlook, we collect here a few observations and conjectures concerning this problem.

11.1 Spectrum in Toda field theory

In order to determine the set of representations of the algebra $\mathcal{W}_N$ appearing in the spectrum of Toda field theory one may follow the example of Liouville theory. For studying the spectral problem of Toda field theories it is natural to consider canonical quantisation on a spacetime having the geometry of a two dimensional cylinder with time coordinate t and a spatial coordinate $\sigma \sim \sigma + 2\pi$. At time $t = 0$ one may decompose the fields $\phi(\sigma) \equiv \phi(0,\sigma)$ as $\phi(\sigma) = \phi_0 + \chi(\sigma)$, where the zero mode is defined as the average $\phi_0 = \frac{1}{2\pi}\int_0^{2\pi} \mathrm{d}\sigma\ \phi(\sigma)$. One may then observe that the interaction term $\int_0^{2\pi} \mathrm{d}\sigma\ \mathrm{e}^{b(e_i,\phi(\sigma))}$ in the Hamiltonian is equal to $2\pi\,\mathrm{e}^{b(e_i,\phi_0)}$ up to terms of order b^2. This means that zero modes and oscillators completely decouple in the limit $b^2 \to 0$. Canonical quantisation of the oscillators yields a Hamiltonian of the form

$$H \;=\; H_0 + \mathsf{N} + \bar{\mathsf{N}} + \mathcal{O}(b^2)\,, \qquad \text{with} \quad H_0 = \frac{1}{2}(p,p) + 2\pi\mu \mathrm{e}^{b(e_i,\phi_0)}\,, \tag{11.1.1}$$

which is defined on the Hilbert space $\mathcal{H} = L^2(\mathbb{R}^{N-1}) \otimes \mathcal{F}$ by choosing the Schrödinger representation on $L^2(\mathbb{R}^{N-1})$ for the operators p_i and ϕ_0^j satisfying $[\phi_0^i, p_j] = \mathrm{i}\delta^i_j$, and by realizing two sets of oscillators a_n^i and $\bar{a}_n^i$, $i = 1,\dots,N-1$, $n \in \mathbb{Z} \setminus \{0\}$, on the Fock space $\mathcal{F}$ in the usual way. The operator N satisfies $[\mathsf{N}, a_n^i] = -n a_n^i$, and commutes with $\bar{a}_n^i$, and similarly for $\bar{\mathsf{N}}$.

The problem of determining the spectrum of the Hamiltonian H therefore reduces in the limit $b^2 \to 0$ to the problem of finding the spectrum of the quantum-mechanical system with Hamiltonian H_0. This system is a well-known quantum integrable model called the open Toda chain, and its spectrum is known exactly [124], [125], [126]. The spectrum is purely continuous, with generalised eigenstates in one-to-one correspondence with the orbits of vectors $\mathfrak{p} \in \mathbb{R}^{N-1}$ under the Weyl group of $SU(N)$. This suggests that the spectrum of Toda field theory will be purely continuous.

Observing furthermore that the interaction terms $\int_0^{2\pi} \mathrm{d}\sigma \ \mathrm{e}^{b(e_i,\phi(\sigma))}$ are closely related to the screening charges of the free field realisation of the $\mathcal{W}_N$ algebra, it becomes straightforward to generalise the arguments used in [127] to determine the spectrum of Liouville theory to Toda field theories with $N > 2$, leading to the conclusion that the spectrum has the form that we stated at the beginning of Chapter 6

$$\mathcal{H} \ = \ \int_{\mathbb{S}} \mathrm{d}\alpha \ \mathcal{V}_\alpha \otimes \bar{\mathcal{V}}_\alpha \, , \tag{11.1.2}$$

where $\mathcal{V}_\alpha$ and $\bar{\mathcal{V}}_\alpha$ are representations of the algebra $\mathcal{W}_N$ generated by holomorphic currents $W_k(z)$ and their anti-holomorphic counterparts $\bar{W}_k(\bar{z})$ and $\mathbb{S}$ denotes the set of Weyl-orbits of vectors of the form $\alpha = \rho_W(b + b^{-1}) + \mathrm{i}\mathfrak{p}$, with $\mathfrak{p} \in \mathbb{R}^{N-1}$. It follows from this form of the spectrum that correlation functions such as

$$\left\langle \, \alpha_\infty \, | \, V_{\alpha_2}(z_2, \bar{z}_2) \, V_{\alpha_1}(z_1, \bar{z}_1) \, | \, \alpha_0 \, \right\rangle , \tag{11.1.3}$$

can be represented in the form

$$\begin{aligned} &\left\langle \, \alpha_\infty \, | \, V_{\alpha_2}(z_2, \bar{z}_2) \, V_{\alpha_1}(z_1, \bar{z}_1) \, | \, \alpha_0 \, \right\rangle \\ &\qquad = \int_{\mathbb{S}} \mathrm{d}\beta \int_{\mathbb{V}} \mathrm{d}s_1 \mathrm{d}s_2 \mathrm{d}\bar{s}_1 \mathrm{d}\bar{s}_2 \ C_{s_2\bar{s}_2}(\alpha_\infty, \alpha_2, \beta) C_{s_1\bar{s}_1}(Q - \beta, \alpha_1, \alpha_0) \\ &\qquad\qquad\qquad \times f\left[{}^{\alpha_2}_{\alpha_\infty} s_2 | \beta | s_1 {}^{\alpha_1}_{\alpha_0}\right](z_2, z_1) \bar{f}\left[{}^{\alpha_2}_{\alpha_\infty} \bar{s}_2 | \beta | \bar{s}_1 {}^{\alpha_1}_{\alpha_0}\right](\bar{z}_2, \bar{z}_1) \, , \end{aligned} \tag{11.1.4}$$

where

$$f\left[{}^{\alpha_2}_{\alpha_\infty} s_2 | \beta | s_1 {}^{\alpha_1}_{\alpha_0}\right](z_2, z_1) = \left\langle \, v_{\alpha_\infty} \, , \, V_{s_2}^{\rho_2}(z_2) \, V_{s_1}^{\rho_1}(z_1) \, v_{\alpha_0} \, \right\rangle_{\alpha_\infty} . \tag{11.1.5}$$

and $\rho_1 = (\beta, \alpha_1, \alpha_0), \ \rho_2 = (\alpha_\infty, \alpha_2, \beta)$. In order to arrive at the expansion (11.1.4) we have inserted a complete set of intermediate states from $\mathcal{H}$ between the two vertex operators $V_{\alpha_2}(z_2, \bar{z}_2)$ and $V_{\alpha_1}(z_1, \bar{z}_1)$, and we have furthermore assumed that the resulting matrix elements can be expanded as

$$\begin{aligned} &\left\langle \, Q - \alpha_3 \, | \, V_{\alpha_2}(z, \bar{z}) \, | \, \alpha_1 \, \right\rangle \ = \\ &\qquad = \int_{\mathbb{V}} \mathrm{d}s \, \mathrm{d}\bar{s} \ C_{s\bar{s}}(\alpha_3, \alpha_2, \alpha_1) \ \left\langle \, v_{\alpha_3} \, , V_s^{(\alpha_3,\alpha_2,\alpha_1)}(z) \, v_{\alpha_1} \, \right\rangle_{\alpha_3} \left\langle \, v_{\alpha_3} \, , V_{\bar{s}}^{(\alpha_3,\alpha_2,\alpha_1)}(\bar{z}) \, v_{\alpha_1} \, \right\rangle_{\alpha_3} . \end{aligned} \tag{11.1.6}$$

The assumption (11.1.6) will hold for any set of chiral vertex operators $V_s^{(\alpha_3,\alpha_2,\alpha_1)}(z)$ labeled by an index s taking values in the set $\mathbb{V}$ with measure $\mathrm{d}s$ which may be continuous or discrete allowing us to define a basis for the space $\mathrm{CB}(\mathcal{C}_{0,3})$ via (6.2.22). If the index set $\mathbb{V}$ or measure $\mathrm{d}s$ depends nontrivially on the choice of α_i, one will have to modify (11.1.4).

It seems likely that the usual consistency conditions of the conformal bootstrap can only be satisfied if the conformal blocks with $\alpha \in \mathbb{S}$ form a basis for the space of conformal blocks $\mathrm{CB}(\mathcal{C}_{0,4})$ on the four-punctured sphere $\mathbb{P}^1 \setminus \{0, z_1, z_2, \infty\}$, as is known to be the case for $N = 2$ (Liouville theory) [54]. It is furthermore easy to show that the Verlinde loop operators associated with the curve γ_s separating punctures z_1 and 0 from z_2 and ∞ act diagonally in this basis, with eigenvalues parameterised in terms of $\alpha = \rho_W(b + b^{-1}) + \mathrm{i}\mathfrak{p}$. The formulas for the eigenvalues look simplest if one represents the vectors $\mathfrak{p} \in \mathbb{R}^{N-1}$ in terms of vectors $\mathfrak{a} \in \mathbb{R}^N$ lying on the plane $\sum_k a_k = 0$, where a_k are the components of $\mathfrak{a}$ with respect to an orthonormal basis for $\mathbb{R}^N$. The eigenvalues $\lambda_{\omega_1}(a)$ of the Verlinde loop operator associated with the curve γ_s and the degenerate fields $D_\imath$, for example, can then be represented as

$$\lambda_{\omega_1}(a) \;=\; \sum_{i=1}^{N} \mathrm{e}^{-2\pi i b a_i} \,. \tag{11.1.7}$$

The considerations above motivate us to propose that the Hilbert space of Toda conformal blocks has the form

$$\mathrm{HCB}(\mathcal{C}_{g,n}) \;=\; \int_{\mathbb{S}} \prod_{\text{edges } e} \mathrm{d}\beta_e \bigotimes_{\text{vertices } v} \mathrm{HCB}(\mathcal{C}^v_{0,3}) \,. \tag{11.1.8}$$

Here $\mathrm{HCB}(\mathcal{C}^v_{0,3})$ is the Hilbert space of conformal blocks on the three-punctured spheres $\mathcal{C}^v_{0,3}$, with $v = 1, \ldots, 2g - 2 + n$, that appear in the pants decomposition of $\mathcal{C}_{g,n}$. The conformal blocks constructed by gluing will diagonalize the Verlinde loop operators for the cutting curves in the pants decomposition.

It should be noted that our conjecture (11.1.8) appears to be necessary for having consistency conditions of the conformal bootstrap like crossing symmetry, modular invariance, or locality realized in the usual way. Let us consider, for example, the condition of mutual locality of the vertex operators $V_\alpha(z, \bar{z})$ within correlation functions such as

$$\big\langle\, \alpha_\infty \,|\, V_{\alpha_2}(z_2, \bar{z}_2)\, V_{\alpha_1}(z_1, \bar{z}_1) \,|\, \alpha_0 \,\big\rangle = \big\langle\, \alpha_\infty \,|\, V_{\alpha_1}(z_1, \bar{z}_1)\, V_{\alpha_2}(z_2, \bar{z}_2) \,|\, \alpha_0 \,\big\rangle \,. \tag{11.1.9}$$

Such relations would hold if (i) the conformal blocks satisfy braid relations of the form

$$\begin{aligned} & f\left[\begin{smallmatrix}\alpha_2 \\ \alpha_\infty\end{smallmatrix} s_2 |\beta| s_1 \begin{smallmatrix}\alpha_1 \\ \alpha_0\end{smallmatrix}\right](z_2, z_1) = \\ & \qquad = \int_{\mathbb{S}} \mathrm{d}\beta' \int_{\mathbb{T}} \mathrm{d}t_2 \mathrm{d}t_1 \; B_{\beta\beta'}\left[\begin{smallmatrix}\alpha_2 & \alpha_1 \\ \alpha_\infty & \alpha_0\end{smallmatrix}\right]^{t_2 t_1}_{s_2 s_1} \; f\left[\begin{smallmatrix}\alpha_1 \\ \alpha_\infty\end{smallmatrix} t_1 |\beta| t_2 \begin{smallmatrix}\alpha_2 \\ \alpha_0\end{smallmatrix}\right](z_1, z_2) \,, \end{aligned} \tag{11.1.10}$$

and (ii) kernels $B_{\beta\beta'}\left[\begin{smallmatrix}\alpha_2 & \alpha_1 \\ \alpha_\infty & \alpha_0\end{smallmatrix}\right]^{t_2 t_1}_{s_2 s_1}$ and structure functions $C_{s\bar{s}}(\alpha_3, \alpha_2, \alpha_1)$ appearing in (11.1.4) satisfy suitable orthogonality relations. Equations (11.1.10) may then be interpreted as relations between two different bases for the space of conformal blocks $\mathrm{HCB}(\mathcal{C}_{0,4})$. The spectrum (11.1.2) thereby gets related to the spectrum (11.1.8) of Verlinde loop operators on the space of conformal blocks.

11.2 Spectrum of quantised trace functions

We have explained in Section 2.6 that a maximal set of commuting Hamiltonians on the symplectic moduli space $\bar{\mathcal{M}}^N_{g,n}$ (with fixed holonomies around the punctures) consists of the cutting

loops that specify a pants decomposition of $\mathcal{C}_{g,n}$ together with the corresponding pants networks. This implies that all these loop and network operators can be simultaneously diagonalized.

We are going to argue that the spectrum of the Hamiltonians associated with the cutting curves coincides with the expected spectrum of the corresponding Verlinde loop operators. To this aim we are going to observe that some essential features of the spectrum can be anticipated without solving the eigenvalue problem explicitly.

Example for $N = 2$: As a warm-up, let us consider the case of $SL(2)$-connections on $\mathcal{C}_{1,1}$. In the polarization $\mathsf{p} = \frac{1}{2}(\hat{B} + \hat{C})$ and $\mathsf{q} = -\frac{1}{2}(\hat{B} - \hat{C})$ with $[\mathsf{p}, \mathsf{q}] = -i\hbar$, the A-cycle operator (4.5.53) becomes

$$\hat{A} \;=\; 2\cosh \mathsf{p} + \mathrm{e}^{-\mathsf{q}}\,, \tag{11.2.11}$$

which defines a positive self-adjoint, but unbounded operator on $L^2(\mathbb{R})$. A complete set of eigenfunctions for this difference operator is known [128], [129]. The spectrum is purely continuous, and supported in the semi-infinite interval $(2, \infty)$. The (generalized) eigenvalues are non-degenerate and may therefore be parameterized in terms of a parameter $s \in \mathbb{R}^+$ as $2\cosh(s)$.

Without having solved the spectral problem explicitly one could still note that the term $\mathrm{e}^{-\mathsf{q}}$ appearing in the definition of $\hat{A}$ decays exponentially for $\mathsf{q} \to \infty$, and that the term $2\cosh \mathsf{p}$ can be seen as a "deformation" of the usual term p^2 in Schrödinger operators. One may therefore expect that the spectral problem for $\hat{A}$ will in some respects be similar to the spectral problem for the Liouville quantum mechanics with Hamiltonian H_0 (11.1.1). The extend to which this is the case was clarified in [129]. In the Schrödinger representation with q represented on wave-functions $\psi(q)$ as an operator of multiplication with q one may construct two linearly independent Jost solutions, eigenfunctions $f_s^{\pm}(q)$ of H_0 that behave for $q \to \infty$ as $f_s^{\pm}(q) = \mathrm{e}^{\pm\frac{i}{\hbar}sq} + o(1)$ [129]. The Jost solutions grow exponentially at the opposite end $q \to -\infty$. One may, however, find a function $R(s)$ such that the linear combination $\psi_s(q) = f_s^+(q) + R(s)f_s^-(q)$ decays rapidly for $q \to -\infty$. Only this linear combination may appear in the spectral decomposition of $\hat{A}$. Note that $\psi_{-s}(q)$ is related to $\psi_s(q)$ by a relation of the form $\psi_{-s}(q) = R(s)\psi_s(q)$, analogous to the case of a Schrödinger operator with repulsive potential.

The fact that the spectrum is bounded from below by 2 follows from the observation that $\hat{A}$ is the sum of two positive self-adjoint operators, and its spectrum therefore bounded from below by the spectrum of $2\cosh \mathsf{p}$.

Example for $N = 3$: Although we will not be able to find explicit diagonal representations for the A-cycle operators for higher rank, we can anticipate features of their spectra by a similar reasoning. In order to see how the observation above generalize, let us next consider the quantisation of the trace functions associated with $SL(3)$-connections on $\mathcal{C}_{1,1}$ in Chapter 4.

In order to represent the trace functions associated with A- and B-cycles in a form that will be convenient for the quantisation, let us start by fixing the eigenvalues of the holonomy M around

the puncture in terms of constants $\gamma_1 = a_1a_2b_1b_2c_1c_2$ and $\gamma_2 = xy$:

$$\left\{\frac{1}{a_1a_2b_1b_2c_1c_2xy}, \frac{1}{xy}, a_1a_2b_1b_2c_1c_2x^2y^2\right\} = \left\{\frac{1}{\gamma_1\gamma_2}, \frac{1}{\gamma_2}, \gamma_1\gamma_2^2\right\} . \tag{11.2.12}$$

We must then choose a polarization with momenta P_i and positions Q_j satisfying $\{P_i, Q_j\} = \delta_{ij}P_iQ_j$. The nice Poisson bracket (4.5.58) between the monomials α_i and β_j appearing in the A- and B-cycle suggests the following choice:

$$\begin{aligned} P_1 &= \alpha_1 = b_1c_1x\,, \qquad Q_1 = \prod_i \beta_i^{-\kappa_{1i}^{-1}} = a_1^{-\frac{2}{3}}a_2^{-\frac{1}{3}}b_1^{-\frac{2}{3}}b_2^{-\frac{1}{3}}x^{-\frac{1}{3}}y^{-\frac{2}{3}}\,,\\ P_2 &= \alpha_2 = b_2c_2y\,, \qquad Q_2 = \prod_i \beta_i^{-\kappa_{2i}^{-1}} = a_1^{-\frac{1}{3}}a_2^{-\frac{2}{3}}b_1^{-\frac{1}{3}}b_2^{-\frac{2}{3}}x^{-\frac{2}{3}}y^{-\frac{1}{3}}\,,\\ P_3 &= x\,, \qquad\qquad Q_3 = (a_2b_2c_2)^{-1}\,. \end{aligned} \tag{11.2.13}$$

The A-cycle trace functions are then expressed as

$$\begin{aligned} A_1 &= P_1^{\frac{1}{3}}P_2^{\frac{2}{3}} + \frac{P_1^{\frac{1}{3}}}{P_2^{\frac{1}{3}}} + \frac{1}{P_1^{\frac{2}{3}}P_2^{\frac{1}{3}}} + \frac{P_1^{\frac{1}{3}}P_2^{\frac{2}{3}}P_3}{\gamma_1\gamma_2^2Q_1Q_2} + P_1^{\frac{1}{3}}P_2^{\frac{2}{3}}\frac{Q_1Q_3}{Q_2^2}\left(1+\frac{1}{\gamma_2}\right) + \frac{P_1^{\frac{1}{3}}Q_2(1+P_3)}{\gamma_1\gamma_2P_2^{\frac{1}{3}}Q_1^2Q_3}\,,\\ A_2 &= P_1^{\frac{2}{3}}P_2^{\frac{1}{3}} + \frac{P_2^{\frac{1}{3}}}{P_1^{\frac{1}{3}}} + \frac{1}{P_1^{\frac{1}{3}}P_2^{\frac{2}{3}}} + \frac{P_2^{\frac{1}{3}}Q_1Q_3}{P_1^{\frac{1}{3}}P_3Q_2^2} + \frac{P_2^{\frac{1}{3}}Q_1Q_3}{P_1^{\frac{1}{3}}Q_2^2}\left(\frac{1}{P_3}+\frac{1}{\gamma_2}\right) + \frac{P_1^{\frac{2}{3}}P_2^{\frac{1}{3}}Q_2}{\gamma_1\gamma_2Q_1^2Q_3}(1+P_3)\,. \end{aligned}$$

If we take the limit $Q_1, Q_2 \to \infty$ with Q_1/Q_2 finite we see that only the first three terms survive. The quantisation of these expressions is straightforward following our discussions above, allowing us to define operators $\hat{A}_i$, $i = 1, 2$.

By generalizing the arguments used in the case $N = 2$ above one finds that the eigenvalues A_i' of the operators $\hat{A}_i$ can be parameterized in terms of a vector $(s_1, s_2) \in \mathbb{R}^2$ as follows

$$A_1' = \xi_1 + \xi_2 + \xi_3\,, \qquad A_2' = \frac{1}{\xi_1} + \frac{1}{\xi_2} + \frac{1}{\xi_3}\,, \tag{11.2.14}$$

where ξ_a are defined for $a = 1, 2, 3$ as

$$\big(\xi_1, \xi_2, \xi_3\big) = \big(\mathrm{e}^{\frac{1}{3}(s_1+2s_2)},\ \mathrm{e}^{\frac{1}{3}(s_1-s_2)},\ \mathrm{e}^{-\frac{1}{3}(2s_1+s_2)}\big)\,. \tag{11.2.15}$$

The expressions for the eigenvalues A_i' are manifestly invariant under Weyl symmetry permuting the ξ_a.

Furthermore, it seems likely that the repulsive nature of the dependence on Q_1, Q_2 will imply that the spectrum is parameterized by the Weyl-orbits of vectors $\mathfrak{s} = (s_1, s_2) \in \mathbb{R}^2$. In order to see this, let $\psi_{\mathfrak{s}}(\mathfrak{q})$, $\mathfrak{q} = (q_1, q_2)$, be a joint eigenfunction of the operators $\hat{A}_i$, $i = 1, 2$, in a Schrödinger-type representation where the quantum operators corresponding to the classical variables $\log Q_i$ are diagonal with eigenvalues q_i. The wave-function $\psi_{\mathfrak{s}}(\mathfrak{q})$ will be of the form

$$\psi_{\mathfrak{s}}(\mathfrak{q}) \;=\; \psi^0_{\mathfrak{s}}(\mathfrak{q}) + \mathcal{O}\big(\mathrm{e}^{-\frac{1}{2}(q_1+q_2)}\big)\,, \tag{11.2.16}$$

where $\psi^0_{\mathfrak{s}}(\mathfrak{q})$ is an eigenfunction of the operators

$$\hat{A}_1^0 = \mathsf{P}_1^{\frac{1}{3}}\mathsf{P}_2^{\frac{2}{3}} + \mathsf{P}_1^{\frac{1}{3}}\mathsf{P}_2^{-\frac{1}{3}} + \mathsf{P}_1^{-\frac{2}{3}}\mathsf{P}_2^{-\frac{1}{3}}\,, \qquad \hat{A}_2^0 = \mathsf{P}_1^{\frac{2}{3}}\mathsf{P}_2^{\frac{1}{3}} + \mathsf{P}_1^{-\frac{1}{3}}\mathsf{P}_2^{\frac{1}{3}} + \mathsf{P}_1^{-\frac{1}{3}}\mathsf{P}_2^{-\frac{2}{3}}\,,$$

where $\mathsf{P}_i = \mathrm{e}^{\frac{\hbar}{\mathrm{i}}\frac{\partial}{\partial q_i}}$. A joint eigenfunction of $\hat{A}_i^0$ is given by $\mathrm{e}^{\frac{\mathrm{i}}{\hbar}(s_1 q_1 + s_2 q_2)} \equiv \mathrm{e}^{\frac{\mathrm{i}}{\hbar}(\mathfrak{s},\mathfrak{q})}$, where $(\mathfrak{s},\mathfrak{q})$ denotes the standard scalar product of the vectors $\mathfrak{s}$ and $\mathfrak{q}$ in $\mathbb{R}^2$. The Weyl-invariance of the eigenvalues of $\hat{A}_i^0$ implies that other joint eigenfunctions of $\hat{A}_i^0$ are given by the functions $\mathrm{e}^{\frac{\mathrm{i}}{\hbar}(w(\mathfrak{s}),\mathfrak{q})}$, where $w(\mathfrak{s})$ is the vector obtained by the action of the element w of the Weyl-group $\mathcal{W}$ of $SL(3)$ on $\mathfrak{s} \in \mathbb{R}^2$. It follows that the most general joint eigenfunction of the $\hat{A}_i^0$ has the form

$$\psi_{\mathfrak{s}}^0(\mathfrak{q}) \;=\; \sum_{w\in\mathcal{W}} C_w(\mathfrak{s}) \mathrm{e}^{\frac{\mathrm{i}}{\hbar}(w(\mathfrak{s}),\mathfrak{q})}\,. \tag{11.2.17}$$

The exponential growth of the terms in $\hat{A}_i$ depending on $q_i \equiv \log Q_i$ will imply that the wave-functions $\psi_{\mathfrak{s}}(\mathfrak{q})$ have to decay very rapidly when $q_1, q_2 \to \infty$. This will imply that $\psi_{\mathfrak{s}}(\mathfrak{q})$ has to satisfy two reflection relations that must be compatible with the structure (11.2.17) of the $\psi_{\mathfrak{s}}^0(\mathfrak{q})$. The reflection relations must therefore be of the form

$$\psi_{w_i(\mathfrak{s})}(\mathfrak{q}) \;=\; R_i(\mathfrak{s})\psi_{\mathfrak{s}}(\mathfrak{q})\,, \qquad i = 1,2\,, \tag{11.2.18}$$

with w_i two different elements of $\mathcal{W}$. By composition of the Weyl reflections w_i, one may generate reflection relations corresponding to all elements of the Weyl group $\mathcal{W}$. The resulting relations will determine the coefficients $C_w(\mathfrak{s})$ in (11.2.17) completely up to an overall normalization. We are thereby led to the conclusion that the spectrum is indeed parameterized by the Weyl-orbits of vectors $\mathfrak{s} \in \mathbb{R}^2$.

A very similar structure is found for the trace functions B_i associated with the B-cycles. The explicit expressions turn out to be of the form

$$B_1 = Q_2 + \frac{Q_1}{Q_2} + \frac{1}{Q_1} + \mathcal{O}\big((P_1P_2)^{\frac{1}{6}}\big), \quad B_2 = \frac{1}{Q_2} + \frac{Q_2}{Q_1} + Q_1 + \mathcal{O}\big((P_1P_2)^{\frac{1}{6}}\big), \tag{11.2.19}$$

suggesting that the eigenvalues can be parameterized in terms of real positive numbers ζ_a, $a = 1,2,3$, satisfying $\zeta_1\zeta_2\zeta_3 = 1$, as

$$B_1 \to \zeta_1 + \zeta_2 + \zeta_3\,, \qquad B_2 \to \frac{1}{\zeta_1} + \frac{1}{\zeta_2} + \frac{1}{\zeta_3}\,. \tag{11.2.20}$$

Our observations above suggest that the spectrum of the trace-functions A_1 and B_1 coincides with the spectrum (11.1.7) of the corresponding Verlinde loop operators.

Higher rank: The remarks above seem to generalize to cases with $N > 3$. In the case $N = 4$, for example, one may note that the trace function A_2 of the A-cycle holonomy in the second antisymmetric representation (see (4.5.65)) has a similar structure as observed in the case $N = 3$ above, with the following leading term:

$$A_2^0 = 2\cosh\frac{1}{2}(p_1 + p_3) + 2\cosh\frac{1}{2}(p_1 - p_3) + 2\cosh\frac{1}{2}(p_1 + 2p_2 + p_3)\,, \tag{11.2.21}$$

where we defined $p_i \equiv \log P_i$. This further strengthens our confidence that the spectra of quantised trace functions will coincide with the spectra of the Verlinde loop operators in Toda CFT.

11.3 Remarks

One of the most important problems is clearly to find useful bases for the space of conformal blocks $\mathrm{CB}(\mathcal{C}_{0,3})$. A natural possibility would be to define such bases by diagonalizing a maximal set of commuting Verlinde network operators. Natural as it may be, it seems technically much harder to analyze the spectrum of network operators along similar lines as described above. As an example let us consider the pants network N_1 on $\mathcal{C}_{0,3}$ in the case $N = 3$. We may use the coordinates

$$p_1 = a_1 \,, \qquad q_1 = y \,, \tag{11.3.22}$$

and denote the eigenvalues of $\mathbf{A}$ by $\tilde{\alpha}_1 = \alpha_1^{1/3}\alpha_2^{2/3}$ and $\tilde{\alpha}_2 = \alpha_1^{1/3}\alpha_2^{-1/3}$, and similarly for $\mathbf{B}$ and $\mathbf{C}$. The pants network function can then be represented as

$$\begin{aligned} N_1 = \frac{p_1}{\tilde{\beta}_1\tilde{\gamma}_1\tilde{\gamma}_2}\Bigg[1 &+ \frac{2\tilde{\beta}_1^2\tilde{\gamma}_1^2\tilde{\gamma}_2^3}{\tilde{\alpha}_1 p_1^3} + \tilde{\alpha}_1\tilde{\beta}_1\tilde{\gamma}_1 \\ &+ \frac{1}{p_1^2}\left(\frac{\tilde{\beta}_1\tilde{\gamma}_1^2\tilde{\gamma}_2^2}{\tilde{\alpha}_1\tilde{\alpha}_2} + \frac{\tilde{\beta}_1^2\tilde{\gamma}_1^2\tilde{\gamma}_2^3}{\tilde{\alpha}_1} + \frac{\tilde{\beta}_1^2\tilde{\gamma}_1\tilde{\gamma}_2}{\tilde{\alpha}_1} + \tilde{\alpha}_2\tilde{\beta}_1\tilde{\gamma}_1^2\tilde{\gamma}_2^2 + \tilde{\beta}_1^2\tilde{\beta}_2\tilde{\gamma}_1\tilde{\gamma}_2^2 + \frac{\tilde{\beta}_1\tilde{\gamma}_1\tilde{\gamma}_2^2}{\tilde{\beta}_2}\right) \\ &+ q_1\left(\frac{\tilde{\alpha}_2\tilde{\beta}_1^2\tilde{\beta}_2\tilde{\gamma}_1^2\tilde{\gamma}_2^4}{\tilde{\alpha}_1 p_1^3} + \frac{\tilde{\alpha}_2\tilde{\beta}_1^2\tilde{\beta}_2\tilde{\gamma}_1\tilde{\gamma}_2^2}{\tilde{\alpha}_1 p_1^2} + \frac{\tilde{\beta}_1\tilde{\beta}_2\tilde{\gamma}_1^2\tilde{\gamma}_2^3}{\tilde{\alpha}_1 p_1^2} + \frac{\tilde{\beta}_1\tilde{\beta}_2\tilde{\gamma}_1\tilde{\gamma}_2}{\tilde{\alpha}_1 p_1} + \frac{\tilde{\alpha}_2\tilde{\beta}_1\tilde{\gamma}_1\tilde{\gamma}_2^3}{p_1^2} + \frac{\tilde{\alpha}_2\tilde{\beta}_1\tilde{\gamma}_2}{p_1} + \frac{\tilde{\gamma}_1\tilde{\gamma}_2^2}{p_1} + 1\right) \\ &+ \frac{1}{q_1}\left(\frac{\tilde{\beta}_1^2\tilde{\gamma}_1^2\tilde{\gamma}_2^2}{\tilde{\alpha}_1\tilde{\alpha}_2\tilde{\beta}_2 p_1^3} + \frac{\tilde{\beta}_1^2\tilde{\gamma}_1^2\tilde{\gamma}_2^2}{\tilde{\alpha}_1\tilde{\alpha}_2\tilde{\beta}_2 p_1^2} + \frac{\tilde{\alpha}_1\tilde{\beta}_1\tilde{\gamma}_1}{p_1} + \tilde{\alpha}_1\tilde{\beta}_1\tilde{\gamma}_1 + \frac{\tilde{\beta}_1^2\tilde{\gamma}_1\tilde{\gamma}_2}{\tilde{\alpha}_2 p_1^2} + \frac{\tilde{\beta}_1^2\tilde{\gamma}_1\tilde{\gamma}_2}{\tilde{\alpha}_2 p_1} + \frac{\tilde{\beta}_1\tilde{\gamma}_1^2\tilde{\gamma}_2}{\tilde{\beta}_2 p_1^2} + \frac{\tilde{\beta}_1\tilde{\gamma}_1^2\tilde{\gamma}_2}{\tilde{\beta}_2 p_1}\right)\Bigg] . \end{aligned} \tag{11.3.23}$$

We see that there is no limit in which the terms depending on q_1 vanish. This might indicate that the spectrum of the corresponding quantum operator is discrete rather than continuous. It would be very interesting if one could describe the spectrum of this operator more precisely.

One may also note that the free field construction of chiral vertex operators gave us families of conformal blocks labeled by a space of parameters which has the same dimension as Lagrangian subspaces of $\mathcal{M}_{0,3}^N$. This indicates that the conformal blocks that can be obtained in this way may represent a basis for $\mathrm{CB}(\mathcal{C}_{0,3})$.

Let us finally note that the geometric engineering of gauge theories of class $\mathcal{S}$ combined with the topological vertex technique discussed in the introduction to this thesis in Section 1.3 has led to a prediction for the structure functions $C_{s\bar{s}}(\alpha_3, \alpha_2, \alpha_1)$ appearing in (11.1.4), see [48], [75]. The labels s for a basis of $\mathrm{CB}(\mathcal{C}_{0,3})$ should thereby be identified with geometric data of the local Calabi-Yau manifold used in the geometric engineering of the class $\mathcal{S}$ theories associated with $\mathcal{C}_{0,3}$. It is very interesting to identify the meaning of this parameter within conformal field theory (we will do so in Part IV), or within the quantum theory obtained by quantising $\mathcal{M}_{0,3}^N$.

Chapter 12

More relations to the quantisation of moduli spaces of flat connections

In this chapter we return briefly to the discussion of relations between the quantisation of moduli spaces of flat connections and Toda CFT. We have explained in the previous chapters how the "quantum monodromy" relations (6.5.41) can be used to define a quantisation of the moduli spaces of flat $SL(3)$-connections on $\mathcal{C}_{0,3}$ and we have proved the isomorphism between the quantised algebra of functions on moduli spaces of flat connections and the algebra of Verlinde network operators on spaces of Toda conformal blocks. Our main goal in this chapter is to explain why the operators u, v representing elementary building blocks of the operator-valued monodromy matrices $M_\gamma(\mathsf{u},\mathsf{v})_i{}^j$ constructed in Chapter 9 are closely related to quantum counterparts of a natural higher rank generalisation of the Fenchel-Nielsen coordinates. To this end and for ease of presentation, we will first briefly review some of the material presented in Part II.

12.1 The notion of Fenchel-Nielsen type coordinates

As a preparation let us first discuss defining properties of a class of coordinate system which will be called coordinates of Fenchel-Nielsen type. In order to motivate our proposal we will briefly review the case of flat $SL(2)$ connections.

Recall that $\mathcal{M}_{\text{flat}}^{SL(2)}(\mathcal{C}_{0,4})$ has the structure of an algebraic variety and that useful coordinates on this moduli space are the trace coordinates, associating to a closed curve γ the trace of the holonomy along γ, that is[1] $L_\gamma = \mathrm{tr}(M_\gamma)$. For $N = 2$ and $\mathcal{C}_{0,4} = \mathbb{P}^1 \setminus \{z_1, z_2, z_3, z_4\}$ one may, for example, introduce the holonomies M_i around the punctures z_i and define the following set of trace functions:

$$L_i = \mathrm{Tr}\, M_i = 2\cos 2\pi m_i, \qquad i = 1, \dots, 4, \tag{12.1.1}$$

$$L_s = \mathrm{Tr}\, M_1 M_2, \qquad L_t = \mathrm{Tr}\, M_1 M_3, \qquad L_u = \mathrm{Tr}\, M_2 M_3, \tag{12.1.2}$$

In order to describe $\mathcal{M}_{\text{flat}}^{SL(2)}(\mathcal{C}_{0,4})$ as an algebraic Poisson variety we need the polynomial

$$\begin{aligned}\mathcal{P}_{0,4}(L_s, L_t, L_u) :&= L_1L_2L_3L_4 + L_sL_tL_u + L_s^2 + L_t^2 + L_u^2 + L_1^2 + L_2^2 + L_3^2 + L_4^2 \\ &\quad - (L_1L_2 + L_3L_4)\, L_s - (L_1L_3 + L_2L_4)\, L_t - (L_2L_3 + L_1L_4)\, L_u - 4\,.\end{aligned} \tag{12.1.3a}$$

[1] To lighten notation, we no longer use bold face letters to denote monodromy matrices, like in Part II.

The polynomial $\mathcal{P}_{0,4}$ allows us to write both the equation describing $\mathcal{M}_{\text{flat}}^{SL(2)}(\mathcal{C}_{0,4})$ as algebraic variety and the Poisson brackets among the regular functions L_s, L_t and L_u in the following form:

$$\text{(i)} \quad \mathcal{P}(L_s, L_t, L_u) = 0 \,, \tag{12.1.3b}$$

$$\text{(ii)} \quad \{L_s, L_u\} = \frac{\partial}{\partial L_t}\mathcal{P}(L_s, L_t, L_u) \ \text{ and cyclic} \,. \tag{12.1.3c}$$

A set of Darboux coordinates λ, κ for $\mathcal{M}_{\text{flat}}^{SL(2)}(\mathcal{C}_{0,4})$ can then be defined by parameterising L_s, L_t and L_u as

$$\begin{aligned}
&(u-u^{-1})^2\, L_t = C_t^+(u)\, v + C_t^0(u) + C_t^-(u)\, v^{-1} \,, \\
&(u-u^{-1})^2\, L_u = C_u^+(u)\, v + C_u^0(u) + C_u^-(u)\, v^{-1} \,, \qquad L_s = u + u^{-1}, \\
&C_u^0(u) = 2\left[\cos 2\pi m_2 \cos 2\pi m_3 + \cos 2\pi m_1 \cos 2\pi m_4\right] \\
&\qquad\quad - (u+u^{-1})\left[\cos 2\pi m_1 \cos 2\pi m_3 + \cos 2\pi m_2 \cos 2\pi m_4\right] , \\
&C_u^\pm(u) = (u + u^{-1} - 2\cos 2\pi(m_1 \mp m_2))(u + u^{-1} - 2\cos 2\pi(m_3 \mp m_4))
\end{aligned}$$

The coordinates defined by representing u, v as $u = e^{\mathrm{i}\lambda}$, $v = e^{\mathrm{i}\kappa}$ are related to the Fenchel-Nielsen coordinates from Teichmüller theory. Restricting λ and κ to the flat $PSL(2,\mathbb{R})$ connections coming from the uniformisation of Riemann surfaces one finds purely imaginary values of these coordinates. $2\mathrm{i}\lambda$ will coincide with the geodesic length along γ_s, and $\mathrm{i}\kappa$ will differ from the Fenchel-Nielsen twist parameter τ only by a simple function of λ, $\mathrm{i}\kappa = \tau + \eta(\lambda)$. Compared to the Fenchel-Nielsen coordinates the parametrisation introduced above has the advantage that the expressions for the trace functions in terms of λ, κ have more favourable analytic properties. In the case of the Fenchel-Nielsen coordinates one would find square-roots in these expressions.

This motivates the following definition. Darboux coordinates (μ, ν), with $\mu = (\mu_1, \ldots, \mu_d)$, $\nu = (\nu_1, \ldots, \nu_d)$ for $\mathcal{M}_{\text{flat}}(\mathcal{C})$ are of "Fenchel-Nielsen type" if

- (R) the expressions for $L_\gamma(\mu, \nu)$ have the best possible analytic structure, being rational functions of $u_a = e^{\mathrm{i}\mu_a}$, $v_a = e^{\mathrm{i}\nu_a}$ or even Laurent polynomials,
- (P) the coordinates are compatible with a pants decomposition of $\mathcal{C}$.

Requirement (R) means that coordinates of Fenchel-Nielsen type are reflecting the Poisson-algebraic structure of $\mathcal{M}_{\text{flat}}(\mathcal{C})$ in an optimal way. Note that this property is shared by the Fock-Goncharov coordinates for $\mathcal{M}_{\text{flat}}(\mathcal{C})$. The main feature referred to in the terminology "Fenchel-Nielsen type" is (P), shared by the Fenchel-Nielsen coordinates for the Teichmüller spaces. Compatibility with a pants decomposition means that appropriate subsets of the coordinates would represent coordinate systems for the surfaces obtained by cutting the surface $\mathcal{C}$ along any simple closed curve defining the pants decomposition. The Fock-Goncharov coordinates for $\mathcal{M}_{\text{flat}}(\mathcal{C})$ do not have this property, since they are associated to triangulations of $\mathcal{C}$.

12.2 Quantum Fenchel-Nielsen type coordinates

In order to relate the operators u and v to quantum counterparts of Fenchel-Nielsen type coordinates for $\mathcal{M}_{\text{flat}}^{SL(3)}(\mathcal{C}_{0,3})$ one mainly needs to observe the following simple consequence of our calculation of

quantum monodromy matrices.

$$\text{(L)} \quad \left\{ \begin{array}{l} \text{The operators } \mathsf{V}_\gamma \text{ generating a representation of } \mathcal{A}_\hbar,\ \hbar = b^2, \text{ on the spaces of} \\ \text{conformal blocks can be represented as Laurent polynomials } \mathcal{V}^\hbar_\gamma(\mathsf{u},\mathsf{v}) \text{ of } \mathsf{u} \text{ and } \mathsf{v}. \end{array} \right\}$$

One may represent u and v as $\mathsf{u} = e^{\mathrm{i}\hat{\mu}}$ and $\mathsf{v} = e^{\mathrm{i}\hat{\nu}}$, with $\hat{\mu}\,\mathcal{F}_{\mu,k} = 2\pi b^2 k \mathcal{F}_{\mu,k}$ and $\hat{\nu}\,\mathcal{F}_{\mu,k} = -\mathrm{i}\frac{\partial}{\partial k}\mathcal{F}_{\mu,k}$, respectively. We will interpret our observation (L) as the statement that $\hat{\mu}$ and $\hat{\nu}$ represent the quantised counterparts of Fenchel-Nielsen type coordinates for $\mathcal{M}^{SL(3)}_{\text{flat}}(\mathcal{C}_{0,3})$.

In order to support this interpretation let us consider the Poisson-algebra $\mathcal{R}_0$ generated by rational functions of two variables u, v with Poisson-bracket $\{u, v\} = -2\pi\, uv$. The classical limit $\mathcal{A}_0$ of the algebras $\mathcal{A}_\hbar$ considered above is a Poisson-algebra which can be identified with the sub-algebra of $\mathcal{R}_0$ generated by the Laurent polynomials $\mathcal{V}^0_\gamma(u, v)$ The logarithmic coordinates $\mu = -\mathrm{i}\log u$, $\nu = -\mathrm{i}\log v$ have Poisson bracket $\{\mu, \nu\} = 2\pi$, identifying them as Darboux-coordinates for $\mathcal{A}_0$. It follows from our observations above that mapping $\mathcal{V}^0_\gamma$ to $\mathcal{L}_\gamma$ defines an isomorphism of Poisson algebras. This means in particular that the functions $\mathcal{V}^0_\gamma(u, v)$ satisfy the relations (6.6.47), and have Poisson brackets that reproduce the Poisson brackets of the trace functions L_γ when L_γ is replaced by $\mathcal{V}^0_\gamma$.

These properties are completely analogous to the description of the moduli space $\mathcal{M}^{SL(2)}_{\text{flat}}(\mathcal{C}_{0,4})$, motivating us to call the coordinates μ, ν Fenchel-Nielsen type coordinates for $\mathcal{M}^{SL(3)}_{\text{flat}}(\mathcal{C}_{0,3})$.

12.3 Yang's functions and isomonodromic tau functions from classical limits

We will now point out further relations between Toda CFT and the theory of flat connections on $\mathcal{C}_{0,3}$, which arise in two different limits. The standard classical limit of Toda field theory corresponds to $b \to 0$. Assuming that the vectors α_i are of the form $\alpha_i = -b^{-1}\eta_i$ for $i = 1, 2, 3$ one may expect that the conformal blocks behave in the limit $b \to 0$, $\alpha_i = \eta_i/b^2$, $k = \mu/2\pi b^2$, with η_i, $i = 1, 2, 3$, and μ finite, as follows:

$$\mathcal{F}^\rho_k(y_0, y)_{\jmath,\imath} \sim e^{-\frac{1}{b^2}\mathcal{Y}(\eta,\mu)}\bar{\chi}_\jmath(y_0)\chi_\imath(y), \tag{12.3.4}$$

where $\chi_\imath(y)$, and $\bar{\chi}_\imath(y)$, $\imath = 1, 2, 3$, are three linearly independent solutions of the differential equations

$$\Big(-\frac{\partial^3}{\partial y^3} + T(y)\frac{\partial}{\partial y} + \frac{1}{2}T'(y) + W(y)\Big)\chi_\imath(y) \;=\; 0\,, \tag{12.3.5}$$

$$\Big(-\frac{\partial^3}{\partial y^3} + T(y)\frac{\partial}{\partial y} + \frac{1}{2}T'(y) - W(y)\Big)\bar{\chi}_\imath(y) \;=\; 0\,, \tag{12.3.6}$$

Differential equations of this form are closely related to a special class of flat $\mathfrak{sl}_3$ connections on $\mathcal{C}_{0,3}$ called *opers*. The action of the operator-valued matrices $M_\gamma(\mathsf{u}, \mathsf{v})$ on $\mathbf{F}^\rho(y_0, y)_{\jmath,\imath}$ turns into the multiplication with the ordinary matrices $M_\gamma(u, v)$ with $u = e^{\mathrm{i}\mu}$ and $v = e^{\mathrm{i}\nu}$ in the limit (12.3.4), where

$$\nu = \frac{\mu}{2} + 2\pi\frac{b^2}{\mathrm{i}}\frac{\partial}{\partial\mu}\mathcal{Y}(\rho, \mu). \tag{12.3.7}$$

The matrices $M_\gamma(u, v)$ represent the monodromy of the differential equation (12.3.5). Equation (12.3.7) describes the image of $\mathrm{Op}_{\mathfrak{sl}_3}(\mathcal{C}_{0,3})$ within $\mathcal{M}^{SL(3)}_{\text{flat}}(\mathcal{C}_{0,3})$ under the holonomy map. It therefore represents

a higher rank analog of the generating function of the variety of $\mathfrak{sl}_2$-opers proposed to represent the Yang's function for the quantised Hitchin system in [130], [70],[109].

Another interesting limit is $b \to i$, where $c = 2$. In this case one finds $q^2 = 1$, so that the operators u and v commute with each other. The transformation

$$\mathcal{G}^\rho(y_0, y; \kappa, \lambda)_{\bar{\imath}u} = \sum_{n \in \mathbb{Z}} e^{\pi \mathrm{i}\, n\lambda} e^{-\frac{\pi}{2}\mathrm{i}\, n^2} \mathcal{F}^\rho_{\kappa+n}(y_0, y)_{\bar{\imath}u} \tag{12.3.8}$$

diagonalises u and v simultaneously with eigenvalues $u = e^{-2\pi \mathrm{i}\, \kappa}$ and $v = \mathrm{i} e^{-\pi \mathrm{i}(\kappa+\lambda)}$, respectively. It follows that the operator-valued monodromy matrices $\mathsf{M}_\gamma = M_\gamma(\mathsf{u}, \mathsf{v})$ are transformed into ordinary matrices $M_\gamma(u, v)$. The conformal blocks $\mathcal{G}^\rho$ represent solutions to the Riemann-Hilbert problem to construct multi-valued analytic functions on $\mathcal{C}_{0,3}$ with monodromies fixed by the data λ, κ. Following [131] one may identify the function

$$G^\rho(\kappa, \lambda) = \sum_{n \in \mathbb{Z}} e^{\pi \mathrm{i}\, n\lambda} e^{-\frac{\pi}{2}\mathrm{i}\, n^2} F^\rho_{\kappa+n} \tag{12.3.9}$$

as the isomondromic tau function.

Chapter 13

Conclusions and outlook

In Part III of this thesis we have defined a convenient natural parametrisation for spaces of Toda conformal blocks in terms of screening charges through the free field representation of $\mathcal{W}_N$ algebras. This has allowed us to construct a family of chiral vertex operators and derive operator valued monodromy matrices from the point of view of $\mathfrak{sl}_3$ Toda CFT. We have then defined Verlinde network operators and, based on our results and also results collected from literature, constructed a proof of the isomorphism between the algebras $\mathcal{A}_V$ of Verlinde network operators on spaces of Toda conformal blocks $\mathrm{CB}(\mathcal{C}_{g,n})$ and the quantised algebras $\mathcal{A}_{\text{flat}}$ of functions on moduli spaces of flat connections $\mathcal{M}_{\text{flat}}^{SL(N)}(\mathcal{C}_{g,n})$, studied in Part II.

Proving this relation was set in Section 1.5 as one of the main goals for this thesis, since it is a key to establishing the isomorphism between $\mathcal{A}_V$ and the algebras of supersymmetric line operators $\mathcal{A}_{\mathfrak{X}}$ in theories $\mathfrak{X}(\mathcal{C}_{g,n}, \mathfrak{sl}_N)$ of class $\mathcal{S}$, by the arguments in Section 1.4. Together with the remarks comparing the spectra of the operators which realise the algebras $\mathcal{A}_V$ and $\mathcal{A}_{\text{flat}}$, it therefore constitutes evidence for a higher-rank AGT correspondence.

We have furthermore found a remarkably simple relation between the screening charges which enter the construction of Toda conformal blocks in the free field representation for $\mathfrak{sl}_3$ Toda CFT and Fenchel-Nielsen type coordinates for the space $\mathcal{M}_{\text{flat}}^{SL(3)}(\mathcal{C}_{0,3})$. This direct link between the free field realisation of CFTs and the (quantum) geometry of flat connections on Riemann surfaces seems to offer a key towards a more direct understanding of the relations between these two subjects. We believe that these relations deserve to be investigated much more extensively.

13.1 More punctures

The generalisation to construct "quantum" monodromy matrices for conformal blocks on surfaces with a higher number of punctures should be straightforward. A simple counting of variables indicates that Fenchel-Nielsen type coordinates for surfaces $\mathcal{C}_{0,n}$ with arbitrary n can be obtained from the Fenchel-Nielsen coordinates of all subsurfaces of type $\mathcal{C}_{0,3}$ and $\mathcal{C}_{0,4}$ appearing in a pants decomposition of $\mathcal{C}_{0,n}$. The previous chapters have introduced all ingredients necessary to compute the monodromies of degenerate fields on any punctured Riemann sphere. Using these ingredients within the set-up of [131] it is not hard to see that the operator valued monodromy matrices can be represented as Laurent polynomials of basic shift and multiplication operators which can be related to Fenchel-Nielsen type coordinates in the

same way as before.

13.2 Continuous bases for spaces of conformal blocks in Toda CFT

The conformal blocks defined above generate a subspace of the space of conformal blocks which is sufficient to describe the holomorphic factorisation for the subset of the physical correlation functions in $\mathfrak{sl}_N$ Toda CFT admitting multiple integral representations of Dotsenko-Fateev type. For the case of Liouville theory it is known that one needs to consider continuous families of conformal blocks in order to construct generic correlation functions in a holomorphically factorised form. The same qualitative feature is expected to hold in Toda CFTs associated to higher rank Lie algebras. Based on the experiences from Liouville theory one may anticipate some essential features of the generalisation from the discrete families of conformal blocks studied in the previous chapters to the cases relevant for generic Toda correlation functions.

13.2.1 Continuation in screening numbers

Recall that the conformal blocks provided by the free field representation can be labelled by the so-called screening numbers, the numbers of screening currents integrated over in the multiple-integral representations. We conjecture that conformal blocks appearing in generic Toda correlation functions are analytic functions of a set of parameters which restrict to the conformal blocks coming from the free field construction when the parameters are specialised to a discrete set of values labelled by the screening numbers.

In order to support this conjecture let us offer the following observations. A variant of the free field construction can be used to construct *continuous* families of conformal blocks. For real and sufficiently small values of the parameter b one may define, following [16], operators $Q_i(\gamma)$, $i = 1, 2$ by integrating along contours γ supported on the unit circle. Following the discussion of the Virasoro case in [17] one may argue that the operators $Q_i(\gamma)$ are densely defined and can be made *positive* self-adjoint with respect to the natural scalar product on the direct sum of unitary Fock modules $\int_{\mathbb{S}} d\alpha\, \mathcal{V}_\alpha$, with $\mathbb{S}$ being the set of vectors α of the form $\alpha = \mathcal{Q} + \mathrm{i}\mathfrak{p}$, $\mathfrak{p} \in \mathbb{R}^2$, $\mathcal{Q} = \rho_W(b + b^{-1})$ and ρ_W being the Weyl vector of $\mathfrak{sl}_3$. The operator $Q_{12}(\gamma)$ defined in (8.1.4) can also be shown to be proportional to a positive operator by expressing it as an ordered double integral and normal-ordering the product $S_1(y)S_2(y')$. For purely imaginary values of n_1, n_{12} and n_2 one may therefore define *unitary* operators denoted by $Q_1^{n_2}(\gamma)$, $Q_{12}^{n_{12}}(\gamma)$, and $Q_2^{n_1}(\gamma)$ by simply taking $Q_i^{n_i}(\gamma) = \exp(n_i \log(Q_i(\gamma))$, for $i = 1, 12, 2$. We conjecture that $Q_i^{n_i}(\gamma)$ can be defined for even more general values of n_i by analytic continuation.

This means in particular that the definition of the conformal blocks $\mathcal{F}_k^\rho$ given in Section 6.5 can be generalised to provide families of conformal blocks for $\mathcal{C}_{0,3}$ labelled by a set of continuous parameters $\rho = (\alpha_3, \alpha_2, \alpha_1)$ and k. We conjecture that the dependence of F_k^ρ on ρ and k is meromorphic. This is consistent with, and supported by the fact that the operator-valued monodromy matrices calculated here have an obvious analytic continuation which is entire analytic in the parameter k and meromorphic in ρ. If the conformal blocks on $\mathcal{C}_{0,3}$ have an analytic continuation in these parameters as conjectured, the quantum monodromies defined from the analytically continued conformal blocks must coincide with the obvious analytic continuation of the monodromy matrices calculated here.

Conformal field theory	Quantum group theory	Moduli space
Liouville theory	Modular double of $\mathcal{U}_q(SL(2,\mathbb{R}))$	$PSL(2,\mathbb{R})$-connections, Fuchsian component.

Table 13.1: *Relations between conformal field theory, quantum group theory and moduli spaces of flat connections relevant for the case of Liouville theory. The Fuchsian component in the moduli space of flat $PSL(2,\mathbb{R})$ connections is the connected component formed by all connections having holonomies $\rho : \pi_1(\mathcal{C}) \to PSL(2,\mathbb{R})$ such that $\mathbb{H}/\rho$ is a Riemann surface of the same topological type as $\mathcal{C}$.*

13.2.2 Relation to quantum group theory and higher Teichmüller theory

There are further encouraging hints that the description of the continuous families of Virasoro conformal blocks relevant for Liouville theory admits a higher rank generalisation representing the analytic continuation of the conformal blocks considered in Part III of this thesis. Let us recall that the conformal blocks needed for generic correlation functions come in families associated to a continuous series of Virasoro representations [19]. The monodromies of conformal blocks can be represented in term of the $6j$-symbols associated to a continuous family of representations of the non-compact quantum group $\mathcal{U}_q(SL(2,\mathbb{R}))$ [16]. The relevant family of quantum group representations [132], [133] is distinguished by remarkable positivity properties closely related [134] to the phenomenon of modular duality [135], [132], [136]. All this is closely related to the quantisation of the Teichmüller spaces [137], [138]: it turns out that the $6j$-symbols of $\mathcal{U}_q(SL(2,\mathbb{R}))$ mentioned above describe the change of pants decompositions on the four-holed sphere in quantum Teichmüller theory [17], [139]. The situation is summarised in Table 13.1.

The mathematical structures appearing in Liouville theory have generalisations associated to Lie algebras of higher ranks. The higher Teichmüller theories [63] can be quantised [140]. A key feature facilitating the quantisation of the higher Teichmüller spaces is the positivity of the coordinates introduced in [63] when restricted to the so-called Teichmüller component, a connected component in the moduli spaces of flat $PSL(N,\mathbb{R})$-connections generalising the Fuchsian component isomorphic to the Teichmüller spaces for $N = 2$ [141]. This generalises similar properties of the ordinary Teichmüller spaces when described in terms of the coordinates going back to [142].

The main new feature in the higher rank cases is the appearance of non-trivial spaces of three point conformal blocks. We expect these spaces to be isomorphic to the multiplicity spaces of Clebsch-Gordan maps for the positive representations of $\mathcal{U}_q(SL(N,\mathbb{R}))$. The study of the positive representations of $\mathcal{U}_q(SL(N,\mathbb{R}))$, $N > 2$, was initiated in [143]. The Clebsch-Gordan maps for this class of representations of $\mathcal{U}_q(SL(N,\mathbb{R}))$ have recently been constructed in [144]. For the case $N = 3$ one gets bases for the space of Clebsch-Gordan maps labelled by one continuous parameter. The constructions in [145], [144] reveal a direct connection between the positive representations of $\mathcal{U}_q(SL(N,\mathbb{R}))$ and the quantised higher Teichmüller theories, generalising what was found for $N = 2$ in [146], [139].

It should be possible to establish a link between the continuous families of conformal blocks introduced above and a suitable basis for the space of Clebsch-Gordan maps between positive representations of $\mathcal{U}_q(SL(3,\mathbb{R}))$ by generalising the constructions in [16] for the case of Liouville theory. The positivity of the screening charges together with the direct relation between Clebsch-Gordan maps and free field representation established in the previous chapters suggests that there is a scalar product on the space of conformal blocks on $\mathcal{C}_{0,3}$ with $\rho = (\alpha_3, \alpha_2, \alpha_1)$, $\alpha_i = \mathcal{Q} + \mathfrak{i}\mathfrak{p}_i$ for which the conformal blocks F_k^ρ with

$k \in \mathrm{i}\mathbb{R}$ generate a basis.

Appendices

Appendix B

Useful relations

We compile here a list of useful relations for the quantum group related calculations in Part III. We wish to compute the action of the raising operators e_i on some generic representation of $\mathcal{U}_q(\mathfrak{sl}_3)$, which is constructed from a highest weight vector v_λ, that is $\mathsf{e}_i e^\lambda_{\mathbf{n}} = \mathsf{e}_i \mathsf{f}_1^{n_1} \mathsf{f}_{12}^{n} \mathsf{f}_2^{n_2} v_\lambda$. To do so we use the notations $\mathbf{n} = (n_1, n, n_2) = (s_1 - k, k, s_2 - k) = ß_k$ and also $\mathbf{s}_1 = (1,0,0)$, $\mathbf{s}_2 = (0,0,1)$, $\mathbf{s}_3 = (1,0,1)$ and $\mathbf{s}_{12} = (0,1,0)$. For $e_{12} = e_1 + e_2$,

$$[\mathsf{e}_1, \mathsf{f}_{12}] = \mathsf{f}_2 \mathsf{k}_1^{-1} , \qquad [\mathsf{e}_2, \mathsf{f}_{12}] = -q \mathsf{f}_1 \mathsf{k}_2 \tag{B.0.1}$$

$$[\mathsf{e}_{12}, \mathsf{f}_1] = -q \mathsf{k}_1 \mathsf{e}_2 , \qquad [\mathsf{e}_{12}, \mathsf{f}_2] = \mathsf{k}_2^{-1} \mathsf{e}_1 \tag{B.0.2}$$

$$[\mathsf{e}_{12}, \mathsf{f}_{12}] = \frac{q}{q - q^{-1}} (\mathsf{k}_1^{-1} \mathsf{k}_2^{-1} - \mathsf{k}_1 \mathsf{k}_2) \tag{B.0.3}$$

$$\mathsf{e}_1 \mathsf{f}_1^m = \mathsf{f}_1^m \mathsf{e}_1 + \frac{[m]}{q - q^{-1}} \mathsf{f}_1^{m-1} (q^{2(1-m)} \mathsf{k}_1 - \mathsf{k}_1^{-1}) \tag{B.0.4}$$

$$\mathsf{e}_2 \mathsf{f}_2^m = \mathsf{f}_2^m \mathsf{e}_2 + \frac{[m]}{q - q^{-1}} \mathsf{f}_2^{m-1} (q^{2(1-m)} \mathsf{k}_2 - \mathsf{k}_2^{-1}) \tag{B.0.5}$$

$$\mathsf{e}_1 \mathsf{f}_{12}^m = \mathsf{f}_{12}^m \mathsf{e}_1 + [m] \mathsf{f}_{12}^{m-1} \mathsf{f}_2 \mathsf{k}_1^{-1} \tag{B.0.6}$$

$$\mathsf{e}_2 \mathsf{f}_{12}^m = \mathsf{f}_{12}^m \mathsf{e}_2 - [m] q^{2-m} \mathsf{f}_1 \mathsf{f}_{12}^{m-1} \mathsf{k}_2 \tag{B.0.7}$$

$$\mathsf{e}_{12} \mathsf{f}_1^m = \mathsf{f}_1^m \mathsf{e}_{12} - [m] q^{-2m+3} \mathsf{f}_1^{m-1} \mathsf{k}_1 \mathsf{e}_2 \tag{B.0.8}$$

$$\mathsf{e}_{12} \mathsf{f}_{12}^m = \mathsf{f}_{12}^m \mathsf{e}_{12} - \frac{[m]}{1 - q^{-2}} \mathsf{f}_{12}^{m-1} (q^{2(1-m)} \mathsf{k}_1 \mathsf{k}_2 - \mathsf{k}_1^{-1} \mathsf{k}_2^{-1}) \tag{B.0.9}$$

$$\mathsf{e}_{12} \mathsf{f}_2^m = \mathsf{f}_2^m \mathsf{e}_{12} + [m] \mathsf{f}_2^{m-1} \mathsf{k}_2^{-1} \mathsf{e}_1 \tag{B.0.10}$$

The matrix elements which give actions of generators e_i on representations of $\mathcal{U}_q(\mathfrak{sl}_3)$ are

$$\begin{aligned}
\mathsf{e}_1 e^\lambda_{ß_k} &= \mathsf{v}^{-1}[k] q^{-s_2 - (e_1, \lambda)} e^\lambda_{ß_k - \mathbf{s}_1} + [s_1 - k][1 - s_1 - k + s_2 + (e_1, \lambda)] q^{1 + 2k - s_2 - (e_1, \lambda)} e^\lambda_{ß_k - \mathbf{s}_1} \\
\mathsf{e}_2 e^\lambda_{ß_k} &= -\mathsf{v}^{-1}[k] q^{2 - 2s_2 + (e_2, \lambda)} e^\lambda_{ß_k - \mathbf{s}_2} + [s_2 - k][1 - s_2 + k + (e_2, \lambda)] q^{1 - (e_2, \lambda)} e^\lambda_{ß_k - \mathbf{s}_2} \\
\mathsf{e}_{12} e^\lambda_{ß_k} &= -[s_1 - k][s_2 - k][1 - s_2 + k + (e_2, \lambda)] q^{3 - 2s_1 + s_2 + (e_1 - e_2, \lambda)} e^\lambda_{ß_k - \mathbf{s}_3} \\
&\quad + \mathsf{v}^{-1}[k] q^{4 - 2k - s_2 + (e_{12}, \lambda)} (q^{-2(s_1 - k)}[s_1 - k] + [s_2 - 1 - (e_{12}, \lambda)]) e^\lambda_{ß_k - \mathbf{s}_3} .
\end{aligned} \tag{B.0.11}$$

The operator v acts on representations $e_{ß_k}$ through $\mathsf{v} e^\lambda_{ß_k} = q^{-k} e^\lambda_{ß_{k+1}}$ and therefore shifts the value of the multiplicity label k. One may note however that k is bounded and when it is zero, any term which includes v^{-1} in equations (B.0.11) vanishes due to the presence of the factor $[k]$. Thus from equations

(B.0.11), for some generic fixed $ß_k$, the matrix elements representing the generators e are non-zero only for particular $ß'_k$

$$R^{\lambda,ß_k}_{(\mathsf{e}_1),ß'_k} \neq 0 \quad \text{iff} \quad ß'_k \in \{ß_k + (1,0,0)\ ,\ ß_{k+1} + (1,0,0)\}\ , \tag{B.0.12}$$

$$R^{\lambda,ß_k}_{(\mathsf{e}_2),ß'_k} \neq 0 \quad \text{iff} \quad ß'_k \in \{ß_k + (0,0,1)\ ,\ ß_{k+1} + (0,0,1)\}\ , \tag{B.0.13}$$

$$R^{\lambda,ß_k}_{(\mathsf{e}_{12}),ß'_k} \neq 0 \quad \text{iff} \quad ß'_k \in \{ß_k + (1,0,1)\ ,\ ß_{k+1} + (1,0,1)\}\ . \tag{B.0.14}$$

When $ß_k = 0$, the values of $ß'_k$ are more restricted, since each component of $ß'_k$ is non-negative

$$R^{\lambda,0}_{(\mathsf{e}_i),ß'_k} \neq 0 \quad \text{iff} \quad ß'_k = \{(1,0,0)\delta_{i,1}, (0,0,1)\delta_{i,2}, (1,0,1)\delta_{i,12}, (0,1,0)\delta_{i,12}\} \tag{B.0.15}$$

If we hold s_i fixed, then equations (B.0.11) set the representations of the e_i generators to be

$$\begin{aligned}
R^{\lambda,ß_{k-1}-\mathbf{s}_1}_{(\mathsf{e}_1),ß_k} &= [k]q^{-s_2+k-(e_1,\lambda)} \qquad\qquad (\text{B.0.16})\\
R^{\lambda,ß_k-\mathbf{s}_1}_{(\mathsf{e}_1),ß_k} &= [s_1-k][1-s_1-k+s_2+(e_1,\lambda)]q^{1+2k-s_2-(e_1,\lambda)}\\
R^{\lambda,ß_{k-1}-\mathbf{s}_2}_{(\mathsf{e}_2),ß_k} &= -[k]q^{2-2s_2+k+(e_2,\lambda)}\\
R^{\lambda,ß_k-\mathbf{s}_2}_{(\mathsf{e}_2),ß_k} &= [s_2-k][1-s_2+k+(e_2,\lambda)]q^{1-(e_2,\lambda)}\\
R^{\lambda,ß_{k-1}-\mathbf{s}_3}_{(\mathsf{e}_{12}),ß_k} &= [k]q^{4-k-s_2+(e_{12},\lambda)}(q^{-2(s_1-k)}[s_1-k]+[s_2-1-(e_{12},\lambda)])\\
R^{\lambda,ß_k-\mathbf{s}_3}_{(\mathsf{e}_{12}),ß_k} &= -[s_1-k][s_2-k][1-s_2+k+(e_2,\lambda)]q^{3-2s_1+s_2+(e_1-e_2,\lambda)}\ .
\end{aligned}$$

The e_i label can be omitted since it is redundant, being implied by the difference of weights. Similarly, the action of generators f_i is represented by

$$R^{\lambda,ß_k+\mathbf{s}_1}_{ß_k} = 1\ ,\ R^{\lambda,ß_{k+1}+\mathbf{s}_3}_{ß_k} = q^{s_1-k}\ ,\ R^{\lambda,ß_k+\mathbf{s}_2}_{ß_k} = q^{2k-s_1}\ ,\ R^{\lambda,ß_{k+1}+\mathbf{s}_2}_{ß_k} = -q^{k-s_1}[s_1-k]\ . \tag{B.0.17}$$

Appendix C

Clebsch-Gordan coefficients

Here we sketch how to compute the Clebsch-Gordan coefficients which enter the construction of chiral vertex operators in Section 7.2, starting from equation (7.2.18) reproduced below

$$0 = \sum_{\mathbf{n}_2'} \left(\begin{smallmatrix} \lambda_3 \\ 0 \end{smallmatrix} \middle| \begin{smallmatrix} \lambda_2 & \lambda_1 \\ \mathbf{n}_2' & \mathbf{n}_1 \end{smallmatrix} \right) q^{(e_i,\nu_1)} R^{\lambda_2,\mathbf{n}_2}_{(\mathsf{e}_i),\mathbf{n}_2'} + \sum_{\mathbf{n}_1'} \left(\begin{smallmatrix} \lambda_3 \\ 0 \end{smallmatrix} \middle| \begin{smallmatrix} \lambda_2 & \lambda_1 \\ \mathbf{n}_2 & \mathbf{n}_1' \end{smallmatrix} \right) R^{\lambda_1,\mathbf{n}_1}_{(\mathsf{e}_i),\mathbf{n}_1'} \ . \tag{C.0.1}$$

To lighten notation, let us drop the first column in the notation $(\cdot|\cdot\cdot)$, which will be everywhere $\left(\begin{smallmatrix} \lambda_3 \\ 0 \end{smallmatrix}\right)$ and where λ_3 is fully determined by the other weights.

C.1 Clebsch-Gordan coefficients for generic weights λ

For generic weights λ, equation (C.0.1) can be used iteratively to determine the CGC $\left(\begin{smallmatrix} \lambda_2 & \lambda_1 \\ \mathbf{n}_2 & \mathbf{n}_1 \end{smallmatrix}\right)$ in terms of $\left(\begin{smallmatrix} \lambda_2 & \lambda_1 \\ \mathbf{n} & 0 \end{smallmatrix}\right)$ by constructing $\mathbf{n}_1$ as $\mathbf{n}_1 = n_{1,1}\mathbf{s}_1 + n_1\mathbf{s}_{12} + n_{1,2}\mathbf{s}_2$. Below we first describe the calculation for $\mathbf{n}_1 \in \{\mathbf{s}_1, \mathbf{s}_2, \mathbf{s}_{12}, \mathbf{s}_3\}$, which represent the first two steps of the iteration, and then describe the general inductive step. Beginning with equation (C.0.1), $\mathbf{n}_1 = 0$ and $i = 1, 2$

$$0 \ = \ \left(\begin{smallmatrix} \lambda_2 & \lambda_1 \\ \mathbb{ß}_k & \mathbf{s}_i \end{smallmatrix}\right) R^{\lambda_1,0}_{\mathbf{s}_i} + \left(\begin{smallmatrix} \lambda_2 & \lambda_1 \\ \mathbb{ß}_k+\mathbf{s}_i & 0 \end{smallmatrix}\right) q^{(e_i,\lambda_1)} R^{\lambda_2,\mathbb{ß}_k}_{\mathbb{ß}_k+\mathbf{s}_i} + \left(\begin{smallmatrix} \lambda_2 & \lambda_1 \\ \mathbb{ß}_{k+1}+\mathbf{s}_i & 0 \end{smallmatrix}\right) q^{(e_i,\lambda_1)} R^{\lambda_2,\mathbb{ß}_k}_{\mathbb{ß}_{k+1}+\mathbf{s}_i} \ . \tag{C.1.2}$$

The resulting system is under-determined, so we solve for a one-parameter family of solutions with the constraint (7.2.19)

$$\left(\begin{smallmatrix} \lambda_2 & \lambda_1 \\ \mathbb{ß}_k & \mathbf{s}_i \end{smallmatrix}\right)_k \ = \ -q^{(e_i,\lambda_1)} \left(R^{\lambda_1,0}_{\mathbf{s}_i}\right)^{-1} R^{\lambda_2,\mathbb{ß}_k}_{\mathbb{ß}_k+\mathbf{s}_i} \ , \ \left(\begin{smallmatrix} \lambda_2 & \lambda_1 \\ \mathbb{ß}_{k-1} & \mathbf{s}_i \end{smallmatrix}\right)_k = -q^{(e_i,\lambda_1)} \left(R^{\lambda_1,0}_{\mathbf{s}_i}\right)^{-1} R^{\lambda_2,\mathbb{ß}_{k-1}}_{\mathbb{ß}_k+\mathbf{s}_i} \tag{C.1.3}$$

The second step sets $\mathbf{n}_1' = \mathbf{s}_{12}, \mathbf{s}_3$ and we use (C.0.1) with $(\mathbf{n}_1 = \mathbf{s}_2, i = 1)$ and $(\mathbf{n}_1 = \mathbf{s}_1, i = 2)$

$$0 \ = \ \sum_{j=3,12} \left(\begin{smallmatrix} \lambda_2 & \lambda_1 \\ \mathbb{ß}_l & \mathbf{s}_j \end{smallmatrix}\right)_k R^{\lambda_1,\mathbf{s}_3-\mathbf{s}_i}_{\mathbf{s}_j} + q^{1+(e_i,\lambda_1)} \sum_{l'=0,1} \left(\begin{smallmatrix} \lambda_2 & \lambda_1 \\ \mathbb{ß}_{l+l'}+\mathbf{s}_i & \mathbf{s}_3-\mathbf{s}_i \end{smallmatrix}\right)_k R^{\lambda_2,\mathbb{ß}_l}_{\mathbb{ß}_{l+l'}+\mathbf{s}_i} \ .$$

These equations alone are not sufficient to fully determine $\left(\begin{smallmatrix} \lambda_2 & \lambda_1 \\ \mathbf{n}_2 & \mathbf{s}_3 \end{smallmatrix}\right)_k$, $\left(\begin{smallmatrix} \lambda_2 & \lambda_1 \\ \mathbf{n}_2 & \mathbf{s}_{12} \end{smallmatrix}\right)_k$. One first needs to insert the solutions (C.1.3) into the right-most coefficients, thereby arriving at a pair of coupled equations

$$\begin{aligned} q^{-1-(e_{12},\lambda_1)} R^{\lambda_1,0}_{\mathbf{s}_i} \sum_{j=3,12} \left(\begin{smallmatrix} \lambda_2 & \lambda_1 \\ \mathbb{ß}_l & \mathbf{s}_j \end{smallmatrix}\right)_k R^{\lambda_1,\mathbf{s}_i}_{\mathbf{s}_j} &= \left(\begin{smallmatrix} \lambda_2 & \lambda_1 \\ \mathbb{ß}_l+\mathbf{s}_3 & 0 \end{smallmatrix}\right)_k R^{\lambda_2,\mathbb{ß}_l}_{\mathbb{ß}_l+\mathbf{s}_3-\mathbf{s}_i} R^{\lambda_2,\mathbb{ß}_l+\mathbf{s}_3-\mathbf{s}_i}_{\mathbb{ß}_l+\mathbf{s}_3} \\ &+ \left(\begin{smallmatrix} \lambda_2 & \lambda_1 \\ \mathbb{ß}_{l+1}+\mathbf{s}_3 & 0 \end{smallmatrix}\right)_k \left(R^{\lambda_2,\mathbb{ß}_l}_{\mathbb{ß}_l+\mathbf{s}_3-\mathbf{s}_i} R^{\lambda_2,\mathbb{ß}_l+\mathbf{s}_3-\mathbf{s}_i}_{\mathbb{ß}_{l+1}+\mathbf{s}_3} + R^{\lambda_2,\mathbb{ß}_l}_{\mathbb{ß}_{l+1}+\mathbf{s}_3-\mathbf{s}_i} R^{\lambda_2,\mathbb{ß}_{l+1}+\mathbf{s}_3-\mathbf{s}_i}_{\mathbb{ß}_{l+1}+\mathbf{s}_3} \right) \\ &+ \left(\begin{smallmatrix} \lambda_2 & \lambda_1 \\ \mathbb{ß}_{l+2}+\mathbf{s}_3 & 0 \end{smallmatrix}\right)_k R^{\lambda_2,\mathbb{ß}_l}_{\mathbb{ß}_{l+1}+\mathbf{s}_3-\mathbf{s}_i} R^{\lambda_2,\mathbb{ß}_{l+1}+\mathbf{s}_3-\mathbf{s}_i}_{\mathbb{ß}_{l+2}+\mathbf{s}_3} \end{aligned} \tag{C.1.4}$$

with three solutions $\left(\begin{smallmatrix}\lambda_2 & \lambda_1\\ ß_l & \mathbf{s}_i\end{smallmatrix}\right)_k$ distinguished by $l \in \{k, k-1, k-2\}$.

Inductive step: Let us consider a pair of equations labeled by two integers (s_1, s_2) which enter the weight $\nu_1' = \lambda_1 - s_1 e_1 - s_2 e_2 < \lambda_1$. If we denote by w' the sum $w' = s_1 + s_2$ of these labels, which enter the CGC under the weight λ_1

$$\left(\begin{smallmatrix}\lambda_2 & \lambda_1\\ \mathbf{n} & \mathbf{s}_m\end{smallmatrix}\right)_k \ , \qquad \left(\begin{smallmatrix}\lambda_2 & \lambda_1\\ \mathbf{n} & \mathbf{s}_{m+1}\end{smallmatrix}\right)_k \ , \tag{C.1.5}$$

then these coefficients are determined by the coupled pair of linear equations with label (s_1, s_2) in terms of coefficients with $w = w' - 1$ and for which $\nu_1 = \lambda_1 - s_1 e_1 - s_2 e_2 + e_i > \nu_1'$. It is thus possible to set up an induction procedure through the pair of equations

$$\sum_{m'=0,1} \left(\begin{smallmatrix}\lambda_2 & \lambda_1\\ \mathbf{n} & ß_{m+m'}\end{smallmatrix}\right)_k R^{\lambda_1, ß_m - \mathbf{s}_i}_{ß_{m+m'}} = -q^{(e_i,\nu_1)} \sum_{\mathbf{n}' \in \{\mathbf{n}+\mathbf{s}_i, \mathbf{n}+\mathbf{s}_{12}-\mathbf{s}_{j\neq i}\}} \left(\begin{smallmatrix}\lambda_2 & \lambda_1\\ \mathbf{n}' & ß_m - \mathbf{s}_i\end{smallmatrix}\right)_k R^{\lambda_2, \mathbf{n}}_{\mathbf{n}'} \tag{C.1.6}$$

for $i = 1, 2$, which corresponds to the actions of the $\mathsf{e}_1, \mathsf{e}_2$ generators respectively. Note that the parameter j can also only take values $1, 2$ depending on the particular value of i. A possible obstruction to inverting this system and solve for the CGC in (C.1.5) could arise if the matrix of coefficients in equations (C.1.6)

$$\begin{pmatrix} R^{\lambda_1, ß_m - \mathbf{s}_1}_{ß_m} & R^{\lambda_1, ß_m - \mathbf{s}_1}_{ß_{m+1}} \\ R^{\lambda_1, ß_m - \mathbf{s}_2}_{ß_m} & R^{\lambda_1, ß_m - \mathbf{s}_2}_{ß_{m+1}} \end{pmatrix} \tag{C.1.7}$$

were not invertible. This is however not the case for generic weights λ_1, λ_2, given the explicit expressions (B.0.16).

C.2 Clebsch-Gordan coefficients for the case $\lambda_2 = \omega_1$

When one of the highest weights is a fundamental weight, specifically $\lambda_2 = \omega_1$, the CGC no longer come in families parametrised by an integer k and they can be computed in a few steps. For example

$$0 = \left(\begin{smallmatrix}\omega_1 & \lambda\\ \mathbf{s}_1 & 0\end{smallmatrix}\right) q^{(e_1,\lambda)} R^{\omega_1,0}_{\mathbf{s}_1} + \left(\begin{smallmatrix}\omega_1 & \lambda\\ 0 & \mathbf{s}_1\end{smallmatrix}\right) R^{\lambda,0}_{\mathbf{s}_1} \quad \Rightarrow \quad \left(\begin{smallmatrix}\omega_1 & \lambda\\ 0 & \mathbf{s}_1\end{smallmatrix}\right) = q^{-1}[-(e_1,\lambda)]^{-1} \left(\begin{smallmatrix}\omega_1 & \lambda\\ \mathbf{s}_1 & 0\end{smallmatrix}\right) \ . \tag{C.2.8}$$

When $\mathbf{n}_1' = \mathbf{s}_{12}, \mathbf{s}_3$, one finds from equation (C.0.1)

$$0 \ = \ \left(\begin{smallmatrix}\omega_1 & \lambda\\ \mathbf{s}_i & \mathbf{s}_3 - \mathbf{s}_i\end{smallmatrix}\right) q^{1+(e_i,\lambda)} R^{\omega_1,0}_{\mathbf{s}_i} + \left(\begin{smallmatrix}\omega_1 & \lambda\\ 0 & \mathbf{s}_3\end{smallmatrix}\right) R^{\lambda, \mathbf{s}_3 - \mathbf{s}_i}_{\mathbf{s}_3} + \left(\begin{smallmatrix}\omega_1 & \lambda\\ 0 & \mathbf{s}_{12}\end{smallmatrix}\right) R^{\lambda, \mathbf{s}_3 - \mathbf{s}_i}_{\mathbf{s}_{12}} \ , \ \ i = 1, 2 \tag{C.2.9}$$

and

$$\begin{aligned} 0 \ = \ & \left(\begin{smallmatrix}\omega_1 & \lambda\\ \mathbf{s}_{12} & 0\end{smallmatrix}\right) q^{(e_{12},\lambda)} R^{\omega_1,0}_{\mathbf{s}_{12}} + \left(\begin{smallmatrix}\omega_1 & \lambda\\ \mathbf{s}_3 & 0\end{smallmatrix}\right) q^{(e_{12},\lambda)} R^{\omega_1,0}_{\mathbf{s}_3} \\ & + \left(\begin{smallmatrix}\omega_1 & \lambda\\ 0 & \mathbf{s}_3\end{smallmatrix}\right) R^{\lambda,0}_{\mathbf{s}_3} + \left(\begin{smallmatrix}\omega_1 & \lambda\\ 0 & \mathbf{s}_{12}\end{smallmatrix}\right) R^{\lambda,0}_{\mathbf{s}_{12}} + (1-q^2) \left(\begin{smallmatrix}\omega_1 & \lambda\\ \mathbf{s}_1 & \mathbf{s}_2\end{smallmatrix}\right) q^{(e_1,\lambda)} R^{\lambda,0}_{\mathbf{s}_2} R^{\omega_1,0}_{\mathbf{s}_1} \ . \end{aligned} \tag{C.2.10}$$

The solution to this system is given by

$$\left(\begin{smallmatrix}\omega_1 & \lambda\\ 0 & \mathbf{s}_{12}\end{smallmatrix}\right) = -[-(e_2,\lambda)] q^{1+(e_{12},\lambda)} \mathsf{c}_\lambda^{-1} \ , \quad \left(\begin{smallmatrix}\omega_1 & \lambda\\ 0 & \mathbf{s}_3\end{smallmatrix}\right) = q^{1+(e_{12},\lambda)} \mathsf{c}_\lambda^{-1} \tag{C.2.11}$$

$$\left(\begin{smallmatrix}\omega_1 & \lambda\\ \mathbf{s}_1 & \mathbf{s}_2\end{smallmatrix}\right) = q^{(e_2-e_1,\lambda)} ([-(e_2,\lambda)] - [1+(e_1,\lambda)]) \mathsf{c}_\lambda^{-1} \ , \tag{C.2.12}$$

for the normalization $\left(\begin{smallmatrix}\omega_1 & \lambda\\ \delta_i & 0\end{smallmatrix}\right) = 1$ and where

$$\mathsf{c}_\lambda = q^{-(e_{12},\lambda)} [(e_2,\lambda)] \left(q^{2+2(e_1,\lambda)} (1 + [-(e_{12},\lambda)]) + (1-q^2) ([-(e_2,\lambda)] - [1+(e_1,\lambda)]) \right) \ .$$

Appendix D

Braid matrix derivation

In this appendix we collect a few of the more technical points that occur in the calculations of the braiding of screened vertex operators in Chapter 9, as was depicted in Figure 8.2 and reproduced below in Figure D.1.

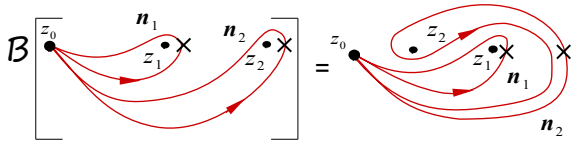

Figure D.1: *Braiding of two generic multi-contours.*

This procedure was described in Section 8.3 as an induction process to deform contours around z_2 in Figure D.1 to pass to linear combinations of the types of loops illustrated in Figure D.2 and then deform the resulting auxiliary loops into a set of basis contours like those in Figure 8.1.

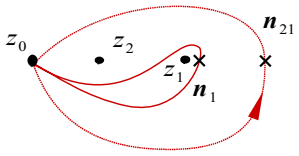

Figure D.2: *A set of auxiliary contours for the braiding calculation.*

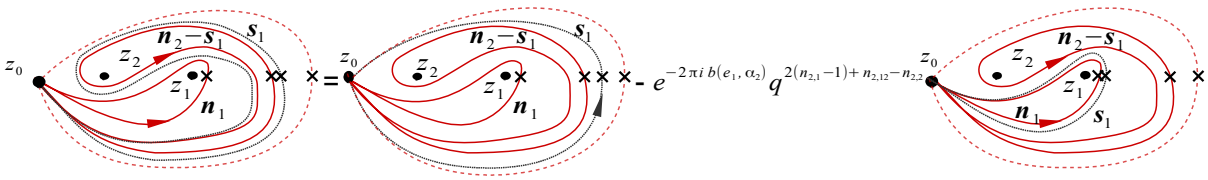

Figure D.3: *Deformation of the outermost of the contours encircling z_2.*

Part 1: The first part of the braiding calculation specifically deforms the contours around z_2 from Figure D.1 to linear combinations of loops like in Figure D.2. An intermediate step of this procedure is depicted in Figure D.3. The ordered marked points x represent normalisation points for the integral over the indicated contours, where the integrand is real. The grey contour being deformed in Figure D.3 is associated with a Q_1 screening charge and carries the label $\mathbf{s}_1$. On the right hand side, this loop turns into a sum of two types of contours. The first is a loop around both points z and has normalisation point x at the same position as on the original contour. The second type however, is a loop around only the point z_1, whose normalization point is related by analytic continuation to the marked point x on the original gray contour. This means that the relative order of the marked points x has changed and as a consequence of the exchange relation (6.4.33), a braiding factor gets generated.

This factor contains a full monodromy $\mathrm{e}^{-2\pi i b(e_1,\alpha_2)}$ due to moving the insertion point of the screening current S_1 counter-clockwise around z_2. The factor $q^{2(n_{2,1}-1)+n_{2,12}-n_{2,2}}$ then arises because one needs to relate the respective integrands defined by using two different choices of normalization points with the help of the exchange relation (6.4.33).

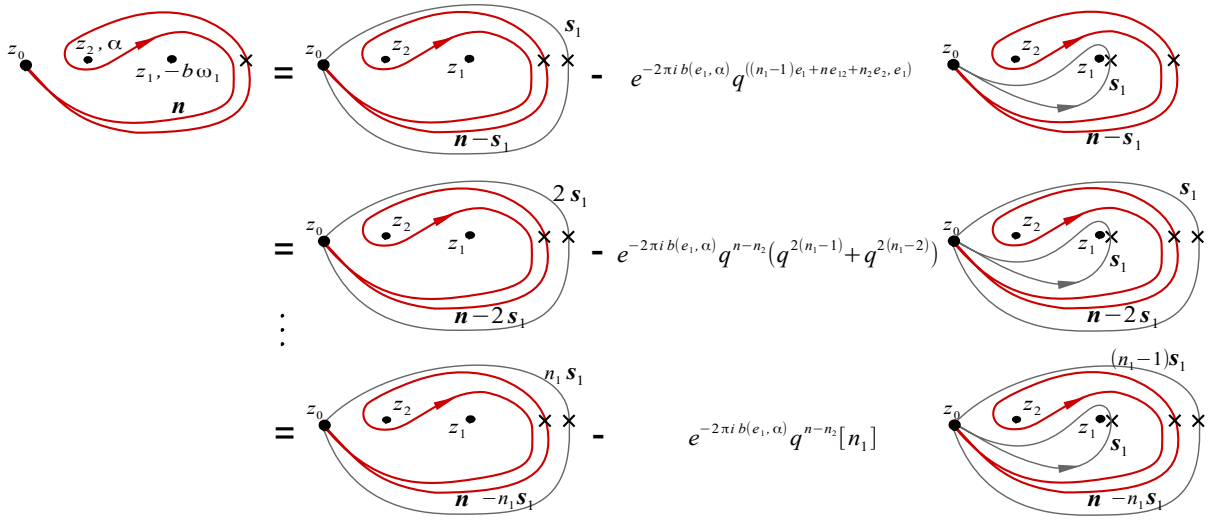

Figure D.4: *Example illustrating how quantum numbers arise in the braiding calculation.*

Repeating the step described in Figure D.3 generates quantum numbers $[n] = \frac{1-q^{2n}}{1-q^2}$, as illustrated in Figure D.4, which has a generic vertex operator at z_2 and a degenerate operator at z_1. Let us explain a few more steps in this example, as it is relevant for one of the braiding calculations in which we are interested. We may denote $\gamma_1^{\mathbf{s}_i}$ the loop around z_1 which is associated with screening charges Q_1 and Q_{12} for $i = 1$ and 12, respectively, and with no charge for $i = 0$. If we then denote $\beta_2^{\mathbf{n}}$ the deformed loop around z_2 and $\beta_{21}^{\mathbf{n}_{21}}$ the loop around both points z and denote $I[\beta_{21}^{\mathbf{n}_{21}}\beta^{\mathbf{n}}\gamma_1^{\mathbf{s}_i}]$ the integral over the indicated contours, then the intermediate results after resolving the contours associated with each type

of screening charge are

$$
\begin{aligned}
I[\beta_2^{\mathbf{n}}\gamma_1^{\mathbf{s}_0}] &= I[\beta_{21}^{n_1\mathbf{s}_1}\beta_2^{\mathbf{n}-n_1\mathbf{s}_1}\gamma_1^{\mathbf{s}_0}] - \mathrm{e}^{-2\pi i b(e_1,\alpha)}q^{n-n_2}[n_1]I[\beta_{21}^{(n_1-1)\mathbf{s}_1}\beta_2^{\mathbf{n}-n_1\mathbf{s}_1}\gamma_1^{\mathbf{s}_1}] \qquad \text{(D.0.1)}\\
&= I[\beta_{21}^{\mathbf{n}-n_2\mathbf{s}_2}\beta_2^{n_2\mathbf{s}_2}\gamma_1^{\mathbf{s}_0}] - \mathrm{e}^{-2\pi i b(e_{12},\alpha)}q^{-2+n_2}[n]I[\beta_{21}^{n_1\mathbf{s}_1+(n-1)\mathbf{s}_{12}}\beta_2^{n_2\mathbf{s}_2}\gamma_1^{\mathbf{s}_{12}}]-\\
&\quad - \mathrm{e}^{-2\pi i b(e_1,\alpha)}(q^{-1}-q)q^{-n_2}[n]I[\beta_{21}^{n_1\mathbf{s}_1+(n-1)\mathbf{s}_{12}+\mathbf{s}_2}\beta_2^{n_2\mathbf{s}_2}\gamma_1^{\mathbf{s}_1}]-\\
&\quad - \mathrm{e}^{-2\pi i b(e_1,\alpha)}q^{n-n_2}[n_1]I[\beta_{21}^{(n_1-1)\mathbf{s}_1+n\mathbf{s}_{12}}\beta_2^{n_2\mathbf{s}_2}\gamma_1^{\mathbf{s}_1}]\\
&= I[\beta_{21}^{\mathbf{n}}\gamma_1^{\mathbf{s}_0}] - \mathrm{e}^{-2\pi i b(e_1,\alpha)}(q^{-1}-q)q^{-n_2}[n]I[\beta_{21}^{\mathbf{n}-\mathbf{s}_{12}+\mathbf{s}_2}\gamma_1^{\mathbf{s}_1}]-\\
&\quad - \mathrm{e}^{-2\pi i b(e_{12},\alpha)}[n]\left(q^{-2+n_2}+(q^{-1}-q)q^{-1-n_2}[n_2]\right)I[\beta_{21}^{\mathbf{n}-\mathbf{s}_{12}}\gamma_1^{\mathbf{s}_{12}}]-\\
&\quad - \mathrm{e}^{-2\pi i b(e_1,\alpha)}q^{n-n_2}[n_1]I[\beta_{21}^{\mathbf{n}-\mathbf{s}_1}\gamma_1^{\mathbf{s}_1}] - \mathrm{e}^{-2\pi i b(e_{12},\alpha)q^{n-1-n_2}}[n_1][n_2]I[\beta_{21}^{\mathbf{n}-\mathbf{s}_3}\gamma_1^{\mathbf{s}_{12}}]\,.
\end{aligned}
$$

Note: There are two additional technical observations here: *i)* contours associated with the composite screening charge $Q_{12} = Q_1Q_2 - qQ_2Q_1$ are most safely treated when considered as linear combinations of contours for simple charges and *ii)* one must take care of the ordering of the newly generated contours, in particular when they are associated with the screening charges Q_{12} and Q_2. Any reordering of contours implies a permutation of their associated normalisation points, which further implies that braiding factors get generated, as illustrated for example by

$$
\int_\gamma dy S_1(y)V_\alpha^{\mathbf{n}}(z) = V_\alpha^{\mathbf{n}+\mathbf{s}_1}(z) \qquad \text{vs.} \qquad \int_\gamma dy S_{12}(y)V_\alpha^{\mathbf{n}}(z) = q^{n_1}V_\alpha^{\mathbf{n}+\mathbf{s}_{12}}(z)\,. \qquad \text{(D.0.2)}
$$

The case where a screening charge Q_2 is added has one additional feature. Changing the order of contours such that the $\mathbf{s}_2$ contour is inside of the loops with labels $\mathbf{s}_1$ means commuting an S_2 screening current past S_1, which by the definition of composite screening charges generates a current S_{12} and thus

$$
\int_\gamma dy S_2(y)V_\alpha^{\mathbf{n}}(z) = q^{n_{12}-n_1}V_\alpha^{\mathbf{n}+\mathbf{s}_2}(z) - q^{-n_1}[n_1]V_\alpha^{\mathbf{n}+\mathbf{s}_{12}-\mathbf{s}_1}(z)\,.
$$

Part 2: Resolving all of the deformed contours around the point z_2 in Figure D.1, that are generated by the braiding procedure, creates a combination of the types of loops in Figure D.2. The second part of the induction procedure described in section 8.3 is then the deformation of any such auxiliary loops that enclose both z_1 and z_2 in Figure D.2 into combinations of the basis contours in Figure 8.1. An intermediate step is depicted in Figure D.5. The same considerations as above apply here when deforming the gray contour on the left hand side. The resulting grey loops on the right have normalisation points x that are either at the same position as on the original curve or moved to a different position and the integrands associated to different choices of normalisation points are related by analytic continuation, which gives rise to a braiding factor. Furthermore, if the grey loop being deformed like in Figure D.5 carries labels $\mathbf{s}_{12}$ or $\mathbf{s}_2$, it is necessary to reorder the resulting contours like we did in equations (D.0.2), (D.0.3) so that they match the order prescribed in Figure 8.1.

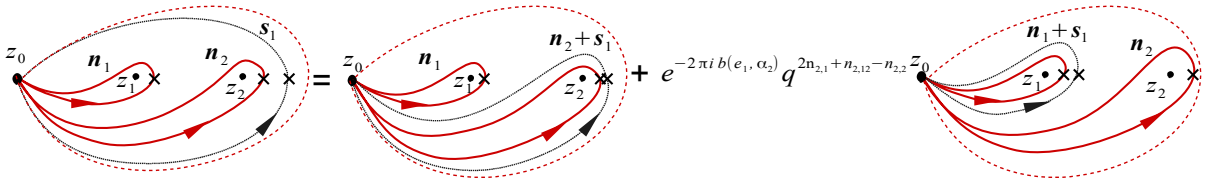

Figure D.5: *Decomposition of a simple contour associated with the root e_1 around two punctures into contours enclosing only one of the punctures.*

Let us now take the contours in Figure D.2 with a generic vertex operator inserted at the position z_2 and a degenerate operator at z_1 and deform the loop enclosing both points z into a combination of basis contours like in Figure 8.1. This case is relevant to the braiding calculation of interest here. If we call $\gamma_1^{\mathbf{s}_i}$ the loop around z_1 and $\beta_{21}^{\mathbf{n}_{21}}$ the loop around both points z, then the resolution of β_{21}-type contours is

$$
\begin{aligned}
I[\beta_{21}^{\mathbf{n}_{21}}\gamma_1^{\mathbf{s}_0}] &= q^{1-n}[n]I[\gamma_2^{\mathbf{n}_{21}-\mathbf{s}_{12}}\gamma_1^{\mathbf{s}_{12}}] + q^{1-n_1-n}[n_1]I[\gamma_2^{\mathbf{n}_{21}-\mathbf{s}_1}\gamma_1^{\mathbf{s}_1}] + q^{-n_1-n}I[\gamma_2^{\mathbf{n}_{21}}\gamma_1^{\mathbf{s}_0}], \qquad \text{(D.0.3)}\\
I[\beta_{21}^{\mathbf{n}_{21}}\gamma_1^{\mathbf{s}_1}] &= q^{n_1-n_2}I[\gamma_2^{\mathbf{n}_{21}}\gamma_1^{\mathbf{s}_1}] - q^{n-n_2}[n_2]I[\gamma_2^{\mathbf{n}_{21}-\mathbf{s}_2}\gamma_1^{\mathbf{s}_{12}}] - q^{-1-n_2}(1-q^2)[n]I[\gamma_2^{\mathbf{n}_{21}+\mathbf{s}_1-\mathbf{s}_{12}}\gamma_1^{\mathbf{s}_{12}}],\\
I[\beta_{21}^{\mathbf{n}_{21}}\gamma_1^{\mathbf{s}_{12}}] &= q^{n_2+n}I[\gamma_2^{\mathbf{n}_{21}}\gamma_1^{\mathbf{s}_{12}}],
\end{aligned}
$$

with notation $I[\beta_{21}^{\mathbf{n}_{21}}\gamma_1^{\mathbf{s}_i}]$ for the integral over the indicated contours and where the loop $\gamma_2^{\mathbf{s}_i}$ is a basis contour enclosing the point z_2. Combining the two parts of the braiding calculation, we reach the main result.

Main result: The two types of braid matrices that we compute following the steps outlined above have a degenerate vertex operator inserted at either the point z_1 or z_2 and are explicitly

$$
\mathsf{B}[W_{\alpha,-b\omega_1}^{ß_k-\delta_i,\mathbf{d}_i}(z_2,z_1)] \;=\; \sum_{j=1}^{3}(\mathsf{b}_+)_{ij}W_{-b\omega_1,\alpha}^{\mathbf{d}_j,ß_k-\delta_j}(z_1,z_2) \qquad \text{(D.0.4)}
$$

$$
\mathsf{B}[W_{-b\omega_1,\alpha}^{\mathbf{d}_i,ß_k-\delta_i}(z_2,z_1)] = \sum_{j=1}^{3}(\mathsf{b}_-)_{ij}W_{\alpha,-b\omega_1}^{ß_k-\mathbf{d}_j,\mathbf{d}_j}(z_1,z_2) \qquad \text{(D.0.5)}
$$

using the notation $ß_k = (s_1-k,k,s_2-k)$ and $\delta_1=(0,0,0),\delta_2=(1,0,0)$ and $\delta_3=(1,0,1)$. The matrix elements of b_+ are

$$
\begin{aligned}
\mathsf{b}_{11}^+ &= q^{(h_1,\nu)}\,, \qquad \mathsf{b}_{22}^+ = q^{(h_2,\nu+e_1)}\,, \qquad \mathsf{b}_{33}^+ = q^{(h_3,\nu+e_{12})} \qquad \text{(D.0.6)}\\
\mathsf{b}_{12}^+ &= q^{(h_2,\nu+e_1)}(q-q^{-1})q^{-s_2-(e_1,\lambda)}\Big(q^{1+2k}[s_1-k][1-s_1+s_2-k+(e_1,\lambda)]+\mathsf{v}^{-1}[k]\Big)\\
\mathsf{b}_{23}^+ &= q^{(h_3,\nu+e_{12})}(q^{-1}-q)\Big([s_2-k][1-s_2+k+(e_2,\lambda)]q^{-(e_2,\lambda)}-\mathsf{v}^{-1}[k]q^{1-2s_2+(e_2,\lambda)}\Big)
\end{aligned}
$$

and

$$
\begin{aligned}
\mathsf{b}_{13}^+ = q^{(h_3,\nu+e_{12})}(1-q^2)\Big([s_1-k][s_2-k][s_2-1-k-(e_2,\lambda)]q^{1+4k-3s_2+(e_2-e_1,\lambda)} \qquad \text{(D.0.7)}\\
+\mathsf{v}^{-1}[k]\big([s_2-2-(e_{12},\lambda)]q^{2-2k-s_2+(e_{12},\lambda)}-[s_2-k]q^{-2-s_2-(e_{12},\lambda)}\\
+[s_1-k]q^{2k-3s_2+(e_2-e_1,\lambda)}+[s_2-k+1]q^{2k-2-3s_2+(e_2-e_1,\lambda)}\big)\\
-q^{-1}\mathsf{v}^{-2}[k][k-1]q^{-3s_2-(e_2-e_1,\lambda)}\Big)\,,
\end{aligned}
$$

while those of b_- are

$$\begin{aligned}
\mathsf{b}^-_{11} &= q^{(h_1,\nu)}\,, \qquad \mathsf{b}^-_{22} = q^{(h_2,\nu+e_1)}\,, \qquad \mathsf{b}^-_{33} = q^{(h_3,\nu+e_{12})} \\
\mathsf{b}^-_{21} &= q^{(h_1,\nu)}(q-q^{-1})\,, \qquad \mathsf{b}^-_{32} = q^{(h_2,\nu+e_1)}(q^2-1)q^{-s_1+1}\left(\mathsf{v}q^{2k}[s_1-1-k]-q^{2k}\right) \\
\mathsf{b}^-_{31} &= q^{(h_1,\nu)}(q-q^{-1})\mathsf{v}q^{s_1-1}
\end{aligned} \tag{D.0.8}$$

for $\alpha = -b\lambda$ and $\nu = \lambda - s_1 e_1 - s_2 e_2$.

Appendix E

Realisation of the generators e_i on screened vertex operators

In this section we derive the identification between the action of L_{-1} on screened vertex operators (8.4.16), which removes one contour of integration, and the action of e_i generators on tensor products of representations (8.4.17). Using notations similar to the ones introduced in Section 8.4.1 for the simpler case of $\mathcal{U}_q(\mathfrak{sl}_2)$, we find that

$$\big[\, L_{-1}\,,\, V_n^\alpha(z)\,\big] - \partial_z V_n^\alpha(z) = S(z_0)(q-q^{-1})\mathsf{k}^{-1}\mathsf{e}V_n^\alpha(z) \tag{E.0.1}$$

by the following considerations. For screening number $n=2$, there are only two contours of integration. L_{-1} acts by the Leibniz rule on each screening current in $V_n^\alpha(z)$, producingtotal derivative terms. The contributions from the two boundaries of the integration contour are related by monodromy factors. In this way it is not hard to arrive at the following equation

$$\big[\, L_{-1}\,,\, V_2^\alpha(z)\,\big] = \oint dy(1-\mathsf{e}^{-4\pi i b(\alpha+b)})S(z_0)S(y) + (1-\mathsf{e}^{-4\pi i b\alpha})S(y)S(z_0)V_\alpha(z) + \partial_z V_2^\alpha(z)\,.$$

By factoring off the operator $S(z_0)$, this simplifies to

$$\big[\, L_{-1}\,,\, V_2^\alpha(z)\,\big] = q^{2(1-\lambda_\alpha)}(q-q^{-1})^{-1}(q^{2\lambda_\alpha-1}-q^{-2\lambda_\alpha+1})(q^2-q^{-2})S(z_0)V_1^\alpha(z) + \partial_z V_2^\alpha(z)\,.$$

More generally, for arbitrary $n\in\mathbb{N}$ units of screening charge, we find by iterating these steps

$$\big[\, L_{-1}\,,\, V_\alpha^n(z)\,\big] = \partial_z V_n^\alpha(z) + q^{2(n-1-\lambda)}(q-q^{-1})^{-1}(q^{2\lambda-n+1}-q^{-2\lambda+n-1})(q^n-q^{-n})S(z_0)V_{n-1}^\alpha(z)\,.$$

To compare now with the actions of the e and k generators, notice that these are

$$\mathsf{e}\; e_n^\lambda = (q-q^{-1})^{-2}(q^{2\lambda-n+1}-q^{-2\lambda+n-1})(q^n-q^{-n})e_{n-1}^\lambda\,,\quad \mathsf{k}^{-1}\; e_{n-1}^\lambda = q^{2(n-1-\lambda)}e_{n-1}^\lambda\,,$$

so we arrive indeed at equation (E.0.1).

At higher rank, for $\mathcal{U}_q(\mathfrak{sl}_3)$, one can similarly show for example

$$\big[\, L_{-1}\,,\, V_{\mathbf{n}}^\alpha(z)\,\big] - \partial_z V_{\mathbf{n}}^\alpha(z) \sim (q-q^{-1})\left(\mathsf{k}_1^{-1}\mathsf{e}_1 + \mathsf{k}_2^{-1}\mathsf{e}_2\right) V_{\mathbf{n}}^\alpha(z) \tag{E.0.2}$$

The final observation to make in order to identify the actions of L_{-1} and e is that the action of L_{-1} on composite screened vertex operators correctly reproduces the action of the co-product

$$\big[\, L_{-1}\,,\, V^{\alpha_m,\ldots,\alpha_1}_{\mathbf{n}_m,\ldots,\mathbf{n}_1}(z_m,\ldots,z_1)\,\big] - \sum_{l=1}^{m} \partial_{z_l} V^{\alpha_m,\ldots,\alpha_1}_{\mathbf{n}_m,\ldots,\mathbf{n}_1}(z_m,\ldots,z_1) \sim (\Delta(x) V^{\alpha_m,\ldots,\alpha_1}_{\mathbf{n}_m,\ldots,\mathbf{n}_1})(z_m,\ldots,z_1),$$

for

$$x = (q-q^{-1})(\mathsf{k}_1^{-1}\mathsf{e}_1 + \mathsf{k}_2^{-1}\mathsf{e}_2),$$

which we verified by direct computation.

In order to see that the boundary terms occurring in the commutators with arbitrary generators of the $\mathcal{W}$-algebra admit a similar representations in terms of the generators e_i the main point to observe is that all commutators between screening currents and $\mathcal{W}$-algebra generators can be represented as total derivatives.

Part IV

Toda conformal blocks and topological strings

Introduction

Parts II and III of this thesis have focused on a proof of the isomorphism between the algebras $\mathcal{A}_{\mathfrak{X}}$ of supersymmetric line operators in $\mathcal{N} = 2$ field theories $\mathfrak{X}(\mathcal{C}_{g,n}, \mathfrak{g})$ in four dimensions, which can be identified with the quantised algebras $\mathcal{A}_{\text{flat}}$ of functions on moduli spaces of flat connections on punctured Riemann surfaces $\mathcal{C}_{g,n}$, and the algebras of Verlinde operators $\mathcal{A}_V$ on spaces of conformal blocks $\mathrm{CB}(\mathcal{C}_{g,n})$ for $\mathfrak{sl}_N$ Toda conformal field theories. Following the arguments presented in Section 1.4, this relation is a key element for the higher rank generalisation of the AGT correspondence [14], [20] between 4d $\mathcal{N} = 2$ supersymmetric field theories and 2d conformal field theories, in particular for non-Lagrangian theories $\mathfrak{X}(\mathcal{C}_{g,n}, \mathfrak{g})$. A part of the foundations that support this result has been the construction in Part III of a natural basis for the space of three point conformal blocks $\mathrm{CB}(\mathcal{C}_{0,3})$ associated to a three punctured sphere, on which the Verlinde operators act.

The introductory sections in Part I have presented another possible way to view the AGT correspondence, though the relation to topological string theory. Section 1.3 in particular described how 4d $\mathcal{N} = 2$ field theories emerge in the geometric engineering limit as low energy descriptions of compactifications of type IIA string theory on non-compact Calabi-Yau threefolds CY_3 [38], [39], [40]. This perspective provides a geometric type IIA picture where it is possible to calculate the topological string partition function using the refined topological vertex formalism [44], [45], [46]. The link between Toda CFT in two dimensions and topological string theory was first proposed by [49], [147] based on the geometric engineering of $\mathcal{N} = 2$ field theories and the AGT correspondence. It comes from the fact that one can write both the topological string partition functions and the conformal blocks through the same type of integral formulation, as briefly mentioned at the end of Section 1.3. Such integrals appear in literature under the name *matrix model* integrals, defined as integrals over eigenvalues of families of matrices. In Part IV of this thesis we aim to study the relation between the topological string theory description of theories $\mathfrak{X}(\mathcal{C}_{g,n}, \mathfrak{g})$, with particular interest for certain non-Lagrangian theories, and the corresponding conformal blocks of Toda CFT.

The gauge theories comprising the class $\mathcal{S}$ introduced by Gaiotto [9], which have $SU(N)$ gauge factors, can be constructed by gluing or equivalently gauging certain basic building blocks (see Table 1.1 for $SU(2)$ theories in Section 1.1). These basic building blocks are the T_N trinion theories, which have been discussed in Chapter 3. They can be seen to descend from the six dimensional $(2, 0)$ superconformal field theory of type A_{N-1} through a twisted compactification of N M5 branes on a sphere with three 'maximal' punctures. Such trinions are therefore represented by three punctured spheres $\mathcal{C}_{0,3}$ in Gaiotto's classification of class $\mathcal{S}$ and the maximal type of the punctures represents their $SU(N)^3$ global symmetry. The T_N trinions have no known weakly-coupled Lagrangian description[1] and thus it is not possible to

[1] Even the $\mathcal{N} = 1$ Lagrangian description for the T_N theories that was proposed in [148] cannot be used for computing the partition function via localization given the state of the art.

compute their partition function via supersymmetric localization [13]. Under a generalisation of the AGT correspondence, their partition functions are expected to correspond to the three point functions of $\mathfrak{sl}_N$ Toda conformal field theory with three generic primaries, the computation of which is a long standing open problem in mathematical physics [149], [106], [150].

Breaking the impasse created by these technical difficulties both on the side of four dimensional field theory and on the side of 2d CFT, the partition functions of the uplift to five dimensions on a circle S^1 of the four dimensional T_N trinion theories have been computed in [74], [151] using the tools of topological string theory. To understand the uplift to five dimensions and the compactification of the fifth dimension on S^1, recall from Section 1.3 that there are various dual string theoretic constructions which engineer the same quantum field theory at low energies. The topological strings partition functions corresponding to the T_N theories can be computed graphically, similarly to Feynman diagrams, using *brane* or *web* diagrams like in the examples which were depicted in Figure 1.2, which we reproduce below. Such web diagrams are dual to the toric diagrams which encode the combinatorial data specifying the CY_3 in the corresponding geometric engineering construction. From the perspective of web diagrams, the low energy dynamics of the uplift to five dimensions of the T_N theories is captured by brane diagrams [47] of the type sketched in Figure 13.1c. The brane configuration listed in the table below shows the 5-branes to intersect in five common spacetime directions: the four spacetime directions $x^0 - x^3$ where the 4d field theory lives and the direction x^5, which is compactified on the circle S^1.

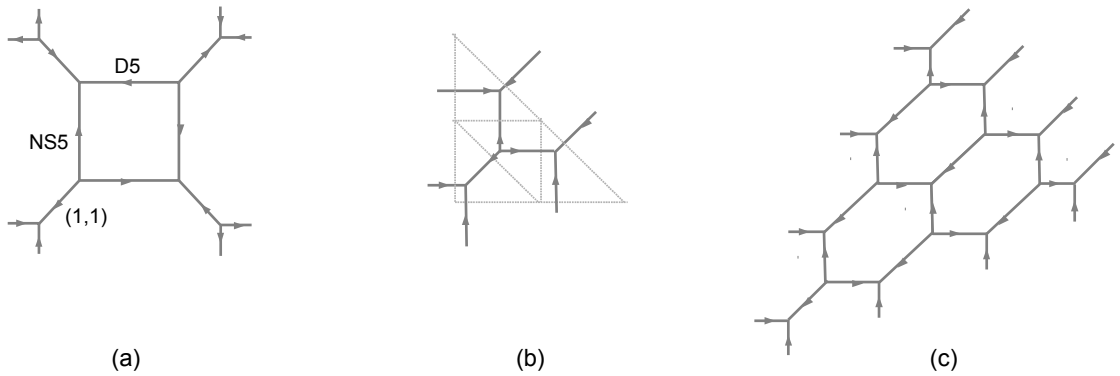

IIB	x^0	x^1	x^2	x^3	x^4	x^5	x^6	x^7	x^8	x^9
NS5-branes	–	–	–	–	–	–	.	.	.	.
D5-branes	–	–	–	–	.	–	–	.	.	.

Figure 13.1: (a) *The type IIB web diagram realising the $d = 4$, $\mathcal{N} = 2$, $SU(2)$ four flavour gauge theory on junctions of NS5, D5 and (1,1) branes.* (b) *The web diagram realising the T_2 theory of class $\mathcal{S}$ and the dual (dashed) toric diagram.* (c) *The web diagram realising the T_4 theory.* Bottom: *The table lists the brane configuration in the spacetime directions and the direction x^5 is compactification on a circle.*

The uplifts to five dimensions of the 4d $\mathcal{N} = 2$ superconformal field theories in class $\mathcal{S}$, such as those engineered by the brane constructions depicted in Figure 13.1, are related [152], [153] to a $\mathfrak{q}$-deformation of Toda theories [154], [155]. We have summarised some of the background regarding the free field construction of *undeformed* Toda field theories and their chiral $\mathcal{W}_N$ algebra in Chapter 6. These correspond to $\mathfrak{q} = 1$. A deformation with $\mathfrak{q} \neq 1$ of such theories was defined in [154], [155] though a $\mathfrak{q}$ deformation of the $\mathcal{W}_N$ algebras, their free field realisations and the screening operators. The deformation parameter $\mathfrak{q}$ enters for example the commutation relations of the modes in the expansion of the free Toda fields and

in the definition of the screening charges. The correlation functions of screened vertex operators in the free field representation of $\mathfrak{q}$-deformed Toda CFT are expressed as matrix model integrals, examples of which will appear in chapters 16 – 19[2]. The relation between the uplifts to five dimensions of the 4d $\mathcal{N} = 2$ superconformal field theories in class $\mathcal{S}$ and $\mathfrak{q}$-deformed Toda theories is a $\mathfrak{q}$-deformed version of the AGT correspondence, which has been studied by many authors [156], [157], [158], [159], [160], [161], [162], [34], [163], [164], [165], [166], [167], [168], [169].

Based on the aforementioned works, the authors of [48], [75] addressed the problem of determining the three point functions of Toda CFT with three generic primary fields using the refined topological vertex formalism. The resulting three point functions have the correct symmetries, zeros and, after appropriate specialisation, give the Fateev-Litvinov semi-degeneration formula [149], [106], [150]. It should be possible to take the $\mathfrak{q} \to 1$ limit in order to obtain the partition functions of the four dimensional T_N theories with non-Lagrangian description, as well as the undeformed three point $\mathfrak{sl}_N$ Toda correlators to which they correspond. The precise way to take this limit is however unclear since the proposed formulas from [48], [75] are given in terms of infinite sums admitting (for $N > 2$) only partial resummations for which convergence is not guaranteed. We aim to offer some clarification for this issue by identifying a way to take the undeformed limit $\mathfrak{q} \to 1$ in the most simple case, where $N = 2$. Once there exists a prescription for taking the limit, it is reasonable to expect that the partition function for the T_N trinions should correspond to a preferred basis on the space of conformal blocks $\mathrm{CB}(\mathcal{C}_{0,3})$ for $\mathfrak{sl}_N$ Toda CFT. A natural next step from this point of view is then to identify the dictionary between the screening numbers $\mathfrak{s}$ that parametrise a natural basis for the space $\mathrm{CB}(\mathcal{C}_{0,3})$ constructed in Chapter 8 with data used in the geometric engineering of the T_N theories, as outlined at the end of Section 1.5.

Contents of Part IV

Part IV of this thesis sets to address some of the problems listed above, beginning with the simplest case of the T_2 theory. The limit $\mathfrak{q} \to 1$ of the topological string partition function appears to be divergent and so it is necessary to find a renormalisation prescription to define a finite and meaningful result. Since most renormalisation procedures leave some freedom in the definition of the finite parts, we should furthermore address the ambiguity of the final result. Moreover, for some applications it is important to determine the normalisation factors in the resulting conformal blocks precisely, which will be particularly important in the higher rank cases. Surprisingly, even in the most simple case of the T_2 trinion it appears that none of the existing proposals concerning the relation between topological string partition functions and Liouville three point conformal blocks is entirely correct, giving additional motivation to present this case in detail. This is furthermore ideal as a warm-up exercise for the study of the higher rank T_N trinions, since it is possible to identify the $\mathfrak{q} \to 1$ limit and the precise parameter dictionary for T_2 trinions though two independent approaches:

(i) the resummation of the T_2 partition function – obtained as an infinite sum from topological vertex techniques – to an infinite product formula [74];

(ii) the realisation of the infinite sum formula for the T_2 partition function from topological strings as a sum over residues for the free field matrix integral representation of $\mathfrak{q}$-deformed Liouville CFT

[2]The use of the term *matrix* might seem confusing here as there is no matrix present explicitly in the integrals. However such integrals have appeared in literature in the past as defined over families of matrices.

[162], [34].

After identifying this link precisely in Chapter 14, we present its derivation through the methods (*i*) and (*ii*) in Chapters 15 – 17. Chapter 15 summarises the necessary background for the refined topological vertex calculations and also the derivation of the infinite product formula [74], proving the convergence of the topological string partition function for T_2. It then uses this product formula to identify a meaningful way to take the limit $\mathfrak{q} \to 1$. Chapter 16 focuses on the integral realisation of the T_2 partition function from topological strings as a matrix model integral, while Chapter 17 studies its relation to Liouville three point conformal blocks. We then focus on the matrix model integral realisation of the partition functions for the higher rank T_N trinions in Chapter 18 and the dictionary of parameters to $\mathfrak{sl}_N$ Toda CFT in Chapter 19.

Part IV of this thesis is based on two upcoming publications [170], [171].

Chapter 14

Liouville conformal blocks and topological strings

In this chapter we take steps to establish the relation between three point blocks of Liouville conformal field theory and the topological string partition function on $\mathbb{C}\times\mathbb{C}^2/\mathbb{Z}_2\times\mathbb{Z}_2$ [47] for the 5d uplift of the T_2 theory, aiming to clarify important previously unresolved issues.

Summary of the results

The topological string partition function of the T_2 theory computed in [74] for the web diagram depicted in Figure 14.1 is a function of three Kähler parameters Q_1, Q_2, Q_3 as well as the Omega deformation parameters ϵ_1, ϵ_2

$$\begin{aligned}&\mathcal{Z}_2^{\text{top}}(Q_1,Q_2,Q_3;\mathfrak{q},\mathfrak{t}) = \\ &= \frac{\mathcal{M}(Q_1Q_2)}{\mathcal{M}(\sqrt{\frac{\mathfrak{t}}{\mathfrak{q}}}Q_1)\mathcal{M}(\sqrt{\frac{\mathfrak{t}}{\mathfrak{q}}}Q_2)}\sum_Y\left(\sqrt{\frac{\mathfrak{t}}{\mathfrak{q}}}Q_3\right)^{|Y|}\frac{\mathcal{N}_{Y\emptyset}\left(\sqrt{\frac{\mathfrak{t}}{\mathfrak{q}}}Q_2\right)\mathcal{N}_{\emptyset Y}\left(\sqrt{\frac{\mathfrak{t}}{\mathfrak{q}}}Q_1\right)}{\mathcal{N}_{YY}(\mathfrak{t}/\mathfrak{q})}\,,\end{aligned} \tag{14.0.1}$$

where

$$\mathfrak{q}=e^{-R\epsilon_1}\,,\qquad \mathfrak{t}=e^{R\epsilon_2} \tag{14.0.2}$$

and R is the radius of the fifth dimension compactified on a circle S^1. The definitions and properties of the Nekrasov functions $\mathcal{N}_{YY'}(Q)$ and also for $\mathcal{M}(Q)$ are collected in Appendix F. It will be useful to work with a reparametrisation in terms of the auxiliary variables M, N, L that are related to the Kähler parameters through:

$$Q_1Q_2=\frac{M_1}{M_2}=M^2\,,\qquad Q_1Q_3=\frac{N_1}{N_2}=N^2\,,\qquad Q_2Q_3=\frac{L_1}{L_2}=L^2\,. \tag{14.0.3}$$

In Section 15.1 we will show that the infinite sum in equation (14.0.1) has a finite radius of convergence and that the result is indeed given by the factorised expression

$$\mathcal{Z}_2^{\text{top}}(M,N,L;q,t)=\frac{\mathcal{M}(M^2)\mathcal{M}(N^2/v^2)\mathcal{M}(L^2)}{\mathcal{M}(ML/Nv)\mathcal{M}(MN/Lv)\mathcal{M}(LN/Mv)\mathcal{M}(LMN/v)}\,, \tag{14.0.4}$$

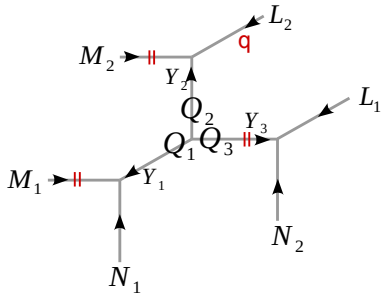

Figure 14.1: *The 5-brane web diagram for T_2 with the choice of the preferred direction and associated Kähler parameters. The edges along the preferred direction are marked by two red strips. The internal edges have corresponding Young tableaux Y_1, Y_2, Y_3.*

with $v = \sqrt{\mathfrak{q}/\mathfrak{t}}$, as has been conjectured in [172], [74]. One goal is to clarify the relation to Virasoro conformal blocks expected to emerge in the limit where $R \to 0$. This is nontrivial since the function $\mathcal{M}$ representing the basic building block of the expression (14.0.4) diverges in this limit. In the case $|\mathfrak{q}| < 1$, $|\mathfrak{t}| < 1$ we will show in Chapter 16 that the limit

$$\mathcal{Z}_2^{\rm 4d}(a_1, a_2, a_3; \beta) = \lim_{R\to 0} (2\pi i)^s \mathcal{M}(\mathfrak{t}/\mathfrak{q}) \left(\frac{\varphi(\mathfrak{t})}{\varphi(\mathfrak{q})}\right)^s \mathcal{Z}_2^{\rm top}(M, N, L; \mathfrak{q}, \mathfrak{t}) \tag{14.0.5}$$

exists if $\beta^2 = -\epsilon_2/\epsilon_1$, assuming that the parameters a_1, a_2, a_3 and N, M, L are related through

$$M^2 = \frac{\mathfrak{t}}{\mathfrak{q}}\mathfrak{q}^{2\beta a_2}\,, \quad L^2 = \frac{\mathfrak{t}}{\mathfrak{q}}\mathfrak{q}^{2\beta a_3}\,, \quad N^2 = \frac{\mathfrak{q}}{\mathfrak{t}}\mathfrak{q}^{-2\beta a_1}\,, \quad \mathfrak{t} = \mathfrak{q}^{\beta^2}\,, \tag{14.0.6}$$

while obeying the condition $a_1 + a_2 + a_3 = (\beta^{-1} - \beta) + s\beta$. This means that some divergent factors in the asymptotic behaviour of $\mathcal{Z}_2^{\rm top}$ for $R \to 0$ depend on s. Different ways of extracting finite quantities from this asymptotic behaviour may differ by functions of s, as thoroughly discussed in Section 15.2.3. We will also discuss the regime where $|\mathfrak{t}| > 1$.

The function $\mathcal{Z}_2^{\rm 4d}(a_1, a_2, a_3)$ is thereby found to be

$$\mathcal{Z}_2^{\rm 4d}(a_1, a_2, a_3; \beta) = \left(\frac{\beta^{1-\beta^2}}{2\pi \mathrm{i}}\Gamma(\beta^2)\right)^{-s} \frac{\Gamma_\beta(\beta)}{\Gamma_\beta((s+1)\beta)} \tag{14.0.7}$$
$$\frac{\Gamma_\beta(\beta^{-1} - 2a_1)\Gamma_\beta(2a_2 + \beta)\Gamma_\beta(2a_3 + \beta)}{\Gamma_\beta(\beta^{-1} - 2a_1 + s\beta)\Gamma_\beta(2a_2 + \beta + s\beta)\Gamma_\beta(2a_3 + \beta + s\beta)}\,,$$

which is the three point conformal block of the Virasoro algebra with $c = 1 - 6(\beta + \beta^{-1})^2 < 1$ central charge. It is interesting to note that a similar limit exists for $|\mathfrak{t}| > 1$, $|\mathfrak{q}| < 1$ corresponding to the Liouville conformal blocks

$$\mathcal{Z}_{\rm Liou}(\alpha_1, \alpha_2, \alpha_3) = \left(\frac{b^{1+b^2}}{2\pi \mathrm{i}}\Gamma(-b^2)\right)^{-s} \frac{\Gamma_b(-sb)}{\Gamma_b(0)} \tag{14.0.8}$$
$$\frac{\Gamma_b(Q - 2\alpha_1 - sb)\Gamma_b(2\alpha_2 + sb)\Gamma_b(2\alpha_3 + sb)}{\Gamma_b(Q - 2\alpha_1)\Gamma_b(2\alpha_2)\Gamma_b(2\alpha_3)}\,.$$

In order to relate the partition function $\mathcal{Z}_2^{\rm top}$ to Liouville conformal blocks, we will use an alternative representation for $\mathcal{Z}_2^{\rm top}$ which is available for the specialisation of parameters

$$v\frac{ML}{N} = \mathfrak{t}^s, \qquad s \in \mathbb{N}. \tag{14.0.9}$$

For this case it was shown in [34], [162] that $\mathcal{Z}_2^{\text{top}}$ has an alternative representation often called $\mathfrak{q}$-deformed matrix integral in terms of a function $\mathcal{I}_2(N, M, L; \mathfrak{q}, \mathfrak{t})$, defined as

$$\mathcal{I}_2 = (2\pi i)^s \sum_{\substack{Y_1,\ldots,Y_s\in\mathbb{N} \\ Y_1>Y_2>\ldots Y_s}} \operatorname*{Res}_{y=y_Y} \mathfrak{q}^{(\zeta+1)|\nu|}\mathcal{I}_{1,1}(y)\mathcal{I}_m(y)\,, \qquad \mathfrak{q}^{\zeta+1} = \sqrt{\frac{\mathfrak{t}}{\mathfrak{q}}}\frac{LN}{M}\,, \tag{14.0.10}$$

where $y_Y = (\mathfrak{t}^{s-1}\mathfrak{q}^{Y_1}, \mathfrak{t}^{s-2}\mathfrak{q}^{Y_2}, \ldots, \mathfrak{q}^{Y_s})$ and

$$\mathcal{I}_{1,1}(y) = \prod_{i\neq j=1}^{s} \frac{\varphi(y_i/y_j)}{\varphi(\mathfrak{t}y_i/y_j)}\,, \quad \mathcal{I}_m(y) = \prod_{i=1}^{s} \frac{\varphi(M^2\mathfrak{q}/y_i\mathfrak{t})}{\varphi(1/y_i)}\,. \tag{14.0.11}$$

The function $\mathcal{I}_2$ is a variant of a multiple Jackson integral defined for meromorphic integrands. The precise relation between $\mathcal{Z}_2^{\text{top}}$ and $\mathcal{I}_2$ will be shown to be

$$\mathcal{Z}_2^{\text{top}}(M, N, L; \mathfrak{q}, \mathfrak{t}) = \frac{\mathfrak{t}^{-\frac{1}{2}s(s-1)(\zeta+1)}}{(2\pi i)^s\mathcal{M}(\mathfrak{t}/\mathfrak{q})}\left(\frac{\varphi(\mathfrak{q})}{\varphi(\mathfrak{t})}\right)^s \mathcal{I}_2(N, M, L; \mathfrak{q}, \mathfrak{t})\,. \tag{14.0.12}$$

Representing $\mathcal{Z}_2^{\text{top}}$ via (14.0.12) offers another way to study the limit (14.0.5). Despite the fact that all the ingredients in the definition of $\mathcal{I}_2(N, M, L; \mathfrak{q}, \mathfrak{t})$ diverge in this limit, we will find that a finite limit exists for $\mathcal{I}_2(N, M, L; \mathfrak{q}, \mathfrak{t})$, giving an independent confirmation for equation (14.0.5). Relations of the form (14.0.5) have previously been proposed in [172], [74]. However, the references above have neither identified a renormalisation prescription giving a finite limit such as (14.0.5), nor correctly identified the precise relation (18.0.17) between the parameters.

Chapter 15

The topological vertex result

In this chapter we review some important points from the computation of the topological string partition function in [74], which are necessary to prove the converge of this partition for the T_2 theory, as a formal sum, and which enable us to determine a meaningful way to take the undeformed limit $\mathfrak{q} \to 1$.

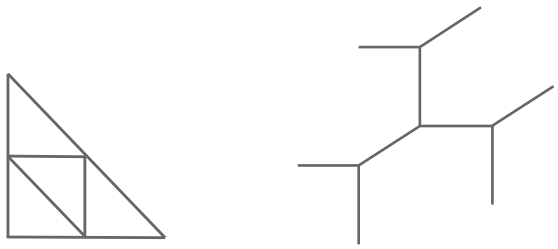

Figure 15.1: *The toric diagram of* $\mathbb{C}^3/\mathbb{Z}_2 \times \mathbb{Z}_2$ (right) *and its dual web diagram* (left) *for the* T_2 *geometry.*

In four dimensions the T_2 theory refers to the theory of 2×2 free hypermultipltes and it is the basic building block to enter the construction of $\mathcal{N} = 2$ gauge theories with $SU(2)$ gauge group [9]. There exists a five dimensional uplift of this theory compactified on S^1, which can be constructed in type IIB string theory via the (p, q) web 5-brane diagram [173], [174] depicted in figure 15.1 and due to [47]. Equivalently, this theory can be constructed in M-theory/type IIA string theory on Calabi-Yau threefold manifolds via geometric engineering [39], [40]. The toric diagram of the corresponding $\mathbb{C}^3/\mathbb{Z}_2 \times \mathbb{Z}_2$ Calabi-Yau manifold has the same shape as the dual of the T_2 web diagram [175]. The partition function of the T_2 theory and any $\mathcal{N} = 2$ theory geometrically engineered with a toric Calabi-Yau compactification can be obtained by computing the topological string partition function on the Calabi-Yau [12], [176], [177]. A very efficient method to compute five dimensional Nekrasov partition functions is the refined topological vertex formalism [45], [43], [46].

The T_2 geometry is parametrised by three independent Kähler parameters Q_1, Q_2 and Q_3 that are related to the 5d gauge theory parameters M, N, L like in equations (14.0.3), and which are further related to the four dimensional gauge theory parameters as

$$M = e^{-Rm} \,. \tag{15.0.1}$$

The topological partition function is also a function of the parameters $\mathfrak{q}, \mathfrak{t}$ which represent the 5d version of the Omega background $\mathfrak{q} = e^{-R\epsilon_1}$, $\mathfrak{t} = e^{R\epsilon_2}$ in equation (14.0.2). For completeness we sketch the

Figure 15.2: *The direction of the arrows determines the way partitions enter the vertex factor. Partitions are counted clockwise to the preferred direction and the variables* $\mathfrak{q},\mathfrak{t}$ *enter the vertex factor in this order for* $\mathfrak{q}$ *associated with the end of the first edge and* $\mathfrak{t}$ *with the end of the second.*

rules for computing the refined topological string partition function from the dual toric diagram. The procedure is very similar to calculating Feynman diagrams where we associate functions of the Kähler parameters, the Omega background as well as Young diagrams to the edges and vertices of the dual toric diagram. The topological partition function is then obtained as the product of all the edge and vertex factors, summed over all possible partitions associated with the internal edges.

In order to compute the refined topological string partition function through the refined topological vertex formalism it is necessary first need to pick a preferred direction on the toric diagram. This was denoted with two red lines in Figure 14.1. Each edge has associated a partition Y and the partitions which correspond to external lines of the diagram are empty. The *edge factor* is the function that we associate to each edge:

$$\text{edge factor} \stackrel{\text{def}}{=} (-Q)^{|Y|} \times \text{framing factor}. \tag{15.0.2}$$

For the T_2 toric diagram depicted in Figure 14.1 the only required *framing factors* are trivial, equal to one. The *refined topological vertex* is the function associated to each vertex:

$$C_{Y_1Y_2Y_3}(\mathfrak{t},\mathfrak{q}) = \mathfrak{q}^{\frac{||Y_2||+||Y_3||}{2}}\mathfrak{t}^{-\frac{||Y_2^t||}{2}}\tilde{Z}_{Y_3}(\mathfrak{t},\mathfrak{q})\sum_{Y}\left(\frac{\mathfrak{q}}{\mathfrak{t}}\right)^{\frac{|Y|+|Y_1|-|Y_2|}{2}} s_{Y_1^t/Y}(\mathfrak{t}^{-\rho}\mathfrak{q}^{-Y_3})s_{Y_2/Y}(\mathfrak{q}^{-\rho}\mathfrak{t}^{-Y_3^t}), \tag{15.0.3}$$

where the functions $\tilde{Z}_{Y_3}(\mathfrak{t},\mathfrak{q})$ are defined in equation (F.0.21) in Appendix F and $s_{Y'/Y}(x)$ are the skew-Schur functions of the infinite vector $x=(x_1,\dots)$. The notation used is such that for a partition Y with $Y=(Y_1,Y_2,\dots)$, the vector $\mathfrak{t}^{-\rho}\mathfrak{q}^{-Y}$ is given by

$$\mathfrak{t}^{-\rho}\mathfrak{q}^{-Y_3} = (\mathfrak{t}^{\frac{1}{2}}\mathfrak{q}^{-Y_1},\mathfrak{t}^{\frac{3}{2}}\mathfrak{q}^{-Y_2},\mathfrak{t}^{\frac{5}{2}}\mathfrak{q}^{-Y_3},\dots). \tag{15.0.4}$$

The topological string partition function is a sum over the partitions $\{Y_1,\cdots,Y_M\}$ of the M internal edges of the toric diagram

$$\mathcal{Z}^{\text{top}} = \sum_{Y_1,\cdots,Y_M}\prod_{\text{edges}}\text{edge factor}\times\prod_{\text{vertices}}\text{vertex factor}. \tag{15.0.5}$$

For the T_2 geometry depicted in Figure 15.1 the refined topological string partition function is

$$\mathcal{Z}^{\text{top}}_{T_2} = \mathcal{Z}^{\text{top}}_2(\boldsymbol{Q}) = \sum_{\mathbf{Y}}\prod_{i=1}^{3}(-Q_i)^{|Y_i|}C_{Y_1^t\emptyset\emptyset}(\mathfrak{q},\mathfrak{t})C_{\emptyset Y_2^t\emptyset}(\mathfrak{q},\mathfrak{t})C_{\emptyset\emptyset Y_3^t}(\mathfrak{q},\mathfrak{t})C_{Y_1Y_2Y_3}(\mathfrak{t},\mathfrak{q}), \tag{15.0.6}$$

where $\boldsymbol{Q}=(Q_1,Q_2,Q_3)$. The T_2 geometry is special and following the work of [178] for the unrefined partition function it is possible to perform some of the sums and achieve a more compact way to write

(15.0.6). The final result [74] can be brought to the form (14.0.1)

$$\mathcal{Z}_2^{\text{top}}(M,N,L;\mathfrak{q},\mathfrak{t}) = \tag{15.0.7}$$
$$= \frac{\mathcal{M}(M^2)}{\mathcal{M}\big(\sqrt{\frac{\mathfrak{t}}{\mathfrak{q}}}\frac{LM}{N}\big)\mathcal{M}\big(\sqrt{\frac{\mathfrak{t}}{\mathfrak{q}}}\frac{NM}{L}\big)} \sum_Y \left(\sqrt{\frac{\mathfrak{t}}{\mathfrak{q}}}\frac{LN}{M}\right)^{|Y|} \frac{\mathcal{N}_{Y\emptyset}\left(\sqrt{\frac{\mathfrak{t}}{\mathfrak{q}}}\frac{LM}{N}\right)\mathcal{N}_{\emptyset Y}\left(\sqrt{\frac{\mathfrak{t}}{\mathfrak{q}}}\frac{NM}{L}\right)}{\mathcal{N}_{YY}(\mathfrak{t}/\mathfrak{q})}\,.$$

In doing so we have applied the relations (14.0.3) of the three Kähler parameters Q_1,Q_2,Q_3 to the five dimensional mass parameters M, N, L and the shorthand notations $\mathcal{M}(Q) = \mathcal{M}(Q;\mathfrak{t},\mathfrak{q})$ and $\mathcal{N}_{YY'}(Q) = \mathcal{N}_{YY'}(Q;\mathfrak{t},\mathfrak{q})$. The partition $Y \equiv Y_3$ is associated with the edge corresponding to the Kähler parameter Q_3.

15.1 Resummation into a product formula

In this section we will show how the partition function of the T_2 theory can be brought to an infinite product formula

$$\mathcal{Z}_2^{\text{top}}(\boldsymbol{Q}) = \prod_{i,j=1}^{\infty} \frac{(1-Q_1Q_2Q_3\mathfrak{q}^{i-\frac{1}{2}}\mathfrak{t}^{j-\frac{1}{2}})\prod_{k=1}^{3}(1-Q_k\mathfrak{q}^{i-\frac{1}{2}}\mathfrak{t}^{j-\frac{1}{2}})}{(1-Q_1Q_2\mathfrak{q}^{i}\mathfrak{t}^{j-1})(1-Q_1Q_3\mathfrak{q}^{i-1}\mathfrak{t}^{j})(1-Q_2Q_3\mathfrak{q}^{i}\mathfrak{t}^{j-1})}. \tag{15.1.8}$$

We begin with the formula (14.0.1) derived using the topological vertex formalism. It is useful to write this, using (F.0.12), as

$$\mathcal{Z}_2^{\text{top}}(\boldsymbol{Q}) = \mathcal{Z}_2^{\text{prod}} \sum_Y (-Q_3)^{|Y|}\mathfrak{q}^{\frac{\|Y\|^2}{2}}\mathfrak{t}^{\frac{\|Y^t\|^2}{2}} \prod_{(i,j)\in Y} \frac{(1-Q_1\sqrt{\frac{\mathfrak{t}}{\mathfrak{q}}}\mathfrak{q}^{1-j}\mathfrak{t}^{i-1})(1-Q_2\sqrt{\frac{\mathfrak{q}}{\mathfrak{t}}}\mathfrak{q}^{j-1}\mathfrak{t}^{1-i})}{(1-\mathfrak{q}^{Y_i-j+1}\mathfrak{t}^{Y_j^t-i})(1-\mathfrak{q}^{Y_i-j}\mathfrak{t}^{Y_j^t-i+1})}\,, \tag{15.1.9}$$

where we denote $\mathcal{Z}_2^{\text{prod}} = \mathcal{M}(M^2)/\mathcal{M}(LM/Nv)\mathcal{M}(NM/Lv)$ the part of the partition function that is already in product form. This sum formula is a formal series

$$\mathcal{Z}_2^{\text{top}}(\boldsymbol{Q}) = \mathcal{Z}_2^{\text{prod}} \sum_{k=0}^{\infty} (-Q_3)^k P_k(Q_1,Q_2) \tag{15.1.10}$$

for which we have not given a proof of convergence yet, where $P_k(Q_1,Q_2)$ is a degree k polynomial in Q_1 and Q_2 which can also be explicitly written as

$$P_k(Q_1,Q_2) = \sum_{\ell=0}^{k} Q_1^\ell P_{k\ell}(Q_2) = \sum_{\ell,m=0}^{k} Q_1^\ell Q_2^m P_{k\ell}\,. \tag{15.1.11}$$

The goal is to find a function that can be expanded as the same formal series, but for which convergence is known. Then, we can use the fact that polynomials of degree k in two variables (Q_1 and Q_2) are completely defined if we know their values at $(k+1)^2$ points.

To try to determine this function, we first specialise Q_1 and Q_2 as

$$\mathfrak{q}^x = Q_1\mathfrak{q}^{-\frac{1}{2}}\mathfrak{t}^{\frac{1}{2}}, \quad \mathfrak{t}^y = Q_2\mathfrak{q}^{\frac{1}{2}}\mathfrak{t}^{-\frac{1}{2}}\,, \tag{15.1.12}$$

with x and y integers. This specialisation is very useful because then we can further rewrite equation (15.1.10) using a specialisation of the Macdonald symmetric polynomials

$$P_Y(\mathfrak{t}^{x-\frac{1}{2}},\mathfrak{t}^{x-\frac{3}{2}},\cdots,\mathfrak{t}^{\frac{1}{2}};\mathfrak{q},\mathfrak{t}) = \mathfrak{t}^{\frac{\|Y^t\|}{2}} \prod_{(i,j)\in Y} \frac{(1-\mathfrak{q}^{j-1}\mathfrak{t}^{x+1-i})}{(1-\mathfrak{q}^{Y_i-j}\mathfrak{t}^{Y_j^t-i+1})} \tag{15.1.13}$$

taken from [179], equation (6.11') on page 337. Then, by further using the Cauchy formula

$$\sum_{\nu} Q^{|Y|} P_Y(\mathfrak{x};\mathfrak{q},\mathfrak{t}) P_Y(\mathfrak{y};\mathfrak{t},\mathfrak{q}) = \prod_{i,j=1}^{\infty} (1+Q\mathfrak{x}_i\mathfrak{y}_j) \tag{15.1.14}$$

for Macdonald symmetric polynomials, we can rewrite

$$\begin{aligned}\mathcal{Z}_2^{\text{top}}(\boldsymbol{Q}) &= \mathcal{Z}_2^{\text{prod}} \sum_{Y} (-Q_3)^{|Y|} P_{Y^t}(\mathfrak{q}^{x-\frac{1}{2}},\mathfrak{q}^{x-\frac{3}{2}},\cdots,\mathfrak{q}^{\frac{1}{2}};\mathfrak{t},\mathfrak{q}) P_Y(\mathfrak{t}^{y-\frac{1}{2}},\mathfrak{t}^{y-\frac{3}{2}},\cdots,\mathfrak{t}^{\frac{1}{2}};\mathfrak{q},\mathfrak{t}) \\ &= \mathcal{Z}_2^{\text{prod}} \prod_{i=1}^{x}\prod_{j=1}^{y} \big(1-Q_3\mathfrak{q}^{i-\frac{1}{2}}\mathfrak{t}^{j-\frac{1}{2}}\big).\end{aligned} \tag{15.1.15}$$

At the same time, due to the specialisation (15.1.12), we can also recast the infinite product

$$\prod_{i,j=1}^{\infty} \frac{(1-Q_3\mathfrak{q}^{i-\frac{1}{2}}\mathfrak{t}^{j-\frac{1}{2}})(1-Q_1Q_2Q_3\mathfrak{q}^{i-\frac{1}{2}}\mathfrak{t}^{j-\frac{1}{2}})}{(1-Q_1Q_3\mathfrak{q}^{i-1}\mathfrak{t}^{j})(1-Q_2Q_3\mathfrak{q}^{i}\mathfrak{t}^{j-1})} = \prod_{i=1}^{x}\prod_{j=1}^{y} \big(1-Q_3\mathfrak{q}^{i-\frac{1}{2}}\mathfrak{t}^{j-\frac{1}{2}}\big) \tag{15.1.16}$$

as the finite product (15.1.15) using the Cauchy formula. Since the polynomials $P_k(Q_1,Q_2)$ are completely defined if their values are known at $(k+1)^2$ points (assuming that $\frac{\epsilon_1}{\epsilon_2}$ is irrational) we can now "analytically continue" the values of Q_1 and Q_2 and reach the product formula for the partition function (15.1.15)

$$\mathcal{Z}_2^{\text{top}}(\boldsymbol{Q}) = \prod_{i,j=1}^{\infty} \frac{(1-Q_1Q_2Q_3\mathfrak{q}^{i-\frac{1}{2}}\mathfrak{t}^{j-\frac{1}{2}})\prod_{k=1}^{3}(1-Q_k\mathfrak{q}^{i-\frac{1}{2}}\mathfrak{t}^{j-\frac{1}{2}})}{(1-Q_1Q_2\mathfrak{q}^{i}\mathfrak{t}^{j-1})(1-Q_1Q_3\mathfrak{q}^{i-1}\mathfrak{t}^{j})(1-Q_2Q_3\mathfrak{q}^{i}\mathfrak{t}^{j-1})}\,, \tag{15.1.17}$$

which can also be written as

$$\mathcal{Z}_2^{\text{top}}(\boldsymbol{Q}) = \frac{\mathcal{M}\big(Q_1Q_2\big)\mathcal{M}(Q_1Q_3\frac{\mathfrak{t}}{\mathfrak{q}})\mathcal{M}\big(Q_2Q_3\big)}{\mathcal{M}\big(Q_1\sqrt{\frac{\mathfrak{t}}{\mathfrak{q}}}\big)\mathcal{M}\big(Q_2\sqrt{\frac{\mathfrak{t}}{\mathfrak{q}}}\big)\mathcal{M}\big(Q_3\sqrt{\frac{\mathfrak{t}}{\mathfrak{q}}}\big)\mathcal{M}\big(Q_1Q_2Q_3\sqrt{\frac{\mathfrak{t}}{\mathfrak{q}}}\big)} \tag{15.1.18}$$

using the function $\mathcal{M}(Q)$ defined in (F.0.6). Note that the function $\mathcal{M}(Q)$ also has a plethystic exponential form, given in equation (F.0.7) and thus the function (15.1.18) is analytic and has a convergent power series expansion in some neighbourhood around $Q_3 = 0$. The key result is that both functions (15.1.18) and (15.1.17) have the same formal power expansion (15.1.10) and we have compared the coefficients of the polynomials at $(k+1)^2$ points. Since term by term the two series coincide, it follows that the two functions are equal.

15.2 The four dimensional limit

We are now going to analyse the 4d limit $R \to 0$. In order to define this limit precisely we find it useful to parametrise the variables $\mathfrak{q}$, $\mathfrak{t}$, L, M and N, as

$$\mathfrak{q} = e^{-\epsilon_1 R}\,, \quad \mathfrak{t} = \mathfrak{q}^{\beta^2}\,, \quad M^2 = \frac{\mathfrak{t}^{\mu}}{\mathfrak{q}}\,, \quad N^2 = \frac{\mathfrak{t}^{\nu}}{\mathfrak{t}}\,, \quad L^2 = \frac{\mathfrak{t}^{\lambda}}{\mathfrak{q}}\,. \tag{15.2.19}$$

The limit of our interest is $R \to 0$ keeping $\epsilon_1, \beta, \lambda, \mu, \nu$ finite. Introducing the notation

$$s = \frac{1}{2}(\lambda + \mu - \nu - \beta^{-2}). \tag{15.2.20}$$

allows us to rewrite the expression for $\mathcal{Z}_2^{\rm top} \equiv \mathcal{Z}_2^{\rm top}(\lambda, \mu, \nu; \epsilon_1, \beta, R)$ in the following useful form

$$\mathcal{Z}_2^{\rm top} = \frac{1}{\mathcal{M}(\mathfrak{t}^{1+s}/\mathfrak{q})} \frac{\mathcal{M}(\mathfrak{t}^{\lambda}/\mathfrak{q})\mathcal{M}(\mathfrak{t}^{\mu}/\mathfrak{q})\mathcal{M}(\mathfrak{t}^{\nu}/\mathfrak{q})}{\mathcal{M}(\mathfrak{t}^{\lambda-s}/\mathfrak{q})\mathcal{M}(\mathfrak{t}^{\mu-s}/\mathfrak{q})\mathcal{M}(\mathfrak{t}^{\nu+s}/\mathfrak{q})} \,. \tag{15.2.21}$$

It turns out that each of the functions $\mathcal{M}$ becomes singular in the limit defined above, see Appendix F.1 for a discussion. It follows that the function $\mathcal{Z}_2^{\rm top}(\lambda, \mu, \nu, \epsilon_1, \epsilon_2, R)$ does not have a finite limit when $R \to 0$. In the rest of this section we will discuss how a meaningful limit can be defined nevertheless.

15.2.1 A useful factorisation

The following will demonstrate that $\mathcal{Z}_2^{\rm top}$ can be factorised in a singular and a regular factor

$$\mathcal{Z}_2^{\rm top}(\lambda, \mu, \nu; \epsilon_1, \beta, R) = \mathcal{Z}_{2,\rm sing}^{\rm top}(s, \epsilon_1, \beta, R)\mathcal{Z}_{2,\rm reg}^{\rm top}(\lambda, \mu, \nu, \epsilon_1, \beta, R), \tag{15.2.22}$$

where $\mathcal{Z}_{2,\rm reg}^{\rm top}(\lambda, \mu, \nu, \epsilon_1, \beta, R)$ stays finite in the limit $R \to 0$ and the singular part $\mathcal{Z}_{2,\rm sing}^{\rm top}$ is

$$\mathcal{Z}_{2,\rm sing}^{\rm top}(s, \epsilon_1, \beta, R) = \frac{1}{\mathcal{M}(\mathfrak{t}/\mathfrak{q})} \frac{(1 - e^{-\epsilon_1 R})^{\beta^2 s}}{(1 - e^{-\epsilon_1 \beta^2 R})^{s}} \,. \tag{15.2.23}$$

In order to prove the factorisation (15.2.22) one may start by rewriting $\mathcal{Z}_2^{\rm top}$ as

$$\mathcal{Z}_2^{\rm top} = \frac{1}{\mathcal{M}(\mathfrak{t}/\mathfrak{q})} \frac{(\mathfrak{t}^{s+1}; \mathfrak{t})_\infty (\mathfrak{q}; \mathfrak{q})_\infty}{(\mathfrak{t}; \mathfrak{t})_\infty (\mathfrak{q}^{\beta^2 s+1}; \mathfrak{q})_\infty} \frac{\mathcal{M}(t^{\lambda}/q)\mathcal{M}(t^{\mu}/q)\mathcal{M}(t^{\nu}/q)\mathcal{M}(1)}{\mathcal{M}(t^{\lambda-s}/q)\mathcal{M}(t^{\mu-s}/q)\mathcal{M}(t^{\nu+s}/q)\mathcal{M}(t^{s})} \,. \tag{15.2.24}$$

The notation $(x; \mathfrak{q})_\infty$ stands for the quantum dilogarithm function defined in equation (F.0.1). The equality between the two expression for $\mathcal{Z}_2^{\rm top}$ above is easily verified using the functional equations

$$\mathcal{M}(u\mathfrak{t}) = (u\mathfrak{q}, \mathfrak{q})_\infty \mathcal{M}(u) \,, \qquad \mathcal{M}(u\mathfrak{q}) = (u\mathfrak{q}, \mathfrak{t})_\infty \mathcal{M}(u) \,. \tag{15.2.25}$$

The middle factor in (15.2.24) may be represented in terms of the $\mathfrak{q}$-Gamma function

$$\Gamma_{\mathfrak{q}}(x) = (1 - \mathfrak{q})^{1-x} \frac{(\mathfrak{q}; \mathfrak{q})_\infty}{(\mathfrak{q}^x; \mathfrak{q})_\infty} \,, \tag{15.2.26}$$

as

$$\frac{(\mathfrak{t}^{s+1}; \mathfrak{t})_\infty (\mathfrak{q}; \mathfrak{q})_\infty}{(\mathfrak{t}; \mathfrak{t})_\infty (\mathfrak{q}^{\beta^2 s+1}; \mathfrak{q})_\infty} = \frac{(1 - \mathfrak{q})^{\beta^2 s}}{(1 - \mathfrak{t})^{s}} \frac{\Gamma_{\mathfrak{q}}(1 + \beta^2 s)}{\Gamma_{\mathfrak{t}}(1 + s)}. \tag{15.2.27}$$

The function $\Gamma_{\mathfrak{q}}(x)$ is known to have the ordinary Gamma-function $\Gamma(x)$ as its limit $\mathfrak{q} \to 1$, so that (15.2.24) displays a factorisation into a simple singular and a finite part for $R \to 0$.

We thereby arrive at the factorisation (15.2.22) with

$$\mathcal{Z}_{2,\rm reg}^{\rm top} = \frac{\Gamma_{\mathfrak{q}}(1 + \beta^2 s)}{\Gamma_{\mathfrak{t}}(1 + s)} \mathcal{Z}_{2,\rm bal}^{\rm top}, \quad \mathcal{Z}_{2,\rm bal}^{\rm top} = \frac{\mathcal{M}(\mathfrak{t}^{\lambda}/\mathfrak{q})\mathcal{M}(\mathfrak{t}^{\mu}/\mathfrak{q})\mathcal{M}(\mathfrak{t}^{\nu}/\mathfrak{q})\mathcal{M}(1)}{\mathcal{M}(\mathfrak{t}^{\lambda-s}/\mathfrak{q})\mathcal{M}(\mathfrak{t}^{\mu-s}/\mathfrak{q})\mathcal{M}(\mathfrak{t}^{\nu+s}/\mathfrak{q})\mathcal{M}(\mathfrak{t}^{s})} \tag{15.2.28}$$

which will be shown to have a finite limit when $R \to 0$.

15.2.2 The limit of the regular part

In order to show that $\mathcal{Z}^{\rm top}_{2,\rm reg}$ has a finite limit when $R \to 0$ it is useful to observe that it is a ratio of products of functions that is "perfectly balanced" in the following sense. For any given function $F(x)$ we may call ratios of the form

$$R(\lambda,\mu,\nu,\delta) = \frac{F(\delta)}{F(\delta-s)}\frac{F(\nu)}{F(\nu-s)}\frac{F(\mu)}{F(\mu+s)}\frac{F(\lambda)}{F(\lambda+s)} \tag{15.2.29}$$

perfectly balanced if (λ,μ,ν,δ) satisfy $\mu+\lambda-\nu-\delta = 2s$. If this is the case one easily finds that the function $\tilde{R}(\lambda,\mu,\nu,\delta)$ obtained by replacing the function $F(x)$ in equation (15.2.29) by $\tilde{F}(x) = e^{\alpha x^2+\beta x}F(x)$ is identically equal to the function $R(\lambda,\mu,\nu,\delta)$. It is easily checked that $\mathcal{Z}^{\rm top}_{2,\rm bal} \equiv \mathcal{Z}^{\rm top}_{2,\rm bal}(\lambda,\mu,\nu,\beta^{-2})$ is perfectly balanced in this sense. It can be represented as the infinite product

$$\mathfrak{T}_s(\delta,\nu,\mu,\lambda) = \prod_{i,j=0} \mathfrak{t}_{ij}(\delta,\nu,\mu,\lambda)\,, \tag{15.2.30}$$

where $\delta = \beta^{-2}$ and

$$\mathfrak{t}_{ij}(\delta,\nu,\mu,\lambda) = \vartheta^+_{ij}(\delta,s)\vartheta^+_{ij}(\nu,s)\vartheta^-_{ij}(\mu,s)\vartheta^-_{ij}(\lambda,s)\,, \quad \vartheta^\pm_{ij}(\mu,s) = \frac{1-\mathfrak{t}^{\mu\pm s+i}\mathfrak{q}^j}{1-\mathfrak{t}^{\mu+i}\mathfrak{q}^j}. \tag{15.2.31}$$

In the limit $R \to 0$ one finds that

$$\mathfrak{T}_s(\delta,\nu,\mu,\lambda) \to \mathfrak{R}_s(\delta,\nu,\mu,\lambda) = \prod_{i,j=0} \mathfrak{r}_{ij}(\delta,\nu,\mu,\lambda)\,, \tag{15.2.32}$$

where

$$\mathfrak{r}_{ij}(\delta,\nu,\mu,\lambda) = \varrho^+_{ij}(\delta,s)\varrho^+_{ij}(\nu,s)\varrho^-_{ij}(\mu,s)\varrho^-_{ij}(\lambda,s)\,, \quad \varrho^\pm_{ij}(\mu,s) = \frac{i+\beta^2(\mu\pm s+j)}{i+\beta^2(\mu+j)}\,. \tag{15.2.33}$$

The crucial point to observe is that the infinite product that defines $\mathfrak{R}_s(\delta,\nu,\mu,\lambda)$ is still absolutely convergent thanks to the fact that it is the product of perfectly balanced factors. In order to see this, let us introduce $\Gamma_\beta(\beta x) = \Gamma_2(x|1,\beta^{-2})$, with $\Gamma_2(x|\epsilon_1,\epsilon_2)$ defined by the absolutely convergent infinite product.

$$\Gamma_2(x|\epsilon_1,\epsilon_2) = \frac{e^{-\alpha x+\frac{\beta x^2}{2}}}{x}\prod_{n_1,n_2\geq 0}{}' \frac{e^{\frac{x}{\epsilon_1 n_1+\epsilon_2 n_2}-\frac{x^2}{2(\epsilon_1 n_1+\epsilon_2 n_2)^2}}}{1+\frac{x}{\epsilon_1 n_1+\epsilon_2 n_2}}\,, \quad \epsilon_1,\epsilon_2 > 0\,. \tag{15.2.34}$$

It is then easy to see that

$$\mathfrak{R}_s(\beta^{-2},\nu,\mu,\lambda) = \frac{\Gamma_\beta(\beta^{-1})}{\Gamma_\beta(\beta^{-1}+\beta s)}\frac{\Gamma_\beta(\beta\nu)}{\Gamma_\beta(\beta(\nu-s))}\frac{\Gamma_\beta(\beta\mu)}{\Gamma_\beta(\beta(\mu+s))}\frac{\Gamma_\beta(\beta\lambda)}{\Gamma_\beta(\beta(\lambda+s))}. \tag{15.2.35}$$

Indeed, each factor in the infinite product over n_1, n_2 obtained by inserting (15.2.34) into (15.2.35) is perfectly balanced, making it easy to see that all exponential factors cancel each other, factor by factor, leaving behind the infinite product defining $\mathfrak{R}_s(\delta,\nu,\mu,\lambda)$, which is of course as absolutely convergent as the infinite products defining the function $\Gamma_\beta(x)$ are.

15.2.3 Renormalising the singular part

One may now be tempted to simply define $\mathcal{Z}_2^{\rm 4d}$ to be $\mathcal{Z}^{\rm top}_{2,reg}(\lambda,\mu,\nu,\epsilon_1,\beta,R)$. However, it is clear that the factorisation (15.2.22) is ambiguous. One could modify $\mathcal{Z}^{\rm top}_{2,sing}$ by multiplying it with an arbitrary function while dividing $\mathcal{Z}^{\rm top}_{2,reg}$ by the same function. Additional requirements have to be imposed in order to arrive at an unambiguous definition for $\mathcal{Z}_2^{\rm 4d}$.

In our case it seems natural to require that the key analytic properties of the function $\mathcal{Z}_2^{\rm top}$ are preserved in the limit. In this regard let us note that the factorisation (15.2.22) has some special features distinguishing it from other possible factorisations. The singular piece, here recalled for convenience

$$\mathcal{Z}^{\rm top}_{2,\rm sing}(s,\epsilon_1,\beta,R)=\frac{1}{\mathcal{M}(\mathfrak{t}/\mathfrak{q})}\frac{(1-e^{-\epsilon_1 R})^{\beta^2 s}}{(1-e^{-\epsilon_1\beta^2 R})^{s}}\,, \tag{15.2.36}$$

depends (i) on the variables λ,μ,ν only through the combination $s=\frac{1}{2}(\lambda+\mu-\nu-\beta^{-2})$ and (ii) depends on the variable s in a very simple way: the dependence of $\mathcal{Z}^{\rm top}_{2,\rm sing}$ on the variable s is entire analytic, $\mathcal{Z}^{\rm top}_{2,\rm sing}$ is nowhere vanishing as function of s and it has at most exponential growth. This means that $\log\mathcal{Z}^{\rm top}_{2,\rm sing}$ is a linear function.

Imposing the requirement that these features are preserved in the limit $R\to 0$ eliminates most of the ambiguities in the renormalisation of $\mathcal{Z}_2^{\rm top}$. The factor $\frac{1}{\mathcal{M}(\mathfrak{t}/\mathfrak{q})}$ does not depend on s at all, while

$$\frac{(1-e^{-\epsilon_1 R})^{\beta^2 s}}{(1-e^{-\epsilon_1\beta^2 R})^{s}}\sim R^{s(\beta^2-1)}\,\beta^{-2s}\,. \tag{15.2.37}$$

We conclude that the most general renormalised limit $R\to 0$ satisfying the requirements formulated above is

$$\lim_{R\to 0}\eta(\rho R^{\beta^2})^{-s}\mathcal{M}(\mathfrak{t}/\mathfrak{q})\mathcal{Z}_2^{\rm top}(\lambda,\mu,\nu;\epsilon_1,\beta,R). \tag{15.2.38}$$

The factors η and ρ^{-s} represent the ambiguity in the definition of the limit that cannot be removed by the requirements above.

Collecting our findings above, introducing the notations

$$\beta\lambda=2a_3+\beta,\qquad \beta\mu=2a_2+\beta,\qquad \beta\nu=\beta^{-1}-2a_1, \tag{15.2.39}$$

and using the identity

$$\frac{\Gamma_\beta(\beta^{-1})}{\Gamma_\beta(\beta^{-1}+\beta s)}=\beta^{-s(1+\beta^2)}\frac{\Gamma(1+s)}{\Gamma(1+\beta^2 s)}\frac{\Gamma_\beta(\beta)}{\Gamma_\beta(\beta+\beta s)} \tag{15.2.40}$$

we arrive at the statement that

$$\begin{aligned}\lim_{R\to 0}\eta(\rho R^{\beta^2})^{-s}\mathcal{M}(\mathfrak{t}/\mathfrak{q})\mathcal{Z}_2^{\rm top}=\eta\big(\beta^{1+\beta^2}\rho\big)^{-s}\frac{\Gamma_\beta(\beta)}{\Gamma_\beta(\beta+\beta s)}\\ \times\frac{\Gamma_\beta(\beta^{-1}-2a_1)}{\Gamma_\beta(\beta^{-1}-2a_1+\beta s)}\frac{\Gamma_\beta(2a_2+\beta)}{\Gamma_\beta(2a_2+\beta-\beta s)}\frac{\Gamma_\beta(2a_3+\beta)}{\Gamma_\beta(2a_3+\beta-\beta s)}\,.\end{aligned} \tag{15.2.41}$$

Recall that the calculation above is performed for the case $\mathfrak{q}=e^{-\epsilon_1 R}<1$ and $\mathfrak{t}=\mathfrak{q}^{\beta^2}<1$. In the regime where $|\mathfrak{t}|>1$ it is more natural to parameterise $\mathfrak{t}=\mathfrak{q}^{-b^2}>1$. In this case we obtain

$$\begin{aligned}\lim_{R\to 0}\eta(\rho R^{\beta^2})^{-s}\mathcal{M}(\mathfrak{t}/\mathfrak{q})\mathcal{Z}_2^{\rm top}=&\eta(b^{1-b^2}\rho)^{-s}\frac{\Gamma_b(-sb^2)}{\Gamma_b(0)}\\ &\frac{\Gamma_b(Q-2\alpha_1-sb)\Gamma_b(2\alpha_2+sb)\Gamma_b(2\alpha_3+sb)}{\Gamma_b(Q-2\alpha_1)\Gamma_b(2\alpha_2)\Gamma_b(2\alpha_3)}\end{aligned} \tag{15.2.42}$$

which looks more like the three point conformal block for the Liouville theory.

Chapter 16

From topological strings to a matrix integral

In this chapter we show an alternative approach towards relating topological strings partition functions to conformal blocks of Liouville conformal field theory, following [34], [162]. The specialisation of one parameter in the topological string partition function allows to rewrite it as the matrix model integral in the Coulomb gas approximation of the three point conformal block $\mathcal{B}_{\mathfrak{q}-\text{Liouv}}$ of $\mathfrak{q}$-deformed Liouville conformal field theory. This specialisation condition is known in the CFT literature as the screening condition.

16.1 Imposing the specialisation condition on the topological strings

We begin with the topological string partition function for T_2 derived in Chapter 15 and written in equation (14.0.1), which we rewrite here for the convenience of the reader:

$$\begin{aligned}&\mathcal{Z}_2^{\text{top}}(M,N,L;\mathfrak{q},\mathfrak{t}) = \\ &= \frac{\mathcal{M}(M^2)}{\mathcal{M}(\sqrt{\frac{\mathfrak{t}}{\mathfrak{q}}}\frac{LM}{N})\mathcal{M}(\sqrt{\frac{\mathfrak{t}}{\mathfrak{q}}}\frac{NM}{L})}\sum_Y\left(\sqrt{\frac{\mathfrak{t}}{\mathfrak{q}}}\frac{LN}{M}\right)^{|Y|}\frac{\mathcal{N}_{Y\emptyset}\left(\sqrt{\frac{\mathfrak{t}}{\mathfrak{q}}}\frac{LM}{N}\right)\mathcal{N}_{\emptyset Y}\left(\sqrt{\frac{\mathfrak{t}}{\mathfrak{q}}}\frac{NM}{L}\right)}{\mathcal{N}_{YY}(\mathfrak{t}/\mathfrak{q})}\,.\end{aligned} \tag{16.1.1}$$

An important first step is to observe that if we impose

$$\sqrt{\frac{\mathfrak{t}}{\mathfrak{q}}}\frac{LM}{N} = \frac{\mathfrak{t}}{\mathfrak{q}}\,\mathfrak{t}^s\,, \tag{16.1.2}$$

with s an integer and $N_Y > s$, the partition function vanishes so, after substituting (16.1.2) in (16.1.1) we can safely replace N_Y by s on the products. By massaging the equation (16.1.1) we can rewrite the topological string partition function into the form

$$\mathcal{Z}_2^{\text{top}} = \frac{\prod_{i=1}^s\varphi(M^2\mathfrak{q}\mathfrak{t}^{-i})}{\mathcal{M}(v^{-2})\prod_{i=1}^s\varphi(\mathfrak{t}^i)}\sum_Y\left(\frac{LN}{vM}\right)^{|Y|}\frac{\mathcal{I}_m(y_Y)}{\mathcal{I}_m(y_\emptyset)}\frac{\mathcal{I}_{1,1}(y_Y)}{\mathcal{I}_{1,1}(y_\emptyset)} \tag{16.1.3}$$

in terms of $v = \sqrt{\mathfrak{q}/\mathfrak{t}}$ and the quantum dilogarithm function $\varphi(x)$ from equation (F.0.1), recalling the definitions (14.0.11)

$$\mathcal{I}_m(y_Y) = \prod_{i=1}^{s} \frac{\varphi(M^2 v^2/y_{Y,i})}{\varphi(1/y_{Y,i})}\,,\ \mathcal{I}_{1,1}(y_Y) = \prod_{i\neq j=1}^{s} \frac{\varphi(\mathfrak{q}^{Y_i-Y_j}\mathfrak{t}^{j-i})}{\varphi(\mathfrak{q}^{Y_i-Y_j}\mathfrak{t}^{j-i+1})} = \prod_{i\neq j=1}^{s} \frac{\varphi(y_{Y,i}/y_{Y,j})}{\varphi(\mathfrak{t} y_{Y,i}/y_{Y,j})}\,, \quad (16.1.4)$$

and where the variables y are defined as

$$y_{Y,i} = \mathfrak{q}^{Y_i}\mathfrak{t}^{s-i}\ . \quad (16.1.5)$$

To prove equation (16.1.3), simply note that using equations (F.0.11) and (F.0.12) we can recast the topological string partition function of T_2 as

$$\begin{aligned} \mathcal{Z}_2^{\text{top}} &= \frac{\prod_{i=1}^{s}\varphi(M^2\mathfrak{q}\mathfrak{t}^{-i})}{\mathcal{M}(v^{-2})\prod_{i=1}^{s}\varphi(\mathfrak{t}^i)} \sum_Y \left(\frac{LN}{vM}\right)^{|Y|} \\ &\quad \times \prod_{i=1}^{s}\frac{\varphi(M^2v^2/y_{Y,i})}{\varphi(M^2v^2/y_{\emptyset,i})}\prod_{i=1}^{s}\frac{\varphi(1/y_{\emptyset,i})}{\varphi(1/y_{Y,i})}\prod_{i,j=1}^{s}\frac{\varphi(\mathfrak{q}^{Y_i-Y_j}\mathfrak{t}^{j-i})}{\varphi(\mathfrak{q}^{Y_i-Y_j}\mathfrak{t}^{j-i+1})}\frac{\varphi(\mathfrak{t}^{j-i+1})}{\varphi(\mathfrak{t}^{j-i})}\,, \end{aligned} \quad (16.1.6)$$

observing that when s is the number of rows of the partition Y, the expansion (F.0.19) of the Nekrasov function $\mathcal{N}_{YY}(\mathfrak{t}/\mathfrak{q})$ into quantum dilogarithms allows to obtain $\mathcal{I}_{1,1}(y)$ from

$$\mathcal{N}_{YY}(\mathfrak{t}/\mathfrak{q})^{-1} = \mathcal{N}_{Y\emptyset}\left(\mathfrak{t}^{1+s}/\mathfrak{q}\right)^{-1}\mathcal{N}_{\emptyset Y}\left(\mathfrak{t}^{1-s}/\mathfrak{q}\right)^{-1}\frac{\mathcal{I}_{1,1}(y_Y)}{\mathcal{I}_{1,1}(y_\emptyset)}\,. \quad (16.1.7)$$

Then, the functions $\mathcal{N}_{Y\emptyset}$ cancel while $\mathcal{N}_{\emptyset Y}$ combine to give the function $\mathcal{I}_m(y)$

$$\frac{\mathcal{N}_{\emptyset Y}(M^2\mathfrak{t}^{-s})}{\mathcal{N}_{\emptyset Y}\left(\mathfrak{t}^{1-s}/\mathfrak{q}\right)} = \frac{\mathcal{I}_m(y_Y)}{\mathcal{I}_m(y_\emptyset)}\,. \quad (16.1.8)$$

16.2 The matrix integral as a sum of residues

We are almost ready to show that the topological string partition function (16.1.3) is related to the matrix integral

$$\mathcal{I}_2 = \int d'_{\mathfrak{q}}y_1\cdots d'_{\mathfrak{q}}y_s \prod_{i=1}^{s} y_i^{\zeta}\,\mathcal{I}_{1,1}(y)\,\mathcal{I}_m(y)\,, \quad (16.2.9)$$

where the parameter ζ is defined by

$$\mathfrak{q}^{\zeta+1} = \sqrt{\frac{\mathfrak{t}}{\mathfrak{q}}}\frac{LN}{M}\,, \quad (16.2.10)$$

and the integrals $\int d'_{\mathfrak{q}}y_1\cdots d'_{\mathfrak{q}}y_s$ are variants of the Jackson integral defined for meromorphic functions $M(y)$ of s variables $y = (y_1,\ldots,y_s)$ as a sum over residues

$$\int \frac{d'_q y_1}{y_1}\cdots\frac{d'_q y_s}{y_s}\,M(y) := (2\pi\mathrm{i})^s \sum_{\substack{Y_1,\ldots,Y_s\in\mathbb{N}\\ Y_1>Y_2>\ldots Y_s}} \operatorname*{Res}_{y=y_Y} M(y)\,. \quad (16.2.11)$$

A simple example

Let us first consider a simple example in order to understand this. We are ultimately interested in evaluating the $\mathfrak{q} \to 1^-$ limit of integrals of the form

$$\mathcal{I}_\mathfrak{q} = \int_\mathcal{C} dx\ \mathcal{R}(x;s,t), \qquad \mathcal{R}(x;s,t) = x^{t+s-2}\frac{\varphi(\mathfrak{q}^{1-s}/x)}{\varphi(1/x)}\,. \tag{16.2.12}$$

where $\mathcal{C}$ is a contour starting and ending at 0, encircling the poles of the integrand in the interval $(0,1)$ in the counterclockwise direction. The integrand (16.2.12) has poles at $x = \mathfrak{q}^n$, $n \in \mathbb{N}$. The integral $\mathcal{I}_\mathfrak{q}$ can therefore be evaluated as a sum of the residues

$$\mathcal{I}_\mathfrak{q} = 2\pi\mathrm{i}\sum_{n=0}^{\infty}\mathcal{R}_n(s,t), \qquad \mathcal{R}_n(s,t) := \operatorname*{Res}_{x=\mathfrak{q}^n}\mathcal{R}(x;s,t)\,, \tag{16.2.13}$$

being a special case of (16.2.9). Evaluating the integral in this way is however tricky because in the limit $\mathfrak{q} \to 1$, the ratio of quantum dilogarithms in the integrand $\mathcal{R}(x;s,t)$ becomes $(1-1/x)$ (see equation (F.1.29)). Therefore, it is precisely in the region of integration that poles condensate on a branch cut and one has to note that the limit formula is valid only in a region which is outside the region of integration in the present case. For what follows we find it useful to introduce a variant of the Jacobi triple product function

$$\vartheta_\mathfrak{q}(z) := \varphi(z)\varphi(\mathfrak{q}/z)\varphi(\mathfrak{q}) = (1-z)\prod_{n=1}(1-z\mathfrak{q}^n)(1-z^{-1}\mathfrak{q}^n)(1-\mathfrak{q}^n) \tag{16.2.14}$$

and the function

$$\vartheta_\mathfrak{q}(x,\mathfrak{q}^\kappa) = x^{\kappa-1}\frac{\varphi(\mathfrak{q}^\kappa x)}{\varphi(\mathfrak{q}x)}\frac{\varphi(\mathfrak{q}^{1-\kappa}/x)}{\varphi(1/x)} = x^{\kappa-1}\frac{\vartheta_\mathfrak{q}(\mathfrak{q}^\kappa x)}{\vartheta_\mathfrak{q}(\mathfrak{q}x)}\,. \tag{16.2.15}$$

The function $\vartheta_\mathfrak{q}(x,\mathfrak{q}^\kappa)$ is a quasi-constant, meaning that it does not depend on multiplicative shifts of the argument by $\mathfrak{q}$,

$$\vartheta_\mathfrak{q}(x,\mathfrak{q}^\kappa) = \vartheta_\mathfrak{q}(\mathfrak{q}x,\mathfrak{q}^\kappa)\,. \tag{16.2.16}$$

We may use this function to rewrite the integrand $\mathcal{R}(x;s,t)$ of $\mathcal{I}_\mathfrak{q}$ as

$$\mathcal{R}(x;s,t) = \vartheta_\mathfrak{q}(x,\mathfrak{q}^s)x^{t-1}\frac{\varphi(\mathfrak{q}x)}{\varphi(\mathfrak{q}^s x)}\,, \tag{16.2.17}$$

which allows us to represent $\mathcal{I}_\mathfrak{q}$ as

$$\mathcal{I}_\mathfrak{q} = 2\pi\mathrm{i}\sum_{n=0}^{\infty}\rho(s)\mathcal{R}'_n(s,t)\,, \qquad \mathcal{R}'_n(s,t) := \left[x^{t-1}\frac{\varphi(\mathfrak{q}x)}{\varphi(\mathfrak{q}^s x)}\right]_{x=\mathfrak{q}^n} \tag{16.2.18}$$

and where $\rho(s)$ is given by

$$\rho(s) = \operatorname*{Res}_{x=\mathfrak{q}^n}\vartheta_\mathfrak{q}(x,\mathfrak{q}^s) = \mathfrak{q}^n\frac{\vartheta_\mathfrak{q}(\mathfrak{q}^s)}{(\mathfrak{q};\mathfrak{q})_\infty^3}\,. \tag{16.2.19}$$

In equation (16.2.18) the singularities are no longer close to the points being evaluated. It follows that the integral (16.2.12) can be rewritten in terms of an integral $\mathcal{I}'_\mathfrak{q}$

$$\mathcal{I}_\mathfrak{q} = \frac{2\pi\mathrm{i}}{1-\mathfrak{q}}\frac{\vartheta_\mathfrak{q}(\mathfrak{q}^s)}{(\mathfrak{q};\mathfrak{q})_\infty^3}\mathcal{I}'_\mathfrak{q}, \qquad \mathcal{I}'_\mathfrak{q} = \int_0^1 d_\mathfrak{q}x\ x^{t-1}\frac{\varphi(\mathfrak{q}x)}{\varphi(\mathfrak{q}^s x)}\,, \tag{16.2.20}$$

where $\mathcal{I}'_{\mathfrak{q}}$ can be evaluated as Jacksons integral

$$\int_0^1 d_{\mathfrak{q}} x f(x) = (1-\mathfrak{q}) \sum_{k=0}^{\infty} \mathfrak{q}^k f(\mathfrak{q}^k) \,. \tag{16.2.21}$$

The right hand side is defined such that, in the limit $\mathfrak{q} \to 1$ the integral on the left becomes its classical counterpart

$$\int_0^1 d_{\mathfrak{q}} x f(x) \;\rightsquigarrow\; \int_0^1 dx f(x) \quad \Rightarrow \quad (1-\mathfrak{q}) \sum_{k=0}^{\infty} f(\mathfrak{q}^k) \;\rightsquigarrow\; \int_0^1 \frac{dx}{x} f(x) \,. \tag{16.2.22}$$

This is the reason that ζ enters the matrix model integral (16.2.9) but it is $\mathfrak{q}^{\zeta+1}$ that is related to the topological string parameters in equation (14.0.10).

Summation over residues

To understand the relation between the integral (16.2.9) and its expression as a sum over residues more precisely, we now discuss the pole structure of the integrand, noting that it parallels the analysis of [34], [162]. Assuming a radial ordering of the poles $|y_i| < |y_{i+1}|$, these originate from:

- $\mathcal{I}_m(y)$: outermost pole $y_s = \mathfrak{q}^{Y_s}$
- $\mathcal{I}_{1,1}(y)$: poles organised by a partition Y, with $y_i = \mathfrak{q}^{Y_i}\mathfrak{t}^{s-i}$, $1 \le i < s$.

The reasoning behind this statement is as follows. The poles of the function $\mathcal{I}_m(y)$ are located at $y_i = \mathfrak{q}^m,\ m \in \mathbb{N}$ while, in the regime where $|\mathfrak{q}|, |\mathfrak{t}| < 1$, those of the function $\mathcal{I}_{1,1}(y)$ satisfy $y_i/y_{i+1} = \mathfrak{q}^n\mathfrak{t}$. The outermost pole y_s therefore has to belong to $\mathcal{I}_m(y)$, since it would otherwise be inconsistent with the radial ordering. Having established this fact, no other poles can originate from $\mathcal{I}_m(y)$ because any such singularities would be cancelled by zeros of $\mathcal{I}_{1,1}(y)$. Consequently, all of the remaining poles belong to the function $\mathcal{I}_{1,1}(y)$ and $y_{s-1}/y_s = \mathfrak{q}^n\mathfrak{t}$ implies $y_{s-1} = \mathfrak{q}^{Y_{s-1}}\mathfrak{t}$, with $Y_{s-1} > Y_s$. Iterating this logic, we find the remaining poles are $y_i = \mathfrak{q}^{Y_i}\mathfrak{t}^{s-i}$, the set of which is therefore labelled by a Young tableau Y

$$y_Y = \left(\mathfrak{q}^{Y_1}\mathfrak{t}^{s-1}, \ldots, \mathfrak{q}^{Y_{s-1}}\mathfrak{t}, \mathfrak{q}^{Y_s}\right) \,. \tag{16.2.23}$$

The matrix integral (16.2.9) is therefore defined through the sum

$$\mathcal{I}_2 = (2\pi i)^s \left(\text{Res}_{\emptyset}\right) \sum_Y \mathfrak{q}^{(\zeta+1)|Y|} \frac{\mathcal{I}_{1,1}(y_Y)}{\mathcal{I}_{1,1}(y_\emptyset)} \frac{\mathcal{I}_m(y_Y)}{\mathcal{I}_m(y_\emptyset)} \,, \tag{16.2.24}$$

where the coefficient

$$\text{Res}_{\emptyset} = \mathfrak{t}^{\frac{1}{2}s(s-1)(\zeta+1)} \left(\frac{\varphi(\mathfrak{t})}{\varphi(\mathfrak{q})}\right)^s \prod_{i=1}^{s} \frac{\varphi(M^2\mathfrak{q}\mathfrak{t}^{i-s-1})}{\varphi(\mathfrak{t}^i)} \tag{16.2.25}$$

is obtained by evaluating the integral (16.2.9) with Y empty.

Relation to the topological strings partition function

The relation between the full partition function (16.1.3) and the integral formulation (16.2.9) is

$$\mathcal{I}_2(a_1,a_2,s;\beta) = (2\pi i)^s \mathfrak{t}^{\frac{1}{2}s(s-1)(\zeta+1)} \left(\frac{\varphi(\mathfrak{t})}{\varphi(\mathfrak{q})}\right)^s \mathcal{M}\big(\mathfrak{t}/\mathfrak{q}\big)\mathcal{Z}_2^{\text{top}}(M,N,L;\mathfrak{q},\mathfrak{t}) \tag{16.2.26}$$

with the parameter identification

$$M^2 = \frac{\mathfrak{t}}{\mathfrak{q}}\mathfrak{q}^{2\beta a_2}\,, \quad L^2 = \frac{\mathfrak{t}}{\mathfrak{q}}\mathfrak{q}^{2\beta a_3}\,, \quad N^2 = \frac{\mathfrak{q}}{\mathfrak{t}}\mathfrak{q}^{-2\beta a_1}\,, \quad \mathfrak{t} = \mathfrak{q}^{\beta^2}\,, \tag{16.2.27}$$

where $a_1 + a_2 + a_3 = (\beta^{-1} - \beta) + s\beta$ and the $\mathfrak{q}$ deformation parameter is identified with the Omega background $\mathfrak{q}$. This identification relates the matrix integral $\mathcal{I}_2(a_1,a_2,s;\beta)$, which we could equivalently call $\mathcal{I}_2(a_1,a_2,a_3;\beta)$ or $\mathcal{I}_2(N,M,L;\beta)$, to three point conformal blocks of $\mathfrak{q}$-deformed Liouville conformal field theory.

Chapter 17

The free field representation

In this chapter we briefly review the elements which enter the free field construction of $\mathfrak{q}$-deformed Liouville three point conformal blocks, relating them to the matrix integral $\mathcal{I}_2$ from the previous chapter. We will then take the undeformed limit $\mathfrak{q} \to 1$, in which the integral $\mathcal{I}_2$ becomes a Selberg integral.

The free field representation of the conformal blocks provides an interpretation for the parameter s as a screening charge and the specialisation of parameters becomes the screening charge condition. A three point conformal block on $\mathbb{CP}^1 \setminus \{z_1, z_2, z_3\}$ with primary fields V_{a_1}, V_{a_2} and V_{a_3} inserted at the locations of the punctures and with V_{a_2} screened by s currents $S(y)$ can be written as

$$\mathcal{B}_{\mathfrak{q}-\text{Liouv}} \equiv \oint dy\, \mathcal{I}_{\mathfrak{q}-\text{Liouv}} \tag{17.0.1}$$

with the integrand

$$\mathcal{I}_{\mathfrak{q}-\text{Liouv}} = \langle V_{a_2}(z_2) V_{a_1}(z_1)\rangle \prod_{k=1}^{2}\prod_{i=1}^{s}\langle S(y_i) V_{a_k}(z_k)\rangle \prod_{j>i=1}^{s}\langle S(y_j)S(y_i)\rangle\,, \tag{17.0.2}$$

where without any loss of generality we send $z_3 \to \infty$. The two point function of $\mathfrak{q}$-Liouville between a primary field and a screening current is

$$\langle S(y_i) V_{\alpha_2}(z)\rangle = (y_i)^{-2\beta a_2}\frac{\varphi(\mathfrak{q}^{2\beta a_2}/y_i)}{\varphi(1/y_i)}\,, \tag{17.0.3}$$

while that between two screening currents is [154], [155]

$$\langle S(y_j)S(y_i)\rangle = (y_j)^{2\beta^2}\,\frac{\varphi(y_i/y_j)\varphi(\mathfrak{q}\mathfrak{t}^{-1}y_i/y_j)}{\varphi(\mathfrak{q}y_i/y_j)\varphi(\mathfrak{t}y_i/y_j)}\,, \quad |y_i| < |y_j|\,,\ i<j\,. \tag{17.0.4}$$

It is worth noting that the latter has been misquoted in some of the relevant literature. To compare with the matrix model it is necessary to rewrite (17.0.4) using the following quasi-constant function

$$\vartheta_{\mathfrak{q}}\left(\frac{y_i}{y_j}, \mathfrak{q}^{1-\beta^2}\right) = \left(\frac{y_j}{y_i}\right)^{\beta^2}\frac{\varphi(\mathfrak{q}\mathfrak{t}^{-1}y_i/y_j)}{\varphi(\mathfrak{q}y_i/y_j)}\frac{\varphi(\mathfrak{t}y_j/y_i)}{\varphi(y_j/y_i)}\,. \tag{17.0.5}$$

If we now introduce the short-hand grouping all quasi-constants

$$\vartheta_{\mathfrak{q}}(y, \mathfrak{q}^s) = \prod_{j>i}^{s}\vartheta_{\mathfrak{q}}\left(\frac{y_i}{y_j}, \mathfrak{q}^{1-\beta^2}\right)\,, \tag{17.0.6}$$

gather the contributions of all floating y_i factors into y_i^ζ with

$$\zeta = -2\beta(a_1+a_2)+\beta^2(s-1) \tag{17.0.7}$$

and set $r_V = \langle V_{\alpha_2}(z_2)V_{\alpha_1}(z_1)\rangle$, then the three point conformal block $\mathcal{B}_{\mathfrak{q}-\text{Liouv}}$ in the free field representation with $z_1=0, z_2=1$ and $z_3=\infty$ can be written

$$\mathcal{B}_{\mathfrak{q}-\text{Liouv}} \;=\; r_V \int d'_{\mathfrak{q}}y_1\cdots d'_{\mathfrak{q}}y_s \prod_{i=1}^{s} y_i^\zeta\, \mathcal{I}_m(y)\mathcal{I}_{1,1}(y)\vartheta_{\mathfrak{q}}(y,\mathfrak{q}^s) = r_V\,\vartheta_{\mathfrak{q}}(y,\mathfrak{q}^s)\,\mathcal{I}_2(a_1,a_2,s;\beta)\,. \tag{17.0.8}$$

17.1 The $\mathfrak{q}\to 1$ limit of the matrix integral

Having established the relation between the topological string partition function and the matrix integral, we wish to learn how to take the $\mathfrak{q}\to 1$ limit of the latter, where this limit is well defined and thus determines the four dimensional limit of the former. Looking at the definition (14.0.10) and (14.0.11) as well as (F.1.23) one will notice that the function $\varphi(z)$ representing the main building block of the integrand diverges for $\mathfrak{q}\to 1$ and that the summation over residues defining $\mathcal{I}_2$ does not have an obvious limit.

Our strategy to resolve this issue is to first rewrite the sum (16.2.24) as a Jackson integral, then recast this in terms of combinations of functions $\varphi(z)$ which are known to have a well-defined limit when $\mathfrak{q}\to 1$, like in the simple example in Section 16.2. As a result we discover the relation to the usual Selberg integral. To achieve our goal we use again the quasi-constants $\vartheta_{\mathfrak{q}}(x,\mathfrak{q}^s)$ defined in equation (16.2.15). The trick is to push all the singularities of the integrant inside the quasi-constants such that the rest of the integral can be safely evaluated with no further singularities close to the evaluation points. Equation (17.0.5) allows us to rewrite the integral (16.2.9) as

$$\begin{aligned}\mathcal{I}_2 = \int d'_{\mathfrak{q}}y_1\cdots d'_{\mathfrak{q}}y_s \prod_{i=1}^{s} y_i^\zeta \frac{\varphi(\mathfrak{q}y_i)}{\varphi(\mathfrak{t}y_i/M^2)}\vartheta_{\mathfrak{q}}\left(y_i,\mathfrak{q}^{1-2\beta a_2}\right)(y_i)^{2\beta a_2} \\ \prod_{j>i}^{s}\frac{\varphi(y_i/y_j)}{\varphi(\mathfrak{t}y_i/y_j)}\frac{\varphi(v^2y_i/y_j)}{\varphi(\mathfrak{q}y_i/y_j)}\vartheta_{\mathfrak{q}}\left(\frac{y_i}{\mathfrak{t}y_j},\mathfrak{q}^{1+\beta^2}\right)\left(\frac{y_i}{\mathfrak{t}y_j}\right)^{-\beta^2}\,,\end{aligned} \tag{17.1.9}$$

where we recall that the integrals $\int d'_{\mathfrak{q}}y_1\cdots d'_{\mathfrak{q}}y_s$ are variants of the Jackson integral (16.2.11). We also recall that as explained in Section 16.2 we have assumed the radial ordering of poles $|y_i|<|y_{i+1}|$, which are labelled by a partition Y

$$y_Y = \{y_1,y_2,\ldots,y_{s-1},y_s\}_Y = \{\mathfrak{t}^{s-1}\mathfrak{q}^{Y_1},\mathfrak{t}^{s-2}\mathfrak{q}^{Y_2},\ldots,\mathfrak{t}\mathfrak{q}^{Y_{s-1}},\mathfrak{q}^{Y_s}\}\,. \tag{17.1.10}$$

Since quasi-constants are independent of multiplicative shifts of the argument by $\mathfrak{q}$, they can be factored

out of the integrant and $\mathcal{I}_2$ becomes

$$\begin{aligned}\mathcal{I}_2 \;=\; & \mathfrak{t}^{\frac{s(s-1)}{2}\beta^2}\left(\frac{2\pi\mathrm{i}}{1-\mathfrak{q}}\right)^s \mathrm{Eval}_{y=y_\emptyset}\left[\prod_{i=1}^{s-1}\vartheta_\mathfrak{q}\left(y_i,\mathfrak{q}^{1-2\beta a_2}\right)\prod_{j-i\geq 2}^{s}\vartheta_\mathfrak{q}\left(\frac{y_i}{ty_j},\mathfrak{q}^{1+\beta^2}\right)\right] \\ & \mathrm{Res}_{y_s=1}\,\vartheta_\mathfrak{q}\left(y_s,\mathfrak{q}^{1-2\beta a_2}\right)\prod_{i=1}^{s-1}\mathrm{Res}_{y_i=\mathfrak{t}y_{i+1}}\vartheta_\mathfrak{q}\left(\frac{y_i}{\mathfrak{t}y_{i+1}},\mathfrak{q}^{1+\beta^2}\right) \\ & \int d'_\mathfrak{q}y_1\cdots d'_\mathfrak{q}y_s\prod_{i=1}^{s}y_i^{2\beta^2(i-1)-2\beta a_1}\frac{\varphi(\mathfrak{q}y_i)}{\varphi(\mathfrak{t}y_i/M^2)}\prod_{i<j}^{s}\frac{\varphi(y_i/y_j)}{\varphi(\mathfrak{t}y_i/y_j)}\frac{\varphi(v^2y_i/y_j)}{\varphi(\mathfrak{q}y_i/y_j)}\,. \quad (17.1.11)\end{aligned}$$

The residues can be evaluated, as we show in Appendix G, and in particular using the definition (17.0.5), whereby we find

$$\mathrm{Res}_{y_i=\mathfrak{t}y_{i+1}}\vartheta_\mathfrak{q}\left(\frac{y_i}{\mathfrak{t}y_{i+1}},\mathfrak{q}^{1+\beta^2}\right)=\frac{\vartheta_\mathfrak{q}(\mathfrak{q}^{-\beta^2})}{\varphi(\mathfrak{q})^3} \quad (17.1.12)$$

and

$$\mathrm{Res}_{y_s=1}\,\vartheta_\mathfrak{q}\left(y_s,\mathfrak{q}^{1-2\beta a_2}\right)=\frac{\vartheta_\mathfrak{q}(\mathfrak{q}^{2\beta a_2})}{\varphi(\mathfrak{q})^3}\,. \quad (17.1.13)$$

These ratios have a well defined limit $\mathfrak{q}\to 1$, see Appendix G, which is generically

$$\frac{\vartheta_\mathfrak{q}(\mathfrak{q}^s)}{\vartheta_\mathfrak{q}(\mathfrak{q}^t)}\xrightarrow{\mathfrak{q}\to 1}\frac{\sin(\pi s)}{\sin(\pi t)}\,,\qquad \frac{2\pi\mathrm{i}}{1-\mathfrak{q}}\frac{\vartheta_\mathfrak{q}(\mathfrak{q}^s)}{\varphi(\mathfrak{q})^3}\xrightarrow{\mathfrak{q}\to 1}2\mathrm{i}\sin(\pi s)\,, \quad (17.1.14)$$

and thus the matrix model integral (17.1.11) using the definition of the Jackson integral and also equation (F.1.29) becomes,

$$\begin{aligned}\mathcal{I}_2\xrightarrow{\mathfrak{q}\to 1}\quad & \prod_{k=0}^{s-1}2\mathrm{i}\sin(\pi\beta(2a_2-k\beta)) \\ & \int_0^1 dy_s\int_0^{y_s}dy_{s-1}\ldots\int_0^{y_2}dy_1\prod_{i=1}^{s}y_i^{-2\beta a_1}(1-y_i)^{-2\beta a_2}\prod_{i<j}(y_j-y_i)^{2\beta^2}\,. \quad (17.1.15)\end{aligned}$$

Obtaining the $\prod_{k=0}^{s-1}\sin(\pi\beta(2a_2-k\beta))$ prefactor in front of the Selberg integral is one of the interesting points of this exercise as it reflects a particular choice for the Liouville conformal block from the point of view of the geometric engineering construction.

The matrix integral as a Selberg integral

We can finally express the limit of $\mathcal{I}_2$ in terms of Γ-functions through the Selberg integral

$$\lim_{\mathfrak{q}\to 1}\mathcal{I}_2=\prod_{k=0}^{s-1}2\mathrm{i}\sin(\pi\beta(2a_2-k\beta))\,\mathcal{I}_{\mathrm{Sel}}(1-2\beta a_1,1-2\beta a_2,\beta^2)\,, \quad (17.1.16)$$

using the definition

$$\mathcal{I}_{\text{Sel}}(1-2\beta a_1, 1-2\beta a_2, \beta^2) = \int_0^1 dy_s \int_0^{y_s} dy_{s-1} \dots \int_0^{y_2} dy_1 \prod_{i=1}^{s} y_i^{-2\beta a_1}(1-y_i)^{-2\beta a_2} \prod_{i<j}(y_j - y_i)^{2\beta^2} = \prod_{j=0}^{s-1} \frac{\Gamma(1-2\beta a_1 + j\beta^2)\Gamma(1-2\beta a_2 + j\beta^2)\Gamma((j+1)\beta^2)}{\Gamma(2-2\beta(a_1+a_2)+(N-1+j)\beta^2)\Gamma(\beta^2)}. \tag{17.1.17}$$

Furthermore, using the shift identities of the Γ function to suppress the products in equation (17.1.16) by rewriting this in terms of the double gamma function Γ_β:

$$\frac{\pi}{\sin(\pi x)} = \Gamma(1-x)\Gamma(x) \tag{17.1.18}$$

and

$$\frac{\Gamma_\beta(x+\beta)}{\Gamma_\beta(x)} = \sqrt{2\pi}\beta^{\frac{1}{2}-\beta x}\Gamma^{-1}(\beta x)\,, \tag{17.1.19}$$

equation (17.1.16) becomes

$$\lim_{\mathfrak{q}\to 1} \mathcal{I}_2 = \left(\frac{2\pi \mathrm{i}}{\beta^{\beta^2-1}\Gamma(\beta^2)}\right)^s \frac{\Gamma_\beta(\beta^{-1}-2a_1)}{\Gamma_\beta(\beta^{-1}-2a_1+s\beta)} \frac{\Gamma_\beta(2a_2+\beta)}{\Gamma_\beta(2a_2-(s-1)\beta)} \frac{\Gamma_\beta(2a_3+\beta)}{\Gamma_\beta(2a_3-(s-1)b)} \frac{\Gamma_\beta(\beta)}{\Gamma_\beta((s+1)\beta)}\,. \tag{17.1.20}$$

We would like to stress that the $\prod_{k=0}^{s-1}\sin(\pi\beta(2a_2 - k\beta))$ prefactor in front of the Selberg integral (17.1.15) played an important role in the precise form of (17.1.20).

Note: Note that this equation is derived and holds in the regime where $|\mathfrak{q}| < 1$, $|\mathfrak{t}| < 1$, where both $\epsilon_1 > 0$ and $\epsilon_2 < 0$ (14.0.2). By definition

$$\mathfrak{t} = \mathfrak{q}^{\beta^2} = \mathfrak{q}^{-b^2}\,, \tag{17.1.21}$$

so if $b \in \mathbb{R}$ this definition implies that the regime of validity is $|\mathfrak{t}| > 1$ and $|\mathfrak{q}| < 1$ and instead of obtaining (17.1.20), equation (17.1.16) would lead to the "upsidedown" form (14.0.8). In the regime $|\mathfrak{q}| < 1$, $|\mathfrak{t}| < 1$, where we now are, $b \in \mathbb{I}$ is purely imaginary. This case was studied in [180] and is known as generalised Minimal Models, as it corresponds to a central charge that is less than one. For a more recent analysis see also [181]. Following [180] the Liouville field theory and the generalised Minimal Models (GMM) are related by the analytic continuation of the parameters

$$b = -\mathrm{i}\beta\,, \quad \alpha = \mathrm{i}a\,, \tag{17.1.22}$$

with the central charge of GMM being $c_{GMM} = 1 - 6(\beta - \beta^{-1})^2 < 1$, while for Liouville field theory $c_{\text{Liouv}} = 1 + 6(b + b^{-1})^2 > 1$.

Chapter 18

Integral form of the T_N topological strings partition function

We generalise here some of the results in Chapters 14 – 17 to higher rank T_N theories and recast the T_N partition function from topological strings $\mathcal{Z}_N^{\text{top}}(\mathbf{A};\mathfrak{q},\mathfrak{t})$ as a matrix integral $\mathcal{I}_N(a_1,a_2,\mathbf{s};\beta)$ through a specialisation of parameters. This will allow to identify in the next chapter some of the geometrical parameters which enter the topological string construction with the parameters $\mathbf{s}$, the screening numbers, appearing in the integral $\mathcal{I}_N(a_1,a_2,\mathbf{s};\beta)$. After briefly describing the geometrical setup and introducing the functions $\mathcal{Z}_N^{\text{top}}(\mathbf{A};\mathfrak{q},\mathfrak{t})$ and $\mathcal{I}_N(a_1,a_2,\mathbf{s};\beta)$, we will state the main result in equation (18.0.20) and then proceed to derive this in the following sections. Let us first introduce the brane web in Figure 18.1 which geometrically engineers the low energy dynamics of the T_N theories, following [48]. The T_N geometry is parametrised by Kähler parameters $Q_{\bullet;a}^{(i)}$, where the symbol $\bullet$ stands for (m,n,l), with $a=1,\dots,N-1$ and $i=1,\dots,N-a$ and which are defined in terms of the Coulomb parameters $A_i^{(j)}$ associated to the faces of the web diagram

$$Q_{m;i}^{(j)}=\frac{A_i^{(j-1)}A_{i-1}^{(j)}}{A_i^{(j)}A_{i-1}^{(j-1)}}\,,\qquad Q_{n;i}^{(j)}=\frac{A_i^{(j)}A_{i-1}^{(j)}}{A_i^{(j-1)}A_{i-1}^{(j+1)}}\,,\qquad Q_{l;i}^{(j)}=\frac{A_i^{(j)}A_i^{(j-1)}}{A_{i-1}^{(j)}A_{i+1}^{(j-1)}}\,, \tag{18.0.1}$$

subject to $A_0^{(0)}=A_N^{(0)}=A_0^{(N)}=1$. They satisfy the following relations for each internal face

$$Q_{l;i}^{(j)}Q_{m;i+1}^{(j)}=Q_{m;i}^{(j+1)}Q_{l;i}^{(j+1)}\,,\ Q_{n;i}^{(j)}Q_{m;i}^{(j+1)}=Q_{m;i+1}^{(j)}Q_{n;i+1}^{(j)}\,,\ Q_{l;i}^{(j)}Q_{n;i}^{(j)}=Q_{l;i}^{(j+1)}Q_{n;i+1}^{(j)}\,, \tag{18.0.2}$$

where any two of these identities imply the third, and they are related to the gauge theory parameters through

$$Q_{m;i}^{(1)}Q_{l;i}^{(1)}=\frac{M_i}{M_{i+1}}\,,\qquad Q_{m;1}^{(i)}Q_{n;1}^{(i)}=\frac{N_i}{N_{i+1}}\,,\qquad Q_{n;i}^{(N-i)}Q_{l;i}^{(N-i)}=\frac{L_i}{L_{i+1}}\,, \tag{18.0.3}$$

$$M_i=\frac{A_i^{(0)}}{A_{i-1}^{(0)}}\,,\qquad N_i=\frac{A_0^{(i)}}{A_0^{(i-1)}}\,,\qquad L_i=\frac{A_i^{(N-i)}}{A_{i-1}^{(N-i+1)}}\,. \tag{18.0.4}$$

It is furthermore useful to introduce the following short-hand notation, with $v=\sqrt{\mathfrak{q}/\mathfrak{t}}$,

$$\mathcal{A}_{a,i}\overset{\text{def}}{=}v^aA_i^{(a)}/A_{i-1}^{(a)}\,. \tag{18.0.5}$$

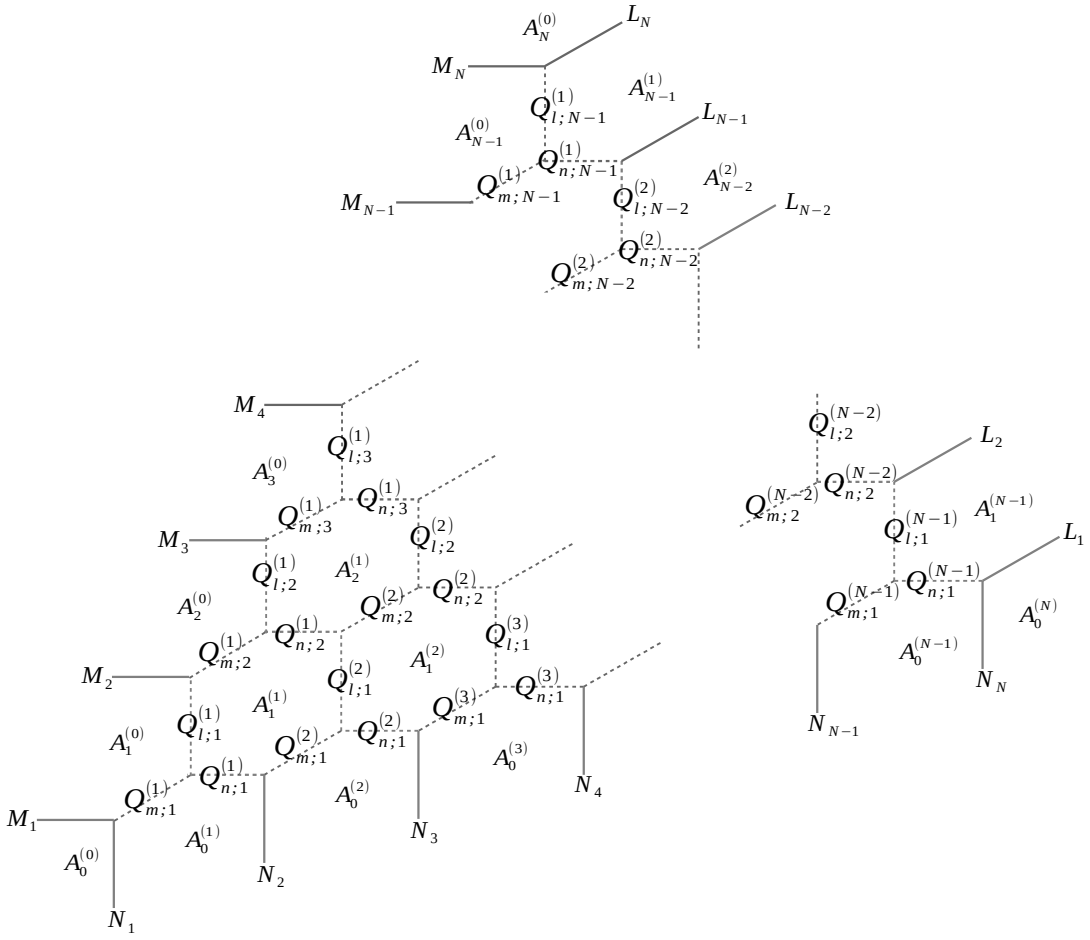

Figure 18.1: (p, q) *5-brane web that engineers the low energy dynamics of the* T_N *theory.*

The T_N topological string partition function is $\mathcal{Z}_N^{\rm top} = \mathcal{Z}_N^{\rm pert}\,\mathcal{Z}_N^{\rm inst}$, where the components are

$$\mathcal{Z}_N^{\rm pert} = \prod_{i\leq j=1}^{N-1} \frac{\mathcal{M}\Big(\frac{M_i}{M_{j+1}}\Big)}{\mathcal{M}\Big(\frac{M_i}{\mathcal{A}_{1,j}}\Big)\mathcal{M}\Big(v^{-2}\frac{\mathcal{A}_{1,i}}{M_{j+1}}\Big)} \prod_{a=1}^{N-2}\prod_{i\leq j=1}^{N-a-1} \frac{\mathcal{M}\Big(\frac{\mathcal{A}_{a,i}}{\mathcal{A}_{a,j+1}}\Big)\mathcal{M}\Big(v^{-2}\frac{\mathcal{A}_{a,i}}{\mathcal{A}_{a,j+1}}\Big)}{\mathcal{M}\Big(\frac{\mathcal{A}_{a,i}}{\mathcal{A}_{a+1,j}}\Big)\mathcal{M}\Big(v^{-2}\frac{\mathcal{A}_{a+1,i}}{\mathcal{A}_{a,j+1}}\Big)} \tag{18.0.6}$$

and

$$\mathcal{Z}_N^{\rm inst} = \sum_{\mathbf{Y}} \mathfrak{f}^{Y}\; z_R\; z_0 \prod_{a=1}^{N-1}\left(\frac{N_a L_{N-a}}{N_{a+1}L_{N-a+1}} v^{-2(N-a)}\right)^{\sum_{i=1}^{N-a}\frac{|Y_{a,i}|}{2}} z_a \prod_{a=1}^{N-2} z_{a,a+1}\ , \tag{18.0.7}$$

where $\{Y_{a,i}\}$ represent a set of Young tableaux associated to the edges of the web diagram and

$$z_a = \prod_{i,j=1}^{N-a}\left[\mathcal{N}_{Y_{a,i}Y_{a,j}}(v^{-2}\mathcal{A}_{a,i}/\mathcal{A}_{a,j})\right]^{-1}\ , \tag{18.0.8}$$

$$z_0 = \prod_{i=1}^{N-1}\prod_{j=1}^{N}\mathcal{N}_{\emptyset Y_{1,i}}(M_j/\mathcal{A}_{1,i})\ , \tag{18.0.9}$$

$$z_{a,a+1} = \prod_{i=1}^{N-a}\prod_{j=1}^{N-a-1}\mathcal{N}_{Y_{a,i}Y_{a+1,j}}(\mathcal{A}_{a,i}/\mathcal{A}_{a+1,j})\ , \tag{18.0.10}$$

$$\mathfrak{f}^Y = \prod_{i=1}^{N-1}\prod_{j=1}^{N}(vM_j/\mathcal{A}_{1,i})^{-\frac{|Y_{1,i}|}{2}} \prod_{a=1}^{N-2}\prod_{i=1}^{N-a}\prod_{j=1}^{N-a-1}(v\mathcal{A}_{a,i}/\mathcal{A}_{a+1,j})^{-\frac{|Y_{a,i}|+|Y_{a+1,j}|}{2}} \ , \tag{18.0.11}$$

$$z_Y = \prod_{a=1}^{N-1}\prod_{i=1}^{N-a}(-1)^{|Y_{a,i}|}\mathfrak{q}^{||Y_{a,i}||/2}\mathfrak{t}^{-||Y^t_{a,i}||/2} \ . \tag{18.0.12}$$

Following the specialisation of parameters $\mathcal{A}_{a,i} = \mathfrak{t}^{N_{a,i}}M_{a+i}$, the partition function $\mathcal{Z}^{\rm top}_N(\mathbf{A};\mathfrak{q},\mathfrak{t})$ can be related to the matrix integral

$$\mathcal{I}_N = \int d'_{\mathfrak{q}}\mathbf{y} \prod_{a=1}^{N-1}\prod_{I=1}^{s_a}(y_I^{(a)})^{\zeta_a}\,\mathcal{I}_{m_a}(y)\mathcal{I}_{a,a}(y)\prod_{a=1}^{N-2}\mathcal{I}_{a,a+1}(y) \tag{18.0.13}$$

where $\mathbf{y} = \{y_I^{(a)}\}$ contains the set of all integration variables and

$$\mathcal{I}_{m_a}(y) = \prod_{I=1}^{s_a}\frac{\varphi(v^2M_a/y_I^{(a)})}{\varphi(M_{a+1}/y_I^{(a)})} \ , \tag{18.0.14}$$

$$\mathcal{I}_{a,a}(y) = \prod_{J\neq I=1}^{s_a}\frac{\varphi(y_I^{(a)}/y_J^{(a)})}{\varphi(\mathfrak{t}y_I^{(a)}/y_J^{(a)})} \ , \quad \mathcal{I}_{a,a+1}(y) = \prod_{I=1}^{s_a}\prod_{J=1}^{s_{a+1}}\frac{\varphi(\mathfrak{t}y_J^{(a+1)}/y_I^{(a)})}{\varphi(y_J^{(a+1)}/y_I^{(a)})} \ , \tag{18.0.15}$$

and

$$\zeta_a = -\beta(a_1+a_2,e_a) - \beta^2 s_{a+1} + \beta^2(s_a-1) \ , \qquad s_N = 0 \ , \tag{18.0.16}$$

with $s_a = \sum_{i=1}^{N-a}N_{a,i}$. The vectors e_a are the simple roots of the algebra $\mathfrak{sl}_N$, the inner products are taken with respect to the Cartan matrix, $a_2 = (a_2^{(1)},\dots,a_2^{(N-1)})$ and $(a_2,e_a) = a_2^{(a)} - a_2^{(a+1)}$. The $(N-1)$ component vectors a_i in equation (18.0.16) are related to the gauge theory parameters M, N, L through

$$\frac{M_a}{M_{a+1}} = \frac{\mathfrak{t}}{\mathfrak{q}}\mathfrak{q}^{\beta(a_2,e_a)} \ , \quad \frac{L_{N-a}}{L_{N-a+1}} = \frac{\mathfrak{t}}{\mathfrak{q}}\mathfrak{q}^{\beta(a_3,e_a)} \ , \quad \frac{N_a}{N_{a+1}} = \frac{\mathfrak{q}}{\mathfrak{t}}\mathfrak{q}^{-\beta(a_1,e_a)} \ , \quad \mathfrak{t} = \mathfrak{q}^{\beta^2} \ , \tag{18.0.17}$$

where

$$a_1 + a_2 + a_3 = 2(\beta^{-1}-\beta)\rho_W + \beta\sum_{a=1}^{N-1}s_a e_a \tag{18.0.18}$$

and ρ_W is the Weyl vector. The integrals $\int d'_{\mathfrak{q}}y$ are variants of the Jackson integral defined for meromorphic functions $M(y^{(a)})$ of s_a variables $y^{(a)} = (y_1^{(a)},\dots,y_{s_a}^{(a)})$ as

$$\int d'_{\mathfrak{q}}\mathbf{y}\prod_{a=1}^{N-1}\prod_{I=1}^{s_a}(y_I^{(a)})^{-1}M(y^{(a)}) := (2\pi\mathrm{i})^{\sum_{a=1}^{N-1}s_a}\sum_{\substack{Y_{a=1,\dots,N-1}\\ Y_{a,1},\dots,Y_{a,s_a}\in\mathbb{N}\\ Y_{a,1}>Y_{a,2}\dots>Y_{a,s_a}}}\prod_{a=1}^{N-1}\operatorname*{Res}_{y^{(a)}=y_{Y_a}}M(y^{(a)}) \ , \tag{18.0.19}$$

where $y_{Y_a} = (M_{a+i}\mathfrak{q}^{Y_{a,i,I}}\mathfrak{t}^{N_{a,i}-I})_{\substack{I=1,\dots,N_{a,i}\\ i=N-a,\dots,1}}$. Finally, the precise relation between the partition function and the integral formulation is

$$\mathcal{I}_N \ = \ \left(2\pi\mathrm{i}\frac{\varphi(\mathfrak{t})}{\varphi(\mathfrak{q})}\right)^{\sum_{a=1}^{N-1}s_a}\vartheta_M\,\mathcal{M}(\mathfrak{t}/\mathfrak{q})^{\frac{N(N-1)}{2}}\prod_{a=1}^{N-1}\prod_{I=1}^{s_a}\left(y_I^{(a)}\right)_{\emptyset}^{\zeta_a+1}\mathcal{Z}^{\rm top}_N \tag{18.0.20}$$

where the term ϑ_M is

$$\vartheta_M = \prod_{a=1}^{N-2}\prod_{j>i=1}^{N-a}\prod_{J=1}^{N_{a,j}}\left(\frac{M_{a+i}}{M_{a+j}}\mathfrak{t}^{-J}\right)^{-\beta^2 N_{a,i}}\vartheta_{\mathfrak{q}}\left(\frac{M_{a+i}}{M_{a+j}}\mathfrak{t}^{-J},\mathfrak{q}^{1+\beta^2 N_{a,i}}\right)$$
$$\prod_{j\geq i=1}^{N-a-1}\prod_{I=1}^{N_{a,i}}\left(\frac{M_{a+i}}{M_{a+1+j}}\mathfrak{t}^{I-1}\right)^{\beta^2 N_{a+1,j}}\vartheta_{\mathfrak{q}}\left(\frac{M_{a+i}}{M_{a+1+j}}\mathfrak{t}^{I-1},\mathfrak{q}^{1-\beta^2 N_{a+1,j}}\right)\,. \tag{18.0.21}$$

18.1 Defining of the functions $\mathcal{I}_a,\ \mathcal{I}_{m_a},\ \mathcal{I}_{a,a}$

We can first observe how the functions $\mathcal{I}_a,\ \mathcal{I}_{m_a},\ \mathcal{I}_{a,a}$ emerge from the T_N topological strings partition function $\mathcal{Z}_N^{\text{top}}(\mathbf{A};\mathfrak{q},\mathfrak{t})$, following [34]. Considering the components (18.0.8)-(18.0.10) that enter this function and defining the following variables

$$(y_{I,i}^{(a)})_Y = \mathcal{A}_{a,i}\mathfrak{q}^{Y_{a,i,I}}\mathfrak{t}^{-I} \tag{18.1.22}$$

leads to the identification of the functions (18.0.15). Notice that starting with z_a in equation (18.0.8) and expanding the Nekrasov functions into products of quantum dilogarithms like in equation (F.0.11), this becomes

$$z_a = \frac{\mathcal{I}_{a,a}(y_Y)}{\mathcal{I}_{a,a}(y_\emptyset)}\prod_{i,j=1}^{N-a}\left(\mathcal{N}_{Y_{a,i}\emptyset}\left(v^{-2}\mathfrak{t}^{N_{a,j}}\frac{\mathcal{A}_{a,i}}{\mathcal{A}_{a,j}}\right)\mathcal{N}_{\emptyset Y_{a,j}}\left(v^{-2}\mathfrak{t}^{-N_{a,i}}\frac{\mathcal{A}_{a,i}}{\mathcal{A}_{a,j}}\right)\right)^{-1} \tag{18.1.23}$$

by setting

$$\mathcal{I}_{a,a}(y) = \prod_{i,j=1}^{N-a}\prod_{I=1}^{N_{a,i}}\prod_{J=1}^{N_{a,j}}\frac{\varphi(y_{I,i}^{(a)}/y_{J,j}^{(a)})}{\varphi(\mathfrak{t}y_{I,i}^{(a)}/y_{J,j}^{(a)})} \equiv \prod_{I\neq J=1}^{s_a}\frac{\varphi(y_I^{(a)}/y_J^{(a)})}{\varphi(\mathfrak{t}y_I^{(a)}/y_J^{(a)})} \tag{18.1.24}$$

and we can define the product of Nekrasov functions with one empty partition label

$$\tilde{z}_a = \prod_{i,j=1}^{N-a}\left(\mathcal{N}_{Y_{a,i}\emptyset}\left(v^{-2}\mathfrak{t}^{N_{a,j}}\frac{\mathcal{A}_{a,i}}{\mathcal{A}_{a,j}}\right)\mathcal{N}_{\emptyset Y_{a,j}}\left(v^{-2}\mathfrak{t}^{-N_{a,i}}\frac{\mathcal{A}_{a,i}}{\mathcal{A}_{a,j}}\right)\right)^{-1}\,. \tag{18.1.25}$$

In writing equation (18.1.24) we gather the parameters

$$\{y_I^{(a)}\}_{I=1,\dots,s_a} \equiv \{y_{I,i}^{(a)}\}_{\substack{I=1,\dots,N_{a,i}\\ i=N-a,\dots,1}} \tag{18.1.26}$$

and set $s_a = \sum_{i=1}^{N-a} N_{a,i}$. Similarly the function $z_{a,a+1}$ (18.0.10) becomes

$$z_{a,a+1} = \mathfrak{t}^{s_a|Y_{a+1}|-s_{a+1}|Y_a|}\,\frac{\mathcal{I}_{a,a+1}(y_Y)}{\mathcal{I}_{a,a+1}(y_\emptyset)}$$
$$\prod_{i=1}^{N-a}\prod_{j=1}^{N-a-1}\mathcal{N}_{Y_{a,i}\emptyset}\left(\mathfrak{t}^{N_{a+1,j}}\frac{\mathcal{A}_{a,i}}{\mathcal{A}_{a+1,j}}\right)\mathcal{N}_{\emptyset Y_{a+1,j}}\left(\mathfrak{t}^{-N_{a,i}}\frac{\mathcal{A}_{a,i}}{\mathcal{A}_{a+1,j}}\right) \tag{18.1.27}$$

for $|Y_a| = \sum_{i=1}^{N-a}|Y_{a,i}|$ and

$$\mathcal{I}_{a,a+1}(y) = \prod_{i=1}^{N-a}\prod_{j=1}^{N-a-1}\prod_{I=1}^{N_{a,i}}\prod_{I=1}^{N_{a+1,j}}\frac{\varphi(\mathfrak{t}y_{J,j}^{(a+1)}/y_{I,i}^{(a)})}{\varphi(y_{J,j}^{(a+1)}/y_{I,i}^{(a)})} = \prod_{I=1}^{s_a}\prod_{J=1}^{s_{a+1}}\frac{\varphi(\mathfrak{t}y_J^{(a+1)}/y_I^{(a)})}{\varphi(y_J^{(a+1)}/y_I^{(a)})}\,. \tag{18.1.28}$$

The second line of equation (18.1.29) defines

$$\tilde{z}_{a,a+1} = \prod_{i=1}^{N-a} \prod_{j=1}^{N-a-1} \mathcal{N}_{Y_{a,i}\emptyset}\left(\mathfrak{t}^{N_{a+1,j}} \frac{\mathcal{A}_{a,i}}{\mathcal{A}_{a+1,j}}\right) \mathcal{N}_{\emptyset Y_{a+1,j}}\left(\mathfrak{t}^{-N_{a,i}} \frac{\mathcal{A}_{a,i}}{\mathcal{A}_{a+1,j}}\right) . \tag{18.1.29}$$

One should observe here the appearance of the factor $\mathfrak{t}^{s_a|Y_{a+1}|-s_{a+1}|Y_a|}$ in equation (18.1.29). Its presence is due to the fact that direct substitution of the parameters $y^{(a)}$ into equation (18.0.10) would yield

$$z_{a,a+1} = \frac{\tilde{\mathcal{I}}_{a,a+1}(y_Y)}{\tilde{\mathcal{I}}_{a,a+1}(y_\emptyset)} \tilde{z}_{a,a+1} , \quad \tilde{\mathcal{I}}_{a,a+1}(y) = \prod_{I=1}^{s_a} \prod_{J=1}^{s_{a+1}} \frac{\varphi(\mathfrak{q} y_I^{(a)}/y_J^{(a+1)})}{\varphi(v^2 y_I^{(a)}/y_J^{(a+1)})} . \tag{18.1.30}$$

However, the following identity for the quasi-constant $\vartheta_{\mathfrak{q}}(x, \mathfrak{q}^\kappa)$

$$\frac{\varphi(\mathfrak{q} y_I^{(a)}/y_J^{(a+1)})}{\varphi(v^2 y_I^{(a)}/y_J^{(a+1)})} = \frac{\varphi(\mathfrak{t} y_J^{(a+1)}/y_I^{(a)})}{\varphi(y_J^{(a+1)}/y_I^{(a)})} \left(\frac{y_J^{(a+1)}}{y_I^{(a)}}\right)^{\beta^2} \vartheta_{\mathfrak{q}}\left(\frac{y_I^{(a)}}{y_J^{(a+1)}}, \mathfrak{q}^{1-\beta^2}\right)^{-1} \tag{18.1.31}$$

implies the relation

$$\frac{\tilde{\mathcal{I}}_{a,a+1}(y_Y)}{\tilde{\mathcal{I}}_{a,a+1}(y_\emptyset)} = \mathfrak{t}^{s_a|Y_{a+1}|-s_{a+1}|Y_a|} \frac{\mathcal{I}_{a,a+1}(y_Y)}{\mathcal{I}_{a,a+1}(y_\emptyset)} , \tag{18.1.32}$$

The difference between equations (18.1.30) and (18.1.29) is the ordering of variables $y^{(a)} \lessgtr y^{(a+1)}$, which determines the regions where the quantum dilogarithm functions have poles at argument $\mathfrak{q}^{-n}$.

Specialisation of parameters: provided the following specialisation of parameters

$$\mathcal{A}_{a,i} = \mathfrak{t}^{N_{a,i}} M_{a+i} , \tag{18.1.33}$$

the product of all the factors $\tilde{z}_a$, $\tilde{z}_{a,a}$ and $\mathfrak{t}^{s_a|Y_{a+1}|-s_{a+1}|Y_a|}$ with the remaining components in $\mathcal{Z}_N^{\text{inst}}(\mathbf{A}; \mathfrak{q}, \mathfrak{t})$ is

$$\mathfrak{f}^Y z_0 z_Y \prod_{a=1}^{N-1} \left(\frac{N_a L_{N-a}}{N_{a+1} L_{N-a+1}} v^{2(a-N)}\right)^{\frac{|Y_a|}{2}} \tilde{z}_a \prod_{a=1}^{N-2} \mathfrak{t}^{(s_a|Y_{a+1}|-s_{a+1}|Y_a|)} \tilde{z}_{a,a} = \prod_{a=1}^{N-1} \mathfrak{q}^{(\zeta_a+1)|Y_a|} \frac{\mathcal{I}_{m_a}(y_Y)}{\mathcal{I}_{m_a}(y_\emptyset)} \tag{18.1.34}$$

and defines the functions

$$\mathcal{I}_{m_a}(y) = \prod_{i=1}^{N-a} \prod_{I=1}^{N_{a,i}} \frac{\varphi(v^2 M_a/y_{I,i}^{(a)})}{\varphi(M_{a+1}/y_{I,i}^{(a)})} = \prod_{I=1}^{s_a} \frac{\varphi(v^2 M_a/y_I^{(a)})}{\varphi(M_{a+1}/y_I^{(a)})} , \tag{18.1.35}$$

and

$$\prod_{a=1}^{N-1} \mathfrak{q}^{(\zeta_a+1)|Y_a|} = \mathfrak{t}^{-\frac{1}{2}\sum_{a=1}^{N-2} s_{a+1}|Y^{(a)}|-s_a|Y^{(a+1)}|} \prod_{a=1}^{N-1} \left(\frac{\mathfrak{t}}{\mathfrak{q}} \frac{M_{a+1} N_a L_{N-a}}{M_a N_{a+1} L_{N-a+1}}\right)^{\frac{1}{2}|Y_a|} . \tag{18.1.36}$$

Before the specialisation (18.1.33), the left hand side of equation (18.1.34) has $N(N-1)(2N-1)/3$ pairs of Nekrasov functions, where the partition labels of each of these include one empty partition. Imposing the specialisation of parameters (18.1.33) cancels $N(N-1)(4N-5)/6$ of the pairs in a process which involves repeated application of the identity (F.0.17) and leaves behind $N(N-2)/2$ pairs of Nekrasov functions on the right hand side of equation (18.1.34). Combining the above results shows that the instanton partition function $\mathcal{Z}_N^{\text{inst}}(\mathbf{A}; \mathfrak{q}, \mathfrak{t})$ can be written as

$$\mathcal{Z}_N^{\text{inst}}(\mathbf{A}; \mathfrak{q}, \mathfrak{t}) = \sum_{Y_a} \prod_{a=1}^{N-1} \mathfrak{q}^{(\zeta_a+1)|Y_a|} \prod_{a=1}^{N-1} \frac{\mathcal{I}_{a,a}(y_Y)\mathcal{I}_{m_a}(y_Y)\mathcal{I}_{a,a+1}(y_Y)}{\mathcal{I}_{a,a}(y_\emptyset)\mathcal{I}_{m_a}(y_\emptyset)\mathcal{I}_{a,a+1}(y_\emptyset)} . \tag{18.1.37}$$

18.2 Reduction of $\mathcal{Z}_N^{\text{pert}}$

After the specialisation (18.1.33), the perturbative part $\mathcal{Z}_N^{\text{pert}}(\mathbf{A};\mathfrak{q},\mathfrak{t})$ of the partition function (18.0.6) depends only on the parameters $M_i, \mathfrak{q}$ and $\mathfrak{t}$ through

$$\begin{aligned}\mathcal{Z}_N^{\text{pert}} &= \prod_{i\leq j=1}^{N-1}\frac{\mathcal{M}\left(\frac{M_i}{M_{j+1}}\right)}{\mathcal{M}\left(\mathfrak{t}^{-N_{1,j}}\frac{M_i}{M_{1+j}}\right)}\times\prod_{a=1}^{N-1}\prod_{i=1}^{N-a}\mathcal{M}(v^{-2}\mathfrak{t}^{N_{a,i}-N_{a-1,i+1}})^{-1}\\ &\quad\prod_{a=1}^{N-2}\prod_{i\leq j=1}^{N-a-1}\frac{\mathcal{M}\left(\mathfrak{t}^{N_{a,i}-N_{a,j+1}}\frac{M_{a+i}}{M_{a+j+1}}\right)\mathcal{M}\left(v^{-2}\mathfrak{t}^{N_{a,i}-N_{a,j+1}}\frac{M_{a+i}}{M_{a+j+1}}\right)}{\mathcal{M}\left(\mathfrak{t}^{N_{a,i}-N_{a+1,j}}\frac{M_{a+i}}{M_{a+1+j}}\right)\mathcal{M}\left(v^{-2}\mathfrak{t}^{N_{a,i}-N_{a-1,j+2}}\frac{M_{a+i}}{M_{a+j+1}}\right)}\ .\end{aligned}\tag{18.2.38}$$

It furthermore greatly simplifies upon applying the shift identities of the function $\mathcal{M}(Q;\mathfrak{t},\mathfrak{q})$ in appendix H to the following form

$$\begin{aligned}\mathcal{Z}_N^{\text{pert}} &= \prod_{a=0}^{N-2}\prod_{i=1}^{N-a-1}\prod_{j=i+1}^{N-a}\frac{\prod_{I=1}^{N_{a+1,j-1}}\varphi(\frac{M_{a+i}}{M_{a+j}}\mathfrak{q}\mathfrak{t}^{N_{a,i}-I})}{\prod_{I=1}^{N_{a,j}}\varphi(\frac{M_{a+i}}{M_{a+j}}\mathfrak{q}\mathfrak{t}^{N_{a,i}-I})}\frac{\prod_{I=1}^{N_{a-1,j+1}}\varphi(\frac{M_{a+i}}{M_{a+j}}\mathfrak{t}^{N_{a,i}-I+1})}{\prod_{I=1}^{N_{a,j}}\varphi(\frac{M_{a+i}}{M_{a+j}}\mathfrak{t}^{N_{a,i}-I+1})}\\ &\quad\frac{1}{\prod_{a=1}^{N-1}\prod_{i=1}^{N-a}\prod_{I=1}^{N_{a,i}-N_{a-1,i+1}}\varphi(\mathfrak{t}^I)}\mathcal{M}(v^{-2})^{-\frac{N(N-1)}{2}}\ .\end{aligned}\tag{18.2.39}$$

The product of equations (18.1.37) and (18.2.39) then gives the full partition function $\mathcal{Z}_N^{\text{top}}(\mathbf{A};\mathfrak{q},\mathfrak{t})$.

18.3 Poles and residues of $\mathcal{I}_N$

The topological strings partition function $\mathcal{Z}_N^{\text{inst}}$ is related to the matrix integral (18.0.13), which is also reproduced below

$$\mathcal{I}_N=\int d'_{\mathfrak{q}}\mathbf{y}\ \prod_{a=1}^{N-1}\prod_{I=1}^{s_a}(y_I^{(a)})^{\zeta_a}\ \mathcal{I}_{m_a}(y)\mathcal{I}_{a,a}(y)\prod_{a=1}^{N-2}\mathcal{I}_{a,a+1}(y)\ ,\tag{18.3.40}$$

with the following identification of parameters

$$\frac{M_a}{M_{a+1}}=\frac{\mathfrak{t}}{\mathfrak{q}}\mathfrak{q}^{\beta(a_2,e_a)}\ ,\quad \frac{L_{N-a}}{L_{N-a+1}}=\frac{\mathfrak{t}}{\mathfrak{q}}\mathfrak{q}^{\beta(a_3,e_a)}\ ,\quad \frac{N_a}{N_{a+1}}=\frac{\mathfrak{q}}{\mathfrak{t}}\mathfrak{q}^{-\beta(a_1,e_a)}\ ,\quad \mathfrak{t}=\mathfrak{q}^{\beta^2}\tag{18.3.41}$$

and where

$$\zeta_a=-\beta(a_1+a_2,e_a)-\beta^2 s_{a+1}+\beta^2(s_a-1)\ ,\qquad s_N=0\ ,\tag{18.3.42}$$

$$a_1+a_2+a_3=2(\beta^{-1}-\beta)\rho_W+\beta\sum_{a=1}^{N-1}s_a e_a\ ,\tag{18.3.43}$$

with ρ_W being the Weyl vector. The matrix integral (18.0.13) is defined by the sum over its residues (18.0.19) at the singular points of the integrand. The locations on these points are [1]

$$\{y_I^{(a)}\}_{I=1,\ldots,s_a}\equiv\{y_{I,i}^{(a)}\}_{\substack{I=1,\ldots,N_{a,i}\\ i=N-a,\ldots,1}}\ ,\qquad a=1,\ldots,N-1\tag{18.3.44}$$

[1] For the example $N=3$ and $a=1$, the poles sit at $y^{(1)}_{I=1,\ldots,s_1}=(y^{(1)}_{1,2},\ldots,y^{(1)}_{N_{1,2},2},y^{(1)}_{1,1},\ldots,y^{(1)}_{N_{1,1},1})$.

and by combining equations (18.1.22) and (18.1.33) they are labelled by partitions $Y_{a,i}$ as

$$(y_{I,i}^{(a)})_Y = M_{a+i}\mathfrak{q}^{Y_{a,i,I}}\mathfrak{t}^{N_{a,i}-I} \ . \tag{18.3.45}$$

This process also groups the set of partitions $\{Y_{a,i}\}$ for $i = 1, \dots, N-a$ into a partition Y_a. We can understand the pole structure of the integrand more in depth through the following considerations [34]. Poles of the functions $\mathcal{I}_{m_a}(y)$ occur when $y_I^{(a)} = M_{a+1}\mathfrak{q}^{Y_{a,I}}$. Repeating then the analysis from Section 16.2 for the locations of poles whose origin is solely in the functions $\mathcal{I}_{m_a}$ and $\mathcal{I}_{a,a}$, for a fixed value of "a", would show these to be located at positions $y_I^{(a)} = M_{a+1}\mathfrak{q}^{Y_{a,I}}\mathfrak{t}^{s_a-I}$. However, the presence of the functions $\mathcal{I}_{a,a+1}$ inside the integrand of equation (18.0.13) brings an additional element to this story. Assuming now that one has integrated over all of the variables $y^{(a)}$, except for the last group $y^{(N-1)}$, the remaining singularities must all come from the functions $\mathcal{I}_{m_{N-1}}$ and $\mathcal{I}_{N-1,N-1}$. Indeed, in this case the singular points occur at

$$y_I^{(N-1)} = M_N\mathfrak{q}^{Y_{N-1,I}}\mathfrak{t}^{s_{N-1}-I} \ . \tag{18.3.46}$$

Then for the second to last group $y^{(N-2)}$, the functions that determine the location of the poles are $\mathcal{I}_{m_{N-2}}$, $\mathcal{I}_{N-2,N-2}$ and also $\mathcal{I}_{N-2,N-1}$, so their locations split into two sets

$$y_I^{(N-2),1} = y_{I'}^{(N-1)}\mathfrak{q}^{Y_{N-2,I}-Y_{N-1,I'}} \ , \qquad y_I^{(N-2),2} = M_{N-1}\mathfrak{q}^{Y_{N-2,I}}\mathfrak{t}^{s_{N-2}-I} \ , \tag{18.3.47}$$

where $I' = N_{N-1,N-2} - N_{N-2,N-1} + 1$. Similarly the group $y^{(N-3)}$ will have three sets of poles

$$y^{(N-3),1} \in \Big[0, y^{(N-2),1}\Big] \ , \ y^{(N-3),2} \in \Big[0, y^{(N-2),2}\Big] \ , \ y^{(N-3),3} = M_{N-2}\mathfrak{q}^{Y_{N-3,I}}\mathfrak{t}^{s_{N-3}-I} \tag{18.3.48}$$

and so on for the remaining integration variables, which places the full set of poles of the integrand (18.0.13) at the locations listed in equations (18.3.45), (18.3.44). The matrix integral (18.3.40) is therefore defined through the sum

$$\mathcal{I}_N = (2\pi i)^{\sum_{a=1}^{N-1} s_a}(\mathrm{Res}_\emptyset)\sum_{Y_a}\prod_{a=1}^{N-1}\mathfrak{q}^{(\zeta_a+1)|Y_a|}\prod_{a=1}^{N-1}\frac{\mathcal{I}_{a,a}(y_Y)\mathcal{I}_{m_a}(y_Y)\mathcal{I}_{a,a+1}(y_Y)}{\mathcal{I}_{a,a}(y_\emptyset)\mathcal{I}_{m_a}(y_\emptyset)\mathcal{I}_{a,a+1}(y_\emptyset)} \ , \tag{18.3.49}$$

where the coefficient $\mathrm{Res}_\emptyset$

$$\begin{aligned}\mathrm{Res}_\emptyset \ = \ & \left(\frac{\varphi(\mathfrak{t})}{\varphi(\mathfrak{q})}\right)^{\sum_{a=1}^{N-1} s_a}\vartheta_M\prod_{a=1}^{N-1}\prod_{I=1}^{s_a}\Big(y_I^{(a)}\Big)_\emptyset^{\zeta_a+1} \\ & \prod_{a=0}^{N-2}\prod_{i=1}^{N-a-1}\prod_{j=i+1}^{N-a}\frac{\prod_{I=1}^{N_{a+1,j-1}}\varphi(\frac{M_{a+i}}{M_{a+j}}\mathfrak{q}\mathfrak{t}^{N_{a,i}-I})}{\prod_{I=1}^{N_{a,j}}\varphi(\frac{M_{a+i}}{M_{a+j}}\mathfrak{q}\mathfrak{t}^{N_{a,i}-I})}\frac{\prod_{I=1}^{N_{a-1,j+1}}\varphi(\frac{M_{a+i}}{M_{a+j}}\mathfrak{t}^{N_{a,i}-I+1})}{\prod_{I=1}^{N_{a,j}}\varphi(\frac{M_{a+i}}{M_{a+j}}\mathfrak{t}^{N_{a,i}-I+1})} \\ & \frac{1}{\prod_{a=1}^{N-1}\prod_{i=1}^{N-a}\prod_{I=1}^{N_{a,i}-N_{a-1,i+1}}\varphi(\mathfrak{t}^I)} \ .\end{aligned} \tag{18.3.50}$$

is obtained by evaluating the integral $\mathcal{I}_N$ with empty partitions. The first line contains the factor

$$\begin{aligned}\vartheta_M = & \prod_{a=1}^{N-2}\prod_{j>i=1}^{N-a}\prod_{J=1}^{N_{a,j}}\left(\frac{M_{a+i}}{M_{a+j}}\mathfrak{t}^{-J}\right)^{-\beta^2 N_{a,i}}\vartheta_\mathfrak{q}\left(\frac{M_{a+i}}{M_{a+j}}\mathfrak{t}^{-J}, \mathfrak{q}^{1+\beta^2 N_{a,i}}\right) \\ & \prod_{j\geq i=1}^{N-a-1}\prod_{I=1}^{N_{a,i}}\left(\frac{M_{a+i}}{M_{a+1+j}}\mathfrak{t}^{I-1}\right)^{\beta^2 N_{a+1,j}}\vartheta_\mathfrak{q}\left(\frac{M_{a+i}}{M_{a+1+j}}\mathfrak{t}^{I-1}, \mathfrak{q}^{1-\beta^2 N_{a+1,j}}\right)\end{aligned} \tag{18.3.51}$$

which is expressed in terms of quasi-constants $\vartheta_{\mathfrak{q}}(x,\mathfrak{q}^{\kappa})$. The main steps required to arrive at the coefficient $\text{Res}_{\emptyset}$ are the evaluation of non-singular terms by directly substituting (18.3.45) and reducing double products using the identities (H.0.4), followed by the computation of residues for the singular terms. The first line of equation (18.3.51) comes from applying the identity

$$\frac{\varphi(\mathfrak{q}^{1-\kappa}/x)}{\varphi(1/x)} = \frac{\vartheta_{\mathfrak{q}}(\mathfrak{q}^{\kappa}x)}{\vartheta_{\mathfrak{q}}(\mathfrak{q}x)}\frac{\varphi(\mathfrak{q}x)}{\varphi(\mathfrak{q}^{\kappa}x)} = x^{1-\kappa}\vartheta_{\mathfrak{q}}(x,\mathfrak{q}^{\kappa})\frac{\varphi(\mathfrak{q}x)}{\varphi(\mathfrak{q}^{\kappa}x)} \ . \tag{18.3.52}$$

to a subset of the terms which appear in the expansion of the function $\mathcal{I}_{a,a}$, while the second line of equation (18.3.51) comes from applying this identity to a subset of the terms in the expansion of $\mathcal{I}_{a,a+1}$. The justification for these two operations comes from the fact that as a result, the second and third lines of equation (18.3.50) precisely equal $\mathcal{M}(v^{-2})^{N(N-1)/2}\mathcal{Z}_N^{\text{pert}}$ from equation (18.2.39)

$$\text{Res}_{\emptyset} \quad = \quad \left(\frac{\varphi(\mathfrak{t})}{\varphi(\mathfrak{q})}\right)^{\sum_{a=1}^{N-1}s_a}\vartheta_M\prod_{a=1}^{N-1}\prod_{I=1}^{s_a}\left(y_I^{(a)}\right)_{\emptyset}^{\zeta_a+1}\ \mathcal{M}(v^{-2})^{\frac{N(N-1)}{2}}\mathcal{Z}_N^{\text{pert}} \ . \tag{18.3.53}$$

This relation leads directly to the identification (18.0.20).

Chapter 19

The free field representation of $\mathfrak{sl}_N$ $\mathfrak{q}$-Toda

The matrix model integral $\mathcal{I}_N(a_1, a_2, \mathbf{s}; \beta)$ determined in the previous chapter is related to the three point conformal block of $\mathfrak{sl}_N$ $\mathfrak{q}$-deformed Toda conformal field theory. We briefly review here the elements that enter the free field construction, similarly to Chapter 17, which provide an interpretation for the parameters $\mathbf{s} = (s_1, \ldots, s_{N-1})$ as screening numbers and which allow to view the specialisation of parameters on the topological strings side as a screening charge condition in CFT. The three point conformal block $\mathcal{B}_{\mathfrak{q}-\text{Toda}}$ on $\mathbb{CP}^1 \backslash \{z_1, z_2, z_3\}$ with primary fields $V_{a_1}, V_{a_2}, V_{a_3}$ inserted at the locations of the punctures, where without loss of generality $z_1 = 0, z_2 = z$ and $z_3 \to \infty$ and V_{a_2} is screened by s_a screening currents $S_a(y^{(a)})$ for $a = 1, \ldots, N-1$, can be written

$$\mathcal{B}_{\mathfrak{q}-\text{Toda}} = \int d'_{\mathfrak{q}} y \, \mathcal{I}_{\mathfrak{q}-\text{Toda}} \,, \tag{19.0.1}$$

with integrand

$$\mathcal{I}_{\mathfrak{q}-\text{Toda}} = r_V \prod_{\substack{1\leq a\leq N-1 \\ 1\leq k\leq 2 \\ 1\leq I\leq s_a}} \langle S_a(y_I^{(a)}) V_{a_k}(z_k)\rangle \prod_{J>I=1}^{s_a} \langle S_a(y_J^{(a)}) S_a(y_I^{(a)})\rangle \prod_{\substack{1\leq a\leq N-2 \\ 1\leq I\leq s_a \\ 1\leq J\leq s_{a+1}}} \langle S_a(y_I^{(a)}) S_{a+1}(y_J^{(a+1)})\rangle \tag{19.0.2}$$

and where $r_V = \langle V_{\alpha_2}(z) V_{\alpha_1}(z_1)\rangle$. The explicit form of the two point function between a primary field and a screening current is

$$\langle S_a(y_I^{(a)}) V_{a_2}(z)\rangle = (y_I^{(a)})^{-\beta(a_2, e_a)} \frac{\varphi(v^{2(a+1)} \mathfrak{q}^{\beta a_2^{(a)}} z / y_I^{(a)})}{\varphi(v^{2(a+1)} \mathfrak{q}^{\beta a_2^{(a+1)}} z / y_I^{(a)})} \,, \quad |y_I^{(a)}| > |z| \,, \tag{19.0.3}$$

where the inner product with the simple roots e_a of the Lie algebra $\mathfrak{sl}_N$ is $(a_2, e_a) = a_2^{(a)} - a_2^{(a+1)}$ and the dictionary to the M gauge theory parameters is $M_a = v^{2a} \mathfrak{q}^{\beta a_2^{(a)}} z$, while the two point functions between screening currents are

$$\langle S_a(y_J^{(a)}) S_a(y_I^{(a)})\rangle = (y_J^{(a)})^{2\beta^2} \, \frac{\varphi(y_I^{(a)}/y_J^{(a)}) \varphi(\mathfrak{q}\mathfrak{t}^{-1} y_I^{(a)}/y_J^{(a)})}{\varphi(\mathfrak{q} y_I^{(a)}/y_J^{(a)}) \varphi(\mathfrak{t} y_I^{(a)}/y_J^{(a)})} \,, \quad |y_I^{(a)}| < |y_J^{(a)}| \,, \; J > I \tag{19.0.4}$$

and

$$\langle S_a(y_I^{(a)}) S_{a+1}(y_J^{(a+1)})\rangle = (y_I^{(a)})^{-\beta^2} \, \frac{\varphi(\mathfrak{t} y_J^{(a+1)}/y_I^{(a)})}{\varphi(y_J^{(a+1)}/y_I^{(a)})} \,, \quad |y_I^{(a)}| > |y_J^{(a+1)}| \,, \; \forall I, J \,. \tag{19.0.5}$$

To compare with the matrix model we first need to rewrite equation (19.0.4) using the quasi-constant function $\vartheta_{\mathfrak{q}}(x,\mathfrak{q}^{\kappa})$ like in equations (17.0.5) and (18.3.52) to replace

$$\frac{\varphi(\mathfrak{q}\mathfrak{t}^{-1}y_I^{(a)}/y_J^{(a)})}{\varphi(\mathfrak{q}y_I^{(a)}/y_J^{(a)})}=\frac{\varphi(y_J^{(a)}/y_I^{(a)})}{\varphi(\mathfrak{t}y_J^{(a)}/y_I^{(a)})}\left(\frac{y_I^{(a)}}{y_J^{(a)}}\right)^{\beta^2}\vartheta_q\left(\frac{y_I^{(a)}}{y_J^{(a)}},\mathfrak{q}^{1-\beta^2}\right)\,. \tag{19.0.6}$$

Then by introducing the short-hand

$$\vartheta_{\mathfrak{q}}(y,\mathfrak{q}^{\mathbf{s}})=\prod_{a=1}^{N-1}\prod_{J>I=1}^{s_a}\vartheta_{\mathfrak{q}}\left(\frac{y_I^{(a)}}{y_J^{(a)}},\mathfrak{q}^{1-\beta^2}\right) \tag{19.0.7}$$

to group all of the resulting quasi-constant terms and combining all of the remaining floating $y_I^{(a)}$ factors in equation (19.0.9) into $(y_I^{(a)})^{\zeta_a}$ with

$$\zeta_a=-\beta(a_1+a_2,e_a)-\beta^2 s_{a+1}+\beta^2(s_a-1)\,,\qquad s_N=0\,, \tag{19.0.8}$$

it is possible to rewrite the three point conformal block $\mathcal{B}_{\mathfrak{q}-\text{Toda}}$ in equation (19.0.1) with

$$\mathcal{I}_{\mathfrak{q}-\text{Toda}}=r_V\prod_{a=1}^{N-1}\prod_{I=1}^{s_a}(y_I^{(a)})^{\zeta_a}\,\mathcal{I}_{m_a}(y;z,a_2)\mathcal{I}_{a,a}(y)\prod_{a=1}^{N-2}\mathcal{I}_{a,a+1}(y)\vartheta_{\mathfrak{q}}(y,\mathfrak{q}^{\mathbf{s}})\,, \tag{19.0.9}$$

such that

$$\mathcal{B}_{\mathfrak{q}-\text{Toda}}=r_V\,\vartheta_{\mathfrak{q}}(y,\mathfrak{q}^{\mathbf{s}})\,\mathcal{I}_N(a_1,a_2,\mathbf{s};\beta)\,. \tag{19.0.10}$$

Limit $\mathfrak{q}\to 1$: As a final comment let us note here that the limit $\mathfrak{q}\to 1$ of the two point functions (19.0.3), (19.0.4) and (19.0.5) gives the expected two point function of $\mathfrak{sl}_N$ Toda CFT, using the formula (F.1.29)

$$\begin{aligned}\langle S_a(y_I^{(a)})V_{a_2}(z)\rangle&=(y_I^{(a)}-z)^{-\beta(a_2,e_a)}\,,\\ \langle S_a(y_J^{(a)})S_a(y_I^{(a)})\rangle&=(y_J^{(a)}-y_I^{(a)})^{2\beta^2}\,,\\ \langle S_a(y_I^{(a)})S_{a+1}(y_J^{(a+1)})\rangle&=(y_I^{(a)}-y_J^{(a+1)})^{-\beta^2}\,.\end{aligned} \tag{19.0.11}$$

The evaluation of the limit $\mathfrak{q}\to 1$ for the integral $\mathcal{I}_N(a_1,a_2,\mathbf{s};\beta)$ is more delicate than the corresponding computation in Section 17.1 for the more simple case where $N=2$. The pole structure so far obscures a possible rewriting of this integral which would push the singularities of the integrant inside of quasi-constants, such that the evaluation points of the integral are not close to any singular points.

19.1 Geometrical interpretation for the screening numbers

The relation between three point conformal blocks $\mathcal{B}_{\mathfrak{q}-\text{Toda}}$ of $\mathfrak{q}$-deformed Toda CFT and the matrix integral $\mathcal{I}_N(a_1,a_2,\mathbf{s};\beta)$ in equation (19.0.10), with the following dictionary

$$\frac{M_a}{M_{a+1}}=\frac{\mathfrak{t}}{\mathfrak{q}}\mathfrak{q}^{\beta(a_2,e_a)}\,,\quad\frac{L_{N-a}}{L_{N-a+1}}=\frac{\mathfrak{q}}{\mathfrak{t}}\mathfrak{q}^{-\beta(a_1+a_2-\beta\sum_{k=1}^{N-1}s_ke_k,e_a)}\,,\quad\frac{N_a}{N_{a+1}}=\frac{\mathfrak{q}}{\mathfrak{t}}\mathfrak{q}^{-\beta(a_1,e_a)}\,, \tag{19.1.12}$$

leads to an identification between the Kähler parameters $Q^{(i)}_{l;j}$ associated to the brane diagram in Figure 19.1 and the screening numbers $\mathfrak{s}$. The geometric interpretation follows from the partition the screening numbers like in Chapter 8

$$s_a = \sum_{i=1}^{a} \sum_{j=a}^{N-1} s_{ij} \ , \tag{19.1.13}$$

such that s_{ij} correspond to the positive roots of $\mathfrak{sl}_N$, and their relation to the parameters $Q^{(i)}_{l;j}$ is

$$\beta s_{ij} = -R^{-1} \ln \left(Q^{(i)}_{l;j-i+1} \right) + Q/2 \ , \qquad i \leq j = 1, \dots N-1 \ . \tag{19.1.14}$$

Here R is the radius of the five dimensional circle for the gauge theory, while $Q = \beta^{-1} - \beta$.

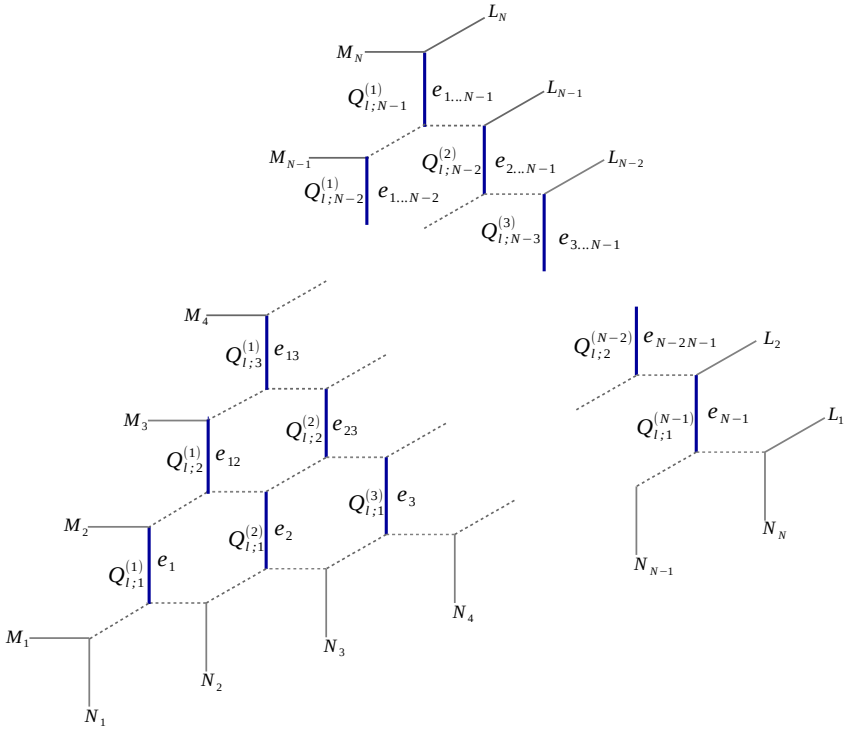

Figure 19.1: *Identification between the Kähler parameters $Q^{(j)}_{l;i}$ and screening numbers s_{ij} that are associated to the positive roots $e_{ij} = \sum_{k=i}^{j} e_k$ of the algebra $\mathfrak{sl}_N$.*

The screening numbers s_{ij} are therefore also related to the lengths of the partitions $Y_{a,i}$ through

$$N_{a,i} = \sum_{j=1}^{a} s_{j,a+i-1} \ . \tag{19.1.15}$$

Proof: To prove equation (19.1.14), we first note that the identifications (19.1.12) can be recast as

$$(a_1, e_a) = \frac{1}{R} \ln \left(\frac{N_a}{N_{a+1}} \right) + Q \ , \quad (a_2, e_a) = \frac{1}{R} \ln \left(\frac{M_{a+1}}{M_a} \right) - Q \tag{19.1.16}$$

and

$$(a_1 + a_2 - \beta \sum_{k=1}^{N-1} s_k e_k, e_a) = \frac{1}{R} \ln \left(\frac{L_{N-a}}{L_{N-a+1}} \right) + Q \ . \tag{19.1.17}$$

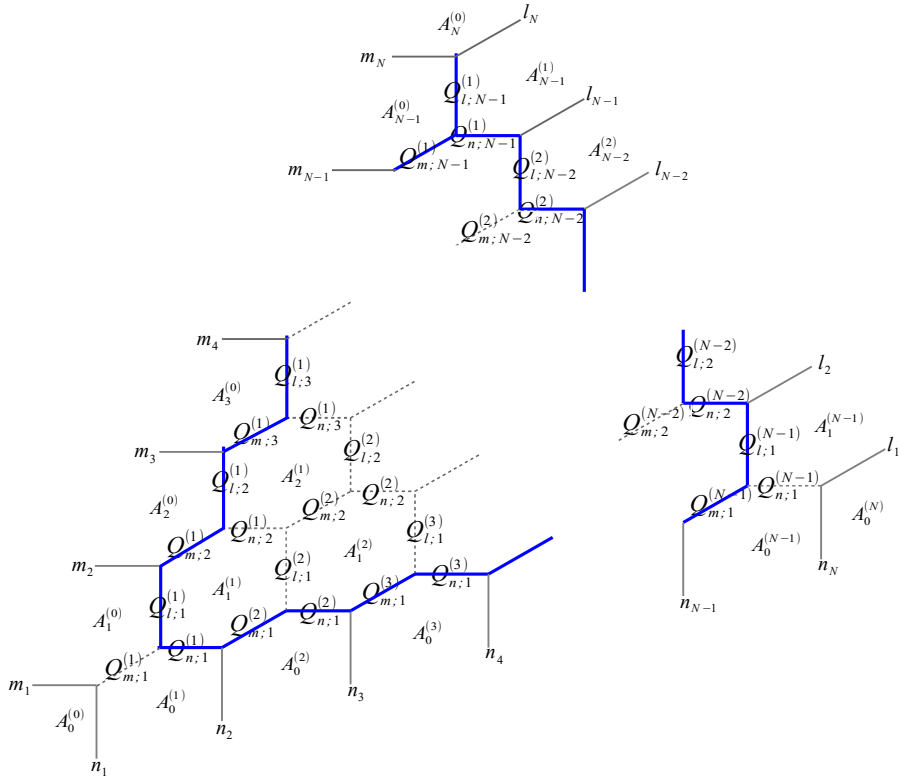

Figure 19.2: *Identification of the Kähler parameters which enter equation* (19.1.21).

These imply that the screening numbers s_k are determined by the system of equations

$$\beta \sum_{k=1}^{N-1} \kappa_{ak} s_k = -\frac{1}{R} \ln \left(\frac{Q^{(1)}_{m;a} Q^{(1)}_{l;a} Q^{(a)}_{n;N-a} Q^{(a)}_{l;N-a}}{Q^{(a)}_{m;1} Q^{(a)}_{n;1}} \right) + Q \;\Rightarrow \tag{19.1.18}$$

$$\beta s_a = -\frac{\kappa^{-1}_{aj}}{R} \ln \left(\frac{Q^{(1)}_{m;j} Q^{(1)}_{l;j} Q^{(j)}_{n;N-j} Q^{(j)}_{l;N-j}}{Q^{(j)}_{m;1} Q^{(j)}_{n;1}} \right) + \frac{a(N-a)}{2} Q \ .$$

in terms of the $\mathfrak{sl}_N$ Cartan matrix κ_{ij} and its inverse

$$\kappa^{-1}_{ij} = \begin{cases} \frac{1}{N}(N-i)j \ , & \text{if } j \leq i \\ \frac{1}{N}(N-j)i \ , & \text{otherwise} \end{cases} \ . \tag{19.1.19}$$

Let us denote

$$\beta \tilde{s}_a = R \beta s_a - \frac{a(N-a)}{2} RQ \tag{19.1.20}$$

and use the explicit form of κ^{-1}_{ij} in equation (19.1.19) to start simplifying the expression (19.1.18) for the screening numbers

$$\beta \tilde{s}_a = -\ln \left(\prod_{j=1}^{a} \left(\frac{Q^{(1)}_{m;j} Q^{(1)}_{l;j} Q^{(j)}_{n;N-j} Q^{(j)}_{l;N-j}}{Q^{(j)}_{m;1} Q^{(j)}_{n;1}} \right)^{\frac{j(N-a)}{N}} \prod_{j=a+1}^{N-1} \left(\frac{Q^{(1)}_{m;j} Q^{(1)}_{l;j} Q^{(j)}_{n;N-j} Q^{(j)}_{l;N-j}}{Q^{(j)}_{m;1} Q^{(j)}_{n;1}} \right)^{\frac{a(N-j)}{N}} \right) . \tag{19.1.21}$$

By expanding the products inside equation (19.1.21), it becomes manifest that the parameters $Q^{(i)}_{\bullet;a}$ correspond to a very particular set of segments on the web diagram in Figure 19.2. The parameter $Q^{(1)}_{l;N-1}$ enters with power N and is associated to the top-most blue line. The remaining Kähler parameters correspond to edges on the web diagram that surround all of the inner faces and that are depicted in the colour blue in Figure 19.2. It is thus possible to apply repeatedly the identities (18.0.2) to reduce equation (19.1.21), where we remind the reader these identities state that the product of parameters $Q^{(i)}_{\bullet;a}$ associated to adjoining edges of a face is equal to the product of $Q^{(i)}_{\bullet;a}$ associated to parallel and opposite adjoining edges of that same face. As a consequence it is possible to derive more general identities on strips of the brane diagram, like those which we present in appendix H.1. Working on such strips and successively substituting the identities (H.1.6) – (H.1.10) for strips $k = 1, \ldots, N-2$ into equation (19.1.21) reduces this to

$$\beta\tilde{s}_a = -\ln\left[\prod_{k=0}^{a-2}\prod_{j=1}^{k+1} Q^{(j)}_{l;N-k-1} \prod_{k=a-1}^{N-a-1}\prod_{j=1}^{a} Q^{(j)}_{l;N-k-1} \prod_{k=N-a}^{N-2}\prod_{j=k+a+2-N}^{a} Q^{(j)}_{l;N-k-1}\right] . \tag{19.1.22}$$

Combining this result with equation (19.1.20) then shows the screening numbers s_a to be related to the $Q^{(i)}_{l;j}$ Kähler parameters. Further partitioning the screening numbers like in Chapter 8

$$s_a = \sum_{i=1}^{a}\sum_{j=a}^{N} s_{ij} \ , \tag{19.1.23}$$

with $i, j = 1, \ldots, N-1$ and $i \leq a \leq j$, then leads to the identification (19.1.14)

$$\beta s_{ij} = -R^{-1}\ln\left(Q^{(i)}_{l;j-i+1}\right) + Q/2 \ , \qquad i \leq j = 1, \ldots N-1 \ . \tag{19.1.24}$$

When $N = 2$, this reduces to $\beta s = -R^{-1}\ln Q_l + Q/2$, which is precisely equation (16.1.2).

Open questions

At the time of writing, it remains an open question how to precisely take the 4d limit, where $R \to 0$ and $\mathfrak{q} \to 1$, of the T_N topological string partition function $\mathcal{Z}^{\text{top}}_N$ from equations (18.0.6)-(18.0.7) and the matrix integral (18.0.13), which is related to the three point conformal block (19.0.1) of $\mathfrak{sl}_N$ Toda CFT through equation (19.0.10). In particular, the contours of integration for the screening charges still need to be determined for the $\mathfrak{q} \to 1$ limit and this will establish the exact relation between the screening numbers in equation (19.1.14) and those defined in Part III of this thesis, in equation (8.1.9).

Chapter 20

Conclusions and outlook

Part IV of this thesis began by determining the precise relation between the topological string partition function for the T_2 trinion theories and $\mathfrak{q}$-deformed Liouville three point conformal blocks. In this case a resummation of the $\mathcal{Z}_2^{\text{top}}$ infinite sum formula to an infinite product formula is possible and allows to show rigorously that the infinite sum has a finite radius of convergence, whereby it can indeed be rewritten as a factorised infinite product. We were furthermore able to realise the infinite sum formula of the topological string as the sum over residues of a matrix integral in the free field representation of $\mathfrak{q}$-deformed Liouville CFT following [162], [34]. Using these two independent representations of $\mathcal{Z}_2^{\text{top}}$ it was possible to take $\mathfrak{q} \to 1$ defining a geometric engineering limit for the 4d partition function of the T_2 trinion, discussing the renormalisation ambiguities of $\mathcal{Z}_2^{\text{top}}$ and identifying a renormalisation prescription. At higher rank, for the case of the T_N trinion theories, we were able to extend the mapping between the topological string partition function $\mathcal{Z}_N^{\text{top}}$ and three point conformal blocks of $\mathfrak{q}$-deformed $\mathfrak{sl}_N$ Toda field theory. The result of this identification was a geometric interpretation of the screening numbers which enter the free field construction of Toda conformal blocks. There remain however many open questions, which are the subject of ongoing work.

Emergence of the Seiberg-Witten curve

The remarkably simple relation (19.1.14) between the screening numbers s_{ij}, which enter the construction of conformal blocks in Chapter 8, and the Kähler parameters $Q^{(i)}_{l;j-i+1}$ associated to segments of the web diagram in Figure 18.1 leads to a nice geometrical interpretation, similarly to the story presented in [49]. The circle uplift to five dimensions of the 4d T_N theories can be constructed equivalently in type IIB string theory via the web diagram of (p,q) 5-branes depicted in Figure 18.1 and in M-theory / type IIA string theory on Calabi-Yau threefolds through geometric engineering. For special gauge groups, like those of $SU(N)$ type, the mirror (IIB) Calabi-Yau data is captured by a Riemann surface which gets identified with the Seiberg-Witten curve. The geometry of this curve emerges in the double scaling limit $\epsilon_1, \epsilon_2 \to 0$ with large screening charges s_{ij}, while keeping parameters $g_s s_{ij}$ finite and where $g_s = \sqrt{-\epsilon_1 \epsilon_2}$. In this limit the background charge Q also vanishes. The parameters $\nu_{ij} \equiv g_s s_{ij}$ are the period integrals corresponding to a natural homology basis of A-cycles and measure the sizes of branch cuts on the Seiberg-Witten curve. They may thus be identified with the Kähler parameters for the Calabi-Yau threefold on the IIA side, wherefrom it emerges that the Seiberg-Witten curve can be viewed as a

thickening of the web diagram 18.1. This line of thought deserves further exploration, as it proposes a refinement of the analysis of multi-matrix models in [49].

The 4d limit

The results from the topological strings calculations identified in equation (18.0.20) the partition function of the 5d uplift of the T_N theories $\mathcal{Z}_N^{\text{top}}(\mathbf{A};\mathfrak{q},\mathfrak{t})$ and the matrix integral $\mathcal{I}_N(a_1,a_2,\mathbf{s};\beta)$, which was then further related to three point conformal blocks of $\mathfrak{q}$-deformed Toda conformal field theory in equation (19.0.10). For the particular case where $N = 2$, it was discussed in Section 17.1 how to take the undeformed $\mathfrak{q} \to 1$ limit of the matrix integral in a meaningful way, whereby one finds Liouville three point conformal blocks. It remains however an open problem to determine which three point conformal blocks are chosen by the topological strings result in the limit $\mathfrak{q} \to 1$ when $N \geq 3$. This would mean in particular to identify the order in which the screening charges Q_{ij} introduced in Chapter 8 enter three point conformal blocks and also to determine precisely the corresponding defining contours of integration for these screening charges.

More punctures

It is known that Liouville conformal blocks on punctured spheres $\mathcal{C}_{0,n}$ with $n \geq 3$ vertex operator insertions can also be obtained from topological strings. The simplest example is the four point block obtained by a gluing two strip geometries like in [74], the result of which gives the correct Nekrasov instanton partition function in the four dimensional limit. This corresponds to the gauge theory with $SU(2)$ gauge symmetry and $N_f = 4$ fundamental hypermultiplets.

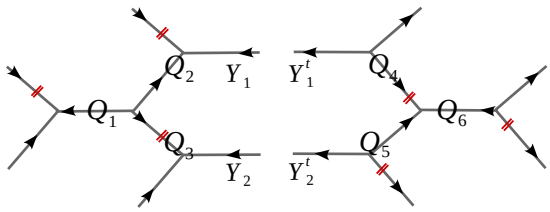

Figure 20.1: *Gluing the web diagrams of two T_2 trinions.*

One should now determine how to arrive at this result by gluing the web diagrams for two T_2 trinions like schematically depicted in Figure 20.1. In order to do so it is necessary to keep the Young diagrams on two of the legs of web diagrams non-empty and recompute the topological string partition function, which will again admit a partial resummation to the form

$$\mathcal{Z}_2^{Y_1Y_2}(Q_1,Q_2,Q_3) = \sum_{k=0}^{\infty}(-Q_3)^k P_k^{Y_1Y_2}(Q_1,Q_2)\ , \tag{20.0.1}$$

with $\mathcal{Z}_2^{\emptyset\emptyset} = \mathcal{Z}_2^{\text{top}}$. The resulting partition function is then schematically

$$\mathcal{Z}_{T_2-T_2} = \sum_{Y_1Y_2} \mathcal{Z}_2^{Y_1Y_2}(Q_1,Q_2,Q_3)\mathcal{Z}_2^{Y_2^tY_1^t}(Q_6,Q_5,Q_4)\ . \tag{20.0.2}$$

Appendices

Appendix F

Special functions

Here we collect definitions and identities for special functions. The quantum dilogarithm

$$\varphi(x) = (x;\mathfrak{q})_\infty = \prod_{n=0}^{\infty}(1-\mathfrak{q}^n x)\,, \qquad |\mathfrak{q}|<1 \tag{F.0.1}$$

is a special case of shifted factorial function

$$(x;\mathfrak{q}_1,\dots,\mathfrak{q}_r)_\infty = \prod_{n_1,\dots,n_r=0}^{\infty}(1-x\mathfrak{q}_1^{n_1},\cdots,\mathfrak{q}_r^{n_r})\,, \quad \forall \quad |\mathfrak{q}_i|<1\,. \tag{F.0.2}$$

A definition that overcomes the need to specify a regime of the $|\mathfrak{q}_i|$ and resolves issues of convergence is the polylogarithm function or the plethystic exponential [182]

$$(x;\mathfrak{q}_1,\dots,\mathfrak{q}_r)_\infty = \exp\left(-\mathrm{Li}_{r+1}(x;\mathfrak{q}_1,\dots,\mathfrak{q}_r)\right)\,, \quad |x|<1 \tag{F.0.3}$$

with the definition

$$\mathrm{Li}_r(z;\mathfrak{q}_1,\dots,\mathfrak{q}_r) = \sum_{j=1}^{\infty}\frac{z^j}{j\prod_{i=1}^r(1-\mathfrak{q}_i^j)}\,, \tag{F.0.4}$$

such that

$$\mathrm{Li}_r(z) = \sum_{n=1}^{\infty}\frac{z^n}{n^r}\,, \quad |z|<1 \tag{F.0.5}$$

for all complex arguments z with $|z|<1$.

The infinite product function $\mathcal{M}(U)\equiv\mathcal{M}(U;\mathfrak{t},\mathfrak{q})$ which appears often in the main text is also defined as a shifted factorial

$$\mathcal{M}(U;\mathfrak{t},\mathfrak{q}) = (U\mathfrak{q};\mathfrak{t},\mathfrak{q})_\infty^{-1} = \begin{cases} \prod_{i,j=1}^{\infty}(1-U\mathfrak{t}^{i-1}\mathfrak{q}^j)^{-1} & \text{for } |\mathfrak{t}|<1, |\mathfrak{q}|<1 \\ \prod_{i,j=1}^{\infty}(1-U\mathfrak{t}^{i-1}\mathfrak{q}^{1-j}) & \text{for } |\mathfrak{t}|<1, |\mathfrak{q}|>1 \\ \prod_{i,j=1}^{\infty}(1-U\mathfrak{t}^{-i}\mathfrak{q}^{j}) & \text{for } |\mathfrak{t}|>1, |\mathfrak{q}|<1 \\ \prod_{i,j=1}^{\infty}(1-U\mathfrak{t}^{-i}\mathfrak{q}^{1-j})^{-1} & \text{for } |\mathfrak{t}|>1, |\mathfrak{q}|>1 \end{cases}\,, \tag{F.0.6}$$

converging for all U. This function can be alternatively written as a plethystic exponential

$$\mathcal{M}(U;\mathfrak{t},\mathfrak{q}) = \exp\left[\sum_{m=1}^{\infty}\frac{U^m}{m}\frac{\mathfrak{q}^m}{(1-\mathfrak{t}^m)(1-\mathfrak{q}^m)}\right], \tag{F.0.7}$$

which converges for all $\mathfrak{t}$ and all $\mathfrak{q}$ provided that $|U| < \mathfrak{q}^{-1+\theta(|q|-1)}\mathfrak{t}^{\theta(|\mathfrak{t}|-1)}$, where only here $\theta(x)$ denotes the step function which is $\theta(x) = 1$ if $x > 0$ and $\theta(x) = 0$ if $x \leq 0$. From the analytic properties of the shifted factorials (F.0.2) we can derive the identities

$$\mathcal{MM}(U;\mathfrak{t}^{-1},\mathfrak{q}) = \frac{1}{\mathcal{M}(U\mathfrak{t};\mathfrak{t},\mathfrak{q})}, \qquad \mathcal{M}(U;\mathfrak{t},\mathfrak{q}^{-1}) = \frac{1}{\mathcal{M}(U\mathfrak{q}^{-1};\mathfrak{t},\mathfrak{q})}, \tag{F.0.8}$$

as well as the following functional relations

$$\mathcal{M}(U\mathfrak{t};\mathfrak{t},\mathfrak{q}) = (U\mathfrak{q};\mathfrak{q})_\infty \mathcal{M}(U;\mathfrak{t},\mathfrak{q}), \qquad \mathcal{M}(U\mathfrak{q};\mathfrak{t},\mathfrak{q}) = (U\mathfrak{q};\mathfrak{t})_\infty \mathcal{M}(U;\mathfrak{t},\mathfrak{q}). \tag{F.0.9}$$

A further useful identity is

$$\mathcal{M}(Q;\mathfrak{q},\mathfrak{t}) = \mathcal{M}(Q\frac{\mathfrak{t}}{\mathfrak{q}};\mathfrak{t},\mathfrak{q})\ . \tag{F.0.10}$$

Nekrasov partition function: The quantum dilogarithm enters the definition of the Nekrasov partition function [43] through the functions $\mathcal{N}_{RP}(Q;\mathfrak{t},\mathfrak{q})$

$$\mathcal{N}_{RP}(Q;\mathfrak{t},\mathfrak{q}) = \prod_{i=1}^{\infty}\prod_{j=1}^{\infty}\frac{\varphi(Q\mathfrak{q}^{R_i-P_j+1}\mathfrak{t}^{j-i})}{\varphi(Q\mathfrak{q}^{R_i-P_j+1}\mathfrak{t}^{j-i-1})}\frac{\varphi(Q\mathfrak{q}\mathfrak{t}^{j-i-1})}{\varphi(Q\mathfrak{q}\mathfrak{t}^{j-i})}\ , \tag{F.0.11}$$

which are equivalent to

$$\mathcal{N}_{RP}(Q;\mathfrak{t},\mathfrak{q}) = \prod_{(i,j)\in R}\left(1-Q\mathfrak{q}^{R_i-j+1}\mathfrak{t}^{P_j^t-i}\right)\prod_{(i,j)\in P}\left(1-Q\mathfrak{q}^{-P_i+j}\mathfrak{t}^{-R_j^t+i-1}\right) \tag{F.0.12}$$

and also to

$$\mathcal{N}_{RP}(Q;\mathfrak{t},\mathfrak{q}) = \prod_{(i,j)\in P}\left(1-Q\mathfrak{q}^{R_i-j+1}\mathfrak{t}^{P_j^t-i}\right)\prod_{(i,j)\in R}\left(1-Q\mathfrak{q}^{-P_i+j}\mathfrak{t}^{-R_j^t+i-1}\right)\ . \tag{F.0.13}$$

In the main text, we label $\mathcal{N}_{RP}(Q;\mathfrak{t},\mathfrak{q}) \equiv \mathcal{N}_{RP}(Q)$ in order not to make our formulas too baroque. The notation in these expressions is as follows: R and P are Young tableaux or partitions, R_i represents the length of row i and R^t is the dual partition to R, with rows and column exchanged with respect to those of R. Furthermore, a box $s \in R$ on row i and column j of R has leg-length $l_R(s) = R_j^t - i$. When one of the partitions in definition (F.0.12) is empty, this becomes one of the following

$$\mathcal{N}_{\emptyset R}(Q) = \prod_{(i,j)\in R}\left(1-Q\mathfrak{q}^{-R_i+j}\mathfrak{t}^{i-1}\right) = \prod_{i=1}^{N_R}\frac{\varphi(Q\mathfrak{q}^{-R_i+1}\mathfrak{t}^{i-1})}{\varphi(Q\mathfrak{q}\mathfrak{t}^{i-1})}\ , \tag{F.0.14}$$

$$\mathcal{N}_{R\emptyset}(Q) = \prod_{(i,j)\in R}\left(1-Q\mathfrak{q}^{R_i-j+1}\mathfrak{t}^{-i}\right) = \prod_{i=1}^{N_R}\frac{\varphi(Q\mathfrak{q}\mathfrak{t}^{-i})}{\varphi(Q\mathfrak{q}^{R_i+1}\mathfrak{t}^{-i})}\ . \tag{F.0.15}$$

Note here for future reference that for $Q = v^{-2}\mathfrak{t}^N$, the partition function

$$\mathcal{N}_{R\emptyset}(Q) = \prod_{i=1}^{N_R}\frac{\varphi(Q\mathfrak{q}\mathfrak{t}^{-i})}{\varphi(Q\mathfrak{q}^{R_i+1}\mathfrak{t}^{-i})} \tag{F.0.16}$$

vanishes if $N_R > N$; the argument for the quantum dilogarithm in the numerator $\varphi(Q\mathfrak{q}\mathfrak{t}^{-i})$ becomes 1 at $i = N+1$ and the numerator vanishes. Similarly, $\mathcal{N}_{\emptyset R}(Q)$ vanishes if $Q = \mathfrak{t}^{-N}$ and $N_R > N$. This follows from the identity

$$\mathcal{N}_{RP}(Qv^{-2}) = \mathcal{N}_{PR}(Q^{-1})(Qv^{-1})^{|R|+|P|}\frac{f_R}{f_P}\,, \tag{F.0.17}$$

where

$$f_R = \prod_{(i,j)\in R}(-1)\mathfrak{q}^{R_i-j+1/2}\mathfrak{t}^{-R_j^t+i-1/2} = (-1)^{|R|}\mathfrak{q}^{||R||/2}\mathfrak{t}^{-||R^t||/2} \tag{F.0.18}$$

for $|R| = \sum_i R_i$ and $||R|| = \sum_i R_i^2$. Finally, note that when the partitions R and P are finite, whereby the Young tableau have a finite number of rows, equation (F.0.11) becomes

$$\mathcal{N}_{RP}(Q) = \prod_{i=1}^{N_R}\prod_{j=1}^{N_P}\frac{\varphi(Q\mathfrak{q}^{R_i-P_j+1}\mathfrak{t}^{j-i})}{\varphi(Q\mathfrak{q}^{R_i-P_j+1}\mathfrak{t}^{j-i-1})}\frac{\varphi(Q\mathfrak{q}\mathfrak{t}^{j-i-1})}{\varphi(Q\mathfrak{q}\mathfrak{t}^{j-i})}\mathcal{N}_{R\emptyset}(\mathfrak{t}^{N_P}Q)\mathcal{N}_{\emptyset P}(\mathfrak{t}^{-N_R}Q)\,. \tag{F.0.19}$$

Similarly to (F.0.14)-(F.0.15), the partition function (F.0.19) also vanishes when $Q = v^{-2}\mathfrak{t}^N$ unless $N_R - N_P \leq N$ (and likewise when $Q = \mathfrak{t}^{-N}$). The function $\mathcal{N}_{RP}$ further satisfies the identity

$$\mathcal{N}_{RP}(Q;\mathfrak{q},\mathfrak{t}) = \mathcal{N}_{P^tR^t}(Q\frac{\mathfrak{t}}{\mathfrak{q}};\mathfrak{t},\mathfrak{q})\,. \tag{F.0.20}$$

Special functions for topological string amplitudes: When writing topological string amplitudes, the following function is ubiquitous

$$\tilde{Z}_\nu(\mathfrak{t},\mathfrak{q}) = \prod_{i=1}^{\ell(\nu)}\prod_{j=1}^{\nu_i}\left(1-\mathfrak{t}^{\nu_j^t-i+1}\mathfrak{q}^{\nu_i-j}\right)^{-1}, \tag{F.0.21}$$

which up to an over all coefficient is the principal specialisation of the Macdonald function.

F.1 The limit $\mathfrak{q} \to 1$

In this section we study how to take the $\mathfrak{q} \to 1$ of $\varphi(z)$ and $\mathcal{M}(z)$. We begin with the quantum dilogarithm $\varphi(z)$ and its plethystic exponential expression

$$\varphi(z) = (z;\mathfrak{q})_\infty = \exp\left[-\sum_{m=1}^{\infty}\frac{z^m}{m}\frac{1}{(1-\mathfrak{q}^m)}\right]\,, \tag{F.1.22}$$

using which we can derive

$$\log\varphi(z) = \frac{1}{\log\mathfrak{q}}\mathrm{Li}_2(z) + \frac{1}{2}\log(1-z) + \mathcal{O}\left(\log\mathfrak{q}\right)\,. \tag{F.1.23}$$

This identity was also derived by Kirillov in [183]. Observe that by forming the ratio $\frac{\varphi(q)}{\varphi(z)}$ we eliminate the leading Li_2 divergence in the $\mathfrak{q} \to 1$ limit and then by further dividing by the subleading $\log$ term we obtain a function

$$\Gamma_\mathfrak{q}(z) = \frac{\varphi(\mathfrak{q})}{\varphi(\mathfrak{q}^z)}(1-\mathfrak{q})^{1-z}\,, \tag{F.1.24}$$

that is finite in the $\mathfrak{q} \to 1$ limit

$$\lim_{\mathfrak{q}\to 1} \Gamma_{\mathfrak{q}}(z) = \exp\left(\zeta(0)(1-x)\left(\log \mathfrak{q}\right) + \mathcal{O}\left(\log \mathfrak{q}\right)^2\right) \tag{F.1.25}$$

with $\zeta(0) = -\frac{1}{2}$. This is a $\mathfrak{q}$-deformed version of the usual Gamma function and satisfies the functional relation

$$\Gamma_{\mathfrak{q}}(z+1) = \frac{1-\mathfrak{q}^z}{1-\mathfrak{q}}\Gamma_{\mathfrak{q}}(z) = [z]\Gamma_{\mathfrak{q}}(z)\,. \tag{F.1.26}$$

It is proved by Koornwinder in the Appendix B of [184] that

$$\lim_{\mathfrak{q}\to 1} \Gamma_{\mathfrak{q}}(z) = \Gamma(z)\,. \tag{F.1.27}$$

Finally, we may compute the $\mathfrak{q} \to 1$ limit of

$$\lim_{\mathfrak{q}\to 1} \left(\varphi(\mathfrak{t})/\varphi(\mathfrak{q})\right) = \left(\Gamma(-b^2)\right)^{-1}(1-\mathfrak{q})^{1+b^2}\,. \tag{F.1.28}$$

We also derive here a useful identity that we need in the main text, the limit for the following ratio of quantum dilogarithm functions

$$\begin{aligned}
\lim_{\mathfrak{q}\to 1} \frac{\varphi(\mathfrak{q}^{\alpha_1}x)}{\varphi(\mathfrak{q}^{\alpha_2}x)} \quad &\to \exp(-\left(\mathrm{Li}_2(e^{-\alpha_1}x) - \mathrm{Li}_2(e^{-\alpha_2}x)\right)/\epsilon) && \text{(F.1.29)}\\
&\approx \exp(-\left(\mathrm{Li}_2(x(1-\alpha_1\epsilon)) - \mathrm{Li}_2(x(1-\alpha_2\epsilon))\right)/\epsilon)\\
&= \exp\left((\alpha_1-\alpha_2)x\mathrm{Li'}_2(x)\right)\\
&= \exp((\alpha_1-\alpha_2)x(-\log(1-x)/x)) = (1-x)^{\alpha_2-\alpha_1}\,, && \text{(F.1.30)}
\end{aligned}$$

where at an intermediate step we use the identity

$$\mathrm{Li}_2(x) = -\int_0^x \frac{dy}{y}\log(1-y)\,. \tag{F.1.31}$$

We can now proceed similarly with the $\mathcal{M}$ function using (F.0.7)

$$\mathcal{M}\big(z\big) = (z\mathfrak{q};\mathfrak{t},\mathfrak{q})_\infty^{-1} = \exp\left[\sum_{m=1}^{\infty}\frac{z^m}{m}\frac{\mathfrak{q}^m}{(1-\mathfrak{t}^m)(1-\mathfrak{q}^m)}\right]\,, \tag{F.1.32}$$

and in the $\mathfrak{q} \to 1$ limit we obtain

$$b^2\log(z;\mathfrak{q},\mathfrak{t})_\infty = -\frac{\mathrm{Li}_3(z)}{(\log\mathfrak{q})^2} - \frac{1}{2}\frac{\mathrm{Li}_2(z)}{\log\mathfrak{q}}(b^2-1) + \frac{\mathrm{Li}_1(z)}{3!}\frac{b^4-3b^2+1}{2} + \mathcal{O}\left(\log\mathfrak{q}\right)\,. \tag{F.1.33}$$

We find that the function

$$\Gamma_{\mathfrak{q},\mathfrak{t}}(x) = \frac{\mathcal{M}(\mathfrak{t}/\mathfrak{q})}{\mathcal{M}(\mathfrak{t}^x/\mathfrak{q})}\varphi(\mathfrak{q})^{x-1}(1-\mathfrak{q})^{\frac{1}{2}(x-1)(2-b^{-2}x)} \tag{F.1.34}$$

has a finite $\mathfrak{q} \to 1$ limit and it furthermore satisfies, using (F.0.9), the functional relation

$$\Gamma_{\mathfrak{q},\mathfrak{t}}(x+1) = \Gamma_{\mathfrak{q}}(x)\Gamma_{\mathfrak{q},\mathfrak{t}}(x)\,. \tag{F.1.35}$$

Appendix G

Variants of Jackson integrals and the $\mathfrak{q} \to 1$ limit

Equation (16.2.20) is useful for studying the limit $\mathfrak{q} \to 1$ of the Jackson integral. We reproduce this here

$$\mathcal{I}'_q = \int_0^1 d_{\mathfrak{q}}x \; x^{t-1} \frac{\varphi(\mathfrak{q}x)}{\varphi(\mathfrak{q}^s x)} \,. \tag{G.0.1}$$

In the limit it corresponds to the integral

$$\lim_{\mathfrak{q}\to 1} \mathcal{I}'_{\mathfrak{q}} = \int_0^1 dx \; x^{t-1}(1-x)^{s-1} \,. \tag{G.0.2}$$

It remains to study the factor in front of $\mathcal{I}'_{\mathfrak{q}}$ in (16.2.20). We first note that $\vartheta_{\mathfrak{q}}(z)$ is closely related to the Jacobi theta function $\theta_1(x,\tau)$ defined as

$$\theta_1(x,\tau) = -e^{\frac{\pi \mathrm{i}}{4}\tau}\, 2\sin(\pi x) \prod_{n=1} (1-e^{2\pi \mathrm{i} n\tau} e^{2\pi \mathrm{i} x})(1-e^{2\pi \mathrm{i} n\tau} e^{-2\pi \mathrm{i} x})(1-e^{2\pi \mathrm{i} n\tau}) \tag{G.0.3}$$

Indeed, the relation between $\vartheta_{\mathfrak{q}}(z)$ and $\theta_1(x,\tau)$ is

$$\vartheta_{\mathfrak{q}}(e^{2\pi \mathrm{i} x}) = \mathrm{i}\, e^{\pi \mathrm{i} x}\, e^{-\frac{\pi \mathrm{i}}{4}\tau}\, \theta_1(x,\tau), \qquad \mathfrak{q} = e^{2\pi \mathrm{i}\tau}. \tag{G.0.4}$$

In order to study the limit $\mathfrak{q} \to 1^-$, or equivalently $\tau \to 0$, $\mathrm{Im}(\tau) > 0$, we may use the modular transformation property of $\theta_1(x,\tau)$,

$$\theta_1(x,\tau) = \mathrm{i}(-\mathrm{i}\tau)^{-\frac{1}{2}} e^{-\frac{\pi \mathrm{i}}{\tau}x^2} \theta_1(x/\tau, -1/\tau). \tag{G.0.5}$$

It follows that

$$\theta_1(s\tau,\tau) = \mathrm{i}\,(-\mathrm{i}\tau)^{-\frac{1}{2}} e^{-\pi \mathrm{i} s^2\tau} \theta_1(s,-1/\tau) \sim -\mathrm{i}\,(-\mathrm{i}\tau)^{-\frac{1}{2}}\, e^{-\frac{\pi \mathrm{i}}{4\tau}}\, 2\sin(\pi s), \tag{G.0.6}$$

leading to

$$\vartheta_{\mathfrak{q}}(\mathfrak{q}^s) \sim (-\mathrm{i}\tau)^{-\frac{1}{2}}\, e^{-\frac{\pi \mathrm{i}}{4\tau}}\, 2\sin(\pi s). \tag{G.0.7}$$

It remains to study the asymptotics of $(\mathfrak{q},\mathfrak{q})_\infty^3$. To this aim we may use the relation between $(\mathfrak{q},\mathfrak{q})_\infty$ and the Dedekind eta-function,

$$(\mathfrak{q},\mathfrak{q})_\infty = e^{-\frac{\pi \mathrm{i}\tau}{12}} \eta(\tau) \,. \tag{G.0.8}$$

Using the modular transformation property $\eta(\tau) = (-i\tau)^{-\frac{1}{2}}\eta(-1/\tau)$, one finds

$$(\mathfrak{q},\mathfrak{q})_\infty = e^{-\frac{\pi \mathrm{i}\tau}{12}}(-i\tau)^{-\frac{1}{2}}\eta(-1/\tau) = e^{-\frac{\pi \mathrm{i}\tau}{12}}(-i\tau)^{-\frac{1}{2}}e^{-\frac{\pi \mathrm{i}}{12\tau}}\prod_{n=1}(1-e^{-2\pi \mathrm{i}/\tau})\,. \tag{G.0.9}$$

which implies

$$(\mathfrak{q},\mathfrak{q})_\infty \sim e^{-\frac{\pi \mathrm{i}}{12\tau}}\,(-i\tau)^{-\frac{1}{2}}\,. \tag{G.0.10}$$

Taken together this yields

$$\frac{2\pi \mathrm{i}}{1-\mathfrak{q}}\,\frac{\vartheta_{\mathfrak{q}}(\mathfrak{q}^s)}{(\mathfrak{q};\mathfrak{q})_\infty^3} \sim \frac{2\pi \mathrm{i}}{(-2\pi \mathrm{i}\tau)}\frac{(-\mathrm{i}\tau)^{-\frac{1}{2}}}{(-i\tau)^{-\frac{3}{2}}}\,2\sin(\pi s) \sim 2\mathrm{i}\sin(\pi s). \tag{G.0.11}$$

Appendix H

Useful identities

Here we collect a set of useful identities which enter the derivation of the main results presented in Section 18.2. The functional shift relations (F.0.9) obeyed by the function $\mathcal{M}(Q;\mathfrak{t},\mathfrak{q})$ imply the shift relation

$$\mathcal{M}(M)=\mathcal{M}(M\mathfrak{t}^{-s})\prod_{I=1}^{s}\varphi(M\mathfrak{q}\mathfrak{t}^{-I})\,, \tag{H.0.1}$$

which further implies the following identities

$$\frac{\mathcal{M}\Big(\frac{M_i}{M_{j+1}}\Big)}{\mathcal{M}\Big(\mathfrak{t}^{-N_{1,j}}\frac{M_i}{M_{1+j}}\Big)}=\prod_{I=1}^{N_{1,j}}\varphi\left(\frac{M_i}{M_{1+j}}\mathfrak{q}\mathfrak{t}^{-I}\right)\,, \tag{H.0.2}$$

$$\frac{\mathcal{M}\Big(\mathfrak{t}^{N_{a,i}-N_{a,j+1}}\frac{M_{a+i}}{M_{a+j+1}}\Big)}{\mathcal{M}\Big(\mathfrak{t}^{N_{a,i}-N_{a+1,j}}\frac{M_{a+i}}{M_{a+1+j}}\Big)}=\frac{\prod_{I=1}^{N_{a+1,j}}\varphi\left(\frac{M_{a+i}}{M_{a+1+j}}\mathfrak{t}^{N_{a,i}-I}\mathfrak{q}\right)}{\prod_{I=1}^{N_{a,j+1}}\varphi\left(\frac{M_{a+i}}{M_{a+1+j}}\mathfrak{t}^{N_{a,i}-I}\mathfrak{q}\right)}\,. \tag{H.0.3}$$

Useful identities: double products that appear in Section 18.3 in the evaluation of the integrand (18.3.40) with empty partitions can be reduced using the following identities

$$\begin{aligned}
&\prod_{I=1}^{s_1}\prod_{J=1}^{s_2}\frac{\varphi(Q\mathfrak{t}^{s_1-s_2+J-I})}{\varphi(Q\mathfrak{t}^{s_1-s_2+J-I+1})}=\prod_{I=1}^{s_1}\frac{\varphi(Q\mathfrak{t}^{I-s_2})}{\varphi(Q\mathfrak{t}^{I})}\,,\quad \prod_{I=1}^{s_1}\prod_{J=1}^{s_2}\frac{\varphi(Q\mathfrak{t}^{s_1-s_2+J-I-1})}{\varphi(Q\mathfrak{t}^{s_1-s_2+J-I})}=\prod_{I=J}^{s_2}\frac{\varphi(Q\mathfrak{t}^{-J})}{\varphi(Q\mathfrak{t}^{s_1-J})}\,,\\
&\prod_{I=1}^{s_1}\prod_{J=1}^{s_2}\frac{\varphi(Q\mathfrak{t}^{s_1-s_2+J-I})}{\varphi(Q\mathfrak{t}^{s_1-s_2+J-I-1})}=\prod_{I=1}^{s_1}\frac{\varphi(Q\mathfrak{t}^{s_1-I})}{\varphi(Q\mathfrak{t}^{s_1-s_2-I})}\,,\quad \prod_{I=1}^{s_1}\prod_{J=1}^{s_2}\frac{\varphi(Q\mathfrak{t}^{s_2-s_1+I-J+1})}{\varphi(Q\mathfrak{t}^{s_2-s_1+I-J})}=\prod_{I=1}^{s_1}\frac{\varphi(Q\mathfrak{t}^{s_2+1-I})}{\varphi(Q\mathfrak{t}^{1-I})}.
\end{aligned} \tag{H.0.4}$$

H.1 Face relations among Kähler parameters

The Kähler parameters $Q^{(i)}_{\bullet;a}$ that are associated to segments on the web diagram in Figure 18.1 obey the relations (18.0.2), which we reproduce below

$$Q^{(j)}_{l;i}Q^{(j)}_{m;i+1}=Q^{(j+1)}_{m;i}Q^{(j+1)}_{l;i}\,,\ Q^{(j)}_{n;i}Q^{(j+1)}_{m;i}=Q^{(j)}_{m;i+1}Q^{(j)}_{n;i+1}\,,\ Q^{(j)}_{l;i}Q^{(j)}_{n;i}=Q^{(j+1)}_{l;i}Q^{(j)}_{n;i+1}\,, \tag{H.1.5}$$

and which relate products of Kähler parameters around a face of the web. Starting from these basic identities, we derive in this section a more general set of face relations, where the faces assemble into strips on the web diagram. Such strips are depicted by solid colourful lines in Figure H.1 and each of them corresponds to a product of Kähler parameters with powers dictated by equation (19.1.21) in Section 19.1.

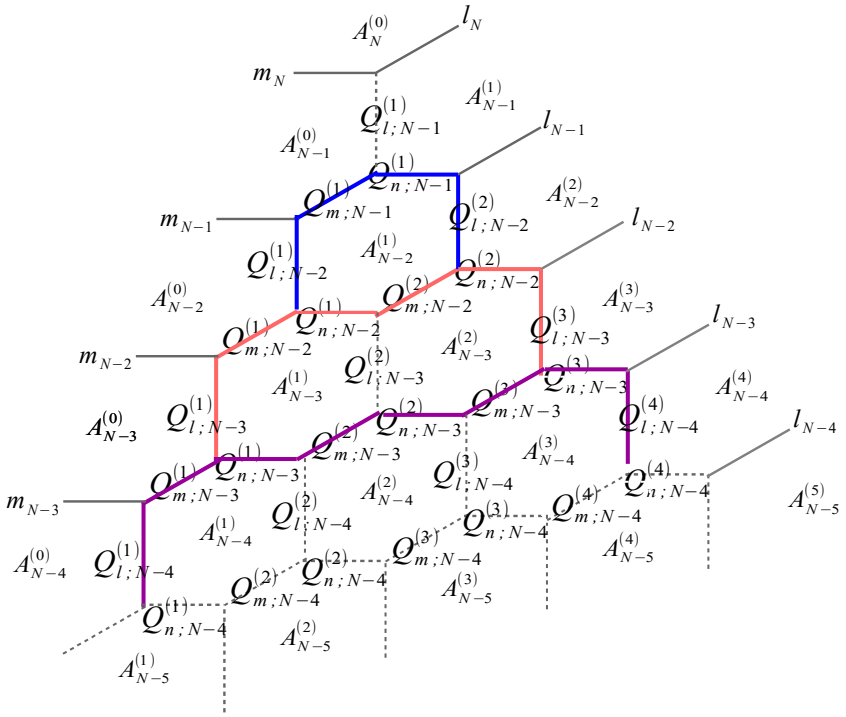

Figure H.1: *Kähler parameters $Q^{(i)}_{\bullet;a}$ associated to strips on the web diagram.*

For example, the most simple such strip relations are

$$\begin{aligned}
\textbf{strip 1 (blue)}: &\ (Q^{(1)}_{n;N-1})^{N-a}(Q^{(1)}_{m;N-1})^{a}(Q^{(1)}_{l;N-2})^{2a}(Q^{(2)}_{l;N-2})^{2(N-a)} = \\
&\ (Q^{(1)}_{n;N-2})^{N-a}(Q^{(2)}_{m;N-2})^{a}(Q^{(1)}_{l;N-2})^{N}(Q^{(2)}_{l;N-2})^{N}\ , \\
\textbf{strip 2 (red)}: &\ \prod_{j=1}^{2}(Q^{(j)}_{n;N-2})^{j(N-a)}(Q^{(j)}_{m;N-2})^{a(3-j)}(Q^{(1)}_{l;N-3})^{3a}(Q^{(3)}_{l;N-3})^{3(N-a)} = \\
&\ \prod_{j=1}^{2}(Q^{(j)}_{n;N-3})^{j(N-a)}(Q^{(j+1)}_{m;N-3})^{a(3-j)}\prod_{j=1}^{3}(Q^{(j)}_{l;N-3})^{N}\ .
\end{aligned} \tag{H.1.6}$$

More generally, the Kähler parameters on a generic strip $k < a-1$ satisfy the identity

$$\begin{aligned}
\textbf{strip k}: &\ \prod_{j=1}^{k}(Q^{(j)}_{n;N-k})^{j(N-a)}(Q^{(j)}_{m;N-k})^{a(k+1-j)}(Q^{(1)}_{l;N-k-1})^{a(k+1)}(Q^{(k+1)}_{l;N-k-1})^{(k+1)(N-a)} = \\
&\ \prod_{j=1}^{k}(Q^{(j)}_{n;N-k-1})^{j(N-a)}(Q^{(j+1)}_{m;N-k-1})^{a(k+1-j)}\prod_{j=1}^{k+1}(Q^{(j)}_{l;N-k-1})^{N}\ .
\end{aligned} \tag{H.1.7}$$

For $k \geq a-1$, there are two cases that should be distinguished. The first of these is

$$\begin{aligned}
&\mathbf{strip\ a-1 \leq k \leq N-a-1}: \qquad (H.1.8)\\
&\prod_{j=1}^{a}(Q^{(j)}_{n;N-k})^{j(N-a)} \prod_{j=a+1}^{k}(Q^{(j)}_{n;N-k})^{a(N-j)} \prod_{j=1}^{k}(Q^{(j)}_{m;N-k})^{a(k+1-j)}\\
&(Q^{(1)}_{l;N-k-1})^{a(k+1)}(Q^{(k+1)}_{l;N-k-1})^{a(N-k-1)} =\\
&\prod_{j=1}^{a}(Q^{(j)}_{n;N-k-1})^{j(N-a)} \prod_{j=a+1}^{k}(Q^{(j)}_{n;N-k-1})^{a(N-j)} \prod_{j=1}^{k}(Q^{(j+1)}_{m;N-k-1})^{a(k+1-j)} \prod_{j=1}^{a}(Q^{(j)}_{l;N-k-1})^{N}\ .
\end{aligned}$$

The second involves the strips in the range $N-a-1 < k \leq N-2$, whose label can be set to $k = N-a-1+k'$

$$\begin{aligned}
&\mathbf{strip\ N-a-1 < k \leq N-2}: \qquad (H.1.9)\\
&(Q^{(1)}_{l;N-k-1})^{(N-a)(N-k-1)} \prod_{j=1}^{a}(Q^{(j)}_{n;N-k})^{j(N-a)} \prod_{j=a+1}^{k}(Q^{(j)}_{n;N-k})^{a(N-j)}\\
&\prod_{j=1}^{k'}(Q^{(j)}_{m;N-k})^{(N-a)(N-k-1+j)} \prod_{j=k'+1}^{k}(Q^{(j)}_{m;N-k})^{a(k+1-j)}(Q^{(k+1)}_{l;N-k-1})^{a(N-k-1)} =\\
&\prod_{j=1}^{a}(Q^{(j)}_{n;N-k-1})^{j(N-a)} \prod_{j=a+1}^{k}(Q^{(j)}_{n;N-k-1})^{a(N-j)}\\
&\prod_{j=1}^{k'}(Q^{(j+1)}_{m;N-k-1})^{(N-a)(N-k-1+j)} \prod_{j=k'+1}^{k}(Q^{(j+1)}_{m;N-k-1})^{a(k+1-j)} \prod_{j=k'+1}^{a}(Q^{(j)}_{l;N-k-1})^{N}\ .
\end{aligned}$$

In particular on the last strip $k = N-2$, equation (H.1.9) becomes

$$\text{(H.1.9)} = (Q^{(a)}_{l;1})^{N} \prod_{j=1}^{a}(Q^{(j)}_{n;1})^{j(N-a)} \prod_{j=a+1}^{N-2}(Q^{(j)}_{n;1})^{a(N-j)} \prod_{j=2}^{a}(Q^{(j)}_{m;1})^{j(N-a)} \prod_{j=a+1}^{N-1}(Q^{(j)}_{m;1})^{a(N-j)}\ . \qquad (H.1.10)$$

after relabelling the limits for the products.

Part V

Final thoughts and perspectives

Concluding remarks

The study of four dimensional quantum field theories with a certain amount of supersymmetry is partly based on the hope that understanding non-perturbative phenomena and developing techniques to compute certain quantities of physical interest exactly will lead to invaluable knowledge which is applicable to more realistic cases. In this context, $\mathcal{N} = 2$ supersymmetric field theories have been at the heart of much recent progress. Such theories have been engineered as low energy limits of different, dual string theory constructions and this perspective has led to surprising insights.

One such example is the correspondence between certain $\mathcal{N} = 2$ supersymmetric field theories $\mathfrak{X}(\mathcal{C}_{g,n}, \mathfrak{g})$ in four dimensions and two dimensional $\mathfrak{sl}_N$ Toda conformal field theories. In this thesis we have begun a program to generalise this correspondence in particular for higher rank cases where no Lagrangian description is known of the former. Quantities protected by supersymmetry, such as partition functions and vacuum expectation values of supersymmetric line operators, play a central role in this endeavour. Motivated by the approach of [54] for $\mathfrak{g} = \mathfrak{sl}_2$ and the relation between line operators and the moduli space of flat connections $\mathcal{M}_{\text{flat}}$ which was investigated there, we took the quantised algebra of functions $\mathcal{A}_{\text{flat}}$ on moduli space of flat $SL(N, \mathbb{C})$ connections on Riemann surfaces $\mathcal{C}_{g,n}$ as an ansatz for the algebra $\mathcal{A}_{\mathfrak{X}}$ of supersymmetric loop observables in theories $\mathfrak{X}(\mathcal{C}_{g,n}, \mathfrak{g})$ of class $\mathcal{S}$ with $\mathfrak{g} = \mathfrak{sl}_N$.

In part II we have described in detail the quantum algebra $\mathcal{A}_{\text{flat}}$ in terms of generators and relations, which the arguments of Gaiotto, Moore and Neitzke relate to $\mathcal{A}_{\mathfrak{X}}$, while in Part III we have proven $\mathcal{A}_{\text{flat}}$ to be isomorphic to the algebra $\mathcal{A}_V$ of Verlinde loop and network operators in $\mathfrak{sl}_N$ Toda conformal field theory. The resulting relations $\mathcal{A}_{\mathfrak{X}} \simeq \mathcal{A}_{\text{flat}} \simeq \mathcal{A}_V$ support a higher rank generalisation of the AGT correspondence, in particular to strongly coupled non-Lagrangian theories $\mathfrak{X}(\mathcal{C}_{g,n}, \mathfrak{g})$.

While parts II and III established an isomorphism between the three algebras of operators, they only briefly touched on their spectra in Chapter 11. This isomorphism should be extended to a higher generalisation of modular functors [185], identifying the Hilbert spaces on which these operators act and the actions of the mapping class group of the Riemann surface on them. The first step would be to compute and compare the spectra of operators. As functions on the moduli space of flat connections, one should find a representation which diagonalises a maximally commuting set of operators (possibly including networks) in terms of canonically conjugate variables.

The results of parts II and III also suggest that suitable Toda conformal blocks represent natural candidates for the partition functions of strongly coupled theories $\mathfrak{X}(\mathcal{C}_{g,n}, \mathfrak{g})$, and together with Part IV of this thesis provide the groundwork for a program to explore this relation further. Part IV has begun addressing connections to topological string theory using the partition functions from topological strings on Calabi-Yau threefolds which appear in the geometric engineering of 4d non-Lagrangian theories $\mathfrak{X}(\mathcal{C}_{g,n}, \mathfrak{g})$ and which have been determined through refined topological vertex techniques by [48], [75]. The corre-

sponding Toda conformal blocks should be obtained as a limit of these partition functions, however, the precise way to take such a limit is still in general an open question and requires a meaningful renormalisation procedure to eliminate divergences. It will become possible to extract useful predictions from the topological strings results only when such questions are fully elucidated.

Bibliography

[1] J. Teschner, *Exact results on $\mathcal{N} = 2$ supersymmetric gauge theories*, [arXiv:1412.7145].

[2] N. Seiberg and E. Witten, *Monopole Condensation, And Confinement In N=2 Supersymmetric Yang-Mills Theory*, *Nucl. Phys.* **B426** (1994) 19–52. [hep-th/9407087].

[3] N. Seiberg and E. Witten, *Monopoles, duality and chiral symmetry breaking in N=2 supersymmetric QCD*, *Nucl. Phys.* **B431** (1994) 484–550. [hep-th/9408099].

[4] Y. Tachikawa, *N=2 supersymmetric dynamics for pedestrians*, Lect. Notes Phys. **890** (2014), [arXiv:1312.2684].

[5] E. Witten, *Solutions of four-dimensional field theories via M- theory*, Nucl. Phys. B500 (1997) 342, [hep-th/9703166].

[6] E. Witten, *Some comments on string dynamics*, *Future perspectives in string theory 501-523*, (1995), [hep-th/9507121].

[7] E. Witten, *Five-branes and M theory on an orbifold*, *Nucl. Phys.* B **463**, 383 (1996), [hep-th/9512219].

[8] A. Strominger, *Open p-branes*, *Phys. Lett. B* **383**, 44 (1996), [hep-th/9512059].

[9] D. Gaiotto, *$\mathcal{N}$=2 dualities*, *JHEP* **1208** (2012) 034, [arXiv:0904.2715].

[10] D. Gaiotto, G. W. Moore, and A. Neitzke, *Wall-crossing, Hitchin systems, and the WKB approximation*, *Adv. Math.* **234** (2013) 239–403, [arXiv:0907.3987].

[11] E. Witten, *Topological Quantum Field Theory*, *Commun. Math. Phys.* **117** (1988) 353.

[12] N. A. Nekrasov, *Seiberg-Witten prepotential from instanton counting*, *Adv. Theor. Math. Phys.* **7** (2004) 831–864. [hep-th/0206161].

[13] V. Pestun, *Localization of gauge theory on a four-sphere and supersymmetric Wilson loops*, *Commun.Math.Phys.* **313** (2012) 71–129, [arXiv:0712.2824].

[14] L. F. Alday, D. Gaiotto, and Y. Tachikawa, *Liouville Correlation Functions from Four-dimensional Gauge Theories*, *Lett.Math.Phys.* **91** (2010) 167–197, [arXiv:0906.3219].

[15] J. Teschner, *A guide to two-dimensional conformal field theory*, arXiv:1708.0068.

[16] J. Teschner, *Liouville theory revisited*, *Class. Quant. Grav.* **18** (2001) R153–R222, [hep-th/0104158].

[17] J. Teschner, *On the relation between quantum Liouville theory and the quantized Teichmüller spaces*, Int. J. Mod. Phys. **A19S2** (2004) 459–477, [hep-th/0303149].

[18] H. Dorn and H. J. Otto, *Two and three point functions in Liouville theory*, *Nucl. Phys. B* **429**, 375 (1994), [hep-th/9403141].

[19] A. B. Zamolodchikov and A. B. Zamolodchikov, *Structure constants and conformal bootstrap in Liouville field theory*, *Nucl. Phys. B* **477**, 577 (1996), [hep-th/9506136].

[20] N. Wyllard, *A_{N-1} conformal Toda field theory correlation functions from conformal $\mathcal{N} = 2$ $SU(N)$ quiver gauge theories*, *JHEP* **0911** (2009) 002, [arXiv:0907.2189].

[21] F. Passerini, *Gauge Theory Wilson Loops and Conformal Toda Field Theory*, *JHEP* **1003** (2010) 125, [arXiv:1003.1151].

[22] C. Kozcaz, S. Pasquetti, and N. Wyllard, *A & B model approaches to surface operators and Toda theories*, *JHEP* **1008** (2010) 042, [arXiv:1004.2025].

[23] S. Kanno, Y. Matsuo, and S. Shiba, *Analysis of correlation functions in Toda theory and AGT-W relation for SU(3) quiver*, *Phys.Rev.* **D82** (2010) 066009, [arXiv:1007.0601].

[24] J. Gomis and B. Le Floch, *'t Hooft Operators in Gauge Theory from Toda CFT*, *JHEP* **1111** (2011) 114, [arXiv:1008.4139].

[25] N. Wyllard, *W-algebras and surface operators in $\mathcal{N} = 2$ gauge theories*, *J.Phys.* **A44** (2011) 155401, [arXiv:1011.0289].

[26] N. Wyllard, *Instanton partition functions in $\mathcal{N} = 2$ $SU(N)$ gauge theories with a general surface operator, and their W-algebra duals*, *JHEP* **1102** (2011) 114, [arXiv:1012.1355].

[27] N. Drukker and F. Passerini, *(de)Tails of Toda CFT*, *JHEP* **1104** (2011) 106, [arXiv:1012.1352].

[28] Y. Tachikawa, *On W-algebras and the symmetries of defects of 6d $\mathcal{N} = (2, 0)$ theory*, *JHEP* **1103** (2011) 043, [arXiv:1102.0076].

[29] V. Fateev and A. Litvinov, *Integrable structure, W-symmetry and AGT relation*, *JHEP* **1201** (2012) 051, [arXiv:1109.4042].

[30] B. Estienne, V. Pasquier, R. Santachiara, and D. Serban, *Conformal blocks in Virasoro and W theories: Duality and the Calogero-Sutherland model*, *Nucl.Phys.* **B860** (2012) 377–420, [arXiv:1110.1101].

[31] H. Zhang and Y. Matsuo, *Selberg Integral and SU(N) AGT Conjecture*, *JHEP* **1112** (2011) 106, [arXiv:1110.5255].

[32] S. Shiba, *Notes on 3-point functions of A_{N-1} Toda theory and AGT-W relation for SU(N) quiver*, *JHEP* **1112** (2011) 108, [arXiv:1111.1899].

[33] S. Kanno, Y. Matsuo, and H. Zhang, *Extended Conformal Symmetry and Recursion Formulae for Nekrasov Partition Function*, *JHEP* **1308** (2013) 028, [arXiv:1306.1523].

[34] M. Aganagic, N. Haouzi, and S. Shakirov, *A_n-Triality*, [arXiv:1403.3657].

[35] J. Gomis, B. Le Floch, *M2-brane surface operators and gauge theory dualities in Toda*, JHEP **1604** (2016) 183, [arXiv:1407.1852].

[36] L. Hollands, *Topological Strings and Quantum Curves*, [arXiv:0911.341].

[37] A. Karch, D. Lust and D. J. Smith, *Equivalence of geometric engineering and Hanany-Witten via fractional branes*, *Nucl. Phys. B* **533**, 348 (1998), [hep-th/9803232].

[38] A. Klemm, W. Lerche, P. Mayr, C. Vafa and N. P. Warner, *Selfdual strings and N=2 supersymmetric field theory*, *Nucl. Phys. B* **477**, 746 (1996), [hep-th/9604034].

[39] S. H. Katz, A. Klemm and C. Vafa, *Geometric engineering of quantum field theories*, *Nucl. Phys. B* **497** (1997) 173, [hep-th/9609239].

[40] S. Katz, P. Mayr and C. Vafa, *Mirror symmetry and exact solution of 4-D N=2 gauge theories I*, *Adv. Theor. Math. Phys.* **1**, 53 (1998), [hep-th/9706110].

[41] M. Aganagic, A. Klemm, M. Marino and C. Vafa, *The Topological vertex*, *Commun. Math. Phys.* **254**, 425 (2005), [hep-th/0305132].

[42] H. Awata and H. Kanno, *Instanton counting, Macdonald functions and the moduli space of D-branes*, *JHEP* **0505**, 039 (2005), [hep-th/0502061].

[43] H. Awata and H. Kanno, *Refined BPS state counting from Nekrasov's formula and Macdonald functions*, *Int. J. Mod. Phys.* A **24**, 2253 (2009), [arXiv:0805.0191].

[44] H. Awata, B. Feigin and J. Shiraishi, *Quantum Algebraic Approach to Refined Topological Vertex*, *JHEP* **1203**, 041 (2012), [arXiv:1112.6074].

[45] A. Iqbal, C. Kozcaz and C. Vafa, *The refined topological vertex*, *JHEP* **0910**, 069 (2009), [hep-th/0701156].

[46] M. Taki, *Refined Topological Vertex and Instanton Counting*, *JHEP* **0803**, 048 (2008), [arXiv:0710.1776].

[47] F. Benini, S. Benvenuti and Y. Tachikawa, *Webs of five-branes and N=2 superconformal field theories*, *JHEP* **0909**, 052 (2009), [arXiv:0906.0359].

[48] V. Mitev, E. Pomoni, *Toda 3-Point Functions From Topological Strings* JHEP **1506** (2015) 049. [arXiv:1409.6313].

[49] R. Dijkgraaf and C. Vafa, *Toda Theories, Matrix Models, Topological Strings, and N=2 Gauge Systems*, [arXiv:0909.2453].

[50] D. Gaiotto, G. W. Moore, and A. Neitzke, *Four-dimensional wall-crossing via three-dimensional field theory*, *Commun.Math.Phys.* **299** (2010) 163–224, [arXiv:0807.4723].

[51] D. Gaiotto, G. W. Moore, and A. Neitzke, *Framed BPS States*, *Adv.Theor.Math.Phys.* **17** (2013) 241–397, [arXiv:1006.0146].

[52] D. Gaiotto, G. W. Moore, and A. Neitzke, *Spectral Networks and Snakes*, *Annales Henri Poincare* **15** (2014) 61–141, [arXiv:1209.0866].

[53] A. Neitzke, *Hitchin systems in $\mathcal{N} = 2$ field theory*, [arXiv:1412.7120].

[54] J. Teschner and G. Vartanov, *Supersymmetric gauge theories, quantization of $\mathcal{M}_{\rm flat}$, and conformal field theory*, *Adv.Theor.Math.Phys.* **19** (2015) 1–135, [arXiv:1302.3778].

[55] J. Teschner, *Supersymmetric gauge theories, quantization of moduli spaces of flat connections, and Liouville theory*, arXiv:1412.7140.

[56] L. F. Alday, D. Gaiotto, S. Gukov, Y. Tachikawa, and H. Verlinde, *Loop and surface operators in $\mathcal{N} = 2$ gauge theory and Liouville modular geometry*, *JHEP* **1001** (2010) 113, [arXiv:0909.0945].

[57] N. Drukker, J. Gomis, T. Okuda, and J. Teschner, *Gauge Theory Loop Operators and Liouville Theory*, *JHEP* **1002** (2010) 057, [arXiv:0909.1105].

[58] J. Gomis, T. Okuda, and V. Pestun, *Exact Results for 't Hooft Loops in Gauge Theories on S^4*, *JHEP* **1205** (2012) 141, [arXiv:1105.2568].

[59] Y. Ito, T. Okuda, and M. Taki, *Line operators on $S^1 \times \mathbb{R}^3$ and quantization of the Hitchin moduli space*, *JHEP* **1204** (2012) 010, [arXiv:1111.4221].

[60] O. Aharony, N. Seiberg, and Y. Tachikawa, *Reading between the lines of four-dimensional gauge theories*, *JHEP* **1308** (2013) 115, [arXiv:1305.0318].

[61] Y. Tachikawa, *On the 6d origin of discrete additional data of 4d gauge theories*, *JHEP* **1405** (2014) 020, [arXiv:1309.0697].

[62] C. Cordova and A. Neitzke, *Line Defects, Tropicalization, and Multi-Centered Quiver Quantum Mechanics*, *JHEP* **1409** (2014) 099, [arXiv:1308.6829].

[63] V. Fock and A. Goncharov, *Moduli spaces of local systems and higher Teichmuller theory*, *Publ. Math. Inst. Hautes Études Sci.* **103** (2006) 1211, [math/0311149].

[64] N. J. Hitchin, *The Selfduality equations on a Riemann surface*, *Proc. Lond. Math. Soc.* **55** (1987) 59?131.

[65] W. M. Goldman, *Topological components of spaces of representations*, *Inventiones Mathematicae* **93**, no. 3, (1988) 557-608.

[66] S. Gukov and E. Witten, *Gauge theory, ramification, and the geometric Langlands program*, in *Current developments in mathematics, 2006*, pp. 35–180. Int. Press, Somerville, MA, 2008, [hep-th/0612073].

[67] N. Hama and K. Hosomichi, *Seiberg-Witten Theories on Ellipsoids*, *JHEP* **1209** (2012) 033, [arXiv:1206.6359].

[68] Y. Tachikawa, *A review on instanton counting and W-algebras*, arXiv:1412.7121.

[69] N. Nekrasov and E. Witten, *The Omega Deformation, Branes, Integrability, and Liouville Theory*, *JHEP* **1009** (2010) 092, [arXiv:1002.0888].

[70] N. Nekrasov, A. Rosly, and S. Shatashvili, *Darboux coordinates, Yang-Yang functional, and gauge theory*, *Nucl. Phys. Proc. Suppl.* **216** (2011) 69–93, [arXiv:1103.3919].

[71] M. Bullimore, *Defect Networks and Supersymmetric Loop Operators*, *JHEP* **1502** (2015) 066, [arXiv:1312.5001].

[72] B. Le Floch, *S-duality wall of SQCD from Toda braiding*, [arXiv:1512.09128].

[73] N. Y. Reshetikhin and V. G. Turaev, *Ribbon graphs and their invariants derived from quantum groups*, *Comm. Math. Phys.* **127** (1990), no. 1 1–26.

[74] L. Bao, V. Mitev, E. Pomoni, M. Taki, and F. Yagi, *Non-Lagrangian Theories from Brane Junctions*, *JHEP* **1401** (2014) 175, [arXiv:1310.3841].

[75] M. Isachenkov, V. Mitev, E. Pomoni, *Toda 3-Point Functions From Topological Strings II*, JHEP **1608** (2016) 066, [arXiv:1412.3395].

[76] O. Chacaltana and J. Distler, *Tinkertoys for Gaiotto Duality*, *JHEP* **1011** (2010) 099, [arXiv:1008.5203].

[77] I. Coman, M. Gabella, J. Teschner, *Line operators in theories of class $\mathcal{S}$, quantized moduli space of flat connections, and Toda field theory*, JHEP **1510** (2015) 143, [arXiv:1505.05898].

[78] W. M. Goldman, *Trace Coordinates on Fricke spaces of some simple hyperbolic surfaces*, *ArXiv e-prints* (Jan., 2009) [arXiv:0901.1404].

[79] A. S. Sikora, *Generating sets for coordinate rings of character varieties*, *ArXiv e-prints* (June, 2011) [arXiv:1106.4837].

[80] S. Lawton, *Generators, Relations and Symmetries in Pairs of 3x3 Unimodular Matrices*, *ArXiv Mathematics e-prints* (Jan., 2006) [math/0601132].

[81] M. Audin, *Lectures on gauge theory and integrable systems*, in *Gauge Theory and Symplectic Geometry* (J. Hurtubise, F. Lalonde, and G. Sabidussi, eds.), vol. 488 of *NATO ASI Series*, pp. 1–48. Springer Netherlands, 1997.

[82] W. Goldman, *Invariant functions on lie groups and hamiltonian flows of surface group representations*, *Inventiones mathematicae* **85** (1986), no. 2 263–302.

[83] S. Lawton, *Poisson Geometry of SL(3,C)-Character Varieties Relative to a Surface with Boundary*, *ArXiv Mathematics e-prints* (Mar., 2007) [math/0703251].

[84] G. Kuperberg, *Spiders for rank 2 Lie algebras*, in *eprint arXiv:q-alg/9712003*, p. 12003, Nov., 1997.

[85] V. G. Turaev, *Skein quantization of poisson algebras of loops on surfaces*, *Annales scientifiques de l'cole Normale Suprieure* **24** (1991), no. 6 635–704.

[86] E. Witten, *Quantum field theory and the jones polynomial*, *Comm. Math. Phys.* **121** (1989), no. 3 351–399.

[87] E. Witten, *Gauge Theories, Vertex Models and Quantum Groups*, *Nucl.Phys.* **B330** (1990) 285.

[88] A. S. Sikora, *Skein theory for SU(n)-quantum invariants*, *ArXiv Mathematics e-prints* (July, 2004) [math/0407299].

[89] H. Murakami, T. Ohtsuki, and S. Yamada, *HOMFLY Polynomial via an Invariant of Colored Plane Graphs*, *L'Enseignement Mathématique* **44** (1998) 325–360.

[90] D. Kim, *Graphical Calculus on Representations of Quantum Lie Algebras*, *ArXiv Mathematics e-prints* (Oct., 2003) [math/0310143].

[91] S. Morrison, *A Diagrammatic Category for the Representation Theory of $U_q(\mathfrak{sl}_N)$*, *ArXiv e-prints* (Apr., 2007) [arXiv:0704.1503].

[92] S. Cautis, J. Kamnitzer, and S. Morrison, *Webs and quantum skew Howe duality*, *Math. Ann.* **360** (2014), no. 1-2 351–390, [arXiv:1210.6437].

[93] Y. Tachikawa, N. Watanabe, *On skein relations in class S theories*, JHEP **1506** (2015) 186, [arXiv:1504.00121].

[94] Y. Teranishi, *The ring of invariants of matrices*, *Nagoya Math. J.* **104** (1986) 149–161.

[95] T. Dimofte and S. Gukov, *Chern-Simons Theory and S-duality*, *JHEP* **1305** (2013) 109, [arXiv:1106.4550].

[96] D. Xie, *Higher laminations, webs and $\mathcal{N} = 2$ line operators*, arXiv:1304.2390.

[97] S. Lawton, *Obtaining the One-Holed Torus from Pants: Duality in an SL(3,C)-Character Variety*, *ArXiv e-prints* (Mar., 2008) [arXiv:0803.3489].

[98] S. Lawton, *Minimal Affine Coordinates for SL(3,C) Character Varieties of Free Groups*, *ArXiv e-prints* (Sept., 2007) [arXiv:0709.4403].

[99] S. Lawton, *Algebraic Independence in SL(3,C) Character Varieties of Free Groups*, *ArXiv e-prints* (July, 2008) [arXiv:0807.0798].

[100] N. Saulina, *Spectral networks and higher web-like structures*, arXiv:1409.2561.

[101] T. Dimofte, M. Gabella, and A. B. Goncharov, *K-Decompositions and 3d Gauge Theories*, arXiv:1301.0192.

[102] W. Goldman, *Convex real projective structures on compact surfaces*, J. Differential Geom. **31** (1990) 126-159.

[103] H.C. Kim, *The symplectic global coordinates on the moduli space of real projective structures*, J. Differential Geom. **53** (1999) 359-401.

[104] L. Hollands, A. Neitzke, *Spectral Networks and Fenchel–Nielsen Coordinates*, Lett. Math. Phys. **106** (2016) 811–877, [arXiv:1312.2979].

[105] L. Hollands, O. Kidwai, *Higher length-twist coordinates, generalized Heun's opers, and twisted superpotentials*, [arXiv:1710.04438].

[106] V. Fateev and A. Litvinov, *Correlation functions in conformal Toda field theory. I.*, *JHEP* **0711** (2007) 002, [arXiv:0709.3806].

[107] I. Coman, E. Pomoni, J. Teschner, *Toda conformal blocks, quantum groups, and flat connections, (2017), [arXiv:1712.10225].*

[108] P. Bouwknegt and K. Schoutens, W symmetry in conformal field theory, Phys.Rept. **223** *(1993) 183–276, [hep-th/9210010].*

[109] J. Teschner A guide to two-dimensional conformal field theory, [arXiv:1708.00680].

[110] E. Frenkel and D. Ben-Zvi, Vertex algebras and algebraic curves, American Mathematical Society, *2004.*

[111] A. Belavin, A. Polyakov, and A. Zamolodchikov, Infinite conformal symmetry in two-dimensional quantum field theory, Nuclear Physics B **241** *(1984), no. 2 333 – 380.*

[112] J. Teschner, Quantization of moduli spaces of flat connections and Liouville theory, ArXiv e-prints *(May, 2014) [arXiv:1405.0359].*

[113] P. Bowcock and G. Watts, Null vectors, three point and four point functions in conformal field theory, Theor.Math.Phys. **98** *(1994) 350–356, [hep-th/9309146].*

[114] V. Chari and A. Pressley, A guide to quantum groups*. Cambridge University Press, 1994.*

[115] C. Gomez, G. Sierra, The Quantum Symmetry of Rational Conformal Field Theories, Nucl.Phys. **B352** *(1991) 791-828 .*

[116] G. Felder, C. Wiecerkowski, Topological representations of the quantum group $U_q(sl(2))$, Comm. Math. Phys. **138** *(1991) 583-605.*

[117] C. Ramirez, H. Ruegg, M. Ruiz-Altaba, The Contour picture of quantum groups: Conformal field theories, Nucl.Phys. **B364** *(1991) 195-233.*

[118] P. Bouwknegt, J. McCarthy, K. Pilch, Free field approach to two-dimensional conformal field theories, Prog. Theor. Phys. Suppl. **102** *(1990) 67-135.*

[119] R. Bezrukavnikov, M. Finkelberg, V. Schechtman, Factorisable sheaves and quantum groups, Lecture Notes in Mathematics **1691***, Springer Verlag, Berlin, 1998.*

[120] G. Felder, BRST approach to minimal models, Nuclear Physics **B317***, (1989), 215-236.*

[121] A. Bilal and J.-L. Gervais, Systematic Construction of Conformal Theories with Higher Spin Virasoro Symmetries, Nucl.Phys. **B318** *(1989) 579.*

[122] E. Cremmer and J.-L. Gervais, The quantum group structure associated with nonlinearly extended virasoro algebras, Comm. Math. Phys. **134** *(1990), no. 3 619–632.*

[123] E. Buffenoir, P. Roche, and V. Terras, Quantum Dynamical coBoundary Equation for finite dimensional simple Lie algebras, ArXiv Mathematics e-prints *(Dec., 2005) [math/0512500].*

[124] M. Semenov-Tian-Shansky, Quantization of open toda lattices, in Dynamical Systems VII *(V. Arnold and S. Novikov, eds.), vol. 16 of* Encyclopaedia of Mathematical Sciences*, pp. 226–259. Springer Berlin Heidelberg, 1994.*

[125] N. Wallach, Real reductive groups II. *Academic Press, 1992.*

[126] K. K. Kozlowski, Unitarity of the SoV Transform for the Toda Chain, Communications in Mathematical Physics *(Aug., 2014) [arXiv:1306.4967].*

[127] T. L. Curtright and C. B. Thorn, Conformally Invariant Quantization of the Liouville Theory, Phys. Rev. Lett. **48** *(1982) 1309.*

[128] R. M. Kashaev, On the Spectrum of Dehn Twists in Quantum Teichmüller Theory, in Physics and Combinatorics *(A. N. Kirillov, A. Tsuchiya, and H. Umemura, eds.), pp. 63–81, Apr., 2001. math/0008148.*

[129] L. D. Faddeev and L. A. Takhtajan, On the spectral theory of one functional-difference operator from conformal field theory, ArXiv e-prints *(Aug., 2014) [arXiv:1408.0307].*

[130] J. Teschner, Quantization of the Hitchin moduli spaces, Liouville theory, and the geometric Langlands correspondence I. Adv. Theor. Math. Phys. **15** *(2011) 471–564, [arXiv:1005.2846].*

[131] N. Iorgov, O. Lisovyy, J. Teschner, Isomonodromic tau-functions from Liouville conformal blocks, Comm. Math. Phys. **336** *(2015) 671-694, [arXiv:1401.6104].*

[132] B. Ponsot and J. Teschner, Liouville bootstrap via harmonic analysis on a noncompact quantum group*, [arXiv:hep-th/9911110].*

[133] B. Ponsot and J. Teschner, Clebsch-Gordan and Racah-Wigner coefficients for a continuous series of representations of $U_q(sl(2,\mathbb{R}))$*, Commun. Math. Phys.* **224** *(2001) 613–655, [math/0007097].*

[134] A. G. Bytsko and J. Teschner, R-operator, co-product and Haar-measure for the modular double of $U_q(\mathfrak{sl}(2,\mathbb{R}))$*. Comm. Math. Phys.* **240** *(2003) 171–196, [math/0208191].*

[135] L. D. Faddeev, Discrete Heisenberg-Weyl Group and Modular Group*, Lett. Math. Phys.* **34** *(1995) 249-254, [hep-th/9504111].*

[136] L. D. Faddeev, Modular double of a quantum group*, Confrence Mosh Flato 1999, Vol. I (Dijon), 149–156, Math. Phys. Stud.,* **21***, Kluwer Acad. Publ., Dordrecht, 2000, [math/9912078].*

[137] L.O. Chekhov, V. Fock: A quantum Teichmüller space, Theor. Math. Phys. **120** *(1999) 1245–1259, [math/9908165].*

[138] R.M. Kashaev: Quantization of Teichmüller spaces and the quantum dilogarithm, Lett. Math. Phys. **43** *(1998) 105-115, [q-alg/9705021]*

[139] I. Nidaiev, T. Teschner, On the relation between the modular double of $U_q(sl(2,R))$ *and the quantum Teichmueller theory, [arXiv:1302.3454].*

[140] Fock, V. V.; Goncharov, A. B. The quantum dilogarithm and representations of quantum cluster varieties. Invent. Math. **175** *(2009) 223–286, [math/0702397].*

[141] N. Hitchin, Lie group and Teichmüller space, Topology **31** *(1992) 449–473.*

[142] R.C. Penner, The decorated Teichmüller space of punctured surfaces, Comm. Math. Phys. **113** *(1987) 299–339.*

[143] I. Frenkel, I. Ip, Positive representation of split real quantum groups and future perspectives, International Mathematics Research Notices, **2014** *(8) (2014) 2126-2164, [arXiv:1111.1033].*

[144] G. Schrader, A. Shapiro, Continuous tensor categories from quantum groups I: algebraic aspects, [arXiv:1708.08107].

[145] G. Schrader, A. Shapiro, A cluster realization of $U_q(\mathfrak{sl}_n)$ from quantum character varieties, [arXiv:1607.00271].

[146] R. M. Kashaev, The quantum dilogarithm and Dehn twists in quantum Teichmüller theory. Integrable structures of exactly solvable two-dimensional models of quantum field theory (Kiev, 2000), 211–221, NATO Sci. Ser. II Math. Phys. Chem., 35, Kluwer Acad. Publ., Dordrecht, 2001.

[147] M. C. N. Cheng, R. Dijkgraaf, and C. Vafa, Non-Perturbative Topological Strings And Conformal Blocks, JHEP **09** *(2011) 022, [arXiv:1010.4573].*

[148] A. Gadde, S. S. Razamat, and B. Willett, "Lagrangian" for a Non-Lagrangian Field Theory with $\mathcal{N} = 2$ Supersymmetry, Phys. Rev. Lett. **115** *(2015), no. 17 171604, [arXiv:1505.0583].*

[149] V. Fateev and A. Litvinov, On differential equation on four-point correlation function in the Conformal Toda Field Theory, JETP Lett. **81** *(2005) 594–598, [hep-th/0505120].*

[150] V. Fateev and A. Litvinov, Correlation functions in conformal Toda field theory II, JHEP **0901** *(2009) 033, [arXiv:0810.3020].*

[151] H. Hayashi, H.-C. Kim, and T. Nishinaka, Topological strings and 5d T_N partition functions, arXiv:1310.3854.

[152] H. Awata and Y. Yamada, Five-dimensional AGT Conjecture and the Deformed Virasoro Algebra, JHEP **1001** *(2010) 125, [arXiv:0910.4431].*

[153] H. Awata and Y. Yamada, Five-dimensional AGT Relation and the Deformed beta-ensemble, Prog.Theor.Phys. **124** *(2010) 227–262, [arXiv:1004.5122].*

[154] B. Feigin and E. Frenkel, Quantum W algebras and elliptic algebras, Commun. Math. Phys. **178** *(1996) 653–678, [q-alg/9508009].*

[155] E. Frenkel and N. Reshetikhin, Deformations of W-algebras associated to simple Lie algebras, (1997), [q-alg/9708006].

[156] R. Schiappa and N. Wyllard, An A(r) threesome: Matrix models, 2d CFTs and 4d N=2 gauge theories, J. Math. Phys. **51** *(2010) 082304, [arXiv:0911.5337].*

[157] A. Mironov, A. Morozov, S. Shakirov, and A. Smirnov, Proving AGT conjecture as HS duality: extension to five dimensions, Nucl.Phys. **B855** *(2012) 128–151, [arXiv:1105.0948].*

[158] L. Bao, E. Pomoni, M. Taki, and F. Yagi, M5-Branes, Toric Diagrams and Gauge Theory Duality, JHEP **1204** *(2012) 105, [arXiv:1112.5228].*

[159] H. Itoyama, T. Oota, and R. Yoshioka, 2d-4d Connection between q-Virasoro/W Block at Root of Unity Limit and Instanton Partition Function on ALE Space, Nucl.Phys. **B877** *(2013) 506–537, [arXiv:1308.2068].*

[160] F. Nieri, S. Pasquetti, and F. Passerini, 3d & 5d gauge theory partition functions as q-deformed CFT correlators, arXiv:1303.2626.

[161] F. Nieri, S. Pasquetti, F. Passerini, and A. Torrielli, 5D partition functions, q-Virasoro systems and integrable spin-chains, arXiv:1312.1294.

[162] M. Aganagic, N. Haouzi, C. Kozcaz, and S. Shakirov, Gauge/Liouville Triality, arXiv:1309.1687.

[163] M. Taki, On AGT-W Conjecture and q-Deformed W-Algebra, arXiv:1403.7016.

[164] M.-C. Tan, An M-Theoretic Derivation of a 5d and 6d AGT Correspondence, and Relativistic and Elliptized Integrable Systems, JHEP **1312** *(2013) 031, [arXiv:1309.4775].*

[165] E. Carlsson, N. Nekrasov, and A. Okounkov, Five dimensional gauge theories and vertex operators, Moscow Math. J. **14** *(2014), no. 1 39–61, [arXiv:1308.2465].*

[166] T. Kimura and V. Pestun, Quiver W-algebras, arXiv:1512.0853.

[167] A. Mironov, A. Morozov, and Y. Zenkevich, Ding-Iohara-Miki symmetry of network matrix models, Phys. Lett. **B762** *(2016) 196–208, [arXiv:1603.0546].*

[168] J.-E. Bourgine, M. Fukuda, Y. Matsuo, H. Zhang, and R.-D. Zhu, Coherent states in quantum $\mathcal{W}_{1+\infty}$ algebra and qq-character for 5d Super Yang-Mills, PTEP **2016** *(2016), no. 12 123B05, [arXiv:1606.0802].*

[169] J.-E. Bourgine, M. Fukuda, K. Harada, Y. Matsuo, and R.-D. Zhu, (p,q)-webs of DIM representations, 5d N=1 instanton partition functions and qq-characters, [arXiv:1703.1075].

[170] I. Coman, E. Pomoni, J. Teschner, Liouville conformal blocks from topological strings, to appear.

[171] I. Coman, E. Pomoni, J. Teschner, Toda conformal blocks from topological strings, in progress.

[172] C. Kozcaz, S. Pasquetti, and N. Wyllard, $A\&B$ model approaches to surface operators and Toda theories, JHEP **1008** *(2010) 042, [arXiv:1004.2025].*

[173] O. Aharony and A. Hanany, Branes, superpotentials and superconformal fixed points, Nucl.Phys. **B504** *(1997) 239–271, [hep-th/9704170].*

[174] O. Aharony, A. Hanany, and B. Kol, Webs of (p,q) five-branes, five-dimensional field theories and grid diagrams, JHEP **9801** *(1998) 002, [hep-th/9710116].*

[175] N. C. Leung and C. Vafa, Branes and toric geometry, Adv.Theor.Math.Phys. **2** *(1998) 91–118, [hep-th/9711013].*

[176] A. Iqbal and A.-K. Kashani-Poor, Instanton counting and Chern-Simons theory, Adv. Theor. Math. Phys. **7** *(2003), no. 3 457–497, [hep-th/0212279].*

[177] A. Iqbal and A.-K. Kashani-Poor, SU(N) geometries and topological string amplitudes, Adv. Theor. Math. Phys. **10** *(2006), no. 1 1–32, [hep-th/0306032]. ,*

[178] P. Sulkowski, Crystal model for the closed topological vertex geometry, JHEP **12** *(2006) 030, [hep-th/0606055].*

[179] I. G. Macdonald, Symmetric Functions and Hall Polynomials, Oxford University Press*, (1998)*

[180] A. B. Zamolodchikov, Three-point function in the minimal Liouville gravity, Theor. Math. Phys. **142***,183 (2005) , hep-th/0505063.*

[181] S. Ribault and R. Santachiara, Liouville theory with a central charge less than one, JHEP **08** *(2015) 109, [arXiv:1503.0206].*

[182] N. Michitomo, Multiple Gamma Function, Its q- and Elliptic Analogue, Rocky Mountain J. Math.*,* **32***, (2002), 2, 793–811, [1030539697].*

[183] A. N. Kirillov, Dilogarithm identities, Prog. Theor. Phys. Suppl. **118** *(1995) 61–142, [hep-th/9408113].*

[184] T. H. Koornwinder, Jacobi functions as limit cases of q-ultraspherical polynomials, Journal of Mathematical Analysis and Applications **148** *(1990), no. 1 44 – 54*

[185] J. Teschner, An analog of a modular functor from quantized Teichmuller theory, [math-qa/0510174].

Acknowledgements

My warmest acknowledgement and sincere gratitude go to my supervisor Joerg Teschner, who gave me the opportunity to join the Theory Group in Desy and patiently answered avalanches of questions over the years. His constant support and encouragement, as well as the many projects discussions and life advice have been invaluable.

I would also like to say thank you to Volker Schomerus for giving me the chance to join the "Gauge Theory as an Integrable System" (GATIS) training network and his unwavering help at crucial moments during my PhD.

Over the course of my time in Desy I had the pleasure to work with some fantastic collaborators, Elli Pomoni, Maxime Gabella, Futoshi Yagi and Masato Taki, whom I thank for the many engaging discussions. I have benefited greatly from their experience.

My work was financially supported by the GATIS training network, the DESY Theory Group and the Research Training Group 1670 "Mathematics inspired by string theory and quantum field theory", at the University of Hamburg. I am grateful to Desy and the University of Hamburg for the excellent working conditions they provided.

I wish to say a big thank you to my friends Jan-Peter Carstensen, Yannick Linke, Troy Figiel, Raphaël Belliard, Rob Klabbers, Madalena Lemos, Ricardo Vaz, Martina Cornagliotto, Lorenzo Bianchi, Alessandra Cagnazzo, Mikhail Isachenkov and Malik Abdullah. You have made days in Desy (and outside) fun and created many fond memories. I am very grateful to Jan-Peter for his help in translating the abstract of my thesis.

I am very grateful to Amelie and Andres for the kindness they have shown me and the moral support they have provided, for welcoming me to Hamburg and into their home.

With all my love I thank my parents Ana and Doru and my little sister Cristina for their unconditional support in the pursuit of dreams. Mami si tati, va multumesc pentru toata sustinerea, incurajearea si pentru ca aveti grija de puiul meu. Fara ajutorul vostru nu as fi putut scrie teza. To my husband Nikolas, rakastan sinua. Olet ihanin aviomies, isä ja paras kaverini. Our daughter Karolina was born in Aug. 2016 and has since turned our life into an absolute adventure. Mama te iubeste mai presus de tot.

Eidesstattliche Versicherung

Hiermit versichere ich an Eides statt, die vorliegende Dissertationsschrift selbst verfasst und keine anderen als die angegebenen Hilfsmittel und Quellen benutzt zu haben. Die eingereichte schriftliche Fassung entspricht der auf dem elektronischen Speichermedium. Die Dissertation wurde in der vorgelegten oder einer ähnlichen Form nicht schon einmal in einem früheren Promotionsverfahren angenommen oder als ungenügend beurteilt.

I hereby declare on oath, that I have written the present dissertation by my own and have not used other than the acknowledged resources and aids. The submitted written version corresponds to the version on the electronic storage medium. I hereby declare that I have not previously applied or pursued for a doctorate (Ph.D. studies).

Hamburg, den 06. März 2018 Unterschrift Ioana Alexandra Coman-Lohi